Bio-based reference façade wall details

Design and analysis of moisture transport and thermal bridges for Dutch residential top-up buildings

Master thesis
MSc. Architecture, Urbanism and Building Sciences
Master track: Buidling Technology
19-06-2025

Mark de Kanter

ABSTRACT

By 2050, the Dutch construction sector is required to be fully circular, where bio-based materials can play a promising role in this transition. However, the implementation of bio-based materials is currently limited due to a lack of technical design knowledge within the sector. Additionally, the hygroscopic properties are insufficiently understood, which further hinders the integration of bio-based materials into building designs. The main objective of this thesis is therefore to develop validated 1:5 scale bio-based façade wall reference details for residential top-up buildings that perform well in reducing thermal bridges and ensuring effective moisture transport.

The research combines a literature review with research-by-design and digital simulations. Initially, the advantages and disadvantages of bio-based construction materials over conventional ones are examined. Following this, five bio-based materials (cork, flax, hemp, straw, and wood) are selected and incorporated into the developed bio-based reference details. Design principles were first established to ensure the correct implementation of these materials.

In total, this thesis presents 11 detail configurations, consisting of 33 validated bio-based reference details. These details were evaluated using the simulation software WUFI for moisture transport, mould growth, surface condensation, and thermal bridges. The thesis outlines both the methodology and the results. The first configuration is discussed in detail in the main report, while the remaining ten validated configurations are included in the appendix. In addition, this thesis presents 33 additional reference details which were not validated but are expected to show similar performance to the validated ones.

Based on the simulation results, most of the detail configurations meet the requirements for moisture regulation and thermal performance. The isopleth analyses indicate that mould growth does not occur within the tested material layers in most configurations. Furthermore, no surface condensation was observed at the most critical points within the details. The results also comply with Dutch regulations regarding limited thermal bridging, with the measured values comparable to those of the 'ISSO reference details'.

These simulation results hereby demonstrate that the developed bio-based reference details can be effectively used in residential top-up buildings. However, the established design principles and vapour permeability must be maintained. When applied correctly, the selected bio-based materials can prevent mould growth and surface condensation, while keeping thermal bridging to a minimum.

Although the simulations provide valuable insights, the validation is limited by the exclusive use of WUFI. Next, only a medium moisture load for indoor climates and the NEN 5060 for outdoor climates are used making the assessments only representative for the Netherlands. Future research could validate the results using alternative simulation software and by considering various climatic and moisture conditions. Before the developed details can be applied in the Dutch market, additional research must explore the remaining building physics aspects and structural requirements. Nevertheless, the developed design principles and validated reference details provide a solid foundation for the further implementation of bio-based construction in Dutch residential buildings.

Keywords: Bio-based details, thermal bridges, moisture-transport, WUFI-simulations, residential top-up buildings

ACKNOWLEDGEMENTS

Firstly, I would like to express my sincerest gratitude to my supervisors Dr. Ing. Olga Ioannou and Prof. Dr. Ir. Martin Tenpierik, for your invaluable guidance. Thanks to your expertise, I have not only grown academically but also developed personally. Throughout my graduation process, you supported me with dedication and professionalism during our meetings, for which I am deeply grateful.

During the course Circular Product Design, I developed a strong interest in bio-based building materials, largely thanks to the enthusiasm of Olga Ioannou. In this course, a bio-based detail must be designed and developed, which I thoroughly enjoyed. This experience was the main reason I decided to focus my graduation project on developing bio-based reference details. I also felt highly motivated to pursue this topic after our first conversation. The weekly group sessions were pleasant and valuable, and I appreciated how you always made time for everyone and provided constructive feedback.

Next, I also have always had a strong interest in building physics, and during our first conversation, Martin Tenpierik encouraged me to explore thermal bridges and moisture transport in the details. I learned a great deal from the individual sessions about, which challenged me to think critically and elevate my work. I especially appreciated the elaborated explanation of the WUFI software, given its less-than-intuitive interface. Our short but effective feedback sessions while picking up and returning the computer with the WUFI software on it were always valuable, and I will remember them fondly.

In addition to my supervisors, I would like to thank Florian Eckardt, Georgios Karvelas, Jan van de Voort, Max Salzberger, Paddy Tomesen, and Pierre Jennen for discussing and providing feedback on my bio-based reference details. The opportunity to consult with you significantly contributed to their quality.

I would also like to thank my friends that I made during my years in Delft. I never expected to meet such a great group of people during my master's. In particular, I want to thank my housemates Bob and Lowie for the motivation you gave me and for the conversations and discussions we shared. I especially cherish the wonderful memories we created together at our home office table in the living room.

I am also deeply grateful to my girlfriend Roos for her never-ending support. Despite both of us working on our graduation projects, we kept encouraging each other. I truly appreciated the meaningful conversations we had and the joyful moments we shared, which brought much-needed relaxation alongside our graduation.

Lastly, I want to thank my amazing parents, my brother Daan, and my girlfriend's mother Jeannette, whom I could always count on. Over the past year, your advice and encouragement have helped me enormously. Even when you didn't fully understand the technical issues I was facing, you always listened and motivated me to take the next step forward.

Delft, University of Technology
June 19, 2025

T.N.M. de Kanter

TABLE OF CONTENTS

1. Introduction

1.1 Background

The Netherlands is facing a significant **housing shortage**, making the construction of new homes a key objective for the national government. This challenge is particularly evident in cities where space is scarce (De Rijksoverheid, 2022). According to the Primos forecast 2023, in total **981,000** additional homes are needed by **2030** (De Rijksoverheid, 2023). Without action, this situation will worsen, with the population expected to increase to 20.6 million by 2070 (Centraal Bureau voor de Statistiek, 2025).

Adding extra floors to existing buildings, known as **top-ups**, could provide approximately **100,000** new homes by **2030** without occupying additional land (Ministerie van Volkshuisvesting en Ruimtelijke Ordening, 2024). But the construction of new buildings involves **energy consumption**, **CO_2 emissions**, and **material use**. According to Hamilton et al. (2024), the construction sector is responsible **40%** of total **CO_2 emissions**. In **the Netherlands**, the sector accounts for **35%** of **national CO_2 emissions** (Nelissen et al., 2018), with **7.7%** attributed to **material-related emissions** (Kuhlmann et al., 2023). To ensure that the temperature rise due to CO_2 emissions remains below 2°C, The Paris Agreement was signed by the Dutch government. It is, therefore, crucial that the **construction sector** also **aims** for **zero CO_2 emissions** by **2050**. To that aim, **bio-based building materials** seems like a **potential** and **suitable candidate** that can contribute to this goal (Hamilton et al., 2021). Only in the Netherlands, these materials have the potential to **reduce CO_2 emissions** by **1.6 Mton annually** (Minister van Binnenlandse Zaken en Koninkrijksrelaties, 2023).

Additionally, humanity is facing a **scarcity of materials**, making it necessary to **reduce** the use of **exhaustible materials** (Bermejo, 2014). **Globally**, the **construction sector** is the **largest consumer** of **materials** (Giesekam et al., 2016). **The Dutch construction sector** significantly contributes to the national raw material use, accounting for **50%** of the **total consumption** (Nelissen et al., 2018). According to Giesekam et al. (2016), **biobased building materials** offer numerous benefits that can help **mitigate** these issues. Bio-based materials are characterized by low environmental impact due to **renewability** (Sandak et al., 2019). Furthermore, most of these materials are **sustainably produced** and are **biodegradable** at the **end** of their **lifecycle** (Jones, 2017). Research by Bosch et al. (2023) indicates that the primary raw material consumption for housing construction could **decrease** by **11.7%** in **the Netherlands** if bio-based materials are adapted.

Due to these advantages, the Dutch government aims to a transition to the use of bio-based materials (Minister van Binnenlandse Zaken en Koninkrijksrelaties, 2023). To achieve this, the **Dutch government** has set goals to realize a **fully circular economy** by **2050**. This includes **halving** the use of **primary abiotic raw building materials** by **2030**. Bio-based building materials can contribute to both objectives (Arnoldusse et al., 2022).

The high demand for housing presents an opportunity to promote sustainable urbanization and meet the ambitions of the Dutch government. The application of bio-based materials in top-up projects contributes to housing needs and helps achieve the goal of a circular economy by 2050 (Budding-Polo Ballinas et al., 2023). However, in general the construction sector is seen as conservative and risk averse. This makes it **challenging** to **implement** and **adopt** new processes and technologies, such as bio-based materials (Dams et al., 2023).

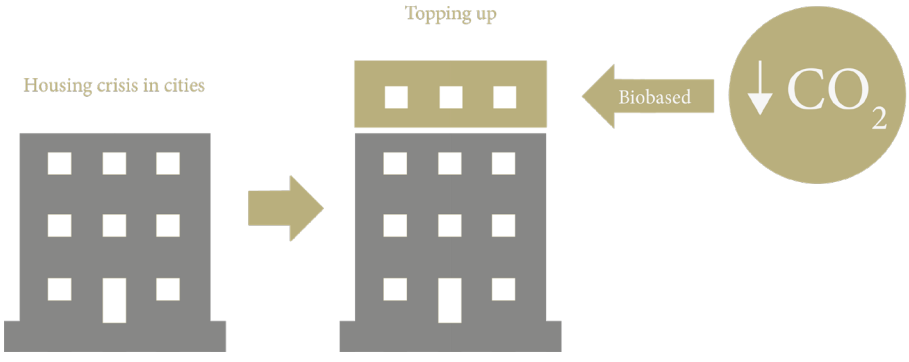

Figure 1, Illustration background, own illustration

1.2 Problem statement

The Dutch construction sector currently **lacks sufficient technical design knowledge** regarding **bio-based construction**, including **standardized details** of **bio-based materials** with wooden building systems. This knowledge gap is a significant **barrier** to achieving **full circularity** by **2050**. To achieve this goal, bio-based building materials must be **applied** in buildings in the short term to gain new insights. At the same time, **technical knowledge competence** must be developed within the Dutch construction sector (Ministerie van Onderwijs & en Wetenschap, 2023).

The lack of knowledge about the technical implementation of bio-based materials is confirmed by research (van der Velde & van Leeuwen, 2019), which also indicates that **little is known** about the **building physics properties** of these materials. The reason for this is that the Dutch construction sector is **not accustomed** to **designing** with these materials (Jones, 2017).

The **construction methods** associated with bio-based materials have **not yet** been **optimized** due to **limited knowledge** and **use**. Compared to traditional construction methods, the design and construction process of bio-based buildings generally proceeds **differently**. As a result, bio-based materials are **not yet applied** in the **early stages** of the **design process**, which is, however, essential. This phase **largely determines** the **environmental performance** of the **design** as the materials are established here (Denac et al., 2018).

Correctly applying bio-based building materials in the design process requires architects to **expand personal competencies** with **specific knowledge** about bio-based materials, including **technical expertise**. However, these **competencies** are often **not yet developed** (Kanters, 2020). The **lack of knowledge** is partly driven by the **difficulty** construction **professionals** face in **obtaining new technical knowledge** about bio-based materials (Dams et al., 2023). Even when buildings are detailed with bio-based materials, the materials are unfortunately **incorrectly implemented** (Hedley-Smith & Stainton, 2024).

These factors can lead to **distrust** and **resistance** to the application of bio-based materials. The knowledge gap is unfortunately **extending** into the material property fields that are related to the **thermal**, **moisture**, and **hygroscopic building properties** (Volf et al., 2015) (Dams et al., 2023). The **limited knowledge** about **hygroscopic properties** further **restricts** the **applications** of these materials (Dams et al., 2021). All in all, this could have the **troublesome effect** of not reaching the desired construction-based **CO_2 reduction goal** (Dams et al., 2023).

Despite its potential, **top-ups** are still **rarely applied** in the Netherlands (Geuting et al., 2023). For a successful top-up building a **lightweight construction**, such as wood, is **important**. Additionally, it is essential to **shorten** the **construction time**. Here **bio-based** materials are posed as an **ideal candidate** due to **lightweight** and **easy prefabrication** making bio-based materials extremely **suitable** in combination with a wooden structure (Beemer et al., 2022). Various **Dutch construction companies** therefore **wish** to use **bio-based materials** for residential top-up buildings. However, the incorporation of bio-based materials is **not feasible** for these companies due to a **lack of knowledge** in this field (Stulen, 2024).

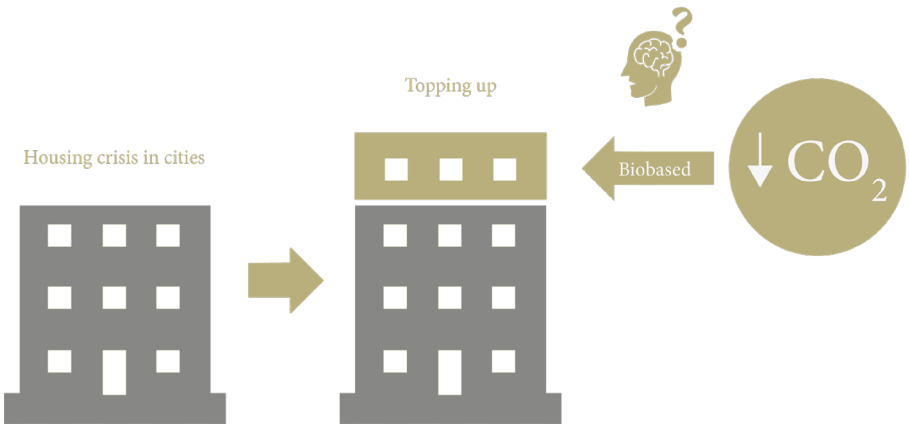

Figure 2, Illustration problem statement, own illustration

1.3 Hypothesis

What if **standardized bio-based façade wall reference details**, **tested** for **thermal** and **moisture performance**, were available for architects to use in designing and detailing bio-based top-up buildings? Developing standardized and building physics-tested bio-based reference details will help **bridge** the **knowledge gap** regarding the **design** and **detailing** of bio-based top-up buildings. By **testing** these details for **thermal bridges** and **moisture accumulation**, **new knowledge** about the **building physics performance** of bio-based materials will be **generated**. Making these details available will not only **increase confidence** in and the application of bio-based materials but will also **contribute** to the **scaling up** of **bio-based top-up projects**. This can help address part of the housing shortage in the Netherlands in a sustainable manner.

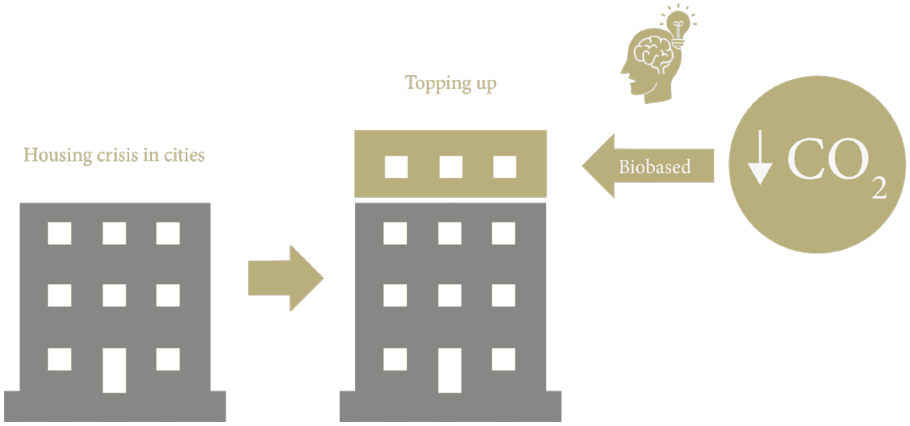

Figure 3, Illustration hypothesis, own illustration

1.4 Research Questions

This thesis investigates how **complete façade wall details** can be developed for residential building top-ups, focusing on **ensuring proper thermal bridge mitigation** and **moisture transport regulation** within the construction. The developed details will be **evaluated** for **thermal performance** and **moisture behaviour**. The following main question is formulated, thereby helping to improve the knowledge of bio-based technical detailing for residential top-up buildings among professionals:

How can bio-based façade wall reference details for residential top-up buildings be developed according to thermal and moisture regulation within the construction?

To give an answer to this question, sub questions have been formulated, which will be addressed in the following chapters of this thesis. **Chapter 2.2** will explain why to use bio-based building materials and will answer the sub-question:

What are the advantages and disadvantages of using bio-based building materials instead of conventional building materials?

Chapter 2.3 discusses why bio-based building materials are appropriate for application in residential top-up buildings and will provide an answer to the sub-question:

What makes bio-based building materials relevant to residential top-up buildings.

Chapter 2.4 will provide the key properties to analyse thermal bridges and moisture in the WUFI-software in detail and will answer the sub-question:

What properties of bio-based building materials are crucial for analysing thermal bridges and moisture in WUFI?

Chapter 2.5 presents a selection of bio-based materials with their products with a focus on analysing thermal bridges and moisture transport and answers the sub-question:

Which bio-based building materials are suitable for bio-based façade wall details with a focus on analysing thermal bridges and moisture transport?

Chapter 2.6 will show which design principles need to be considered when designing with the selection of bio-based building materials and **chapter 3** will show the developed details in order to answer the following sub-question:

How can the selected bio-based materials be effectively applied to develop validated bio-based façade wall details?

Chapter 5 will show the simulations of the developed reference details and will answer the following sub-question:

How do moisture transport and thermal bridges behave in the developed biobased reference details?

1.5 Objective

The **primary objective** of this research is to **develop technical horizontal** and **vertical façade wall reference details** that architects can use in the technical elaboration of designs for residential top-up buildings. These details will be **validated** to ensure that **no thermal bridges** occur, and that **moisture transport functions optimally** to **prevent condensation** and **moisture problems**. Hereby the research contributes to the transition to a circular economy and supports the reduction of CO_2 emissions and material use in the construction sector.

The associated sub-objectives are:

1. Developing standardized bio-based details suitable for application in Dutch construction practice and compliant with the Building Decree.

2. Analysing and optimizing the details for thermal bridges and moisture transport using building physics simulation software such as WUFI.

3. Compiling an overview of used bio-based products with their building physics properties, including relevant standards and certifications.

4. Translating the research results into a practical guide for designers and construction professionals.

1.6 Scope

It must be noted that this study focuses **only** on **horizontal** and **vertical bio-based façade wall details**. Other building components, such as floors or roofs, are excluded within the simulations. The tested details will be evaluated **solely** for **moisture transport** and **thermal bridges** using **WUFI exclusively**. In that regard, no other validations will be performed using different software programs than WUFI. Moreover, other building physics aspects, such as acoustics, fire safety, and structural performance, including structural strength and stability, are beyond the scope of this research.

Additionally, a selected group of **five bio-based materials** will be used in the design and testing of the façade wall details: **cork**, **flax**, **hemp**, **straw**, and **wood**. Various configurations of details will be developed with these materials. Materials not included in this selection will not be considered in this research.

1.7 Methodology

This thesis is divided into **two parts** to answer the main research question: a **literature review** and the **development** of **bio-based façade wall details tested** with **WUFI**. The literature review combines various methodologies to gather the necessary knowledge for developing and analysing the reference façade wall details. In the second part, the reference details will be developed and tested for thermal bridges and moisture transport using WUFI. This involves applying **research through design** and **conducting simulations**. This chapter first describes the methodologies from the literature review. Subsequently, it will outline the methodologies for designing the details.

For the sub-questions '*What are the advantages and disadvantages of using bio-based building materials instead of conventional building materials?*' and '*What makes bio-based building materials relevant to residential top-up buildings.*', a combination of Dutch policy documents and scientific literature has been consulted.

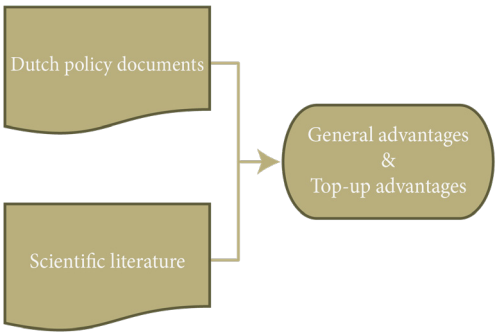

Dutch policy documents have been used to **describe** the **ambitions** regarding the use of bio-based building materials in the construction sector and the addition of extra homes to address the housing shortage in cities through top-ups. Subsequently, the scientific literature outlines the **advantages** and **disadvantages** of **bio-based materials** compared to **conventional materials** in the construction sector. The focus has been on **material density**, **phase shift**, **temperature amplitude damping**, **prefabrication possibilities**, and the **reduction** of **disturbances** for nearby residents. Additionally, the **hygroscopic properties** have been investigated, such as **thermal conductivity**, **diffusivity**, **specific heat capacity**, **vapour permeability**, and **vapour diffusion resistance**. Specific literature has been consulted for each property.

For the third sub-question, '*What properties of bio-based building materials are crucial for analysing thermal bridges and moisture in WUFI?*', scientific literature has been reviewed along with consulting the WUFI database.

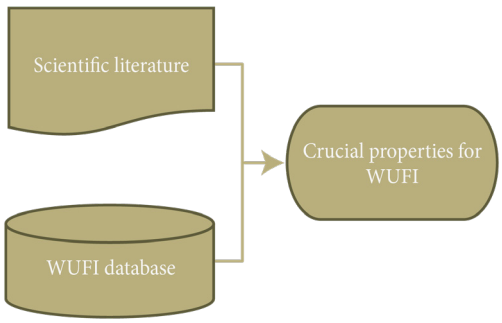

Scientific sources have been consulted that describe the **thermal performance** of **thermal bridges** in lightweight constructions and the **consequences** of thermal bridges for heat loss. Additionally, the **impact** of **mold formation** on **thermal bridges** and how **correct detailing** can **influence thermal bridges** have been investigated. Furthermore, the **WUFI database** has been **consulted** to obtain the necessary **hygroscopic properties** required for **assessing thermal bridges** and **moisture transport**. Important terms for the scientific literature in this context include **Moisture Storage Function**, **Liquid Transport Coefficient**, **Water Vapour Diffusion Resistance Factor**, **Thermal Conductivity** and **Enthalpy**.

The sub-question '*Which bio-based building materials can be used for bio-based façade wall details with a focus on analysing thermal bridges and moisture transport?*' combines Dutch policy documents, the WUFI database, scientific literature, and material desk research.

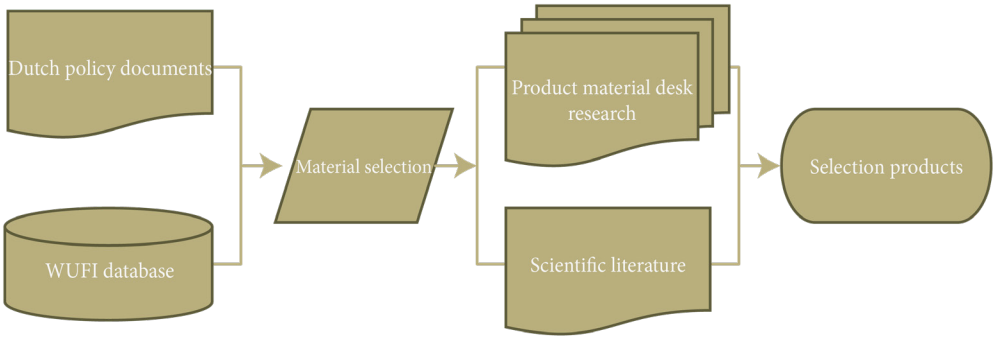

Dutch policy documents have been consulted to **select bio-based materials** with which the Dutch construction sector already has some design and construction knowledge. For further material reduction, the **WUFI database** has been **consulted**. This is because many specific properties required for the analyses are often not yet known.

The selection of materials is included in the scientific literature, with **explanations** about the **materials products**, and **applications**. Subsequently, material desk research was conducted to describe **various suppliers** along with **product properties**. Properties not shared by suppliers can be supplemented with values from the WUFI database.

For the final sub-question, '*How can the selected bio-based materials be effectively applied to develop validated bio-based façade wall details?*', the material and product selection was used to conduct a literature review. This review was specified to technical manuals and scientific literature that together provide guidelines on detailing with the specific materials.

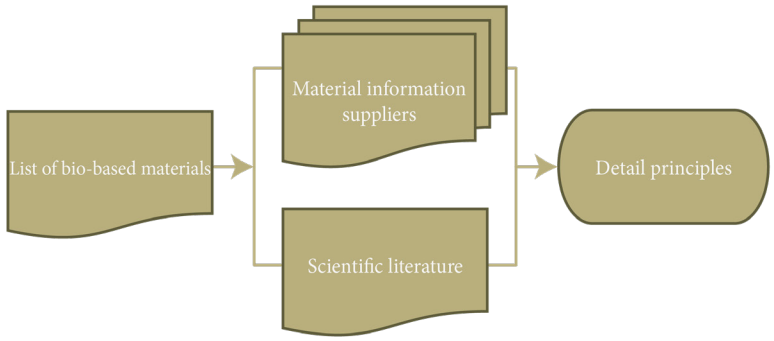

Development of bio-based façade wall details

Following the literature review, the technical details of the horizontal and vertical façade wall details will be **developed** and **tested** for **thermal bridges** and **moisture transport**. During this phase **different combinations** of **materials** will be **experimented** to identify the most effective solution. If certain design detail challenges are not sufficiently understood, additional literature research will be conducted. This method aligns with the approach used during the literature review for the final sub-question.

The **building physics research** focuses on **setting up** and **analysing simulations** using **WUFI** software. Utilizing this software, the **thermal bridges** and **moisture transport** within the details will be **analysed** and **evaluated**. Through an iterative process, the details will be continuously adjusted and improved based on the simulation results. The iterative process consists of multiple cycles of design, simulation, and adjustment.

By following this process, **thermal bridges** are **prevented**, and **moisture built-up** and **mold formation** are **excluded**. Ultimately, the details will be **validated** based on the **simulation outcomes**. Multiple rounds will take place in which different configurations of details are **drafted**, **tested**, **improved**, and **validated**.

The obtained details and the corresponding simulation results will eventually be **documented** and **published** in the thesis. In this way, designers can benefit from the acquired knowledge and make the application in future projects possible.

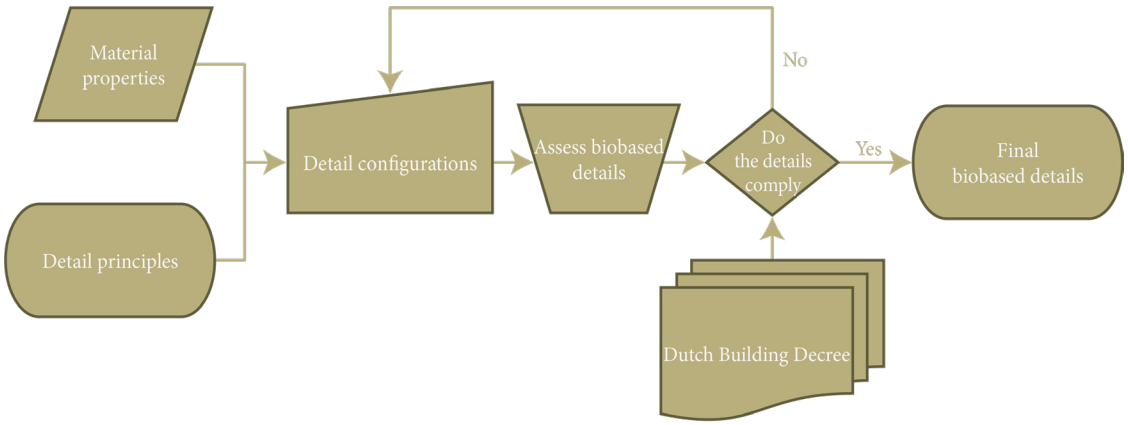

Literature review approach

To answere the questions, a proper **literature review approach** is necessary. Academic search engines such as **Scopus**, **Google Scholar**, and the **TU Delft Library** were used to collect relevant literature. Each sub question contained specific **keywords**, which were then incorporated into tailored search queries for each database. To provide clarity, the table below includes the **key terms** and **corresponding synonyms**.

Research question	Main search keywords
1	"bio-based materials" AND "advantages" AND "disadvantages" AND "conventional materials"
2	"bio-based materials" AND "residential" AND "top-up" AND "advantages"
3	"bio-based materials" AND "thermal" AND "moisture" AND "hygrothermal" AND "properties" AND "heat flow" AND "buffering" AND "WUFI"
4	"bio-based materials" AND "bio-based façade construction" AND "thermal bridge" AND "moisture transport" AND "Dutch bio-based materials" AND "thermal performance" AND "moisture movement"
5	"façade wall construction" AND "thermal bridge" AND "moisture transport" AND "material suitability" AND "thermal performance" AND "moisture movement" AND "cork" AND "flax" AND "hemp" AND "straw" AND "wood" AND "designing" AND "building" AND "implementation"

Each concept is associated with a range of **synonyms** and related **terms**. The diversity of sources consulted allowed for the integration of information from **multiple perspectives**, facilitating a more comprehensive understanding of specific topics.

To evaluate the relevance and quality of a source, both the **abstract** and **conclusion** were reviewed. This approach helped determine whether a source met the **criteria** for inclusion. Additionally, when key statements within a paper were supported by **referenced sources**, those **references** were also examined. If deemed relevant and classified as academic literature, they were included in the review.

1.8 Research outcomes

The achieved results of this research encompass various aspects that **contribute** to the **development** and **application** of **bio-based construction techniques**. Arguments have been presented for the transition to bio-based construction and the value of bio-based materials for residential top-up buildings. Following the presentation of these arguments, the important building physics properties necessary for assessing thermal bridges and moisture transport through the construction using WUFI have been outlined. Subsequently, a selection of bio-based materials has been presented along with the corresponding products and how these products can be applied in façade walls.

Additionally, bio-based products from various suppliers have been listed with the associated product properties. If these properties were not clear or available from the suppliers, a similar product from WUFI can be used to obtain the necessary properties. This is less accurate but helps to analyse the details.

The expected results of this research **include several aspects** that **contribute** to the **development** and **application** of **bio-based construction techniques**. Firstly, **design principles** have been presented on how to **detail** with the various selected bio-based products. Secondly, a series of **validated horizontal** and **vertical 1:5 façade wall details** will be **designed**, specifically for bio-based residential top-up buildings.

Furthermore, the research provides an **analysis** of the **behaviour** of **thermal bridges**, **moisture accumulation**, and **condensation formation** in the **developed bio-based façade wall details**, obtained through simulations in WUFI. With this analysis, the details will be further optimized to **prevent thermal bridges** and **ensure effective moisture transport**, **avoiding moisture accumulation** and **condensation** in the developed details.

Upon completion, this research contributes to the energy transition and circularity by promoting bio-based materials in the built environment and offers sustainable solutions for housing shortages in urban areas.

1.9 Research outputs

Eventually, **multiple horizontal** and **vertical 1:5 façade wall details** will be **developed** and **validated** for **thermal bridges** and **moisture transport** using **WUFI**. These validated details will be presented as reference details that can serve as tools for designers and architects in the **technical elaboration** of bio-based residential top-up buildings.

The details should be **easily applicable** in practice, which means the details will be **drafted** in accordance with the **Dutch Building Decree**. The **results** of the **assessments** on **thermal bridges**, **moisture accumulation**, and **condensation formation** will be presented **clearly** and **comprehensively** as an addition to the reference details. The overall outcome provides insight into the mentioned **building physics performance** of bio-based materials and the application in various configurations.

Finally, all of the above results will be **documented** in a **detailed report**, listing the details along with the corresponding building physics properties. Visualisations, such such as **3D axonometric images**, and **simulation results** will be added to the report to better illustrate the **applicability** and **performance** of the details.

1.10 Impact

Recent research has demonstrated that **traditional construction activities significantly contribute** to **various environmental challenges** (Ingrao et al., 2019). This research seeks to **address** these environmental concerns within the construction sector by developing reference details that utilize bio-based materials instead of conventional materials. This approach **contributes** to the **reduction** of **construction material-related carbon dioxide emissions**, which account for **10%** of the **total 37% carbon dioxide emissions** associated with the construction sector (Hamilton et al., 2021). By **replacing** traditional building materials with bio-based materials, **material scarcity** will also be **mitigated**. Bio-based materials enable a **transition** to a **circular system** to end the **linear** and **depleting use** of **resources** (Yadav & Agarwal, 2021).

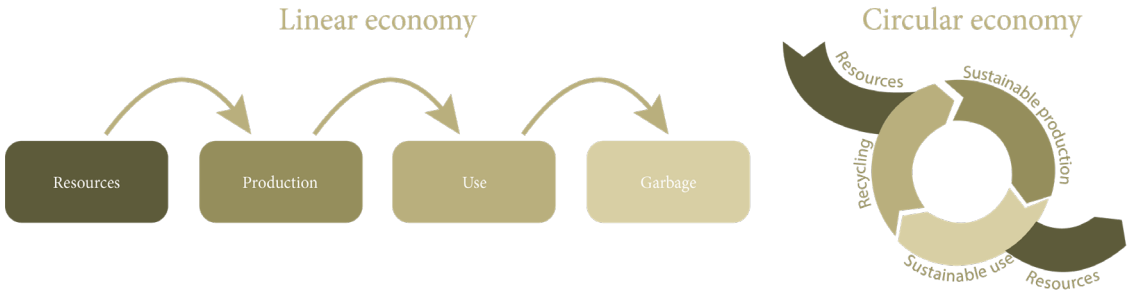

Figure 4, Visualisation of linear and circular economy, derived from: (Stichting Agrodome, 2024).

With the **current trend** towards sustainable buildings and increasing environmental awareness, building with bio-based materials is **gaining** some **popularity** as an **alternative** to **traditional construction methods** (Sandak et al., 2019). However, as previously stated, the **conservative attitude** within the **construction sector** poses an **obstacle** to the **full acceptance** of **bio-based materials** (Dams et al., 2023). By presenting reference façade wall details, this research **aims** to **reduce** the **risks** and **uncertainty** about bio-based construction. The impact of this research, therefore, lies in the potential increase in the use of bio-based materials, not only with a focus on residential top-up buildings but also across the entire construction sector.

Personal competencies are developed through this research, which will enhance the application of bio-based building materials in future projects. This will **reduce** the **CO_2 emissions** of **future designs** and **ensure** that these **designs** use **regenerative building materials**. The personal goal is to strive for a future where environmentally friendly construction practices are the norm and to promote a biobased circular economy.

1.11 Relevance

The problem statement shows that the application of **bio-based materials** in **construction projects** is **hindered** by **limited technical design knowledge** and the need to **apply new construction techniques**. This research is relevant because it indicates that the **limited R**esearch & **D**evelopment **capacities** of **construction companies** and **poor knowledge exchange** from **academia** to **industry** result in limited knowledge about the technical elaboration of designs with bio-based materials (Giesekam et al., 2016).

This research develops **façade wall reference details** that are **publicly** available for use in various designs of residential top-up buildings. This contributes to the **expansion** of **technical design knowledge**, resulting in a **broader application** of **bio-based materials** in **designs**. Currently, designers do not know how to design buildings with bio-based materials, which **hinders** the **application** of these materials (Ipsen et al., 2021).

Additionally, the research provides a **solid foundation** for **further studies** within academia. The used methodology in this research can be used to develop and analyse more **bio-based details** using WUFI. Furthermore, it can **serve** as a **starting point** for **developing details** for **floors** and **roofs**. Finally, it can **act** as a **starting point** for **elaborating other building physics elements**, such as **fire safety**, **acoustics**, or **structural** aspects. The focus on sustainable and environmentally friendly building materials also supports academic goals related to sustainability. The research contributes to scientific efforts to achieve a sustainable world.

Regarding the social relevance, the research addresses reducing CO_2 emissions, decreasing the dependency on critical raw materials, and reducing construction waste. This **supports** the **transition** to a **more sustainable** construction sector and **helps reduce** the construction industry's **impact** on the **environment**. Promoting bio-based materials supports the principles of a circular economy (Min et al., 2022).

Bio-based materials can offer benefits for the health and safety of residents, such as improved air quality and the reduction of harmful substances. This improves the living environment and contributes to people's well-being (Cascione et al., 2022). Thus, the research not only partially addresses the housing shortage in the Netherlands but also provides healthy housing. By ensuring that **no thermal bridges** occur, **more energy-efficient buildings** are **created** as well (Zerari et al., 2024).

2. The literature research

2. Why bio-based building materials?

2.1 Definition bio-based building material

Biobased materials are becoming proliferate, yet there is hardly only one definition that **describes** what biobased materials are. Lee et al. (2023) argue that biobased materials are:

"*Materials wholly or partly derived from renewable biological origins, or by-products and biowaste of plant and/or animal biomass that can be used as raw building materials and decorating items in construction, in their original forms or after being reprocessed*"
(Le et al., 2023)

A bio-based building material does not need to be entirely made of biological raw materials. According to **NEN-EN16575: 2014**, a **bio-based building material** must **consist** of at least **70% renewable mass** (Ministerie van Binnenlandse Zaken en Koninkrijksrelaties et al., 2023). Other criteria for bio-based materials include that they must come from **regenerative cultivation**, which should ensure the ecologically healthy conditions of the harvest location, both now and in the future. Additionally, the materials should be **produced** from **living natural raw materials** that **grow back within one century** after harvest. Furthermore, abiotic raw materials from geological formations are excluded. Finally, bio-based materials must later be **reusable** as raw materials in new building materials or in nature (College van Rijksbouwmeester en Rijksadviseurs, 2022).

2.2 Benefits bio-based building materials in the construction sector

Global environmental impact analyses show that **traditional construction materials** such as concrete, sand, gravel, iron, and steel have **significant impacts** on **air** and **water pollution**, **climate change**, **energy consumption**, **human health**, and **toxicity** of **water** and **land** (OECD, 2018). Many of these and other issues faced by the construction industry today can be **addressed** using **bio-based building materials** (Budding-Polo Ballinas et al., 2023). In addition to solving problems in the construction sector, bio-based materials also **improve residents' well-being** in various ways (Yadav & Agarwal, 2021). This sub-question will explain the improvements of bio-based building materials compared to conventional building materials.

CO_2-reduction

The construction sector significantly contributes to CO_2 emissions. When looking at the material-bound emissions of the entire construction sector, it is calculated that this accounts for **7.7%** of the **total Dutch CO_2 emissions**. If no actions are taken, this is likely to grow by 2030 due to an expected **increase** in **material demand** of **18.75%**, compared to 2019 (Kuhlmann et al., 2023)

The **application** of **bio-based building materials** can lead to various **CO_2 reductions**. Bio-based materials reduce CO_2 emissions in a twofold manner. Firstly, **less CO_2-intensive alternatives** are **used** such as hemp, straw, cork, wood **instead** of **conventional CO_2-intensive materials** like concrete and steel. Secondly, **bio-based materials store carbon absorbed** during the **growth** of the **plants** from which they are made. This stored CO_2 **remains sequestered** in the **building structure** for as long as the materials are in use.

In addition, the Netherlands is dealing with **emission-intensive agricultural activities**, such as livestock farming, which can be partly **displaced** by the **cultivation** of **biobased resources**, resulting in further CO_2 reductions (Minister van Binnenlandse Zaken en Koninkrijksrelaties, 2023). Consequently, CO_2 emissions per **m²** of **gross floor area decrease** by **36%** by building with bio-based materials, excluding the CO_2 storage capacity of the materials. When this **storage** is **considered**, the CO_2 reduction can even reach **77%** (Bosch et al., 2023).

For fast-growing bio-based materials, carbon absorption during their lifecycle can even be greater than the carbon emissions generated during the production of the building material (Cosentino et al., 2024). Fast-growing bio-based materials are found to be more efficient in storing carbon compared to slow-growing bio-based materials, such as wood (Pittau et al., 2018). As described in the background, bio-based building materials can contribute to achieving the objectives of the Paris Agreement.

NO_2-reduction

Despite the housing shortage, **high nitrogen emissions** in **construction hinder** the **granting** of **building permits**. Bio-based building materials indirectly contribute to nitrogen reduction by enabling lighter construction, thereby reducing emissions on construction sites (Building Balance, 2023). Generally, bio-based materials are five times lighter than abiotic alternatives, resulting in a weight reduction of 50% (Bosch et al., 2023).

This **weight reduction leads** to **decreased nitrogen emissions** as equipment can be less heavily executed, and transportation emissions decrease due to lighter loads (Vermeulen et al., 2020). Additionally, there are **better possibilities** for **electrification** of **construction equipment** such as electric cranes and drills, which will further reduce nitrogen emissions (Ministerie van Binnenlandse Zaken en Koninkrijksrelaties et al., 2023).

Regenerative materials

Currently, there is a **high dependency** on critical **raw materials** (Ministerie van Infrastructuur en Waterstaat, 2023b). Research by Van der Lugt (2021) shows when certain construction materials will run out. The results are presented in the diagram below:

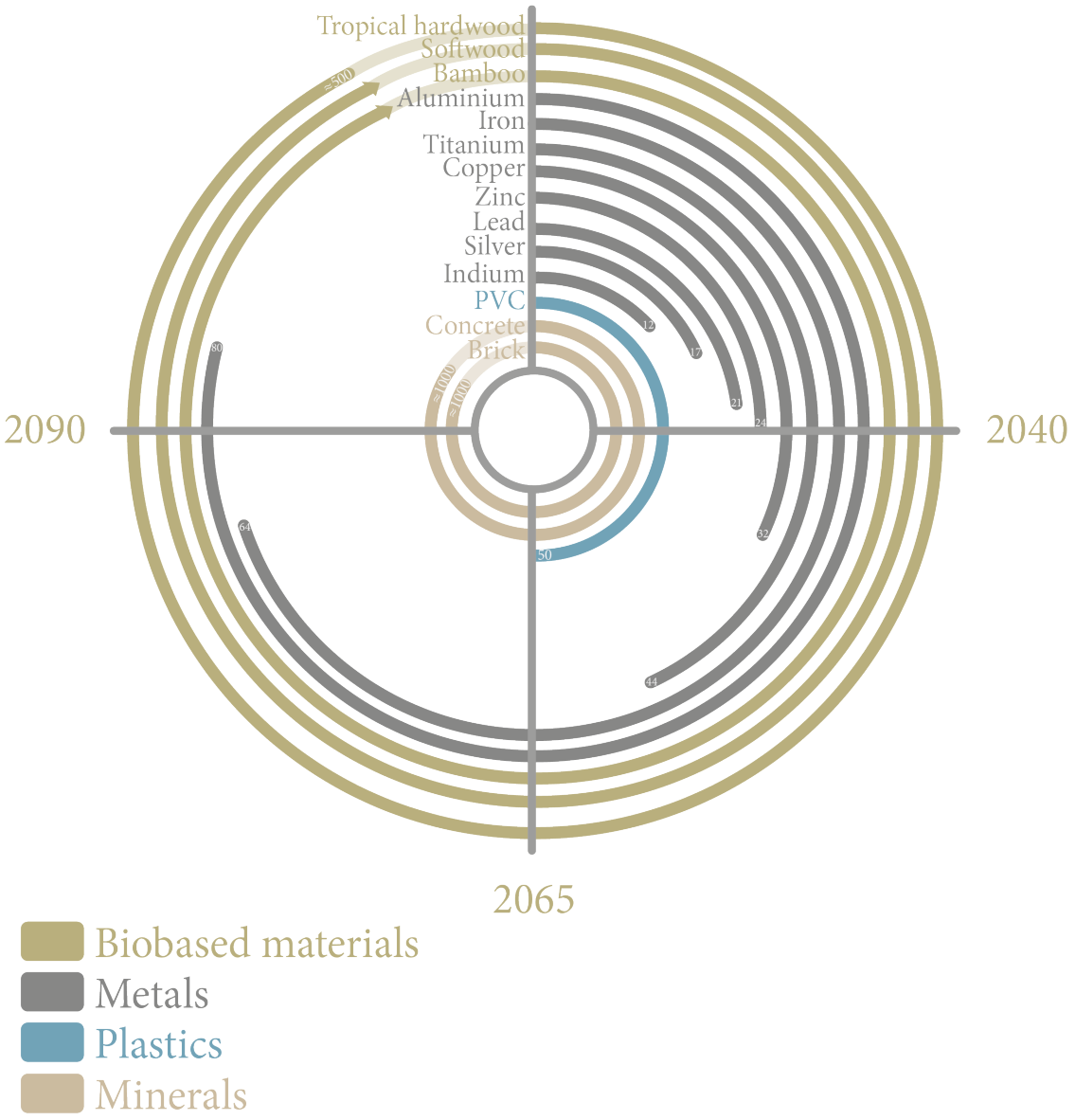

Figure 5, Time till running out of building materials, derived from: (Van der Lugt, 2021)

This implies that concrete will be available for a long time. However, it should be noted that this **availability** might be **lower** if no measures are taken to reduce the use of sand, which is scarce, in concrete (Van der Lugt, 2021). Other **important construction materials** are **beginning** to **deplete** as well: gravel (Rutte Groep, 2021) limestone, which is a key component of cement as well as calcium silicate blocks (Cobouw, 2024).

Despite some **crucial construction materials running out**, the **construction sector** is **responsible** for **50%** of **raw material** use in **the Netherlands** (Ministerie van Infrastructuur en Waterstaat, 2023a). Of this **50%**, **Civil Engineering** (GWW) accounts for **71%** (57 Mton) and **Building & Utility Construction** (B&U) accounts for **29%** (23 Mton) of **material consumption**. This research specifically focuses on housing construction, a part of B&U. The **pie chart** below **shows** the **contribution** of **materials** in **B&U** to total **material consumption**, many of which are **scarce** and **depleting**:

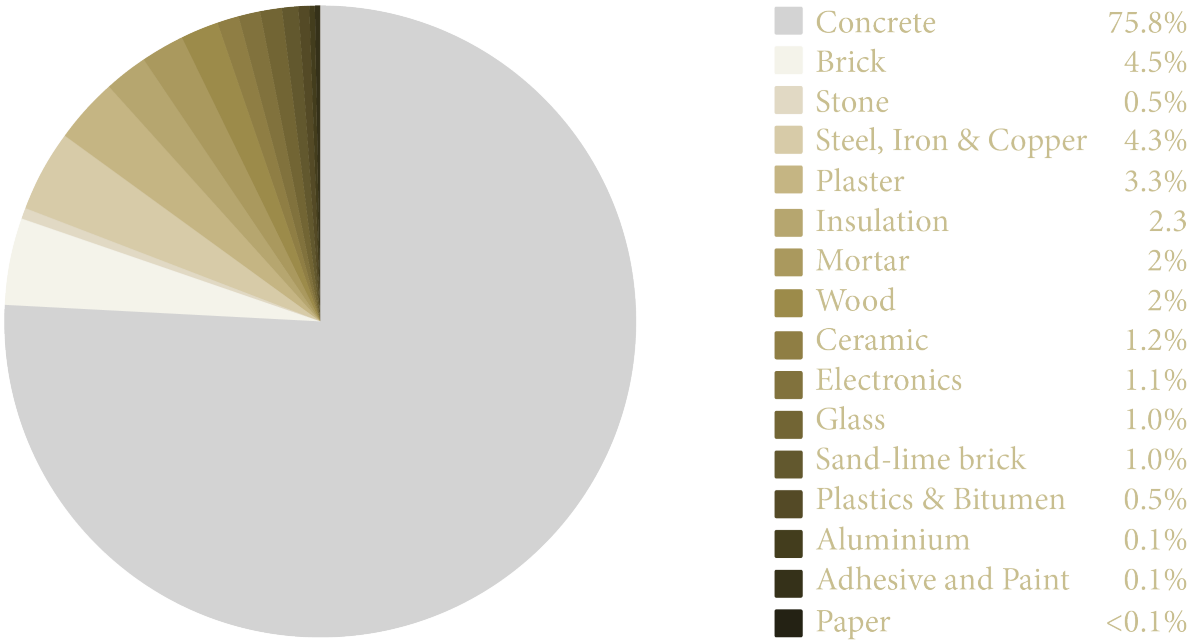

Figure 6 Contribution of different materials in the B&U to the total material consumption, derived from: (Arnoldusse et al., 2022)

Even with full recycling, wear, downcycling, and **new construction** will **create** a **continued need** for **new materials** (Schik et al., 2022). Using bio-based building materials is seen as a way to **reduce dependence** on **fossil resources** (Majer et al., 2018). Research shows that using **bio-based materials** can **reduce primary raw material consumption** for housing construction by **11.7%** (Ministerie van Binnenlandse Zaken en Koninkrijksrelaties et al., 2023).

This is due to the **regenerative nature** of **bio-based building raw material recources** (Jones, 2017). Bio-based materials should **regrow** within **100 years after harvest** (College van Rijksbouwmeester en Rijksadviseurs, 2022). **Fast-growing** bio-based materials, such as straw and hemp, can **fully renew** within **a year** after **harvest**. This **reduces** the **risk** of **material scarcity** and can **meet** the **demand** for future new construction (Pittau et al., 2018).

However, **renewability** of bio-based materials is **only achieved** through **sustainable** and **responsible management** (Cascione et al., 2022). Currently, the **share** of bio-based materials in the **Dutch construction sector** is **low**: **wood** accounts for **2%** of the weight, while **other bio-based materials** represent only **0.1%** (Van der Velde & Van Leeuwen, 2019). Due to a short growth period, it is possible to quickly scale up the use of these materials (Göswein et al., 2022).

Less transportation-emissions

The **energy-intensive processes** of **extraction**, **production**, and **transportation** of construction raw materials significantly contribute to CO_2 emissions (Orsini & Marrone, 2019). Currently, the Netherlands imports many raw materials from abroad, which are associated with high embodied carbon emissions (Ministerie van Infrastructuur en Waterstaat, 2023b) To reduce emissions, **construction materials** should be **produced domestically** or **nearby** (Dams et al., 2023). This is often the case with bio-based materials, which **minimizes emissions associated** with the **transportation** of **materials** (Budding-Polo Ballinas et al., 2023). Therefore, the **Dutch government aims** to establish **regional bio-based chains** to reduce material transportation emissions. Where necessary, materials should come from surrounding countries (Building Balance, 2023).

Transportation emissions are **further reduced** by the **lightweight properties** of **bio-based materials**, leading to **less fuel consumption** during **transport** (Suttie et al., 2017). Bio-based materials are also **well-suited** for **prefabrication**, which can result in a **net reduction** of **20%** in **transport movements** (Miles & Krug, 2013).

Improved energy efficiency

Insulation materials with a **low thermal conductivity**, λ, are crucial for **improving thermal performance** and **reducing energy consumption** in buildings (Schulte et al., 2021). Thermal conductivity indicates a material's ability to **conduct heat**. A **low thermal conductivity** demonstrates **how well heat** can be **retained** in a structure (Hung Anh & Pásztory, 2021). The demand for insulation materials with favorable λ-values has increased to reduce energy consumption in buildings. When **thermal conductivity** has a value of **0.045** or **lower**, the **material** can be **characterized** by **good thermal insulation performance** (Lu et al., 2024).

Research by De Visser et al., (2015) compared the thermal conductivity between synthetic, mineral, and bio-based materials, showing that **bio-based materials generally** have **good λ-values** comparable to traditional materials. Research by Lawrence et al., (2013) also suggests that **bio-based insulation** materials **do not significantly underperform** compared to conventional insulation materials.

Table 1, Thermal conductivity values of synthetic- mineral and natural insulation materials, derived from: (De Visser et al., 2015)

	Material	Thermal conductivity (λ) [W/mK]	Density (ρ) [kg/m³]	Specific heat capacity (c) [J/kgK]
Synthetic	EPS	0.032 - 0.040	15 - 30	1200
	PUR / PIR	0.020 - 0.040	15 - 38	1400
	XPS	0.030 - 0.040	20 - 60	1200
Mineral	Foam Glass	0.040 - 0.090	105 - 165	830
	Mineral Foam Sheet	0.045	115	1000
	Glass Wool	0.032 - 0.040	20 - 140	840
	Rock Wool	0.032 - 0.050	25 - 400	840
Natural	Cellulose Plates	0.040	70 - 100	2000
	Cellulose Flakes	0.039 - 0.045	35 - 60	2200
	Grass	0.042	53 - 68	2200
	Hemp Mats	0.040 - 0.050	30 - 42	1600 - 1700
	Hemp Loose	0.048	40 - 80	1600 - 2200
	Wood Fibre Board	0.040 - 0.052	140 - 180	2100
	Wood Fibre Boad Flexible	0.040 - 0.052	40 - 55	2100
	Wood Fibre Loose	0.040	30 - 40	2100
	Coir	0.045	80 - 120	1300
	Cork Plate	0.040 - 0.045	70 - 140	1800
	Reed	0.038 - 0.055	190 - 225	1300
	Sheep's Wool	0.035 - 0.040	18 - 30	1700
	Straw Bales	0.052 - 0.080	400	2000
	Flax	0.038 - 0.050	15 - 60	1600

Although the thermal conductivity of bio-based insulation materials is generally slightly higher, these materials offer other benefits that enhance the indoor climate and improve the energy efficiency of buildings (Lawrence et al.,2013). These benefits will be described in the next chapter.

Improved indoor climate

The RIVM (Rijksinstituut voor Volksgezondheid en Milieu) reports that **Dutch persons** spend an average of **90%** of their **time indoors**, with **70%** of that **time** in their **own homes**. Therefore, the **quality** of the **indoor environment** is **essential** for **health** (Weterings et al., 2005). These values are still relevant. However, both **new** and **older homes suffer** from **poor indoor climates**, partly due to **conventional building materials** and **constructions** that **limit** the **exchange** of **indoor** and **outdoor air** (De Visser et al., 2015). Additionally, **one in five** Dutch people **suffers** from **damp spots** or **mold indoors** (Vermeulen et al., 2020). Among other things, **building materials** have a **significant effect** on **indoor climate quality** (Van Dam & Van den Oever, 2019).

Bio-based materials can **contribute** to an **improved indoor environment** in various ways (Yadav & Agarwal, 2021). Bio-based materials can **buffer moisture**, **achieving** a **low humidity level**. This contributes to a **less stuffy experience** and **improves indoor air quality** (De Visser et al., 2015). Additionally, compared to conventional flexible lightweight insulation materials, most bio-based materials can also **buffer heat well**, **providing internal stability** to the **environment** which also **benefits** the **indoor climate** (Dams et al., 2023). How bio-based materials can buffer moisture, and heat will be described later. Furthermore, **Volatile Organic Compounds emissions** (VOCs) can **lead** to **health problems** and **reduced cognitive functions**. **Reducing** these **air pollutants** is necessary to **improve Indoor Air Quality** (Czerwinska, 2024).

Both **building materials** and **additives** have **VOC emissions** (De Visser et al., 2015). Although **bio-based materials** also have **VOC emissions**, these are **generally lower** than those of **conventional building materials** with a chemical structure (Raja et al., 2023). Besides emitting fewer VOCs, bio-based materials have a **significant potential** to **absorb various VOC emissions** and **transport** them **out** of **the construction**. This is due to the **breathability** of bio-based materials (Maskell et al., 2015). Therefore, most bio-based materials have a **low emission classification** for **VOC's**. When **VOC emissions decrease**, a **lower ventilation airflow rate** is **possible**, leading to **energy savings** while **maintaining good indoor climate**. Although individual bio-based building materials meet standards, **their combinations** in **practice** can lead to **unacceptable emission levels**. **Further optimizations** are **needed** here (De Visser et al., 2015). To keep emission levels within acceptable limits, ventilation remains necessary (Maskell et al., 2015)

By using natural materials, bio-based materials **promote** a **strong connection** with **nature**. This **supports healing processes** and can **reduce** both **psychological** and **physical stress** (Yadav & Agarwal, 2021). This connection can even contribute to the **recovery** from **physical** and **psychological stress** (Vermeulen et al., 2020). Additionally, **positive effects** have been observed on **child development**, **healthcare**, and **improved performance** in **work efficiency**, **learning**, and **productivity** (Sandak et al., 2019).

Finally, **working** with **artificial** and **chemical conventional building materials** is **detrimental** to **health** (Schik et al., 2022). When buildings need to be **demolished**, the **removal** of these materials is also **harmful** to **health** (Yadav & Agarwal, 2021).

Less waste

With over **24 Mtons** of **waste** in **2020**, the construction sector was responsible for **40%** of the **waste** in the **Dutch economy**, with **21%** coming from **residential** and **utility construction** (Van der Schuit et al., 2023) For this reason, the Netherlands has set a goal to become **fully circular** by **2050**, creating a closed loop of materials (Ministerie van Binnenlandse Zaken en Koninkrijksrelaties et al., 2023). In a fully circular economy, materials and products are utilized optimally and recycled if possible (Centraal Bureau voor de Statistiek, 2019).

Currently, **87%** of construction materials have a **primary origin** (direct or initial source), and only **8%** of materials have a **secondary origin** (derived source). Although about 99% of concrete is recycled, it primarily undergoes downcycling to road construction. Because concrete is difficult to reuse for the same function, only 3% of concrete comes from secondary sources. Steel, on the other hand, can be reused well, with 70% coming from secondary sources (Arnoldusse et al., 2022). For artificial and chemical building materials, this figure is 37.5%, with the rest mostly ending up as waste. The same applies to plastic construction waste, of which only 25% is recycled, while the rest will be burned (Van der Schuit et al., 2023).

Construction waste can be **drastically reduced** by using **bio-based building materials** instead of the a forementioned traditional materials (Le et al., 2023). These materials are **suitable** for **recycling** and **reuse**, thus reducing waste production (Dams et al., 2023). However, this is only applicable if no unnatural materials such as glue are added (College van Rijksadviseurs, 2023).

Even when recycling and reuse are not possible, bio-based materials offer **alternative applications**, such as **biofuel production** (Rabbat et al., 2022). As these materials are **biodegradable**, they can potentially serve as **compost** or **fertilizer** (Cascione et al., 2022). In conclusion, using bio-based materials results in **minimal waste**. Regarding **downcycling**, attention must still be paid to the **lifespan**, **disassembly**, **reusability**, and **recyclability** of materials to enable proper reuse (Ministerie van Binnenlandse Zaken en Koninkrijksrelaties et al., 2023).

2.3 Disadvantages of bio-based building materials

Even though biobased building materials offer several environmental benefits, the implementation of the materials is also associated with various **barriers** and **drawbacks**. Some of these **disadvantages** are outlined below.

Firstly, the construction sector is strongly driven by **cost considerations**, with a predominant focus on **minimising** the **construction costs**. At present, biobased materials generally do have **higher** material **prices** and require **additional investments** in adapted construction methods or building services engineering. Moreover, certain biobased materials necessitate **specific machinery** or **tools** for processing, which may be more expensive or less available than standard equipment used for conventional materials. These additional costs represent a **barrier** to the **adoption** of biobased building materials (Dams et al., 2023).

The use of biobased materials often demands **more specialised knowledge** than conventional construction practices. This is primarily due to the need for **specific fastening** and **processing techniques**. As a result, **specialised craftsmen** are often required, which can lead to **increased labour costs**. Furthermore, **training opportunities** in this field remain **limited**, meaning that **expertise** and **practical experience** with biobased materials are **not** yet widely **embedded** within the construction sector.

Another obstacle is the **limited availability** of biobased materials on the **market**. While **interest** in sustainable construction is **growing**, the **supply chains** for biobased materials are **not** yet fully **developed** or **standardised**. Additionally, some of these materials rely on agricultural by-products or specific crops, making the production dependent on seasonal cycles, regional conditions, and agricultural yields. This can result in **inconsistent** availability and **supply fluctuations** throughout the year. Furthermore, scaling up production to meet the growing demand presents additional logistical and infrastructural challenges. (Sandak et al., 2019).

Furthermore, there are technical performance **limitations** that **restrict applicability**. Most notably, the use of biobased materials is constrained by relatively **low fire resistance classification**. This can limit the application in certain building typologies, particularly where strict fire safety regulations apply. Although considerable research and innovation efforts are in progress to improve the fire performance of biobased materials, existing standards and certification processes continue to pose obstacles to large-scale implementation (Sandak et al., 2019).

The last drawback concerns the **thermal insulation properties** of biobased insulation materials. Compared to conventional insulation materials, biobased alternatives generally exhibit a **higher λ-value**. As a result, **thicker insulation layers** are required to achieve the desired **RC-value**. However, this comes at the **expense** of **usable floor area** (Le et al., 2023).

Conclusion

By applying bio-based building materials, various societal challenges can be addressed. Bio-based building materials can **reduce CO_2** and **NO_2 emissions**. Additionally, the materials are **regenerative** and can be **grown locally**. Furthermore, these materials have **good thermal conductivity properties** and are **capable** of **buffering moisture**, **heat**, and **VOC's**. Bio-based materials have **lower VOC emissions** than conventional materials. Finally, a great advantage of these materials is that bio-based materials can be used in a **circular manner**.

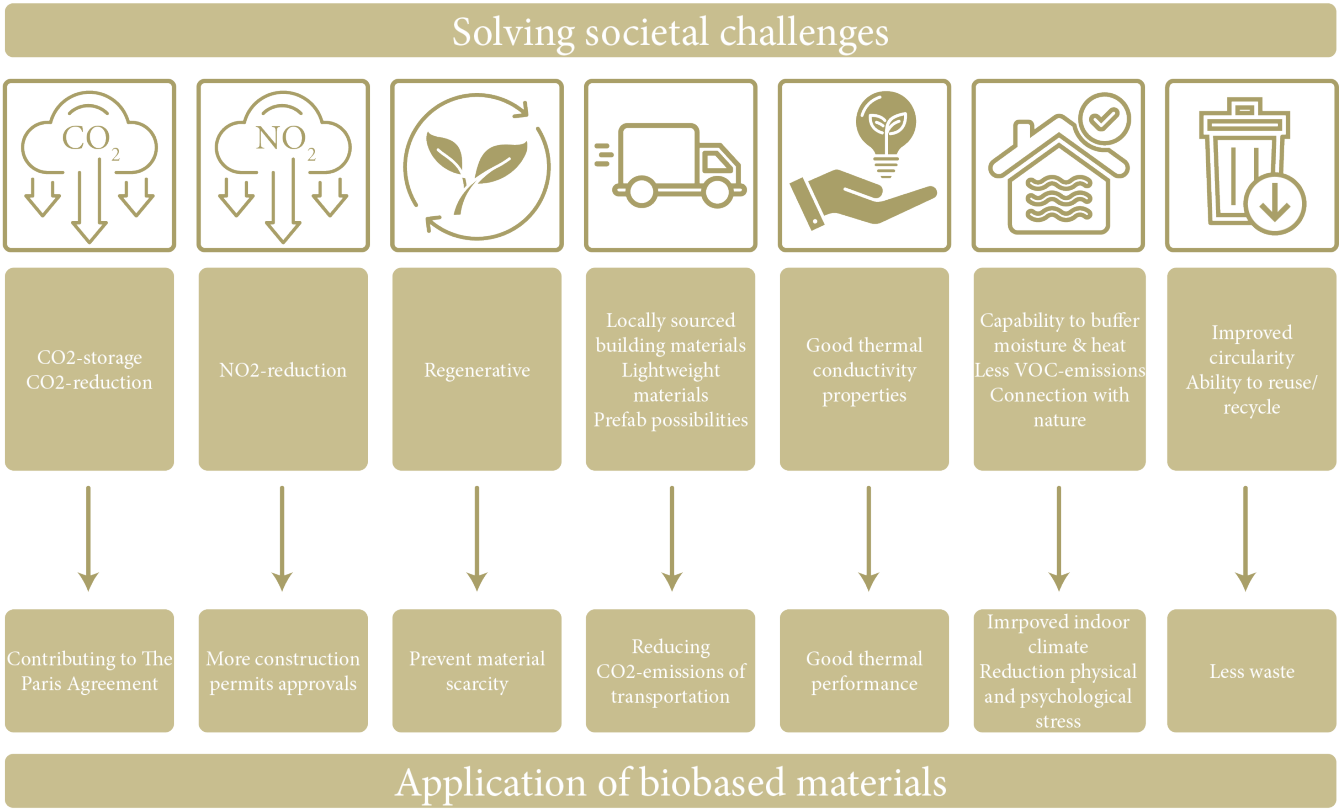

Figure 7, Conclusion advantages application bio-based materials, own illustration

3. Using bio-based for residential top-ups

3.1 Definition top-up building

Top-ups refers to **increasing** an **existing building** with **one** or **more floors**, adding extra residences to the top floors, or repurposing spaces on the ground floor (Ministerie van Binnenlandse Zaken en Koninkrijksrelaties, 2024a). This research will focus on adding residences by increasing an existing building with one or more floors.

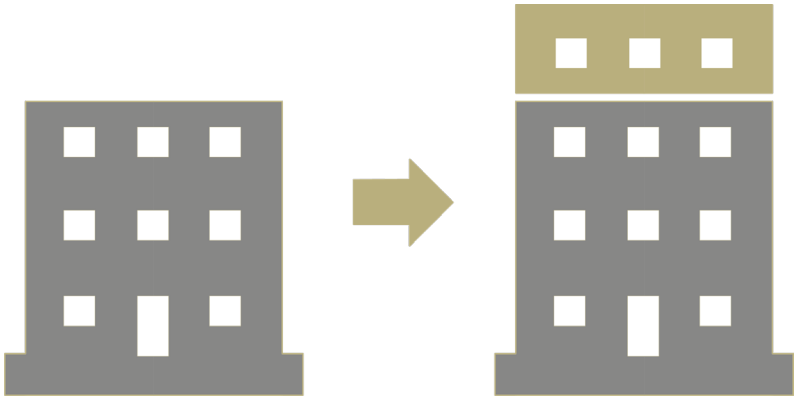

Figure 8, Explanation of a top-up building, own illustration

3.2 Reasons for residential top-up buildings in the Netherlands

Due to urbanization, the Netherlands faces **increased pressure** on housing in cities where land scarcity also plays a role. As a result, **residential top-up buildings** in **cities** becomes **necessary** (Centraal Bureau voor de Statistiek, n.d.). However, top-up buildings are currently only applied to a limited extent, while it offers many opportunities, especially in large cities (Bosch et al., 2023). Therefore, it is important to choose **municipalities** with a **high population** and a **high degree** of **urbanization** (Geuting et al., 2023).

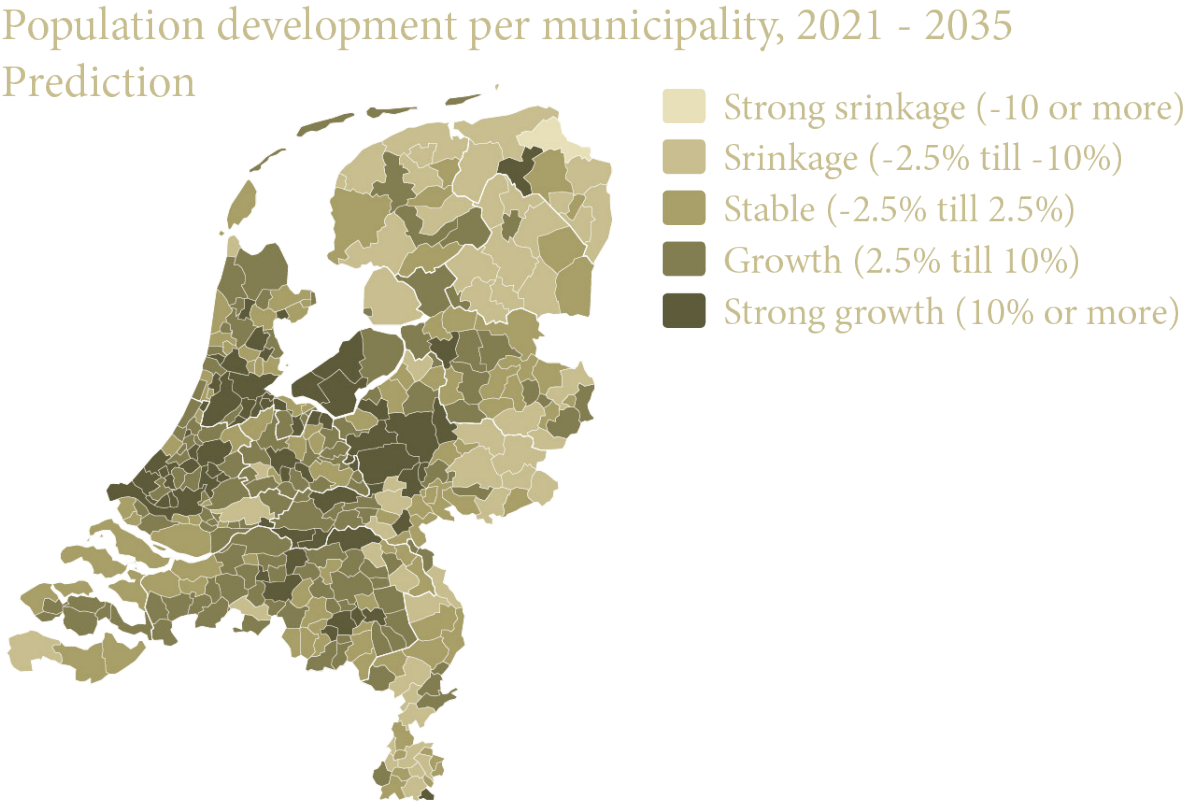

Figure 9, Population development per municipality 2021 - 2035, derived from: (Planbureau voor de Leefomgeving, 2022)

The forecast of the map on the previous page shows that a strong **growth** of nearly **70%** is expected in municipalities with a high population until **2035**. This makes top-up buildings highly applicable in these municipalities in the future. These are also municipalities with many **large cities** (Planbureau voor de Leefomgeving, 2022). Due to the growing population and the limited number of available construction sites in cities, it is **difficult** to **meet** the **housing needs** in **urban areas** (Artés et al., 2017). Regarding the **lack of space** in **cities**, this problem will persist, as it is **expected** that **80%** of the **current buildings** will still **exist** in **2050** (Rijksdienst voor Ondernemend Nederland, 2024). For these reasons, it is important to **utilize existing buildings** more **efficiently** (Ministerie van Volkshuisvesting en Ruimtelijke Ordening, 2024).

Residential top-up buildings **utilize existing locations efficiently**, **increasing usable floor space** in **cities** without using **new construction sites**. In addition to reducing the housing shortage, top-ups can be excellently combined with **renovation** and **sustainability upgrades** of **existing buildings** (Ministerie van Binnenlandse Zaken en Koninkrijksrelaties, 2024a) This not only **improves** the **quality** of the **existing apartments** but also **reduces energy costs**, making it financially attractive (Ministerie van Binnenlandse Zaken en Koninkrijksrelaties, 2024b). The revenues from renting or selling top-up dwellings can finance renovations and sustainability efforts. This process **transforms neighbourhoods** and **improve facilities**.

When applied to 3- and 4-story residential buildings without elevators, an **elevator** can be **added** during the **top-up process**. For buildings with four stories or more, this is even **mandatory**. As a result, **current residents** can **continue living** at **home** for **longer** (Ministerie van Binnenlandse Zaken en Koninkrijksrelaties, 2024a).

Finally, **top-ups** also offers **benefits** for **material** and **CO_2 reduction**, with reductions of **80%** and **26%**, respectively, **compared** to **new-build apartments** (Bosch et al., 2023). This is shown by the image below:

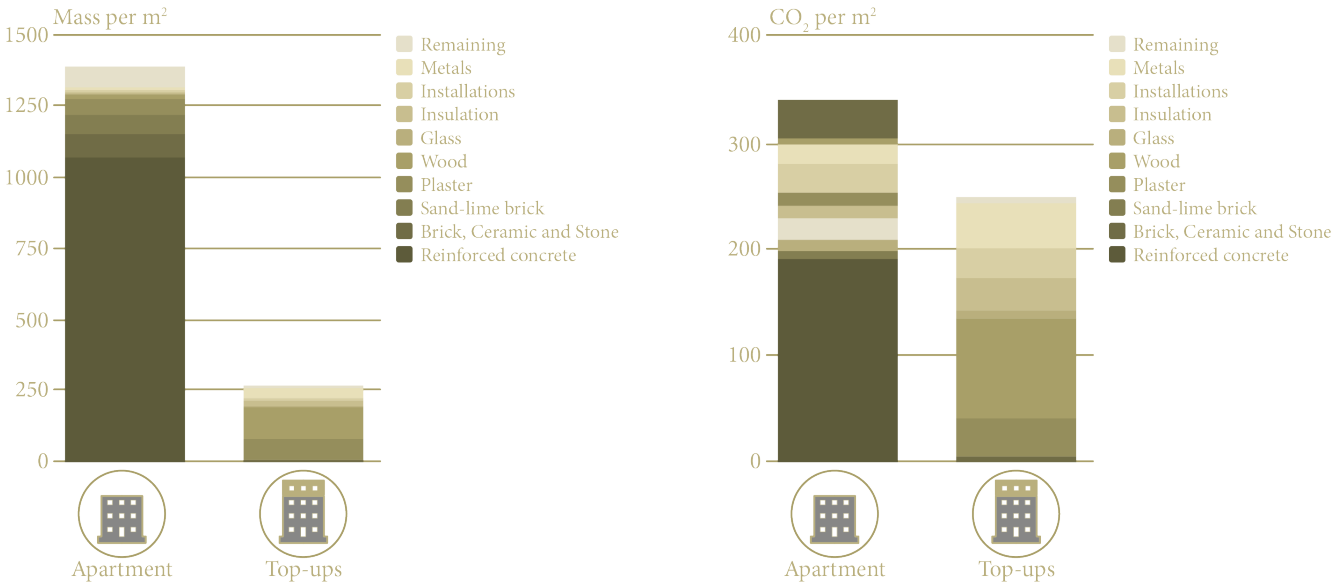

Figure 10, Difference mass and CO_2-reduction between apartment and top-up, derived from (Bosch et al., 2023)

Due to **extensive permitting procedures**, the **nitrogen crisis**, and **zoning plans**, **new housing projects** are currently **experiencing delays**. This **limits housing construction** in certain areas and **hinders** the **resolution** of **housing density issues** (Novogradac, 2024). To speed up the permitting process, municipalities are willing to lower the **threshold** for **granting permits** for **residential top-up buildings** (Geuting et al., 2023). Although there is a **desire** from the **government** and **construction companies** to use bio-based materials for top-ups, there is **insufficient expertise** (Stulen, 2024).

3.3 Potential residential top-up buildings

Since not all residential buildings are suitable for additional floors, it is important to determine which types of apartment buildings can be used for top-ups. To determine which technical characteristics are relevant for top-ups, the **ideal number** of **floors** of the **existing building** for applying top-ups will first be investigated. Next, the **construction year** of the existing building and the **number of floors** that **can** be **added** will be established.

Topping-up is primarily limited by the **physical properties** of the **current** residential building, and it must therefore be **technically** sound, which must be checked for each building. The existing residential building must have a **flat roof** with **sufficient surface area**, and the **structure** must be able to **bear** the **weight** of **additional floors**, so costly adjustments are unnecessary (Greve & Koning, 2024). According to NEN87-7, the **load** can **increase** by up to **15%** without the need for intervention (Koppenhol, Müller, et al., 2024).

Building floors

The research by Geuting et al., (2023) analyses the **top-up possibilities** based on the **number of floors**. As shown in the figure below, four floors (30%) are the most ideal:

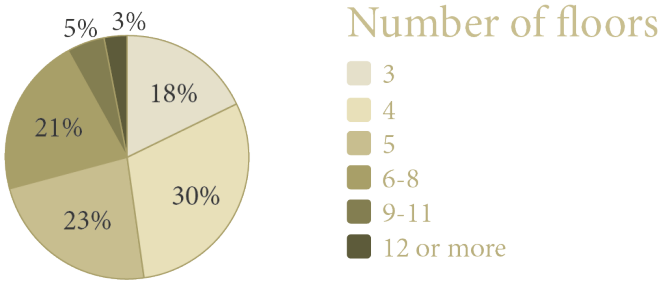

Figure 11, Top-up possibilities based on the number of floors, derived from (Geuting et al., 2023).

Since **NEN 13501-1** states that buildings **taller** than **13 meters** must comply with **fire class B** to ensure fire safety, it has been decided to stay **below 13 meters**. For buildings **lower than 13 meters**, **fire classes C** and **D** are allowed for the **inner façade** and **outer façade**, respectively. The following table explains what each fire class prescribes.

Table 2, Fire Classification according to NEN 13501-1

Fire Classification according to NEN 13501-1	Contribution to Fire	Flammability
A1	No contribution	Non-flammable
A2	Barely any contribution	Virtually non-flammable
B	Very limited contribution	Very difficult to burn
C	Limited contribution	Flammable
D	High contribution	Flammable

Depending on the height of each floor, which varies per building, it can be concluded that **five floors** are the **maximum** to remain under 13 meters and thus fall within the less stringent fire regulations. For this reason, only **three** or **four floors** of the **existing structure** are **permitted**. The above research shows that four floors are the most ideal for residential top-up buildings, thus this is taken as the starting point. These buildings can be **extended** by **one layer**, considering the fire requirements.

Year of construction

Residential buildings constructed **before 1964** are generally **not structurally suitable** for a top-up building, unless costly and significant structural adjustments are made. **From 1964 onwards**, primarily concrete frames were used, which allow the addition of lightweight residential floors, such as those made of wood or steel, without significant structural interventions (Greve & Koning, 2024).

Research by Geuting et al., (2023) has examined the realistic top-up potential for buildings **from 1964 onwards** based on the construction period of the current residential building, see the figure below.

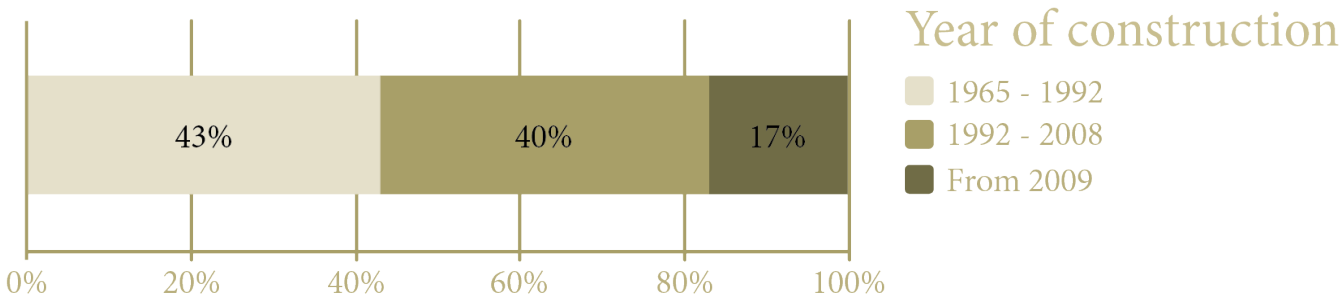

Figure 12, Realistic top-up task based on the construction period of the existing building, derived from: (Geuting et al., 2023).

This shows that buildings from the **period 1965-1992** have the **greatest potential** for top-ups with **43%**. Practical experience, however, shows that adding additional floors is generally more suitable for buildings constructed **after 1992**. **After 1992**, 'Bouwbesluit fase 1' was implemented, which imposed **stricter structural requirements** on buildings. As a result, it can be stated with certainty that buildings constructed **after 1992** have **foundations** that **meet** the **requirements** for **adding extra floors** (Geuting et al., 2023). Finally, **66%** of the realistic top-up tasks consist of buildings from **housing corporations** that have used **standard dimensions**. These dimensions **simplify** the **standardization** and **industrialization** of top-up buildings, benefiting bio-based materials (Ministerie van Binnenlandse Zaken en Koninkrijksrelaties, 2024a).

3.4 Benefits bio-based materials for residential top up buildings

Section 2.2 outlined the general advantages of bio-based materials compared to conventional building materials. This section focuses specifically on the reasons why bio-based building materials are exceptionally suitable for residential top-up buildings. This thesis highlights the **key properties** of bio-based construction materials in relation to **lightweight construction**, **effective moisture regulation**, the **prevention** of **indoor overheating**, and the **reduction** of **construction-related disturbance**. Before listing the benefits of bio-based materials, certain terms will be briefly explained.

Table 3, Explanation building physical properties, derived from: (Bourbia et al., 2023) & (De Visser et al., 2015)

Symbol	Name	Explanation	Units
ρ	Density	Mass per unit volume	Kg/m^3
R	Thermal resistance	The ratio of the temperature difference across an insulator and the heat flux through it	m^2K/W
λ	Thermal conductivity	The heat flow through a unit area of a homogeneous material with a thickness of 1 meter, induced by a temperature difference of 1 Kelvin on the surfaces	W/mK
U	Overall heat transfer coefficient	The amount of heat that flows through a unit area of a complex component or heterogeneous material as a result of a temperature gradient of 1 Kelvin	W/m^2K
α	Thermal diffusivity	The ability of a material to transport heat relative to its capacity to store heat	m^2/s
c	Specific heat capacity	The energy needed to raise the temperature of 1 kg of material by 1 K	J/kgK
δ	Vapour permeability	The amount of water vapour passing through a material per unit thickness, per unit time and per unit vapour pressure difference across the material.	Kg/(msPa)
μ	Vapour diffusion resistance factor	Ratio of the water vapour diffusion coefficient (δ) of the air to the δ value of the building material in question	-

Lightweight materials

Due to the limited structural capacity of existing buildings, **minimizing** the **weight** of the **top-up building** is the **most crucial aspect** of top-up buildings (Julistiono et al., 2023). Currently, for the construction of residential top-up buildings with bio-based materials, only wood is suitable due to the limited mechanical properties of other bio-based materials (Yadav & Agarwal, 2021). Due to the **low density**, ρ, **wooden constructions reduce** the **gravitational load** on **existing buildings** and are therefore a suitable option for the construction of top-ups (Ministerie van Binnenlandse Zaken en Koninkrijksrelaties, 2024a).

When considering traditional, non-bio-based materials, a **concrete construction** is **unfeasible** due to the **much higher density** of **concrete compared** to **wood**. Concrete is on average **five times heavier**, which may exceed the load-bearing capacity of the existing structure (Ministerie van Binnenlandse Zaken, 2022). Besides wood, steel can also be considered for construction due to its lower weight and the possibility for larger spans. However, wood offers significant **climate advantages** (renewable and absorbs CO_2) and aligns with the Dutch government's ambition to **promote bio-based buildings** (Koppenhol, Müller, et al., 2024).

Although the structure accounts for a substantial part of the weight, other construction component functions will also be examined (Brischke & Humar, 2017). Bio-based insulation materials typically have **higher density** and **higher thermal conductivity**, λ, than mineral wool insulation materials. Higher thermal conductivity leads to **more heat conduction**, requiring **thicker insulation** layers to meet the **U-** and **R-requirements** from the Dutch Building Decree. Although the structure carries most of the weight in the total wall construction, this makes bio-based insulation materials **less suitable** (Arup, 2024).

For exterior wall finishes, bio-based materials have a **lower density** than stone finishes, such as brick, concrete, or natural stone. Additionally, bio-based materials are generally **thinner**, further reducing weight. Due to the **better insulating properties** of bio-based materials compared to stone finishes, bio-based exterior finishes can **reduce insulation thickness** (Sandak et al., 2019).

Conventional constructions often use **vapour-tight membranes** on the **inside** and **vapour-open membranes** on the **outside** of the **insulation layer** to **prevent moisture** from condensing between the layers. This keeps both the insulation and the inner layer of the construction dry. However, **small openings** around cables and nails can **allow moisture** to **enter**, **causing** it to be **trapped** by the **vapour-tight construction**. This can lead to **moisture damage** and **mold growth** within the **construction** (De Visser et al., 2015).

Additionally, **high relative humidity indoors** can cause **moisture accumulation** and **mold formation** in **constructions** with **vapour-tight membranes** (CORDIS, 2018). **Relative humidity measures** the amount of **water vapour** in the **air relative** to the **maximum amount** at a given **temperature** and is a crucial aspect of indoor air quality (KNMI, n.d.). The urgency for **good relative humidity** has **increased** because insulation measures in many homes have **further raised** the **relative humidity**. These measures have resulted in a **higher airtightness** (CORDIS, 2018). Other factors affecting relative humidity in homes include daily **temperature fluctuations** and **heating methods** (Brischke & Humar, 2017). Together, this emphasizes the need to keep **relative humidity low**.

Vapour-open construction

Vapour-open constructions are strongly recommended to **prevent moisture accumulation** and **ensure indoor air quality**. Such constructions **allow moisture** to be **transported from** the **inside to** the **outside**, **effectively expelling moisture** (De Visser et al., 2015). A **vapour-open construction** does **not require** a **vapour barrier** between the **insulation material** and the **indoor environment**, meaning there is **direct interaction** between the **outside air**, the **construction**, and the **indoor air** (De Kort et al., 2023). However, it is important to emphasise that **vapour-open constructions** are **not without risks** and require **careful building physics analysis**, as the literature presents varying definitions and interpretations of what constitutes a vapour-open construction.

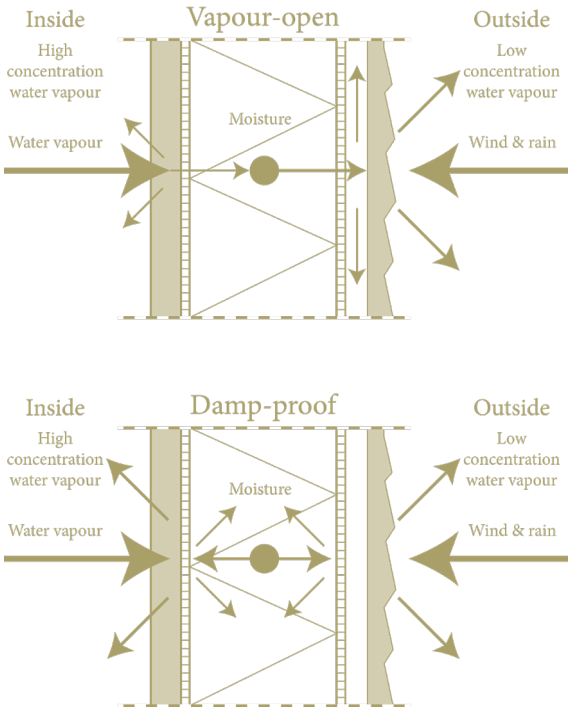

Figure 13, Principle of vapour-open & damp-proof construction, derived from (Bouke, 2020)

For an **effective** vapour-open construction, the use of **hygroscopic materials** is **recommended** (Bardage, 2017). The **hygrothermal performance** of building materials includes the **absorption**, **storage**, and **release** of **heat** and **moisture**. Due to the **ability** to **absorb**, **store**, and **release moisture**, **hygroscopic materials** can **act** as an **effective moisture buffer**, **reducing** the **risk** of **condensation** and **mold growth**. The applicability of this phenomenon is **restricted** to materials that are **capillary active**. (Palumbo et al., 2016). Additionally, these materials **reduce peaks** and **troughs** in **humidity levels**, leading to a **healthy indoor climate** (Dams et al., 2023).

Bio-based materials stand out due to their **excellent hygrothermal properties**, allowing **moisture** in **constructions** to be **managed**. As a result, bio-based materials help **maintain stable moisture levels** in wall constructions, significantly **reducing** the **risk** of **moisture-related problems**. By **regulating moisture**, bio-based materials **improve indoor comfort** and **air quality**. Moreover, these materials can **reduce energy consumption** for **heating** and **cooling** by **5%** and **30%**, respectively (Fischer & Korjenic, 2023).

The hygrothermal properties are partly due to the **natural fibers** in bio-based materials, which can **bind 5 to 40%** of their **dry weight** in **moisture** (Sandak et al., 2019). Fossil or mineral insulation materials have only a **fraction** of this moisture accumulation capacity (Cascione et al., 2022).

Vapour diffusion resistance factor

The hygrothermal properties of bio-based materials include **vapour diffusion properties**. Vapour diffusion is the **process** by which **water vapour** moves through a material from an **area** of **high relative humidity** to an **area** of **lower relative humidity** (Worch, 2004). This phenomenon can be seen in the figure below.

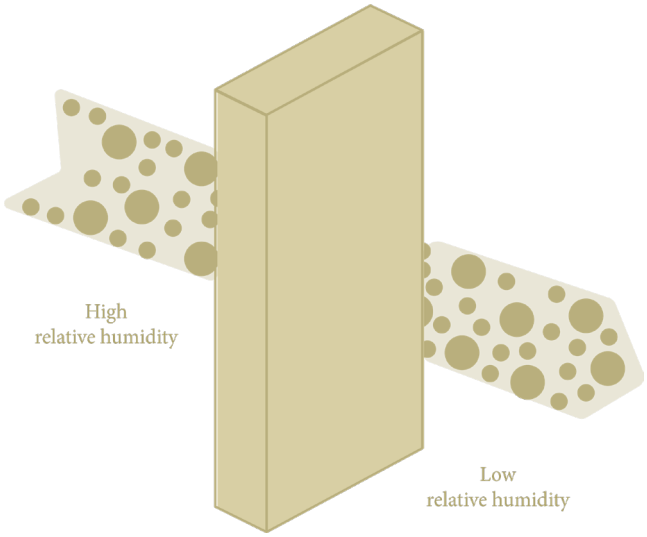

Figure 14, Vapour diffusion resistance factor, own illustration

Vapour diffusion occurs because **higher absolute humidity** has a **higher water vapour pressure**, and **vapour transport** always **moves** towards the **lower vapour pressure**, **regardless** of **gravity** (Vinha & Käkelä. Pasi, 1999). To indicate how much **water vapour** a material **resist**, the **vapour diffusion** of a material is **expressed** with the **vapour diffusion resistance factor**, μ-factor (Fedorik et al., 2021). The factor is a **dimensionless measure**, with air having a μ-value of 1 (Bourbia et al., 2023). The **high porosity** of bio-based materials **results** in a **low μ-factor**, which can be seen in table 3, indicating **high vapour permeability** (The Wit, 2008).

With a **low μ-factor**, **moisture** can be **easily absorbed** and **released** to the **outside** in **response** to **fluctuating relative humidity** and **vapour pressure gradients** in a space. Due to this **low μ-factor**, **bio-based materials** in a construction can **combat moisture** and **mold problems** (Lawrence et al.,2013).

De Visser et al., (2015) conducted research on the μ-factor of various insulation materials. The table on the next page, table 4, shows that the μ-factor of bio-based materials is comparable or often lower than that of stone wool and glass wool. Additionally, **bio-based materials perform better** in this area than **synthetic insulation materials**.

Table 4, Vapour diffusion resistance factor of different insulation materials, derived from: (De Visser et al., 2015)

	Material	Vapour diffusion resistance factor (μ) [-]
Synthetic	EPS	20 - 100
	PUR / PIR	30 - 200
	XPS	80 - 300
Mineral	Foam Glass	-
	Mineral Foam Sheet	5
	Glass Wool	1
	Rock Wool	25 - 400
Natural	Cellulose Plates	2 - 3
	Cellulose Flakes	1 - 1,5
	Grass	1 - 2
	Hemp Mats	1 - 2
	Hemp Loose	1 - 2
	Wood Fibre Board	1 - 2
	Wood Fibre Boad Flexible	2 - 5
	Wood Fibre Loose	1 - 2
	Coir	1
	Cork Plate	2 - 10
	Reed	2
	Sheep's Wool	1 - 2
	Straw Bales	2

Vapour permeability

Another **important hygrothermal property** of bio-based materials is the **high water vapour permeability**, δ. This property **contributes** to **moisture management** in **building constructions** and **enhances** the **functioning** of **vapour-open constructions**. The δ indicates how much **water vapour** can **move through** a **material** per **unit** of **time** at a given **vapour pressure difference**. The **internal fibrous structure** of bio-based materials **contributes** to the **high δ-value** (Bourbia et al., 2023). Due to the long fibers interwoven with spaces, **water vapour** can **diffuse** up to **three times** more **efficiently compared** to **synthetic materials**. This **enables** bio-based materials to effectively transport water vapour from a **moist** to a **drier environment** (Lafond & Blanchet, 2020).

Capillary

Finally, the last **important hygrothermal property** of bio-based materials is **capillary action**. Due to the **fibrous structure** of most bio-based building materials, there are **small individual pores** between the fibers. These **pores allow** the materials to **retain air** or **moisture**, making most bio-based materials **porous** and **capillary**. The **degree** of **porosity** can vary, depending on the **type** of **bio-based material** and the **arrangement** or **compression** of the **fibers** (Brischke & Humar, 2017). **Porous materials** contain **microscopic pores** where **capillary forces** ensure that **moisture** is **absorbed** and **transported** through the **pore structure**. Due to **temperature differences** and **capillary movement**, **moisture spreads through** a **material**, with some **moisture remaining** in the material. This ensures **uniform moisture distribution**, resulting in **more efficient evaporation** from **constructions** and **reduction** of **moisture problems** (The Wit, 2008). The figure below provides a visual representation of this phenomenon.

Figure 15, Capillary movement, own illustration

Heat

Due to the necessity to use lightweight building materials such as wooden construction, this requires extra attention to **prevent overheating**. With respect to the construction, wood, due to its **relatively low density**, has a **limited thermal mass** compared to concrete (Sandak et al., 2019). Additionally, homes are increasingly being built airtight, further increasing the risk of overheating in residences (Farrokhirad et al., 2024).

A **high thermal mass** is essential to **counteract overheating** in residential top-ups. **Thermal mass** is **defined** as the **ability** of a **mass** to **absorb**, **store**, and **release energy** in the **form** of **heat** or **cold**. A **combination** of **convection**, **radiation**, and the **surface area** of the **thermal mass influences** how **quickly heat** is **transferred** between the **thermal mass** and the **indoor air** (Li & Xu, 2006). It is one of the most **efficient passive methods** to **regulate indoor temperature**, **reduce temperature fluctuations**, and **prevent overheating** (Farrokhirad et al., 2024).

The **lower** the **thermal mass** of a **material**, the **less energy** it can **store**, causing **rooms** to **heat up** more **quickly** (Kuczyński & Staszczuk, 2020). A **high thermal mass**, on the other hand, ensures a **greater phase shift** and **damping** of **temperature amplitude** in top-up residences, as illustrated in the figure below (Koppenhol, Hertzberger, et al., 2024). In the illustration below on the **left** is a **lower thermal mass** which results in a **shorter phase shift** and **higher temperature amplitude**. On the **right**, is a **higher thermal mass** which results in a **longer phase shift** and **lower temperature amplitude**.

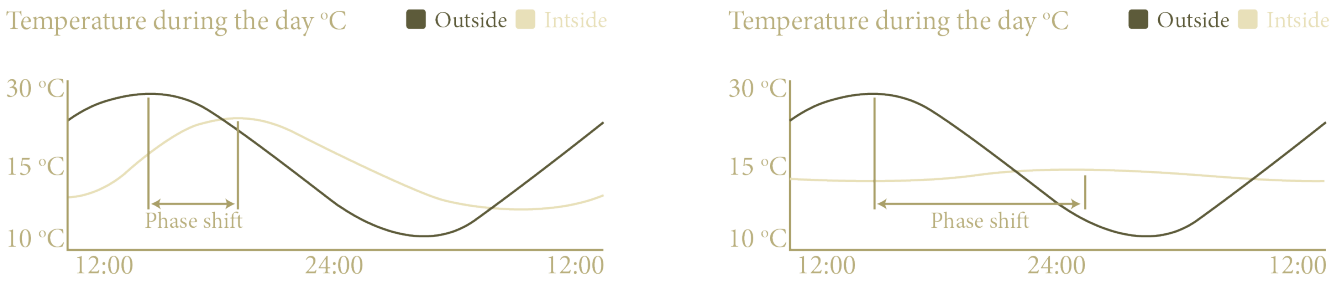

Figure 16, Illustration phase shift and temperature amplitude, derived from (Koppenhol, Hertzberger, et al., 2024)

Due to the **low thermal mass** of **wood**, **thermal mass** must be **added** through **other wall layers**. **Bio-based insulation materials** are extremely **suitable** for this purpose and **ensure** a **stable indoor temperature** in residential top-ups. The contribution of these materials is due to the increased phase shift and temperature amplitude, which will be explained below.

Phase shift

Phase shift refers to the **time delay** with which **fluctuations** in **outside temperature** and **solar radiation** on the **exterior face** of the construction affect the **surface temperature** and **thermal conductivity** to the **indoor air**. A **greater phase shift** leads to a **longer time span** after which the **indoor temperature** is **affected**. As the **phase shift increases**, **temperature fluctuations decrease**, resulting in a more **favourable indoor climate** (Arup, 2024). Besides **density**, **phase shift**, and **thermal conductivity**, **thermal diffusivity** is a crucial factor for **thermal mass**. It determines how **quickly heat moves through** a **material**. Materials with **low thermal diffusivity spread heat more slowly**, resulting in a **longer phase shift** (Owczarek et al., 2021).

Although the Dutch Building Decree currently does not set requirements regarding phase shift, it remains an **important parameter** that should be considered, particularly in lightweight constructions. The following formula can be used to calculate the phase shift.

$$\varphi = (\sum_{i=1}^{n} \left(\frac{d_i}{2\pi d^*}\right) \times t_0)/3600$$

With:

$$d^* = \sqrt{\frac{\alpha_i t_0}{\pi}}$$

$$\alpha_i = \frac{\lambda_i}{\rho_i \times c_i}$$

$$t_0 = 24 \times 3600$$

Where:
φ = Phase shift [h]
d_i = Material thickness of material i [m]
d^* = Characteristic penetration depth of the heat [m]
α_i = Thermal diffusivity [m^2/s]
t_0 = Period of the temperature fluctuation of 24h [s]
λ_i = Thermal conductivity [W/mK]
ρ_i = Density material of material i [kg/m^3]
c_i = Specific heat capacity of material i [J/kgK]
n = Number of layers of the construction [-]
(The Wit, 2008)

While the above formula may provide an indication of the phase shift, it is important to note the **limitations**. For an accurate determination **simulation** is essential. This is because the **material layers thermally influence one another**. Additionally, the use of timber cladding with a **ventilated cavity** results in **partial heat dissipation** through **ventilation** behind the façade. This effect can also be calculated by the use of **simulations**. Finally, the applied formula does not take into account **short-wave radiation absorptivity** or **long-wave radiation emissivity**, both of which significantly affect the thermal performance of the façade.

Due to the **high thermal mass** and **low thermal diffusivity**, the **insulation materials** have the **greatest impact** on the **phase shift**. Although the insulation layer is central to this research, it is important to note that in conventional façades it usually has a limited impact on the phase shift. In bio-based constructions, such as those examined in this thesis, its influence is relatively **greater**. This is also the reason why this thesis only focuses on the manual calculation of the phase shift of bio-based insulation materials. Although software simulations are required for an accurate overall assessment, the scope of this thesis is **limited** to the **insulation material**. Consequently, in the applied formula, the variable 'i' refers exclusively to the insulation layer.

De Visser et al., (2015) researched the various properties of insulation materials that are also relevant for calculating the phase shift, such as density, specific heat capacity, and the overall heat transfer coefficient

Table 5, Thermal conductivity, density and specific heat capacity of different insulation materials, derived from: (De Visser et al., 2015)

	Material	Thermal conductivity (λ) [W/mK]	Density (ρ) [kg/m³]	Specific heat capacity (c) [J/kgK]
Synthetic	EPS	0.032 - 0.040	15 - 30	1200
	PUR / PIR	0.020 - 0.040	15 - 38	1400
	XPS	0.030 - 0.040	20 - 60	1200
Mineral	Foam Glass	0.040 - 0.090	105 - 165	830
	Mineral Foam Sheet	0.045	115	1000
	Glass Wool	0.032 - 0.040	20 - 140	840
	Rock Wool	0.032 - 0.050	25 - 400	840
Natural	Cellulose Plates	0.040	70 - 100	2000
	Cellulose Flakes	0.039 - 0.045	35 - 60	2200
	Grass	0.042	53 - 68	2200
	Hemp Mats	0.040 - 0.050	30 - 42	1600 - 1700
	Hemp Loose	0.048	40 - 80	1600 - 2200
	Wood Fibre Board	0.040 - 0.052	140 - 180	2100
	Wood Fibre Boad Flexible	0.040 - 0.052	40 - 55	2100
	Wood Fibre Loose	0.040	30 - 40	2100
	Coir	0.045	80 - 120	1300
	Cork Plate	0.040 - 0.045	70 - 140	1800
	Reed	0.038 - 0.055	190 - 225	1300
	Sheep's Wool	0.035 - 0.040	18 - 30	1700
	Straw Bales	0.052 - 0.080	400	2000
	Flax	0.038 - 0.050	15 - 60	1600

Bio-based materials generally have a **higher density** than synthetic and mineral insulation materials, contributing to **greater thermal mass**. Similar results are provided by the research of Brischke & Humar, (2017). Additionally, bio-based insulation materials generally have **higher specific heat capacities** than synthetic or mineral materials, which also contributes to high thermal mass (Arup, 2024). This can also be seen in table 5 and is confirmed by (CORDIS, 2018).

Table 5 also shows that bio-based insulation materials generally have **higher**, and thus **less favorable, λ-values**. This conflicts with the need to **reduce** the **thermal conductivity** of materials but is **desirable** in terms of **heat storage**. Studies emphasize that both **high specific heat capacity** and **high thermal conductivity** values are necessary to **activate** the **thermal mass** in a material (Reilly & Kinnane, 2017).

The difference between the λ-values of common synthetic and mineral insulation materials and bio-based insulation materials is, however, minimal, making them still suitable for thermal insulation. This is partly due to the **high porosity** of bio-based materials, where **cavities** in the materials are **filled** with **air** or **gas**. Since **air** and **gas** have much **lower thermal conductivity** than solid materials, this **reduces** the **overall thermal conductivity** of the material. **Potential thermal bridges** due to **lower λ-values** are negligible and can be **resolved** with **thicker insulation layers** or **effective detailing**. This **thicker layer** further **improves** the **thermal mass** of the construction (Liu & Zhao, 2022). (Johra, 2021) conducted research on the **thermal diffusivity** of building materials, where wood and bio-based insulation materials exhibit **low**, thus **positive**, **values**. Similar results are achieved according to the information in table 5.

Temperature amplitude damping

In addition to a longer phase shift, **temperature amplitude** is also important. This refers to the **ability** of **materials** to **minimize outdoor temperature fluctuations**, keeping the **indoor climate stable**. **High thermal mass** also influences this (Koppenhol, Hertzberger, et al., 2024). As previously mentioned, bio-based materials have **low thermal diffusivity**, which **reduces temperature amplitude** (Owczarek et al., 2021).

Next to that, bio-based materials **buffer moisture**, which also has **beneficial effects** on **heat buffering**. During **condensation**, **heat** is **released**, and during **evaporation**, **heat** is **absorbed**, **storing thermal energy** in the material. This ability **mitigates temperature fluctuations**, resulting in a **stabilized indoor temperature** between **day** and **night**. Compared to conventional insulation materials, **less energy** is **transferred**. As a result, it helps to **keep heat out** during the **summer** and **retain heat** during the **winter**. This **positively** contributes to **heating** and **cooling loads** (Lawrence et al.,2013). This is reinforced as the materials can partly **absorb heat** in the **summer** and **release** it in the **winter** and vice versa (De Visser et al., 2015).

Less disturbance

The biggest obstacle for topping up is the **inconvenience** for **existing residents**. The residents do not directly benefit from the additional dwellings but do experience **disturbances** during and after the construction, such as **noise disturbance**, **prolonged inaccessibility** of the **elevator**, and **increased pressure** on **amenities**. Therefore, it is essential to **minimise** the **inconvenience** during the **construction** of top-up buildings.(Greve & Koning, 2024).

The construction process causes **noise** and **environmental issues** due to the **arrival** and **departure** of **workers** and **materials**. Bio-based materials are excellent for the **prefabrication** of building elements, which can **reduce transport movements** by **20%** (Miles & Krug, 2013). Furthermore, **waste** can be **reduced** by **90%** with **bio-based prefab elements**, causing **less disturbance** to existing residents due to construction waste (College van Rijksbouwmeester en Rijksadviseurs, 2022).

Additionally, with prefabrication, parts are produced in the factory and can be directly assembled on the construction site (TNO, n.d.). This **quick assembly** of prefab elements can **significantly shorten** the **construction time**. Moreover, **minimal adjustments** are needed on-site due to the industrial precision of the bio-based prefab elements that are manufactured. This also contributes to an **accelerated construction process** (Brischke & Humar, 2017).

Bio-based prefab elements also make the construction process **less weather-dependent**, further **improving speed** and **quality** (Vermeulen et al., 2020). The lightweight nature of **bio-based prefab elements** and **bio-based materials** allows them to be processed with **simple tools**, **limiting noise disturbance** (Sandak et al., 2019). All of this enhances the **efficiency** of building residential top-ups, thereby reducing the duration of inconvenience for the immediate surroundings.

Regarding the **positive hygroscopic properties** of bio-based materials, it should be noted that the benefits are written in general terms. The **properties** can **vary** per **bio-based material**. The hygroscopic properties of each selected bio-based product will be described later in the report.

Conclusion

For top-up buildings, it is ideal to use **lightweight materials** to **minimise** the **load** on the **foundation**, which is possible with bio-based materials. Additionally, bio-based materials enable the creation of **vapour-open constructions**, **allowing moisture within** the **construction** to be **transported outside**. Furthermore, bio-based materials have **good hygrothermal properties**, which ensure **effective moisture regulation** and create a **healthy indoor climate**. Moreover, bio-based materials achieve a **higher thermal mass**, resulting in a **longer phase shift** and **lower temperature amplitude**. Finally, bio-based materials allow for **prefabrication**, which results in **less disturbance**, **waste**, **transport**, and **faster construction**.

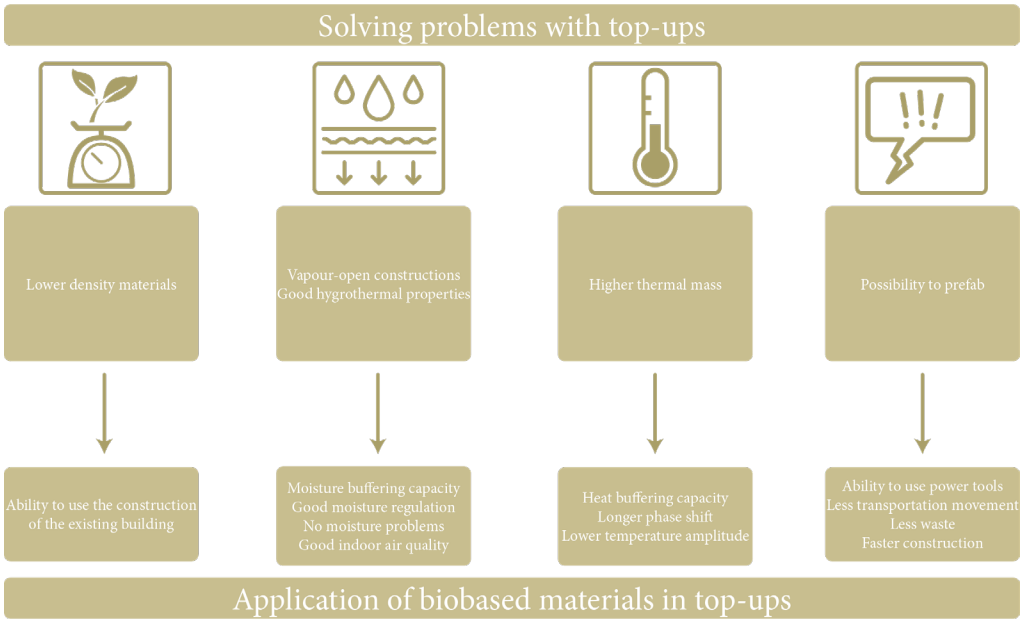

Figure 17, Conclusion advantages application bio-based materials in residential top-up buildings, own illustration

4. Crucial properties for analysing the details in WUFI

Avoiding **thermal bridges** and ensuring **effective moisture transport** are critical **aspects** of all building constructions. To assess the details on these aspects, **WUFI** is used. This is a simulation software that **models heat** and **moisture transport** in **building components**. WUFI allows for **dynamic analysis** based on **real climate data**, **material properties**, and **boundary conditions**, making it a reliable tool for **identifying** and **evaluating risks** related to **thermal bridging** and **moisture accumulation**. A **thermal bridge** refers to a **section** of the **building envelope** that experiences **greater heat transfer** than the **surrounding materials**. This phenomenon arises from **variations** in **thermal conductivity** between **construction elements**, leading to **increased heat transfer**. As a result, **thermal bridges** can contribute to **energy inefficiency**, **indoor temperature inconsistencies**, and potential moisture-related problems such as **mold formation**. The next figure schematically illustrates the concept of a thermal bridge.

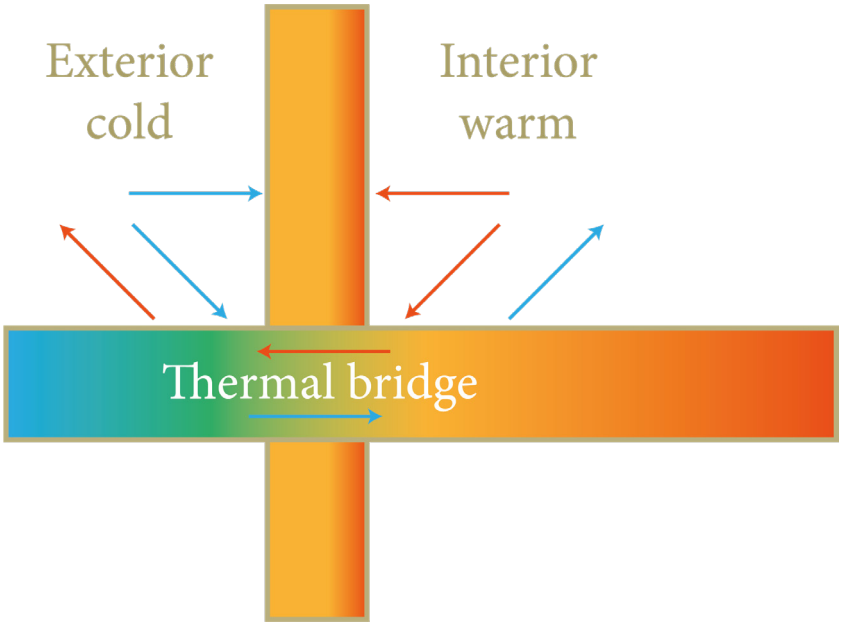

Figure 18, Schematic illustration thermal bridge, derived from (Mousdell, 2024)

This chapter will first explain why these elements are particularly important for residential top-up buildings. Subsequently, the properties required to analyse thermal bridges and moisture transport using the WUFI software will be elaborated upon.

4.1 Avoiding thermal bridges and managing moisture transport in top-ups

There are several reasons why **reducing thermal bridges** and **ensuring effective moisture transport** are particularly important for residential top-ups. First, research by Ingeli et al., (2016) shows that **thermal bridges** are **common** in **lightweight constructions** such as timber. In the context of this research, which focuses on residential top-up buildings using timber structures and other lightweight bio-based materials, it is **essential** to **map thermal bridges** and **eliminate thermal bridges** through **detailing** (Alhawari & Mukhopadhyaya, 2018). **Thermal bridges** significantly **impact overall heat loss transmission**, which must be **minimized** (Asdrubali et al., 2012). Research by Šadauskienė et al., (2015) indicates that **thermal bridges** can **increase heating demand** by up to **30%**. Consequently, **reducing** the effects of **thermal bridges** in façades is crucial to **minimizing heat loss** in building envelopes (Xue et al., 2023). Moreover, **thermal bridges** can **increase** the **risk** of **moisture problems**, eventually leading to **mold growth** (Fantucci et al., 2017).

Thermal bridges occur where the building envelope has **high thermal transmissions**. Adding more layers of insulation to the building envelope **without taking thermal bridges** into account is **unlikely** to significantly **reduce heat loss** and may even **increase** the **influence** of **thermal bridges**. **Correct detailing**, however, is an effective way to **decrease** the **thermal bridges** in constructions (Alhawari & Mukhopadhyaya, 2018). In addition, adding excessive insulation materials **increases weight**, which should be **avoided** as much as possible in top-up buildings. **Identifying thermal bridges** allows for **targeted insulation** or other technical adjustments to both **reduce thermal bridges** and **maintain** a **lightweight construction**.

Eliminating **thermal bridges** also provides benefits for **reducing** the **load** on the busy **electricity grid** in the Netherlands, which is **becoming** increasingly **overloaded**. Chapter 2 highlights that top-ups are mainly applied in urban areas where **grid congestion** is **highest** (Van Hooft, 2023). The share of electricity in the **total energy demand** of the Netherlands is expected to **rise** from **less than 20%** in **2020** to **over 40–60%** by **2050**. This is driven by Dutch climate policy aiming to phase out natural gas and achieve a climate-neutral, CO_2-free energy supply by **2050** (Sijm, 2024). The 'Energieagenda 2016' emphasizes the growing role of electricity in heating and cooling buildings in the coming decades.

Electric heat pumps are an important option for **heating** and **cooling**, but they will **further burden** the **electricity grid**. By **identifying** and **insulating thermal bridges**, **proper insulation** for residential top-up buildings can be **guaranteed**. This will **reduce** the **electricity demand** for **heating** and thus relieve the electricity grid in cities (Ministerie van Economische Zaken, 2016). As previously discussed, bio-based materials contribute to a **damping** of the **temperature amplitude** which can further **reduce** the **energy demand** for **heating** and **especially cooling** (Lawrence et al.,2013).

Thermal bridges negatively impact **heat loss transmission** which can result in higher heating costs. **Moisture** in constructions can **alter** the **properties** of **heat transfer**. Factors such as the **hygrothermal properties** of various materials and **gravity influence** the **moisture content** in constructions. This leads to a **non-uniform distribution** of **water vapour** in different parts of the construction. In general, it can be stated that the **more water vapour** a material in a construction contains, the **higher the thermal conductivity** (Xue et al., 2023).

Besides the negative effects of **moisture** on **mould growth** and a **healthy indoor environment**, it is also **crucial** to ensure **effective moisture transport** to maintain **good thermal properties**. **Excess moisture** is undesirable in terms of **weight** as well. Initially, the **absorption** of **water** by organic building components **increases** the **weight**, which can **impose** additional **stress** on the structure. Therefore, **effective moisture transport** from the **interior** to the **exterior** is essential (Brischke & Humar, 2017).

4.2 Essential properties for WUFI-analysis

Now that the importance of **avoiding thermal bridges** and ensuring **effective moisture transport** in residential top-up buildings has been described, the **key properties** required to **analyse thermal bridges** and **moisture transport** using **WUFI** can be elaborated.

The basic properties of **bulk density**, ρ [kg/m^3], **specific heat capacity**, c [j/kgK], **thermal conductivity**, λ [W/mK] and **water vapour diffusion resistance factor**, μ [-], are essential material characteristics required for the simulations, as explained in chapter 2. Next to these, the **linear thermal transmittance** of the **thermal bridge**, Ψ [W/mK], the **thermal diffusivity**, α [m^2/s], and **porosity**, φ [m^3/m^3], are also important.

Linear thermal transmittance of the thermal bridge

First, the **linear thermal transmittance** of the **thermal bridge**, Ψ [W/mK], will be explained which can be calculated using **WUFI**. This value describes the **amount** of **heat passing through** a **construction component**. The Ψ is derived from the **two-dimensional thermal coupling coefficient**, L^{2D}. The L^{2D} indicates the **total amount** of **heat flowing** through a construction **per metre length**, **divided** by the **temperature difference** between **both sides** of the **construction**. The Ψ is calculated as follows:

$$\Psi = L^{2D} - \sum_{j=1}^{i} U_j l_j$$

Where:
Ψ = Linear thermal transmittance of the thermal bridge [W/mK]
L^{2D} = Two-dimensional thermal coupling coefficient [W/mK]
U_j = Thermal transmittance of the 1-D element j [W/(m^{2}K)]
l_j = The length of the 1-D element j [m]
(Ingeli et al., 2016)

Thermal diffusivity

Thermal diffusivity, α, is the **ratio** of **thermal conductivity** to the **product** of **density** and **specific heat capacity** used to **measure thermal diffusivity**. It is a derived **quantity** composed of the **intrinsic properties** of the **material** (Bourbia et al., 2023). It indicates how **quickly heat diffuses** through a material **after** a **change** in **temperature**. A **high diffusivity** leads to **rapid changes** in **temperature** and is determined using the following formula:

$$\alpha_i = \frac{\lambda_i}{\rho_i \times c_i}$$

Where:
α = Thermal diffusivity [m^2/s]
λ = Thermal conductivity [W/mK]
ρ = Density [kg/m^3]
c = Specific heat capacity [J/kgK]
(Cosentino et al., 2023)

Porosity

Porosity, Ψ, is the **volume** of the **pores** in a **dry material divided** by the **total volume**. Materials with **high porosity** generally have **low μ-factors** (The Wit, 2008). Additionally, a **high porosity**, which many bio-based materials possess, is usually accompanied by **high air content**, which benefits **thermal conductivity**. (Fedorik et al., 2021). **Open porosity** also determines the **maximum water content** the **material** can **hold**, and is determined using the following formula:

$$\varphi = \frac{w_{max}}{\rho_{water}}$$

Where:
φ = Porosity of a material [m^3/m^3]
w_{water} = Maximum water content [-]
ρ_{water} = Density of water [kg/m^3]

Additionally, by using the **true density**, ρ_{true}, and the **bulk density**, ρ_{bulk}, the **porosity**, Ψ, can be estimated as follows:

$$\varphi = 1 - \rho_{bulk}/\rho_{true}$$

Where:
φ = Porosity of a material [m^3/m^3]
ρ_{bulk} = Bulk density [kg/m^3]
ρ_{true} = True density [kg/m^3]
(Schmidt & Hartwig, 2006)

Next to the basic properties the **hygrothermal functions** are also important within WUFI, which are the **Moisture Storage Function**, **Liquid Transport Coefficient** (**Suction** and **Redistribution**), **Water Vapour Diffusion Resistance Factor**, **Thermal Conductivity** (**Moisture**- and **Temperature-dependent** and **Enthalpy**).

Moisture Storage Function

In **porous hygroscopic materials**, the **pore system accumulates water molecules** until the **equilibrium moisture content**, EMC, is reached (WUFI, n.d.-b). The **EMC** describes when the **moisture content** of a **porous hygroscopic material** is in **balance** with the **relative humidity** and **temperature** (Ashour, 2007). With **increasing relative humidity**, **water** first **condenses** in **smaller capillaries** and then in **larger ones** due to the **reduction** of the **saturation vapor pressure** (The Wit, 2008) Consequently, this leads to a significant **increase** in the **EMC** at a relative humidity of **60 – 80%** (WUFI, n.d.-b).

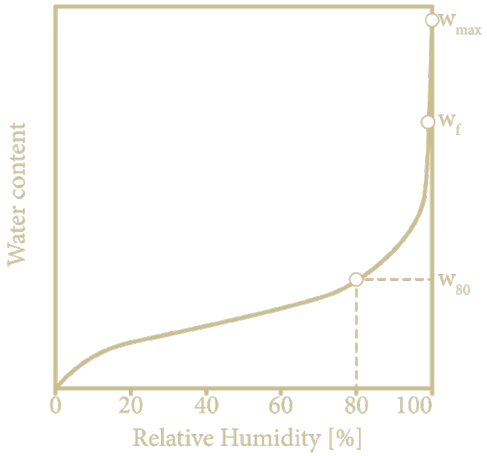

Figure 19, Graph Water Content & Relative Humidity [%], derived from (WUFI, n.d.)

A **capillary-active** material absorbs water until it reaches the **free saturation point**, w_f, which corresponds to a **relative humidity** of **100%**. Additionally, the **porosity** of materials determines the **percentage** of **open spaces** in the **pore structure** that can be **filled** with **air** or **water**. The $\mathbf{w_f}$ is **lower** than the **maximum water content**, w_{max}, as **pores** still can be **filled** with **air**. **Moisture levels above** $\mathbf{w_f}$ can occur due to **condensation** during **temperature differences**, especially in **non-bio-based insulation materials** that do **not absorb water**. **Capillary-active materials**, such as most bio-based materials, **can absorb** this. The $\mathbf{w_f}$ is considered a **standard value** for materials and is therefore usually known. The **practical moisture content**, w_{80}, is another commonly used standard value and corresponds to the **moisture content** at a **relative humidity** of **80%** which is a **common** environmental condition(WUFI, n.d.-b).

WUFI displays the **relative humidity**, φ [-], and the corresponding **moisture contents**, w [kg/m³], in a table where the **points** are **linearly interpolated**. From this, the **moisture storage function**, can be constructed. This function **combines** the **sorption isotherm** (up to 98%) with the **moisture retention curve** (>98%). The **sorption isotherm curve** actually consists of **two** combined **curves**: the **adsorption** and **desorption** of **water**. Due to the **difference** in **porosity** and **permeability** of the **material**, the two curves can **differ**. However, the **difference** is often **small**, so only the **adsorption isotherm** curve is **used** (Taher & Brouwers, 2023).

The generated table can be **extended** to include **moisture contents** in **supersaturated** regions that occur during **condensation**. In these areas, there is no direct **relationship** between **relative humidity** and **moisture content**. The **relative humidity** remains at **1**, and the **moisture content** varies between $\mathbf{w_f}$ and $\mathbf{w_{max}}$ due to **condensation** and **evaporation conditions**. WUFI adds the following extra note for values that exceed $\mathbf{w_f}$:

$$\varphi = 1.01 \text{ gives } w_{max}$$

A **fictive relative humidity** between **100%** and **101%** allows WUFI to assign a **unique relative humidity** to **each moisture content** in oversaturated regions. When the **moisture storage function** can be described using the formula below, the values of $\mathbf{w_{80}}$ and $\mathbf{w_f}$ are sufficient to define the **moisture storage function** in WUFI (WUFI, n.d.-b):

$$w = w_f \frac{(b - 1) * \varphi}{b - \varphi}$$

w = Moisture content corresponding to relative humidity [kg/m³]
w_f = Moisture content at free saturation [kg/m³]
φ = Relative Humidity [-]
b = Approximation factor [-]

By entering the values of $\mathbf{w_f}$, and **b**, the **moisture content** at **different relative humidity levels** can be determined. This allows the **moisture storage function** and thus the **sorption isotherm** curve of materials to be established (The Wit, 2008).

Liquid Transport Coefficient (Suction & Redistribution)

The **moisture transport** in **capillary porous** materials is primarily driven by **capillary liquid transport**. For calculation purposes, it is sufficiently **accurate** to consider **liquid transport** as a **diffusion phenomenon**:

$$g_w = -D_w(w)\nabla w$$

Where:
g_w = Liquid transport flux density [kg/m²s]
w = Moisture content corresponding to relative humidity [kg/m3]
D_w = Liquid transport coefficient [m²/s]

The **Liquid Transport Coefficient**, D_w, strongly depends on the **moisture content** but can be accurately predicted based on how **moisture** is **absorbed**. This is because the above diffusion equation exhibits the same **behaviour** as the **capillary suction process**:

$$s = \sqrt{\frac{\sigma r \cos\theta}{2\eta} t}$$

Where:
s = Water penetration depth [m]
σ = Surface tension of the water [N/m]
r = Capillary radius [m]
θ = Contact angle [°]
η = Viscosity of water [kg/ms]
t = Suction time [s]

The comparison between the two formulas can be made because $\mathbf{D_w}$ is based on the temperature **dependence** of the **surface tension**, σ, and the **viscosity** of the **water**, η. Consequently, the following relationship between the two equations can be established: (Künzel, 1995):

$$D_w(\theta) = \frac{\eta_{ref}}{\eta_\theta} \times D_{w,ref}$$

The **interface** between **water** and **air** in the **capillary**, known as the **contact angle**, can be either **concave** or **convex**. In the case of a **concave surface**, the **pressure** within the **water** is **lower** than the **ambient pressure**, causing the **water** to be **drawn** into the **capillary**, which generates significant **adhesion**. For a **convex surface**, an **external force** is required to drive the water **inward**. The **pressure difference** across the **surface** is referred to as **capillary pressure**, where a **smaller radius** or **contact angle** results in a **higher capillary pressure** (The Wit, 2008).

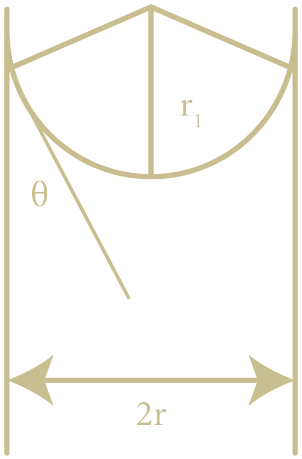

Figure 20, Illustration contact angle because of capillary pressure, derived from (The Wit, 2008)

The **liquid transport coefficient** describes the **rate** at which water is **transported** through a material with **two types** of liquid transport coefficients:

- **Capillary absorption**, primarily through **large** capillaries, D_{ws}.
- The **redistribution** of water after absorption has stopped, primarily through **small** capillaries, D_{ww}.

Due to the **higher flow resistance** in **smaller** capillaries, the **moisture transport process** occurs more **slowly** with D_{ww} than with D_{ws}. For this reason, WUFI uses **distinct liquid transport coefficients**. WUFI applies a **logarithmic interpolation** between the **liquid transport coefficient**, D_w, and **moisture content**, w, as the liquid transport coefficient shows almost an **exponential** dependence on the moisture content.

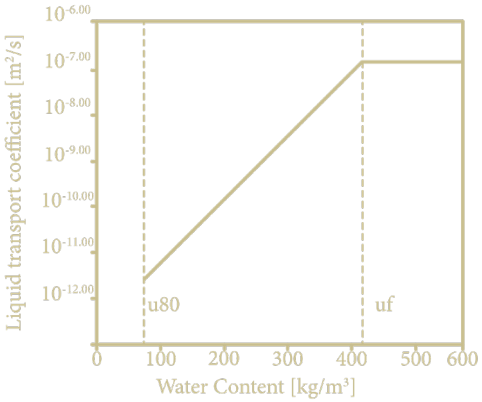

Figure 21, Graph Liquid Transport Coefficient & Water Content, derived from (Coelho & Henriques, 2022)

However, the **liquid transport coefficients** are only available for a few materials, which is why these numbers are often **estimated** based on standard material data. The formulas below are a **rough estimate** that is often successful.

The D_{ws} can be determined by the following formula:

$$D_{ws}(w) = 3.8 \times (\frac{A}{w_f})^2 \times 1000\ (\frac{w}{w_f})^{-1}$$

Next to this, the D_{ww} can be determined by the following formula:

$$D_{ww}(w_f) = \frac{D_{ws}(w_f)}{10}$$

Where:
D_{ws} = Liquid transport coefficient for suction [m^2/s]
D_{ww} = Liquid transport coefficient for redistribution [m^2/s]
A = Water absorption coefficient [$kg/m^2\sqrt{s}$]
w = Moisture content [kg/m^3]
w_f = Free water saturation [kg/m^3]
(WUFI, n.d.-a)

Water Vapour Diffusion Resistance Factor

The **water vapour diffusion resistance factor**, μ, indicates the **resistance** of a **building material** to **water vapour diffusion**. The **constant** is **independent** of **temperature** and **pressure**, making it only dependent on the material. The **μ-value** is used to **compare** the **diffusion resistance** of a **material** with that of an **air** layer of the same thickness (Fedorik et al., 2021).

For **ideal** gases, a **direct relationship** can be found between the **mass fraction**, which indicates the amount of mass of a specific component relative to the total gas mixture, and its **share** of the **total pressure**. As a result, the **diffusion** of **water vapour** can be described as follows:

$$g_v = -\delta \times \frac{dp}{dx}$$

Where:
g_v = Water vapour flux density [kg/m^2s]
p = Water vapour partial pressure [Pa]
$\delta = \frac{2.0 \times 10^{-7}\ T^{0.81}}{P_L}$ = Water vapour diffusion coefficient in air [kg/(msPa)],

Where:
T = Ambient temperature [K]
P_L = Ambient air pressure [Pa]

In **porous** building materials, the **diffusion** of **water vapour** in the **large** pores can be **compared** to that in **air**. However, in the **small** pores, the situation is **different**. Here, **molecules collide more frequently** with the **walls**. In building physics, it is **sufficient** to just use a **diffusion resistance factor**, μ:

$$g_v = (\frac{-\delta}{\mu}) \times \frac{dp}{dx}$$

Where:
g_v = Water vapour flux density [kg/m^2s]
p = Water vapour partial pressure [Pa]
δ = Water vapour diffusion coefficient in air [kg/(msPa)]
μ = Water vapour diffusion resistance factor [-]
(Künzel, 1995)

Variations in the **μ-factor** due to different **relative humidities** indicate how the **vapour diffusion** in a building material is **affected**. The **diffusion flow** of a material can be calculated as follows assuming a **constant temperature** and **μ-value**:

$$g_{v,mat} = \left(\frac{-\delta}{\mu \times s}\right) \times \Delta p$$

The **diffusion flow** through a **stagnant air layer**, μ =1, with a thickness of sd is as follows:

$$g_{v,air} = \left(\frac{-\delta}{1 \times sd}\right) \times \Delta p$$

Where:
$g_{v,mat}$ = Diffusion flux through the material layer [kg/m²s]
p = Difference in water vapour partial pressure [Pa]
δ = Water vapour diffusion coefficient in air [kg/(msPa)]
μ = Water vapour diffusion resistance factor [-]
s = Thickness of the material layer [m]
sd = Thickness of the air layer [m]

By dividing the above formulas with each other, the following arises:

$$\frac{g_{v,mat}}{g_{v,air}} = \frac{sd}{\mu \times s}$$

This then results in **sd = μ × s**, where the **air layer** is chosen such that the **vapor diffusion resistance** is **equal** to that of the **material layer** with a **thickness** of '**s**' (WUFI, n.d.-c).

The **permeance**, Δ [kg/m²sPa], can be introduced through the formula and **depends** on the **thickness** and **properties** of the **material**:

$$\Delta = \frac{\delta}{sd}$$

In WUFI, a graph is plotted between the **Water Vapour Diffusion Resistance factor** [-] and the **Relative Humidity** [-]:

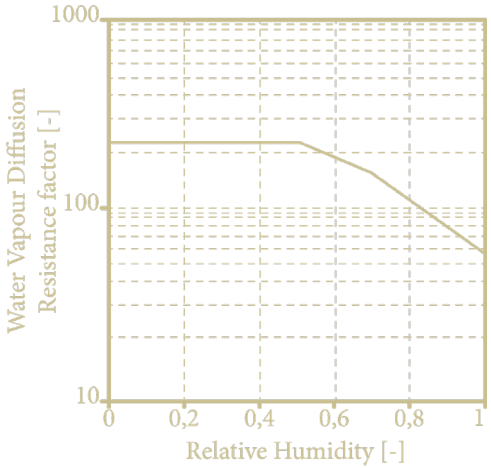

Figure 22, Graph Water vapour resistance factor & Relative humidity, derived from WUFI Database

Thermal Conductivity (moisture- & temperature-dependent)

For a complete understanding of the **thermal conductivity properties**, λ, it is first essential to know the **thermal conductivity** of a **dry material**, λ_0. At the same time, it is important that **humidity influences** the **thermal conductivity**, and this can be calculated using the following formula:

$$\lambda(w) = \lambda_0(1 + \frac{bw}{\rho_s})$$

Where:
λ(w) = Thermal conductivity of moist material [W/mK]
λ_0 = Thermal conductivity of dry material [W/mK]
ρ_s = Bulk density of dry material [kg/m³]
b = Moisture-induced thermal conductivity supplement [%/m-%]
w = Moisture content [kg/m³]

Within WUFI, the graph is constructed by a **relationship** between the **thermal conductivity** of **moist material**, λ(w), and the **water content**, w.

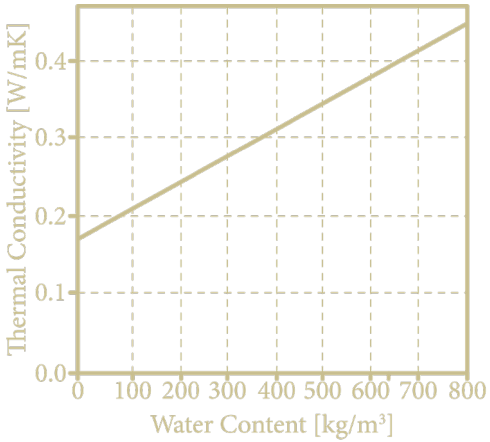

Figure 23, Graph thermal conductivity of moist material & Water content, derived from WUFI Database

When **thermal conductivity** of **moist materials** is mentioned, it refers to how **stationary water** in the material affects **heat transport**. **Water vapour diffusion** is also included in standard **measurement techniques**. Especially for **permeable materials**, an **interpretation** from these **measurement techniques** is taken. In addition, there may be no detailed data on the **moisture dependence** so estimation values can be used to take some **account** of the **moisture content**. It is important that the **thermal conductivity** values with a **moisture content** of **0** correspond to the **thermal conductivity** of **dry material** (WUFI, n.d.-a).

Enthalpy (temperature-dependent)

Enthalpy is referred to as the **heat content** of a material at **constant pressure**, where there is almost a **linear relationship** between the **enthalpy** of a **material** and the **temperature**. Therefore, the **enthalpy** of a **dry** building material is written as follows:

$$H_s = \rho_s \times C_s \times \vartheta$$

Where:
H_s = Enthalpy of the dry building material [J/m³]
ρ_s = Bulk density of dry material [kg/m³]
c_s = Specific heat capacity of the building material [J/kgK]
ϑ = temperature [°C]

For **moist** building materials, the **enthalpy** of the **water present** in the **material** must also be considered. However, this **enthalpy** of water depends on **physical states** in the **micropores** that are difficult to define. To determine the **enthalpy** of water in building materials, the following formula can be used:

$$H_w = \left[(w - w_e) \times C_w + w_e \times C_e - h_e \times \frac{dw_e}{d\vartheta}\right] \times \vartheta$$

Where:
H_w = Enthalpy of moisture in the building material [J/m³]
c_w = Specific heat capacity of liquid water [J/kgK]
c_e = Specific heat capacity of ice [J/kgK]
h_e = Specific melting enthalpy [J/kg]
w = Total water content [kg/m³]
w_e = Content of frozen water [kg/m³]
ϑ = temperature [°C]
(Künzel, 1995).

5. Selected bio-based materials

This sub-question investigates **which bio-based building materials** are **available** on the **Dutch market** and which are the most **promising** for **bio-based façade details**, with a focus on analysing **thermal bridges** and **moisture transport**. Based on this, a selection is made of **products** and **suppliers** that are suitable for developing the reference details, taking into account the **required properties** to **analyse thermal bridges** and **moisture transport** in WUFI.

5.1 Most suitable bio-based materials

Before selecting the suppliers of the various bio-based products, it is necessary to think about which bio-based products have the most **potential** for **application** in **the Netherlands**. The Dutch government has listed these potential products in a clear visualization. Many of these materials are already being harvested or have the potential to be harvested in the Netherlands (College van Rijksadviseurs, 2023).

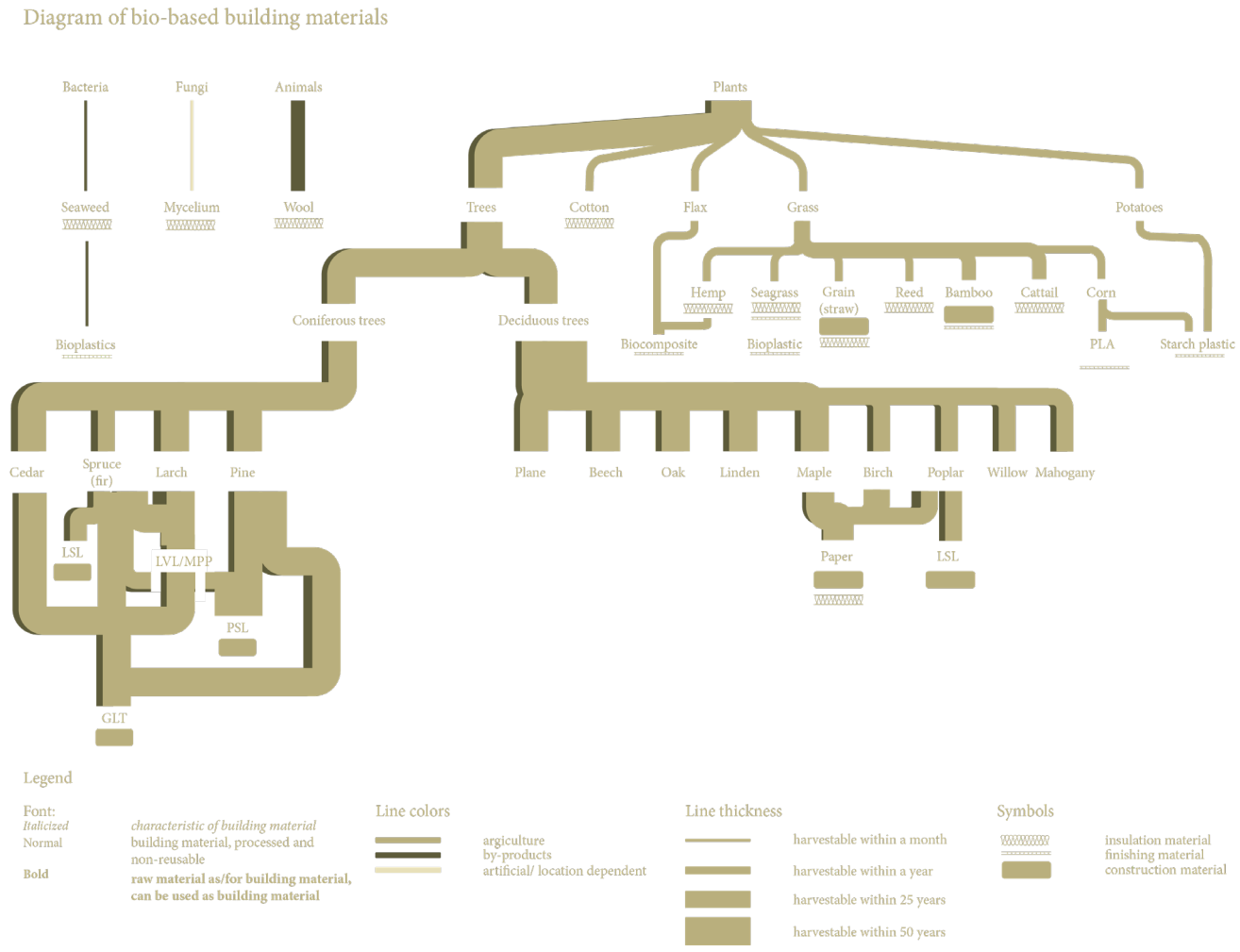

Figure 24, Potential bio-based materials for the Dutch construction market, derived from (College van Rijksadviseurs, 2023)

Among other things, these materials are **included** to make a **final selection** of **bio-based materials**. The final selection is based on the **WUFI 2D database**. To **analyse thermal bridges** and **moisture transport** in façade details, specific **values** are **needed**. These are explained in the previous sub-question. Since many of these specific values are not yet known, the bio-based products in the WUFI database will also be used.

To conclude, research will be conducted into the following **bio-based main components**, which can be used for the **production** of various **bio-based products**. These are based on both the most **promising** bio-based materials according to the Dutch government and the WUFI database:

- ***Cork;***
- ***Flax;***
- ***Hemp;***
- ***Straw;***
- ***Wood.***

These selected materials have been **included** in a **market research study**, where the **suppliers** of different **bio-based products** are collected. For each product, the **supplier**, the **origin** of the **ingredients**, and the **key technical properties** of the bio-based products are mentioned. While doing the research study it was important that the suppliers of the various materials were **located** in **the Netherlands as much as possible**. If this is not possible, it should be **located** as **close** to **the Netherlands as possible**. Another **criterion** is that **only** bio-based materials can be used. As determined in the first sub-question, a bio-based material must consist of at least **70% renewable mass**. Furthermore, to **minimise transportation**, the materials should be **sourced** as **locally** as possible to the factory.

This market research shows that **Dutch suppliers** alone are currently **not sufficient** to meet the **demand** for various bio-based building materials for the various layers of a façade wall construction. For this reason, **suppliers** from **Western European manufacturers** have also been **included**. However, this selection included as many Dutch suppliers as possible.

Additionally, this research examined the **origin** of the **components** of each **bio-based product**. The results show that, although some **ingredients** can be harvested in **the Netherlands**, various **Dutch companies** still choose to source materials from **other countries**. This is because the **climate** of some regions results in **better properties** for these **materials**. The market research has been compiled in an **Excel file**, where for each layer of the façade wall construction, the different suppliers with **corresponding** information are listed.

Firstly, the materials applied in the detail configurations are **briefly** introduced in this chapter. **Chapter 3** presents the developed detail configurations, in which the selected materials are illustrated within the corresponding construction details.

5.2 Explanation materials

Cork

The outer bark of the cork oak, Quercus suber, is used to harvest cork and is becoming popular for a variety of applications in construction (Woolley, 2013). The tree contains phellogen, a continuous and regular tissue layer that surrounds the tree. After removal, a new phellogen layer with the same properties forms, allowing the tree to be repeatedly exploited for cork without damage (Knapic et al., 2016). Thanks to the regrowth of the bark after removal, the tree can absorb 3 to 5 times more CO_2 than other trees (Hanenburg, 2022).

Cork distinguishes itself by a unique combination of good properties including **low density**, **low permeability** for **liquids** and **gases**, and **low thermal conductivity** (Knapic et al., 2016). Additionally, cork is **resistant** to **moisture** and has excellent **fire-resistant qualities** (Van Dam & Van den Oever, 2019). The increase in the use of cork for wall cladding and insulation material has led to innovative design approaches and product development. The various cork-based materials used in construction can be grouped as follows:

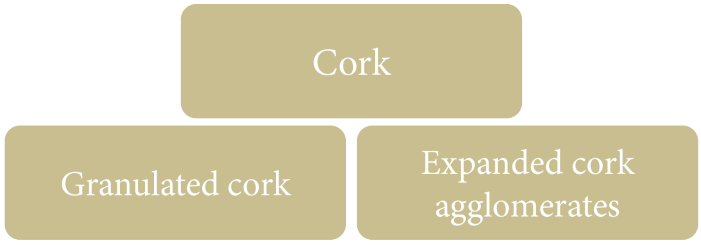

Granulated cork

Cork granules are produced by adjusting the particle size and cleaning the grains using shredders. The granules are then dried with a forced air flow to achieve the desired moisture content (Gil, 2014).

The granules can be used as a final product for **thermal insulation**, for **filling empty spaces** between double walls by blowing it in the construction (Knapic et al., 2016).

Figure 25, Granulated cork (Densities Of Cork Granules, 2022)

Expanded cork agglomerates

Expanded cork panels are created by thermal treatment of ground cork bark in which a natural chemical compound causes the granules to bond together. As no adhesives are used, this is a 100% natural product (Knapic et al., 2016).

The material has excellent **thermal properties** for both **interior** and **exterior walls** and be used as an **insulation** can material. A **more porous** plate, with a **lower thermal conductivity** can serve as an **insulation plate**. The **finishing** plate is **less porous**, with a **higher thermal conductivity**, but can be used as **finishing layer**. (Van Dam & Van den Oever, 2019).

Figure 26, Expanded cork agglomerates (Stichting Nationale Milieudatabase, 2024)

Flax

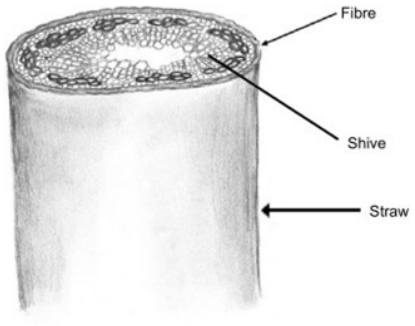

Flax, a plant species, grows quickly and can be harvested within three to four months. The entire plant can be used, as shown in the image below, with flax seeds being used for food production and to make paints and linoleum. Additionally, the flax shives can be used for chipboard where the flax fibres are made into various insulation materials (MNEXT, n.d.-b).
The complex and porous microstructure of flax ensures that building products made from flax have excellent **thermal properties** and serve as **good moisture regulators** (Benmahiddine et al., 2020). The various products which can be manufactured from flax are elaborated below.

Figure 27, Different parts of the flax plant (Nunes, 2017)

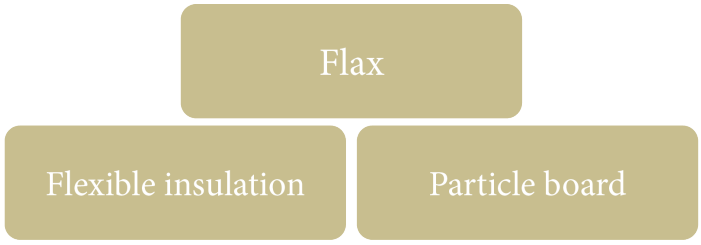

Insulation

Flax fibres can be used as **flax wool insulation** products or the manufacture of flax wool, short fibers are used, which are connected by friction, cohesion, or adhesion (Yadav & Agarwal, 2021). Then, the fibers are mixed with a binder, flame retardant, and mold inhibitor (Grow2Build, n.d.).

Thermal conductivity and **heat capacity properties** of the flax insulation products are **influenced** by **fibre density**, **temperature** and **moisture content** (Hamrouni et al., 2024).

Figure 28, Flax insulation (Isovlas, 2023)

Particle board

Additionally, the **long flax fibers** can be used in **particle boards**. These fibers are obtained by breaking down the flax, where the fibers are separated from the wooden core. The shives from flax plant residues from the linen industry can also be used (Aghamohammadi & Shahmohammadi, 2023).

These shives are then melted with an artificial resin or a natural binder and pressed into molds to form boards which have **good thermal**, **fire-resistant**, and **hygrothermal properties** (Yadav & Agarwal, 2021).

Figure 29, Flax particle board (Database, n.d.)

Hemp

The hemp plant offers a diversity of materials such as fibres, shives and seeds with each component being useful different building materials. The stem consists of long, sturdy fibres used for insulation materials and biocomposites, the shives are used in hempcrete. Next to that, the seeds are mainly used for oils and nutritional supplements. Hemp is an ideal building material due to its **high insulating** and **mechanical properties**, **low density**, and **high water absorption capacity** (Nunes, 2017). Another big advantage of the plant is that it can be harvested in just 60 days (Barbhuiya & Bhusan Das, 2022). The hemp plant can be processed in various ways to create different construction materials:

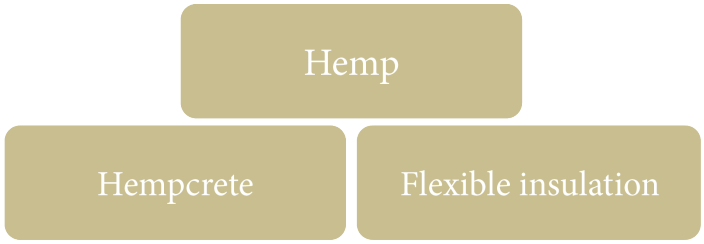

Hempcrete

Hempcrete is a **lightweight**, **insulating biocomposite** made by mixing hemp shives with lime binder and water. It can be cast in **formwork**, made into **blocks**, or used as **insulating plaster** (Woolley, 2013). Hemp blocks are joined together with gypsum or lime and finished with gypsum and lime (Nunes, 2017).

Due to its limited mechanical properties, it is only allowed for **non-structural purposes** (Barbhuiya & Bhusan Das, 2022). Although the lime in the material increases **thermal conductivity**, it does contribute to **good moisture regulation** (Walker & Pavía, 2014).

Figure 30, Hempcrete (NBS_Admin, 2023)

Insulation

Hemp fiber-based insulation is as an environmentally friendly alternative to mineral wool (Nunes, 2017). It is produced by mixing short fibers with flax and/or wood fibers. This fiber combination can be made with natural additives (Woolley, 2013). A combination of carding, cross-laying, and needling allows the fibres to be processed into non-woven insulation mats (Grow2Build, n.d.). During this process, boron or phosphate can be added under thermal pressure to treat the fibres in order to improve the fire resistance. The flexible mats can easily be applied in walls as **thermal-** and **acoustic insulation** (Woolley, 2013).

Figure 31, Hemp flexible insulation (Admin, 2023)

Straw

Straw is considered a by-product of various cereal crops. Only the grain and the husk are used for food production, leaving the dry stems behind (Woolley, 2013). These can be used as bedding for livestock, soil improver, or biomass energy (Sutton et al., 2011). However, a better application is to use this straw as a building material, which not only stores carbon but also reduces reliance on energy-intensive materials (Koh & Kraniotis, 2020). Straw is suitable for construction without the need for additives and is free from toxic substances (Klijn et al., 2017).

Straw is a heterogeneous and porous material, with its chemical composition depending on the **location** and **type** of **straw**. These two together determine the **stability**, **moisture content**, and **thermal** and **mechanical properties** of the **material** (Koh & Kraniotis, 2020). It is possible to build **vapour-open structures** with straw, but it must be well **protected** against **moisture absorption** (Sandak et al., 2019). Finally straw can be used in various ways, as shown in the visualization below:

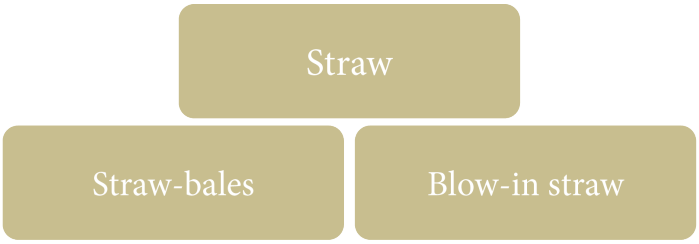

Straw-bales

Straw can be processed into **straw bales** by binding it tightly with wire or a rope. In the Netherlands straw bales are primarily used as an **infill method** in **Timber Frame Construction wall elements**, where the bales can be finished with breathable lime plaster or wooden cladding. This method is well-suited for **prefabrication** (MNEXT, n.d.-a).

The blocks weigh approximately 20 kg and are generally laid dry where the internal anchoring of the straw fibres and the vertical compression between the bales provides stability (Nunes, 2017).

Figure 32, Straw bale (Coastal Farm - New, n.d.)

Blow-in straw

Straw can also be used as **prefabricated elements** as **blow-in straw**, where finely chopped fibres are compacted with air pressure into a wooden frame. A plaster layer improves structural integrity, limits movement, and protects against decay and fire (Sutton et al., 2011).

With respect to blow-in straw, the **compactness** of the **material** and the **type** of **straw** determine the **technical properties**. The **thermal conductivity** of the straw **varies** with **density**, **moisture content**, and **fibre orientation**, differing by supplier (Koh & Kraniotis, 2020).

Figure 33, Blow-in straw (EcoCocon Prefab Stropanelen - Kennisbank Biobased Bouwen, 2023)

Wood

Wood is the most well-known renewable material but many buildings contain unnecessary amounts of wood, such as thicker frames for better insulation and decorative wood. Careful design and the use of composite wood products make wood usage more economical and efficient. Composite wood products can be made from wood chips, sawdust, wood waste, and recycled wood. These are often combined with natural binders, water, or adhesives and are created through heat or pressure (Woolley, 2013).

Like most bio-based materials, wood is **hygroscopic**, meaning it can **absorb** and **desorb water** from the environment to reach a **moisture equilibrium** at stable **relative humidity** (Popescu, 2017). As long as the **moisture content** remains **below 20%**, **fungal degradation** is **not** a **risk** for the wood (Ramage et al., 2017). Wood products for construction are primarily manufactured by sawing, peeling, or shredding. Sawing and peeling require uniform logs with larger diameters, while shredding is suitable for homogeneous logs with smaller diameters (Pramreiter et al., 2023). During the processing of wood, approximately 50% is converted into board and plank products. The remaining material, such as shavings and fibers, is typically used for biomass fuel or processed into engineered wood panels (Ramage et al., 2017). For these products, a distinction is made between the various wood processing methods:

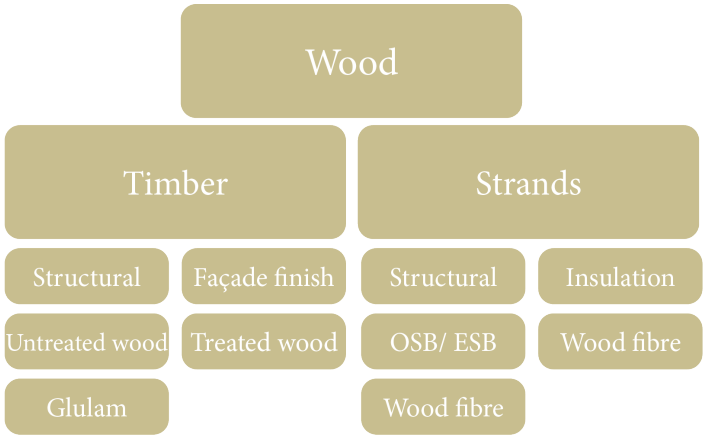

Structural

Figure 34, Untreated wood (Spruce Lumber - Hanford Lumber, 2025)

Untreated wood

Untreated wood, usually spruce wood, is commonly used as a **structural component** in a **timber construction frame**. Which is the applied type of **construction**.

In this type of construction, the untreated wooden beams are typically placed vertically at regular distances between two horizontal beams. Since the **wood** is used **untreated**, **correct detailing** is **essential**, along with **proper protection** against **moisture ingress** (Popescu, 2017).

Figure 35,Ttreated wood (Spruce Lumber - Hanford Lumber, 2025)

Treated wood

Properties of wood, such as **dimensional stability**, **resistance** to **biological decay**, **thermal stability**, **fire resistance**, **UV resistance**, and **mechanical performance** can be **enhanced** through various **treatments**.

Techniques such as **thermal** and **chemical modification**, **impregnation**, and **coating** are possible treatments.

These **improve** the wood **properties** in varous ways depending on the purpose of the wood (Popescu, 2017).

Figure 36, Glulam (Glued Laminated Timber - dataholz.eu, 2024)

Glulam

Glulam can be defined as a **structural wooden element** composed of at least two parallel laminates consisting of one or two planks (Ramage et al., 2017).

The wood layers are **continuously** glued together and cured in a mold. By using strength-graded wood using finger joints, consistent strength is ensured (Lyons, 2006). **Glulam** can be used as **columns** in wall constructions for **larger** spans in the construction (Koppenhol, Hertzberger, et al., 2024).

Façade finish

Figure 37, Timber cladding (Timber Cladding | Wood Cladding, n.d.)

Cladding

Wooden cladding is made from sawn wood, with **properties varying** due to the **natural structure**, **mechanical** and **biophysical characteristics**, and **fiber orientation** of the material. Important properties that make the planks **suitable** for **outdoor applications** are **high hardness** at **low weight**, **high thermal resistance**, and **good hygroscopic properties**. Additionally, the planks can be used **without** the need for **extra protection** (Ivanovic-Sekularac et al., 2016). However, panels that are **thermally** or **chemically** modified or **coated** will show **fewer** problems (Brookes et al., 2008).

Thermal modification improves stability and **resistance** to **decay** but **reduces hygroscopicity**. **Chemical modification changes** the wood's **molecular structure** by reacting with hydroxyl groups. **Impregnation enhances water** and **fungal resistance** without altering the wood's chemistry. **Coatings** act as **physical barriers**, **protecting** wood from **weathering** and making it **suitable** for **outdoor use** (Popescu, 2017).

Strands

Figure 38, Eco Strand Board (NextChapter Software B.V., n.d.)

OSB (Oriented Strand Board) & ESB (Eco Strand Board)

OSB is a layered wood composite made from long wood strands bonded with polymer adhesives OSB has good **strength properties** and is comparable to plywood, but it has higher **shear strength** and is more **hygroscopic**. It can withstand fastenings well, offers reasonable resistance to **biological degradation**, and can be treated with **fire retardants**. OSB is widely used as a **structural wood panel** and as a **web** in **I-beams** (Popescu, 2017). Its alternative, **ESB**, contains a **higher percentage** of **bio-based materials** and is bonded with formaldehyde-free resin. With excellent **vapour diffusion properties**, ESB is well-suited for **vapour-open constructions** and is suitable for **relatively humid** environments.

Wood fibre

Board

For all wood fiber products, wood is reduced to fibres that are then bonded together using water or resin with heat and pressure. Wood fibers can be produced using two methods: the **wet** process, used for **softboard** and **hardboard**, and the **dry** process, used for **MDF** and **HDF** (Popescu, 2017). In the wet process, a mix of water and additives is pressed and heated, with the lignin in the wood acting as a natural binder. In the dry process, a synthetic binder is used instead. In both processes, chemical fire retardants can be added (O'Brien et al., 2025).

Figure 39, Medium Density Fibre board (BouwOnline.com, n.d.)

MDF (Medium Density Fibreboard)

In the production of **MDF**, wood is first shredded into small chips and then washed. Then the fibres are treated with steam and mixed with resins and additives. After drying, the fibres are hot-pressed into a mat that has a consistent density throughout the panel. The formed board is then sanded to get a smooth surface.

The end product is suitable for **wall panels** that need **mechanical resistance** (Popescu, 2017).

Figure 40, Wood fibre insulation (STEICO Insulation Materials, n.d.)

Insulation

Wood fibre insulation can be manufactured using both dry and wet production processes (O'Brien et al., 2025). It contains more than 80% wood fibres and is made from waste wood, such as chips and board from sawmills, with adhesives or additives added if necessary. **Flexible wood fibre insulation** is mainly used as **thermal**- and **acoustic insulation** in construction and is available in rolls, mats, and boards (dataholz, 2022a).

There is also a variant in which the wood fibre can be plastered. In this case, the applied flexible wood fibre must be **water-repellent** and **breathable**.

Conclusion

Based on the conducted literature review, a selection of **five** biobased materials has been established, which will be **integrated** into the **detail configurations**. These materials offer a **range** of **application possibilities**, resulting in varied uses within architectural detailing. Since not all biobased products are suitable for integration into the detail configurations, only the described materials are applied. Materials outside this selection are not considered further and fall beyond the scope of this study.

Later in the report, the **detail configurations** are shown with the materials that are used within each configuration. In addition to this, the **next chapter explaines** the important **design principles** of these materials and are also shown next to each detail configuration.

Within various façade wall construction assemblies, these materials are **combined** and **analysed** through simulations using **WUFI**. The aim of these simulations is to **evaluate** the **performance** of the **materials**, both **individually** and in **combination** with other biobased materials. The focus is on **moisture transport**, the **risk** of **mould growth**, and the **mitigation** of **thermal bridging**.

Figure 41, Conclusion selection of bio-based materials for the detail configurations, own illustration

6. Design principles of the bio-based materials

Based on the selection of bio-based materials, it is essential to investigate how these materials can be **effectively** applied. This requires a research on the specific **application methods** and **design principles** associated with each material. Given that biobased materials are primarily derived from organic sources, specific requirements are necessary on architectural detailing. It is therefore essential that construction details are designed to **prevent moisture accumulation** and to **ensure** that **hygrothermal conditions** remain within **safe** and **acceptable thresholds** (Fedorik et al., 2021).

To achieve this, the material composition must **align** with the **principles** of **vapour diffusion**. Hereby materials with **higher vapour permeability** are positioned towards the **exterior** of the construction, in contrast to **less permeable** materials on the **interior** side (De Visser et al., 2015). Next, various design principles must be applied to effectively integrate the materials in the details.

6.1 Wood

Timber frame construction

Although timber can serve a variety of structural purposes, this thesis limits its scope to the application of timber frame construction. The primary motivation for selecting this system lies in the ability to place insulation between the vertical studs, thereby reducing the overall wall thickness and weigth compared to solid timber constructions. This structural system is used for the varous detail configurations.

Timber frame constructions consist of a **framework** of **vertical studs** and **horizontal plates**, which together form the **structural framework**. This framework is capable of resisting both **vertical** and **lateral loads** while providing **space** for the **integration** of **insulation materials**. Figure 42 illustrates this construction system including the standard **centre-to-centre** distance of **600 mm** and the use of **timber boarding** to provide additional **rigidity**. Figure 43 illustrates the different elements of a timber frame construction.

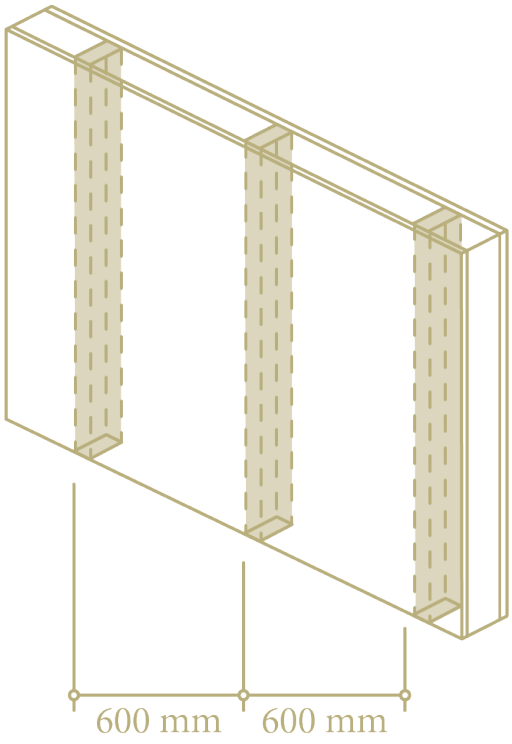

Figure 42, Timber frame construction axonometric, own illustration

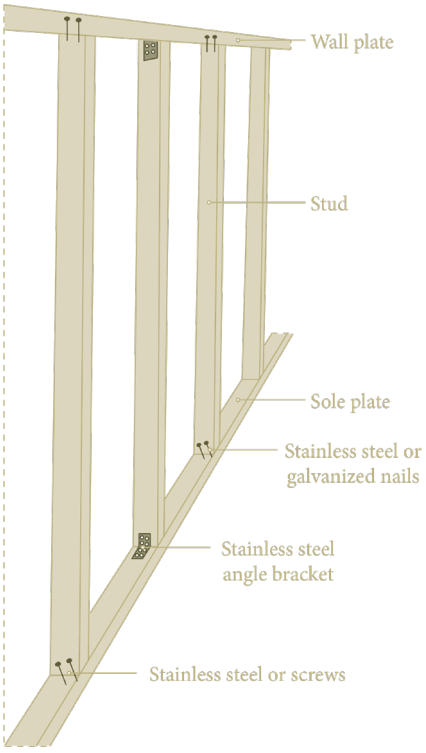

Figure 43, Elements of a timber frame construction, derived from (Stanwix & Sparrow, 2014)

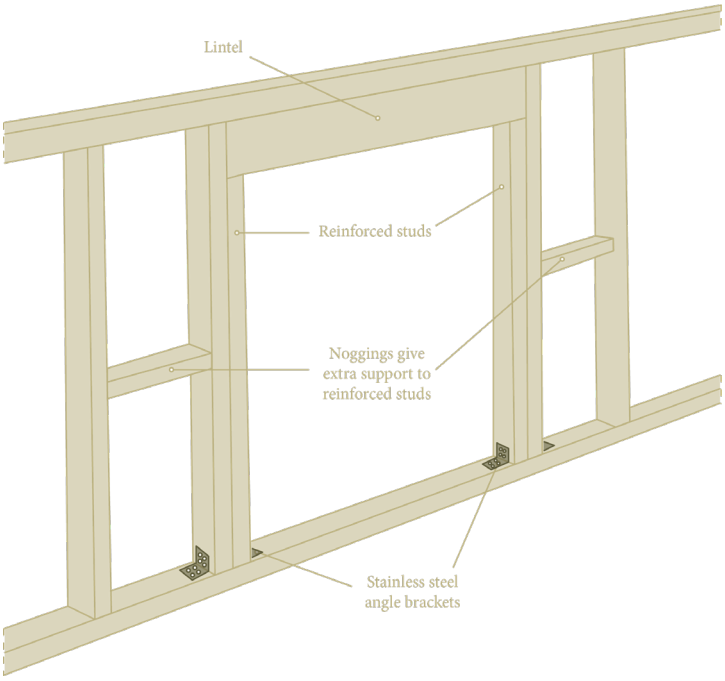

To accommodate **door** and **window openings**, **additional studs** may be incorporated to support a lintel. When structurally required, this approach is illustrated schematically in figure 44. In all cases, the **lintel** must be fully **supported** by the underlying **studs** to ensure a correct **load transfer** and **structural integrity** (Stanwix & Sparrow, 2014)

Figure 44, Timber frame construction with support of a lintel, derived from (Stanwix & Sparrow, 2014)

Outer corner connections

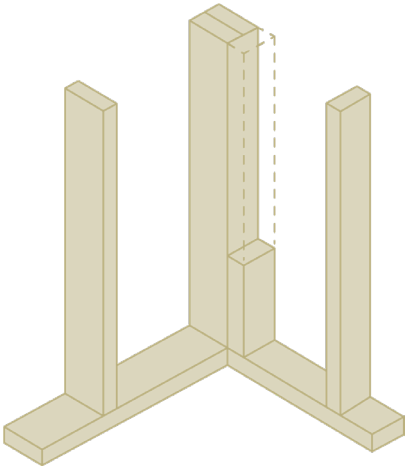

With regard to **corner joints**, it is recommended to add an **additional stud** at the **corner** to enhance structural stability, this is illustrated in figure 45.

The connection at the corner can be easily done bij a screw connection where the **penetration depth** must be to the **half** of the **width** of the wooden **frame**.

Figure 45, Timber frame construction corner, own illustration

Floor to foundation connections

To prevent **rising damp** and **rainwater accumulation**, the timber frame construction is **elevated**. This reduces the **risk** of **moisture damage** and facilitates **drying**. Figure 46 illustrates an incorrect application in option A. Options B and C show common solutions with a steel column embedded in concrete and a mechanically fastened steel support, respectively. Due to weight reduction considerations, option C has been selected for this project. To avoid **capillary moisture transfer**, the timber is **positioned** at least **150 - 300 mm above** the **roof surface**. It is also noted later in the report that this elevation is required for the other biobased materials.

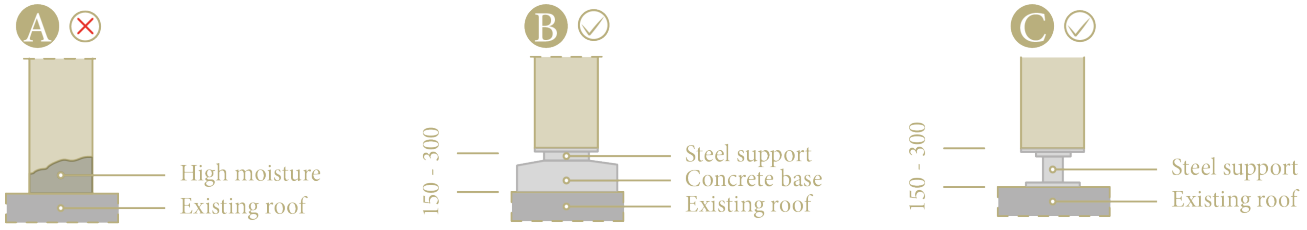

Figure 46, Protection column, derived from (Crocetti et al., 2024)

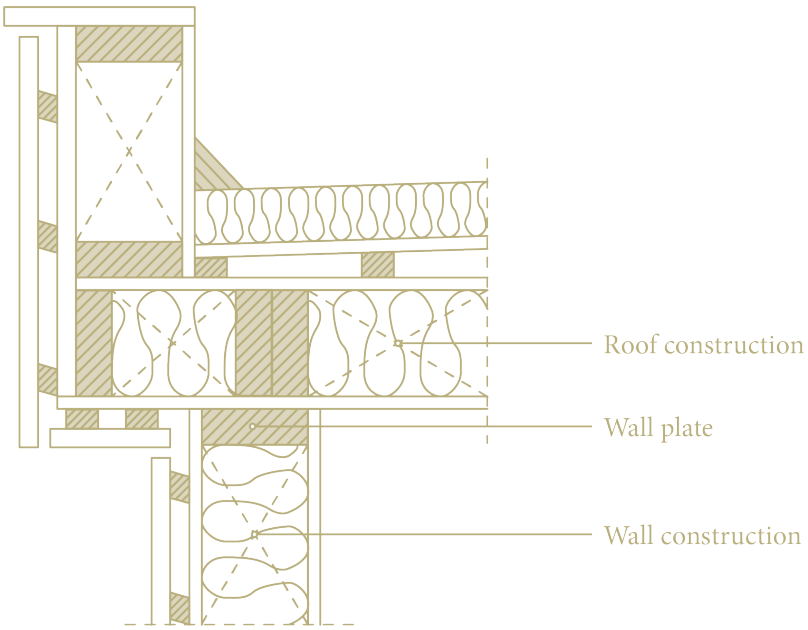

The top of the timber frame structure consists of a **top plate** that serves as a **support** for a **flat roof**.

The roof construction is screwed on this top plate where the **penetration depth** must be to the **half** of the **width** of the wooden **frame**.

The figure on the left, figure 47 shows schematically how a roof structure can be attached to the timber frame structure (Crocetti et al., 2024).

Figure 47, Timber frame construction, roof connection, derived from (Crocetti et al., 2024)

Insulation

There are various types of wood fibre insulation materials. First, **flexible wood fibre insulation** is discussed, which is **compressed** between the **studs** of the **timber frame construction** to ensure that all joints and gaps are fully sealed. The materials should be **protected** agains **moisture penetration**. To ensure optimal **performance**, a **compression factor** of **1%** is required in both **width** and **height**.

On the **interior** side of a timber frame, a **biobased construction board** can serve as a **finishing** layer. On the **exterior** side, **wood fibre boards** are often fixed directly to the studs. These contribute to **thermal insulation** and act as a **wind** and **moisture-regulating layer**. Depending on the application, there are plasterable and pressure-resistance variants available. If the joint between the boards exceeds 2 mm, it is necessary to fill these with a special joint sealer to prevent moisture ingress and air infiltration.

To ensure proper installation, the boards are placed with a **minimum overlap** of **300 mm** and a **maximum centre-to-centre distance** of **250 mm**. At least **three fasteners** per board are needed and is shown in figure 48. For pressure-resistance wood fibre boards, **screws** are commonly used, while special **insulation roses** are ideal for plasterable boards. The fasteners must have a **minimum length equal** to the **thickness** of the **board**, and a **minimum penetration** depth of **31 mm** (GUTEX Holzfaserplattenwerk, n.d.). Figure 49 shows both the fastening of the flexible wood fibre and the wood fibre plate.

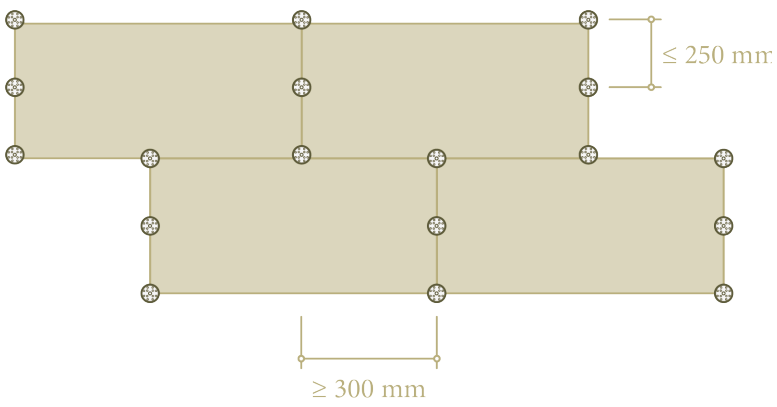

Figure 48, Wood fibre plates with staggered joints and fasteners, own illustration

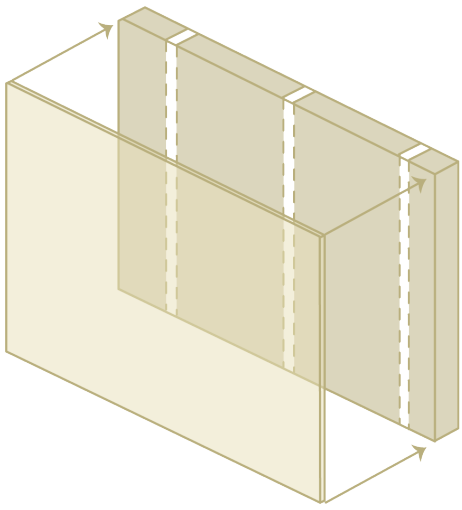

Figure 49, Attachment wood fibre plates, own illustration

A plasterable wood fibre variant must be used, for plaster finishes. The first layer is a **base coat**, **5** to **8 mm** thick, with a **reinforcement mesh** to prevent **cracking**, The mesh should ideally be placed **centrally** of this layer. Optionally, a **primer** can be applied to improve **adhesion**, **suction regulation** and **weather resistance**. The finishing layer, a **final render** of **1.5** to **3 mm**, protects against **weathering** and is finished with a **paint** system to make the wall construction more **durable**. (GUTEX Holzfaserplattenwerk, n.d.).

Cladding

Wood is commonly used as **cladding**, with a **thickness** of **18 mm** being the most common. The wooden boards can vary in **width**, although boards **wider** than **150 mm** are generally **discouraged** due to the increased risk of **swelling** and **shrinkage** caused by **moisture fluctuations**.

There are **two types** of **systems** for wooden cladding, **open** and **closed systems**. In an **open** system, **narrow joints** are used between the wooden cladding boards to provide ventilation. In a **closed** system, on the other hand, the boards fit **tightly** together. Typically, a **tongue** and **groove** or a rebate joint is used to provide space for the movement of the wood (Brookes et al., 2008).

The image below shows both systems including various façade profiles. Here, A and B are open façade systems, while C, D, E, F, and G are closed systems.

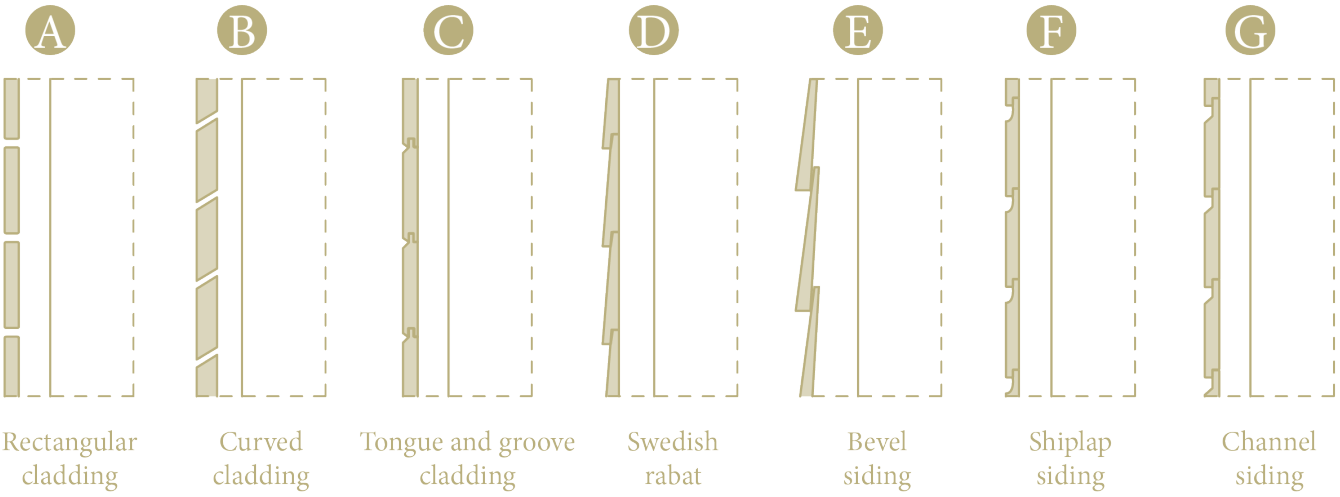

Figure 50, Types of open and closed timber cladding, derived from (Brookes et al., 2008)

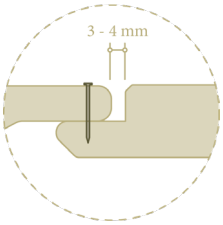

Due to **swelling** and **shrinkage**, a joint of **7** - **10 mm** should be used with an **open** façade system, see figure 51. According to the Dutch Building Decree, the **maximum joint** is **10 mm** because of insect pests. With a **closed** façade system, sufficient **expansion space** should be maintained between the sections, approximately **3** to **4 mm** (Brookes et al., 2008).

Figure 51, Expansion space for closed systems, own illustration

A **framework** of **battens** is used to attach the wooden cladding to the construction. Common dimensions for the battens are **28** x **44 mm** and are mounted onto a **underlayment** of a **load-bearing structure**.

To prevent **moisture accumulation** behind the wooden cladding, a **minimum ventilation gap** of **200 mm²** per **m²** of **façade surface** is required which can be achieved with an **air cavity** of **20** to **40 mm**. For horizontal cladding vertical battens are sufficient. For vertical cladding, additional horizontal battens should be used as well as vertical ones to ensure continuous ventilation flow. The **horizontal battens** should be preferbably **sloped** at an angle of **15** to **30°** for effective water drainage. Figure 52 shows that for both framework systems the maximum **centre-to-centre** distance is **600 mm** (Centrum Hout, 2024).

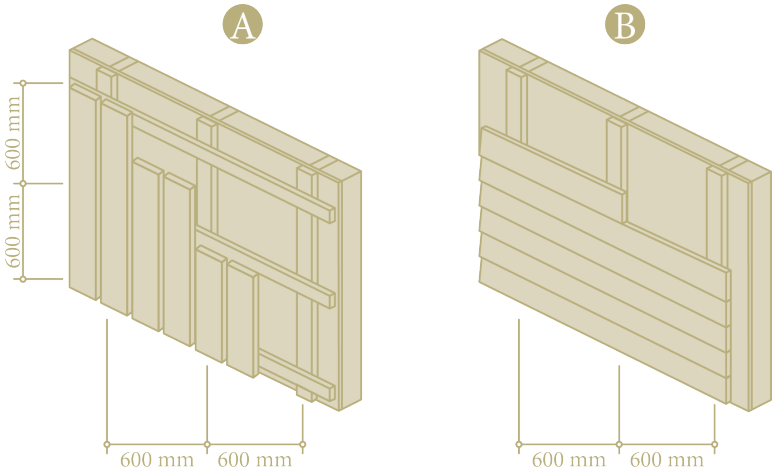

Figure 52, Vertical and horizontal wooden cladding with center-to-center of studs, own illustration

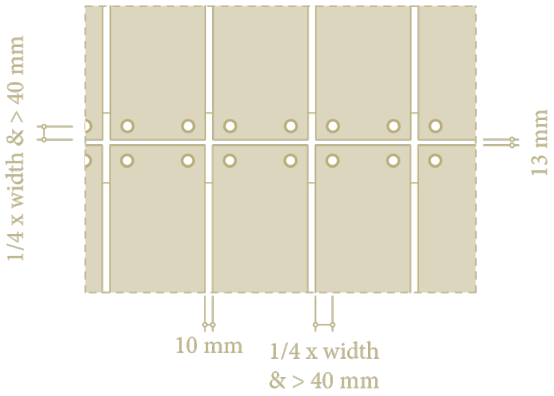

Timber cladding can be fixed using nails, screws, bolts or clips. For boards **wider** than **150 mm two** fixings per board are required.

Nails are generally **preferred** due to the **flexibility** in accommodating timber **expansion** and **contraction**. In open cladding systems, fixings must be positioned at one-quarter of the board width from the edge and at least 40 mm from the end, as illustrated in figure 53 (Brookes et al., 2008).

Figure 53, Spaces between planks and mechanical attachment of fasteners, derived from (Brookes et al., 2008)

In a **closed** cladding systems a **single** fastener per board is required. This should be **positioned** within the **overlapping edge** of the board to provide **space** for the **natural expansion** and **contraction** of the overlapping board. When **nails** are used, the length should be **2.5 times** the **thickness** of the **cladding**. This **length** is **2 times** the cladding **thickness** for **screws**. The figure below illustrates the required **nail** and **screw penetration depth** and how to correctly apply the fasteners (Brookes et al., 2008).

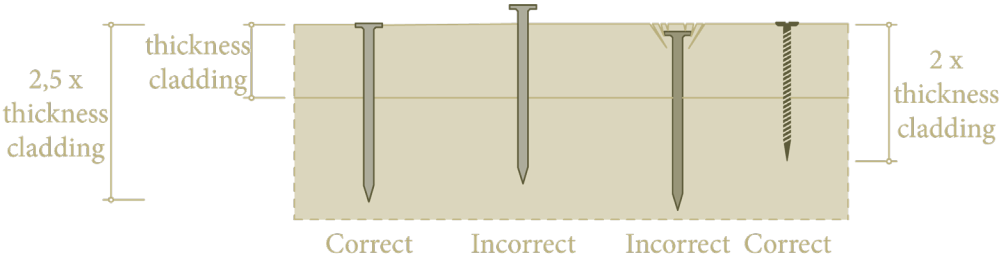

Figure 54, Correct mechanical attachment of nails & screws with penetration depth, derived from (Brookes et al., 2008)

Wall to roof connections

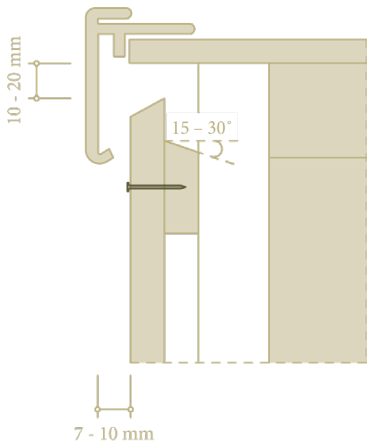

As told before, a proper ventilation is necessary if a wooden finish is applied. In order to provide this, a **minimum space** of **10 mm** is necessary between the **cladding** and the **roof trim**. This is shown in the figure below, figure 55.

Figure 55, Space between cladding and roof trim, derived from (Brookes et al., 2008)

Corner connections

At **corner connections** a **joint width** of 7 to **10 mm** must also be maintained between timber cladding elements for the same purpose. The illustration below show this for both **external** and **internal** corners.

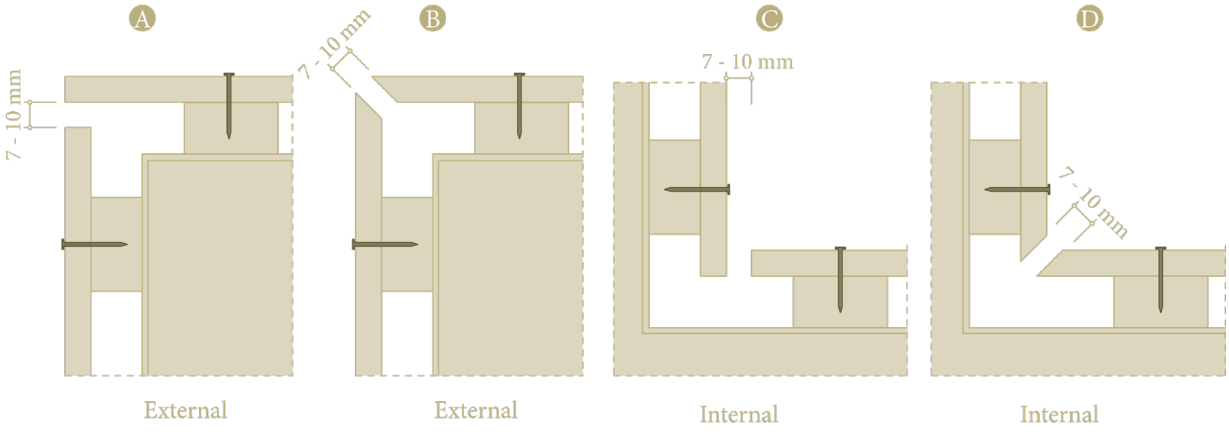

Figure 56, External and internal corner connections, derived from (Brookes et al., 2008)

Wall to window frame connections

Additionally, at **door** and **window frame connections** a **joint width** of 7 to **10 mm** should also be maintained as can be seen in figure 57. To protect **against rainwater**, it is important to provide a **sloped drip sill** above the frame. Furthermore, the frames must be finished with **waterproof membranes** to ensure **long-term protection** against **moisture infiltration**.

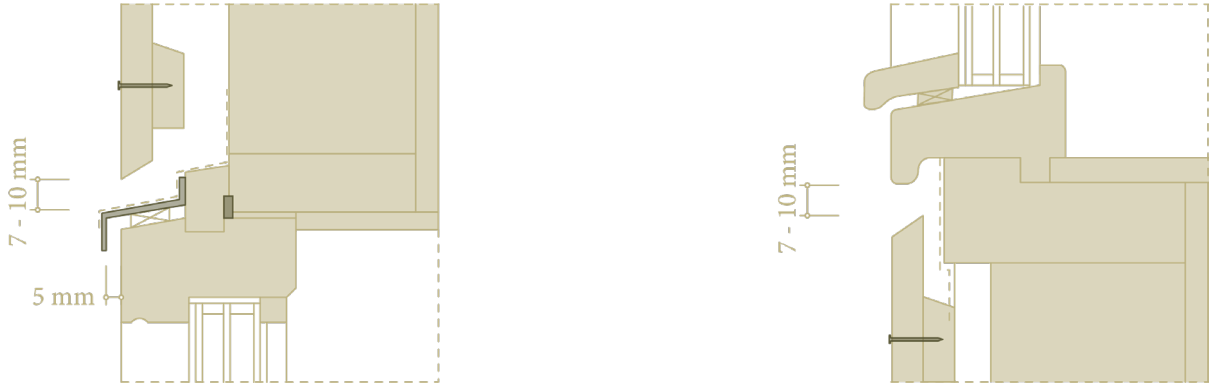

Figure 57, Spaces between cladding and window, derived from (Brookes et al., 2008)

6.2 Hemp

There are various ways to incorporate hempcrete into façade wall constructions, which will shown below.

Cast-in-situ

Cast-in-situ hempcrete is mechanically mixed on-site and poured into formwork. Hempcrete must always be placed around a structural frame. It can be **compressed** to achieve the **desired density**, **strength**, and **insulating properties** (Stanwix & Sparrow, 2014). Hempcrete can support its own weight after approximately 30 minutes. However, it is recommended to leave the formwork for 12-14 hours so the hempcrete can harden due to the carbonisation of the lime. When used as plaster, the wall must be sufficiently dry which takes much time making hempcrete blocks more suitable (Woolley, 2013).

If cast-in-situ hempcrete is desired, a temporary formwork is necessary where a step-by-step plan is explained below.

- Use 2400 mm x 600 mm formwork sheets;
- Fix the first slab with long screws and spacers on both sides of the stud around the building;
- When the formwork do not align, fix the corners as figure 58 where two methods are presented;
- Fill the formwork with hempcrete to the height 100 to 150 mm and compress it;
- Repeat the previous step until the height of the formwork slab is reached;
- After 30 minutes, the temporary formwork can be removed;
- Repeat previous step until the desired height is reached.

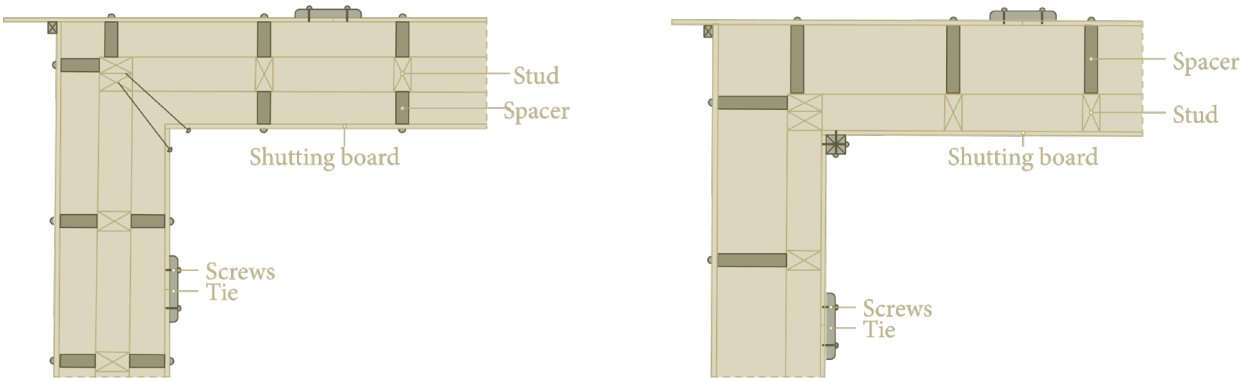

Figure 58, Parts of the cast-in-situ of a hempcrete wall, derived from (Stanwix & Sparrow, 2014)

Hempcrete blocks

Placement blocks

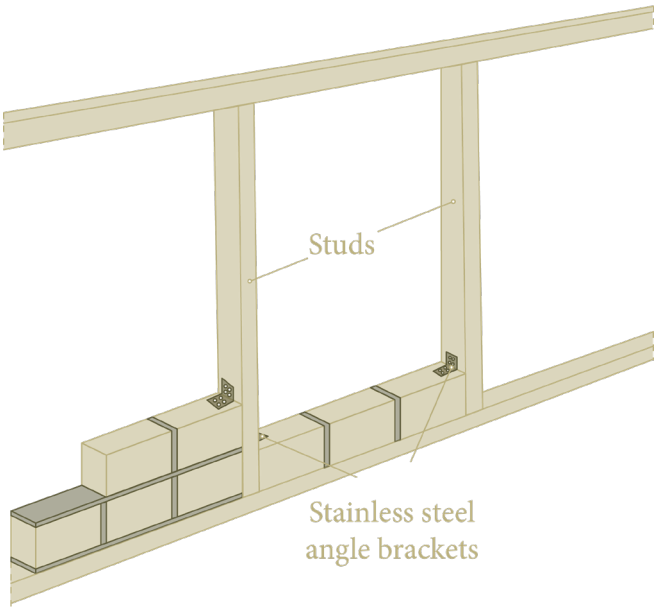

Hempcrete blocks offer advantages such as a controlled drying process that ensures **consistency** and **reliability**. Due to precise mixtures and production processes in prefabrication, the **quality** is also **higher**. The main benefit of prefab hempcrete is that it no longer requires drying, allowing for **immediate application** of façade finishes. This positively impacts construction time (Stanwix & Sparrow, 2014).

The **blocks** are placed between a **wooden structural frame** using connecting angles, as shown in the figure below, figure 58. When a wooden façade cladding is applied, **five** connecting angles per **square meter** are required to provide surficcient support (IsoHemp. (n.d.).

Figure 59, Connection hempcrete blocks and wooden frame, derived from IsoHemp. (n.d.).

The hempcrete blocks must be **protected** against **rising moisture** by a **20 mm damp proof course**. Next, a **10** to **20 mm mortar bed** is applied to ensure the blocks are perfectly **level**. The connection between a floor and a hempcrete block wall is shown in figure 60.

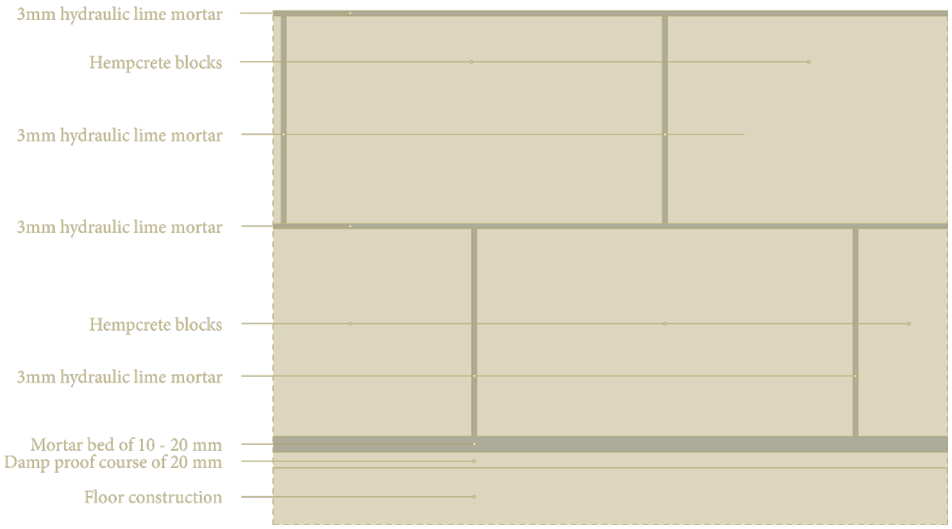

Figure 60, Connection blocks and floor, own illustration

Because of the placement of the last hempcrete blocks, a **minimum gap** of around **20 mm** should be maintained between the **wall** and the **top plane** of the timber frame construction. This cap can be filled with **flexible hemp insulation** after the placement of the hempcrete blocks, this is shown in figure 61.

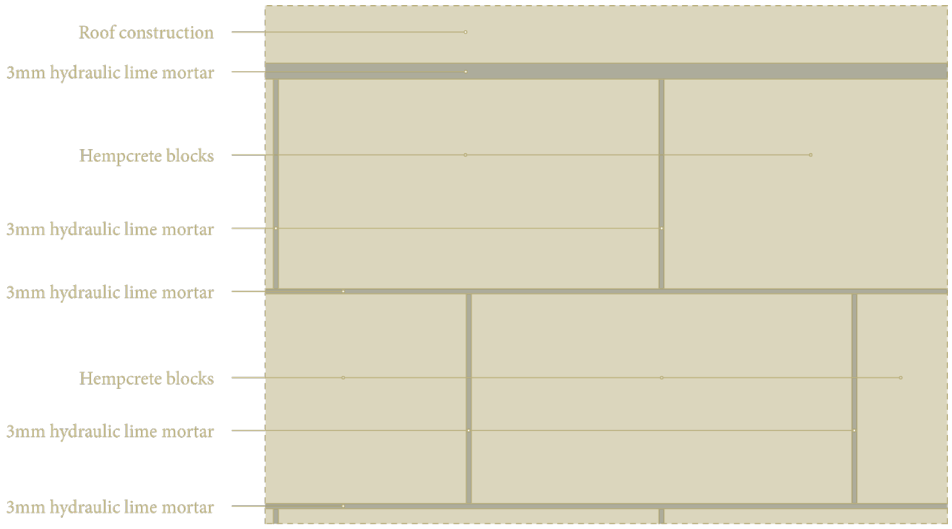

Figure 61, Connection blocks and roof, own illustration

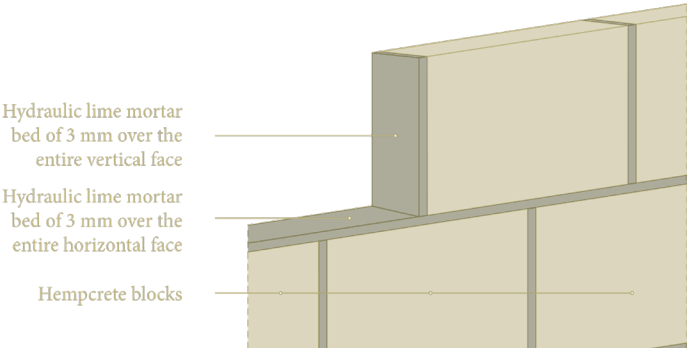

The blocks are **interlocked** by applying a **hydraulic lime** over the **entire surfaces** of the block to ensure a watertight joint.

To minimize thermal bridges, it is essential to **stagger** the **blocks** with a **minimum overlap** of **one third** of the **length** of the block. A **joint thickness** of **3 mm** should be maintained for both the **horizontal** and **vertical joints**, as shown in the figure on the left, figure 62 (IsoHemp. (n.d.).

Figure 62, Placement of hempcrete blocks, own illustration

To protect the **timber frame constuction** against **moisture**, the **frame** must be covered by at least **70 mm** of **hempcrete**. The wall construction must be **vapour-permeable**, with detailing focused on preventing **water ingress** and facilitating **moisture drainage**. **Roofs** should have a minimum **overhang** of **150 mm** for single-storey buildings, and **drip details** must be applied above **window openings**. Additionally, hempcrete should **never** be **directly exposed** to rain and must therefore always be **protected** with an appropriate **exterior finish**.

The hempcrete can be **protected** by a **vapour-permeable membrane** but this solution is less durable Figure 63A resolves this by using a 20 mm thick lime plaster instead. This **hydraulic lime plaster** must have **anti-fungal properties** and should be specifically developed for **outdoor** use to withstand **weather exposure** and **fluctuations** in **relative humidity**. It must also **resist microbial growth** under **high moisture conditions**. The plaster layer typically consists of a **10** to **12 mm base coat** and an **8** to **10 mm finish coat** (Piot et al., 2017). With regard to a wooden, the façade is fixed to the timber frame using long, alkaline-resistant screws where the **battens** should have a **center-to-center** of **600 mm** (Stanwix & Sparrow, 2014).

However, with both finished the **timber frame** is not sufficient protected. Therefore, it should be **recessed 50 mm** into the wall when using plaster, and 70 mm when using timber cladding.

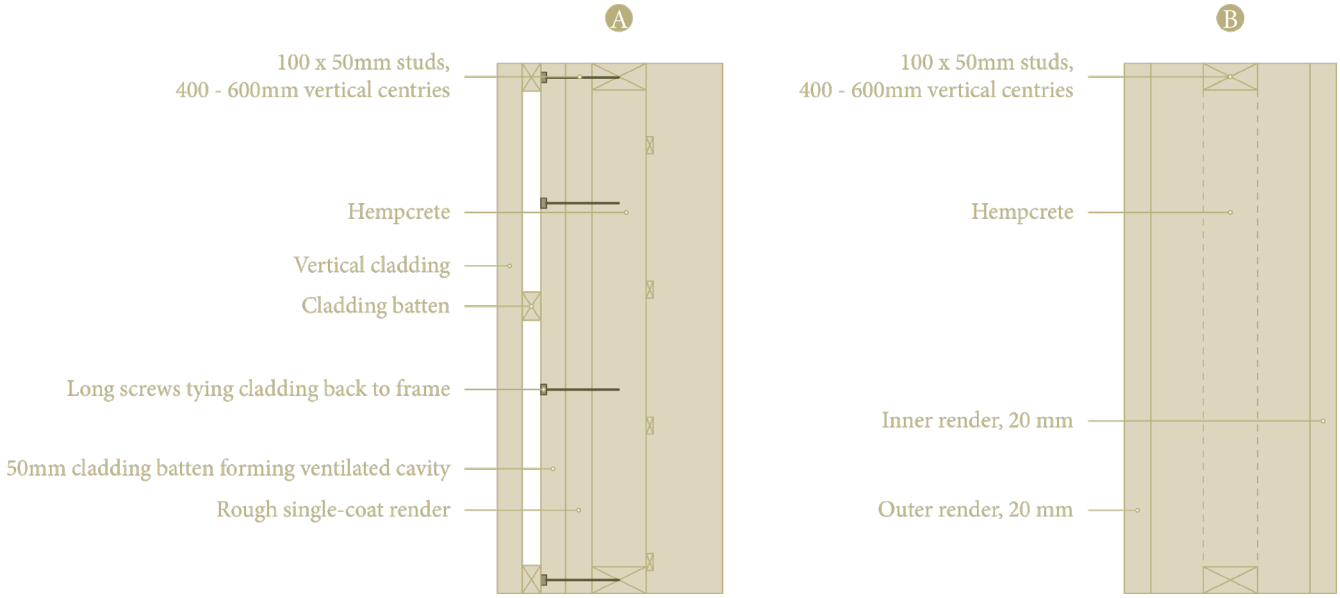

Figure 63, Possible wall constructions with hempcrete, derived from (Stanwix & Sparrow, 2014)

Openings

Window and door **frames should** be fixed to the **timber frame construction**. If the support frame is at the desired position of the frame, fixing can be done easily. In other cases, a supporting sub-frame made of studs is used to create a framed opening, as illustrated in figure 64.

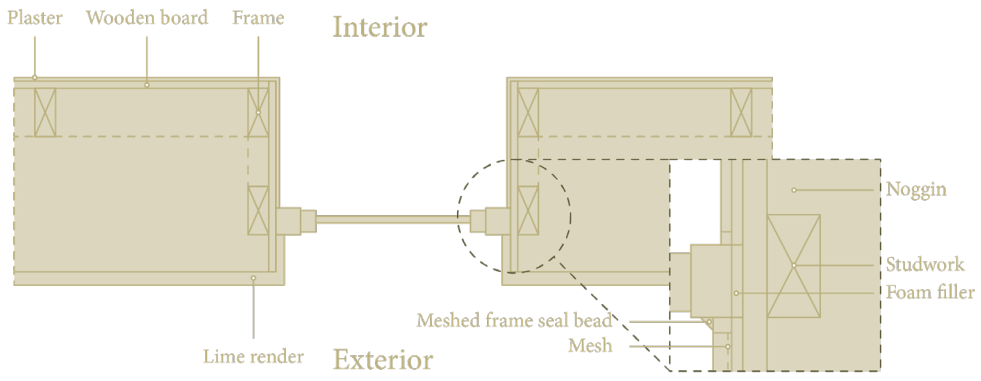

Figure 64, Connection between hempcrete and a window frame, derived from: (Stanwix & Sparrow, 2014)

6.3 Cork

Expanded cork boards can be used both as **insulation** and **finishing**. The **difference** between the application of the boards is the **density** and thus **porosity**. **Insulating** cork is **more porous** and **moisture-absorbent**, while **façade cork** is **more weather-resistant** and **moisture-repellent**. Due to the **softness** of the boards, it is to cut the panels to size.

Insulation

The expanded insulation boards are placed **between** the **structural timber frame** and must be **enclosed** on **both sides** to ensure **stability** and to **secure** the insulation. **Internally** an **18 mm biobased construction board** is typically used to allow for fixings. **Externally structurally**, **vapour-open** boards are required.

Additionally, **expanded cork granules**, ranging from **3** to **15 mm** in size, can be **sprayed** between the construction boards and the structure. At a density of 60 to 70 kg/m³, a λ-value of 0.041 W/(mK) can be achieved. The detailing principles are the same for both cork boards and granules. However, the granules can also be used to **fill cavities** within the construction to prevent **thermal bridging** (Hanenburg, 2022).

Façade

Expanded cork panels can also be applied as **façade cladding** where **two** possible **options** are available. The **first method** involves **mechanically fastening** the cork panels with **screws** onto a vapour-open structural board in combination with a wooden batten framework. Figure 65 shows that the panels are mounted with **three horizontal** and **two vertical screws** per **panel**. Since these are designed with a tongue and groove joint, both a seamless connection and an interlocking structural connection is achieved.

For mechanical fastening, the **centre-to-centre distance** of the **battens** should not exceed **237.5 mm**, as shown in figure 66 below. To strengthen the structural bond and protect against **weathering**, a **6 mm** layer of **cork mortar** over the entire surface of the cork panel must be applied (Amorim, n.d.).

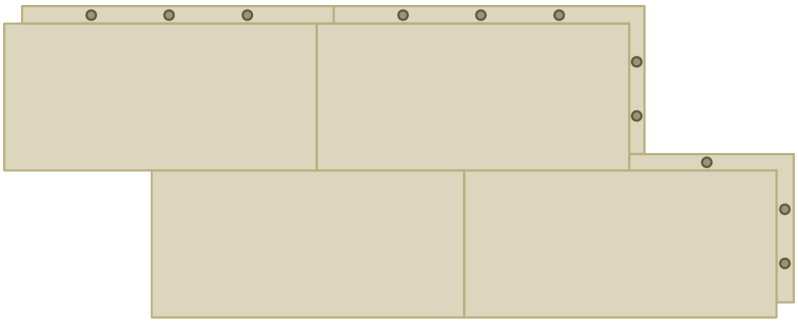

Figure 65, Cork front view with mechanical connection, own illustration

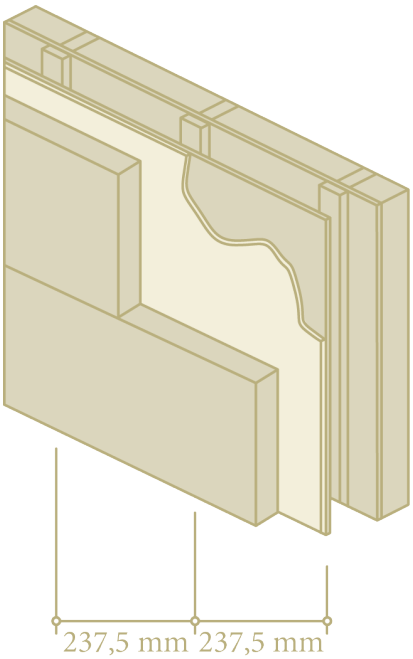

Figure 66, Cork cladding with battens, own illustration

An alternative method for installing cork façade panels involves **bonding** the façade panels to a cork insulation board using a **3 mm** of **cork mortar**. This is then bonded to a vapour-open structural backing board also using a **3 mm** thick layer of **cork mortar**. This principle can be seen in figure 68.

Additional fixing anchors are used to ensure the **stability** of the façade system. These anchors provide **mechanical anchoring** of the insulation boards to the underlying structure. The fixing anchors should have a **minimum length equal** to the **thickness** of the insulation board **plus** at least **30 mm anchoring penetration depth** in the supporting structure.

To ensure a sufficiently strong bond and good wind load resistance, a requirement of **six** fixing **anchors per square metre** of **cork insulation board** applies, as can be seen in figure 67.

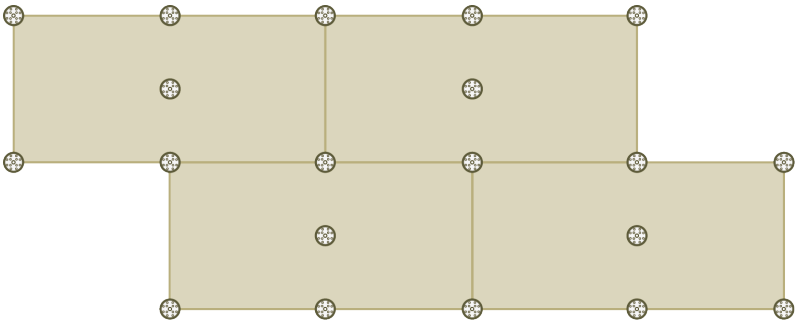

Figure 67, Cork front view with insulation roses, own illustration

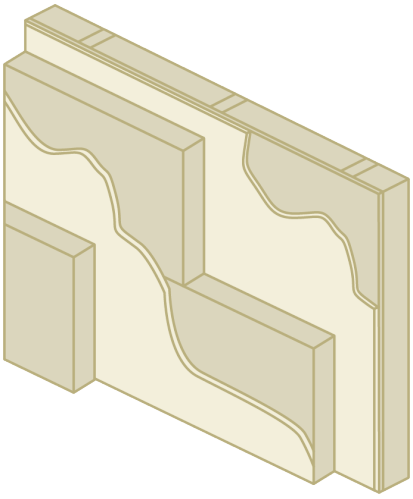

Figure 68, Cork cladding with mortar, own illustration

For both methods, a level surface is essential to ensure correct installation of the panels. Installation begins with a perforated L-profile supporting the bottom row of cork panels and should be the same width as the cork panels. Additionally, the profile should be placed at a **minimum height** of **50 mm** above ground level to prevent **water** and **capillary absorption**. The perforations in the profile ensure drainage in order to prevent moisture problems at the base of the façade.

Furthermore, the **cork panels** should be laid in a **staggered joint** to prevent **thermal bridges**. At **corner connections**, the boards can be placed in **staggered boards**, option A. The other possibility is to cut the boards in a **mitre joint**, this is shown in figure 69 below, at option B.

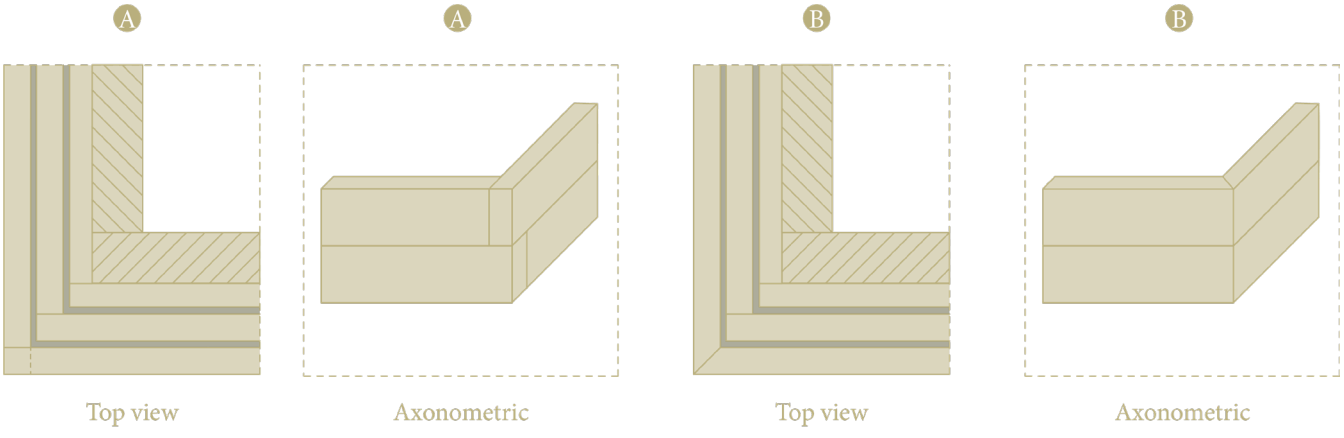

Figure 69, Corner connections, staggered joints & 45° cut, own illustration

Around **window frames**, a **minimum distance** of **5 mm** should be maintained between cork panels and window frame to prevent **water accumulation** and ensure good **drainage**. Next, **window drip caps** should be used around window frames for the same reason and are shown in figure 80 (Mike Wye, 2014).

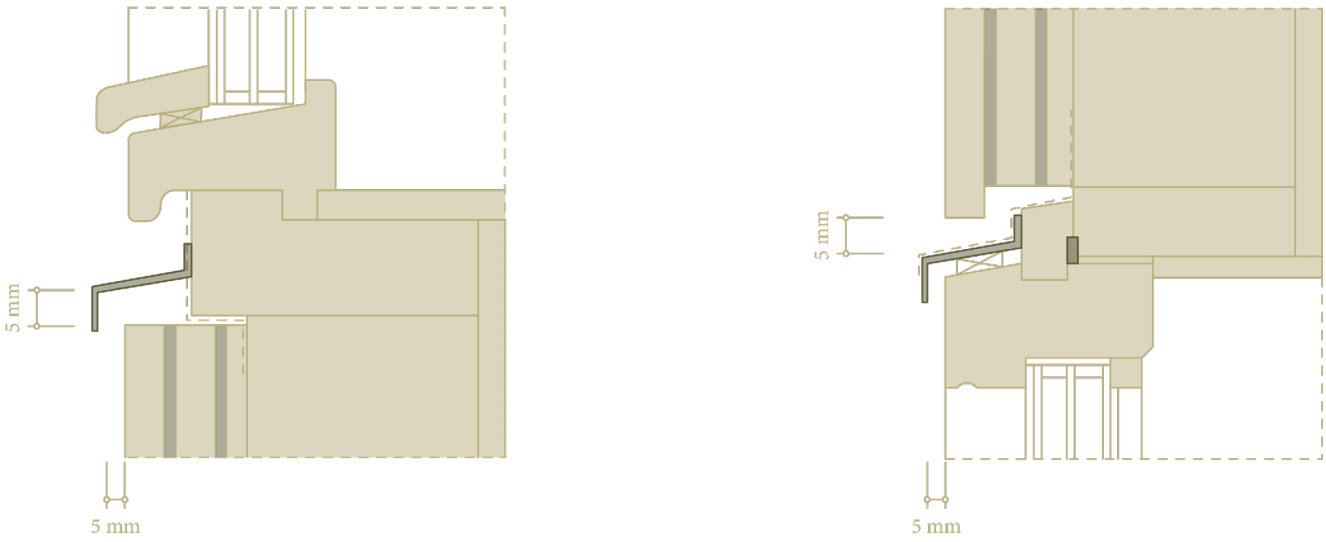

Figure 70, Distance between cork panels and window frame, own illustration

6.4 Flax

Flax is a **flexible insulation material** which can be easily placed **between** the **studs** of the **timber frame construction**. As with flexible wood fibre and flexible hemp, it is a **requirement** to use a **clamp allowance** to ensure effective performance. For flax insulation, this requires an excess of **30** to **40 mm plus** the **centre-to-centre distance** of the **studs** at both the **horizontal** plane and the **vertical** plane. This is shown schematically in the figure below, where 'L' indicates the stud centre-to-centre distance and 'X' the clamp allowance. Flax can easily be cut to size with a special flax knife or saw. To **avoid thermal bridges** and **condensation**, it is important to lay the insulation with a **staggered joint**, as also shown in the illustration.

To **prevent mould formation**, a **water-resistant vapour permeable membrane** should be used on the **outside** of the timber frame construction. On the **inside**, a **biobased construction board** is sufficient to enable interior hangings (Isovlas, 2022).

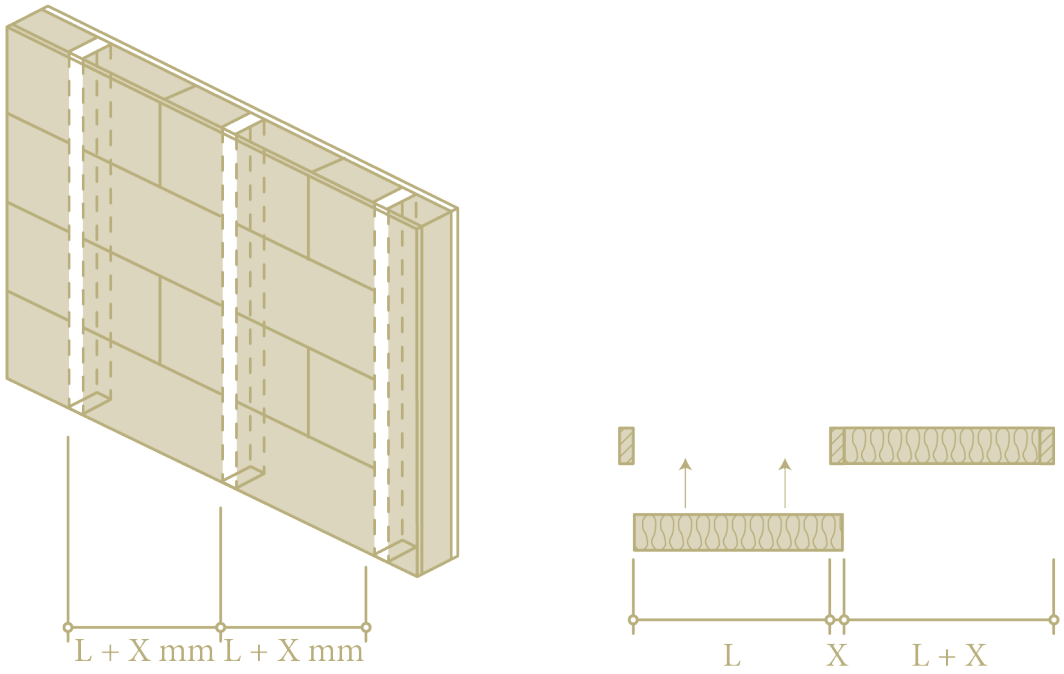

Figure 71, Flax insulation between timber frame, derived from: (Isovlas, 2022)

6.5 Straw

Straw can act as insulation material that can be **placed** between a **wooden frame**. There are **two** possible options to apply straw **between studs** such as **stacked straw bales** and **blown-in straw**.

As straw is **sensitive** to **moisture**, this requires extra attention regarding detailing and should **not** be in **direct contact** with the ground. So, it must be placed at least **300 mm above ground level** to prevent **rising damp** and **splashing rainwater**. A **roof overhang** is **recommended** for straw to protect against **rain**. Window and door frames should be placed near the external surface and feature **drip caps** at the **top** and **bottom**. Finally, **vapour permeability** must be ensured to prevent **vapour pressure** (Sutton et al., 2011).

Straw bale

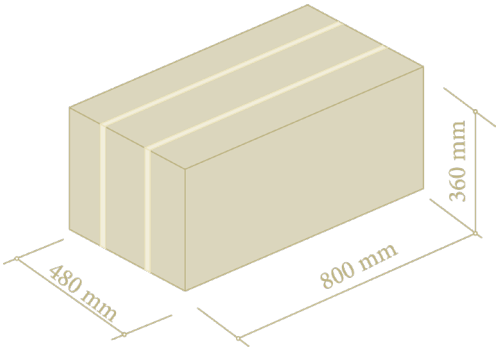

The first straw option comprises straw bales where the **dimensions** and **properties** of the bale should be used as the **starting point**.

A commonly used straw bale in the Netherlands has the following dimensions, as shown in the figure on the left, figure 72.

Figure 72, Dimensions straw bale, derived from: (Vereniging Strobouw Nederland, n.d.)

There are **two** proper ways for the implementarion in a wooden frame. **Firstly**, the position of the **posts** must **align** with the **straw bale dimensions**. **Secondly**, the **straw bales** must be properly **stabilised**. To minimise **thermal bridging** and **condensation**, it is important to **stagger** the **bales** (Sutton et al., 2011).

Although the **posts** can also be placed on the inside and or outside, **central placement** is **preferred**. As the straw bales are often thicker than the wooden studs, the straw bales are cut. To minimise incising, the studs should be as small as possible, usually 100 x 100 mm or 50 x 150 mm (Lierman, 2021). Additionally, unsupported length should not exceed a 13:1 thickness ratio (Ashour & Wu, 2011).

Straw bales can be **plastered directly** on the **outside** and **inside**. For the **exterior**, a **mould-resistant waterproof vapour permeable plaster** is necessary. The **inside** can be finished with a **clay plaster**. It is recommended to embed a **jute mesh** in the wet plaster to **reduce** the **risk** of **cracking**. Alternatively, the straw bales can be finished with wooden cladding, where the **screws** of the post and **battening** should reach into the **centre** of the **wooden structural frame** for sufficient **anchoring** (Lierman, 2021).

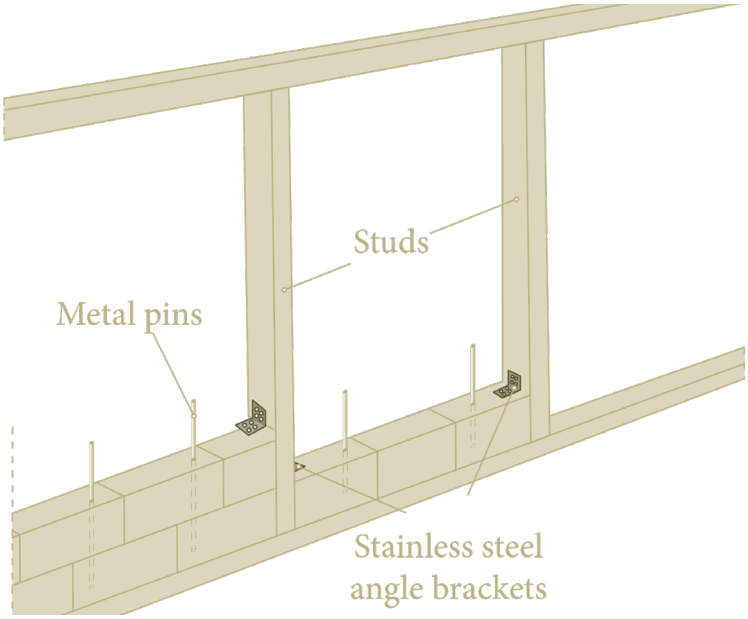

It is necessary to attach the straw bales to the timber frame construction for structural purposes. This can be done using anchors and special metal pins (Lierman, 2021). The attachment of straw bales to the timber frame construction is shown in figure 73.

However, working with straw bales is quite labour-intensive due to their weight. Depending on the type of grain used, moisture level and degree of compression, straw bales can have a density of 81 to 123.6 kg/m^3 (Ashour & Wu, 2011). Moreover, the straw bales should be stacked piece by piece and cut in some places. So, a more suitable way for top-up buildings is to apply blow-in straw between the studs of the timber frame construction and the biobased construction boards on both sides.

Figure 73, Connection straw bales to construction frame, own illustration

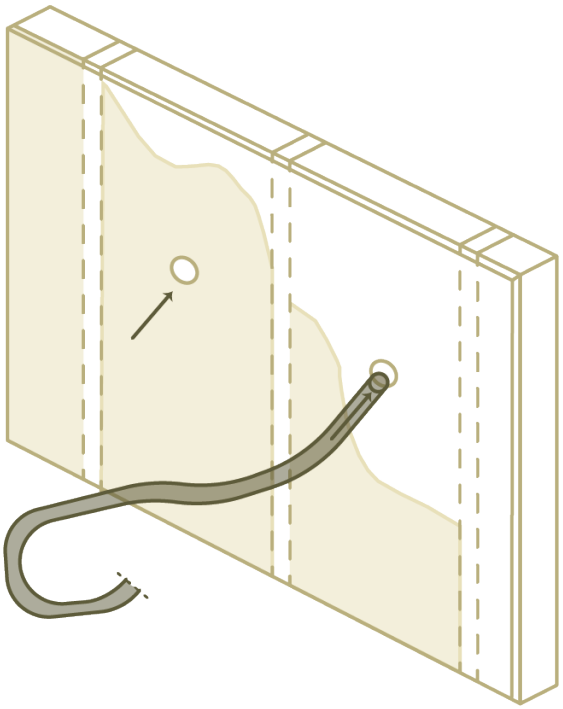

Figure 74, Blow-in straw, own illustration

When using **blow-in straw**, the timber frame construction board should be **covered** on **both** sides with a **biobased construction board**. Straw fibres of various lengths can be used for blow-in straw, usually varying between 10 and 30 mm. Blowing-in is done through an **opening** in the construction, which ensures the fibres are inserted under high pressure and fills the hollow space completely and gap-free.

Blown-in straw with a **density** of **105 kg/m³** achieves a **λ-value** of **0.043 W/mK** and is completely **settlement-free**. Due to this compaction, all hollow spaces are completely filled which benefits the elimination of thermal bridges. Blown-in straw can be used in constructions with a **minimum thickness** of **100 mm**. Using a special blow-in machine, the straw fibres are injected into the construction, with a processing speed of 7 to 10 m³ per hour. However, prefabricated blow in straw between two construction boards and between the timber frame construction is also available. (Klijn, n.d.).

Conclusion

Although the specific design principles may vary depending on the material used, **general guidelines** can be established that apply to all bio-based materials. Based on the literature, all constructions should be **vapour-open** to ensure proper **moisture regulation**. This prevents **moisture accumulation** while allowing **excess moisture** to be effectively **transported outside**. It is crucial that **materials** on the **exterior** are more **vapour-open** than those on the **interior** and that **vapour-tight foils** are **never** applied on both sides, as this could trap moisture and compromise structural integrity. Additionally, air leaks can significantly negatively affect the performance of the structure which makes **high airtightness** a **crucial aspect** in **biobased structures**. Air leaks can be reduced by flexible insulation materials or with blow in insulation.

The installation of bio-based insulation in timber frame constructions follows a relatively straightforward process, similar to conventional insulation methods. However, **façade walls** must be **protected** against **splashing rainwater** and **rising damp**. To achieve this, a **minimum elevation** of **300 mm** is required for most materials, **except cork**, where **50 mm** is considered **sufficient**. Furthermore, an **overhang** of at least **150 mm** is recommended to **protect** the construction from **rain exposure**. The use of **window drip caps** further contributes in proper **rainwater drainage**, and positioning window frames on the external façade enhances overall protection.

Lastly, it is essential that bio-based materials are **protected** from **precipitation** during the **construction phase**. Excess moisture absorption during this period can elevate relative humidity levels and increase the risk of mould growth. These findings, along with insights from existing literature, are confirmed by Loussos et al. (2022). Proper design and construction strategies help **optimize** the **durability** and performance of bio-based materials while maintaining a healthy indoor environment.

In the next chapter, **design principles** will be applied to the detail configurations. For each detail, the design principles used are showcased through a small visualisation placed alongside the details, providing an immediate overview of the implemented concepts. For further clarification regarding the design principles, the explanation is provided in this chapter. Additionally, a clear illustration of the materials used in the details is presented.

3. The detail configurations

3.1 SBR-reference details

Before presenting the developed bio-based reference details, a brief introduction is provided regarding the existing **SBR-reference details**. Furthermore, the importance of having SBR-reference details comprising bio-based materials is given aswell.

SBR details (Standard Architectural Reference Details) are a widely used set of **standardized construction details**. These details serve as a **technical reference** for architects, engineers, and contractors, providing reliable solutions for the **design** and **construction** of **building components**. The SBR database includes **2D detail drawings**, supplemented by **technical specifications**. Due to their accessibility, SBR details are frequently used as a standard reference in practice, particularly in the early technical design phase.

To effectively integrate SBR details into the technical elaboration of designs, architects consult these reference details as a **guide** for **construction methods**, **material selection**, and **connection detailing**. The standardization of SBR details enables their seamless **incorporation** into the **design process**, supporting interdisciplinary collaboration. The same approach is applied when using reference details.

However, SBR details have been predominantly developed using conventional construction materials such as concrete, steel, masonry, synthetic, and mineral-based insulation materials. The **absence** of **SBR details** incorporating **bio-based materials** presents a significant **barrier** to the **integration** of **sustainable building materials** in the design process. Architects and designers aiming to work with renewable materials such as timber, hempcrete, straw, cork, or flax insulation currently **lack** access to equivalent, **validated technical reference details**. This thesis therefore introduces a series of bio-based reference details that align with the format of existing SBR details. The corresponding **simulation results**, presented in **chapter 5** and **appendix A**, ensure the **validation** of the developed details.

In order to ensure effective and accurate implementation, the details have been developed in the same **drawing style** as the existing SBR reference details. As a result, they can be easily incorporated into the technical design process.

Detail configuration 1 - hempcrete blocks with wooden façade

The first detail configuration consists of hempcrete blocks, bonded with a hydraulic lime mortar within a timber construction frame. To protect the timber structure against moisture penetration, a pressure-resistant wood fibre board is used. The horizontal and vertical battens, on which the vertical cladding is fixed, can then be attached to this board. On the inside, the hempcrete blocks can be directly finished with a clay plaster, consisting of a rough base layer and a finer finishing layer.

Used materials in this configuration

Façade finish

Wooden cladding is used as the finish of this detail configuration providing both aesthetic appeal and the first protection against the weather. It is mechanically fixed agains horizontal and vertical wooden battens.

Treated wood

Treated wood is used to form the horizontal and vertical framework. Since this wood is in direct contact with the weather, it must be resistant to weather influences. The techniques to treat the wood are able to make the wood weather resistant.

Glulam

Glulam serves as a structural element in this configuration, allowing for larger spans than a timber frame construction. Its strength and flexibility make it ideal for supporting heavy loads in this configuration. Glulam makes it possible to place the hempcrete blocks within the construction.

Pressure resistant wood fibre plate

Placed on the exterior surface of the structure, a pressure resistant wood fibre plate serve multiple purposes. First it protects the underlying construction, allows for secure mechanical attachment of the wooden cladding, and secondly it adds an insulating layer to improve thermal performance.

Hempcrete blocks

These blocks are positioned within the wooden frame and stacked to form an insulating layer. The prefabricated blocks can be used immediatally at the construction site and are bonded to each other by a 3 mm hydraulic lime mortar.

Flexible hemp insulation

Flexible hemp insulation is used to fill the gaps between the hempcrete blocks and the wooden element. This both enhances the insulation of the construction and eliminates the thermal bridges by providing a continous inuslation layer.

Clay plaster

Hempcrete blocks can remain unfinished, but an optional clay plaster provides a clean finish. The plaster must be applied in 2 layers consisting of a rough base layer of 15 mm and a finishing layer of 5 mm. In between a jute reinforcement mesh is recommended to prevent cracking.

Necessary design principles

Façade wooden finish

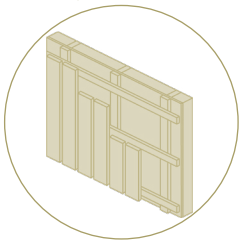

Attachment vertical wooden cladding

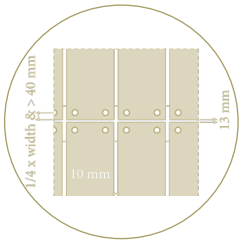

Spaces façade cladding for mechanical attachment

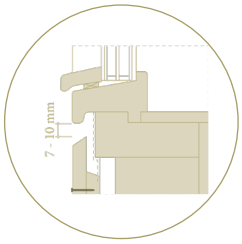

Connection façade bottom window frame

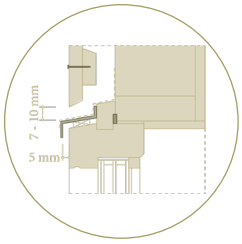

Connection façade top window frame

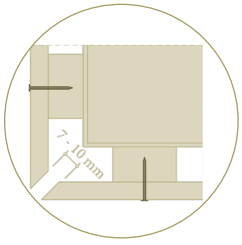

Connection corner façade

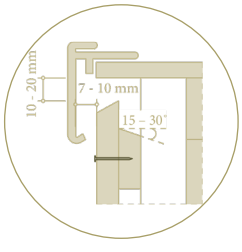

Connection façade roof

Wood fibre plate

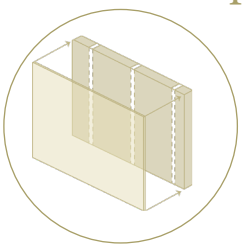

Attachment wooden wood fibre board

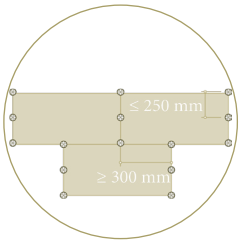

Distances placement wooden wood fibre board

Hempcrete insulation blocks

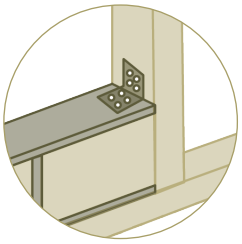

Hempcrete blocks in construction frame

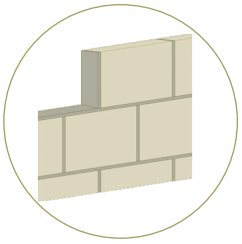

Application of hydraulic lime mortar

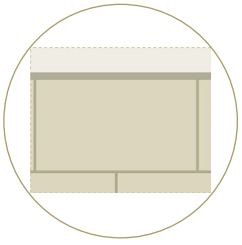

Connection hempcrete blocks roof

Clay finish

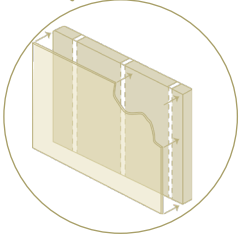

Plastering of clay finish

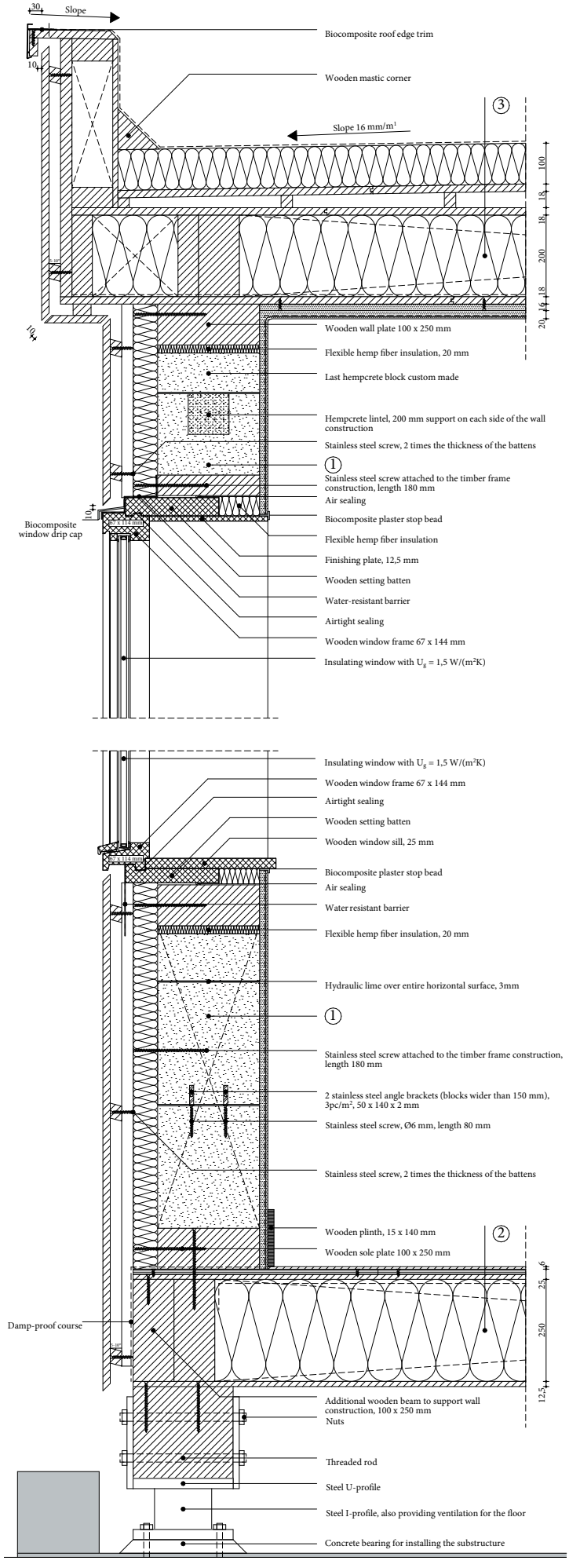

Figure 75, Detail of V1 (below) & V2 (top) configuration 1, own illustration

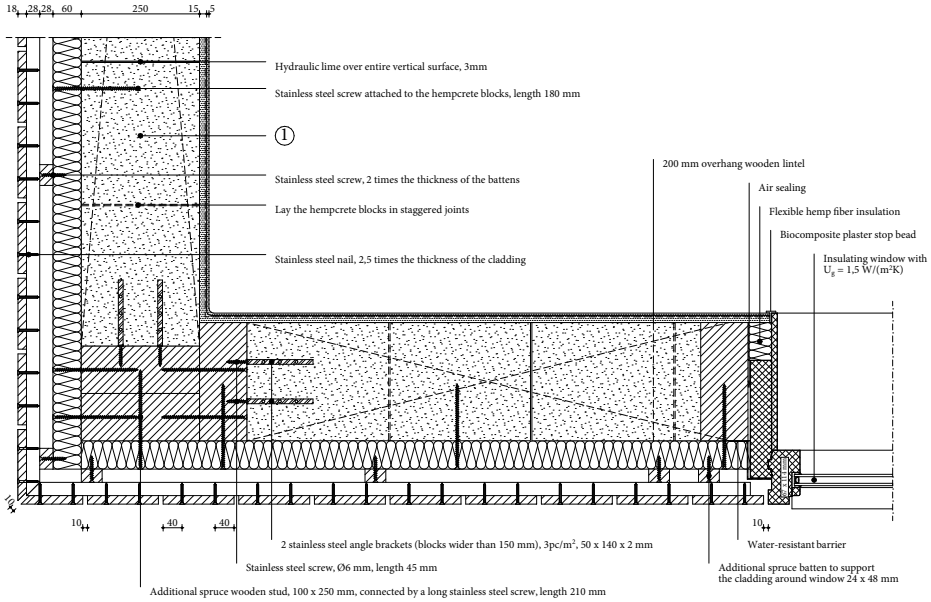

Figure 76, Detail of H1 configuration 1, own illustration

1 Wall construction build-up, RC-value: 4.88 (m²K)/W

- Vertical wooden cladding, 18 mm;
- Horizontal spruce cladding batten cavity, 28 x 44 mm, center-to-center 600 mm;
- Vertical spruce cladding batten forming ventilated cavity, 28 x 44 mm, center-to-center 600 mm;
- Pressure-resistant woodfibre insulation plate (λ ≤ 0.042 W/mK), 60 mm;
- Timber frame construction, 100 x 250 mm, center-to-center 3000 mm;
- Hempcrete blocks (λ ≤ 0.071 W/mK), 250 mm;
- Rough base clay plaster, 15 mm;
- Jute reinforcement mesh;
- Finishing clay plaster, 5 mm.

2 Floor construction build-up, RC-value: 4.65 (m²K)/W

- Finishing board, 6 mm;
- Biobased wooden construction board, 12.5 mm;
- Biobased wooden construction board, perpendicular on the other plate, 12.5 mm;
- Vapour-retarding and airtight membrane with a variable vapour diffusion resistanance;
- Flexible hemp fiber insulation placed between construction (λ ≤ 0.043 W/(mK), 250 mm;
- Wooden beams 100 x 250 mm, center-to-center 600 mm;
- Biobased wooden construction board, 12.5 mm.

3 Roof construction build-up, RC-value: 6.71 (m²K)/W

- EPDM glued on underlayment to prevent roof covering from lifting;
- Pressure-resistant woodfibre insulation plate (λ ≤ 0.042 W/(mK), 100 mm;
- Biobased wooden construction board, 18 mm;
- Sloped wooden battens for drainage at an angle of 16 mm/m[1], 28 x 24 mm;
- Biobased wooden construction board, 18 mm;
- Flexible hemp fiber insulation placed between construction (λ ≤ 0.043 W/(mK), 200 mm;
- Wooden beams 100 x 200 mm, center-to-center 600 mm;
- Vapour-retarding and airtight membrane with a variable vapour diffusion resistanance;
- Biobased wooden construction board, 18 mm;
- Clay base plate, 16 mm;
- Rough base clay plaster, 15 mm;
- Jute reinforcement mesh;
- Finishing clay plaster, 5 mm.

Detail configuration 2 - hempcrete with plaster

The second detail configuration consists of hempcrete blocks, bonded with a hydraulic lime mortar within a timber construction frame. To protect the wooden structure from moisture penetration, the wood must be covered with at least 70 mm of hempcrete. Since the exterior consists of hempcrete blocks, the blocks can, in this configuration, be finished directly with a hydraulic lime plaster on the outside and a clay plaster on the inside. For both finishes, a rough base layer should first be applied, followed by a finer finishing layer.

Used materials in this configuration

Plaster finish

The hempcrete blocks can be finished with a hydraulic lime plaster. It must have anti-fungal properties and should be specifically developed for outdoor use to withstand weather exposure and fluctuations in relative humidity. The plaster layer typically consists of a 10 to 12 mm base coat and an 8 to 10 mm finish coat.

Glulam

Glulam serves as a structural element in this configuration, allowing for larger spans than a timber frame construction. Its strength and flexibility make it ideal for supporting heavy loads in this configuration. Glulam makes it possible to place the hempcrete blocks within the construction.

Hempcrete blocks

These blocks are positioned within the wooden frame and stacked to form an insulating layer. The prefabricated blocks can be used immediatally at the construction site and are bonded to each other by a 3 mm hydraulic lime mortar.

Flexible hemp insulation

Flexible hemp insulation is used to fill the gaps between the hempcrete blocks and the wooden element. This both enhances the insulation of the construction and eliminates the thermal bridges by providing a continuous inuslation layer.

Clay plaster

Hempcrete blocks can remain unfinished, but an optional clay plaster provides a clean finish. The plaster must be applied in 2 layers consisting of a rough base layer of 15 mm and a finishing layer of 5 mm. In between a jute reinforcement mesh is recommended to prevent cracking

Necessary design principles

Façade plastering finish

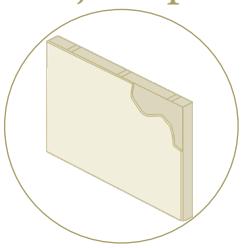

Plastering of hydaulic lime

Hempcrete insulation blocks

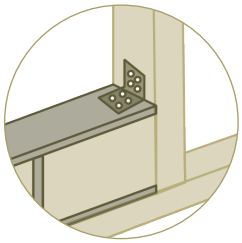

Hempcrete blocks in construction frame

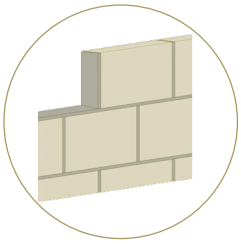

Application of hydraulic lime mortar

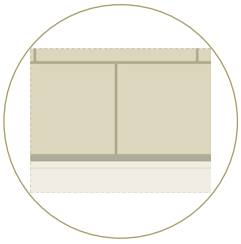

Connection hempcrete blocks floor

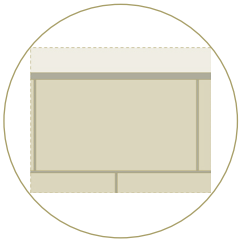

Connection hempcrete blocks roof

Clay finish

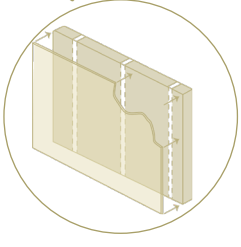

Plastering of clay finish

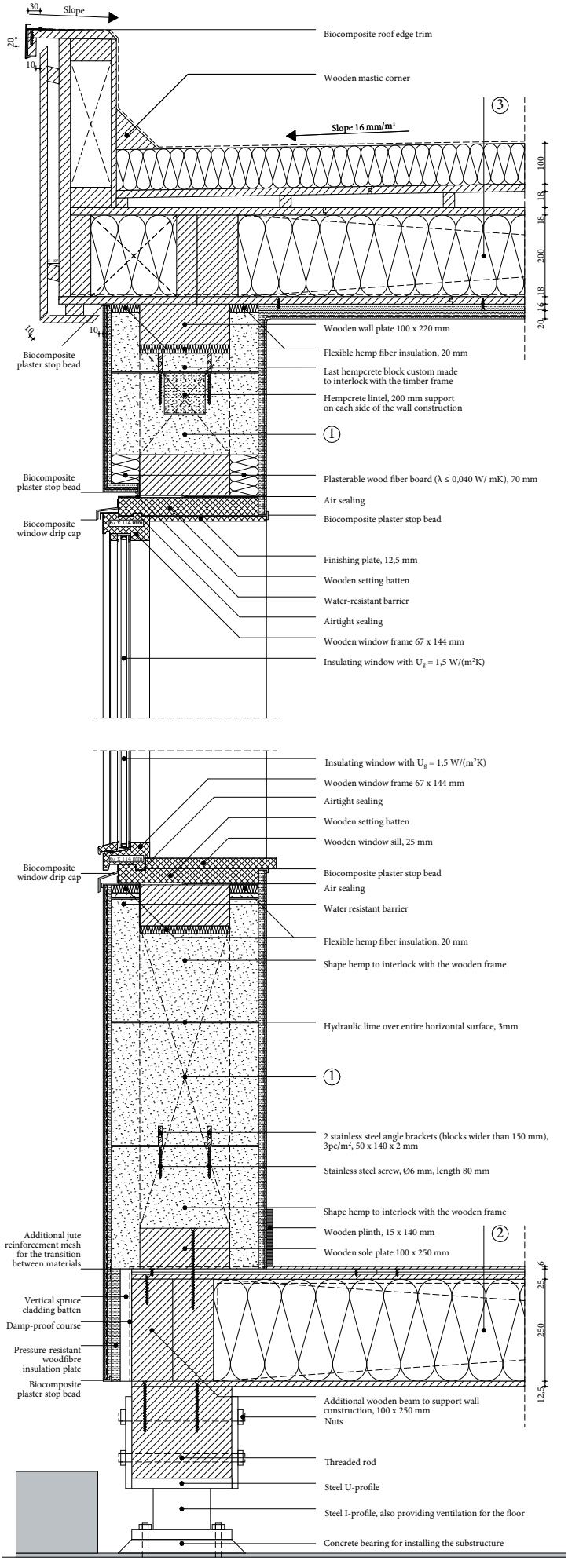

Figure 77, Detail of V1 (below) & V2 (top) configuration 2, own illustration

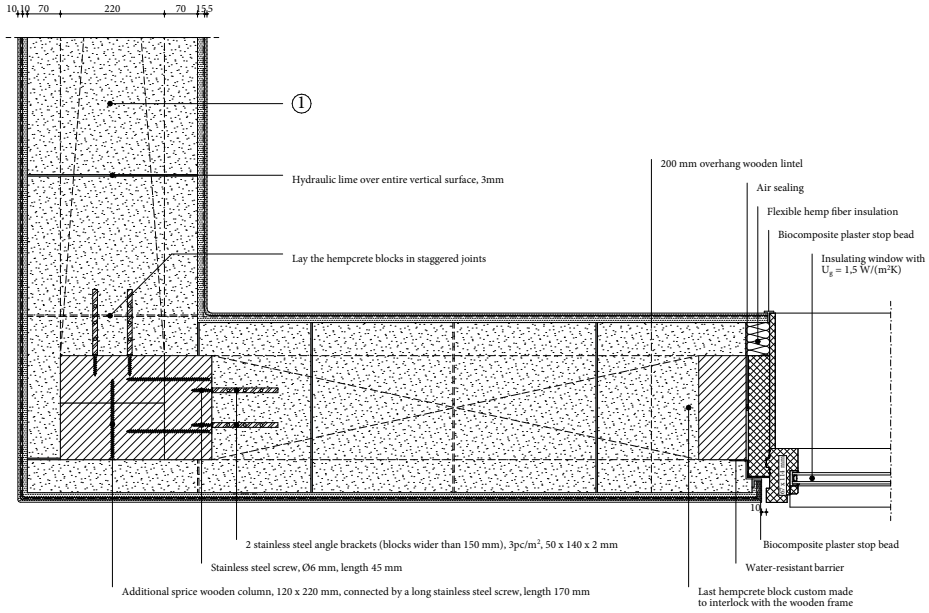

Figure 78, Detail of H1 configuration 2, own illustraion

1 Wall construction build-up, RC-value: 5.53 (m²K)/W

- Finishing lime plaster, 5 mm;
- Jute reinforcement mesh;
- Rough base lime plaster, 5 mm;
- Rough bonding lime plaster, 10 mm;
- Timber frame construction, 100 x 220 mm, center-to-center 3000 mm, placed 70 mm from outside;
- Hempcrete blocks (λ ≤ 0.071 W/mK), 360 mm;
- Rough base clay plaster, 15 mm;
- Jute reinforcement mesh;
- Finishing clay plaster, 5 mm.

2 Floor construction build-up, RC-value: 4.65 (m²K)/W

- Finishing board, 6 mm;
- Biobased wooden construction board, 12.5 mm;
- Biobased wooden construction board, perpendicular on the other plate, 12.5 mm;
- Vapour-retarding and airtight membrane with a variable vapour diffusion resistanance;
- Flexible hemp fiber insulation placed between construction (λ ≤ 0.043 W/(mK), 250 mm;
- Wooden beams 100 x 250 mm, center-to-center 600 mm;
- Biobased wooden construction board, 12.5 mm.

3 Roof construction build-up, RC-value: 6.71 (m²K)/W

- EPDM glued on underlayment to prevent roof covering from lifting;
- Pressure-resistant woodfibre insulation plate (λ ≤ 0.042 W/(mK), 100 mm;
- Biobased wooden construction board, 18 mm;
- Sloped wooden battens for drainage at an angle of 16 mm/m[1], 28 x 24 mm;
- Biobased wooden construction board, 18 mm;
- Flexible hemp fiber insulation placed between construction (λ ≤ 0.043 W/(mK), 200 mm;
- Wooden beams 100 x 200 mm, center-to-center 600 mm;
- Vapour-retarding and airtight membrane with a variable vapour diffusion resistanance;
- Biobased wooden construction board, 18 mm;
- Clay base plate, 16 mm;
- Rough base clay plaster, 15 mm;
- Jute reinforcement mesh;
- Finishing clay plaster, 5 mm.

Detail configuration 3 - flexible hemp with wooden façade

The third detail configuration consists of flexible hemp fibre placed between the studs of the timber construction frame. The timber construction frame is then finished on the exterior with a pressure-resistant wood fibre board. This board protects the timber construction frame against moisture penetration and allows for the attachment of the wooden cladding. On the interior, the timber construction frame is finished with a biobased diffusion-open construction board to which a clay plate is screwed. A clay plaster can be applied on this plate, consisting of a rough layer and a finishing layer.

Used materials in this configuration

Façade finish

Wooden cladding is used as the finish of this detail configuration providing both aesthetic appeal and the first protection against the weather. It is mechanically fixed agains horizontal and vertical wooden battens.

Treated wood

Treated wood is used to form the horizontal and vertical framework. Since this wood is in direct contact with the weather, it must be resistant to weather influences. The techniques to treat the wood are able to make the wood weather resistant.

Untreated wood

Untreated spruce wood is mostly used as the structural component in timber frame constructions. This system consists of vertically placed wooden beams, regularly spaced between a horizontal sole plate and a top wall plate. Since untreated wood is used, it must be protected against moisture ingress

Pressure resistant wood fibre plate

Placed on the exterior surface of the structure, a pressure resistant wood fibre plate serve multiple purposes. First it protects the underlying construction, allows for secure mechanical attachment of the wooden cladding and gives stability, lastly it adds an insulating layer to improve thermal performance.

Flexible hemp insulation

Flexible hemp insulation forms the insulating layer which can be placed between the horizontal wooden beams of the timber frame construction. Additionally the material can also be used to fill gaps within the structure.

ESB

ESB is placed on the interior surface of the structure. Next to the pressure resistant wood fibre plate is also gives stability to the structure. The main purpose, however, is to allow for secure mechanical attachment for indoor hangings. The board is also suitable for relatively humid environments.

Clay plaster

To apply a clay paster a clay is first needed to form a correct underlayment for the clay plaster. The plaster must be applied in 2 layers consisting of a rough base layer of 15 mm and a finishing layer of 5 mm. In between a jute reinforcement mesh is recommended to prevent cracking.

Necessary design principles

Façade wooden finish

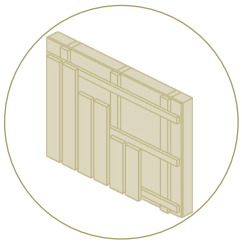

Attachment
vertical
wooden cladding

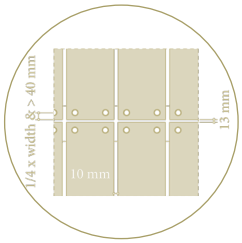

Spaces façade cladding
for
mechanical attachment

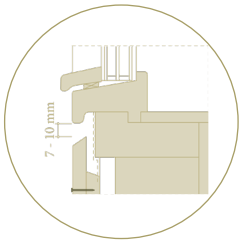

Connection
façade
bottom window frame

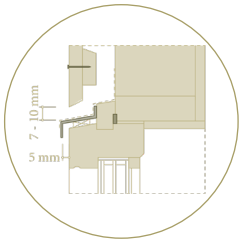

Connection
façade
top window frame

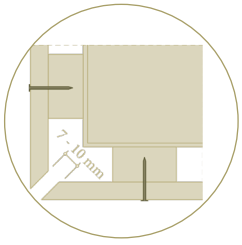

Connection
corner
façade

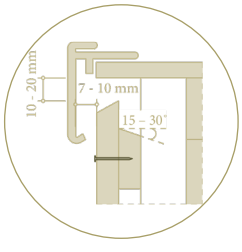

Connection
façade
roof

Wood fibre plate

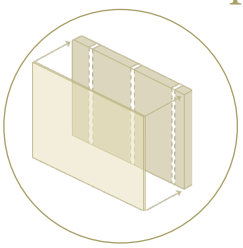

Attachment
wooden wood fibre board

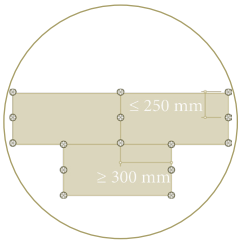

Distances
placement
wooden wood fibre board

Timber frame construction

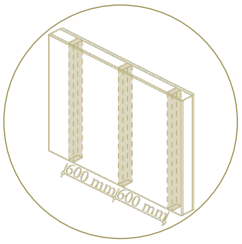

Distances
wooden studs in the
timber frame construction

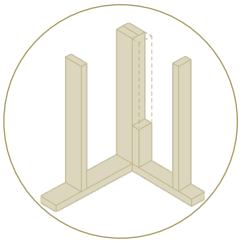

Corner connection
of the
timber frame construction

Flexible hemp fibre insulation

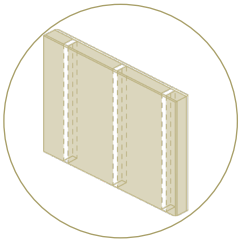

Placement
flexible hemp fibre
insulation plates

ESB board & clay finish

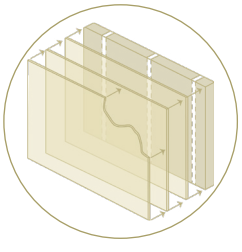

Attachment
ESB construction board &
clay plaster finish

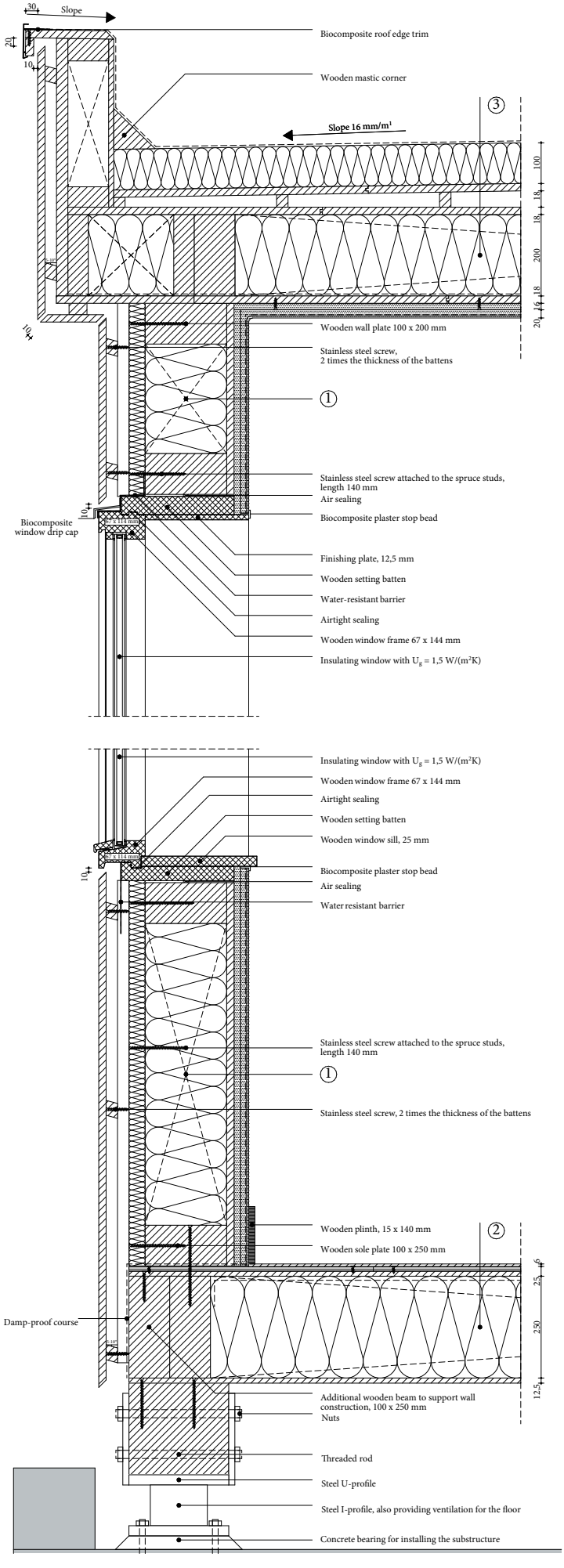

Figure 79, Detail of V1 (below) & V2 (top) configuration 3, own illustration

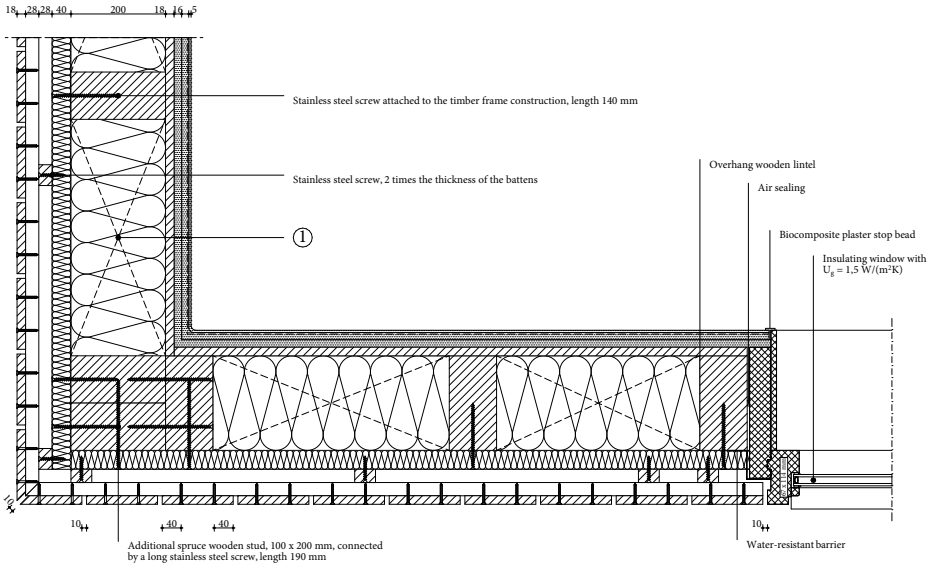

Figure 80 ,Detail of H1 configuration 3, own illustration

1 Wall construction build-up, RC-value: 5.22 (m²K)/W

- Vertical wooden cladding, 18 mm;
- Horizontal spruce cladding batten cavity, 28 x 44 mm, center-to-center 600 mm;
- Vertical spruce cladding batten forming ventilated cavity, 28 x 44 mm, center-to-center 600 mm;
- Pressure-resistant woodfibre insulation plate (λ ≤ 0.042 W/mK), 40 mm;
- Timber frame construction, 100 x 200 mm, center-to-center 600 mm;
- Flexible hemp fibre insulation, placed between construction (λ ≤ 0.043 W/mK), 200 mm;
- Clay base plate, 16 mm;
- Rough base clay plaster, 15 mm;
- Jute reinforcement mesh;
- Finishing clay plaster, 5 mm.

2 Floor construction build-up, RC-value: 4.65 (m²K)/W

- Finishing board, 6 mm;
- Biobased wooden construction board, 12.5 mm;
- Biobased wooden construction board, perpendicular on the other plate, 12.5 mm;
- Vapour-retarding and airtight membrane with a variable vapour diffusion resistanance;
- Flexible hemp fiber insulation placed between construction (λ ≤ 0.043 W/(mK), 250 mm;
- Wooden beams 100 x 250 mm, center-to-center 600 mm;
- Biobased wooden construction board, 12.5 mm.

3 Roof construction build-up, RC-value: 6.71 (m²K)/W

- EPDM glued on underlayment to prevent roof covering from lifting;
- Pressure-resistant woodfibre insulation plate (λ ≤ 0.042 W/(mK), 100 mm;
- Biobased wooden construction board, 18 mm;
- Sloped wooden battens for drainage at an angle of 16 mm/m[1], 28 x 24 mm;
- Biobased wooden construction board, 18 mm;
- Flexible hemp fiber insulation placed between construction (λ ≤ 0.043 W/(mK), 200 mm;
- Wooden beams 100 x 200 mm, center-to-center 600 mm;
- Vapour-retarding and airtight membrane with a variable vapour diffusion resistanance;
- Biobased wooden construction board, 18 mm;
- Clay base plate, 16 mm;
- Rough base clay plaster, 15 mm;
- Jute reinforcement mesh;
- Finishing clay plaster, 5 mm.

Detail configuration 4 - cork insulation with cork façade

In the fourth detail configuration, cork insulation boards are placed between the timber frame studs, which are finished with a pressure-resistant wood fibre board to protect the structure against moisture. This board also enables the attachment of the cork cladding board, which is bonded using a cork mortar to a bio-based, diffusion-open MDF construction board with water-repellent properties. On the interior, the timber frame is finished with a diffusion-open construction board, onto which a clay board is screwed. A clay plaster, consisting of a rough base layer and a finishing layer, is then applied.

Used materials in this configuration

Expanded cork agglomerates finishing & insulating plate

These boards can serve both as insulation and finishing, differing in density and porosity. Insulating cork is more porous with better thermal conductivity, while façade cork is weather-resistant. The finishing plate is mechanically attached and glued to a MDF underlayment. The insulating plate fits between the horizontal wooden timber frame beams. Optionally, cork granules can be blown into the construction to fill gaps.

MDF

The bio-based, diffusion-open MDF construction board forms a suitable underlayment for the cork mortar to glue and mechanically attach the cork finishing plates.

Treated wood

Treated wood is used to form the horizontal and vertical framework. Since this wood is in direct contact with the weather, it must be resistant to weather influences. The techniques to treat the wood are able to make the wood weather resistant.

Untreated wood

Untreated spruce wood is mostly used as the structural component in timber frame constructions. This system consists of vertically placed wooden beams, regularly spaced between a horizontal sole plate and a top wall plate. Since untreated wood is used, it must be protected against moisture ingress.

Pressure resistant wood fibre plate

Placed on the exterior surface of the structure, a pressure resistant wood fibre plate serve multiple purposes. First it protects the underlying construction, allows for secure mechanical attachment of the wooden cladding and gives stability, lastly it adds an insulating layer to improve thermal performance.

ESB

ESB is placed on the interior surface of the structure. Next to the pressure resistant wood fibre plate is also gives stability to the structure. The main purpose, however, is to allow for secure mechanical attachment for indoor hangings. The board is also suitable for relatively humid environments.

Clay plaster

To apply a clay paster a clay is first needed to form a correct underlayment for the clay plaster. The plaster must be applied in 2 layers consisting of a rough base layer of 15 mm and a finishing layer of 5 mm. In between a jute reinforcement mesh is recommended to prevent cracking.

Necessary design principles

Façade cork finish

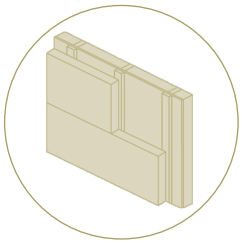

Attachment expanded cork finishing plate

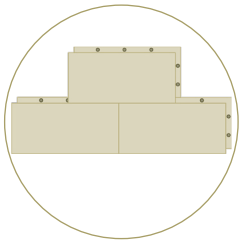

Distances placement cork plates

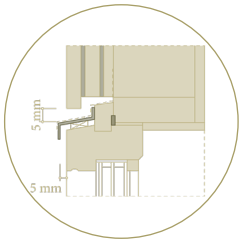

Connection façade bottom window frame

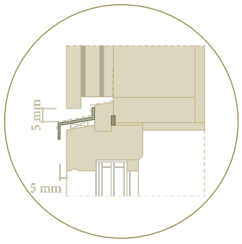

Connection façade top window frame

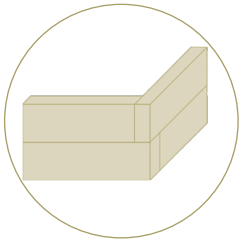

Connection corner cork plates

Cork insulation

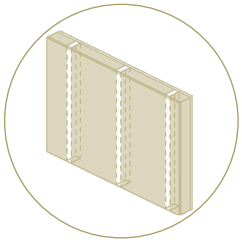

Placement expanded cork insulation plate

Wood fibre plate

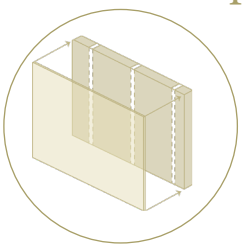

Attachment wooden wood fibre board

MDF

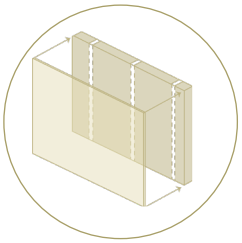

Attachment MDF board

Timber frame construction

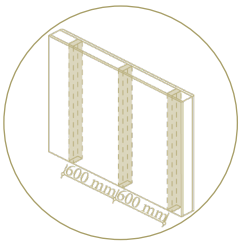

Distances wooden studs in the timber frame construction

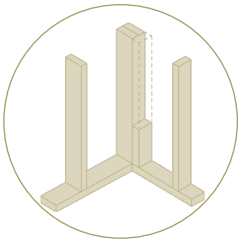

Corner connection of the timber frame construction

ESB board & clay finish

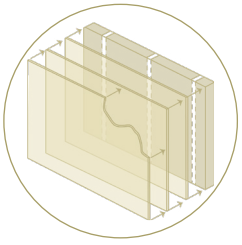

Attachment ESB construction board & clay plaster finish

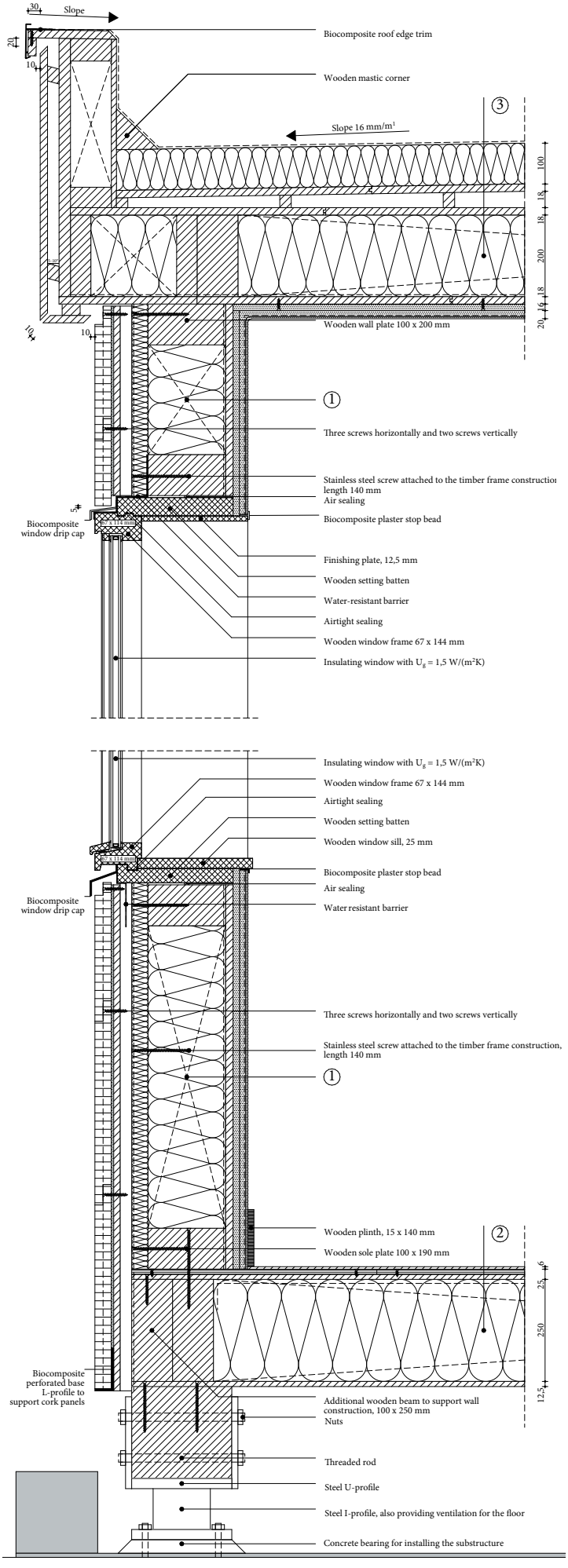

Figure 81, Detail of V1 (below) & V2 (top) configuration 4, own illustration

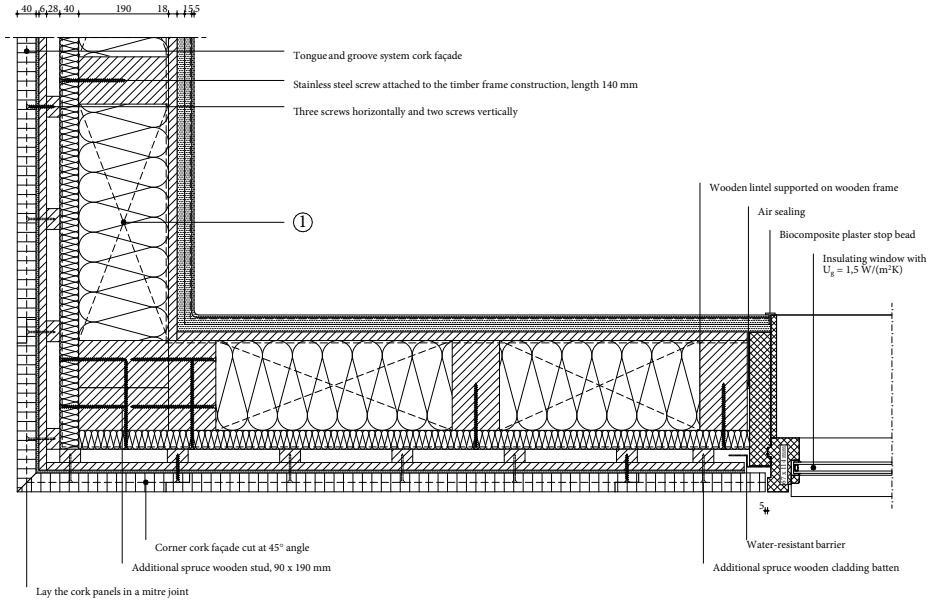

Figure 82, Detail of H1 configuration 4, own illustration

❶ Wall construction build-up, RC-value: 4.98 (m²K)/W

- Tongue and groove cork cladding panels (λ ≤ 0.043 W/mK), 40 mm;
- Cork mortar, 6mm;
- Biobased diffusion open construction board, 16mm;
- Vertical spruce cladding batten forming ventilated cavity, 28 x 44 mm, center-to-center 237 mm;
- Water resistant vapour-permeable membrane;
- Pressure-resistant woodfibre insulation plate (λ ≤ 0.042 W/mK), 40 mm;
- Timber frame construction, 100 x 190 mm, center-to-center 600 mm;
- Expanded insulation corkboard, placed between construction (λ ≤ 0.039 W/mK), 190 mm;
- Biobased construction board, 18 mm;
- Clay base plate, 16 mm;
- Rough base clay plaster, 15 mm;
- Jute reinforcement mesh;
- Finishing clay plaster, 5 mm.

❷ Floor construction build-up, RC-value: 4.65 (m²K)/W

- Finishing board, 6 mm;
- Biobased wooden construction board, 12.5 mm;
- Biobased wooden construction board, perpendicular on the other plate, 12.5 mm;
- Vapour-retarding and airtight membrane with a variable vapour diffusion resistanance;
- Flexible hemp fiber insulation placed between construction (λ ≤ 0.043 W/(mK), 250 mm;
- Wooden beams 100 x 250 mm, center-to-center 600 mm;
- Biobased wooden construction board, 12.5 mm.

❸ Roof construction build-up, RC-value: 6.71 (m²K)/W

- EPDM glued on underlayment to prevent roof covering from lifting;
- Pressure-resistant woodfibre insulation plate (λ ≤ 0.042 W/(mK), 100 mm;
- Biobased wooden construction board, 18 mm;
- Sloped wooden battens for drainage at an angle of 16 mm/m[1], 28 x 24 mm;
- Biobased wooden construction board, 18 mm;
- Flexible hemp fiber insulation placed between construction (λ ≤ 0.043 W/(mK), 200 mm;
- Wooden beams 100 x 200 mm, center-to-center 600 mm;
- Vapour-retarding and airtight membrane with a variable vapour diffusion resistanance;
- Biobased wooden construction board, 18 mm;
- Clay base plate, 16 mm;
- Rough base clay plaster, 15 mm;
- Jute reinforcement mesh;
- Finishing clay plaster, 5 mm.

Detail configuration 5 - cork insulation with cork façade

The fifth detail configuration consists of cork insulation boards placed between the studs of the timber construction frame. A water-resistant, vapour-permeable membrane is used to protect the structure against moisture penetration, followed by a bio-based, diffusion-open board for stability and cork façade application. This board allows the expanded insulation corkboard to be attached and bonded with cork mortar. A second layer of mortar secures the cork cladding panels. On the interior, the timber frame is finished with a diffusion-open construction board and a clay board together with a two-layer clay plaster

Used materials in this configuration

Expanded cork agglomerates finishing & insulating plate

The boards serve both as insulation and finishing, differing in density and porosity. Insulating cork is more porous with better thermal conductivity, while façade cork is weather-resistant. The finishing plate is mechanically attached and glued to a cork insulation plate, both attached on a MDF-plate. The insulating plate fits between the horizontal timber frame beams, with optional cork granulates that can fill gaps.

MDF

The bio-based, diffusion-open MDF construction board forms a suitable underlayment for the cork mortar to glue and mechanically attach the cork finishing plates. Next this gives the structure the required stability but can not fully protect the structure against moisture so a water-resistant, vapour-permeable membrane is necessary.

Untreated wood

Untreated spruce wood is mostly used as the structural component in timber frame constructions. This system consists of vertically placed wooden beams, regularly spaced between a horizontal sole plate and a top wall plate. Since untreated wood is used, it must be protected against moisture ingress.

ESB

ESB is placed on the interior surface of the structure. Next to the pressure resistant wood fibre plate is also gives stability to the structure. The main purpose, however, is to allow for secure mechanical attachment for indoor hangings. The board is also suitable for relatively humid environments.

Clay plaster

To apply a clay paster a clay is first needed to form a correct underlayment for the clay plaster. The plaster must be applied in 2 layers consisting of a rough base layer of 15 mm and a finishing layer of 5 mm. In between a jute reinforcement mesh is recommended to prevent cracking.

Necessary design principles

Façade cork finish

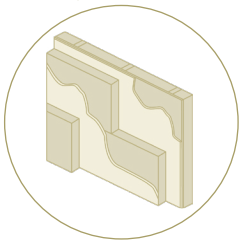

Attachment expanded cork finishing plate

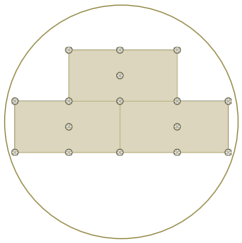

Distances placement cork plates

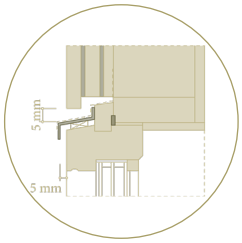

Connection façade bottom window frame

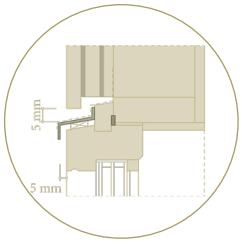

Connection façade top window frame

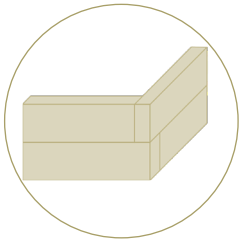

Connection corner cork plates

Cork insulation

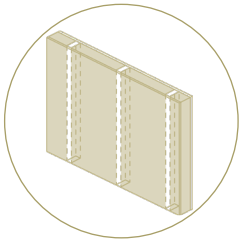

Placement expanded cork insulation plate

MDF board

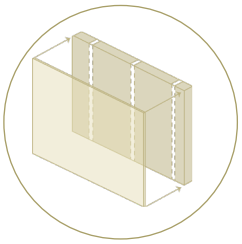

Attachment MDF board

Timber frame construction

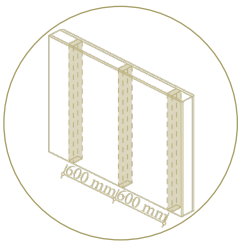

Distances wooden studs in the timber frame construction

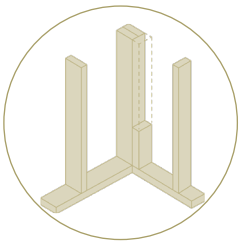

Corner connection of the timber frame construction

ESB board & clay finish

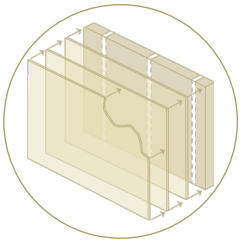

Attachment ESB construction board & clay plaster finish

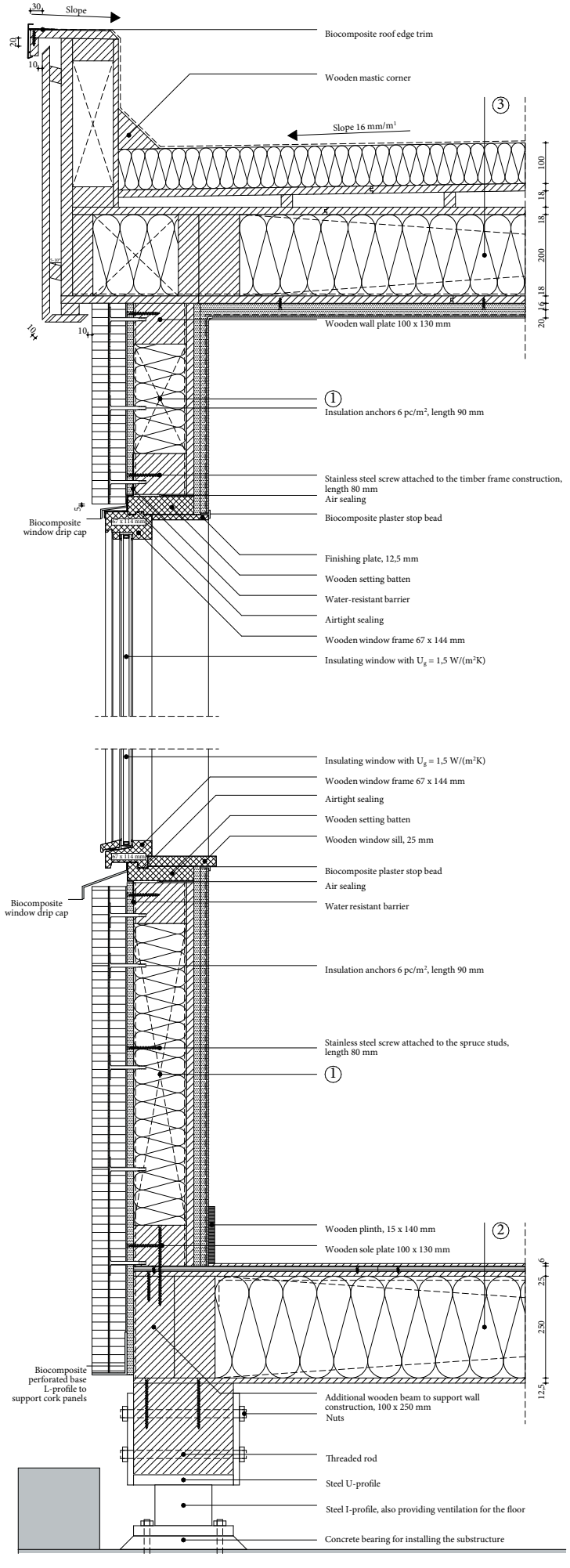

Figure 83, Detail of V1 (below) & V2 (top) configuration 5, own illustration

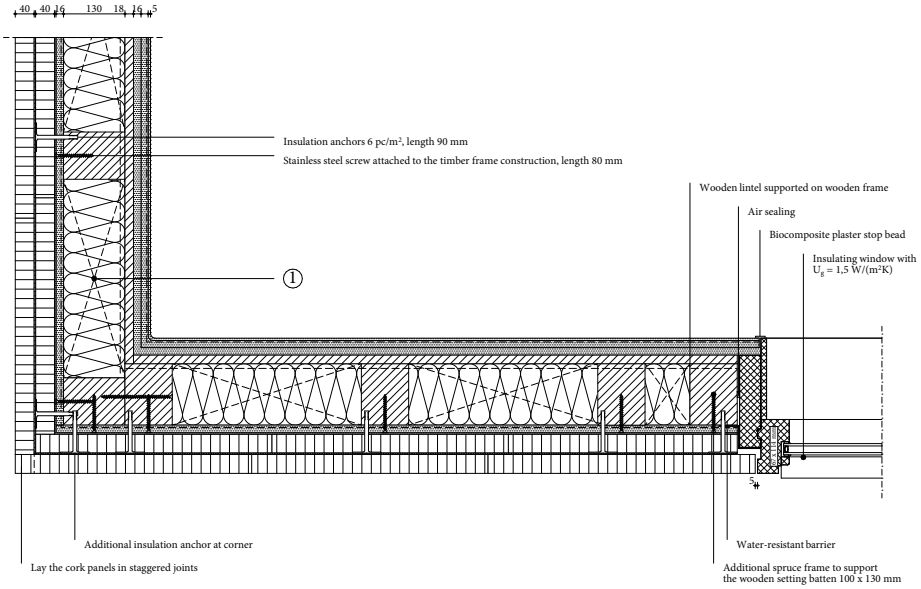

Figure 84, Detail of H1 configuration 5, own illustration

❶ Wall construction build-up, RC-value: 4.94 (m²K)/W

- Cork cladding panels (λ ≤ 0.043 W/mK), 40 mm;
- Cork mortar, 3 mm;
- Expanded insulation corkboard (λ ≤ 0.039 W/mK), 40 mm;
- Cork mortar, 3 mm;
- Biobased diffusion open construction board, 16mm;
- Water resistant vapour-permeable membrane;
- Timber frame construction, 100 x 130 mm, center-to-center 500 mm;
- Expanded insulation corkboard, placed between construction (λ ≤ 0.039 W/mK), 130 mm;
- Vapour-retarding and airtight membrane with a variable vapour diffusion resistance;
- Biobased construction board, 18 mm;
- Clay base plate, 16 mm;
- Rough base clay plaster, 15 mm;
- Jute reinforcement mesh;
- Finishing clay plaster, 5 mm.

❷ Floor construction build-up, RC-value: 4.65 (m²K)/W

- Finishing board, 6 mm;
- Biobased wooden construction board, 12.5 mm;
- Biobased wooden construction board, perpendicular on the other plate, 12,5 mm;
- Vapour-retarding and airtight membrane with a variable vapour diffusion resistanance;
- Flexible hemp fiber insulation placed between construction (λ ≤ 0.043 W/(mK), 250 mm;
- Wooden beams 100 x 250 mm, center-to-center 600 mm;
- Biobased wooden construction board, 12.5 mm.

❸ Roof construction build-up, RC-value: 6.71 (m²K)/W

- EPDM glued on underlayment to prevent roof covering from lifting;
- Pressure-resistant woodfibre insulation plate (λ ≤ 0.042 W/(mK), 100 mm;
- Biobased wooden construction board, 18 mm;
- Sloped wooden battens for drainage at an angle of 16 mm/m[1], 28 x 24 mm;
- Biobased wooden construction board, 18 mm;
- Flexible hemp fiber insulation placed between construction (λ ≤ 0.043 W/(mK), 200 mm;
- Wooden beams 100 x 200 mm, center-to-center 600 mm;
- Vapour-retarding and airtight membrane with a variable vapour diffusion resistanance;
- Biobased wooden construction board, 18 mm;
- Clay base plate, 16 mm;
- Rough base clay plaster, 15 mm;
- Jute reinforcement mesh;
- Finishing clay plaster, 5 mm.

Detail configuration 6 - flax insulation with wooden façade

The sixth detail configuration consists of flexible flax insulation placed between the studs of the timber construction frame. The flax is protected against water and mould growth by a water-resistant vapour-permeable membrane at the outside of the construction. In this configuration the horizontal wooden cladding is placed against vertical battens which are attached to the construction. The construction frame is inside finished with a bio-based, diffusion-open construction board to which a clay board is screwed. A clay plaster can then be applied to this board, consisting of a rough layer and a finishing layer.

Used materials in this configuration

Façade finish

Wooden cladding is used as the finish of this detail configuration providing both aesthetic appeal and the first protection against the weather. It is mechanically fixed agains horizontal and vertical wooden battens.

Treated wood

Treated wood is used to form the vertical framework. Since this wood is in direct contact with the weather, it must be resistant to weather influences. The techniques to treat the wood are able to make the wood weather resistant.

Untreated wood

Untreated spruce wood is mostly used as the structural component in timber frame constructions. This system consists of vertically placed wooden beams, regularly spaced between a horizontal sole plate and a top wall plate. Since untreated wood is used, it must be protected against moisture ingress.

Flax insulation

Flexible flax insulation forms the insulating layer which can be placed between the horizontal wooden beams of the timber frame construction. Hereby it is important to apply a clamp. Additionally the material can also be used to fill gaps within the structure.

ESB

ESB is placed on the interior surface of the structure. Next to the pressure resistant wood fibre plate is also gives stability to the structure. The main purpose, however, is to allow for secure mechanical attachment for indoor hangings. The board is also suitable for relatively humid environments.

Clay plaster

To apply a clay paster a clay is first needed to form a correct underlayment for the clay plaster. The plaster must be applied in 2 layers consisting of a rough base layer of 15 mm and a finishing layer of 5 mm. In between a jute reinforcement mesh is recommended to prevent cracking.

Necessary design principles

Façade wooden finish

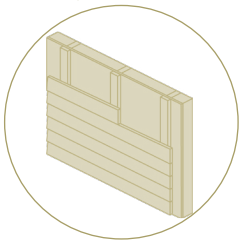

Attachment horizontal wooden cladding

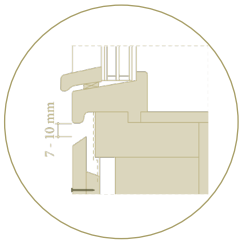

Connection façade bottom window frame

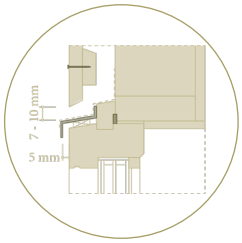

Connection façade top window frame

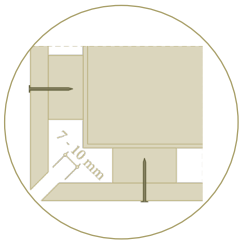

Connection corner façade

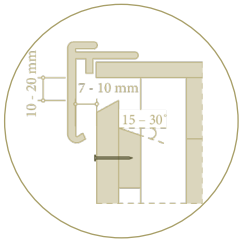

Connection façade roof

Timber frame construction

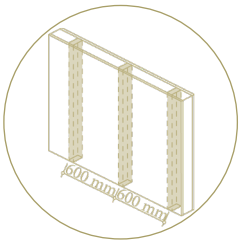

Distances wooden studs in the timber frame construction

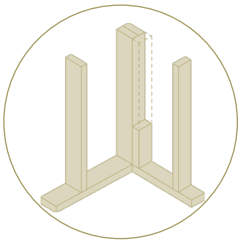

Corner connection of the timber frame construction

Flexible flax insulation

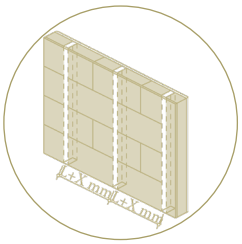

Placement flexible flax insulation plates

ESB board & clay finish

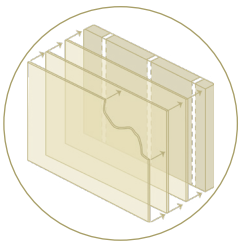

Attachment ESB construction board & clay plaster finish

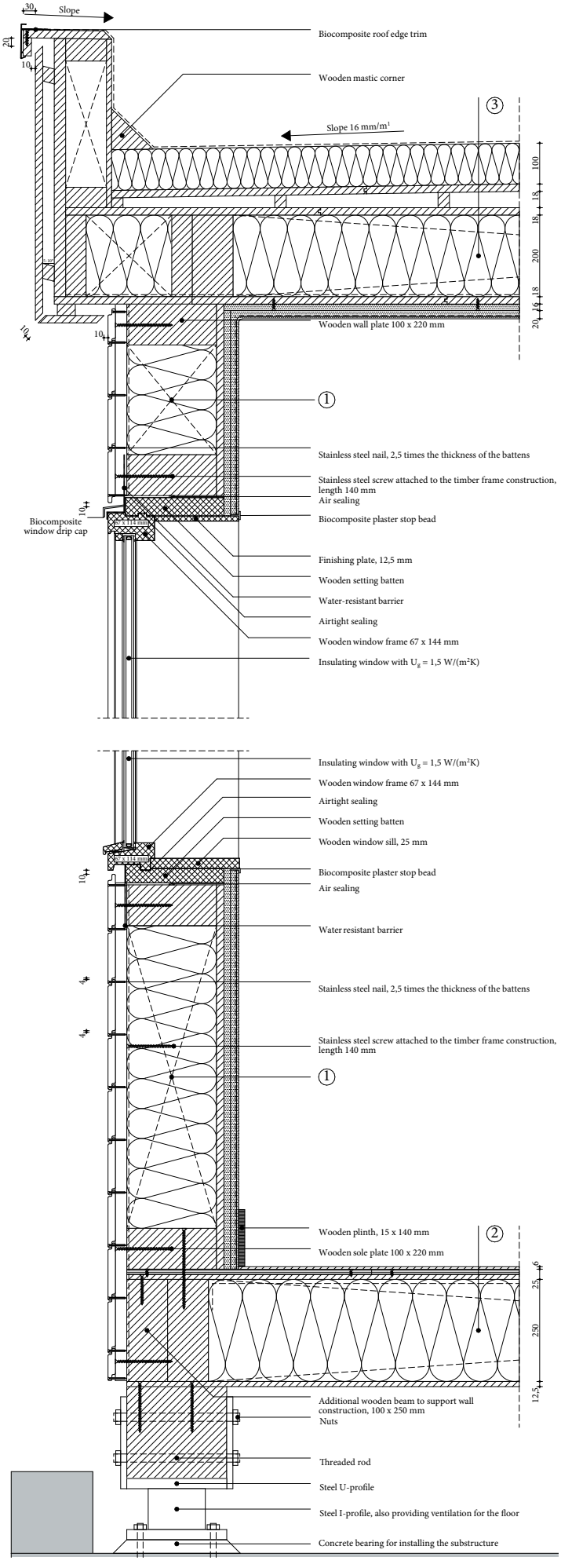

Figure 85, Detail of V1 (below) & V2 (top) configuration 6, own illustration

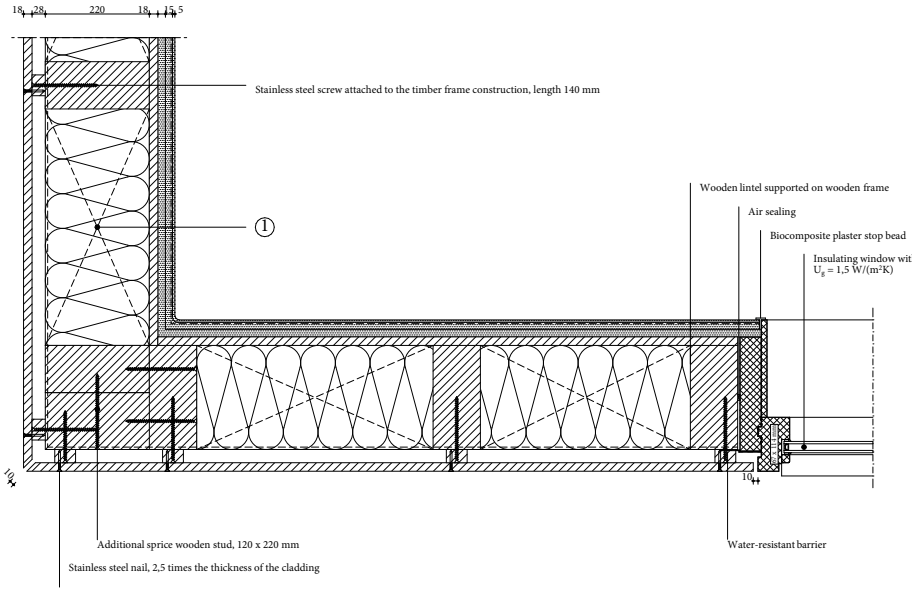

Figure 86, Detail of H1 configuration 6, own illustration

❶ Wall construction build-up, RC-value: 5.09 (m²K)/W

- Horizontal wooden cladding, 18 mm;
- Vertical spruce cladding batten forming ventilated cavity, 28 x 44 mm, center-to-center 600 mm;
- Water resistant vapour-permeable membrane;
- Timber frame construction, 100 x 220 mm, center-to-center 600 mm;
- Flexible flax insulation, placed between construction (λ ≤ 0.035 W/mK), 180 + 40 mm;
- Biobased construction board, 18 mm;
- Clay base plate, 16 mm;
- Rough base clay plaster, 15 mm;
- Jute reinforcement mesh;
- Finishing clay plaster, 5 mm.

❷ Floor construction build-up, RC-value: 4.65 (m²K)/W

- Finishing board, 6 mm;
- Biobased wooden construction board, 12.5 mm;
- Biobased wooden construction board, perpendicular on the other plate, 12.5 mm;
- Vapour-retarding and airtight membrane with a variable vapour diffusion resistanance;
- Flexible hemp fiber insulation placed between construction (λ ≤ 0.043 W/(mK), 250 mm;
- Wooden beams 100 x 250 mm, center-to-center 600 mm;
- Biobased wooden construction board, 12.5 mm.

❸ Roof construction build-up, RC-value: 6.71 (m²K)/W

- EPDM glued on underlayment to prevent roof covering from lifting;
- Pressure-resistant woodfibre insulation plate (λ ≤ 0.042 W/(mK), 100 mm;
- Biobased wooden construction board, 18 mm;
- Sloped wooden battens for drainage at an angle of 16 mm/m[1], 28 x 24 mm;
- Biobased wooden construction board, 18 mm;
- Flexible hemp fiber insulation placed between construction (λ ≤ 0.043 W/(mK), 200 mm;
- Wooden beams 100 x 200 mm, center-to-center 600 mm;
- Vapour-retarding and airtight membrane with a variable vapour diffusion resistanance;
- Biobased wooden construction board, 18 mm;
- Clay base plate, 16 mm;
- Rough base clay plaster, 15 mm;
- Jute reinforcement mesh;
- Finishing clay plaster, 5 mm.

Detail configuration 7 - flax insulation with cork façade

The seventh detail configuration consists of flexible flax insulation placed between the studs of the timber construction frame. A water-resistant, vapour-permeable membrane is used to protect the structure against moisture penetration, followed by a bio-based, diffusion-open board for stability and cork façade application. This board allows the expanded insulation corkboard to be attached and bonded with cork mortar. A second layer of mortar secures the cork cladding panels. On the interior, the timber frame is finished with a diffusion-open construction board and a clay board together with a two-layer clay plaster

Used materials in this configuration

Expanded cork agglomerates finishing plate

The boards serve both as insulation and finishing, differing in density and porosity. Insulating cork is more porous with better thermal conductivity, while façade cork is weather-resistant. The finishing plate is mechanically attached and glued to a cork insulation plate, both attached on a MDF-underlayment plate.

MDF

The bio-based, diffusion-open MDF construction board forms a suitable underlayment for the cork mortar to glue and mechanically attach the cork finishing plates. Next this gives the structure the required stability but can not fully protect the structure against moisture so a water-resistant, vapour-permeable membrane is necessary.

Untreated wood

Untreated spruce wood is mostly used as the structural component in timber frame constructions. This system consists of vertically placed wooden beams, regularly spaced between a horizontal sole plate and a top wall plate. Since untreated wood is used, it must be protected against moisture ingress

Flax insulation

Flexible flax insulation forms the insulating layer which can be placed between the horizontal wooden beams of the timber frame construction. Hereby it is important to apply a clamp. Additionally the material can also be used to fill gaps within the structure.

ESB

ESB is placed on the interior surface of the structure. Next to the pressure resistant wood fibre plate is also gives stability to the structure. The main purpose, however, is to allow for secure mechanical attachment for indoor hangings. The board is also suitable for relatively humid environments.

Clay plaster

To apply a clay paster a clay is first needed to form a correct underlayment for the clay plaster. The plaster must be applied in 2 layers consisting of a rough base layer of 15 mm and a finishing layer of 5 mm. In between a jute reinforcement mesh is recommended to prevent cracking.

Necessary design principles

Façade cork finish

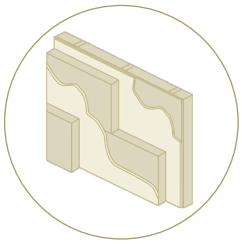

Attachment expanded cork finishing plate

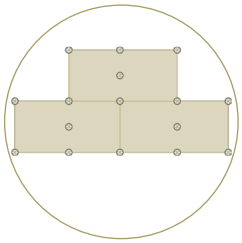

Distances placement cork plates

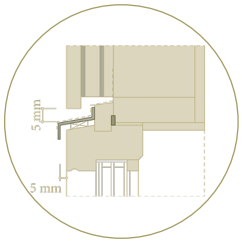

Connection façade bottom window frame

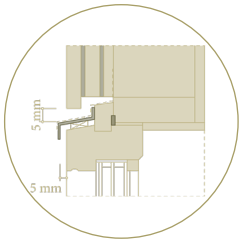

Connection façade top window frame

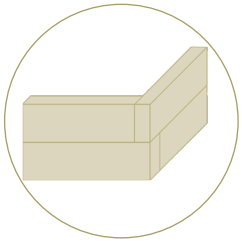

Connection corner cork plates

Cork insulation

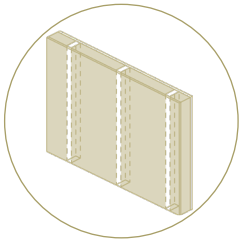

Placement expanded cork insulation plate

MDF board

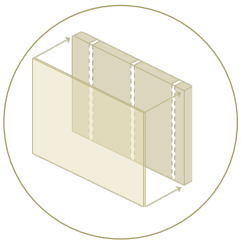

Attachment MDF board

Timber frame construction

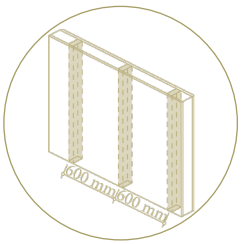

Distances wooden studs in the timber frame construction

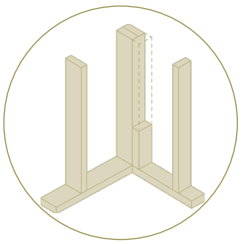

Corner connection of the timber frame construction

Flexible flax insulation

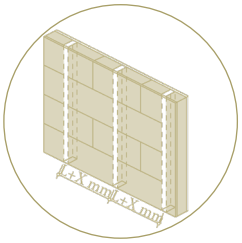

Placement flexible flax insulation plates

ESB board & clay finish

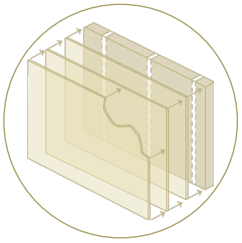

Attachment ESB construction board & clay plaster finish

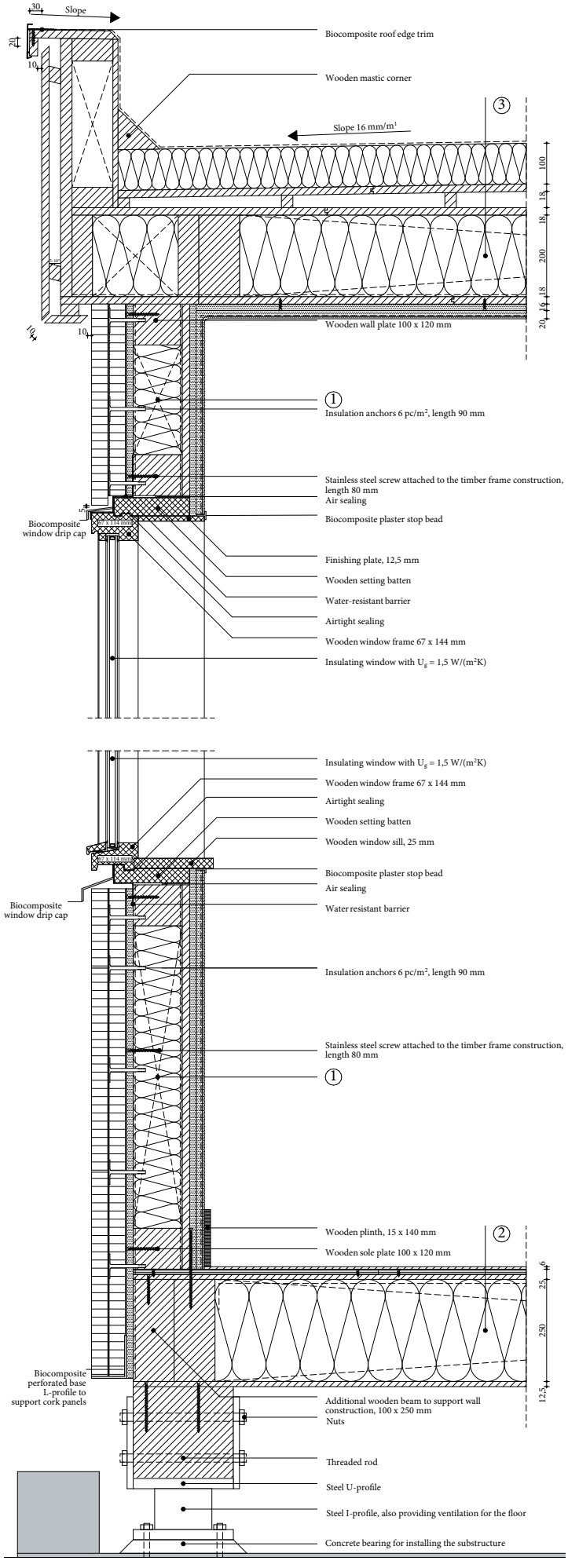

Figure 87, Detail of V1 (below) & V2 (top) configuration 7, own illustration

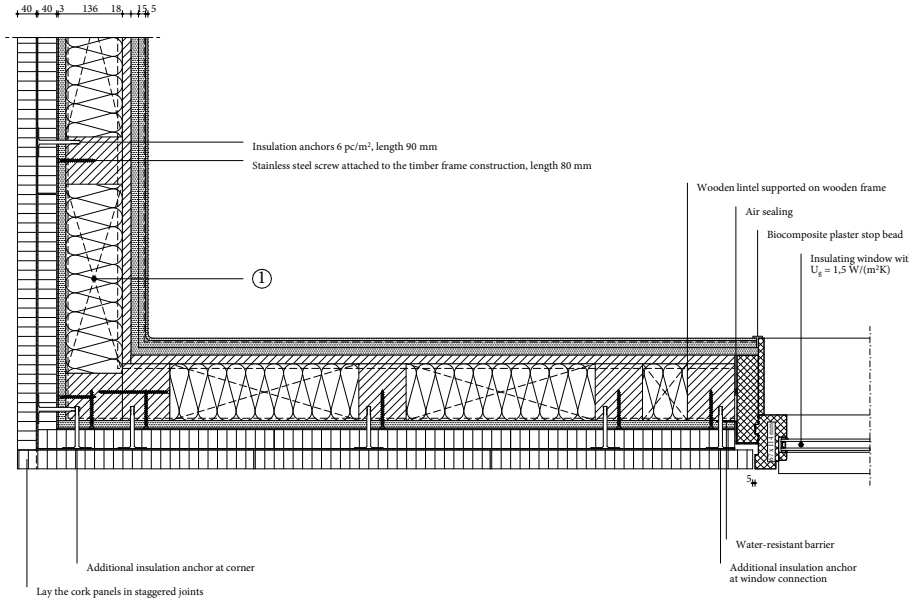

Figure 88, Detail of H1 configuration 7, own illustration

❶ Wall construction build-up, RC-value: 4.89 (m²K)/W

- Cork cladding panels (λ ≤ 0.043 W/mK), 40 mm;
- Cork mortar, 3 mm;
- Expanded insulation corkboard (λ ≤ 0.039 W/mK), 40 mm;
- Cork mortar, 3 mm;
- Biobased diffusion open construction board, 16mm;
- Water resistant vapour-permeable membrane;
- Timber frame construction, 100 x 120 mm, center-to-center 500 mm;
- Flexible flax insulation, placed between construction (λ ≤ 0.035 W/mK), 120 mm;
- Vapour-retarding and airtight membrane with a variable vapour diffusion resistance;
- Biobased construction board, 18 mm;
- Clay base plate, 16 mm;
- Rough base clay plaster, 15 mm;
- Jute reinforcement mesh;
- Finishing clay plaster, 5 mm.

❷ Floor construction build-up, RC-value: 4.65 (m²K)/W

- Finishing board, 6 mm;
- Biobased wooden construction board, 12.5 mm;
- Biobased wooden construction board, perpendicular on the other plate, 12.5 mm;
- Vapour-retarding and airtight membrane with a variable vapour diffusion resistanance;
- Flexible hemp fiber insulation placed between construction (λ ≤ 0.043 W/(mK), 250 mm;
- Wooden beams 100 x 250 mm, center-to-center 600 mm;
- Biobased wooden construction board, 12.5 mm.

❸ Roof construction build-up, RC-value: 6.71 (m²K)/W

- EPDM glued on underlayment to prevent roof covering from lifting;
- Pressure-resistant woodfibre insulation plate (λ ≤ 0.042 W/(mK), 100 mm;
- Biobased wooden construction board, 18 mm;
- Sloped wooden battens for drainage at an angle of 16 mm/m[1], 28 x 24 mm;
- Biobased wooden construction board, 18 mm;
- Flexible hemp fiber insulation placed between construction (λ ≤ 0.043 W/(mK), 200 mm;
- Wooden beams 100 x 200 mm, center-to-center 600 mm;
- Vapour-retarding and airtight membrane with a variable vapour diffusion resistanance;
- Biobased wooden construction board, 18 mm;
- Clay base plate, 16 mm;
- Rough base clay plaster, 15 mm;
- Jute reinforcement mesh;
- Finishing clay plaster, 5 mm.

Detail configuration 8 - wood fibre insulation with wooden façade

The eighth detail configuration consists of flexible wood fibre insulation placed between the studs of the timber construction frame. To protect the construction against water and mould growth a pressure-resistant wood fibre board is placed at the outside of the construction. This board also enables the attachment of the wooden battens and the wooden façade. On the interior, the timber frame is finished with a diffusion-open construction board and a clay board together with a two-layer clay plaster

Used materials in this configuration

Façade finish

Wooden cladding is used as the finish of this detail configuration providing both aesthetic appeal and the first protection against the weather. It is mechanically fixed agains horizontal and vertical wooden battens.

Treated wood

Treated wood is used to form the vertical framework. Since this wood is in direct contact with the weather, it must be resistant to weather influences. The techniques to treat the wood are able to make the wood weather resistant.

Untreated wood

Untreated spruce wood is mostly used as the structural component in timber frame constructions. This system consists of vertically placed wooden beams, regularly spaced between a horizontal sole plate and a top wall plate. Since untreated wood is used, it must be protected against moisture ingress.

Pressure resistant wood fibre plate

Placed on the exterior surface of the structure, a pressure resistant wood fibre plate serve multiple purposes. First it protects the underlying construction, allows for secure mechanical attachment of the wooden cladding and gives stability, lastly it adds an insulating layer to improve thermal performance.

Flexible wood fibre insulations

Flexible wood fibre insulation forms the insulating layer which can be placed between the horizontal wooden beams of the timber frame construction. Hereby it is important to apply a clamp. Additionally the material can also be used to fill gaps within the structure

ESB

ESB is placed on the interior surface of the structure. Next to the pressure resistant wood fibre plate is also gives stability to the structure. The main purpose, however, is to allow for secure mechanical attachment for indoor hangings. The board is also suitable for relatively humid environments.

Clay plaster

To apply a clay paster a clay is first needed to form a correct underlayment for the clay plaster. The plaster must be applied in 2 layers consisting of a rough base layer of 15 mm and a finishing layer of 5 mm. In between a jute reinforcement mesh is recommended to prevent cracking.

Necessary design principles

Façade wooden finish

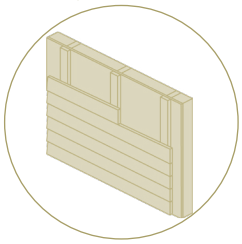

Attachment horizontal wooden cladding

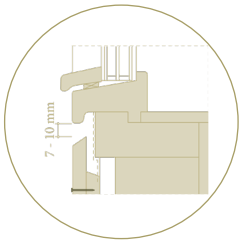

Connection façade bottom window frame

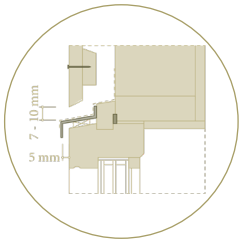

Connection façade top window frame

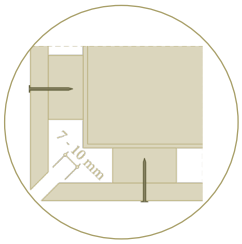

Connection corner façade

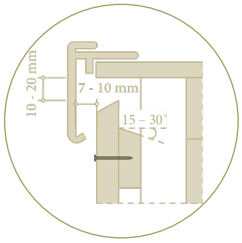

Connection façade roof

Wood fibre plate

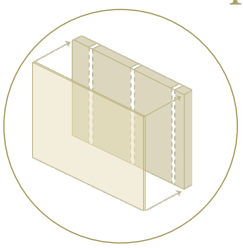

Attachment wooden wood fibre board

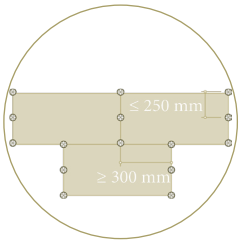

Distances placement wooden wood fibre board

Timber frame construction

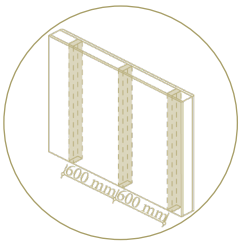

Distances wooden studs in the timber frame construction

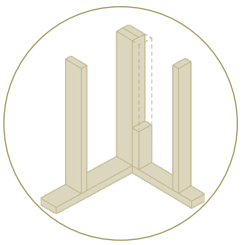

Corner connection of the timber frame construction

Flexible wood fibre insulation

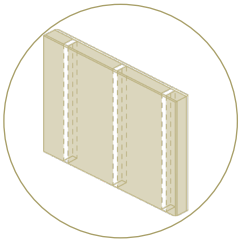

Placement flexible wood fibre insulation plates

ESB board & clay finish

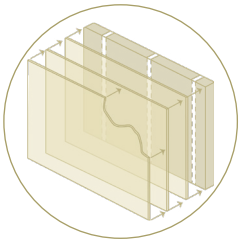

Attachment ESB construction board & clay plaster finish

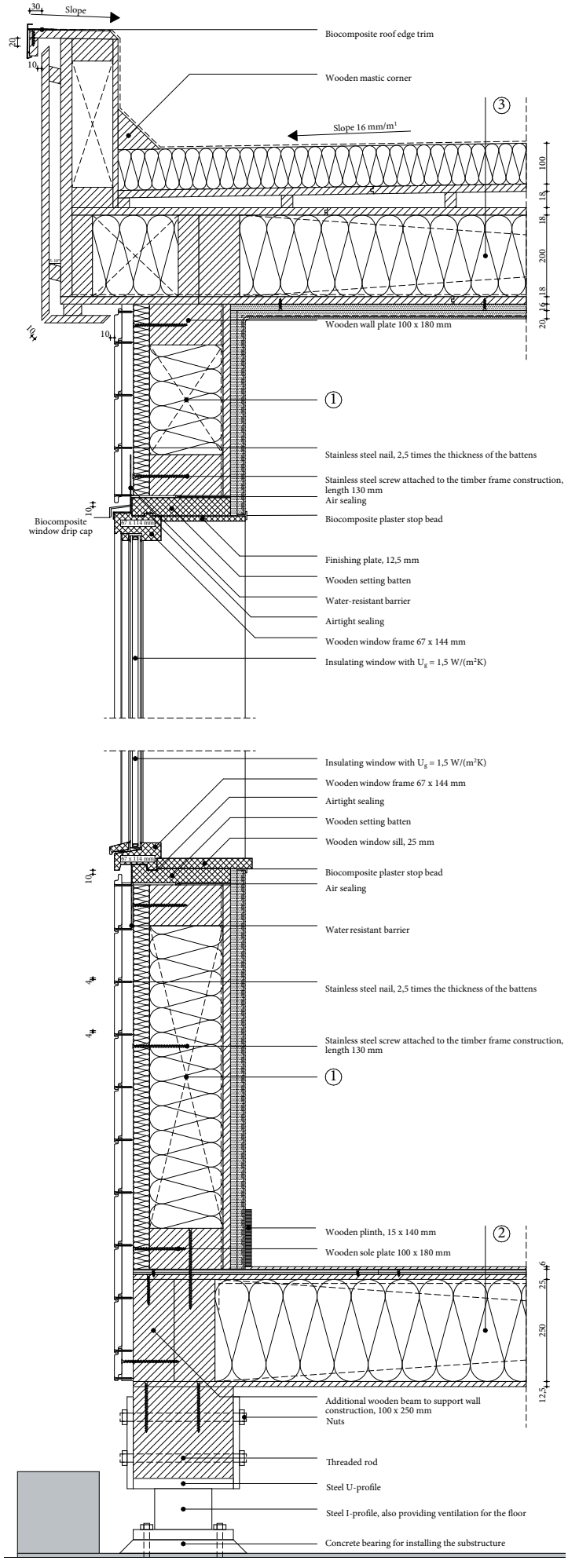

Figure 89, Detail of V1 (below) & V2 (top) configuration 8, own illustration

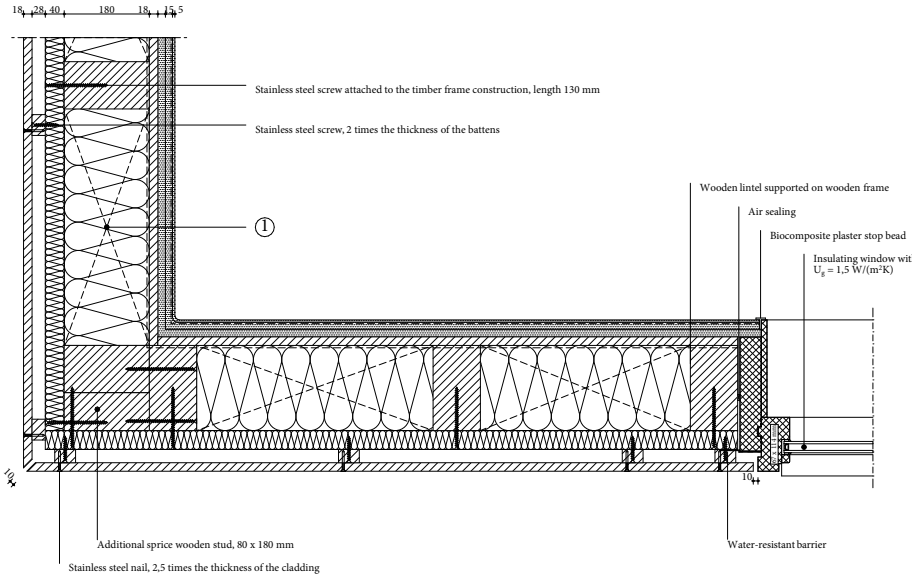

Figure 90, Detail of H1 configuration 8, own illustration

❶ Wall construction build-up, RC-value: 5.08 (m²K)/W

- Horizontal wooden cladding, 18 mm;
- Vertical spruce cladding batten forming ventilated cavity, 28 x 44 mm, center-to-center 600 mm;
- Pressure-resistant woodfibre insulation plate (λ ≤ 0.042 W/mK), 40 mm;
- Timber frame construction, 100 x 180 mm, center-to-center 600 mm;
- Flexible wood fibre insulation, placed between construction (λ ≤ 0.038 W/mK), 180 mm;
- Vapour-retarding and airtight membrane with a variable vapour diffusion resistance;
- Biobased construction board, 18 mm;
- Clay base plate, 16 mm;
- Rough base clay plaster, 15 mm;
- Jute reinforcement mesh;
- Finishing clay plaster, 5 mm.

❷ Floor construction build-up, RC-value: 4.65 (m²K)/W

- Finishing board, 6 mm;
- Biobased wooden construction board, 12.5 mm;
- Biobased wooden construction board, perpendicular on the other plate, 12.5 mm;
- Vapour-retarding and airtight membrane with a variable vapour diffusion resistanance;
- Flexible hemp fiber insulation placed between construction (λ ≤ 0.043 W/(mK), 250 mm;
- Wooden beams 100 x 250 mm, center-to-center 600 mm;
- Biobased wooden construction board, 12.5 mm.

❸ Roof construction build-up, RC-value: 6.71 (m²K)/W

- EPDM glued on underlayment to prevent roof covering from lifting;
- Pressure-resistant woodfibre insulation plate (λ ≤ 0.042 W/(mK), 100 mm;
- Biobased wooden construction board, 18 mm;
- Sloped wooden battens for drainage at an angle of 16 mm/m[1], 28 x 24 mm;
- Biobased wooden construction board, 18 mm;
- Flexible hemp fiber insulation placed between construction (λ ≤ 0.043 W/(mK), 200 mm;
- Wooden beams 100 x 200 mm, center-to-center 600 mm;
- Vapour-retarding and airtight membrane with a variable vapour diffusion resistanance;
- Biobased wooden construction board, 18 mm;
- Clay base plate, 16 mm;
- Rough base clay plaster, 15 mm;
- Jute reinforcement mesh;
- Finishing clay plaster, 5 mm.

Detail configuration 9 - wood fibre insulation with cork façade

The ninth detail configuration consists of flexible wood fibre insulation placed between the studs of the timber construction frame. A water-resistant, vapour-permeable membrane is used to protect the structure against moisture penetration, followed by a bio-based, diffusion-open board for stability and cork façade application. This board allows the expanded insulation corkboard to be attached and bonded with cork mortar. A second layer of mortar secures the cork cladding panels. On the interior, the timber frame is finished with a diffusion-open construction board and a clay board together with a two-layer clay plaster

Used materials in this configuration

Expanded cork agglomerates finishing plate

The boards serve both as insulation and finishing, differing in density and porosity. Insulating cork is more porous with better thermal conductivity, while façade cork is weather-resistant. The finishing plate is mechanically attached and glued to a cork insulation plate, both attached on a MDF-underlayment plate.

MDF

The bio-based, diffusion-open MDF construction board forms a suitable underlayment for the cork mortar to glue and mechanically attach the cork finishing plates. Next this gives the structure the required stability but can not fully protect the structure against moisture so a water-resistant, vapour-permeable membrane is necessary.

Untreated wood

Untreated spruce wood is mostly used as the structural component in timber frame constructions. This system consists of vertically placed wooden beams, regularly spaced between a horizontal sole plate and a top wall plate. Since untreated wood is used, it must be protected against moisture ingress.

Flexible wood fibre insulations

Flexible wood fibre insulation forms the insulating layer which can be placed between the horizontal wooden beams of the timber frame construction. Hereby it is important to apply a clamp. Additionally the material can also be used to fill gaps within the structure.

ESB

ESB is placed on the interior surface of the structure. Next to the pressure resistant wood fibre plate is also gives stability to the structure. The main purpose, however, is to allow for secure mechanical attachment for indoor hangings. The board is also suitable for relatively humid environments.

Clay plaster

To apply a clay paster a clay is first needed to form a correct underlayment for the clay plaster. The plaster must be applied in 2 layers consisting of a rough base layer of 15 mm and a finishing layer of 5 mm. In between a jute reinforcement mesh is recommended to prevent cracking.

Necessary design principles

Façade cork finish

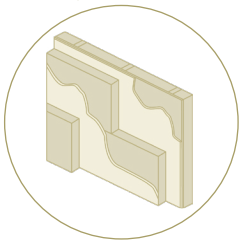

Attachment expanded cork finishing plate

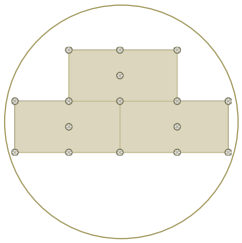

Distances placement cork plates

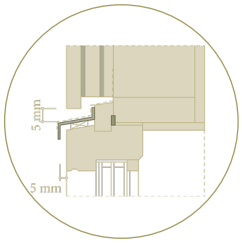

Connection façade bottom window frame

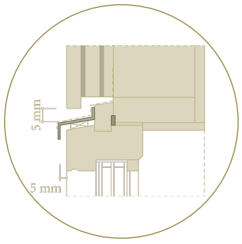

Connection façade top window frame

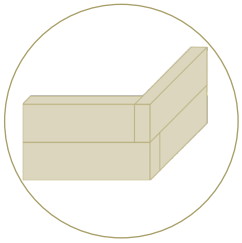

Connection corner cork plates

MDF board

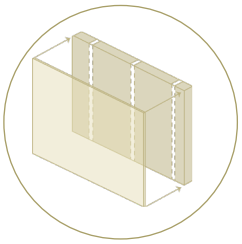

Attachment MDF board

Timber frame construction

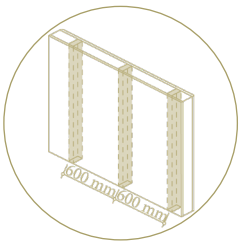

Distances wooden studs in the timber frame construction

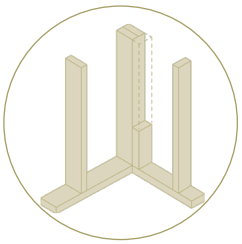

Corner connection of the timber frame construction

Flexible wood fibre insulation

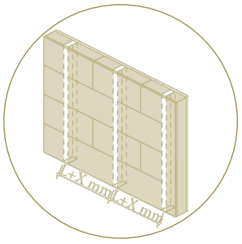

Placement wood fibre insulation plates

ESB board & clay finish

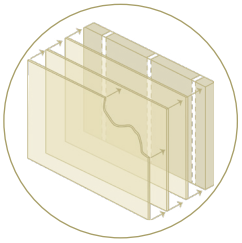

Attachment ESB construction board & clay plaster finish

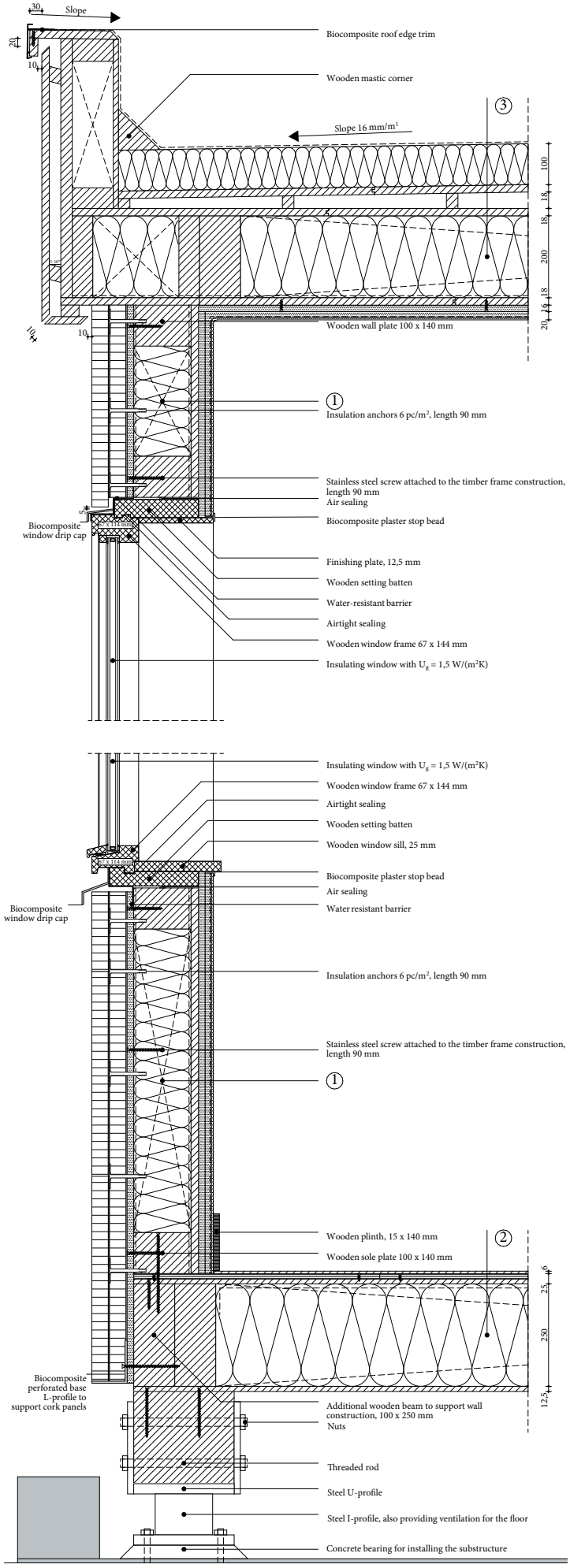

Figure 91, Detail of V1 (below) & V2 (top) configuration 9, own illustration

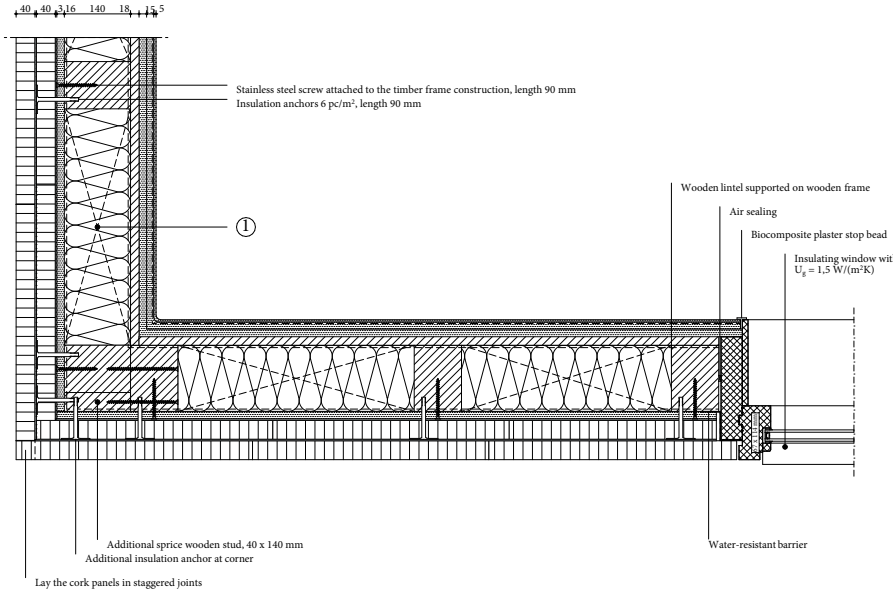

Figure 92, Detail of H1 configuration 9, own illustration

❶ Wall construction build-up, RC-value: 5.28 (m²K)/W

- Cork cladding panels (λ ≤ 0.043 W/mK), 40 mm;
- Cork mortar, 3 mm;
- Expanded insulation corkboard (λ ≤ 0.039 W/mK), 40 mm;
- Cork mortar, 3 mm;
- Biobased diffusion open construction board, 16mm;
- Water resistant vapour-permeable membrane;
- Timber frame construction, 100 x 140 mm, center-to-center 600 mm;
- Wood fibre insulation, placed between construction (λ ≤ 0.038 W/mK), 140 mm;
- Vapour-retarding and airtight membrane with a variable vapour diffusion resistance;
- Biobased construction board, 18 mm;
- Clay base plate, 16 mm;
- Rough base clay plaster, 15 mm;
- Jute reinforcement mesh;
- Finishing clay plaster, 5 mm.

❷ Floor construction build-up, RC-value: 4.65 (m²K)/W

- Finishing board, 6 mm;
- Biobased wooden construction board, 12.5 mm;
- Biobased wooden construction board, perpendicular on the other plate, 12.5 mm;
- Vapour-retarding and airtight membrane with a variable vapour diffusion resistanance;
- Flexible hemp fiber insulation placed between construction (λ ≤ 0.043 W/(mK), 250 mm;
- Wooden beams 100 x 250 mm, center-to-center 600 mm;
- Biobased wooden construction board, 12.5 mm.

❸ Roof construction build-up, RC-value: 6.71 (m²K)/W

- EPDM glued on underlayment to prevent roof covering from lifting;
- Pressure-resistant woodfibre insulation plate (λ ≤ 0.042 W/(mK), 100 mm;
- Biobased wooden construction board, 18 mm;
- Sloped wooden battens for drainage at an angle of 16 mm/m[1], 28 x 24 mm;
- Biobased wooden construction board, 18 mm;
- Flexible hemp fiber insulation placed between construction (λ ≤ 0.043 W/(mK), 200 mm;
- Wooden beams 100 x 200 mm, center-to-center 600 mm;
- Vapour-retarding and airtight membrane with a variable vapour diffusion resistanance;
- Biobased wooden construction board, 18 mm;
- Clay base plate, 16 mm;
- Rough base clay plaster, 15 mm;
- Jute reinforcement mesh;
- Finishing clay plaster, 5 mm.

Detail configuration 10 - straw insulation with wooden façade

The tenth detail configuration consists of blow-in straw insulation that is sprayed between the studs of the timber construction frame and the construction boards with a density of 100 kg/m³. The straw only needs to be protected against water and mould growth by placing a diffusion-open construction board on the exterior side of the timber frame. This board also provides structural stability and serves as a base for the timber façade system. On the interior, the timber frame is finished with a diffusion-open construction board and a clay board together with a two-layer clay plaster.

Used materials in this configuration

Façade finish

Wooden cladding is used as the finish of this detail configuration providing both aesthetic appeal and the first protection against the weather. It is mechanically fixed agains horizontal and vertical wooden battens.

Treated wood

Treated wood is used to form the vertical framework. Since this wood is in direct contact with the weather, it must be resistant to weather influences. The techniques to treat the wood are able to make the wood weather resistant.

Untreated wood

Untreated spruce wood is mostly used as the structural component in timber frame constructions. This system consists of vertically placed wooden beams, regularly spaced between a horizontal sole plate and a top wall plate. Since untreated wood is used, it must be protected against moisture ingress.

MDF

The bio-based, diffusion-open MDF construction board forms a suitable underlayment for the attachment of the vertical battens for the wooden finish. Next, it gives the structure the required stability. Blow-in straw resists moisture and humidity fluctuations, ensuring sufficient protection by the MDF.

Blow-in straw insulation

Blow-in straw is blown between the vertical studs of the timber frame construction which is covered on both sides with a biobased construction board. Straw fibres of various lengths are blown in the construction where the density determines the thermal conductivity of the straw

ESB

ESB is placed on the interior surface of the structure. Next to the pressure resistant wood fibre plate is also gives stability to the structure. The main purpose, however, is to allow for secure mechanical attachment for indoor hangings. The board is also suitable for relatively humid environments.

Clay plaster

To apply a clay paster a clay is first needed to form a correct underlayment for the clay plaster. The plaster must be applied in 2 layers consisting of a rough base layer of 15 mm and a finishing layer of 5 mm. In between a jute reinforcement mesh is recommended to prevent cracking.

Necessary design principles

Façade wooden finish

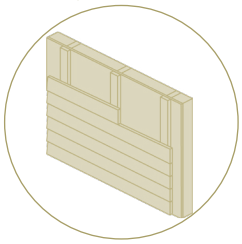

Attachment horizontal wooden cladding

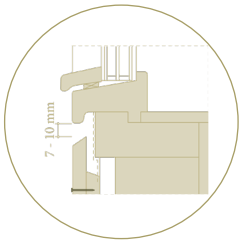

Connection façade bottom window frame

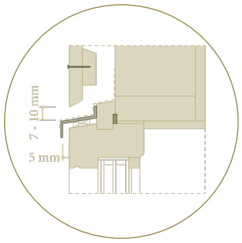

Connection façade top window frame

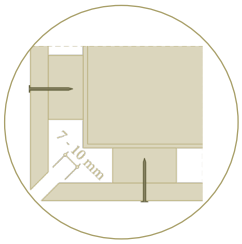

Connection corner façade

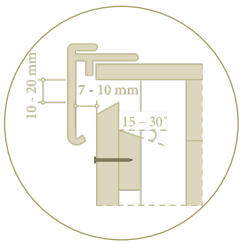

Connection façade roof

MDF board

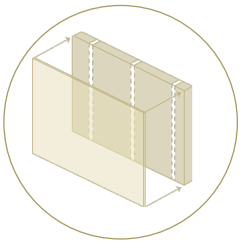

Attachment MDF board

Timber frame construction

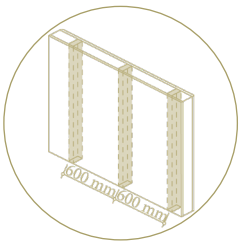

Distances wooden studs in the timber frame construction

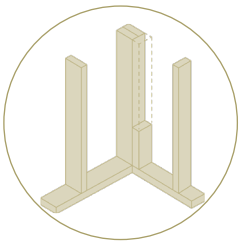

Corner connection of the timber frame construction

Blow-in straw

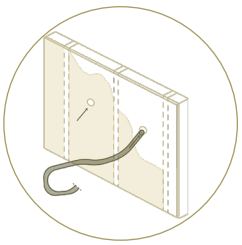

Application blow-in straw

ESB board & clay finish

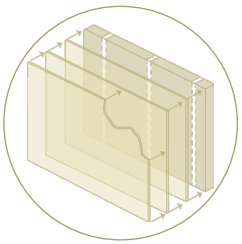

Attachment ESB construction board & clay plaster finish

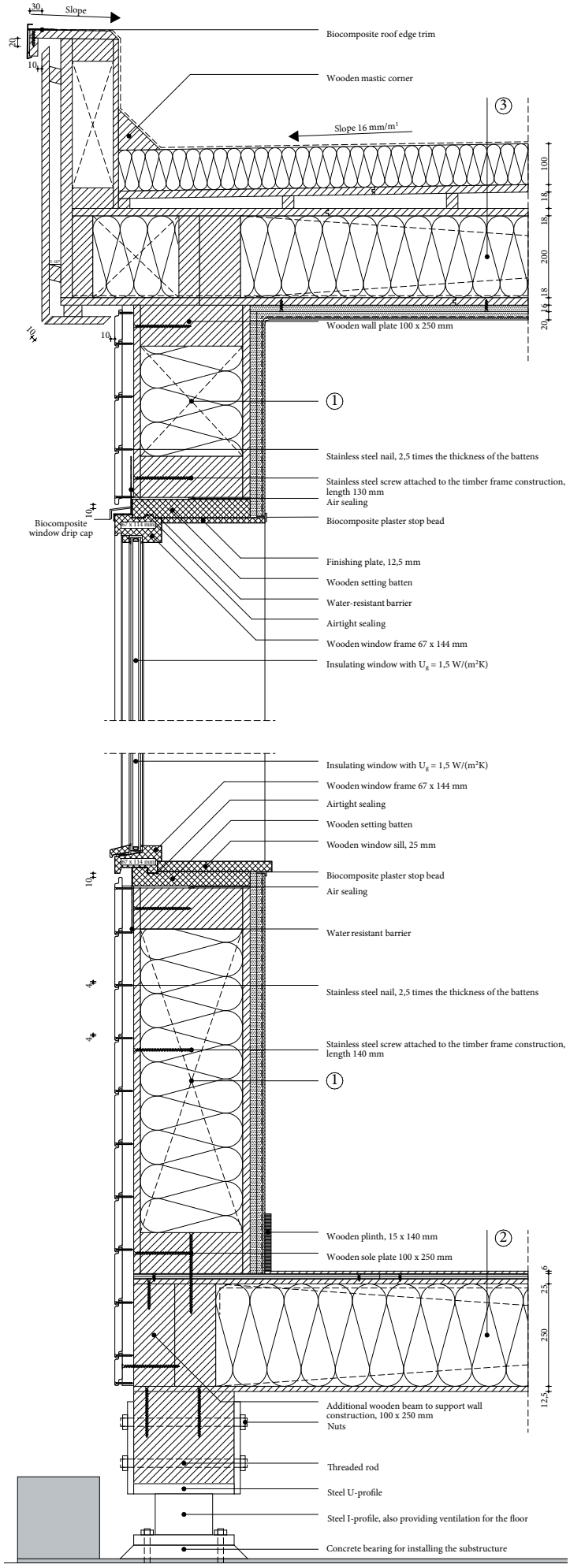

Figure 93, Detail of V1 (below) & V2 (top) configuration 10, own illustration

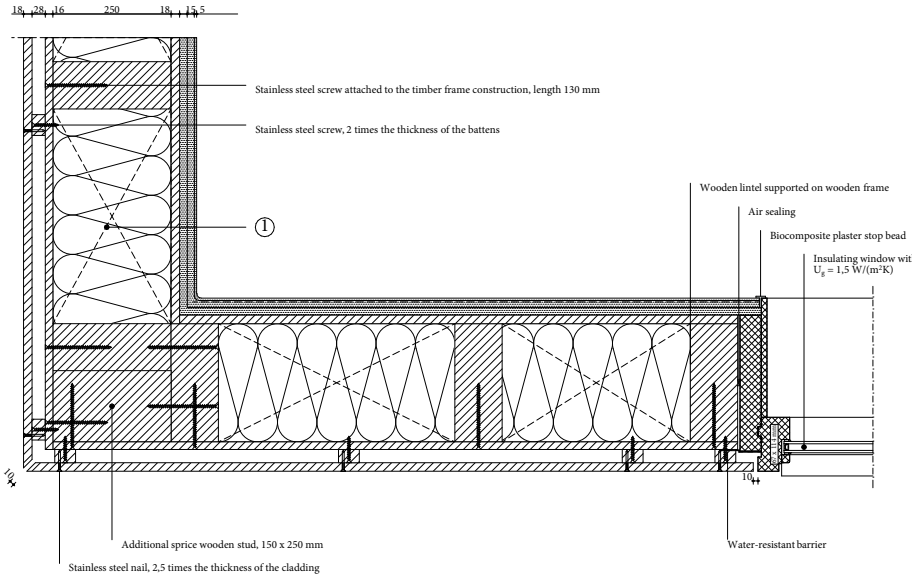

Figure 94 ,Detail of H1 configuration 10, own illustration

1 Wall construction build-up, RC-value: 4.92 (m²K)/W

- Horizontal wooden cladding, 18 mm;
- Vertical spruce cladding batten forming ventilated cavity, 28 x 44 mm, center-to-center 600 mm;
- Biobased diffusion open construction board, 16mm;
- Timber frame construction, 100 x 250 mm, center-to-center 600 mm;
- Blow in straw blown between construction & construction boards (λ ≤ 0.043 W/mK), 250 mm;
- Biobased construction board, 18 mm;
- Clay base plate, 16 mm;
- Rough base clay plaster, 15 mm;
- Jute reinforcement mesh;
- Finishing clay plaster, 5 mm.

2 Floor construction build-up, RC-value: 4.65 (m²K)/W

- Finishing board, 6 mm;
- Biobased wooden construction board, 12.5 mm;
- Biobased wooden construction board, perpendicular on the other plate, 12.5 mm;
- Vapour-retarding and airtight membrane with a variable vapour diffusion resistanance;
- Flexible hemp fiber insulation placed between construction (λ ≤ 0.043 W/(mK), 250 mm;
- Wooden beams 100 x 250 mm, center-to-center 600 mm;
- Biobased wooden construction board, 12.5 mm.

3 Roof construction build-up, RC-value: 6.71 (m²K)/W

- EPDM glued on underlayment to prevent roof covering from lifting;
- Pressure-resistant woodfibre insulation plate (λ ≤ 0.042 W/(mK), 100 mm;
- Biobased wooden construction board, 18 mm;
- Sloped wooden battens for drainage at an angle of 16 mm/m[1], 28 x 24 mm;
- Biobased wooden construction board, 18 mm;
- Flexible hemp fiber insulation placed between construction (λ ≤ 0.043 W/(mK), 200 mm;
- Wooden beams 100 x 200 mm, center-to-center 600 mm;
- Vapour-retarding and airtight membrane with a variable vapour diffusion resistanance;
- Biobased wooden construction board, 18 mm;
- Clay base plate, 16 mm;
- Rough base clay plaster, 15 mm;
- Jute reinforcement mesh;
- Finishing clay plaster, 5 mm.

Detail configuration 11 - straw insulation with cork façade

The eleventh detail configuration consists of blow-in straw insulation that is sprayed between the studs of the timber construction frame and the construction boards with a density of 100 kg/m³. A water-resistant, vapour-permeable membrane is used to protect the structure against moisture penetration, followed by a bio-based, diffusion-open board for stability and cork façade application. This board allows the expanded insulation corkboard to be attached and bonded with cork mortar. A second layer of mortar secures the cork cladding panels. On the interior, the timber frame is finished with a diffusion-open construction board and a clay board together with a two-layer clay plaster

Used materials in this configuration

Expanded cork agglomerates finishing plate

The boards serve both as insulation and finishing, differing in density and porosity. Insulating cork is more porous with better thermal conductivity, while façade cork is weather-resistant. The finishing plate is mechanically attached and glued to a cork insulation plate, both attached on a MDF-underlayment plate.

MDF

The bio-based, diffusion-open MDF construction board forms a suitable underlayment for the cork mortar to glue and mechanically attach the cork finishing plates. Next this gives the structure the required stability but can not fully protect the structure against moisture so a water-resistant, vapour-permeable membrane is necessary.

Untreated wood

Untreated spruce wood is mostly used as the structural component in timber frame constructions. This system consists of vertically placed wooden beams, regularly spaced between a horizontal sole plate and a top wall plate. Since untreated wood is used, it must be protected against moisture ingress.

Blow-in straw insulation

Blow-in straw is blown between the vertical studs of the timber frame construction which is covered on both sides with a biobased construction board. Straw fibres of various lengths are blown in the construction where the density determines the thermal conductivity of the straw.

ESB

ESB is placed on the interior surface of the structure. Next to the pressure resistant wood fibre plate is also gives stability to the structure. The main purpose, however, is to allow for secure mechanical attachment for indoor hangings. The board is also suitable for relatively humid environments.

Clay plaster

To apply a clay paster a clay is first needed to form a correct underlayment for the clay plaster. The plaster must be applied in 2 layers consisting of a rough base layer of 15 mm and a finishing layer of 5 mm. In between a jute reinforcement mesh is recommended to prevent cracking.

Necessary design principles

Façade cork finish

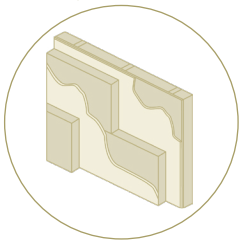

Attachment expanded cork finishing plate

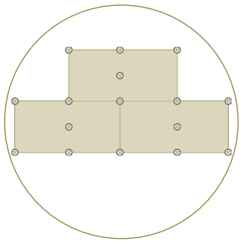

Distances placement cork plates

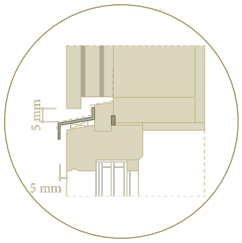

Connection façade bottom window frame

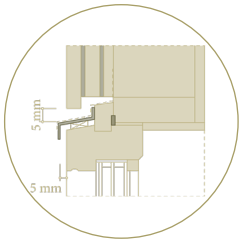

Connection façade top window frame

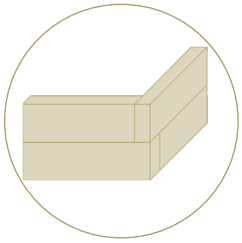

Connection corner cork plates

MDF board

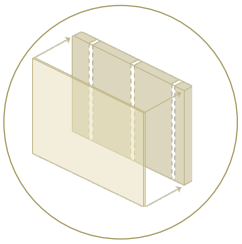

Attachment MDF board

Timber frame construction

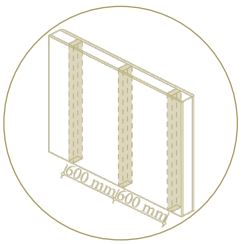

Distances wooden studs in the timber frame construction

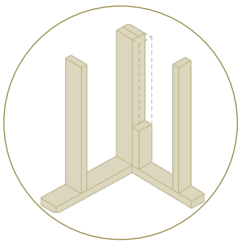

Corner connection of the timber frame construction

Flexible wood fibre insulation

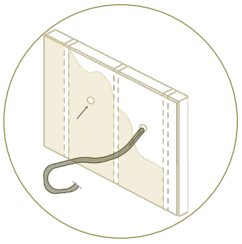

Application blow-in straw

ESB board & clay finish

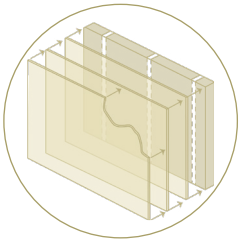

Attachment ESB construction board & clay plaster finish

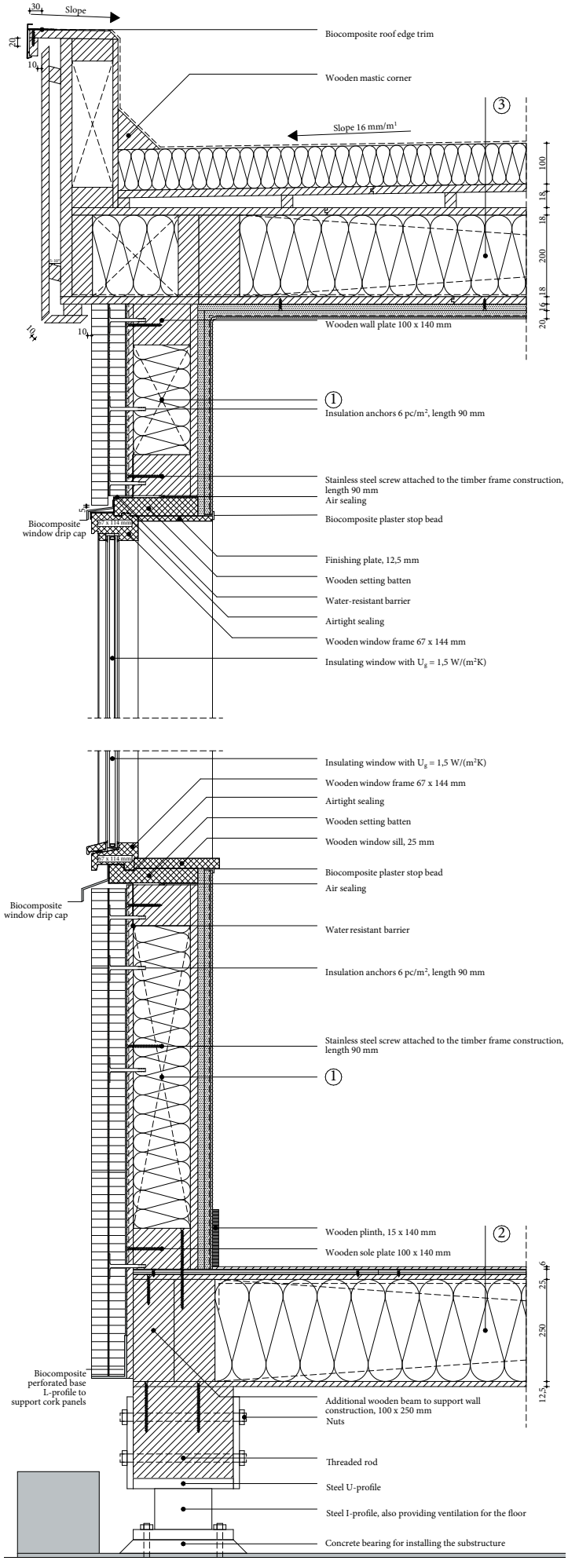

Figure 95, Detail of V1 (below) & V2 (top) configuration 11, own illustration

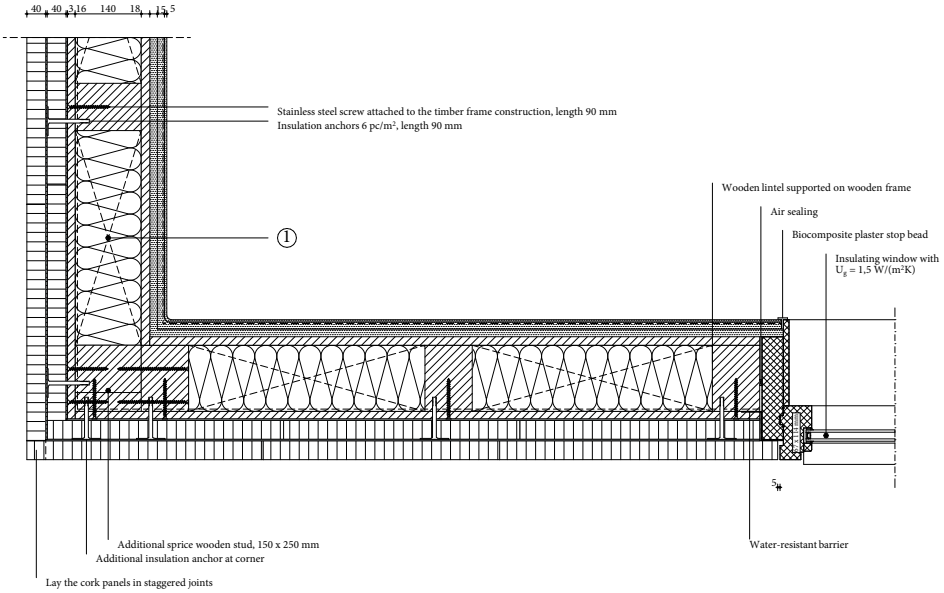

Figure 96, Detail of H1 configuration 11, own illustration

1 Wall construction build-up, RC-value: 4.78 (m²K)/W

- Cork cladding panels (λ ≤ 0.043 W/mK), 40 mm;
- Cork mortar, 3 mm;
- Expanded insulation corkboard (λ ≤ 0.039 W/mK), 40 mm;
- Cork mortar, 3 mm;
- Biobased diffusion open construction board, 16mm;
- Water resistant vapour-permeable membrane;
- Timber frame construction, 100 x 140 mm, center-to-center 600 mm;
- Blow in straw placed between construction & construction boards (λ ≤ 0.043 W/mK), 140 mm;
- Biobased construction board, 18 mm;
- Clay base plate, 16 mm;
- Rough base clay plaster, 15 mm;
- Jute reinforcement mesh;
- Finishing clay plaster, 5 mm.

2 Floor construction build-up, RC-value: 4.65 (m²K)/W

- Finishing board, 6 mm;
- Biobased wooden construction board, 12.5 mm;
- Biobased wooden construction board, perpendicular on the other plate, 12.5 mm;
- Vapour-retarding and airtight membrane with a variable vapour diffusion resistanance;
- Flexible hemp fiber insulation placed between construction (λ ≤ 0.043 W/(mK), 250 mm;
- Wooden beams 100 x 250 mm, center-to-center 600 mm;
- Biobased wooden construction board, 12.5 mm.

3 Roof construction build-up, RC-value: 6.71 (m²K)/W

- EPDM glued on underlayment to prevent roof covering from lifting;
- Pressure-resistant woodfibre insulation plate (λ ≤ 0.042 W/(mK), 100 mm;
- Biobased wooden construction board, 18 mm;
- Sloped wooden battens for drainage at an angle of 16 mm/m[1], 28 x 24 mm;
- Biobased wooden construction board, 18 mm;
- Flexible hemp fiber insulation placed between construction (λ ≤ 0.043 W/(mK), 200 mm;
- Wooden beams 100 x 200 mm, center-to-center 600 mm;
- Vapour-retarding and airtight membrane with a variable vapour diffusion resistanance;
- Biobased wooden construction board, 18 mm;
- Clay base plate, 16 mm;
- Rough base clay plaster, 15 mm;
- Jute reinforcement mesh;
- Finishing clay plaster, 5 mm.

4. Simulation set-up

4. Simulation set-up for WUFI

4.1 Design parameters

Prior to developing the details, it is crucial to establish the parameters used to assess these details. A distinction is made between parameters that are specific to the detail level and those that are relevant at the square metre package level. These are outlined in the table below. The associated boundary conditions are provided for each element, and an explanation is given for calculating these parameters according to the Dutch Building Decree and the NEN-, and ISSO-standards.

Table 6, Design parameters for configuration details, own table

Detail	Square meter package
Linear thermal transmittance	Thermal resistance factor
Moisture transport over several years	Weight
Phase shift	Construction time

4.2 Square metre package level

Thermal resistance factor

Since this research focuses on residential top-up buildings in the Netherlands, it must comply with the minimum requirements specified in the **Dutch Building Decree**. According to **article 4.152**, the following **minimum thermal resistance** values, RC-values, apply to new residential buildings:

- Façades: 4.7 (m^2K)/W
- Roofs: 6.3 (m^2K)/W
- Floors: 3.7 (m^2K)/W

In order to calculate the total RC-value of the various components within a construction, the **R-value** of **each individual material layer** must first be determined. This value is calculated using the following formula:

$$R = \frac{d}{\lambda}$$

When a component of the construction is intersected by another element, for example when insulation material is placed between wooden columns, the configuration of the external wall is no longer homogeneous. The Dutch standard **NTA 8800:2024** takes such components into account and considers the **equivalent thermal resistance** of walls composed of multiple materials. In this context, the equivalent thermal conductivity coefficient is calculated according to the following formula:

$$\lambda' = \frac{(\lambda_{layer} * A_{layer} + \lambda_{fa} * A_{fa})}{(A_{layer} + A_{fa})}$$

Where:
λ' = The equivalent thermal conductivity of the layer [W/(mK)]
λ_{layer} = The thermal conductivity of the insulation layer [W/(mK)]
A_{layer} = The surface of the insulation layer [m^2]
λ_{fa} = The thermal conductivity of the penetrating structural element [W/(mK)]
A_{fa} = The surface of the penetrating structural element [m^2]

Subsequently, the **total thermal resistance** of the entire construction, the R_T, is calculated as follows:

$$R_T = R_{si} + \sum_{i=1}^{n} \frac{d_i}{\lambda_i} + R_{cav} + R_{se}$$

Where:
R_T = The total thermal resistance of the construction [(m²K)/W]
R_{si} = Boundary thermal resistance inside surface [(m²K)/W]
d_i = Thickness layer i [m]
λ_i = Thermal conductivity layer i [W/(mK)]
i = Number of layers within the construction [-]
R_{cav} = Thermal resistance factor cavity [(m²K)/W]
R_{se} = Boundary thermal resistance outside surface [(m²K)/W]

If a construction contains an **air cavity**, the **corresponding thermal conductivity coefficient** should be determined using the following method:

$$R_{cav} = \frac{d_{cav}}{\lambda_{cav}}$$

Where:
λ_{cav} = Thermal conductivity of the air cavity [W/(mK)], which is always: λ_{sp} < 25 W/(mK)
d_{cav} = Thickness of the air cavity [m]
R_{cav} = Thermal resistance of the air cavity [(m²K)/W]

The **NEN NTA 8800:2024-standard** gives the following R_{cav} for cavities of 20 mm or more, based on the ventilation strength:

Table 7, Thermal resistance factor cavity based on strength ventilation, derived from NTA 8800:2024

R_{cav}		
No	Weak	Strong
0.18	0.16	0.13

The strength of the cavity is defined as follows:
- No-ventilated cavity: ≤ 500 mm²/m;
- Weak-ventilated cavity: ≥ 500 mm²/m & < 1500 mm²/m;
- Strong- ventilated cavity: ≥1500 mm²/m.

In addition to the calculated R_T, standard **NTA 8800:2024** also specifies that the following **thermal transition resistance factors** must also be included in the calculations:

- External surface resistance, R_{se} = 0.04 (m²K)/W.
- Internal surface resistance:
  a. R_{si} = 0.13 (m²K)/W for walls and glazing between indoor and outdoor air;
  b. R_{si} = 0.50 (m²K)/W for all closed interior surfaces lower than 1500 mm above floor level with the following exceptions relevant to this study:
     • A section of interior surface at a triangular corner (two facades and a floor) adjacent to outdoor air, consisting of three 500 × 500 mm squares with a common corner (i);
     • An area within 100 mm of doors, windows and frames reveals (ii).
  c. R_{si} = 0.25 (m²K)/W for all surfaces not covered under a or b.

To illustrate the exceptions mentioned in point b, the following illustration is made on the next page.

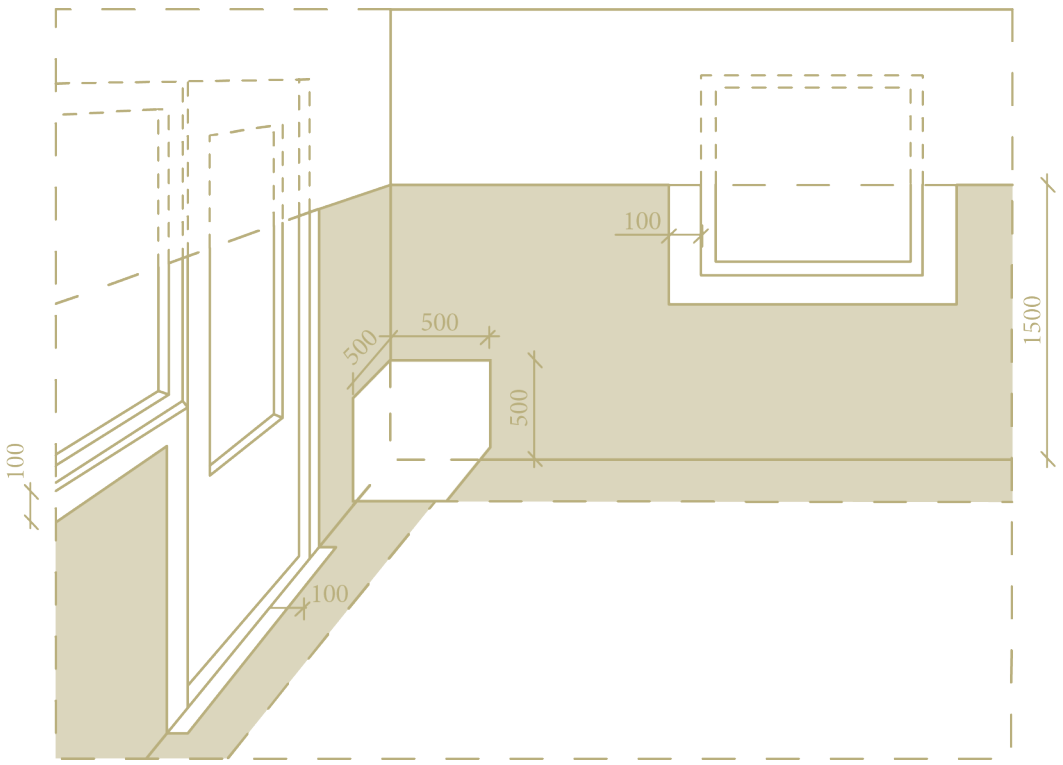

Figure 97, Exceptions transition resistance factors, derived from NTA 8800:2024

From the calculated $\mathbf{R_T}$, the $\mathbf{U_T}$ can be calculated as follows:

$$U_T = \frac{1}{R_T}$$

Where:
U_T = Total overall heat transfer coefficient [W/(m²K)]
R_T = Total thermal resistance [(m²K)/W]

The **NTA 8800:2024-standard** also specifies the **supplementary factors** that must be included in the calculations. These have a negative impact on the overall U-value of the construction. To calculate these factors, the following formula needs to be used:

$$\Delta U = \Delta U_a + \Delta U_{fa} + \Delta U_r + \Delta U_w$$

Where:

ΔU = The total supplementary factor [W/(m²K)]
ΔU_a = Supplementary factor for air voids [W/(m²K)]
ΔU_{fa} = Supplementary factor for fasteners [W/(m²K)]
ΔU_r = Supplementary factor for an 'inverted roof' [W/(m²K)]
ΔU_w = Supplementary factor for construction quality [W/(m²K)]

However, this thesis uses for all **ΔU-values** a value of **0** can be taken. The **correct overall heat transfer coefficient** of the **entire construction**, including the supplementary factors, can be calculated as follows:

$$U_c = U_T + \Delta U$$

From this value, the correct **thermal resistance** of the **construction** can be derived:

$$R_c = \frac{1}{U_c}$$

In addition to the requirements for wall, floor, and roof constructions, the **Dutch Building Decree** also defines requirements for the **overall heat transfer coefficient** of **windows**, **doors**, and **frames**, as specified in **article 4.153**. This thesis only focusses on details with a connection between a façade wall construction with a window. The following **performance requirement** applies to these building elements:

- A maximum U-value of 2.2 W/(m²K) for individual components.

Since this thesis only considers **windows without glazing bars**, the following formula, as specified in the **NTA 8800**, can be used to determine the **window's thermal transmittance**:

$$U_w = \frac{\sum A_{gl} \times \frac{U_{gl}}{f_{prac}} + \sum A_{fr} \times U_{fr} + \sum l_{gl} \times \psi_{gl}}{A_{gl} + A_{fr}}$$

Where:
U_w = Overall heat transfer coefficient of a window [W/(m²K)]
A_{gl} = The smallest of the visible surfaces of the glazing [m²]
U_{gl} = Overall heat transfer coefficient glazing [W/(m²K)]
f_{prac} = The practical performance factor for opaque construction elements with, $f_{prac} = 1$
A_{fr} = The projected frame surface area [m²]
U_{fr} = Overall heat transfer coefficient frame [W/(m²K)]
l_{gl} = The visible outlines of the glazing [m]
ψ_{gl} = The linear heat transfer coefficient as a result of the combined effects of glazing, spacer, and frame [W/(mK)]

To determine the **U_w-factor**, the **glazed area**, A_{gl}, and its corresponding **perimetre**, l_{gl}, are first defined in accordance with the guidelines of **NTA 8800:2024**. When determining the A_{gl}, the **smallest** of the **visible surface areas** should be used. Overlaps caused by sealant joints or glazing gaskets are excluded from this calculation.
Moreover, **l_{gl}** represents the **sum** of the **visible perimetres** of the **glass panes** within the window.

The figure below, figure 98, schematically shows the l_{gl} en A_{gl} for a glazing element. Since all thermal bridge analyses are conducted at a depth of **1 metre**, this results in a **l_{gl}** of **1 metre**. Additionally, the **adiabatic boundary** is **positioned** at a **height** of **0.175 metres**, with sealant joints and glazing gaskets excluded from the assessment. Consequently, the corresponding **A_{gl}** is therefore **0.175 square metres**.

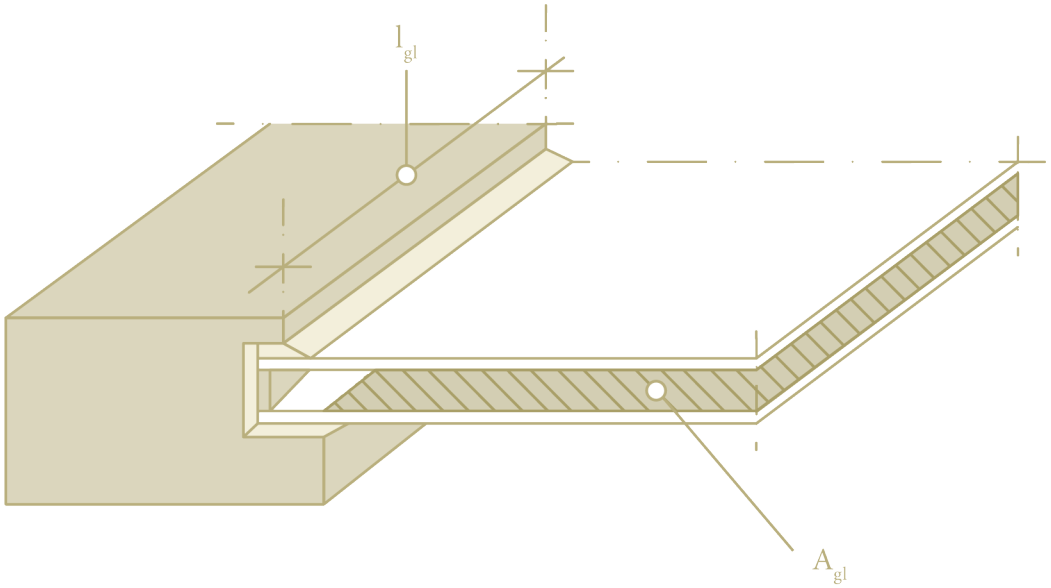

Figure 98, Illustration of glazed area and perimetre, derived from NTA 8800:2024

For the **heat transfer coefficient** of the glazing, U_{gl}, the table on the next page is used taken from the **NTA 8800:2024**. Because an air cavity with an **emissivity factor** of **≤ 0.1** with a **width** of **14 mm** and the type of **argon** cavity of a **double glazing** is used, the **U_{gl}** will be **1.5 W/(m²K)**.

Table 8, Heat transfer coefficient of the glazing, U_g, derived from NTA 8800:2024

				Heat transfer coefficient of the glazing, U_{gl} [W/(m²K)]			
Type of glazing	Coating layer	Emissivity factor	Cavity width	Type of cavity fill (gas concentration ≥ 90%)			
				Air	Argon	Krypton	SF6
Single glazing	-	-	-	5.8			
Double glazing	None (normal glass)	0.89	6	3.3	3.0	2.8	3.0
			9	3.0	2.8	2.6	3.1
			12	2.9	2.7	2.6	3.1
			15	2.7	2.6	2.6	3.1
			20	2.7	2.6	2.6	3.1
	1 pane with heat-reflective coating	≤ 0.4	6	2.9	2.6	2.2	2.6
			9	2.6	2.3	2.0	2.7
			12	2.4	2.1	2.0	2.7
			15	2.2	2.0	2.0	2.7
			20	2.2	2.0	2.0	2.7
		≤ 0.2	6	2.7	2.3	1.9	2.3
			9	2.3	2.0	1.6	2.4
			12	1.9	1.7	1.5	2.4
			15	1.8	1.6	1.6	2.5
			20	1.8	1.7	1.6	2.5
		≤ 0.1	6	2.6	2.2	1.7	2.1
			9	2.1	1.7	1.3	2.2
			12	1.8	1.5	1.3	2.3
			15	1.6	1.4	1.3	2.3
			20	1.6	1.4	1.3	2.3
		≤ 0.05	6	2.5	2.1	1.5	2.0
			9	2.0	1.6	1.3	2.1
			12	1.7	1.3	1.1	2.2
			15	1.5	1.2	1.1	2.2
			20	1.5	1.2	1.2	2.2
Triple glazing	None (normal glass)	0.89	6 & 6	2.3	2.1	1.8	2.0
			9 & 9	2.0	1.9	1.7	2.0
			12 & 12	1.9	1.8	1.6	2.0
	1 pane with heat-reflective coating	≤ 0.4	6 & 6	2.0	1.7	1.4	1.6
			9 & 9	1.7	1.5	1.2	1.6
			12 & 12	1.5	1.3	1.1	1.6
		≤ 0.2	6 & 6	1.8	1.5	1.1	1.3
			9 & 9	1.4	1.2	0.9	1.3
			12 & 12	1.2	1.0	0.8	1.4
		≤ 0.1	6 & 6	1.7	1.3	1.0	1.2
			9 & 9	1.3	1.0	0.8	1.2
			12 & 12	1.1	0.9	0.6	1.2
		≤ 0.05	6 & 6	1.6	1.3	0.9	1.1
			9 & 9	1.2	0.9	0.7	1.1
			12 & 12	1.0	0.8	0.5	1.1

To determine the U_f, the **NEN-EN-ISO 10077:2017** is applied. The following graph is used, which illustrates the thermal transmittance at various thicknesses of the frame. The **X-axis** represents the **frame thickness**, while the corresponding **thermal transmittance** of the **frame** can be derived from the **Y-axis**.

Line 1 represents the thermal transmittance of a hardwood frame (with a density of 700 kg/m³ and a λ of 0.18 W/(mK)).
Line 2 represents the thermal transmittance of a softwood frame (with a density of 500 kg/m³ and a λ of 0.13 W/(mK)).

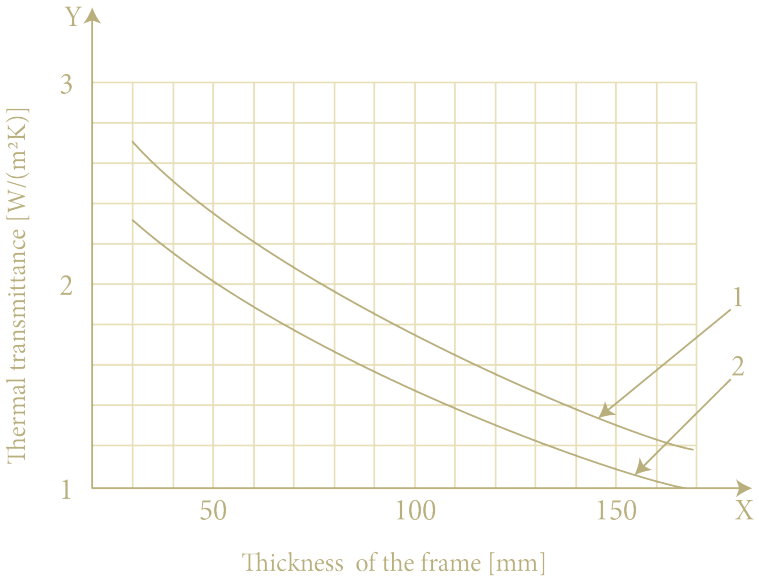

Figure 99, Determination of thermal transmittance of the frame, derived from NEN-EN-ISO 10077: 2017

Based on a **frame thickness** of **114 mm** and the selection of a **softwood frame** with a **λ-value** of **0.13 W/(mK)**, the **U_f-value** is approximately **1.35 W/(m²K)**. Furthermore, for the determination of **A_{fr}**, a standard wooden frame of **67 x 114 mm** is used, to which a **surface area** of **0.067 m²** is assigned.

The previously determined thermal **transmittance** of the **glazing**, U_g, applies to the central part of the glass but does **not account** for the **effect** of **edge spacers** or any **glazing bars** integrated into the glass. Moreover, the **thermal transmittance** of the **frame**, U_f, does **not account** for the **influence** of the **glazing**.

As a result, the **linear thermal transmittance**, Ψ_{gl}, must be applied in the calculation. This value describes the **additional heat transfer** that **arises** from the **interaction** between the **frame**, the **glazing**, and the **spacer**. The thermal properties of each of these components influence the Ψ_{gl}-value, which must be included in the formula for the window's overall thermal transmittance.
In this thesis, plastic **PVC spacers** are used in combination with **uncoated double glazing** consisting filled **air** or **gas**. According to the **NTA 8800**, the corresponding **Ψ_{gl}** value that may be applied is **0.05**.

Once all values are applied to the formula, a **U_w** of **1.66 W/(m²K)** is obtained. These values are summarized in the table below.

Table 9, Calculation of the overall heat transfer coefficient of the window, own table

Surface glazing [m²]	Overall heat transfer coefficient glazing [(W/m²K)]	Practival performance factor	Surface frame [m²]	Overall heat transfer coefficient frame [(W/m²K)]	Length outlines glazing [m]	Linear heat transfer coefficient glazing [(W/m²K)]
0.175	1.5	1	0.067	1.35	1	0.05

Overall heat transfer coefficient window [W/(m²K)]
1.66

Thermal resistance [(m²K)/W]
0.60

Weight

A **critical parameter** in the realisation of a residential top-up building is the **weight** of the **construction**. As the existing foundation remains unchanged, the additional load introduced by the new structure must be limited. According to the literature, **NEN 8707:2018** specifies a maximum allowable weight increase of **15%**.

Given that each reference detail applies identical floor and roof assemblies, as well as window frames with glazing, and since this thesis specifically focuses on the composition of façade wall constructions, only the weight of the wall assemblies is analysed.

For each referenced construction detail, the weight of the façade wall assembly is calculated per **square metre** (m^2), considering the **mass** of the **individual material layers** included in the detail. To calculate the weight of the construction per m^2, the following formula is used:

$$m' = \sum_{i=1}^{n} (\rho_i \times d_i)$$

Where:
m' = Mass per unit area [kg/m^2]
ρ_i = Density of material i [kg/m^3]
d_i = Thickness of material i [m]

At the end of each detail configuration, the relevant configuration will be **assessed** among others, on the **total weight**.

4.3 Detail level

Linear thermal transmittance

For **linear thermal transmittance**, **two concepts** are explained that act as parameters and should be explained first: the **temperature factor**, f, and the **linear thermal transmittance coefficient**, ψ.

Temperature factor

First, the Dutch Building Decree includes a **performance requirement** for the **thermal quality** of wall constructions aimed to **prevent moisture** and **allergen-related issues**. This is expressed by a temperature factor, **f-factor**. This factor is a dimensionless quantity on a scale of 0 to 1 and is defined as follows:

$$f = \frac{\theta_{io} - \theta_e}{\theta_i - \theta_e}$$

Where:
f = The temperature factor [-]
θ_{io} = The lowest interior surface temperature [˚C]
θ_i = The indoor air temperature [˚C]
θ_e = The outdoor air temperature [˚C]
(Van Herpen, 2005)

For **residential buildings**, the following requirement is set for the temperature factor:

$$f \geq 0.65$$

For an accurate determination of the temperature factor and to meet the requirements set, the **guidelines** described in the **NEN 2778:2015** standard should be followed. This describes the **calculation method** along with the associated **boundary conditions** and **assumptions** for performing **thermal calculations** on thermal bridge details. In this context, the following **boundary conditions** should be applied:

Table 10, Boundary condition temperature factor, derived from the NEN 2778:2015

Location	Sub-location	Temperature	Surface heat transfer coefficient on the inside
Interior side	From floor level to 1.5 m above floor level	θ_i = 18˚C	α_i = 2 W/(m²K)
	Above 1.5 m floor level	θ_i = 18˚C	α_i = 4 W/(m²K)
	3-plane outer corners in a cube of 0.5 x 0.5 x 0.5 m	θ_i = 18˚C	α_i = 4 W/(m²K)
	A strip of 0.25 m around windows and frames	θ_i = 18˚C	α_i = 4 W/(m²K)
	Glazing	θ_i = 18˚C	α_i = 7.7 W/(m²K)
Exterior side	-	θ_e = 0˚C	α_e = 25 W/(m²K)
Ground	At a depth of 3 m	θ_g = 10˚C	α_g = ∞ W/(m²K)

Next, the calculation detail must include the core element and the connection elements. Each connection element is adjacent to the core element on one side and to a cutting plane on the other side, which forms the boundary of the calculation detail. In this context, the connection element must be at least 1000 mm long in the calculated direction, with some **exceptions**:

- If there is a symmetrical plane within 1000 mm that meets the conditions, that distance is maintained.
- If another core element of a thermal bridge is present within 1000 mm, it must be fully incorporated into the calculation model and considered part of the connection element.
- The dimensions of the base must meet specific requirements according to 8.2.2.2 within the NEN 2778:2015 standard but are not relevant for this thesis.

Once the calculation detail is specified, **numerical calculations** can be performed using the **finite element method** or any other relevant method.. To achieve this, the calculation detail is first divided into core and connection elements. In the core elements, a **maximum orthogonal grid** of **25 x 25 x 25 mm** is allowed. Regarding the connection elements, **larger grid sizes** are **allowed** as the distance from the core element increases. The following visualization has been prepared for illustration and is applied within WUFI as the numerical grid.

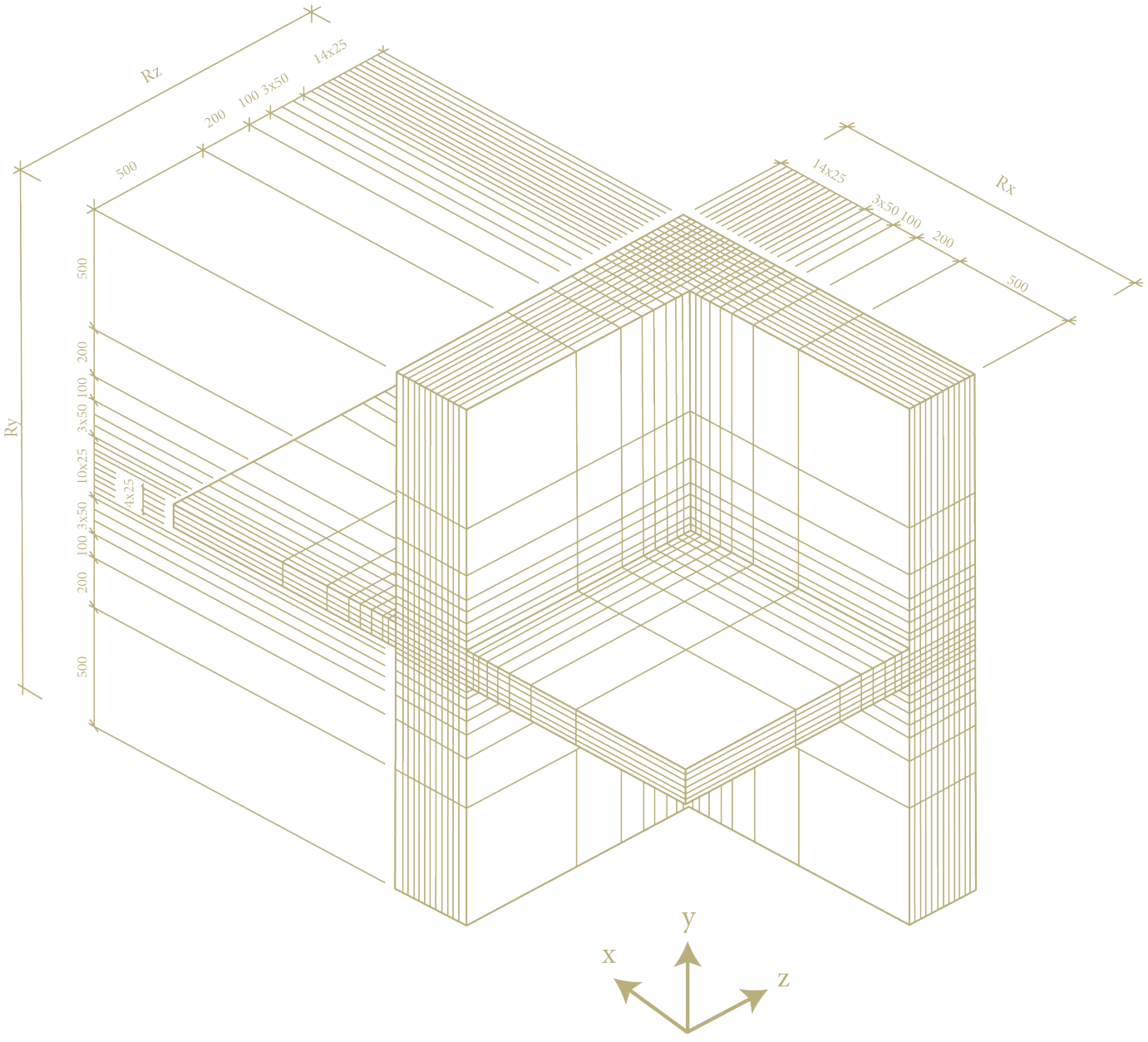

Figure 100, The finite element method, derived from NEN 2778:2015

According to the **NTA 8800:2019 standard**, the **law** of **conservation** of **energy**, Fourier's law, needs to be applied in the calculation model that is divided into material cells. This model leads to a **system** of **equations** that **describe** the **temperatures** at specific points, **nodes**. The solution to this system provides the **temperatures** at the **nodes**. Between the nodes, the **temperature** is determined by **linear interpolation**. Using Fourier's law, the **heat flux** can also be calculated based on the **temperature distribution**. The **heat flux** refers to the **unwanted transfer** of **heat** through a **construction detail** where the **thermal resistance** is **lower** than in the **adjacent structure**, and can be schematized as follows:

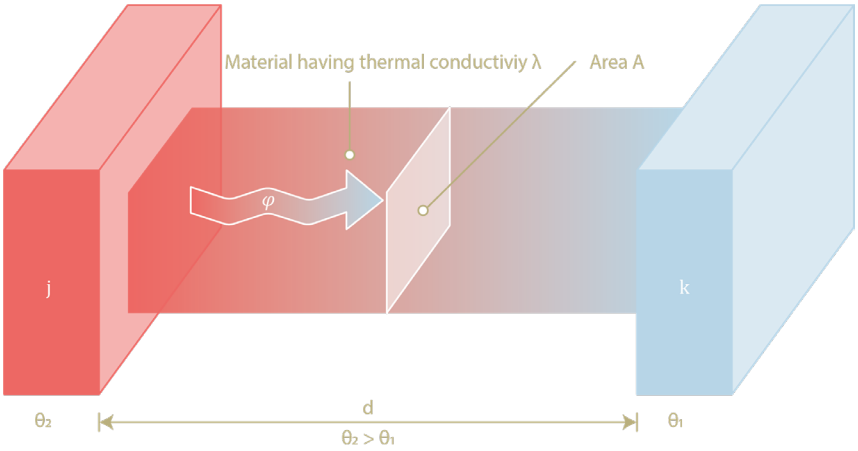

Figure 101, Schematic illustration of heat flux, derived from (Hukseflux, n.d.)

Between the **nodes** of **two adjacent material cells** '**j**' and '**k**' with **node temperatures** θ_j and θ_k a **heat flux** appears as follows:

$$\varphi_{j;k} = c_{j;k} \times (\theta_j - \theta_k)$$

The constant $\mathbf{c_{j;k}}$ is determined under the following conditions:

$$div\ \varphi = 0$$

$$\varphi = -\lambda \times grad\ \theta$$

Where:
φ = Heat flux density [W/m²]
θ = Temperature [°C]
λ = Thermal conductivity [W/(mK)]

The **heat flux density perpendicular** to the **interface** between a **material cell** and the **adjacent air** satisfies for an **incoming heat flow**:

$$\varphi_i = \frac{(\theta_i - \theta_s)}{R_{si}}$$

And satisfies for an **outgoing heat flow**:

$$\varphi_e = \frac{(\theta_s - \theta_e)}{R_{se}}$$

Where:
Φ_i = Incoming heat flux density [W/m²]
Φ_e = Outcoming heat flux density [W/m²]
θ_i = Temperature of the adjacent air on the side of the incoming heat flow [°C]
θ_s = The surface temperature at the interface [°C]
θ_e = Temperature of the adjacent air on the side of the outcoming heat flow [°C]
R_{si} = Heat transfer resistance on the internal surface [(m²K)/W]
R_{se} = Heat transfer resistance on the external surface [(m²K)/W]

Linear thermal transmittance coefficient

NTA 8800:2019 specifies the following formulas for calculating the **linear thermal transmittance**, ψ. The ψ-value of a junction between (construction) components is calculated using:

$$\psi = L^{2D} - \sum_i (U_{T;i} \times l_i)$$

Furthermore, in this thesis, the **linear heat transfer coefficient** of a **glass edge**, ψ_{gl}, is also important and is calculated as follows:

$$\psi_{gl} = L^{2D} - U_{fr} \times l_{fr} - U_{gl} \times l'_{gl}$$

Where:
L^{2D} = Linear thermal coupling coefficient [W/(mK)]
l_i = The width of the part of the (construction) component i included as a flanking element in the calculation detail [m]
$U_{T;i}$ = The heat transfer coefficient of (construction) component i [W/(m²K)]
U_{fr} = The heat transfer coefficient of the frame cross-section [W/(m²K)]
l_{fr} = The projected width of the frame cross-section [m]
U_{gl} = The heat transfer coefficient of the glazing [W/(m²K)]
l'_{gl} = The visible length of the part of the glazing included in the calculation [m]

Since the $\mathbf{L^{2D}}$ of the detail is calculated using the '**Heat Flow**' from **WUFI**, the formula for calculating ψ can be rewritten as follows:

$$\psi = \frac{Q_{WUFI} - Q_{ideal\ condition}}{L \times \Delta T}$$

The value of $\mathbf{Q_{ideal\ condition}}$ is obtained using the following equation:

$$Q_{ideal\ condition} = \sum_{i=1}^{n} \frac{A_{construction} \times \Delta T}{R_{construction}}$$

Where:
Q_{WUFI} = The total heat flow of the detail calculated within WUFI [W]
$Q_{ideal\ condition}$ = The total ideal heat flow of the construction without thermal bridge [W]
$A_{construction}$ = The surface of the construction without thermal bridge [m²]
L = The length of the thermal bridge [m]
ΔT = The difference in temperature between inside and outside [K]
$R_{construction}$ = The total thermal resistance of the construction [(m²K)/W]
n = Number of different constructions within the detail [-]

Additionally, $\mathbf{Q_{WUFI}}$ is determined based on the **sum** of the **heat flow [W/m]**. Since the **depth** is set to **1 metre**, the **length** over which the **heat flow** is **calculated** must be **multiplied** by **1 metre** to determine the **surface area** in WUFI. When this 1 metre is included in the calculation of Q_{WUFI}, the value can be expressed in [W].

In order to calculate the $\mathbf{R_{construction}}$, the **formulas** for $\mathbf{R_{construction,\ wall}}$, $\mathbf{R_{construction,\ floor}}$, $\mathbf{R_{construction,\ roof}}$ and $\mathbf{U_w}$ are used to determine the thermal resistance of the wall-, floor-, and roof constructios, respectively.

To determine the **surface** of the **construction without thermal bridge**, it is important to specify the **length** of the **linear thermal bridges** for both **WUFI simulations** and **manual thermal bridge calculations**.

The **NTA 8800:2024** describes principles to be observed for **determining** the **projected area**, A_l, and the **area** of a **(construction) component**, A_{con}. For **manual calculations**, the $\mathbf{A_{con}}$ is used, and the $\mathbf{A_T}$ should be used in the **simulations** in **WUFI**. For the method of schematisation the correct surfaces, the standard uses the 'ISSO-referentiedetails'. The relevant schematisations of the details for this thesis are presented in the illustrations on the next pages.

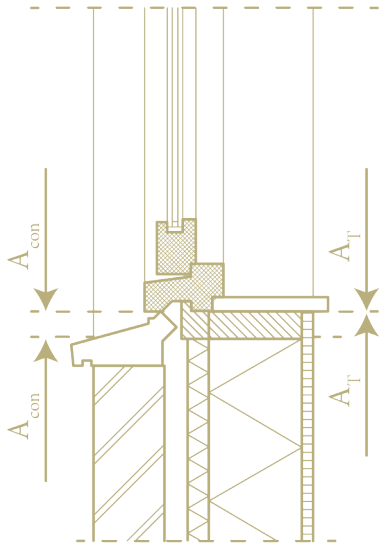

Figure 102, Determination of the surface of the construction foundation, derived from NTA 8800:2024

As shown in the figure above for details with floor overlays, the floor area, A_{con} is bounded by the inside of the floor overlay. In this case, the difference between A_{con} and A_T is attributed to ψ. Although this detail illustrates the placement of a floor on the foundation, the principle is the same for determining the ψ-value.

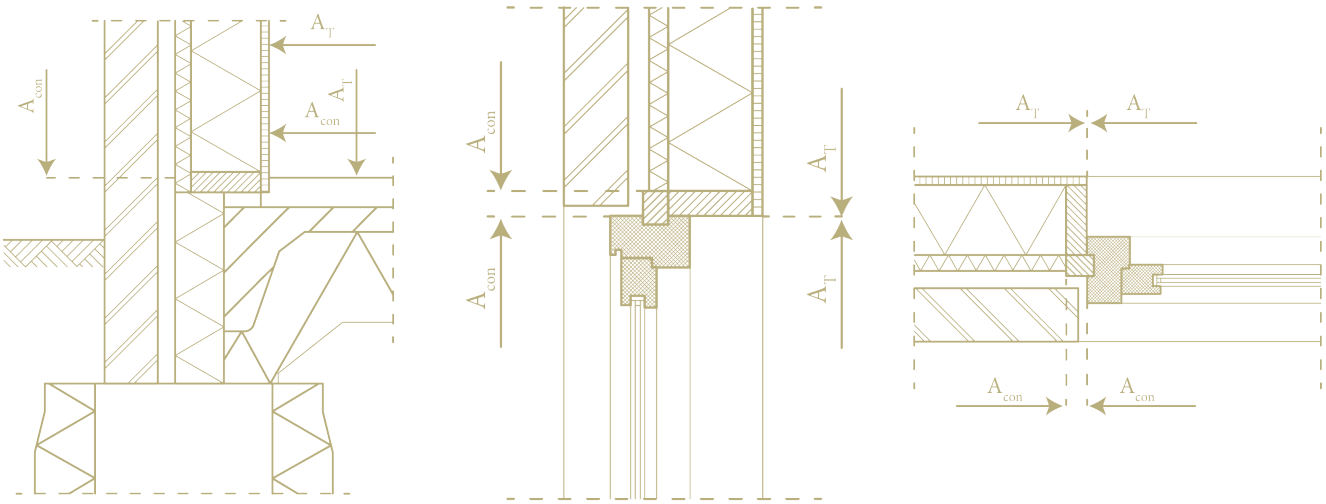

Figure 103, Determination of the surface of the bottom, top and side window frame construction, derived from NTA 8800:2024

As the figures above show for details with connections between windows and a façade, the façade area, A_{con}, is bounded by the bottom side of the setting battens. The frame area, A_{con}, is bounded by the bottom side of the frame. In this case, the difference between A_{con} and A_T attributed to ψ.

Since window frames need to be **simplified**, the boundary of a simplified window frame is more clearly visualised in the illustration below of the **NTA 8800:2019**.

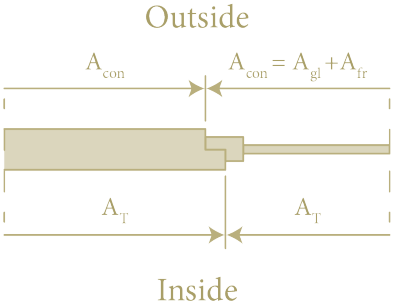

Figure 104, Connection window frame and wall construction, derived from the NTA 8800:2019

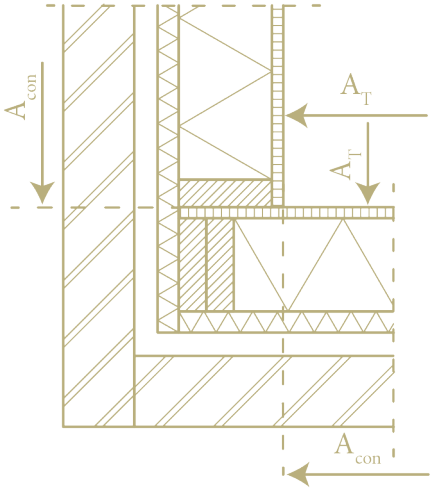

Figure 105, Determination of the corner wall construction, derived from NTA 8800:2019

As shown in the figure above for details with external corners, the façade area, A_{con}, is bounded by the inner side of the façades.

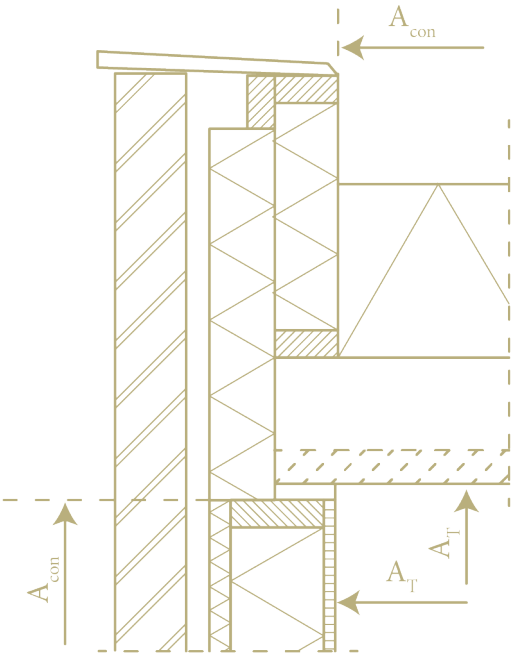

Figure 106, Determination of the flat roof construction, derived from NTA 8800:2019

As shown in the figure above for details with connections between a façade and a flat roof, the façade area, A_{con}, is bounded by the underside of the roof slab. The roof area, A_{con}, is bounded by the inner side of the façade area. In this case, the difference between A_{con} and A_T is attributed to ψ.

For consistency across analysis of the details, the lengths of A_T and A_{con}, should be equal in both the manual calculations and the simulations in WUFI.

Moisture transport over several years

Various aspects need to be considered when calculating **moisture transport** within the structure. The Dutch Building Decree states that **constructions** must be **resistant** to **condensation problems**. To assess this, **simulations** are performed over a **ten-year period** to evaluate whether **moisture accumulation** occurs within the construction during this period.

Although the **Dutch Building Decree** does **not** set explicit **requirements** for **moisture accumulation**, this research focuses on **preventing condensation problems**. In this context, the following aspects are analysed: **surface condensation**, **interstitial condensation**, and the **risk** of **mould growth** (using **isopleths**). These aspects are incorporated into the long-term simulations.

First, the **surface condensation** is addressed by applying the **NEN-EN ISO 13788:2013 standard** for testing. This standard prescribes the **determination** of the **external mean temperature**, **internal mean temperature** and the **relative humidity**. First, for determination of the **external mean temperature**, θ_e, the values for each month are taken from the **weather file** of the **NEN 5060:2018 standard**.

The **internal mean temperature**, θ_i, and **internal relative humidity**, φ_i, are determined over a period of **ten years** using **WUFI** analyses. For determining the θ_i, the method described in **NEN-EN ISO 13788:2013** is applied. This method calculates the **internal mean temperature** based on the previously determined **external mean temperatures**, as visualized in the figure below:

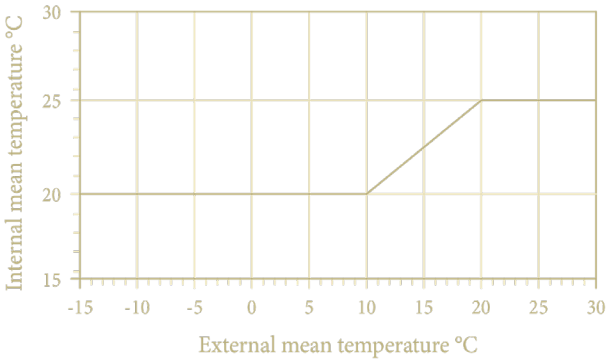

Figure 107, Determination internal mean temperature, derived from the NEN-EN ISO 13788:2013

Based on the determined θ_i the **internal relative humidity**, φ_i, can be established. For this determination, the **methodology** described in **NEN-EN ISO 13788:2013** is **followed**. For determining the correct φ_i, a **moisture load** must be selected, where this thesis assumes a **medium moisture load**, the **normal moisture load**. The φ_i, can be derived using the figure below based on the previously determined θ_i:

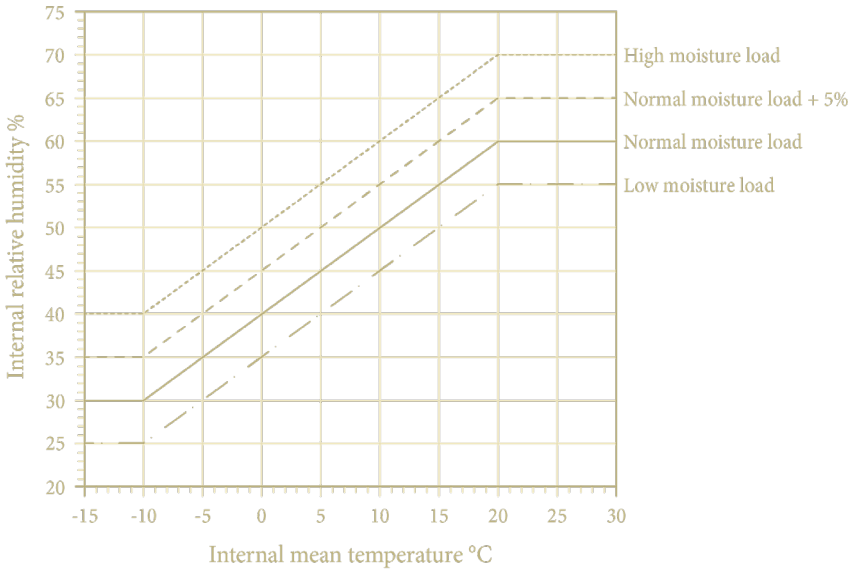

Figure 108, Determination internal relative humidity, derived from the NEN-EN ISO 13788:2013

The next step is to calculate the **external vapour pressure**, p_e, using the following formula:

$$p_e = \varphi_e \times p_{sat}(\theta_e)$$

Where:
p_e = The external vapour pressure [Pa]
φ_e = The external mean relative humidity of the month [%]
θ_e = The external mean temperature of the month [°C]
$p_{sat(\theta e)}$ = The saturation vapour pressure at θ_e [Pa]

With:

$$p_{sat}(\theta) = 610.5 \times e^{\frac{17.269 \times \theta}{237.3+\theta}}, \text{ for } \theta \geq 0\ C°$$
$$p_{sat}(\theta) = 610.5 \times e^{\frac{21.875 \times \theta}{265.5+\theta}}, \text{ for } \theta < 0\ C°$$

Once the **external vapour pressure** has been calculated, the **internal vapour pressure**, p_i, for each month can be determined by:

$$p_i = p_e + \Delta p$$

Where:
p_i = The internal vapour pressure [Pa]
Δp = The difference of the internal- and external vapour pressure [Pa]

For the **Δp**, a **humidity class 2** has been used which is representative of a dwelling. The following graph is used, starting at a Δp of 640 Pa. As the graph shows a linear decrease, the following formula is used to determine the Δp at different outdoor temperatures which is valid between 0 and 20 °C.

$$\Delta p(T) = -27T + 640$$

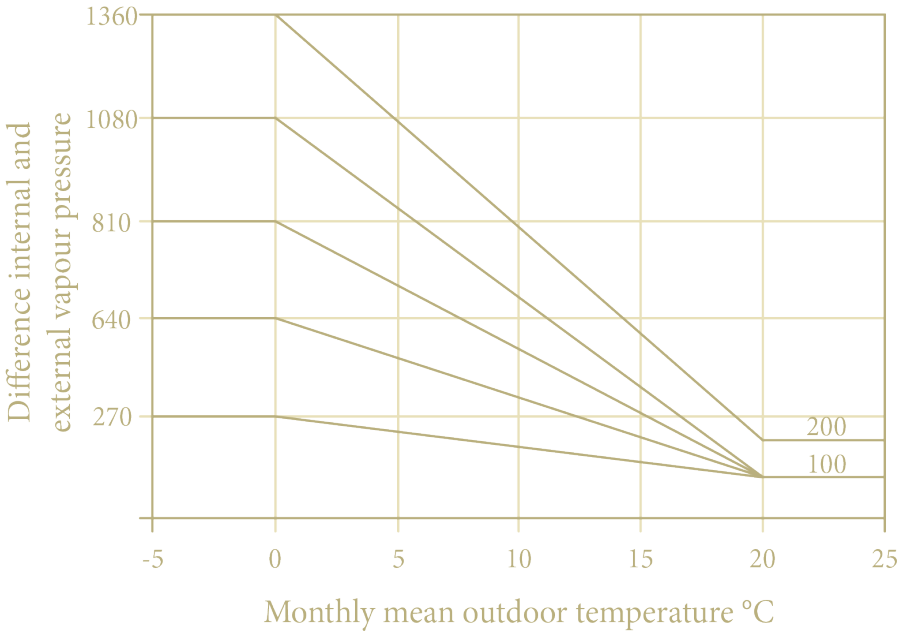

Figure 109, Determination difference internal and external vapour pressure, derived from the NEN-EN ISO 13788:2013

Next, the **saturation pressure**, $p_{sat}(\theta_{si})$, for the **surface temperature**, θ_{si}, is calculated as follows:

$$p_{sat}(\theta_{si}) = \frac{p_i}{\varphi_{si,crit}} = \frac{p_i}{0.8}$$

Where:
$p_{sat(\theta si)}$ = The saturation vapour pressure at θ_{si} [Pa]
$\varphi_{si,crit}$ = The critical relative humidity [%]

Next, the **minimum acceptable surface temperature**, $\theta_{si,min}$, for the minimum acceptable saturation vapour pressure, must be determined. This is calculated as follows:

$$\theta_{si,min} = \frac{237.3 \times ln\frac{p_{sat(\theta_{si})}}{610.5}}{17.269 - ln\frac{p_{sat(\theta_{si})}}{610.5}}, \text{ for } p_{sat}(\theta_{si}) \geq 610.5 \text{ Pa}$$

$$\theta_{si,min} = \frac{237.3 \times ln\frac{p_{sat(\theta_{si})}}{610.5}}{21.875 - ln\frac{p_{sat(\theta_{si})}}{610.5}}, \text{ for } p_{sat}(\theta_{si}) < 610.5 \text{ Pa}$$

The next step is to determine the **minimum f-factor**, $f_{Rsi,min}$, for each month:

$$f_{Rsi,min} = \frac{\theta_{si,min} - \theta_e}{\theta_i - \theta_e}$$

The **critical $f_{Rsi,crit}$** can be determined as the **month** with the **highest required value** of **$f_{Rsi,min}$**. This gives the termperature factor for this month as **$f_{Rsi,max}$**.

$$f_{Rsi,max} = f_{Rsi,crit}$$

Since **moisture accumulation** has a **negative effect** on the **interior surface temperature**, θ_{si} of the construction, a check is performed for each construction detail based on a **ten-year simulation**. For each detail, the **most critical point** is **identified**, and the **temperature variation** at this point is analysed and visualised over the entire simulation period. Based on this temperature curve, the **lowest surface temperature** is determined. This value is then used to **verify** whether the **resulting f_{Rsi}** is **higher** than the **allowable $f_{Rsi,max}$**.

Isopleths

Other than checking the risk of mould at the interior surface, the **isopleths** over **different material layers** are calculated in detail. These calculations are based on **moisture content**, **partial vapour pressure**, **indoor** and **outdoor temperatures** and **relative humidity**. These parameters are evaluated over the various material layers and over a given period of time to see if there is a change of mould growth over these layers. In order to assess this, the **isopleths** are **tested** based on the **IBP-model**.

Moisture transport through the material is calculated using **diffusion** and **capillary movement**. **Vapour pressure** is calculated for each layer within the material, based on **temperature** and **relative humidity**. Over time, the changes of both terms are calculated. By presenting the simulation results on isopleths, the **risk** of **mould growth** is assessed at **various layers** within the **detail** in a graph.

This **isopleths** graph plots **lighter yellow** representing time steps **close** to the **start** of the **simulation**. **Darker colours** represent conditions at the **end** of the **ten-year simulation**. The presented **isopleth diagrams** can be used as an **indicator** of **mould resistance**. **Above** the **LIM II line**, there is an **increased risk** of **mould growth**. **Between** the **LIM I** and **LIM II lines**, **mould growth** is **possible**, depending on the duration and frequency of exposure. When the isopleths remain **below both lines**, **mould growth** is **not** to be **expected**. To conclude that no mould formation occurs over the different material layers in the detail, the detail must fall below both LIM lines over these layers (Sedlbauer et al., 2011). Later in the report, the isopleths for the established details will be presented.

4.4. Simulation WUFI

This sub-chapter will describe the conditions used in WUFI 2D to perform the simulations.

Climate data

In order to make **accurate moisture simulations** and **thermal bridge analyses** of the developed details, it is necessary to use **climate data** that is **representative** for **the Netherlands**. Therefore, this research uses the **NEN 5060:2018 standard**, which utilizes detailed **Dutch climate data**. The standard contains **reference climate data** which are **composite datasets** representing **typical historical climatic conditions** over a certain period. The most **averages** of the **weather conditions** have been **summarised** and **converted** into **one extreme year** which serves as the reference year.

This reference year helps ensure that the details are resistant to extreme Dutch weather conditions concerning **moisture transport** and **thermal bridges**. This accurate and representative climate data are **essential** for **reliable analyses** within WUFI. The values that are used from the **NEN 5060:2018** are:

- Air temperature [°C];
- Relative humidity [%];
- Global solar radiation [W/m^2];
- Normal rain [Ltr/m^{2}h];
- Wind direction [°];
- Wind speed [m/s];
- Air pressure at mean sea level [hPa];
- Cloud Index [-].

Since **NEN 5060:2018** measures the values from a weather station at De Bilt, a **longitude** of **52.27°** and a latitude of **5.18°** are defined in WUFI.

To apply the **NEN 5060:2018 standard** in WUFI, the climate data must be converted into a **.WAC file**, which serves as **input** for the **hygrothermal simulations**. WUFI uses this data to analyse the **behaviour** of **moisture** and **temperature** in building materials under realistic weather conditions. Because certain values in the NEN 5060:2018 standard are defined differently from the units used in the .WAC file, some data were **converted** to the **correct units** prior the simulation. In order to simulate a **ten-year period** in WUFI, the dataset was then **repeated ten times**.

Geometry

The next step is to **define** the **geometries** of the details in WUFI. Since the level of detail in WUFI cannot match that of the established details, the **geometries** need to be **simplified**. This is also necessary due to **calculation time** considerations and considering that only rectangles can be drawn in WUFI.

ISO 10077:2017 outlines the **method** for **calculating** the **thermal performance** of **window** and **door components**. The standard provides **guidelines** for **simplifying geometries** and **omitting** certain **elements** to keep the calculation practically feasible without significantly affecting the accuracy of the results.

The standard first specifies that protrusions of window frames that **overlap** with walls or other building elements should be **disregarded**, as illustrated in figure 110. Additionally, **small geometric details** may be **omitted** to improve the mesh construction and simulation efficiency. An abstract representation of the details is created.

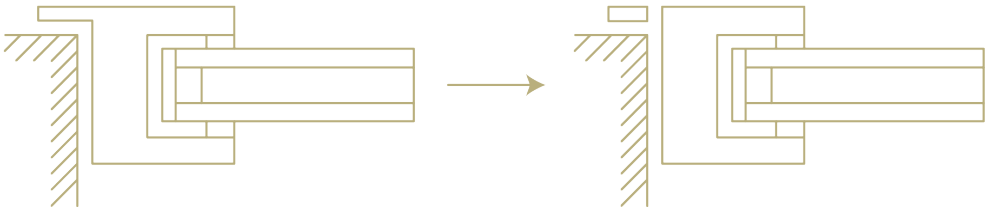

Figure 110, Simplification of window frame, derived from ISO 10077:2017

Air cavities are considered **non-ventilated** when the **cavities** are completely **sealed** or only **connected** to the **interior** or **exterior** through a **gap** of a **maximum** of **2 mm**. Based on this definition, the space beneath glazing should be classified as a **non-ventilated air cavity**. The figure below, figure 111, schematically illustrates the different boundaries, cavities, and grooves of a frame section:

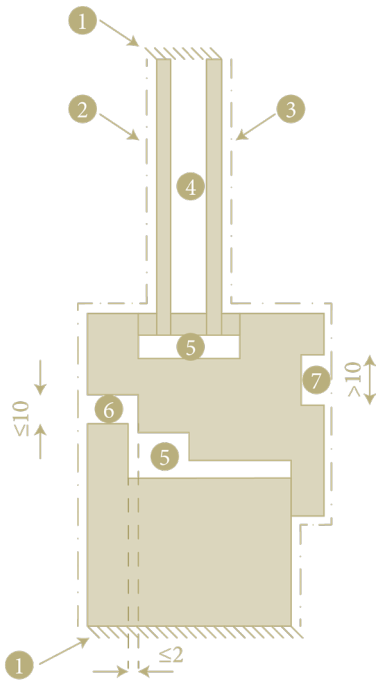

Figure 111, Boundaries, cavities and grooves window derived from ISO 10077:2017

The following boundaries, cavities and grooves are being used:

1. Adiabatic boundary;
2. External surface resistance;
3. Internal surface resistance;
4. Glazing;
5. Unventilated cavity;
6. Slightly ventilated cavity;
7. Well-ventilated cavity.

When an air cavity is non-rectangular, it should be transformed into a **rectangular air cavity** with the **same area** and **aspect ratio** as illustrated in the figure below:

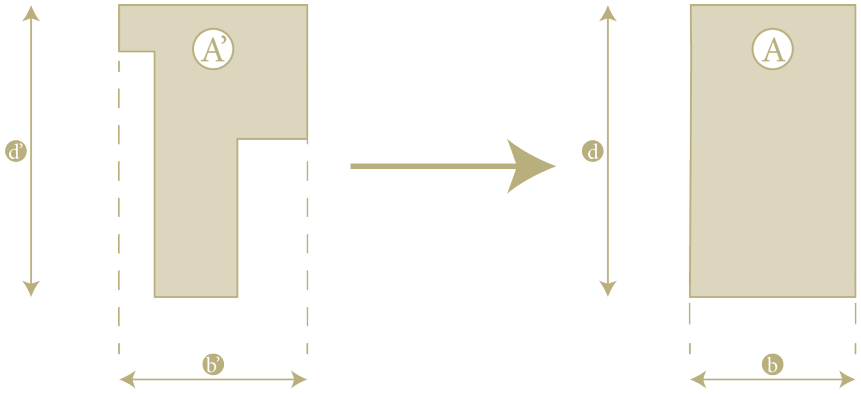

Figure 112, Transformation of non-rectangular air cavities, derived from ISO 10077:2017

The following distancess are being used:

d' b'. Depth and width of the smallest circumscribing rectangle [m];
A'. Area of the true cavity [m²];
d b. Depth and width of the equivalent air cavity [m];
A. Area of the equivalent air cavity [m²].

Additionally, in several architectural details, both **horizontal** and **vertical framing** is applied. Since it is **not possible** in WUFI to specifically **define** the **center-to-center distance** of the framing, the **vertical framing** is **extended** in **horizontal cross-sections**, while the **horizontal framing** is **extended** in **vertical cross-sections**. If this adjustment is not made, WUFI will interpret the framing as a solid wooden element. A ventilated air cavity, with the corresponding thickness, is incorporated between the framing members.

Numerical Grid

Once the geometries have been defined, the **numerical grid** can be established. In doing so, the **finite element method** previously presented, figure 100, is taken into account **as much as possible** when setting up the grid in WUFI, in accordance with the **NEN 2778:2015 standard**. The figure below, figure 113, is an small illustration of the numerical grid of the finite element method.

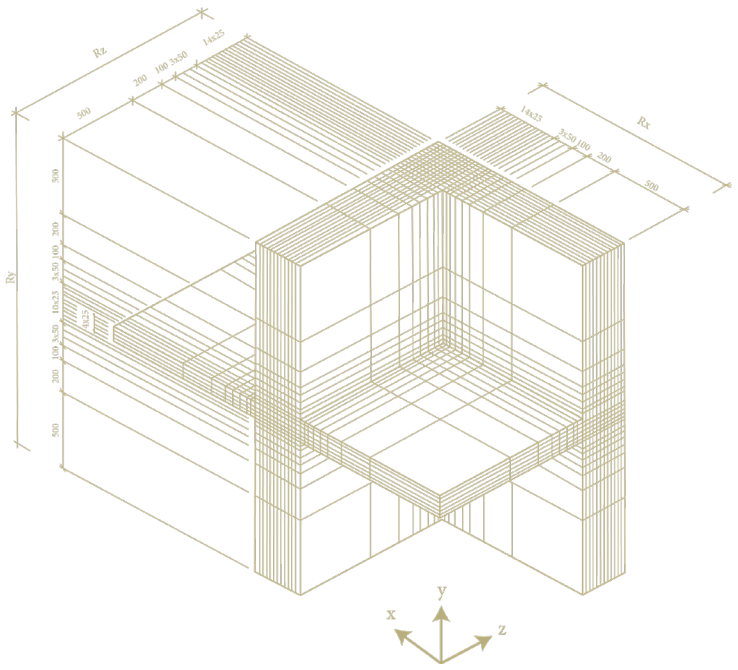

Figure 113, The finite element method, derived from NEN 2778:2015

Materials

The next step is to **assign** the correct **materials** to the previously defined geometries. This primarily utilizes the **database** within **WUFI**. As described earlier, both the **standard properties** (Bulk Density, Porosity, Heat Capacity, Thermal Conductivity, Vapour Resistance) and the **hygrothermal functions** (Moisture Storage Function, Liquid Transport Coefficient Suction & Redistribution, Water Vapour Diffusion Resistance Factor, Thermal Conductivity moisture-dependent and temperature-dependent, and Enthalpy) are **needed** for the analyses.

Since the required material properties are not available for all materials, similar materials from the database are used in WUFI. These are then **adjusted** based on **available data** from suppliers. This approach aims to achieve the **most accurate approximation** of **material behaviour** in the simulation. Nevertheless, it should be noted that the results **may show deviation** from **actual performance**. Within this study, it is not possible to experimentally determine the hygrothermal properties of the biobased materials. Therefore, it was decided to consult the WUFI database as a basis for completing missing material properties.

Regarding the **window constructions**, the different components must be specified separately. As previously explained, the **window details** in this study are **simplified**. In WUFI, the following **abstract representation** is used for this purpose.

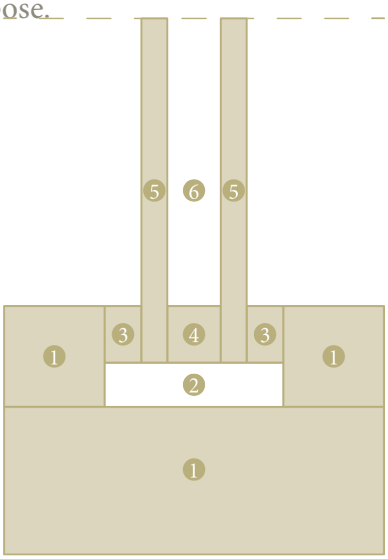

Figure 114, Abstract image of the window geometry within WUFI, own illustration

This involves the use of the following materials:

1. Wooden window frame with an U_f of 1.35 W/(m²K);
2. Unventilated cavity;
3. Glazing rubber;
4. Plastic spacer;
5. HR ++-glazing with a total U-value of 1.5 W/(m²K);
6. Cavity filling.

As previously described, the U_f is determined using the **NEN-EN-ISO 10077:2017 standard**, which results in a **U_f-factor** of **1.35 W/(m²K)**.

The **thermal resistance** of a **non-ventilated air gap**, R_{sp}, is determined according to **NTA 8800:2024**, where the **equivalent thermal conductivity** of an **air space** is **calculated**. In this determination, **heat transfer** through **conduction**, **convection**, and **radiation** is considered within the **unventilated cavity**, which is defined in the table on the next page, table 11.

Table 11, Thermal resistance R_{sp} [(m²K)/W] of an unventilated cavity, derived from NTA 8800:2024

d [mm]	d/b							
	10	5	3	2	1	0.5	0.3	≤ 0.1
2	0.07	0.07	0.07	0.07	0.06	0.06	0.06	0.06
5	0.14	0.14	0.13	0.13	0.13	0.12	0.12	0.11
7	0.17	0.17	0.17	0.16	0.15	0.14	0.14	0.13
10	0.21	0.21	0.20	0.20	0.18	0.17	0.16	0.15
15	0.26	0.25	0.24	0.24	0.22	0.20	0.19	0.17
25	0.29	0.28	0.27	0.26	0.24	0.22	0.20	0.18
25 - 500	0.29	0.28	0.27	0.26	0.24	0.22	0.20	0.18

The dimensions of '**d**' and '**b**' are shown in the figure below and relate to a **heat flow direction**.

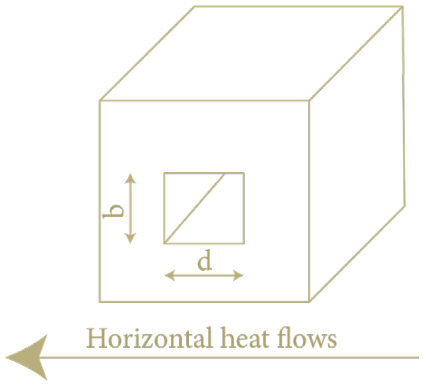

Figure 115, Section of the air layer with the direction of heat flow, derived from NTA 8800:2024

In the details, a value of **32 mm** for **d** and **15 mm** for **b** is applied. By interpolating this value, an R_{sp} of **0.26 (m²K)/W** is obtained. From this, the **equivalent thermal conductivity coefficient**, λ_{eq}, can be calculated using the following formula:

$$\lambda_{eq} = \frac{d_{sp}}{R_{sp}}$$

Based on this, an **equivalent thermal conductivity coefficient**, λ_{eq}, of **0.12 W/(mK)** is derived. Within WUFI, the **material property** of **air** is **adjusted** accordingly to this value, thereby facilitating a realistic simulation of an unventilated air cavity.

Subsequently, **EPDM rubber** is selected for the **glazing seals**, while **polyurethane** is applied for the **plastic spacer**.

Additionally, **EPDM** is used for **sealing** the **frame**, thereby creating a **water-resistant barrier**.

In order to determine the **λ-value** of the **cavity filling**, the following formula must be utilized:

$$R_{tot} = R_{si} + R_{glass} + R_{cav} + R_{se}$$

$$R_{cav} = R_{tot} - R_{si} - R_{glass} - R_{se}$$

The **total thermal resistance**, R_{tot} is calculated based on the **U-value** of the **HR++ glazing**, which results in a **total thermal resistance** of **0.67 (m²K)/W**. Additionally for the R_{si} and R_{se} the values specified in the **NTA 8800:20224 standard** are used, which are **0.13 (m²K)/W** and **0.04 (m²K)**, respectively. For the **glazing**, a **λ-value** of **1 W/(mK)** is applied, with a **thickness** of **2 x 5 mm**, resulting in an **R-value** of **0.01 (m²K)/W**.

From this, a R_{cav} of **0.49 (m²K)/W** is derived combined with a **thickness** of **14 mm**, this results in a **λ-value** of **0.029 W/(mK)**. Similarly, within WUFI, the **material property** for **air** is **adjusted** to this value to adequately model the correct cavity filling.

Besides cavities at the location of windows, the details also contain cavities between other building components. When **cavities** and **grooves** are connected to the **inside** or **outside** with a **gap** between **2 mm** and **10 mm** wide, this is classified as **slightly ventilated cavities** and **grooves**. In this case, it is assumed that the entire surface is exposed to the environment and a surface resistance of $\mathbf{R_s = 0{,}30\ (m^2K)/W}$ is applied to the developed surface.

For situations where the **cavities** and **grooves exceed 10 mm**, this is classified as **well-ventilated cavities** and **grooves**, and the standard $\mathbf{R_{si}}$ en $\mathbf{R_{se}}$ should be applied. The **material properties** for the **components** of a **window** are derived from the values listed in **Table D.1** of the **ISO 10077:2017 standard**.

Materials specified in WUFI

For each detail configuration, the materials used in WUFI have been specified based on their **physical properties**. For each material, the following **parameters** were defined: **bulk density**, **porosity**, **specific heat capacity**, **thermal conductivity**, and the **water vapour diffusion resistance factor**.

Materials were primarily selected from the WUFI database. If the default values in the database did not sufficiently correspond to the properties of the actual material applied (particularly in the case of bio-based materials), these **parameters** were **manually adjusted**. For each detail configuration, it is indicated whether a material was modified or used as provided in the database.

Table 12, Used materials with corresponding properties in WUFI for the floor construction, own table

Layer name	Created/ Changed in WUFI	WUFI material name	Bulk Density [kg/m³]	Porosity [m³/m³]	Specific Heat Capacity [J/kgK]	Thermal Conductivity [W/mK]	Water Vapour Diffusion Resistance Factor
Wooden construction	No	Scandinavian spruce transverse direction	420	0.75	1600	0.13	50
Flexible hemp fibre insulation	Yes	HemKor flexible insulation	42	0.73	2300	0.043	1
Vapour-retarding and airtight membrane	No	Intello Plus	1100	0.086	2500	2.4	34000
Biobased construcion board	No	Esb-Platte elka strong board P5	621	0.57	2000	0.102	91.58
Plinth	No	Scandinavian spruce transverse direction	420	0.75	1600	0.13	50

Table 13, Used materials with corresponding properties in WUFI for the window construction, own table

Layer name	Created/ Changed in WUFI	WUFI material name	Bulk Density [kg/m³]	Porosity [m³/m³]	Specific Heat Capacity [J/kgK]	Thermal Conductivity [W/mK]	Water Vapour Diffusion Resistance Factor
Wooden setting batten	No	Scandinavian spruce transverse direction	420	0.75	1600	0.13	50
Wooden window frame	No	Scandinavian spruce transverse direction	420	0.75	1600	0.13	50
Water resistant barrier	No	EPDM, 45 mil, black	1500	0.001	1500	0.2	99000
Unventilated cavity	Yes	Air layer	1.3	0.999	1000	0.048	0.73
Glazing rubber	No	EPDM, 45 mil, black	1500	0.001	1500	0.2	99000
Plastic spacer	No	Membrane of polyurethan	130	0.001	1500	3	170
HR ++ glazing	Yes	Glass	2500	0.0001	1000	1	1E9
Cavity filling	Yes	Cavity filling	1.3	0.999	1000	0.0211	0.73

Table 14, Used materials with corresponding properties in WUFI for the roof construction, own table

Layer name	Created/ Changed in WUFI	WUFI material name	Bulk Density [kg/m³]	Porosity [m³/m³]	Specific Heat Capacity [J/kgK]	Thermal Conductivity [W/mK]	Water Vapour Diffusion Resistance Factor
Biobased construcion board	No	Esb-Platte elka strong board P5	621	0.57	2000	0.102	91.58
Vapour-retarding and airtight membrane	No	Intello Plus	1100	0.086	2500	2.4	34000
Wooden construction	No	Scandinavian spruce transverse direction	420	0.75	1600	0.13	50
Flexible hemp fibre insulation	Yes	HemKor flexible insulation	42	0.73	2300	0.043	1
Sloped wooden battens	No	Scandinavian spruce transverse direction	420	0.75	1600	0.13	50
Pressure-resistant wood fibre plate	Yes	GUTEX Thermoflat	140	0.91	2100	0.04	3
Cladding panels	No	Scandinavian spruce transverse direction	420	0.75	1600	0.13	50
Cladding cavity batten	No	Scandinavian spruce transverse direction	420	0.75	1600	0.13	50
Air cavity	No	Air Layer 60 mm	1.3	0.999	1000	0.337	0.27

Table 15, Used materials with corresponding properties in WUFI for the detail configuration 1, own table

Layer name	Created/ Changed in WUFI	WUFI material name	Bulk Density [kg/m³]	Porosity [m³/m³]	Specific Heat Capacity [J/kgK]	Thermal Conductivity [W/mK]	Water Vapour Diffusion Resistance Factor
Cladding panels	No	Scandinavian spruce transverse direction	420	0.75	1600	0.13	50
Cladding cavity batten	No	Scandinavian spruce transverse direction	420	0.75	1600	0.13	50
Air cavity	No	Air Layer 30 mm	1.3	0.999	1000	0.18	0.46
Wood fibre plate	No	PAVATEX-ISOLAIR (35 - 80 mm)	198	0.863	1400	0.041	2.7
Hempcrete blocks	Yes	ISOHEMP Hempcrete Block	320	0.83	1600	0.071	2.8
Hydraulic lime	Yes	Hydaulic Lime Mortar, coarse	1830	0.27	850	0.7	19.99
Wooden construction	No	Scandinavian spruce transverse direction	420	0.75	1600	0.13	50
Clay plaster	Yes	Clay plaster	1500	0.42	1000	5	11.3

Table 16, Used materials with corresponding properties in WUFI for the detail configuration 2, own table

Layer name	Created/ Changed in WUFI	WUFI material name	Bulk Density [kg/m³]	Porosity [m³/m³]	Specific Heat Capacity [J/kgK]	Thermal Conductivity [W/mK]	Water Vapour Diffusion Resistance Factor
Lime plaster	No	Exterior Plaster A layer 1 of 4 (exterior)	1310	0.36	850	0.87	8
Lime plaster	No	Exterior Plaster A layer 2 of 4	1300	0.36	850	0.87	8
Lime plaster	No	Exterior Plaster A layer 3 of 4	1219	0.3	850	0.25	10.8
Lime plaster	No	Exterior Plaster A layer 4 of 4 (interior)	1219	0.3	850	0.25	10.8
Hempcrete blocks	Yes	ISOHEMP Hempcrete Block	320	0.83	1600	0.071	2.8
Hydraulic lime	Yes	Hydaulic Lime Mortar, coarse	1830	0.27	850	0.7	19.99
Wooden construction	No	Scandinavian spruce transverse direction	420	0.75	1600	0.13	50
Flexible hemp fibre insulation	Yes	HemKor flexible insulation	42	0.73	2300	0.043	1
Clay plaster	Yes	Clay plaster	1500	0.42	1000	5	11.3

Table 17, Used materials with corresponding properties in WUFI for the detail configuration 3, own table

Layer name	Created/ Changed in WUFI	WUFI material name	Bulk Density [kg/m³]	Porosity [m³/m³]	Specific Heat Capacity [J/kgK]	Thermal Conductivity [W/mK]	Water Vapour Diffusion Resistance Factor
Lime plaster	No	Exterior Plaster A layer 1 of 4 (exterior)	1310	0.36	850	0.87	8
Lime plaster	No	Exterior Plaster A layer 2 of 4	1300	0.36	850	0.87	8
Lime plaster	No	Exterior Plaster A layer 3 of 4	1219	0.3	850	0.25	10.8
Lime plaster	No	Exterior Plaster A layer 4 of 4 (interior)	1219	0.3	850	0.25	10.8
Hempcrete blocks	Yes	ISOHEMP Hempcrete Block	320	0.83	1600	0.071	2.8
Hydraulic lime	Yes	Hydaulic Lime Mortar, coarse	1830	0.27	850	0.7	19.99
Wooden construction	No	Scandinavian spruce transverse direction	420	0.75	1600	0.13	50
Flexible hemp fibre insulation	Yes	HemKor flexible insulation	42	0.73	2300	0.043	1
Clay plaster	Yes	Clay plaster	1500	0.42	1000	5	11.3

Table 18, Used materials with corresponding properties in WUFI for the detail configuration 4, own table

Layer name	Created/ Changed in WUFI	WUFI material name	Bulk Density [kg/m³]	Porosity [m³/m³]	Specific Heat Capacity [J/kgK]	Thermal Conductivity [W/mK]	Water Vapour Diffusion Resistance Factor
Cork cladding panels	No	Thermacork 100% Natural Cork Insulation, MD Façade Density, 50 mm	143	0.22	1900	0.0417	28.3
Biobased diffusion open construction board	No	AGEPAN THD	226	0.79	2100	0.047	3.4
Cladding cavity batten	No	Scandinavian spruce transverse direction	420	0.75	1600	0.13	50
Air cavity	No	Air Layer 30 mm	1.3	0.999	1000	0.18	0.46
Water-resistant vapour-permeable membrane	No	DELTA-FOXX	270	0.001	2300	2.3	18.9
Wood fibre plate	No	PAVATEX-ISOLAIR (35 - 80 mm)	198	0.863	1400	0.041	2.7
Insulation corkboard	No	Thermacork 100% Natural Cork Insulation, Standard Density, 50 mm	107	0.22	1900	0.0397	28.3
Vapour-retarding and airtight membrane	No	INTELLO PLUS (ETA)	100	0.086	2500	2.4	34000
Wooden construction	No	Scandinavian spruce transverse direction	420	0.75	1600	0.13	50
Biobased construction board	No	Esb-Platte elka strong board P5	621	0.57	2000	0.102	91.58
Clay plaster	Yes	Clay plaster	1500	0.42	1000	5	11.3

Table 19, Used materials with corresponding properties in WUFI for the detail configuration 5, own table

Layer name	Created/ Changed in WUFI	WUFI material name	Bulk Density [kg/m³]	Porosity [m³/m³]	Specific Heat Capacity [J/kgK]	Thermal Conductivity [W/mK]	Water Vapour Diffusion Resistance Factor
Cork cladding panels	No	Thermacork 100% Natural Cork Insulation, MD Façade Density, 50 mm	143	0.22	1900	0.0417	28.3
Cork underlayment mortar	No	Diathonite Thermactive.037	252	0.65	974	0.037	3
Insulation corkboard	No	Thermacork 100% Natural Cork Insulation, Standard Density, 50 mm	107	0.22	1900	0.0397	28.3
Biobased diffusion open construction board	No	AGEPAN THD	226	0.79	2100	0.047	3.4
Water-resistant vapour-permeable membrane	No	DELTA-FOXX	270	0.001	2300	2.3	18.9
Insulation corkboard	No	Thermacork 100% Natural Cork Insulation, Standard Density, 50 mm	107	0.22	1900	0.0397	28.3
Wooden construction	No	Scandinavian spruce transverse direction	420	0.75	1600	0.13	50
Vapour-retarding and airtight membrane	No	INTELLO PLUS (ETA)	100	0.086	2500	2.4	34000
Biobased construction board	No	Esb-Platte elka strong board P5	621	0.57	2000	0.102	91.58
Clay plaster	Yes	Clay plaster	1500	0.42	1000	5	11.3

Table 20, Used materials with corresponding properties in WUFI for the detail configuration 6, own table

Layer name	Created/ Changed in WUFI	WUFI material name	Bulk Density [kg/m³]	Porosity [m³/m³]	Specific Heat Capacity [J/kgK]	Thermal Conductivity [W/mK]	Water Vapour Diffusion Resistance Factor
Cladding panels	No	Scandinavian spruce transverse direction	420	0.75	1600	0.13	50
Cladding cavity batten	No	Scandinavian spruce transverse direction	420	0.75	1600	0.13	50
Air cavity	No	Air Layer 30 mm	1.3	0.999	1000	0.18	0.46
Water-resistant vapour-permeable membrane	No	DELTA-FOXX	270	0.001	2300	2.3	18.9
Flax insulation	Yes	Flax Insulation Board - Isovlas PN	45	0.95	1600	0.035	5.7
Wooden construction	No	Scandinavian spruce transverse direction	420	0.75	1600	0.13	50
Biobased construction board	No	Esb-Platte elka strong board P5	621	0.57	2000	0.102	91.58
Clay plaster	Yes	Clay plaster	1500	0.42	1000	5	11.3

Table 21, Used materials with corresponding properties in WUFI for the detail configuration 7, own table

Layer name	Created/ Changed in WUFI	WUFI material name	Bulk Density [kg/m³]	Porosity [m³/m³]	Specific Heat Capacity [J/kgK]	Thermal Conductivity [W/mK]	Water Vapour Diffusion Resistance Factor
Cork cladding panels	No	Thermacork 100% Natural Cork Insulation, MD Façade Density, 50 mm	143	0.22	1900	0.0417	28.3
Cork underlayment mortar	No	Diathonite Thermactive.037	252	0.65	974	0.037	3
Insulation corkboard	No	Thermacork 100% Natural Cork Insulation, Standard Density, 50 mm	107	0.22	1900	0.0397	28.3
Biobased diffusion open construction board	No	AGEPAN THD	226	0.79	2100	0.047	3.4
Water-resistant vapour-permeable membrane	No	DELTA-FOXX	270	0.001	2300	2.3	18.9
Flax insulation	Yes	Flax Insulation Board - Isovlas PN	45	0.95	1600	0.035	5.7
Wooden construction	No	Scandinavian spruce transverse direction	420	0.75	1600	0.13	50
Vapour-retarding and airtight membrane	No	INTELLO PLUS (ETA)	100	0.086	2500	2.4	34000
Biobased construction board	No	Esb-Platte elka strong board P5	621	0.57	2000	0.102	91.58
Clay plaster	Yes	Clay plaster	1500	0.42	1000	5	11.3

Table 22, Used materials with corresponding properties in WUFI for the detail configuration 8, own table

Layer name	Created/ Changed in WUFI	WUFI material name	Bulk Density [kg/m³]	Porosity [m³/m³]	Specific Heat Capacity [J/kgK]	Thermal Conductivity [W/mK]	Water Vapour Diffusion Resistance Factor
Cladding panels	No	Scandinavian spruce transverse direction	420	0.75	1600	0.13	50
Cladding cavity batten	No	Scandinavian spruce transverse direction	420	0.75	1600	0.13	50
Air cavity	No	Air Layer 30 mm	1.3	0.999	1000	0.18	0.46
Wood fibre plate	No	PAVATEX-ISOLAIR (35 - 80 mm)	198	0.863	1400	0.041	2.7
Wood fibre insulation	Yes	GUTEX Thermoflex	50	0.95	1600	0.035	5.7
Wooden construction	No	Scandinavian spruce transverse direction	420	0.91	2100	0.038	2
Biobased construction board	No	Esb-Platte elka strong board P5	621	0.57	2000	0.102	91.58
Clay plaster	Yes	Clay plaster	1500	0.42	1000	5	11.3

Table 23, Used materials with corresponding properties in WUFI for the detail configuration 9, own table

Layer name	Created/ Changed in WUFI	WUFI material name	Bulk Density [kg/m³]	Porosity [m³/m³]	Specific Heat Capacity [J/kgK]	Thermal Conductivity [W/mK]	Water Vapour Diffusion Resistance Factor
Cork cladding panels	No	Thermacork 100% Natural Cork Insulation, MD Façade Density, 50 mm	143	0.22	1900	0.0417	28.3
Cork underlayment mortar	No	Diathonite Thermactive.037	252	0.65	974	0.037	3
Insulation corkboard	No	Thermacork 100% Natural Cork Insulation, Standard Density, 50 mm	107	0.22	1900	0.0397	28.3
Biobased diffusion open construction board	No	AGEPAN THD	226	0.79	2100	0.047	3.4
Water-resistant vapour-permeable membrane	No	DELTA-FOXX	270	0.001	2300	2.3	18.9
Wood fibre insulation	Yes	GUTEX Thermoflex	50	0.95	1600	0.035	5.7
Wooden construction	No	Scandinavian spruce transverse direction	420	0.75	1600	0.13	50
Vapour-retarding and airtight membrane	No	INTELLO PLUS (ETA)	100	0.086	2500	2.4	34000
Biobased construction board	No	Esb-Platte elka strong board P5	621	0.57	2000	0.102	91.58
Clay plaster	Yes	Clay plaster	1500	0.42	1000	5	11.3

Table 24, Used materials with corresponding properties in WUFI for the detail configuration 10, own table

Layer name	Created/ Changed in WUFI	WUFI material name	Bulk Density [kg/m³]	Porosity [m³/m³]	Specific Heat Capacity [J/kgK]	Thermal Conductivity [W/mK]	Water Vapour Diffusion Resistance Factor
Cladding panels	No	Scandinavian spruce transverse direction	420	0.75	1600	0.13	50
Cladding cavity batten	No	Scandinavian spruce transverse direction	420	0.75	1600	0.13	50
Air cavity	No	Air Layer 30 mm	1.3	0.999	1000	0.18	0.46
Biobased construction board	No	Esb-Platte elka strong board P5	621	0.57	2000	0.102	91.58
Blow in straw insulation	Yes	Blow in straw insulation	105	0.9	2000	0.043	2
Wooden construction	No	Scandinavian spruce transverse direction	420	0.91	2100	0.038	2
Biobased construction board	No	Esb-Platte elka strong board P5	621	0.57	2000	0.102	91.58
Clay plaster	Yes	Clay plaster	1500	0.42	1000	5	11.3

Table 25, Used materials with corresponding properties in WUFI for the detail configuration 11, own table

Layer name	Created/ Changed in WUFI	WUFI material name	Bulk Density [kg/m³]	Porosity [m³/m³]	Specific Heat Capacity [J/kgK]	Thermal Conductivity [W/mK]	Water Vapour Diffusion Resistance Factor
Cork cladding panels	No	Thermacork 100% Natural Cork Insulation, MD Façade Density, 50 mm	143	0.22	1900	0.0417	28.3
Cork underlayment mortar	No	Diathonite Thermactive.037	252	0.65	974	0.037	3
Insulation corkboard	No	Thermacork 100% Natural Cork Insulation, Standard Density, 50 mm	107	0.22	1900	0.0397	28.3
Biobased diffusion open construction board	No	AGEPAN THD	226	0.79	2100	0.047	3.4
Water-resistant vapour-permeable membrane	No	DELTA-FOXX	270	0.001	2300	2.3	18.9
Blow in straw insulation	Yes	Blow in straw insulation	105	0.9	2000	0.043	2
Wooden construction	No	Scandinavian spruce transverse direction	420	0.75	1600	0.13	50
Vapour-retarding and airtight membrane	No	INTELLO PLUS (ETA)	100	0.086	2500	2.4	34000
Biobased construction board	No	Esb-Platte elka strong board P5	621	0.57	2000	0.102	91.58
Clay plaster	Yes	Clay plaster	1500	0.42	1000	5	11.3

Surface conditions

In WUFI, various **boundary conditions** are applied to simulate **heat** and **moisture transport** through building constructions. These **boundary conditions** determine the **interaction** of the **construction** with the **environment** and are crucial for an accurate analysis. To achieve this, the edges of the detail must be correctly defined, with a distinction made between **exterior surface**, **interior surface**, and **adiabatic surface**. Given that simulations are conducted for both a **ten-year calculation** and a **steady state calculation**, a distinction is made between these two types of simulations.

Ten-year simulation

The ***exterior surfaces*** of a structure, edges directly exposed to the environment, must be defined. These surfaces are linked to weather data from the NEN 5060:2018 standard, enabling simulations of external influences on moisture transport and thermal bridges. At these the thermophysical properties, the **short-wave radiation absorptivity** and the **long-wave radiation emissivity**, must be determined for each material.

The ***short-wave radiation absorptivity*** refers to the absorption of incoming short-wave radiation, where a value of 0 means the material reflects all radiation, and a value of 1 indicates the material absorbs all radiation. The ***long-wave radiation emissivity*** indicates how well a material emits its own energy as long-wave infrared radiation, where a value of 0 implies that a material does not emit heat, and a value of 1 means the material radiates heat excellently.

Furthermore, edges that separate the building structure from indoor spaces must be defined as ***interior surfaces*** and are linked to the indoor climate conditions of the NEN-EN ISO 13788:2013 standard Finally, edges with no heat or moisture transport are ***adiabatic boundaries***. In WUFI these surfaces are thermally and hygric insulated, meaning no energy loss occurs and are applied at cutting planes.

For exterior surfaces, orientation plays a key role due to climate exposure. A south-western orientation is chosen, as per ISSO 75 which identifies this orientation as the most critical in the Netherlands. Accordingly, the **azimuth** is set at **45°**.

The following inclinations should be applied for the orientation of the detail in WUFI:
- **0°** for **horizontal** details;
- **90°** for **vertical** details.

Finally, in WUFI, the building height is set to '**Tall Building, middle part, up to 10-20 m**' as the details are being evaluated for top-up residential buildings within this height range.

For the ***surface transfer coefficient***, a heat transfer coefficient of **25 W/(m²K)** is used for exterior surfaces. Additionally, the **adhering fraction of rain** is set to **0.7**, adjusted depending on the component inclation For the ***interior surface***, the following conditions must be considered.

Given that the details are specifically for residential top-up buildings, the '**Medium Moisture Load**' should be used for **relative humidity**. Furthermore, in the Netherlands, a heat transfer coefficient of **7.8 W/(m²K)** should be applied for the surface transfer coefficient.

To conduct simulations over a period of ten years, the **number of time steps** is set to **87600 hours**, with **time steps** of **3600 seconds**. For the analysis of moisture transport and thermal bridging, both heat transport calculation and moisture transport calculation must be selected.

Steady state simulation

In the **steady state simulation**, however, most of the assumptions applied in the ten-year simulation are maintained. However, several specific adjustments are made that characterize the steady state approach. The differences are outlined below, while all other assumptions remain consistent with those used in the ten-year simulation.

In the steady state simulation, the ***surface conditions*** are adjusted by replacing the **exterior temperature**, **interior temperature**, and **relative humidity** with **constant values**. These adjustments are necessary to eliminate the sinusoidal variation in the WUFI model.

For the ***exterior conditions***, the **outdoor temperature** is set to **0°C** with a **relative humidity** of **80%**. In **both cases**, the **amplitude** is set to **zero**, ensuring that these values remain constant throughout the simulation period. For the ***interior conditions***, the **indoor temperature** is set at **18°C**, and the **relative humidity** is set at **50%**, also with an **amplitude** of **0**.

These adjustments allow for the calculation of the psi-factor, ψ, and the f-factor for the details.

5. Simulation results and assessment

Detail configuration 1 - hempcrete blocks with wooden façade

This chapter discusses the WUFI simulations to assess the developed details on **isopleths**, **surface condensation**, **f-factor** and **ψ-value**. As a **total** of **33** details were analysed, this chapter describes the methodology used for all tests which is demonstrated using the first configuration. The same methodology is applied to the remaining 32 simulations which are listed in **appendix A**. The conclusions on all 33 details are summarised in the sub-conclusion in this chapter. Each configuration contains two vertical details, **V1** and **V2** and one horizontal detail, **H1**, respectively illustrated in, **figure 116**, **figure 117** and **figure 118**. Since not all 63 developed details could be assessed, the remaining 30 details are listed in **appendix B**. Although these details are not tested in WUFI, similar results can be expected for these details based on the simulation results. However, full validation requires further research.

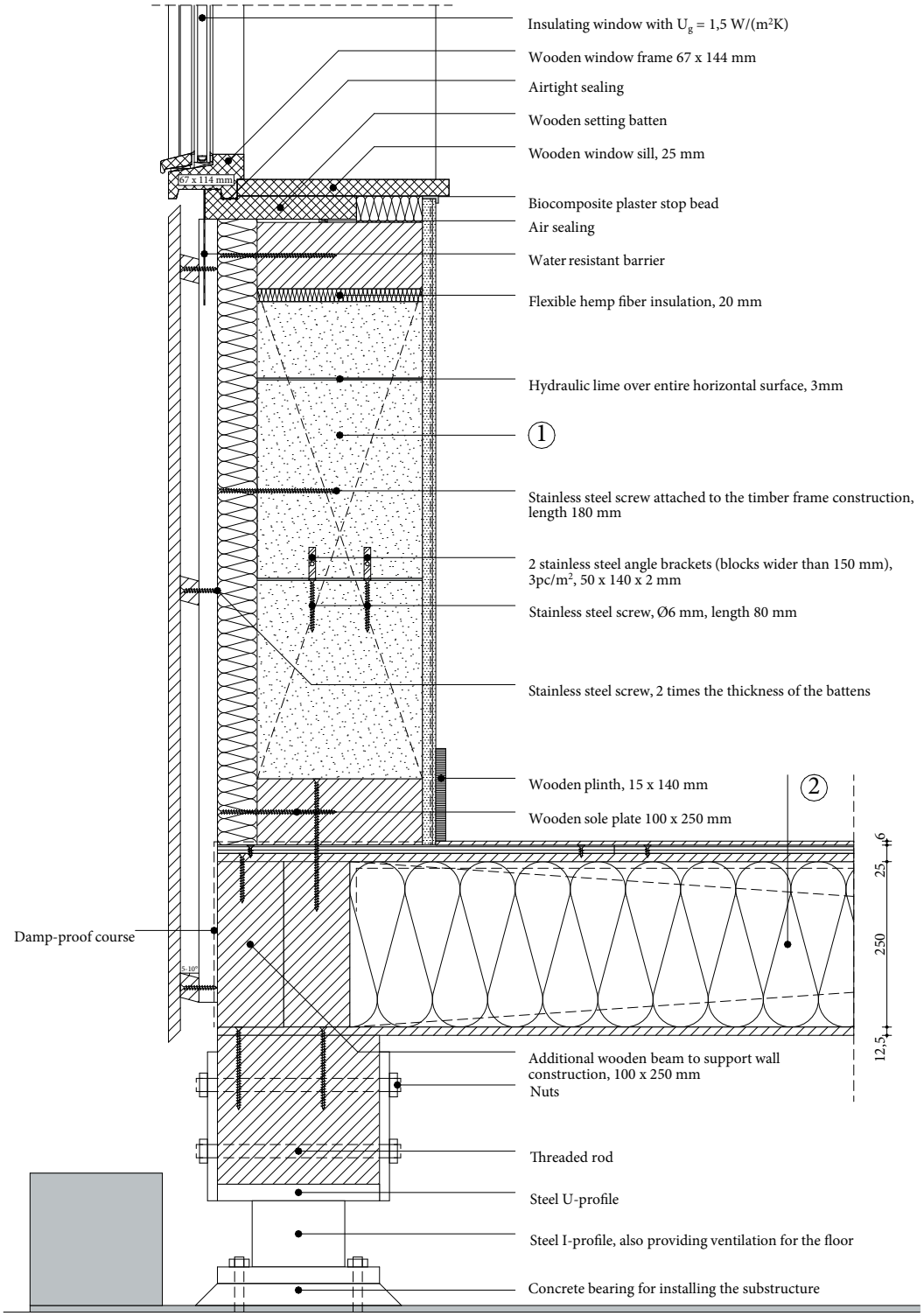

Figure 116, 1:10 detail of V1, configuration 1, own illustration

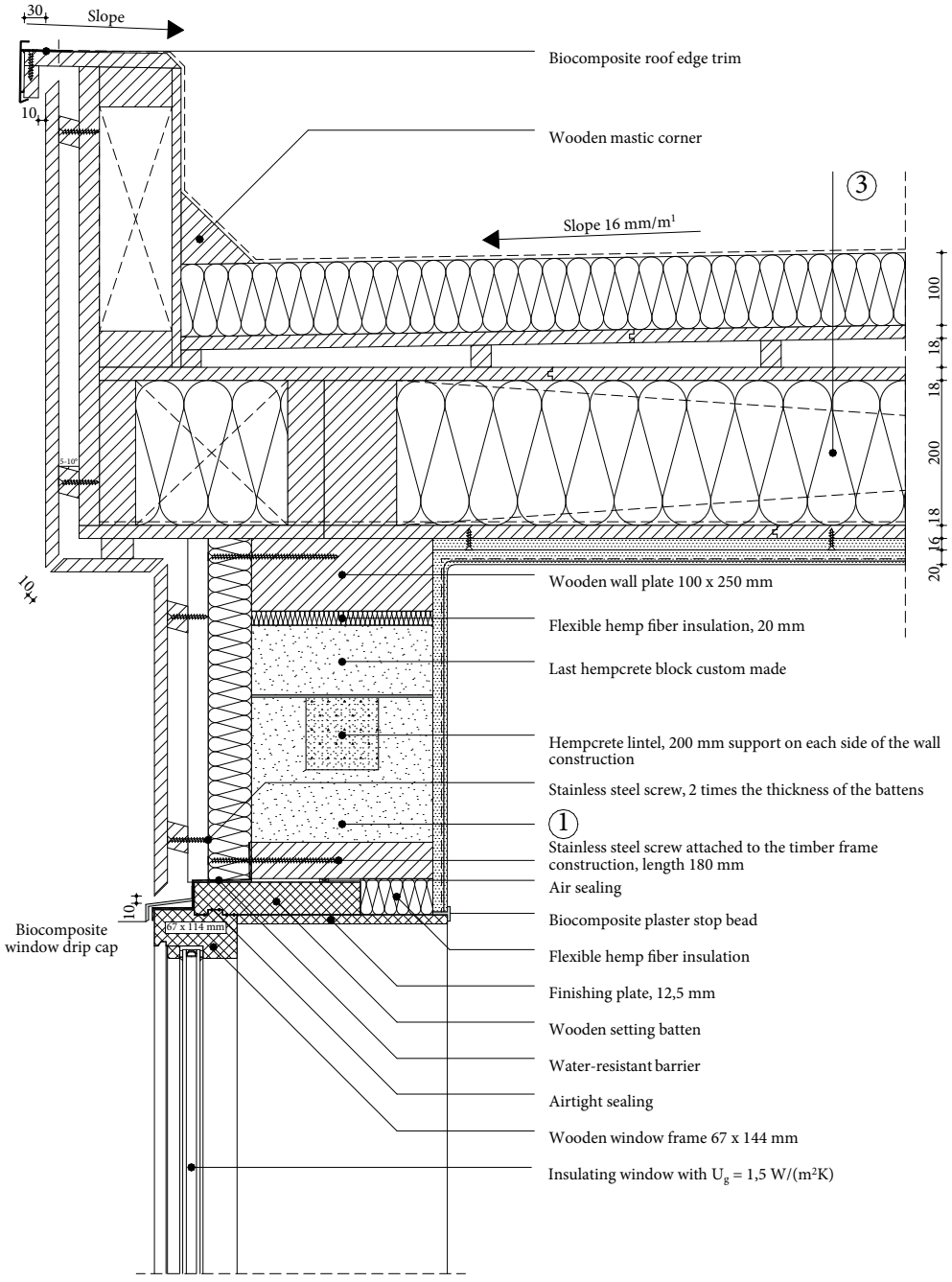

Figure 117, 1:10 detail of V2, configuration 1, own illustration

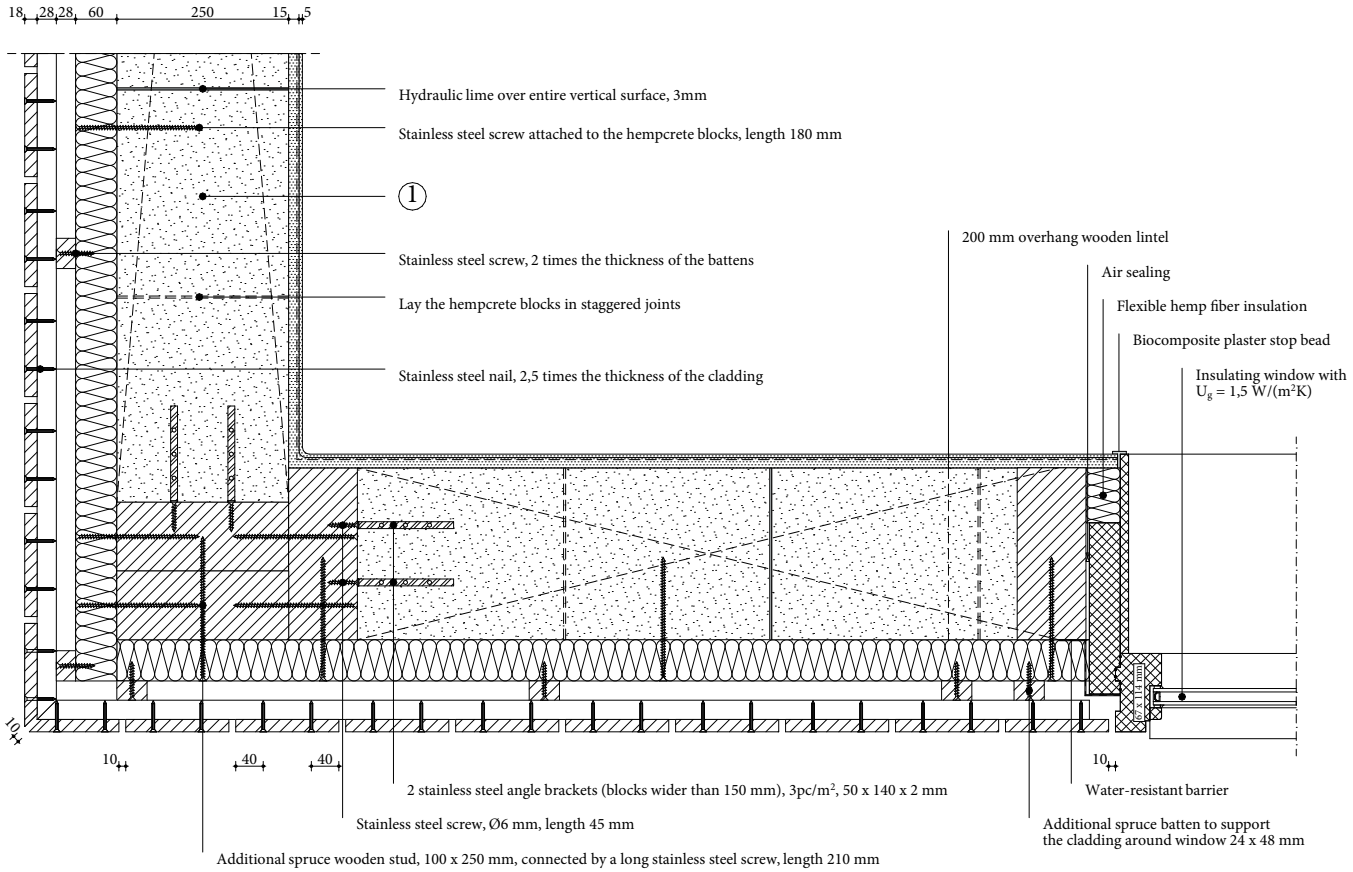

Figure 118, 1:10 detail of H1, configuration 1, own illustration

❶ Wall construction build-up, RC-value: 4.88 (m²K)/W

- Vertical wooden cladding, 18 mm;
- Horizontal spruce cladding batten cavity, 28 x 44 mm, center-to-center 600 mm;
- Vertical spruce cladding batten forming ventilated cavity, 28 x 44 mm, center-to-center 600 mm;
- Pressure-resistant woodfibre insulation plate (λ ≤ 0.042 W/mK), 60 mm;
- Timber frame construction, 100 x 250 mm, center-to-center 3000 mm;
- Hempcrete blocks (λ ≤ 0.071 W/mK), 250 mm;
- Rough base clay plaster, 15 mm;
- Jute reinforcement mesh;
- Finishing clay plaster, 5 mm.

❷ Floor construction build-up, RC-value: 4.65 (m²K)/W

- Finishing board, 6 mm;
- Biobased wooden construction board, 12.5 mm;
- Biobased wooden construction board, perpendicular on the other plate, 12.5 mm;
- Vapour-retarding and airtight membrane with a variable vapour diffusion resistanance;
- Flexible hemp fiber insulation placed between construction (λ ≤ 0.043 W/(mK), 250 mm;
- Wooden beams 100 x 250 mm, center-to-center 600 mm;
- Biobased wooden construction board, 12.5 mm.

❸ Roof construction build-up, RC-value: 6.71 (m²K)/W

- EPDM glued on underlayment to prevent roof covering from lifting;
- Pressure-resistant woodfibre insulation plate (λ ≤ 0.042 W/(mK), 100 mm;
- Biobased wooden construction board, 18 mm;
- Sloped wooden battens for drainage at an angle of 16 mm/m^1, 28 x 24 mm;
- Biobased wooden construction board, 18 mm;
- Flexible hemp fiber insulation placed between construction (λ ≤ 0.043 W/(mK), 200 mm;
- Wooden beams 100 x 200 mm, center-to-center 600 mm;
- Vapour-retarding and airtight membrane with a variable vapour diffusion resistanance;
- Biobased wooden construction board, 18 mm;
- Clay base plate, 16 mm;
- Rough base clay plaster, 15 mm;
- Jute reinforcement mesh;
- Finishing clay plaster, 5 mm.

U_g = 1.5 W/(m²K)

U_w = 1.76 W/(m²K)

f-factor ≥ 0.65

Ψ_{V1}: 0.059 W/(mK) Ψ_{V2}: 0.068 W/(mK) Ψ_{H1}: 0.077 W/(mK)

Isopleths: no risk of mould $f_{R,si} > f_{R,si,\,max}$; no risk of mould

Phase shift of the wall construction: 16.0 h

Density of the wall construction 136 kg/m³

Calculation RC-value

The first step required for the evaluation of the façade wall construction configurations is to determine the correct **thermal resistance value, RC-value**. This parameter forms a fundamental basis for all subsequent simulations presented later in this chapter.

To obtain accurate simulation results, material properties were based on the literature review focused on the physical properties of the different biobased materials that are used for the reference details. Hereby, the following formula is used. This formula is also used for all the other detail configurations.

$$R_T = R_{si} + \sum_{i=1}^{n} \frac{d_i}{\lambda_i} + R_{cav} + R_{se}$$

Sometimes, a layer within the wall construction build-up consist of multiple materials. When this is the case within the detail, **the equivalent thermal conductivity** should be calculated as follows. Subsequently, this value is used as the thermal conductivity for the relevant layer within the construction build-up.

$$\lambda' = \frac{(\lambda_{layer} * A_{layer} + \lambda_{fa} * A_{fa})}{(A_{layer} + A_{fa})}$$

The table below presents the calculated thermal resistance values, RC-values, of the wall construction build-up of **detail configuration 1**, taking into account both internal, R_{si}, and external, R_{se}, surface resistances. These calculations are performed for all the different established detail configurations.

❶ Wall construction build-up, RC-value: 4.88 (m²K)/W

Table 26, Calculation of the RC-value of the wall construction build-up, own table

Material	Thickness [m]	Thermal conductivity [W/(mK)]	Thermal resistance [W/(m²K)]
Vertical wooden cladding	0,018	0,130	0,078
Ventilated cavity with horizontal wooden cladding batten, center-to-center 600 mm	0,028	0,322	0,087
Ventilated cavity with vertical wooden cladding batten, center-to-center 600 mm	0,028	0,322	0,087
Pressure-resistant woodfibre insulation plate	0,060	0,041	1,463
Timber frame construction, with hempcrete blocks	0,250	0,079	3,147
Clay plaster	0,020	0,910	0,022

Table 27, Calculation of the equivalent thermal conductivity of the individual layers in the relevant build-up, own table

	Layer 1		Layer 2	
Material	Area [m²]	Thermal conductivity [W/(mK)]	Area [m²]	Thermal conductivity [W/(mK)]
Ventilated cavity with horizontal wooden cladding batten, center-to-center 600 mm	0,0168	0,337	0,0012	0,130
Ventilated cavity with vertical wooden cladding batten, center-to-center 600 mm	0,0012	0,130	0,0168	0,337
Timber frame construction, with hempcrete blocks	0,1500	0,071	0,0250	0,130

As explained earlier, this thesis focuses only on the design and evaluation of different wall configurations. Nevertheless, **one floor build-up** and **one roof build-up** have also been prepared. This allows insight into the connection details between wall and floor, as well as between wall and roof.

To obtain reliable simulation results, the thermal performance of both the roof and floor is important. Therefore, RC-values are also calculated for these building components using the same methodology as applied for the wall structures. The table below presents the calculated RC-values of the specific superstructures.

Within these build-ups, as with the walls, the equivalent thermal conductivity should be determined at the locations where the insulation material with a wooden frame and vertical studs occur. In addition, $\mathbf{R_{si}}$ and $\mathbf{R_{se}}$ are also taken into account when calculating the total thermal resistance.

❷ Floor construction build-up, RC-value: 4.65 (m²K)/W

Table 28, Calculation of the RC-value of the floor construction build-up, own table

Material	Thickness [m]	Thermal conductivity [W/(mK)]	Thermal resistance [W/(m²K)]
Finishing board	0,0060	0,230	0,026
Biobased wooden construction board	0,0125	0,120	0,104
Biobased wooden construction board	0,0125	0,120	0,104
Timber frame construction, with flexible hemp fibre	0,2500	0,060	4,139
Biobased wooden construction board	0,0125	0,120	0,104

Table 29, Calculation of the equivalent thermal conductivity of the individual layers in the relevant build-up, own table

	Layer 1		Layer 2	
Material	Area [m²]	Thermal conductivity [W/(mK)]	Area [m²]	Thermal conductivity [W/(mK)]
Timber frame construction, with flexible hemp fibre	0,200	0,043	0,05	0,130

❸ Roof construction build-up, RC-value: 6.44 (m²K)/W

Table 30, Calculation of the RC-value of the roof construction build-up, own table

Material	Thickness [m]	Thermal conductivity [W/(mK)]	Thermal resistance [W/(m²K)]
Pressure resistanct wood fibre insulation plate	0,1000	0,042	2,381
Biobased wooden construction board	0,0180	0,120	0,150
Sloped wooden battens for drainage	0,0240	0,325	0,074
Biobased wooden construction board	0,0180	0,120	0,150
Timber frame construction, with flexible hemp fibre	0,2000	0,060	3.311
Biobased wooden construction board	0,0180	0,120	0,150
Clay base plate	0,0160	0,470	0,034
Clay plaster	0,0200	0,910	0,022

Table 31, Calculation of the equivalent thermal conductivity of the individual layers in the relevant build-up, own table

	Layer 1		Layer 2	
Material	Area [m²]	Thermal conductivity [W/(mK)]	Area [m²]	Thermal conductivity [W/(mK)]
Sloped wooden battens for drainage	0,0013	0,130	0,0220	0,337
Timber frame construction, with flexible hemp fibre	0,1600	0,043	0,0400	0,130

In addition to the structure of the wall, floor and roof, the detail drawings also show the connections between the wall construction and the window frame. These intersections are included in the analysis, which requires calculating both the overall heat transfer coefficient, U-value, and the thermal resistance, RC-value, of the window. The U-value of the window is determined using the formula below which was discussed earlier in the report. The corresponding R-value can then be easily calculated as the inverse of this U-value.

$$U_w = \frac{\sum A_{gl} \times \frac{U_{gl}}{f_{prac}} + \sum A_{fr} \times U_{fr} + \sum l_{gl} \times \psi_{gl}}{A_{gl} + A_{fr}}$$

The table below, **table 32**, presents the calculated overall heat transder coefficient and thermal resistance value of the window. Given that the same window is used in all details, the corresponding values are applied to each configuration.

Table 32, Calculation of the overall heat transfer coefficient and thermal resistance of the window, own table

Surface glazing [m²]	Overall heat transfer coefficient glazing [(W/m²K)]	Practival performance factor	Surface frame [m²]	Overall heat transfer coefficient frame [(W/m²K)]	Length outlines glazing [m]	Linear heat transfer coefficient glazing [(W/m²K)]
0.175	1.5	1	0.067	1.35	1	0.05

Overall heat transfer coefficient window [W/(m²K)]
1.66

Thermal resistance [(m²K)/W]
0.60

Density mass per unit area of the wall construction

As weight is a crucial factor in top-up buildings, the mass per unit area of each wall construction is determined for every detail. When a layer consists of multiple materials, the equivalent density is calculated to obtain a representative value for the mass. This equivalent density is then used in the formula provided below. The necessary values for this calculation are presented in **table 33**.

$$m' = \sum_{i=1}^{n} (\rho_i \times d_i)$$

Table 33, Calculation of the density mass per unit area, own table

Material	Thickness [m]	Density [kg/m³]
Vertical wooden cladding	0,018	520
Ventilated cavity with horizontal wooden cladding batten, center-to-center 600 mm	0,024	35
Ventilated cavity with vertical wooden cladding batten, center-to-center 600 mm	0,024	35
Pressure-resistant woodfibre insulation plate	0,040	140
Timber frame construction, with hempcrete blocks	0,250	348
Clay plaster	0,020	1600

This formula, gives a **m'-value** of **136 kg/m²** for the **first detail configuration**.

Phase-shift

The last step of the manual calculations is the calculation of the phase shift, **φ-value,** of the insulation materials. As the calculation of the phase shift requires a higher level of accuracy, which can be achieved using specialised software, a simplified formula is applied in this study. Given that the various layers within the construction influence one another, and thereby affect the total phase shift, a detailed calculation falls outside the scope of this thesis. Nevertheless, by applying the simplified formulas, an approximate phase shift of the insulation materials is determined and gives a good approximation.

Table 34 shows the **values** that are used for the phase shift calculation of the **insulation materials** of the detail configuration.

$$\varphi = (\sum_{i=1}^{n} \left(\frac{d_i}{2\pi d^*}\right) \times t_0)/3600$$

With:

$$d^* = \sqrt{\frac{\alpha_i t_0}{\pi}}$$

$$\alpha_i = \frac{\lambda_i}{\rho_i \times c_i}$$

$$t_0 = 24 \times 3600$$

Table 34, Calculation of the phase shift, own table

Material	Thickness [m]	Thermal conductivity [W/(mK)]	Density [kg/m³]	Specific heat capacity [J/(kgK)]
Timber frame construction, with hempcrete blocks	0,250	0,0794	348,6	1771

By using the first presented formula, the resulting **φ-value** for **the first configuration** is **16,0 h.**

Geometry WUFI

As previously described, the geometry of each detail must be simplified. **Figures 121, 120,** and **119** below show the simplified geometries of **detail V1**, **detail V2**, and **detail H1**, respectively. These visualisations also indicate the **applied surface conditions** and the **positions of the isopleths**, the results of which are presented and discussed later.

To ensure correct **simplification** of the details, the ISSO 10077:2017 standard was applied. This allows the adjusted geometries to be correctly validated within WUFI.

Additionaly, the **NEN 2778:2015** standard has been followed for the numerical grid used in this analysis.

With regard to the assignment of materials within the details, materials from the WUFI database were assigned wherever possible. In cases where specific materials were not available in the database, comparable materials were selected as a basis. The known material properties of the original material were then manually assigned to the selected material in the database, in order to ensure the most accurate possible representation within the simulations.

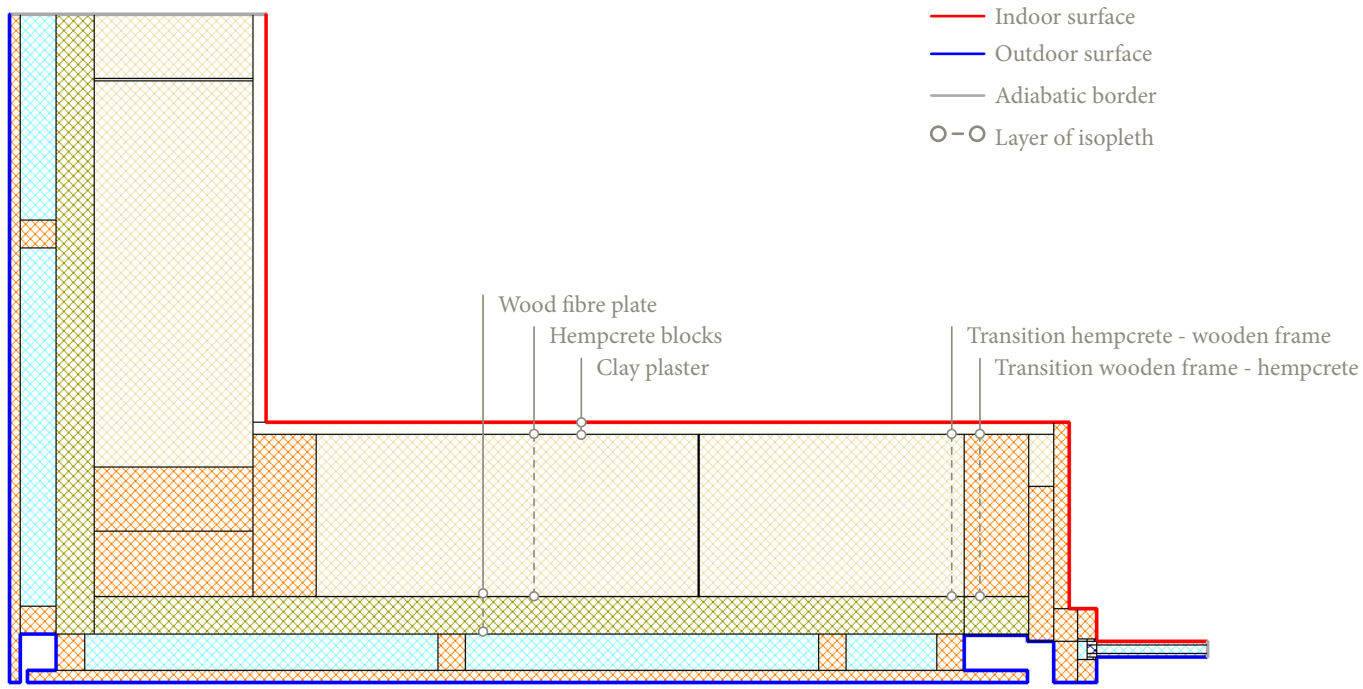

Figure 119, Geometry detail H1 including location isopleths, screenshot WUFI

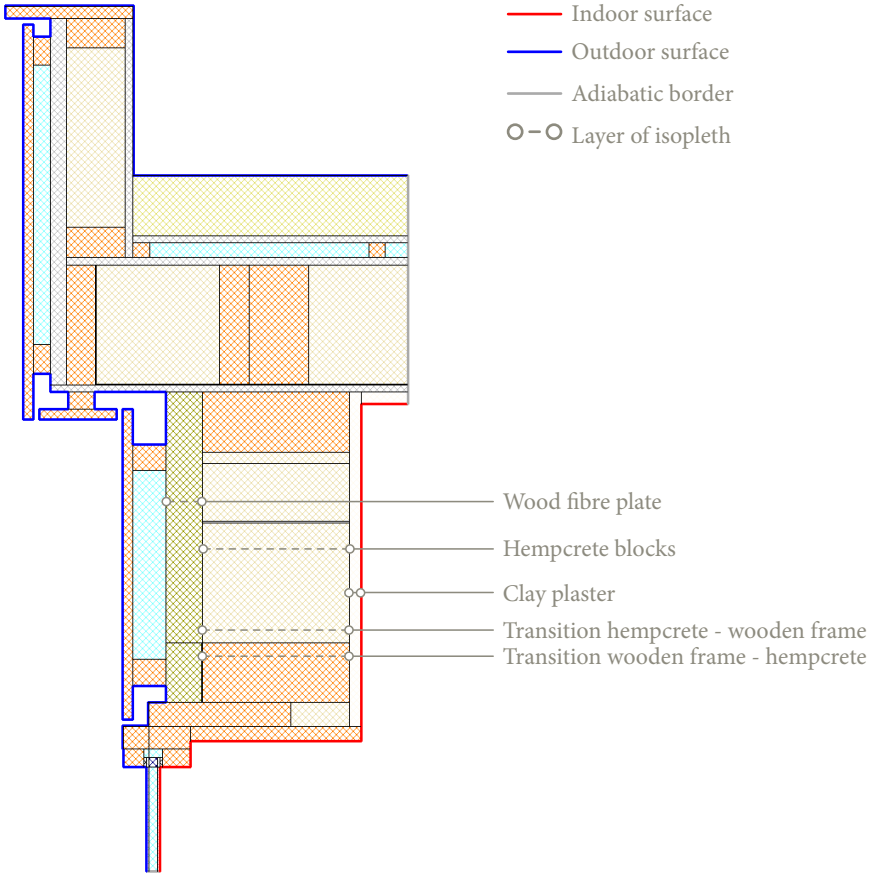

Figure 120, Geometry detail V2 including location isopleths, screenshot WUFI

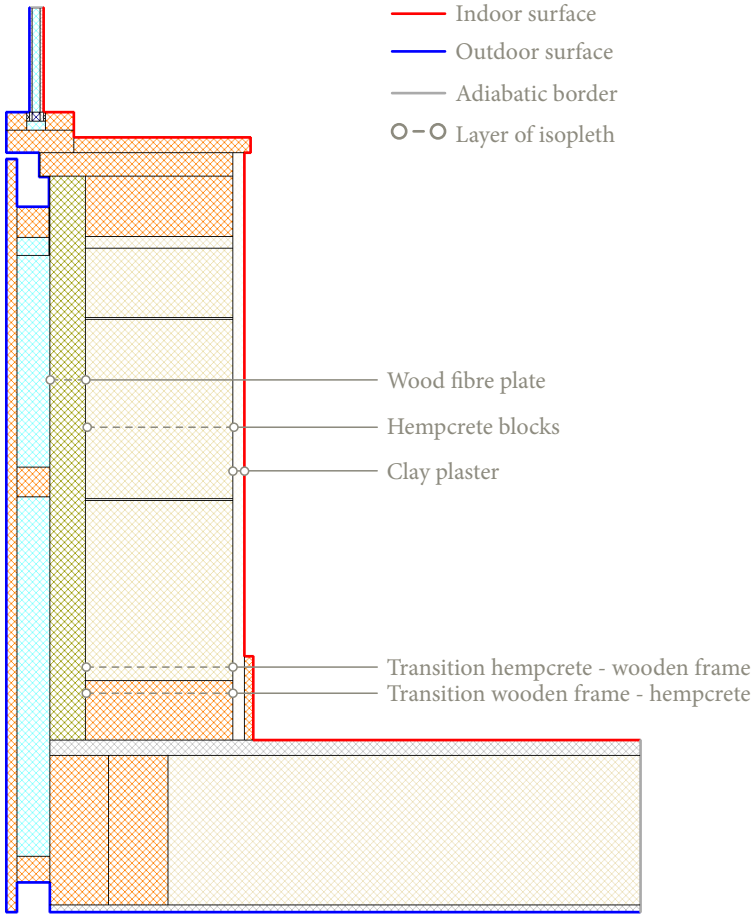

Figure 121, Geometry detail V1 including location isopleths, screenshot WUFI

Isopleths

Each detail is analysed in WUFI based on **isopleths**, using the climate file defined by the NEN 5060 standard, which is used to run a simulation over a ten-year period. To assess the risk of mould growth within the façade construction, the **various layers** within each detail are evaluated using the isopleth analysis.

If the isopleth values remain **below** the **LIM-threshold values**, it can be concluded with reasonable certainty that there is no significant risk of mould development in the respective layer. The analysed layers are shown in **figure 119, figure 120**, and **figure 121**. The results of the isopleth analysis, as simulated in WUFI over the ten-year period, are presented below for each detail within the first detail configuration.

Isopleths - V1

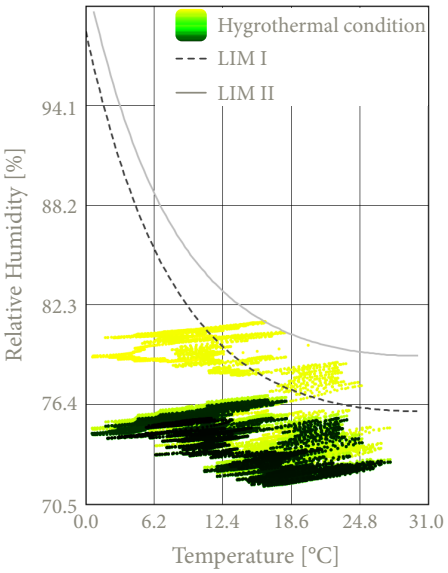

Figure 122, Isopleths wood fibre plate

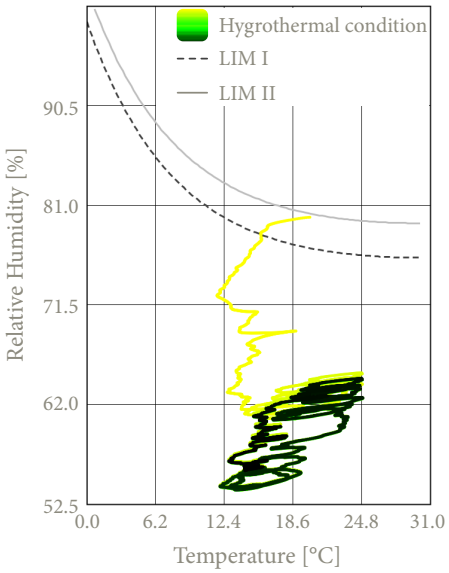

Figure 123, Isopleths hempcrete blocks

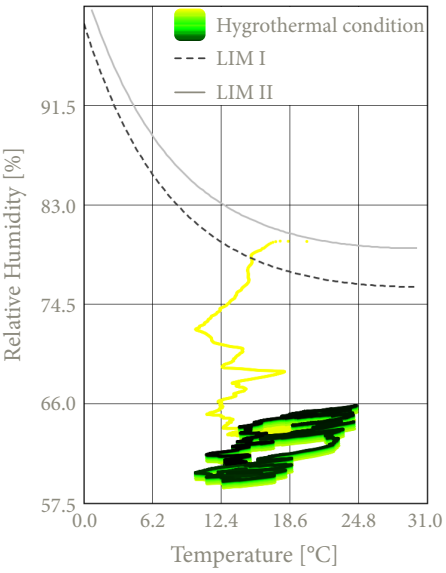

Figure 124, Isopleths transition hempcrete & frame

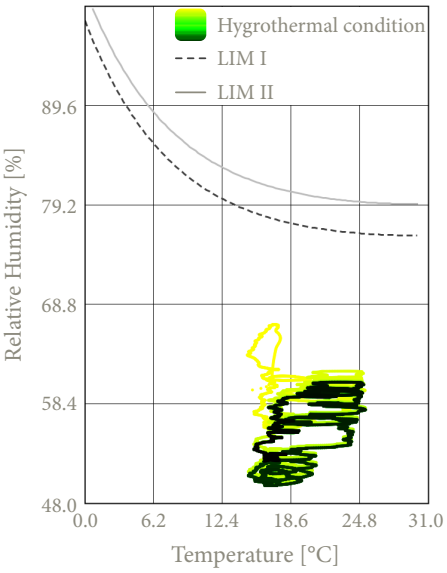

Figure 125, Isopleths transition frame & hempcrete

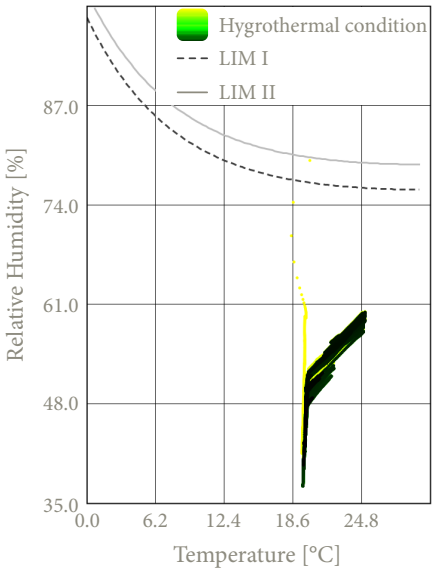

Figure 126, Isopleths clay plaster

Isopleths - V2

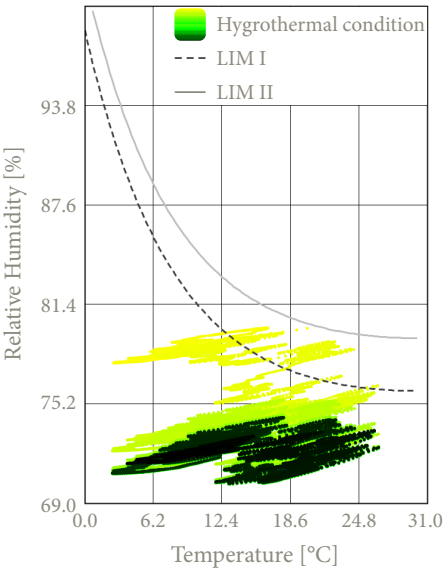

Figure 127, Isopleths wood fibre plate

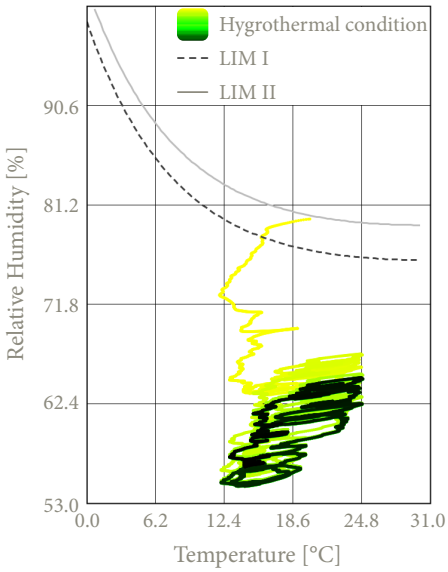

Figure 128, Isopleths hempcrete blocks

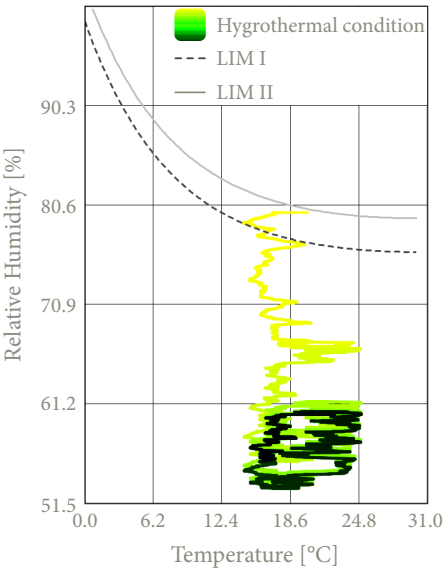

Figure 129, Isopleths transition hempcrete & frame

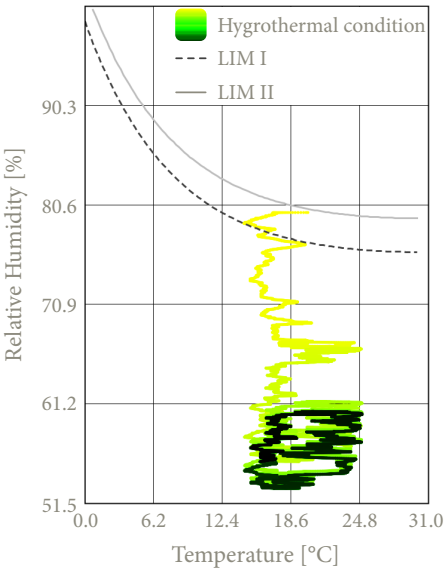

Figure 130, Isopleths transition frame & hempcrete

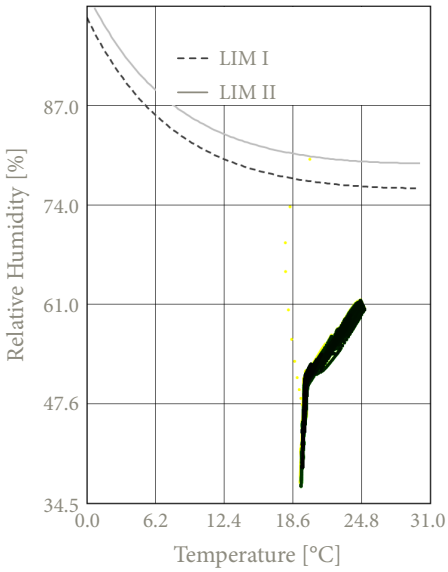

Figure 131, Isopleths clay plaster

Isopleths - H1

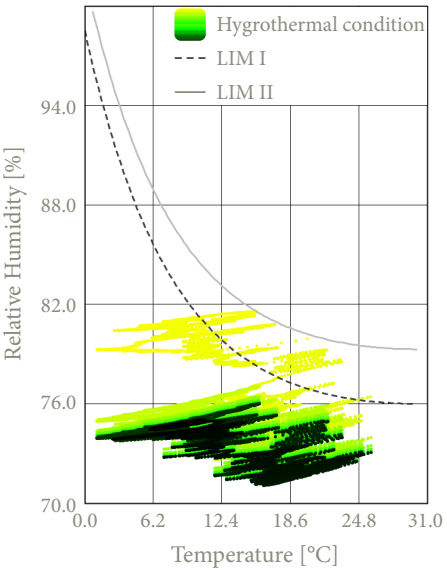

Figure 132, Isopleths wood fibre plate

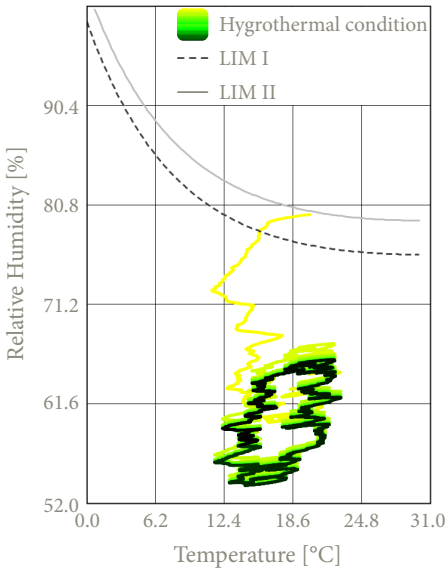

Figure 133, Isopleths hempcrete blocks

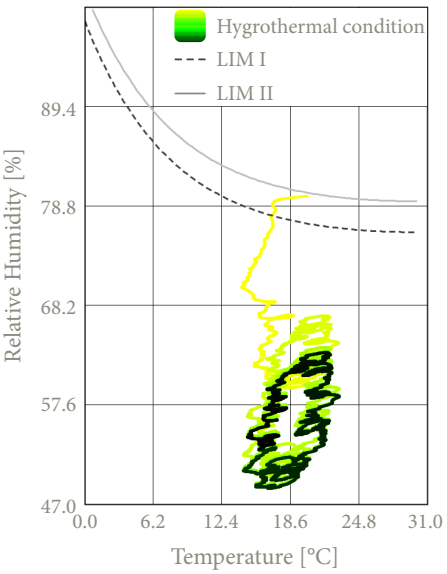

Figure 134, Isopleths transition hempcrete & frame

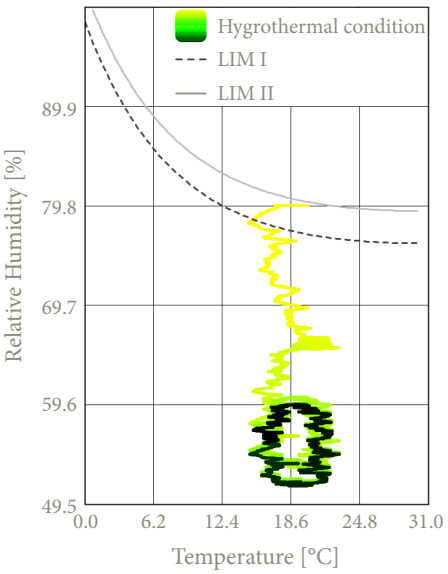

Figure 135, Isopleths transition frame & hempcrete

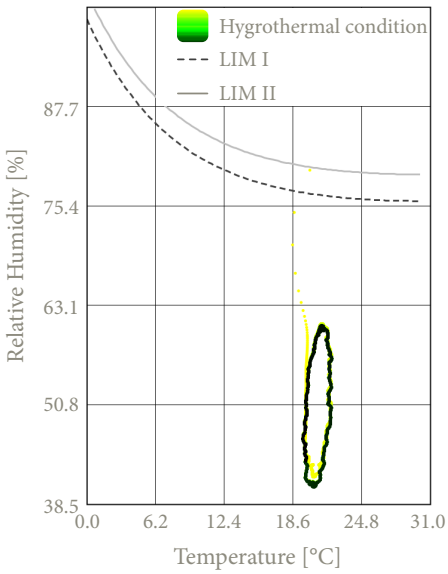

Figure 136, Isopleths clay plaster

Conclusion isoplteths

Based on the analysed isopleths for details **V1**, **V2**, and **H1**, it can be concluded with a high degree of certainty that **no mould growth** is to be expected within the **various material layers** of **this construction configuration**. In all cases, the **isopleth values** for all layers remain **below** the critical threshold values **LIM I** and **LIM II**, indicating that the details meet the established criteria.

With regard to the isopleths related to the **wood fibre plate** in every detail, it can be observed that the relative humidity exceeds the LIM I threshold at the beginning of the simulation. This trend can potentially be attributed to the initial conditions where an initial moisture content of approximately 80% was present in the wood fibre. During the simulation, however, the relative humidity gradually decreases below both LIM I and LIM II indicating that moisture is transportated. This continuously decreasing trend suggests that there is no long-term risk of mould development.

Regarding the isopleths of the **hempcrete blocks**, as well as the **transition zones between the hempcrete blocks** and the **wooden frame**, and the **clay plaster**, values remain well below both LIM-thresholds. At the level of the hemp blocks and at the transition between the blocks and the timber frame, the isopleths show a slight upward trend. However, this increase gradually levels off across all three isopleths with values staying below the critical LIM threshold values.

An interesting result is that the isopleth values for the wood fibre insulation in **detail V2** are **lower** than those in **detail V1** possibly due to a roof overhang that offers protection against direct rain exposure. This suggests that architectural features such as overhangs can have a positive effect on the hygrothermal performance of the façade construction.

In conclusion, it can be stated that this configuration poses no risk of mould growth, thereby complying with the specified isopleth requirements.

Surface condensation - V1

Based on the previously presented formula for determining the minimum surface temperature factor, $f_{Rsi,min}$, the month November has been identified as the most critical period regarding the risk of surface condensation. In order to prevent condensation from occurring in the assessed construction detail, the f_{Rsi} must exceed the threshold value of **0.61**.

To determine the f_{Rsi}, the most critical interior surface temperature of the detail must be considered. This refers to the coldest point within the construction, as illustrated in **figure 137**, below. A time-series plot was generated in WUFI based on this specific point, showing the surface temperature development over a ten-year simulation period and is shown below as well in **figure 138**:

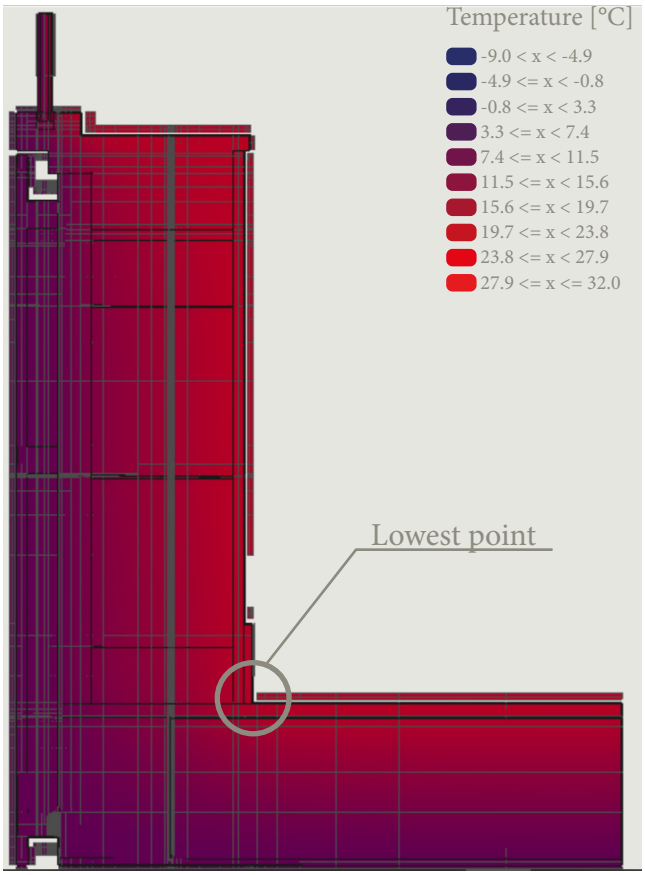

Figure 137, Highlight lowest point, V1

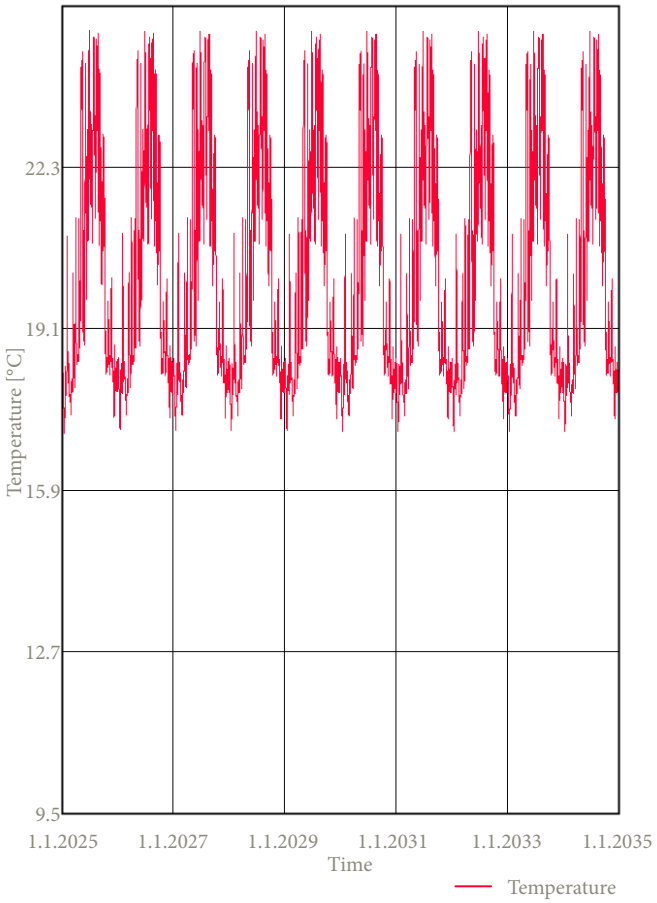

Figure 138, Temperature at the critical surface temperature, V1

From this plot, the lowest surface temperature of **15.94 °C** was obtained and subsequently applied in the following formula:

$$f_{Rsi} = \frac{\theta_{si} - \theta_e}{\theta_i - \theta_e}$$

The resulting f_{Rsi} for this detail is **0.66**. Since this value exceeds the previously established minimum of **0.61**, it can be concluded that the risk of mold growth in this construction detail is negligible.

F-factor - V1

For the calculation of the **f-factor,** the same reference point previously established during the analysis of surface condensation was used. A steady-state calculation was conducted based on this point, using the corresponding **interior surface temperature**. Since the calculation assumes **steady-state conditions**, a temperature value was selected at the point where the temperature remains constant.

Based on this stabilized temperature, an interior surface temperature of **17.07 °C** was determined. This value was subsequently applied in the formula below to calculate the f-factor.

$$f_{factor} = \frac{\theta_{io} - \theta_e}{\theta_i - \theta_e}$$

The resulting **f-factor** is **0.94**, indicating a very limited thermal bridge in the assessed detail. Given that this value significantly exceeds the required threshold of **0.65**, it can be concluded that the detail complies with the thermal performance requirements set by the Dutch Building Decree

PSI-value - V1

The final step in the assessment of the detail within this configuration involves determining the **linear thermal transmittance**, the **Ψ-value**. This calculation is performed using the formula provided below.

$$\psi = \frac{Q_{WUFI} - Q_{ideal\ condition}}{L \times \Delta T}$$

First, the $\mathbf{Q_{ideal\ condition}}$ must be determined, which is calculated using the following formula:

$$Q_{ideal\ condition} = \sum_{i=1}^{n} \frac{A_{construction} \times \Delta T}{R_{construction}}$$

In the context of **detail V1**, the **window, wall, and floor constructions** are relevant for determing the $Q_{ideal\ condition}$. The **thermal resistances** for these building components are presented at the beginning of the detail assessment. The construction areas, $\mathbf{A_{construction}}$, are derived based on the previously defined surface of the construction, $\mathbf{A_{con}}$. Lastly a **ΔT** of **18 K** is assumed.

The table below, **table 35,** presents the used values in the calculation of $\mathbf{Q_{ideal\ condition}}$.

Table 35, Calculation of the $Q_{ideal\ condition}$ V1, own table

$R_{construction,\ window}$ [(m²K)/W]	$A_{construction,\ window}$ [m²]	$R_{construction,\ wall}$ [(m²K)/W]	$A_{construction,\ wall}$ [m²]	$R_{construction,\ floor}$ [(m²K)/W]	$A_{construction,\ floor}$ [m²]
0.600	0.2425	4.884	0.943	4.648	0.685

The resulting $\mathbf{Q_{ideal\ condition}}$ is **13.403 W**

Based on the simulation in WUFI, $\mathbf{Q_{WUFI}}$ is determined by analysing the **heat flow** across the entire detail, taking into account the projected surface area, $\mathbf{A_T}$.

Q_{WUFI} represents the sum of all heat flows through the detail, resulting in a total heat flow of **14.464 W**.

By using the first presented formula, the resulting **Ψ-value** for **detail V1** is **0.059 W/(mK)**, indicating that the detail can be characterised as a well-insulated building component, which reflects limited heat transfer and favourable thermal performance.

Surface condensation - V2

Based on the previously presented formula for determining the minimum surface temperature factor, $f_{Rsi,min}$, the month November has been identified as the most critical period regarding the risk of surface condensation. In order to prevent condensation from occurring in the assessed construction detail, the f_{Rsi} must exceed the threshold value of **0.61**.

To determine the f_{Rsi}, the most critical interior surface temperature of the detail must be considered. This refers to the coldest point within the construction, as illustrated in **figure 139**, below. A time-series plot was generated in WUFI based on this specific point, showing the surface temperature development over a ten-year simulation period and is shown below as well in **figure 140**:

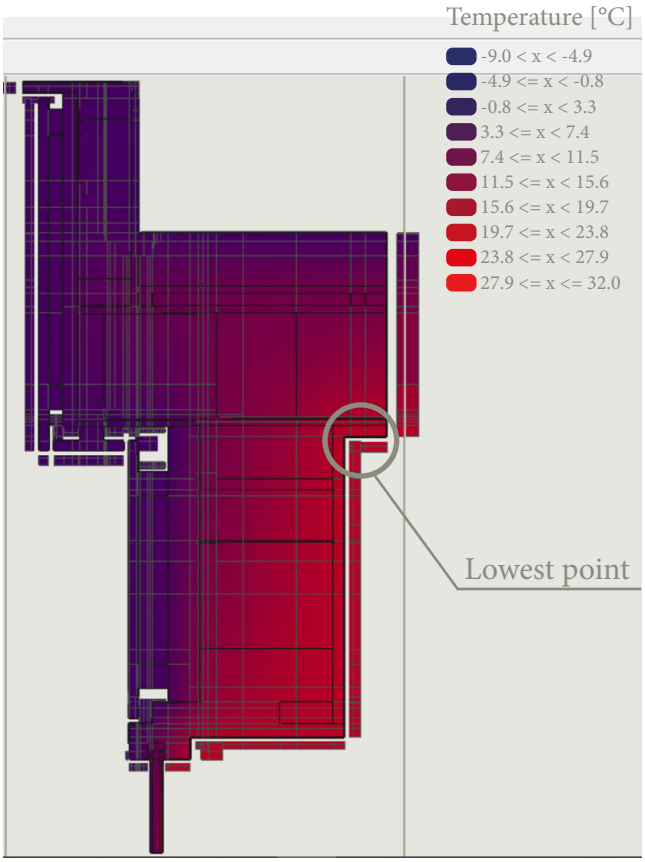

Figure 139, Highlight lowest point, V2

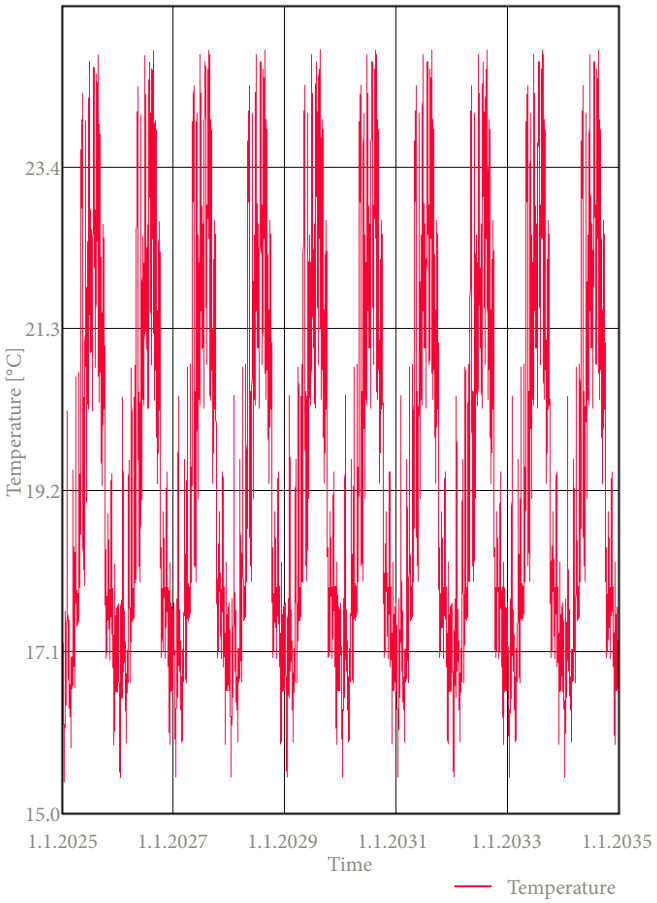

Figure 140, Temperature at the critical surface temperature, V2

From this plot, the lowest surface temperature of **15.40 °C** was obtained and subsequently applied in the following formula:

$$f_{Rsi} = \frac{\theta_{si} - \theta_e}{\theta_i - \theta_e}$$

The resulting f_{Rsi} for this detail is **0.62**. Since this value exceeds the previously established minimum of **0.61**, it can be concluded that the risk of mold growth in this construction detail is negligible.

F-factor - V2

For the calculation of the **f-factor,** the same reference point previously established during the analysis of surface condensation was used. The steady-state calculation was conducted based on this point, using the corresponding **interior surface temperature**. Since the calculation assumes **steady-state conditions**, a temperature value was selected at the point where the temperature remains constant.

Based on this stabilized temperature, an interior surface temperature of **16.92 °C** was determined. This value was subsequently applied in the formula below to calculate the f-factor.

$$f_{factor} = \frac{\theta_{io} - \theta_e}{\theta_i - \theta_e}$$

The resulting **f-factor** is **0.94**, indicating a very limited thermal bridge in the assessed detail. Given that this value significantly exceeds the required threshold of **0.65**, it can be concluded that the detail complies with the thermal performance requirements set by the Dutch Building Decree

PSI-value - V2

The final step in the assessment of the detail within this configuration involves determining the **linear thermal transmittance**, the **Ψ-value**. This calculation is performed using the formula provided below.

$$\psi = \frac{Q_{WUFI} - Q_{ideal\ condition}}{L \times \Delta T}$$

First, the $\mathbf{Q_{ideal\ condition}}$ must be determined, which is calculated using the following formula:

$$Q_{ideal\ condition} = \sum_{i=1}^{n} \frac{A_{construction} \times \Delta T}{R_{construction}}$$

In the context of **detail V2**, the **window, wall, and roof constructions** are relevant for determing the $Q_{ideal\ condition}$. The **thermal resistances** for these building components are presented at the beginning of the detail assessment. The construction areas, $\mathbf{A_{construction}}$, are derived based on the previously defined surface of the construction, $\mathbf{A_{con}}$. Lastly a **ΔT** of **18 K** is assumed.

The table below, **table 37,** presents the used values in the calculation of $\mathbf{Q_{ideal\ condition}}$.

Table 37, Calculation of the $Q_{ideal\ condition}$ V2, own table

$R_{construction,\ window}$ [(m²K)/W]	$A_{construction,\ window}$ [m²]	$R_{construction,\ wall}$ [(m²K)/W]	$A_{construction,\ wall}$ [m²]	$R_{construction,\ roof}$ [(m²K)/W]	$A_{construction,\ roof}$ [m²]
0.600	0.2425	4.884	0.274	6.442	0.090

The resulting $\mathbf{Q_{ideal\ condition}}$ is **8.536 W**

Based on the simulation in WUFI, $\mathbf{Q_{WUFI}}$ is determined by analysing the **heat flow** across the entire detail, taking into account the projected surface area, $\mathbf{A_T}$.

Q_{WUFI} represents the sum of all heat flows through the detail, resulting in a total heat flow of **9.770 W**.

By using the first presented formula, the resulting **Ψ-value** for **detail V2** is **0.068 W/(mK)**, indicating that the detail can be characterised as a well-insulated building component, which reflects limited heat transfer and favourable thermal performance.

Surface condensation - H1

Based on the previously presented formula for determining the minimum surface temperature factor, $\mathbf{f_{Rsi,min}}$, the month November has been identified as the most critical period regarding the risk of surface condensation. In order to prevent condensation from occurring in the assessed construction detail, the $\mathbf{f_{Rsi}}$ must exceed the threshold value of **0.61**.

To determine the $\mathbf{f_{Rsi}}$, the most critical interior surface temperature of the detail must be considered. This refers to the coldest point within the construction, as illustrated in **figure 141**, below. A time-series plot was generated in WUFI based on this specific point, showing the surface temperature development over a ten-year simulation period and is shown below as well in **figure 142**:

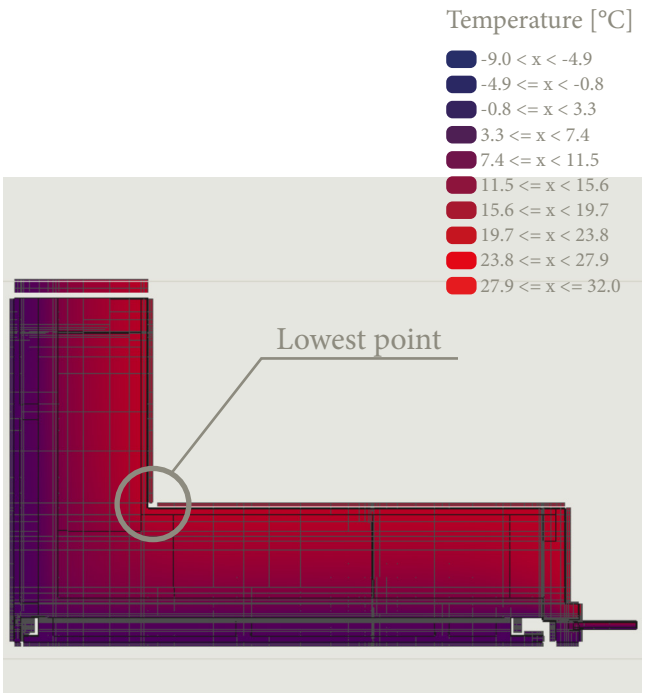

Figure 141, Highlight lowest point, V3

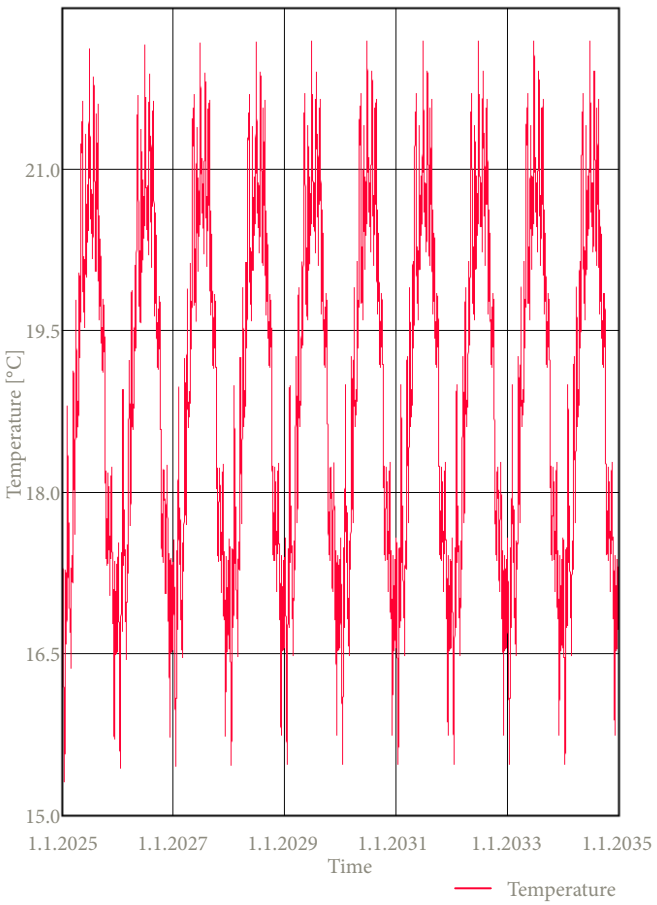

Figure 142, Temperature at the critical surface temperature, V3

From this plot, the lowest surface temperature of **15.31 °C** was obtained and subsequently applied in the following formula:

$$f_{Rsi} = \frac{\theta_{si} - \theta_e}{\theta_i - \theta_e}$$

The resulting $\mathbf{f_{Rsi}}$ for this detail is **0.61**. Since this value is the same as the previously established minimum of **0.61**, it can be concluded that the risk of mold growth in this construction detail is negligible. However since the value is the same as the minimum, extra attention is needed if the value drops below 0.61. This situation may occur under different indoor climate conditions and can be prevented by applying a thicker insulation layer or by adding extra insulation at the relevant location. Under the given indoor climate conditions, however, the detail in question is surficcient.

F-factor - H1

For the calculation of the **f-factor,** the same reference point previously established during the analysis of surface condensation was used. The steady-state calculation was conducted based on this point, using the corresponding **interior surface temperature**. Since the calculation assumes **steady-state conditions**, a temperature value was selected at the point where the temperature remains constant.

Based on this stabilized temperature, an interior surface temperature of **16.99 °C** was determined. This value was subsequently applied in the formula below to calculate the f-factor.

$$f_{factor} = \frac{\theta_{io} - \theta_e}{\theta_i - \theta_e}$$

The resulting **f-factor** is **0.94**, indicating a very limited thermal bridge in the assessed detail. Given that this value significantly exceeds the required threshold of **0.65**, it can be concluded that the detail complies with the thermal performance requirements set by the Dutch Building Decree

PSI-value - H1

The final step in the assessment of the detail within this configuration involves determining the **linear thermal transmittance**, the **Ψ-value**. This calculation is performed using the formula provided below.

$$\psi = \frac{Q_{WUFI} - Q_{ideal\ condition}}{L \times \Delta T}$$

First, the $\mathbf{Q_{ideal\ condition}}$ must be determined, which is calculated using the following formula:

$$Q_{ideal\ condition} = \sum_{i=1}^{n} \frac{A_{construction} \times \Delta T}{R_{construction}}$$

In the context of **detail H1**, the **window and wall constructions** are relevant for determing the $Q_{ideal\ condition}$. The **thermal resistances** for these building components are presented at the beginning of the detail assessment. The construction areas, $\mathbf{A_{construction}}$, are derived based on the previously defined surface of the construction, $\mathbf{A_{con}}$. Lastly a **ΔT** of **18 K** is assumed.

The table below, **table 38,** presents the used values in the calculation of $\mathbf{Q_{ideal\ condition}}$.

Table 38, Calculation of the $Q_{ideal\ condition}$ H1, own table

$R_{construction,\ window}$ [(m²K)/W]	$A_{construction,\ window}$ [m²]	$R_{construction,\ wall}$ [(m²K)/W]	$A_{construction,\ wall}$ [m²]
0.600	0.2425	4.884	2.229

The resulting $\mathbf{Q_{ideal\ condition}}$ is **15.489 W**

Based on the simulation in WUFI, $\mathbf{Q_{WUFI}}$ is determined by analysing the **heat flow** across the entire detail, taking into account the projected surface area, $\mathbf{A_T}$.

Q_{WUFI} represents the sum of all heat flows through the detail, resulting in a total heat flow of **16.886 W**.

By using the first presented formula, the resulting **Ψ-value** for **detail H1** is **0.077 W/(mK)**, indicating that the detail can be characterised as a well-insulated building component, which reflects limited heat transfer and favourable thermal performance.

Assessment detail configuration

Important notes about the details

For the given configuration, **key considerations** are presented below in the form of bullet points. These points highlight specific aspects that need to be taken into account during detailing and construction.

- Apply 3 mm of hydraulic lime to all contact surfaces to ensure proper adhesion between the blocks.
- Place the blocks in staggered joints to distribute load correctly and minimize the thermal bridge.
- The blocks can be easily cut to size to fit for every project.
- Fill the gaps between the blocks and the timber structural frame with 20 mm of flexible hemp.
- Attach the water-resistant barrier of the window frame to the timber structural frame.
- The hempcrete lintel is equipped with a concrete core and needs to have 200 mm bearing.
- The screws of the wood fibre must reach the center of the timber frame to ensure secure attachment.
- Use stainless steel screws with 2 times the thickness of the battens to sufficient load-bearing capacity.
- Stainless steel nails must be at least 2.5 times the thickness of the cladding.
- The stainless steel nails must be placed 40 mm from the outer edge of the cladding.
- Ensure 10 mm gaps for ventilation both between cladding boards and at the window frame.
- Use a jute reinforcement mesh between the rough and finishing clay plaster to prevent cracking.

Assessment of the configuration

Additionally, the configuration is evaluated based on the following criteria:

1. **Weight**: The total mass per unit area of the wall construction.
2. **Construction time**: The time required for assembling the construction.
3. **Resistance Construction-value:** The combined thermal resistance of all layers in the construction.
4. **Phase shift**: The heat transfer delay of the structure.

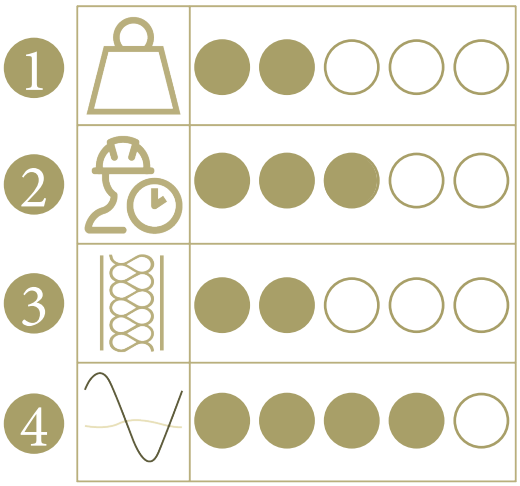

Axonometric view of the detail configuration

In addition to the presented details, an axonometric view of the respective detail is also shown. This is presented in the figure below, **figure 143**, and is intended to provide more clarity and insight into **detail V1**, **detail V2**, and **detail H1**.

Figure 143, Axonometric view of detail configuration 1

Conclusion

The conclusion below applies to **all eleven detail configurations**. **Chapter 5** highlights one configuration, in which the applied methodology and corresponding results are explained. The remaining ten configurations, comprising thirty details in total, are included in **appendix A**. For these configurations the same methodology has been applied. In the **same appendix** the corresponding graphs and results are shown as well.

Isopleths

Based on the analysed **isopleth simulations**, it can be concluded that the **bio-based materials** show a **low risk of mould growth** under the simulated climate conditions. Over the **ten-year simulation period**, **most isopleth simulations** remain **below** the **critical LIM I** and **LIM II thresholds**, indicating that **no harmful moisture accumulation** is **likely** to **occur** that could lead to **mould growth within** the **layer**. The conclusion below clusters the outcomes of the various configurations according to material layers.

Finishing

In **detail configuration 2**, the **plaster finish exceeds** the **critical LIM thresholds** which **indicates** that **conventional plasters** are **not sufficiently resistant** to **moisture build-up**. Consequently, a **mould-resistant** and **vapour-open plaster** should be **applied**, which must also be **resistant** to **weathering** and **fluctuations** in **relative humidity** (Piot et al., 2017).

The **cork façade finish** used in configurations **4**, **5**, **7**, **9**, and **11** also **exceeds** the **threshold values**. However, research by Hon (2024) indicates that **cork** is **resistant** to **mould growth**, and due to its porosity, it can **buffer fluctuations** in **relative humidity**. Nevertheless, **further research** is **needed** to confirm with certainty that no mould growth occurs in either of the finishing layers.

As shown in configurations **5**, **7**, **9**, and **11**, the **expanded insulation cork board** behind the cork façade panel is **better protected** against **moisture ingress**. Over time, the **isopleths** drop **below** the **LIM thresholds** and show a **declining trend**.

Outdoor biobased construction board/ wood fibre board

The outer boards initially show a **temporary exceedance** of **LIM I** and, in **some cases**, **LIM II**, likely due to the initial 80% moisture content in the material. Over time, the isopleths fall **below** the **LIM thresholds**. An **exception** is **V1** in **configuration 3**, where a **slight upward trend** is observed, although it **stagnates**. Overall, it can be stated that both board types have a **minor risk** of **mould formation**.

Insulation and transition to timber frame

For the **insulation materials** and the **transitions** between **insulation** and the **timber window frame**, all graphs remain **below** the **LIM thresholds** and show a **downward trend**. **Exceptions** are **V1** in **configurations 1**, **2**, **3**, **6**, and **10**, where a **slight increase** is visible. However, this trend **stagnates** over time. Additionally, the graphs stay **below** the **LIM thresholds** in all cases indicating a **limited risk** of **mould formation** in these layers.

Interior biobased construction board & clay plaster

All simulations show that the **indoor bio-based construction boards** and **clay plaster** remain **well below** the **LIM thresholds**. The slight decrease in moisture content at the interior board suggests some drying, which is unfavourable for mould growth. Therefore, these layers pose **no risk** of **mould formation** and contribute positively to a healthy indoor climate.

Surface condensation

Regarding surface condensation, it can be concluded that **none** of the tested details have **condensation** at the coldest surface point. For all details, the calculated $\mathbf{f_{Rsi}}$**-value** is **above** the **minimum requirement** of **0.61**, indicating a **negligible risk**.

However, detail **H1** in configuration **1** and detail **V1** in configurations **7** and **8** show a $\mathbf{f_{Rsi}}$ of exactly **0.61**. This means that, under **current climate conditions**, **no surface condensation** occurs but these locations are **vulnerable**. A minor drop in surface temperature, for example due to variable conditions (at a bathroom) or user behaviour, could result in an $\mathbf{f_{Rsi}}$ **below 0.61**, **increasing** the **risk** of **condensation**.

According to the NEN-EN-ISO 13788:2013 standards applied in this study, there is **no risk** of **surface condensation** under this simulated conditions. If **lower f_{Rsi}-values** occur, **improvements** must be made. While increasing insulation thickness is one option, it would add additional weight on the existing foundation. A better alternative is to apply additional insulation locally at the critical point.

Finally, it is noteworthy that **V1 details** in most configurations show **lower f_{Rsi}-values** than the **V2** and **H1** details within the same configurations. This may indicate weaker thermal performance at the V1 locations, **increasing** the **risk** of **surface condensation**. Nonetheless, the **values** remain within **acceptable limits** so within the scope of this study no further measures are necessary.

F-factor

As stated previously, the **Dutch Building Decree** sets a performance requirement with regard to the thermal quality of junctions, requiring a **minimum f-factor** of **0.65**. To calculate this steady-state simulations are carried out in accordance with NEN 2778. The outcome of this study confirms that all assessed details meet this requirement.

The **calculated f-factors** are around **0.90**, indicating **very good thermal quality** of the analysed junctions and a negligible risk of thermal bridge in the details. These high values are likely the result of designs where insulation is nearly continuous across the connections. The simulation results therefore confirm that the applied insulation thicknesses are adequate and that it is feasible to achieve thermally high-performing construction connections using bio-based materials. In conclusion, the **thermal quality** of the detail configurations can be **guaranteed**.

When examining the results of the **f-factor** and **surface condensation**, same results will be expected, as the same geometries and boundary conditions were used in both calculations. However, a **difference** can be observed. A possible **explanation** for this is that the **surface condensation** simulation includes **dynamic effects** and **accounts** for the **moisture conditions** of the **materials**. These **two factors** may explain the **difference** between the **f_{Rsi}-value** derived from **surface condensation** and the calculated **f-factor**.

PSI-value

The calculated **ψ-values** provide **information** regarding the **additional heat loss** occurring at **connections** between **construction elements** in each detail. While the f-factor indicates the risk of surface condensation, the **ψ-value** quantifies **linear thermal transmittance** (W/mK) caused by thermal bridging.

The simulations show that the developed details, **V1** (floor–wall connection & wall–window frame connection), **V2** (roof–wall connection & wall–window frame connection), and **H1** (corner–wall connection & wall–window frame connection), have moderate ψ-values across all **11 configurations**.

The **ψ-values** for these developed details range between **0.051** and **0.098 W/mK**. This suggest that there are no extreme thermal bridges. This aligns with expectations, as **none** of the **details** exhibit an **f-factor below 0.65**. Detail V1 of configuration 4 shows the lowest ψ-value, indicating an efficient floor–wall connection. The **highest value** was found at detail **V2** of configuration **2**. This suggests potential for improvement at the roof–wall connection in this detail.

When compared with the '**ISSO reference details**', **similar ψ-values** are observed, indicating **good thermal performance**. If desired, the details exceeding 0.07 W/mK could be improved to minimise thermal bridging. This ensured uniform heat loss across all details. However, this is not necessary.

Lastly, an important **note** must be given regarding the calculated **Ψ-values**. These values represent the thermal performance of the **entire** construction detail as a whole. While it is **common practice** to **separate** and calculate **Ψ-values** for each **individual** connection within a detail, in this study the values have been aggregated into a **total** value per construction detail.

For the **V1 details**, this includes both the **connection** between the **bottom of the window frame** and **the wall construction**, **and** the **connection** between the **floor**- and the **wall construction**. In the case of the **V2 details**, it refers to the **connection** between the **top of the window frame** and the **wall construction**, **as well as** the **connection** between the **roof**- and the **wall construction**. Finally, the calculated **Ψ-value** for **H1** covers both the **connection** between the **side window frame** and the **wall construction**, **and** the **corner connection** within the **wall construction**.

6. Conclusion

Conclusion

This master's thesis focused on the following central research question:

"*How can bio-based façade wall details for residential top-up buildings be developed according to thermal and moisture regulation within the construction?*"

Based on the research conducted and the simulations performed, it can be concluded that bio-based façade wall reference details can be **effectively** applied within Dutch construction. This is feasible as long as the **vapour permeability** of the construction and the established **design principles** are considered to ensure correct **moisture transport** and **thermal performance**. The results of this study thereby confirm the hypothesis that the proposed **bio-based reference details** can be **used** for **Dutch residential top-up buildings**.

Firstly, the research highlights the various **advantages** that bio-based materials offer compared to conventional materials. These materials are distinguished by **renewability**, the potential for **local cultivation**, **circular applicability**, and the **contribution** to **reducing CO_2**- and **NO_2-emissions**. Moreover, the materials possess **excellent thermal** and **moisture-regulating properties**, including **low thermal conductivity**, effective ability to **buffer moisture** and **volatile organic compounds**, and significant **thermal mass** as compared to many other insulation materials. These characteristics make the materials **suitable** for application in **lightweight** and **vapour-open façade wall constructions**. The aspects of **lightweight** design, **extended phase shift**, and **vapour permeability** are of great importance for residential top-up buildings.

The suitability of a selection of five bio-based materials consisting of **cork**, **flax**, **hemp**, **straw**, and **wood** was subsequently substantiated and applied in **eleven detail configurations**. Each configuration contains **three details** that show the **connection** between the **façade wall** and the **floor** and **roof construction**, as well as the **window frame**. Each detail within the configuration was analysed for **moisture transport**, **risk** of **mould growth**, **condensation**, and **thermal performance**. Simulations conducted using WUFI indicate that **most materials** remain **below** the critical **LIM I** and **LIM II** threshold values. This suggests a **low** risk of **mould formation** within the **respective layer**. Only some exterior finishes, such as conventional plasters and cork panels, an excess was detected.

Surface condensation analysis shows that **none** of the **details** experience **condensation** under simulated conditions. All **f_{Rsi}-values exceed** the **minimum threshold $f_{Rsi,min}$** of **0.61**. In some cases, the **f_{Rsi}-value** is **at** the **limit boundary** of the **threshold** implying increased **vulnerability** under extreme climate conditions. Regarding the **f-factor**, the simulations indicate a value of **0.90**, which indicates **very good thermal quality** of the details. The reference details therefore amply comply with the **requirement** of the **Dutch Building Decree**, which requires a **minimum** of **0.65**. Finally, simulations for determining **ψ-values** reveal values between **0.051** and **0.098** W/mK, indicating that the details have **similar** results as the '**ISSO reference details**' and consequently have a **low thermal bridge** effect.

Moreover, the study highlights the essential importance of the correct implementation of the materials within a façade wall construction. A build-up characterised by **increasing vapour permeability from** the **interior to** the **exterior**, while **avoiding vapour-retarding layers** on **both sides**, is crucial for preventing **moisture-related issues**. Additionally, the presented **design principles** should also be followed for **effective implementation** of bio-based materials. **General design principles** such as adequate ventilation, a minimum elevation of 300 mm, a minimum overhang of 150 mm, and the use of window drip caps, all contribute to **protect** against **splashing rainwater**, **rising damp**, and **correct water drainage**.

Through this design-based research and the execution of simulations, it has been demonstrated that **bio-based façade wall reference details** can be **effectively implemented** in **residential top-up buildings**. The careful application of selected bio-based materials according to the described design principles is crucial. The **simulation results** provide **supporting arguments** for the hypothesis and confirm both the correct movement of moisture transport and the thermal performance of the proposed details.

Discussion

This research provides an answer to **how bio-based façade wall reference details** can be **developed** that **ensure both effective moisture regulation** and **sufficient thermal resistance**. As outlined in the problem statement, there is **limited knowledge** regarding the **application** of these materials in the construction sector. Furthermore, there is **insufficient understanding** of **moisture behaviour** within building assemblies and how **thermal bridges** can be **avoided**.

The **first sub-question** presents **arguments** for choosing bio-based materials over conventional building materials. The conducted literature review highlights the **benefits** of bio-based materials and **provides arguments** for the **application** of these materials. Since many sources describe these advantages in general terms, a variety of references were consulted to make the intended argument useful for the specific topic this thesis focuses on, residential top-up buildings. These arguments are especially relevant given the Dutch government's ambition to achieve a fully circular economy by 2050, where bio-based materials can significantly contribute to sustainability in the built environment.

The **properties** of bio-based materials that make them **suitable** for **top-up applications** are subsequently **addressed**. The literature reveals several advantages of residential bio-based top-ups, particularly in urban areas where housing shortages are critical. This aligns with various Dutch governmental publications that promote top-up buildings in cities. However, the literature usually describes generally the benefits of bio-based materials and rarely discusses one particular material specifically. For this reason, this chapter is described in general terms where possible future research can highlight one bio-based material.

In order to simulate the reference details in WUFI, the **crucial material properties** were first **identified**. These were obtained primarily from WUFI documentation with additional insights from relevant scientific sources. The chapter outlines the **key equations** and **graphs** used by WUFI during simulations. The **required material properties** were subsequently **integrated** into a market study of bio-based materials. The **market research** is mainly based on **product information** from **suppliers** and is **supplemented by literature**. The results were compiled into an **Excel** database **listing each material** and its **properties** together with a **brief description**. This information contributes to a **better understanding** among building professionals by addressing the current knowledge gap regarding bio-based materials.

To **encourage** broader **acceptance** and **implementation**, a set of **design principles** is developed and illustrated with detailed information on how the materials can be effectively applied. The problem statement highlighted that many **architects** and **engineers lack sufficient knowledge** of how to **design** with **bio-based materials**. To gain the necessary knowledge, books were often consulted. As there is currently no book covering all bio-based materials, a book was applied for each material. Due to the limited availability of detailed literature, supplier datasheets and direct communication with manufacturers were also utilised to obtain additional information. Although this information is not scientifically substantiated, the product information must comply with the applicable regulations, which means it can be considered as verified information.

The **design principles informed** the **development** of the **reference details**, which were produced in a drawing style consistent with 'ISSO reference details'. In addition to the design guidelines, **personal technical knowledge** was applied to construct the drawings. **These details** were subsequently **validated** by **five architects** and **several bio-based material suppliers**.

For the **WUFI simulations**, both **NEN**- and **ISSO-guidelines** were followed to **ensure accurate** and **reliable results**. While the simulations provide **valuable insights** into **mould growth**, **condensation risks** and **thermal bridging**, the validation remains **limited** because **only WUFI** was used. Other simulation can validate the results. Nonetheless, the aim is to remove uncertainty among building professionals by presenting the simulation results with the details.

Overall, the **validity** of this **study** is **supported** by an **extensive literature review** based on **scientific papers**, **books**, **government documents** and **product information from suppliers**. This **diversity** of information sources has provided a **broad theoretical framework**. The use of **recognised NEN**- and **ISSO-guidelines**, in **combination** with **WUFI** as a **reliable software** for **hygrothermal analyses**, **strengthens** the **reliability** of the presented methodology for future research applications.

Overall, the results **confirm** the initial **hypothesis** that a set of **1:5 scale bio-based reference details** can be developed which are **physically suitable** for residential top-up applications. This hypothesis has been confirmed by architects and by simulation outcomes. The materials cork, flax, hemp, straw and wood all demonstrate **good performance** in terms of **moisture transport** and **thermal insulation**. A key finding is that the **vapour-open construction** combined with the **natural properties** of these materials results in **positive outcomes** for **mould prevention**, **condensation control** and **thermal performance**. While certain **finishes exceeded LIM values**, **most materials** remained **within** acceptable **thresholds**. The **f_{Rsi}-values**, **f-factor** and **ψ-values comply** or **exceeded Dutch Building Code requirements**. This demonstrates that **bio-based details** are **useful** for **Dutch construction**. It must be stated, however, that these positive results are only achieved when the proposed design principles are properly implemented.

Limitations

Despite these positive results, the research has **some limitations**. The results were **solely** validated using **WUFI** and therefore **lack confirmation** through **alternative simulation software**. Additionally, the simulations are based on '**normal moisture load**' for indoor conditions. In some cases, it is necessary to understand how the constructions perform under '**high moisture load**' scenarios for example in bathrooms. Secondly, the analyses were performed with climatic data according to **NEN 5060**, which is **only representative** for the **Dutch climate**. As a result, applicability in **other climate zones** remains **uncertain**.

Findings from the **isopleths** analysis indicate that **some bio-based materials exceed** the **LIM-thresholds** which implies there is a **higher change** on **mould-growth**. In these cases, it is recommended to conduct **additional material research** or **evaluate alternative finishes** that are more water-repellent and mold-resistant.

Moreover, **phase shift calculations** were conducted **manually** and based on a **single insulation layer**. As such, the **interactions between layers** and the **effects** of **ventilated cavities** are **not considered**. For **more accurate** phase shift assessments, **simulation software** is **required**. It should also be noted that **other building physics aspects**, such as **acoustics**, **fire safety**, and **structural requirements**, were not within the scope of this research. To enable full implementation of these bio-based reference details in construction practice, future work must **address** these **criteria**. Finally, the details have been limited to **a single façade configuration** where the window frame aligns with the outer façade surface, and a single roof and floor build-up was included. Furthermore, this research is **limited** to **five bio-based materials**, which can be expanded by applying the same methodology as presented in this thesis. As a result, alternative configurations have not been considered and the research can be elaborated by implementing additional bio-based materials.

The calculated **Ψ-value** refers to the **entire** construction detail. **Typically**, this value is divided and calculated **separately** for each component within the detail. However, in this study, the **Ψ-values** have been **combined** into a **total** value per detail. So for further research the seperate components should be calculated to give more **accurate** results.

The implications of this research provide **validated bio-based reference details** and **design principles** that contribute to the sustainability of housing construction and the circular ambitions for 2050. The **established design principles**, **technical evidence** and **simulation results promote** the **acceptance** of **bio-based materials**. This aligns with findings from the literature, which emphasise that the adoption of bio-based materials strongly depends on technical evidence.

For **future research**, it is **recommended** to **validate** the developed **reference details** using **other simulation tools** and to **evaluate** their **performance** under **varying climatic conditions** and **moisture loads**. This will ensure **broader applicability**. Finally, **further investigation** is needed into the **building physics** aspects that were **beyond** the **scope** of **this thesis**, so that the proposed details can be fully implemented in the Dutch construction sector. The established **methodology** for both **developing** and **testing** the details using WUFI may serve as a **foundation** for the development of **additional validated bio-based reference details**.

Reflection

This final chapter **reflects** on the graduation research in terms of both the **methodology** and the **results**. Furthermore, it positions the graduation work within the Building Technology (BT) master track of the MSc Architecture, Urbanism, and Building Sciences programme, placing it within a **broader academic context**. This research has focused on the **development** of **bio-based façade wall reference details** for residential top-up buildings. These details have been **validated** through **analyses** on **thermal bridging** and **moisture transport** using **WUFI simulations**.

Graduation process

The BT track's focus on sustainable building materials and advanced building physics is **strengthened** by this project, which examines how **bio-based materials** can **serve** as a **viable alternative** to **conventional materials**. Through the **development** and **validation** of bio-based construction details, this research makes a valuable **contribution** to **promoting sustainable building practices** and **environmentally responsible solutions** in architecture and building engineering. The thesis therefore aligns well with the **Building Technology track**, which emphasises **innovation** and **sustainable construction methods**, integrating **technical**, **architectural**, and **environmental** considerations.

The research methodology combined **literature review**, **research-by-design**, and **digital simulations** using WUFI. This methodological approach proved effective, as it resulted in sufficient **design knowledge** to accurately **develop** bio-based construction **details**. Additionally, the **design decisions** were **validated** by **simulations**. The combination of theoretical and practical approaches has led to **applicable** and **validated** architectural **bio-based details**.

Moreover, the research provides a solid **foundation** for **further academic work**. A key strength of the research is the clearly described **methodology**, which ensures that the results are **reproducible** and can be used for **future development** of bio-based reference details. The developed details may also be further expanded upon to address **other aspects** of **building physics**, such as **fire safety**, **acoustics**, or **structural performance**. As such, the research fits well with Building Technology, where empirical validation, design-based research, and simulation-based analysis are one of the key elements.

Societal impact

The applied **methodology** led to the intended results set out in the hypothesis regarding the development of **1:5 bio-based reference façade details validated** for **moisture transport** and **thermal performance**. The validated details are applicable in practice within the Dutch construction sector, provided they meet additional building physics and structural requirements. Because the details have been drafted in the same graphical **style** as the existing '**ISSO reference details**', the details are practically **applicable** among building professionals. The **implementation** of bio-based building materials in design processes is further supported by a set of developed **design principles**, offering designers concrete **guidance**. In this way, this research contributes in **reducing** the **knowledge gap** regarding **technical design** using **bio-based** materials.

This research provides façade wall reference details that are publicly **available** for use in various residential top-up building **designs**. Furthermore, the **simulation results** offer clear **insights** into the **hygrothermal behaviour** of these constructions. The **design principles**, **reference details**, and **simulation results** together contribute to a **broader implementation** of **bio-based materials** in architectural design. This makes the research **societally** relevant, as currently many designers **lack** the necessary **knowledge** on how to **design** with bio-based materials or how these materials **perform** in terms of **hygrothermal behaviour**, both of which **hinder** the application of bio-based materials.

The **validated performance** of the developed details can be used as a strong **argument** for **integrating bio-based materials** in the design process. Increased use of bio-based materials contributes to a more sustainable future. The **use** of renewable, locally available materials **reduces** dependence on fossil resources, which is positive for the environment.

Because these reference details are specifically developed for top-up buildings, the research also contributes to **addressing** the **housing shortage**. Top-up buildings can contribute to more housing to **solve** a **part** of the **housing shortage problem**. The validated details **reduce** the **risk** of **mould growth** and **surface condensation**, **contributing** to a **healthier indoor climate**, ultimately benefiting future residents. This **enhances** the living environment and contributes to people's **well-being**. Thus, the research not only partially helps **tackle** the housing crisis in the Netherlands but also **supports** the creation of healthy and energy-efficient dwellings by eliminating thermal bridges.

In conclusion, this research contributes not only to the academic field but also to the urgent transition towards circular and sustainable buildings.

Bibliography

References

Aghamohammadi, N., & Shahmohammadi, M. (2023). Towards sustainable development goals and role of bio-based building materials. *Bio-Based Materials and Waste for Energy Generation and Resource Management: Present and Emerging Waste Management Practices: Volume 5 of Advanced Zero Waste Tools*, 243–279. https://doi.org/10.1016/B978-0-323-91149-8.00004-1

Alhawari, A., & Mukhopadhyaya, P. (2018). Thermal bridges in building envelopes – An overview of impacts and solutions. *International Review of Applied Sciences and Engineering*, *9*(1), 31–40. https://doi.org/10.1556/1848.2018.9.1.5

Amorim. (n.d.). *MD FACADE-Installation Manual Index*. Retrieved May 8, 2025, from https://assets.ctfassets.net/2her2xma2kgl/39dd3wTZYdoiALNoUiVxKQ/3584212e012999e2a1b59cb5bde24126/ACI_-_Facade_Installation_Manual.pdf

Arnoldusse, J., Endhoven, T., Kok, J., Groot, P., Blok, M., & Kamps, M. (2022). *Materiaalstromen in de bouw en infra*.

Artés, J., Wadel, G., & Martí, N. (2017). Vertical Extension and Improving of Existing Buildings. *The Open Construction and Building Technology Journal*, *11*(1), 83–94. https://doi.org/10.2174/1874836801711010083

Arup. (2024). *Onderzoek NTA 8800*.

Asdrubali, F., Baldinelli, G., & Bianchi, F. (2012). A quantitative methodology to evaluate thermal bridges in buildings. *Applied Energy*, *97*, 365–373. https://doi.org/10.1016/j.apenergy.2011.12.054

Ashour, T. (2007). *Equilibrium Moisture Content for Some Natural Insulating Materials*. https://www.researchgate.net/publication/275464595

Ashour, T., & Wu, W. (2011). *Using barley straw as building material*. https://www.researchgate.net/publication/287478964_Using_barley_straw_as_building_material

Asokan, R., Rathanasamy, R., Paramasivam, P., Chinnasamy, M., Pal, S. K., & Palaniappan, S. K. (2023). Hemp composite. *Green Sustainable Process for Chemical and Environmental Engineering and Science: Natural Materials Based Green Composites 1: Plant Fibers*, 89–112. https://doi.org/10.1016/B978-0-323-95167-8.00007-7

Barbhuiya, S., & Bhusan Das, B. (2022). A comprehensive review on the use of hemp in concrete. *Construction and Building Materials*, *341*, 127857. https://doi.org/10.1016/J.CONBUILDMAT.2022.127857

Bardage, S. L. (2017). Performance of buildings. *Performance of Bio-Based Building Materials*, 335–383. https://doi.org/10.1016/B978-0-08-100982-6.00006-9

Bekin, M. (2024, August 26). *What Are the Pros and Cons of Interior Timber Cladding*. Eco Choise.

Benmahiddine, F., Cherif, R., Bennai, F., Belarbi, R., Tahakourt, A., & Abahri, K. (2020). Effect of flax shives content and size on the hygrothermal and mechanical properties of flax concrete. *Construction and Building Materials*, *262*, 120077. https://doi.org/10.1016/J.CONBUILDMAT.2020.120077

Bosch, S., Jansen, L., Aartsma, G., Schouten, N., Rohmer, M., van Hoof, S., van Munster, L., Spitsbaard, M., van den Broek, B., Schillemans, P., van Leeuwen, M., Hartmann, T., van Grinsven, J., & van Laar, D. (2023). *Woningbouw binnen planetaire grenzen*.

Bourbia, S., Kazeoui, H., & Belarbi, R. (2023). A review on recent research on bio-based building materials and their applications. *Materials for Renewable and Sustainable Energy*, *12*(2), 117–139. https://doi.org/10.1007/s40243-023-00234-7

Bredenoord, J. (2024). Bamboo as a Sustainable Building Material for Innovative, Low-Cost Housing Construction. *Sustainability*, *16*(6), 2347. https://doi.org/10.3390/su16062347

Brischke, C., & Humar, M. (2017). Performance of the bio-based materials. *Performance of Bio-Based Building Materials*, 249–333. https://doi.org/10.1016/B978-0-08-100982-6.00005-7

Brookes, A. J., Brookes, A. J., & Meijs, M. (2008). *Cladding of Buildings*. Taylor & Francis. https://doi.org/10.4324/9780203099780

Budding-Polo Ballinas, M., Garcia Chavez, L., & Molenaar, R. (2023). *Synergies & trade-offs of Wageningen climate solutions in primary production systems: Urban case study biobased construction materials: contributing to a sustainable housing system in Europe and enhancing climate neutral and resilient cities.*

Building Balance. (2023). *Advies Interdepartementaal Opschalingsplan Biobased Bouwen (IDOBB) 2023 — 2030*. https://www.centrumhout.nl/wp-content/uploads/2023/11/Advies-Interdepartementaal-Opschalingsplan-Biobased-Bouwen-IDOBB-DEF.pdf

Cascione, V., Roberts, M., Allen, S., Dams, B., Maskell, D., Shea, A., Walker, P., & Emmitt, S. (2022). Integration of life cycle assessments (LCA) in circular bio-based wall panel design. *Journal of Cleaner Production*, *344*, 130938. https://doi.org/10.1016/J.JCLEPRO.2022.130938

Centraal Bureau voor de Statistiek. (n.d.). *Dossier Verstedelijking*. Retrieved January 18, 2025, from https://www.cbs.nl/nl-nl/dossier/dossier-verstedelijking

Centraal Bureau voor de Statistiek. (2019, November 4). *Meeste afval en hergebruik materialen in bouwsector*. https://www.cbs.nl/nl-nl/nieuws/2019/45/meeste-afval-en-hergebruik-materialen-in-bouwsector

Centrum Hout. (2024). *Gevelbekleding van massief hout*.

Cobouw. (2024, April 30). *Zijn er genoeg grondstoffen voor de bouw van 900.000 woningen?* https://www.cobouw.nl/304105/zijn-er-genoeg-grondstoffen-voor-de-bouw-van-900-000-woningen

College van Rijksadviseurs. (2023). *Inspiratieboek biobased en natuurinclusief bouwen*.

College van Rijksbouwmeester en Rijksadviseurs. (2022, February 2). *Wat is biobased bouwen?* https://www.collegevanrijksadviseurs.nl/projecten/nieuwe-bouwcultuur/voorbeeldprojecten/wat-is-biobased-bouwen#:~:text=Biobased%20bouwmaterialen%20zijn%20bouwmaterialen%20gemaakt,Deal%20Circulair%20en%20Conceptueel%20Bouwen

CORDIS. (2018, July 10). *Bio-based insulation materials facts & myths*. https://cordis.europa.eu/article/id/123721-biobased-insulation-materials-facts-myths

Cosentino, L., Fernandes, J., & Mateus, R. (2023). A Review of Natural Bio-Based Insulation Materials. *Energies*, *16*(12), 4676. https://doi.org/10.3390/en16124676

Cosentino, L., Fernandes, J., & Mateus, R. (2024). Fast-Growing Bio-Based Construction Materials as an Approach to Accelerate United Nations Sustainable Development Goals. *Applied Sciences*, *14*(11), 4850. https://doi.org/10.3390/app14114850

Czerwinska, N. (2024). *Sustainable materials for improving Indoor Air Quality*. Università Politecnica Delle Marche.

Dams, B., Maskell, D., Shea, A., Allen, S., Cascione, V., & Walker, P. (2023). Upscaling bio-based construction: challenges and opportunities. *Building Research & Information*, *51*(7), 764–782. https://doi.org/10.1080/09613218.2023.2204414

dataholz. (2022a, May 10). *Wood-fibre insulation board*.

dataholz. (2022b, October 5). *Light composite wood-based beams and columns*.

De Kort, J., Gauvin, F., Loomans, M., & Brouwers, J. (2023). *Emission rates of bio-based building materials, a comparison between cork panels and reference building materials*.

De Visser, C., Van Wijk, K., & Van der Voort, M. (2015). *Health, comfort, energy use and sustainability issues related to the use of biobased building materials*.

Deshmukh, G. S. (2022). Advancement in hemp fibre polymer composites: a comprehensive review. *Journal of Polymer Engineering*, *42*(7), 575–598. https://doi.org/10.1515/polyeng-2022-0033

Fantucci, S., Isaia, F., Serra, V., & Dutto, M. (2017). Insulating coat to prevent mold growth in thermal bridges. *Energy Procedia*, *134*, 414–422. https://doi.org/10.1016/j.egypro.2017.09.591

Farrokhirad, E., Gao, Y., Pitts, A., & Chen, G. (2024). A Systematic Review on the Risk of Overheating in Passive Houses. *Buildings*, *14*(8), 2501. https://doi.org/10.3390/buildings14082501

Fedorik, F., Zach, J., Lehto, M., Kymäläinen, H. R., Kuisma, R., Jallinoja, M., Illikainen, K., & Alitalo, S. (2021). Hygrothermal properties of advanced bio-based insulation materials. *Energy and Buildings*, *253*, 111528. https://doi.org/10.1016/J.ENBUILD.2021.111528

Fischer, H., & Korjenic, A. (2023). Hygrothermal Performance of Bio-Based Exterior Wall Constructions and Their Resilience under Air Leakage and Moisture Load. *Buildings*, *13*(10), 2650. https://doi.org/10.3390/buildings13102650

Geuting, E., Wevers, J., Thomasia, M., & Dul, A. (2023). *De potentie van splitsen en optoppen*.

Gil, L. (2014). *Materials for Construction and Civil Engineering*. Springer.

Göswein, V., Arehart, J., Phan-huy, C., Pomponi, F., & Habert, G. (2022). Barriers and opportunities of fast-growing biobased material use in buildings. *Buildings and Cities*, *3*(1), 745–755. https://doi.org/10.5334/bc.254

Grabner, M., Nemestothy, S., & Wächter, E. (2022). Wooden Roofing: Split Shingles versus Sawn Boards. *International Journal of Wood Culture*, *2*(1–3), 19–37. https://doi.org/10.1163/27723194-bja10002

Greve, M., & Koning, M. (2024). *Meer woningen door verbouw -Potentie en belemmeringen bij optoppen, splitsen en transformeren*.

Grow2Build. (n.d.). *BOUWEN MET VLAS EN HENNEP*. www.nibe.org

Hamrouni, I., Jalili, H., Ouahbi, T., Taibi, S., Jamei, M., & Mabrouk, A. (2024). Thermal properties of a raw earth-flax fibers building material. *Construction and Building Materials*, *423*, 135828. https://doi.org/10.1016/J.CONBUILDMAT.2024.135828

Hanenburg, A. (2022). *Biobased Bouwen met Kurk*.

Hon, K. C. (2024). *Development of insulation materials for sustainable building performance* [Eindhoven University of Technology]. www.tue.nl/taverne

Hung Anh, L. D., & Pásztory, Z. (2021). An overview of factors influencing thermal conductivity of building insulation materials. *Journal of Building Engineering*, *44*, 102604. https://doi.org/10.1016/J.JOBE.2021.102604

Ingeli, R., Podhorec, J., & Čekon, M. (2016). Thermal Bridges Impact on Energy Need for Heating in Low Energy Wooden House. *Applied Mechanics and Materials*, *820*, 139–145. https://doi.org/10.4028/www.scientific.net/AMM.820.139

Isovlas. (2022). *Verwerkingsvoorschrift PL &PN Bouwisolatie*.

Ivanovic-Sekularac, J., Šekularac, N., & Tovarovic, J. C. (2016). *Wood as element of façade cladding in modern architecture*. https://www.researchgate.net/publication/294647271

Johra, H. (2021). *Thermal properties of building materials - Review and database*. https://doi.org/10.54337/aau456230861

Jones, D. (2017). Introduction to the performance of bio-based building materials. *Performance of Bio-Based Building Materials*, 1–19. https://doi.org/10.1016/B978-0-08-100982-6.00001-X

Julistiono, E. K., Oldfield, P., & Cardellicchio, L. (2023). Up on the roof: a review of design, construction, and technology trends in vertical extensions. *Architectural Science Review*, *67*(1), 63–77. https://doi.org/10.1080/00038628.2023.2240289

Kain, G., Idam, F., Federspiel, F., Réh, R., & Krišťák, Ľ. (2020). Suitability of Wooden Shingles for Ventilated Roofs: An Evaluation of Ventilation Efficiency. *Applied Sciences*, *10*(18), 6499. https://doi.org/10.3390/app10186499

Kaminski, S., Lawrence, A., & Trujillo, D. (2016). Structural use of bamboo. Part 1: Introduction to bamboo. *The Structural Engineer*, *94*(8), 40–43. https://doi.org/10.56330/PNSC8891

Klijn, W. (n.d.). *Isoleren met stro*.

Klijn, W., Spaan, R., & Eickmeier, C. (2017). *BOUWEN MET STRO Stro als ecologisch isolatiemateriaal*.

Knapic, S., Oliveira, V., Machado, J. S., & Pereira, H. (2016). Cork as a building material: a review. *European Journal of Wood and Wood Products*, *74*(6), 775–791. https://doi.org/10.1007/s00107-016-1076-4

KNMI. (n.d.). *Vochtigheid*. Retrieved January 18, 2025, from https://www.knmi.nl/kennis-en-datacentrum/uitleg/vochtigheid#:~:text=De%20relatieve%20vochtigheid%20geeft%20aan,De%20lucht%20is%20dan%20verzadigd

Koh, C. H. (Alex), & Kraniotis, D. (2020). A review of material properties and performance of straw bale as building material. *Construction and Building Materials*, *259*, 120385. https://doi.org/10.1016/J.CONBUILDMAT.2020.120385

Koppenhol, L., Hertzberger, B., Müller, T., & El Ayadi, Y. (2024). *Technische richtlijnen en overwegingen bij het optoppen*.

Koppenhol, L., Müller, T., & El Ayadi, Y. (2024). *Optoppen: de constructie en fundering, uitdagingen en oplossingen voor duurzame stadsontwikkeling*.

Kuczyński, T., & Staszczuk, A. (2020). Experimental study of the influence of thermal mass on thermal comfort and cooling energy demand in residential buildings. *Energy*, *195*, 116984. https://doi.org/10.1016/J.ENERGY.2020.116984

Kuhlmann, T., Heisma, R., & Rohmer, M. (2023). *Routekaarten voor een duurzame bouw*. www.metabolic.nl

Künzel, H. (1995). *Simultaneous heat and moisture transport in building components : one- and two-dimensional calculation using simple parameters* [Fraunhofer Institute]. https://www.researchgate.net/publication/41124856_Simultaneous_heat_and_moisture_transport_in_building_components_One-_and_two-dimensional_calculation_using_simple_parameters

Lafond, C., & Blanchet, P. (2020). Technical Performance Overview of Bio-Based Insulation Materials Compared to Expanded Polystyrene. *Buildings*, *10*(5), 81. https://doi.org/10.3390/buildings10050081

Lawrence, M., Shea, A., Walker, P., & De Wilde, P. (2013). Hygrothermal performance of bio-based insulation materials. *Proceedings of the Institution of Civil Engineers - Construction Materials*, *166*(4), 257–263. https://doi.org/10.1680/coma.12.00031

Le, D. L., Salomone, R., & Nguyen, Q. T. (2023). Circular bio-based building materials: A literature review of case studies and sustainability assessment methods. *Building and Environment*, *244*, 110774. https://doi.org/10.1016/J.BUILDENV.2023.110774

Li, Y., & Xu, P. (2006). Thermal Mass Design in Buildings – Heavy or Light? *International Journal of Ventilation*, *5*(1), 143–150. https://doi.org/10.1080/14733315.2006.11683731

Lierman, R. (2021). *Het circulaire potentieel van regeneratieve bouwmaterialen - de case van stro*. Universiteit Hasselt.

Liu, H., & Zhao, X. (2022). Thermal Conductivity Analysis of High Porosity Structures with Open and Closed Pores. *International Journal of Heat and Mass Transfer*, *183*, 122089. https://doi.org/10.1016/J.IJHEATMASSTRANSFER.2021.122089

Loussos, P., Van der Aa, A., & Van der Spoel, W. (2022, March). *Voorkomen van aantasting en degradatie van biobased materialen en constructies*. https://abt.eu/wp-content/uploads/2023/06/Artikel-aantasting-biobased-materialen-1.pdf

Lu, Z., Hauschild, M., Ottosen, L. M., Ambaye, T. G., Zerbino, P., Aloini, D., & Lima, A. T. (2024). Climate mitigation potential of biobased insulation materials: A comprehensive review and categorization. *Journal of Cleaner Production*, *470*, 143356. https://doi.org/10.1016/J.JCLEPRO.2024.143356

Lyons, A. (2006). Timber and timber products. *Materials for Architects and Builders*, 96–148. https://doi.org/10.1016/B978-075066940-5/50031-9

Majer, S., Wurster, S., Moosmann, D., Ladu, L., Sumfleth, B., & Thrän, D. (2018). Gaps and Research Demand for Sustainability Certification and Standardisation in a Sustainable Bio-Based Economy in the EU. *Sustainability*, *10*(7), 2455. https://doi.org/10.3390/su10072455

Maskell, D., Da Silva, C. F., Mower, K., Rana, C., Dengel, A., Ball, R. J., Ansell, M. P., Walker, P., & Shea, A. (2015). Properties of bio-based insulation materials and their potential impact on indoor air quality. *First International Conference on Bio-Based Building Materials*. https://www.researchgate.net/publication/279196144_PROPERTIES_OF_BIO-BASED_INSULATION_MATERIALS_AND_THEIR_POTENTIAL_IMPACT_ON_INDOOR_AIR_QUALITY

Mike Wye. (2014). *SecilVit Cork Insulation*. www.mikewye.co.uk

Miles, J., & Krug, D. (2013). *OFFSITE CONSTRUCTION: Sustainability Characteristics*. https://www.buildoffsite.com/content/uploads/2015/03/BoS_offsiteconstruction_1307091.pdf

Minister van Binnenlandse Zaken en Koninkrijksrelaties, S. van I. en W. M. voor K. en E. M. van E. Z. en K. (2023). *Nationale Aanpak Biobased Bouwen Van boerenland tot bouwmateriaal*.

Ministerie van Binnenlandse Zaken. (2022, February 25). *Pablo van der Lugt: De noodzaak van een nieuwe, biobased bouwcultuur*. https://www.collegevanrijksadviseurs.nl/projecten/nieuwe-bouwcultuur/aan-het-woord/pablo-van-der-lugt

Ministerie van Binnenlandse Zaken en Koninkrijksrelaties. (2024a). *Landelijke aanpak Optoppen*. www.volkshuisvestingnederland.nl/optoppen

Ministerie van Binnenlandse Zaken en Koninkrijksrelaties. (2024b, May 31). *Wat is de landelijke aanpas optoppen*. https://www.volkshuisvestingnederland.nl/onderwerpen/optoppen/wat-is-de-landelijke-aanpak-optoppen

Ministerie van Binnenlandse Zaken en Koninkrijksrelaties, Ministerie van Infrastructuur en Waterstaat, Ministerie van Landbouw, N. en V., & Ministerie van Economische Zaken en Klimaat. (2023). *Nationale aanpak biobased bouwen: Van boerenland tot bouwmateriaal.*

Ministerie van Economische Zaken. (2016). *Energieagenda - Naar een CO_2-arme energievoorziening*. https://www.rijksoverheid.nl/documenten/rapporten/2016/12/07/ea

Ministerie van Infrastructuur en Waterstaat. (2023a, May 4). *Omslag naar circulaire economie versnellen*. https://www.rijksoverheid.nl/onderwerpen/circulaire-economie/omslag-naar-circulaire-economie-versnellen

Ministerie van Infrastructuur en Waterstaat. (2023b, October 24). *Noodzaak van circulaire economie*. Circulaire Economie | Rijksoverheid.Nl.

Ministerie van Volkshuisvesting en Ruimtelijke Ordening. (2024, September 13). *Kabinet pakt woningnood aan: sneller, slimmer en met minder regels bouwen*. https://www.rijksoverheid.nl/actueel/nieuws/2024/09/13/kabinet-pakt-woningnood-aan-sneller-slimmer-en-met-minder-regels-bouwen

MNEXT. (n.d.-a). *Stro als biobased bouwmateriaal*. MNEXT. Retrieved January 22, 2025, from https://www.mnext.nl/wiki/stro-als-biobased-bouwmateriaal/

MNEXT. (n.d.-b). *Vlas*.

Novogradac, M. (2024). Affordable Housing Developers Facing Increased Development Challenges. *Journal of Tax Credits*, *15*(5).

Nunes, L. (2017). Nonwood bio-based materials. *Performance of Bio-Based Building Materials*, 97–186. https://doi.org/10.1016/B978-0-08-100982-6.00003-3

O'Brien, L., Li, L., Friess, W., Snow, J., Herzog, B., & O'Neill, S. (2025). Review of bio-based wood fiber insulation for building envelopes: Characteristics and performance assessment. *Energy and Buildings*, *328*, 115114. https://doi.org/10.1016/J.ENBUILD.2024.115114

OECD. (2018, October 22). *Raw materials use to double by 2060 with severe environmental consequences*. Organisation for Economic Co-Operation and Development (OECD). https://www.oecd.org/en/about/news/announcements/2018/10/raw-materials-use-to-double-by-2060-with-severe-environmental-consequences.html#:~:text=severe%20environmental%20consequences-

,Raw%20materials%20use%20to%20double%20by%202060%20with%20severe%20environmental,to%20a%20new%20OECD%20report

Orsini, F., & Marrone, P. (2019). Approaches for a low-carbon production of building materials: A review. *Journal of Cleaner Production*, *241*, 118380. https://doi.org/10.1016/J.JCLEPRO.2019.118380

Owczarek, M., Owczarek, S., Baryłka, A., & Grzebielec, A. (2021). Measurement Method of Thermal Diffusivity of the Building Wall for Summer and Winter Seasons in Poland. *Energies*, *14*(13), 3836. https://doi.org/10.3390/en14133836

Palumbo, M., Lacasta, A. M., Holcroft, N., Shea, A., & Walker, P. (2016). Determination of hygrothermal parameters of experimental and commercial bio-based insulation materials. *Construction and Building Materials*, *124*, 269–275. https://doi.org/10.1016/J.CONBUILDMAT.2016.07.106

Piot, A., Béjat, T., Jay, A., Bessette, L., Wurtz, E., & Barnes-Davin, L. (2017). Study of a hempcrete wall exposed to outdoor climate: Effects of the coating. *Construction and Building Materials*, *139*, 540–550. https://doi.org/10.1016/J.CONBUILDMAT.2016.12.143

Pittau, F., Krause, F., Lumia, G., & Habert, G. (2018). Fast-growing bio-based materials as an opportunity for storing carbon in exterior walls. *Building and Environment*, *129*, 117–129. https://doi.org/10.1016/J.BUILDENV.2017.12.006

Planbureau voor de Leefomgeving. (2022, July 6). *Prognose: in 2035 vooral meer inwoners in en om grotere gemeenten*. https://www.pbl.nl/actueel/nieuws/prognose-in-2035-vooral-meer-inwoners-in-en-om-grotere-gemeenten

Popescu, C. M. (2017). Wood as bio-based building material. *Performance of Bio-Based Building Materials*, 21–96. https://doi.org/10.1016/B978-0-08-100982-6.00002-1

Pramreiter, M., Nenning, T., Malzl, L., & Konnerth, J. (2023). A plea for the efficient use of wood in construction. *Nature Reviews Materials*, *8*(4), 217–218. https://doi.org/10.1038/s41578-023-00534-4

Rabbat, C., Awad, S., Villot, A., Rollet, D., & Andrès, Y. (2022). Sustainability of biomass-based insulation materials in buildings: Current status in France, end-of-life projections and energy recovery potentials. *Renewable and Sustainable Energy Reviews*, *156*, 111962. https://doi.org/10.1016/J.RSER.2021.111962

Raja, P., Murugan, V., Ravichandran, S., Behera, L., Mensah, R. A., Mani, S., Kasi, A., Balasubramanian, K. B. N., Sas, G., Vahabi, H., & Das, O. (2023). A Review of Sustainable Bio-

Based Insulation Materials for Energy-Efficient Buildings. *Macromolecular Materials and Engineering*, *308*(10). https://doi.org/10.1002/mame.202300086

Ramage, M. H., Burridge, H., Busse-Wicher, M., Fereday, G., Reynolds, T., Shah, D. U., Wu, G., Yu, L., Fleming, P., Densley-Tingley, D., Allwood, J., Dupree, P., Linden, P. F., & Scherman, O. (2017). The wood from the trees: The use of timber in construction. *Renewable and Sustainable Energy Reviews*, *68*, 333–359. https://doi.org/10.1016/J.RSER.2016.09.107

Reilly, A., & Kinnane, O. (2017). The impact of thermal mass on building energy consumption. *Applied Energy*, *198*, 108–121. https://doi.org/10.1016/J.APENERGY.2017.04.024

Rijksdienst voor Ondernemend Nederland. (2024). *Sectorstudie: Duurzame gebouwen en openbare ruimte*.

Rutte Groep. (2021, November 1). *Circulair beton*. Circulariteit in de bouw. https://themasites.pbl.nl/o/circulariteit-in-de-bouw/rutte-groep/

Šadauskienė, J., Ramanauskas, J., Šeduikytė, L., Daukšys, M., & Vasylius, A. (2015). A Simplified Methodology for Evaluating the Impact of Point Thermal Bridges on the High-Energy Performance of a Passive House. *Sustainability*, *7*(12), 16687–16702. https://doi.org/10.3390/su71215840

Sandak, A., Sandak, J., Brzezicki, M., & Kutnar, A. (2019). *Bio-based Building Skin*. Springer Singapore. https://doi.org/https://doi.org/10.1007/978-981-13-3747-5_2

Schik, W., Meijer, K., Verkerk, D., Paardekooper, D., Grim, L., & Peek, T. (2022). *De urgente belofte van biobased bouwen*.

Schmidt, S., & Hartwig, K. (2006). *Welcome to WUFI* (4.1.). WUFI. https://wufi.de/download/WUFI41_help_e.pdf

Schulte, M., Lewandowski, I., Pude, R., & Wagner, M. (2021). Comparative life cycle assessment of bio-based insulation materials: Environmental and economic performances. *GCB Bioenergy*, *13*(6), 979–998. https://doi.org/10.1111/gcbb.12825

Sedlbauer, K., Hofbauer, W., Krueger, N., Mayer, F., & Breuer, K. (2011). *Material Specific Isopleth-systems as Valuable Tools for the Assessment of the Durability of Building Materials Against Mould Infestation-The "Isopleth-traffic Light."*

Sharma, B., Gatóo, A., Bock, M., & Ramage, M. (2015). Engineered bamboo for structural applications. *Construction and Building Materials*, *81*, 66–73. https://doi.org/10.1016/J.CONBUILDMAT.2015.01.077

Sijm, J. (2024). *Verkenning van toekomstige ontwikkelingen en uitdagingen voor een klimaatneutraal elektriciteitssysteem in Nederland, 2030-2050*. www.tno.nl

Stanwix, W., & Sparrow, A. (2014). *The Hempcrete Book - Designing and building with hemp-lime*. Green Books.

Sun, X., He, M., & Li, Z. (2020). Novel engineered wood and bamboo composites for structural applications: State-of-art of manufacturing technology and mechanical performance evaluation. *Construction and Building Materials*, *249*, 118751. https://doi.org/10.1016/J.CONBUILDMAT.2020.118751

Suttie, E., Hill, C., Sandin, G., Kutnar, A., Ganne-Chédeville, C., Lowres, F., & Dias, A. C. (2017). Environmental assessment of bio-based building materials. *Performance of Bio-Based Building Materials*, 547–591. https://doi.org/10.1016/B978-0-08-100982-6.00009-4

Sutton, A., Black, D., & Walker, P. (2011). Straw bale - An introduction to low-impact building materials. *BRE Publications*.

Taher, A., & Brouwers, H. J. H. (2023). Sorption isotherm measurements for porous materials: A new hygroscopic method. *Construction and Building Materials*, *379*, 131166. https://doi.org/10.1016/J.CONBUILDMAT.2023.131166

The Wit, M. H. (2008). *Heat and Moisture in Building Envelopes*.

Thoemen, H., Irle, M., & Sernek, M. (2010). *Wood-based Panels - An Introduction for Specialists*. Brunel University Press.

TNO. (n.d.). *Bio-based building materials market in development*. Retrieved January 18, 2025, from https://www.tno.nl/en/sustainable/circular-industrial-construction/bio-based-building-materials-market/

van Dam, J., & van den Oever, M. (2019). *Catalogus biobased bouwmaterialen 2019 : Het groene en circulaire bouwen*. https://doi.org/10.18174/461687

Van der Lugt, P. (2021). *Houtbouwmythes ontkracht het onderscheid tussen fabels en feiten*. www.ams-institute.org

Van der Schuit, J., Van Hoorn, A., Sorel, N., & Rood, T. (2023). *Kenmerken, voorraad en materiaalketens van de bouw*. https://www.pbl.nl/uploads/default/downloads/pbl-2023_kenmerken-voorraad-en-materiaalketens-van-de-bouw_4853_.pdf

Van der Velde, O., & Van Leeuwen, M. (2019). *Potentie van biobased materialen in de bouw*.

Van Herpen, R. (2005). *Koudebruggen, berekenen van F-waarden onder stationaire condities*.

Van Hooft, T. (2023, September 16). *Waarom raakt het stroomnet in Nederland enorm overbelast?* energie kennis. https://energie-kennis.nl/waarom-raakt-het-stroomnet-overbelast/

Vermeulen, M., Van der Waal, J., Van Woerden, B., & Voorter, L. (2020). *Ruimte voor Biobased Bouwen*.

Vinha, J., & Käkelä. Pasi. (1999). *Water vapour transmission in wall structures due to diffusion and convection*.

Walker, R., & Pavía, S. (2014). Moisture transfer and thermal properties of hemp–lime concretes. *Construction and Building Materials*, *64*, 270–276. https://doi.org/10.1016/J.CONBUILDMAT.2014.04.081

Wang, J. S., Demartino, C., Xiao, Y., & Li, Y. Y. (2018). Thermal insulation performance of bamboo- and wood-based shear walls in light-frame buildings. *Energy and Buildings*, *168*, 167–179. https://doi.org/10.1016/J.ENBUILD.2018.03.017

Weterings, M., Van den Bogaard, J., Duijm, F., Van den Elsen, G., & Lops, S. (2005). *GGD Richtlijn Gezonde Woningbouw*. https://www.rivm.nl/sites/default/files/2018-11/Richtlijn%20Gezonde%20Woningbouw%20%282005%29.pdf

Woolley, T. (2013). Low Impact Building: Housing Using Renewable Materials. In *Low Impact Building: Housing Using Renewable Materials*. Wiley. https://doi.org/10.1002/9781118524169.advert2

Worch, A. (2004). The Behaviour of Vapour Transfer on Building Material Surfaces: The Vapour Transfer Resistance. *Journal of Thermal Envelope and Building Science*, *28*(2), 187–200. https://doi.org/10.1177/1097196304044398

WUFI. (n.d.-a). *Details: Heat Conductivity Moisture Dependent*.

WUFI. (n.d.-b). *Details: Liquid Transport Coefficients*. Retrieved January 20, 2025, from https://www.wufi-wiki.com/mediawiki/index.php/Details:LiquidTransportCoefficients

WUFI. (n.d.-c). *Details: Moisture Storage Function*.

WUFI. (n.d.-d). *Details: Water Vapor Diffusion*. Retrieved January 20, 2025, from https://www.wufi-wiki.com/mediawiki/index.php/Details:WaterVaporDiffusion

Xue, Y., Fan, Y., Chen, S., Wang, Z., Gao, W., Sun, Z., & Ge, J. (2023). Heat and moisture transfer in wall-to-floor thermal bridges and its influence on thermal performance. *Energy and Buildings*, *279*, 112642. https://doi.org/10.1016/j.enbuild.2022.112642

Yadav, M., & Agarwal, M. (2021). Biobased building materials for sustainable future: An overview. *Materials Today: Proceedings*, *43*, 2895–2902. https://doi.org/10.1016/J.MATPR.2021.01.165

Figure references

1. Illustration background. Own illustration
2. Illustration problem statemen. Own illustration
3. Illustration hypothesis. Own illustration
4. Visualisation of linear and circular economy. Stichting Agrodome. (2024, 6 March). Kennis delen - Stichting Agrodome. https://stichting.agrodome.nl/kennisdelen/
5. Time till running out of building materials. Van Der Lugt, P. (2021). Houtbouwmythes ontkracht: het onderscheid tussen fabels en feiten. Amsterdam Institute for Advanced Metropolitan Solutions (AMS). https://pure.tudelft.nl/ws/portalfiles/
6. Contribution of different materials in the B&U to the total material consumption. EIB. (2022, 29 April). *Materiaalstromen in de bouw en infra - EIB.* https://www.eib.nl/publicaties/materiaalstromen-in-de-bouw-en-infra/
7. Conclusion advantages application bio-based materials. Own illustration
8. Explanation of a top-up building. Own illustration
9. Population development per municipality 2021 – 2035. Prognose: in 2035 vooral meer inwoners in en om grotere gemeenten. (2022, 6 July). Planbureau Voor de Leefomgeving. https://www.pbl.nl/actueel/nieuws/prognose-in-2035-vooral-meer-inwoners-in-en-om-grotere-gemeenten#:~:text=Nederland%20zal%20in%202035%20naar,randgemeenten%20rond%20de%20grote%20steden
10. Difference massa and CO2-reduction between apartment and top-up. Bosch, S., Jansen, L., & Aartsma, G. (2023, 2 November). *Woningbouw binnen planetaire grenzen - Copper8.* Copper8. https://www.copper8.com/woningbouw-binnen-planetaire-grenzen/
11. Top-up possibilities based on the number of floors. Geuting, E., Wevers, J., Thomasia, M., & Dul, A. (2023, 12 September). *De potentie van splitsen en optoppen.* Rapport | Rijksoverheid.nl. https://www.rijksoverheid.nl/documenten/rapporten/2023/03/20/de-potentie-van-splitsen-en-optoppen
12. Realistic top-up task based on the construction period of the existing building. Geuting, E., Wevers, J., Thomasia, M., & Dul, A. (2023, 12 September). *De potentie van splitsen en optoppen.* Rapport | Rijksoverheid.nl. https://www.rijksoverheid.nl/documenten/rapporten/2023/03/20/de-potentie-van-splitsen-en-optoppen
13. Principle of vapour-open & damp-proof construction. Bouke. (2020, 3 November). Wanden: waar dienen ze eigenlijk voor!? Deel 2 - Het Bewuste Stel. Het Bewuste Stel. https://hetbewustestel.nl/tiny-house-wanden-deel-2/
14. Vapour diffusion resistance factor. Own illustration
15. Capillary movement. Own illustration
16. Illustration phase shift and temperature amplitude, Lower themal mass: shorter Koppenhol, L., Hertzberger, B., Thijs, M., & El Ayadi, Y. (n.d.). Technische richtlijnen en overwegingen bij het optoppen. In *Technische Richtlijnen en Overwegingen Bij het Optoppen | Creative City Solutions.* https://www.volkshuisvestingnederland.nl/binaries/volkshuisvestingnederland/docum

enten/publicaties/2024/09/12/technische-richtlijnen-en-overwegingen-bij-het-optoppen/CCS_Rapport+2024+02+aansluitingen.pdf
17. Conclusion advantages application bio-based materials in residential top-up buildings. Own illustration
18. Schematic illustration thermal bridge, Mousdell, D. (2024, 11 november). *Understanding Thermal Bridging and Its Impact on Building Heat Loss.* H2x Engineering. https://www.h2xengineering.com/blogs/understanding-thermal-bridging-impact-building-heat-loss/
19. Graph Water Content & Relative Humidity [%], from WUFI Database
20. Illustration and contact angle because of capillary pressure. De Wit, M. H. (2009). Heat, air and moisture in building envelopes. https://research.tue.nl/en/publications/heat-air-and-moisture-in-building-envelopes
21. Graph liquid transport coefficient & water content. Coelho, G. B. A., & Henriques, F. M. A. (2022). The importance of moisture transport properties of wall finishings on the hygrothermal performance of masonry walls for current and future climates. Applied Sciences. https://doi.org/10.3390/app13106318
22. Graph water vapour resistance factor & Relative humidity. From WUFI Database
23. Graph thermal conductivity of moist material & Water content. From WUFI Database
24. Potential bio-based materials for the Dutch construction market. College van Rijksadviseurs. (2023). Inspiratieboek biobased en natuurinclusief bouwen. Publicatie | College van Rijksadviseurs. https://www.collegevanrijksadviseurs.nl/adviezen-publicaties/publicatie/2023/2/14/inspiratieboek-biobased-bouwen-en-natuurinclusief-bouwen
25. Granulated cork. Densities of cork granules. (2022, 7 July). CorkLink - Cork Products Direct From Portugal. https://www.corklink.com/index.php/densities-of-cork-granules/
26. Expanded cork agglomerates. Stichting Nationale Milieudatabase. (2024, 22 mei). Pro Suber biobased insulation from expanded cork with CAT-1 data in NMD. NMD. https://milieudatabase.nl/en/database/featured-category-1-product-card-holder-in-dutch/pro-suber-biobased-insulation-from-expanded-cork-with-cat-1-data-in-nmd/
27. Different parts of the flax plant. Nunes, L. (2017). Nonwood bio-based materials.
28. Flax insulation. Isovlas. (2023, 14 February). Bouwisolatie - Isovlas. https://www.isovlas.nl/bouwisolatie/
29. Flax particle board. Database, B. (n.d.). Flax Particle Board | Biobased Database. Copyright 2025 All-in-media | Creatief Maatwerk. https://www.biobasedconsultancy.com/en/database/flax-particle-board
30. Hempcrete. NBS_Admin. (2023, 14 April). IsoHemp pre-cast hempcrete blocks (full pallet - various sizes) - Natural Building Store. Natural Building Store. https://naturalbuildingstore.com/shop/isohemp-pre-cast-hempcrete-blocks/
31. Hemp insulation. Admin. (2023, 22 May). Inditherm: Carbon capturing locally made insulation - Firstplanit. Firstplanit. https://resources.firstplanit.com/inditherm-carbon-capturing-locally-made-insulation/

32. Straw bale. Coastal Farm - New. (n.d.). 2-Tie Straw hay Bale - Horse & Livestock Feed & Treats | Coastal | CoastalCountry. CoastalCountry https://www.coastalcountry.com/products/pet-animal/livestock/feed-treats/2-tie-straw-hay-bale
33. Blow-in straw. EcoCocon prefab Stropanelen - Kennisbank Biobased Bouwen. (2023, 28 August). Kennisbank Biobased Bouwen. https://www.biobasedbouwen.nl/producten/ecococon-prefab-stropanelen/
34. Untreated wood. Spruce Lumber - Hanford Lumber. (2025, 14 maart). Hanford Lumber. https://www.hanfordlumber.com/product/spruce-lumber/
35. Treated wood. Johal, J. (2024, 13 March). Treated Timber: What is it and What is it Used For? - BuildingMaterials.co.uk. BuildingMaterials.co.uk. https://www.buildingmaterials.co.uk/info-hub/timber-joinery/treated-timber-guide
36. Glulam. Glued laminated timber - dataholz.eu. (2024, 7 September). https://www.dataholz.eu/en/building-materials/beams-columns/glued-laminated-timber.htm
37. Timber cladding. Timber cladding | Wood cladding. (n.d.). https://www.tdca.org.uk/timber-cladding/
38. Eco Strand Board. NextChapter Software B.V. (n.d.). Elka ESB plus - duurzame constructieplaat. Copyright © NextChapter Software B.V. - All Rights Reserved. https://www.houtmarkt.nl/nl/3654672/elka-esb-plus-duurzame-constructieplaat/
39. Medium Density Fibre board. BouwOnline.com. (n.d.). MDF Plaatmateriaal 18 mm 305 x 122 cm kopen? https://www.bouwonline.com/mdf-plaat-18mm-305x122cm.html
40. Wood fibre insulation. STEICO Insulation Materials. (n.d.). https://www.steico.com/en/solutions/product-advantages/steico-insulation-materials
41. Conclusion selection of bio-based materials for the detail configurations. Own illustration
42. Figure 42, Timber frame construction axonometric. Own illustration
43. Figure 43, Elements of a timber frame construction. Stanwix, W., & Sparrow, A. (2014). *The Hempcrete Book: Designing and building with hemp-lime*. Green Books. https://www.ukhempcrete.com/the-hempcrete-book/
44. Timber frame construction with support of a lintel. Stanwix, W., & Sparrow, A. (2014). *The Hempcrete Book: Designing and building with hemp-lime*. Green Books. https://www.ukhempcrete.com/the-hempcrete-book/
45. Timber frame construction corner. Own illustration
46. Protection column. Fröbel, J., Swedish Wood, Crocetti, R., & Lund University. (2024). *The Glulam Handbook – Volume 2* (1st edition). Swedish Wood. https://www.swedishwood.com
47. Timber frame construction, roof connection. Fröbel, J., Swedish Wood, Crocetti, R., & Lund University. (2024). *The Glulam Handbook – Volume 2* (1st edition). Swedish Wood. https://www.swedishwood.com
48. Wood fibre plates with staggered joints and fasteners. Own illustration
49. Attachment wood fibre plates. Own illustration

50. Types of open and closed timber cladding. Brookes, A. J., & Meijs, M. (2008). Cladding of Buildings. In *Routledge & CRC Press*. Taylor & Francis. https://www.routledge.com/Cladding-of-Buildings/Brookes-Brookes-Meijs/p/book/9780415383875?srsltid=AfmBOooMjM2RL9yGKvdhhXu9ubH2swfphTH1GUf6fZAObvqokDmm9Ksm
51. Expansion space for closed systems. Own illustration
52. Vertical and horizontal wooden cladding with center-to-center of studs. Own illustration
53. Spaces between planks and mechanical attachment of fasteners. Brookes, A. J., & Meijs, M. (2008). Cladding of Buildings. In *Routledge & CRC Press*. Taylor & Francis. https://www.routledge.com/Cladding-of-Buildings/Brookes-Brookes-Meijs/p/book/9780415383875?srsltid=AfmBOooMjM2RL9yGKvdhhXu9ubH2swfphTH1GUf6fZAObvqokDmm9Ksm
54. Correct mechanical attachment of nails & screws with penetration depth. Brookes, A. J., & Meijs, M. (2008). Cladding of Buildings. In *Routledge & CRC Press*. Taylor & Francis. https://www.routledge.com/Cladding-of-Buildings/Brookes-Brookes-Meijs/p/book/9780415383875?srsltid=AfmBOooMjM2RL9yGKvdhhXu9ubH2swfphTH1GUf6fZAObvqokDmm9Ksm
55. Space between cladding and roof trim. Brookes, A. J., & Meijs, M. (2008). Cladding of Buildings. In *Routledge & CRC Press*. Taylor & Francis. https://www.routledge.com/Cladding-of-Buildings/Brookes-Brookes-Meijs/p/book/9780415383875?srsltid=AfmBOooMjM2RL9yGKvdhhXu9ubH2swfphTH1GUf6fZAObvqokDmm9Ksm
56. External and internal corner connections. Brookes, A. J., & Meijs, M. (2008). Cladding of Buildings. In *Routledge & CRC Press*. Taylor & Francis. https://www.routledge.com/Cladding-of-Buildings/Brookes-Brookes-Meijs/p/book/9780415383875?srsltid=AfmBOooMjM2RL9yGKvdhhXu9ubH2swfphTH1GUf6fZAObvqokDmm9Ksm
57. Spaces between cladding and window. Brookes, A. J., & Meijs, M. (2008). Cladding of Buildings. In *Routledge & CRC Press*. Taylor & Francis. https://www.routledge.com/Cladding-of-Buildings/Brookes-Brookes-Meijs/p/book/9780415383875?srsltid=AfmBOooMjM2RL9yGKvdhhXu9ubH2swfphTH1GUf6fZAObvqokDmm9Ksm
58. Parts of the cast-in-situ of a hempcrete wall. Stanwix, W., & Sparrow, A. (2014). *The Hempcrete Book: Designing and building with hemp-lime*. Green Books. https://www.ukhempcrete.com/the-hempcrete-book/
59. Connection hempcrete blocks and wooden frame. IsoHemp. (n.d.). *Installation Instructions Insulating Hemp Block*.
60. Connection blocks and floor. Own illustration
61. Connection blocks and roof. Own illustration
62. Placement of hempcrete blocks. Own illustration

63. Possible wall constructions with hempcrete. Stanwix, W., & Sparrow, A. (2014). *The Hempcrete Book: Designing and building with hemp-lime.* Green Books. https://www.ukhempcrete.com/the-hempcrete-book/
64. Connection between hempcrete and a window frame. Stanwix, W., & Sparrow, A. (2014). *The Hempcrete Book: Designing and building with hemp-lime.* Green Books. https://www.ukhempcrete.com/the-hempcrete-book/
65. Cork front view with mechanical connection. Own illustration
66. Cork cladding with battens. Own illustration
67. Cork front view with insulation roses. Own illustration
68. Cork cladding with mortar. Own illustration
69. Corner connections, staggered joints & 45° cut. Own illustration
70. Distance between cork panels and window frame. Own illustration
71. Flax insulation between timber frame. Isovlas. (n.d.). *Verwerkingsvoorschrift Isovlas PL & PN bouwisolatie.* https://www.isovlas.nl/wp-content/uploads/2022/09/pl-pn-bouwisolatie_2022-web.pdf
72. Dimensions straw bale. Vereniging Strobouw Nederland. (n.d.). BOUWEN MET STRO.
73. Connection straw bales to construction frame. Own illustration
74. Blow-in straw. Own illustration
75. Detail of V1 (below) & V2 (top), configuration 1. Own illustration
76. Detail of H1, configuration 2. Own illustration
77. Detail of V1 (below) & V2 (top), configuration 2. Own illustration
78. Detail of H1, configuration 2. Own illustration
79. Detail of V1 (below) & V2 (top), configuration 3. Own illustration
80. Detail of H1, configuration 3. Own illustration
81. Detail of V1 (below) & V2 (top), configuration 4. Own illustration
82. Detail of H1, configuration 4. Own illustration
83. Detail of V1 (below) & V2 (top), configuration 5. Own illustration
84. Detail of H1, configuration 5. Own illustration
85. Detail of V1 (below) & V2 (top), configuration 6. Own illustration
86. Detail of H1, configuration 6. Own illustration
87. Detail of V1 (below) & V2 (top), configuration 7. Own illustration
88. Detail of H1, configuration 7. Own illustration
89. Detail of V1 (below) & V2 (top), configuration 8. Own illustration
90. Detail of H1, configuration 8. Own illustration
91. Detail of V1 (below) & V2 (top), configuration 9. Own illustration
92. Detail of H1, configuration 9. Own illustration
93. Detail of V1 (below) & V2 (top), configuration 10. Own illustration
94. Detail of H1, configuration 10. Own illustration
95. Detail of V1 (below) & V2 (top), configuration 11. Own illustration
96. Detail of H1, configuration 11. Own illustration

97. Exceptions transition resistance factors. NEN Connect - NTA 8800:2024 nl. (n.d.). https://connect.nen.nl/Standard/Detail/3701862?compId=10037&collectionId=0

98. Illustration of glazed area and perimeter. NEN Connect - NTA 8800:2024 nl. (n.d.). https://connect.nen.nl/Standard/Detail/3701862?compId=10037&collectionId=0

99. Determination of thermal transmittance of the frame. NEN-EN-ISO 10077-1:2017 en. (n.d.). https://www.nen.nl/nen-en-iso-10077-1-2017-en-236364

100. The finite element method. NEN 2778:2015 nl. (n.d.). https://www.nen.nl/nen-2778-2015-nl-206260

101. Schematic illustration of heat flux. Hukseflux. (n.d.). What is heat flux? https://www.hukseflux.com/library/what-is-heat-flux

102. Determination of the surface of the construction foundation. NEN Connect - NTA 8800:2024 nl. (n.d.). https://connect.nen.nl/Standard/Detail/3701862?compId=10037&collectionId=0

103. Determination of the surface of the bottom, top and side window frame construction. NEN Connect - NTA 8800:2024 nl. (n.d.). https://connect.nen.nl/Standard/Detail/3701862?compId=10037&collectionId=0

104. Connection window frame and wall construction. NEN Connect - NTA 8800:2024 nl. (n.d.). https://connect.nen.nl/Standard/Detail/3701862?compId=10037&collectionId=0

105. Determination of the corner wall construction. NEN Connect - NTA 8800:2024 nl. (n.d.). https://connect.nen.nl/Standard/Detail/3701862?compId=10037&collectionId=0

106. Determination of the flat roof construction. NEN Connect - NTA 8800:2024 nl. (n.d.). https://connect.nen.nl/Standard/Detail/3701862?compId=10037&collectionId=0

107. Determination internal mean temperature. NEN-EN-ISO 13788:2013 en. (n.d.). https://www.nen.nl/nen-en-iso-13788-2013-en-179390

108. Determination internal relative humidity. NEN-EN-ISO 13788:2013 en. (n.d.). https://www.nen.nl/nen-en-iso-13788-2013-en-179390

109. Determination difference internal and external vapour pressure. NEN-EN-ISO 13788:2013 en. (n.d.). https://www.nen.nl/nen-en-iso-13788-2013-en-179390

110. Simplification of window frame. NEN-EN-ISO 10077-1:2017 en. (n.d.). https://www.nen.nl/nen-en-iso-10077-1-2017-en-236364

111. Boundaries, cavities and grooves window. NEN-EN-ISO 10077-1:2017 en. (n.d.). https://www.nen.nl/nen-en-iso-10077-1-2017-en-236364

112. Transformation of non-rectangular air cavities. NEN-EN-ISO 10077-1:2017 en. (n.d.). https://www.nen.nl/nen-en-iso-10077-1-2017-en-236364

113. The finite element method. NEN 2778:2015 nl. (n.d.). https://www.nen.nl/nen-2778-2015-nl-206260

114. Abstract image of the window geometry within WUFI, own illustration

Table references

1. Thermal conductivity values of synthetic- mineral and natural insulation materials, De Visser, C., Van Wijk, K., & Van der Voort, M. (2015). *Health, comfort, energy use and sustainability issues related to the use of biobased building materials.*
2. Fire Classification according to NEN 13501-1, (*NEN-EN 13501-1:2019 En*, n.d.)
3. Explanation building physical properties, De Visser, C., Van Wijk, K., & Van der Voort, M. (2015). *Health, comfort, energy use and sustainability issues related to the use of biobased building materials.*
4. Vapour diffusion resistance factor of different insulation materials, De Visser, C., Van Wijk, K., & Van der Voort, M. (2015). *Health, comfort, energy use and sustainability issues related to the use of biobased building materials.*
5. Thermal conductivity, density and specific heat capacity of different insulation materials, De Visser, C., Van Wijk, K., & Van der Voort, M. (2015). *Health, comfort, energy use and sustainability issues related to the use of biobased building materials.*
6. Design parametres for configuration details. Own table
7. Thermal resistance factor cavity based on strength ventilation. NEN Connect - NTA 8800:2024 nl. (n.d.). https://connect.nen.nl/Standard/Detail/3701862?compId=10037&collectionId=0
8. Heat transfer coefficient of the glazing, U_g. NEN Connect - NTA 8800:2024 nl. (n.d.). https://connect.nen.nl/Standard/Detail/3701862?compId=10037&collectionId=0
9. Calculation of the overall heat transfer coefficient of the window. Own table
10. Boundary condition temperature factor. *NEN 2778:2015 nl.* (n.d.). https://www.nen.nl/nen-2778-2015-nl-206260
11. Thermal resistance R_{sp} [$(m^2K)/W$] of an unventilated cavity. NEN Connect - NTA 8800:2024 nl. (n.d.). https://connect.nen.nl/Standard/Detail/3701862?compId=10037&collectionId=0
12. Used materials with corresponding properties in WUFI for the floor construction. Own table
13. Used materials with corresponding properties in WUFI for the window construction. Own table
14. Used materials with corresponding properties in WUFI for the roof construction. Own table
15. Used materials with corresponding properties in WUFI for detail configuration 1. Own table
16. Used materials with corresponding properties in WUFI for detail configuration 2. Own table
17. Used materials with corresponding properties in WUFI for detail configuration 3. Own

18. Used materials with corresponding properties in WUFI for detail configuration 4. Own table
19. Used materials with corresponding properties in WUFI for detail configuration 5. Own table
20. Used materials with corresponding properties in WUFI for detail configuration 6. Own table
21. Used materials with corresponding properties in WUFI for detail configuration 7. Own table
22. Used materials with corresponding properties in WUFI for detail configuration 8. Own table
23. Used materials with corresponding properties in WUFI for detail configuration 9. Own table
24. Used materials with corresponding properties in WUFI for detail configuration 10. Own table
25. Used materials with corresponding properties in WUFI for detail configuration 11. Own table
26. Calculation of the RC-value of the wall construction build-up. Own table
27. Calculation of the equivalent thermal conductivity of the individual layers in the relevant build-up. Own table
28. Calculation of the RC-value of the floor construction build-up. Own table
29. Calculation of the equivalent thermal conductivity of the individual layers in the relevant build-up. Own table
30. Calculation of the RC-value of the roof construction build-up. Own table
31. Calculation of the equivalent thermal conductivity of the individual layers in the relevant build-up. Own table
32. Calculation of the overall heat transfer coefficient and thermal resistance of the window. Own table
33. Calculation of the density mass per unit area. Own table
34. Calculation of the phase shift. Own table
35. Calculation of the $Q_{ideal\ condition}$ V1. Own table
36. Calculation of the $Q_{ideal\ condition}$ V2. Own table
37. Calculation of the $Q_{ideal\ condition}$ H1. Own table

Appendix A
Simulation results and assessment

Detail configuration 2 - hempcrete with plaster

The second detail configuration consists of hempcrete blocks, bonded with a hydraulic lime mortar within a timber construction frame. To protect the wooden structure from moisture penetration, the wood must be covered with at least 70 mm of hempcrete. Since the exterior consists of hempcrete blocks, the blocks can, in this configuration, be finished directly with a hydraulic lime plaster on the outside and a clay plaster on the inside. For both finishes, a rough base layer should first be applied, followed by a finer finishing layer.

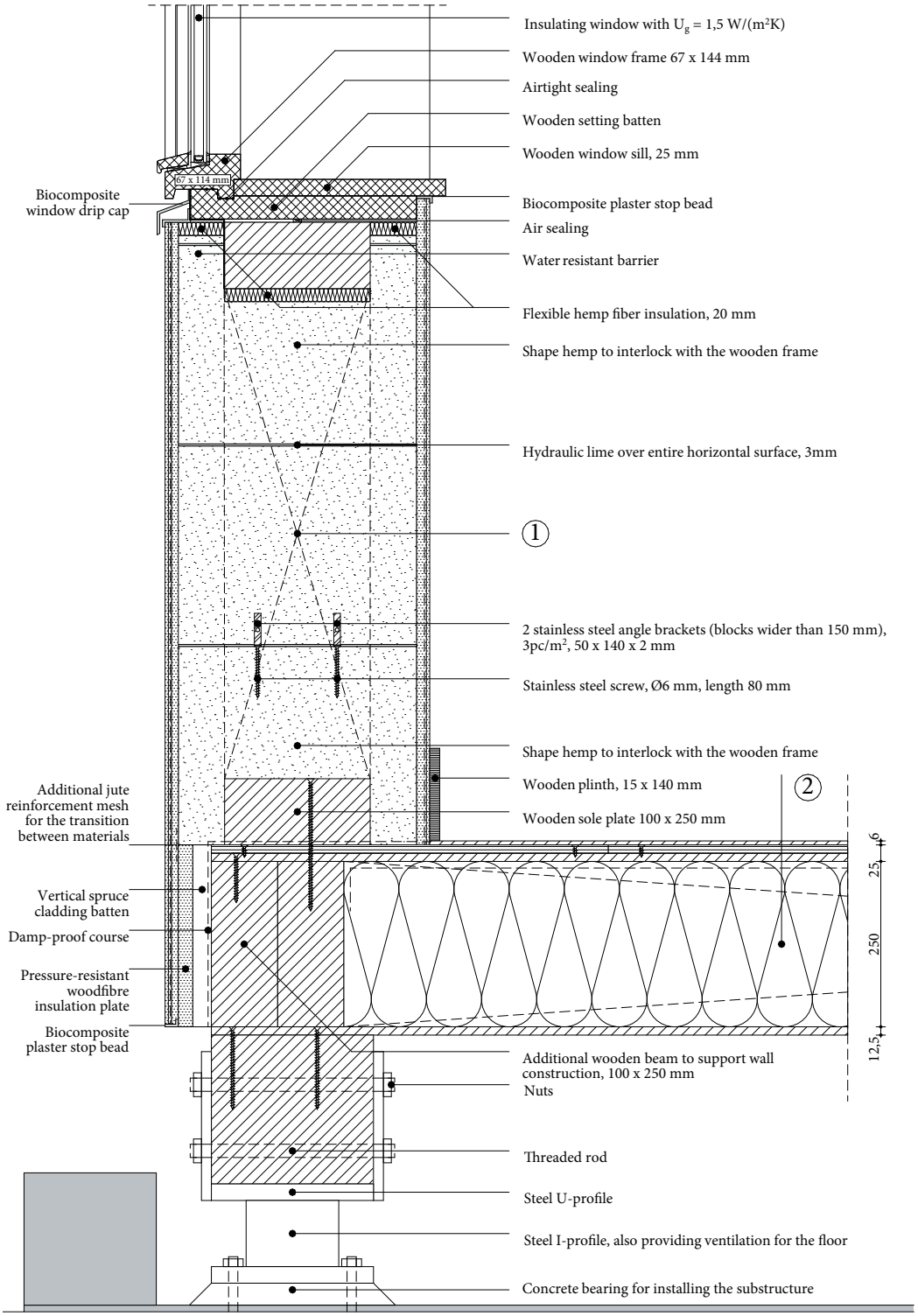

Figure A1, 1:10 detail of V1, configuration 2, own illustration

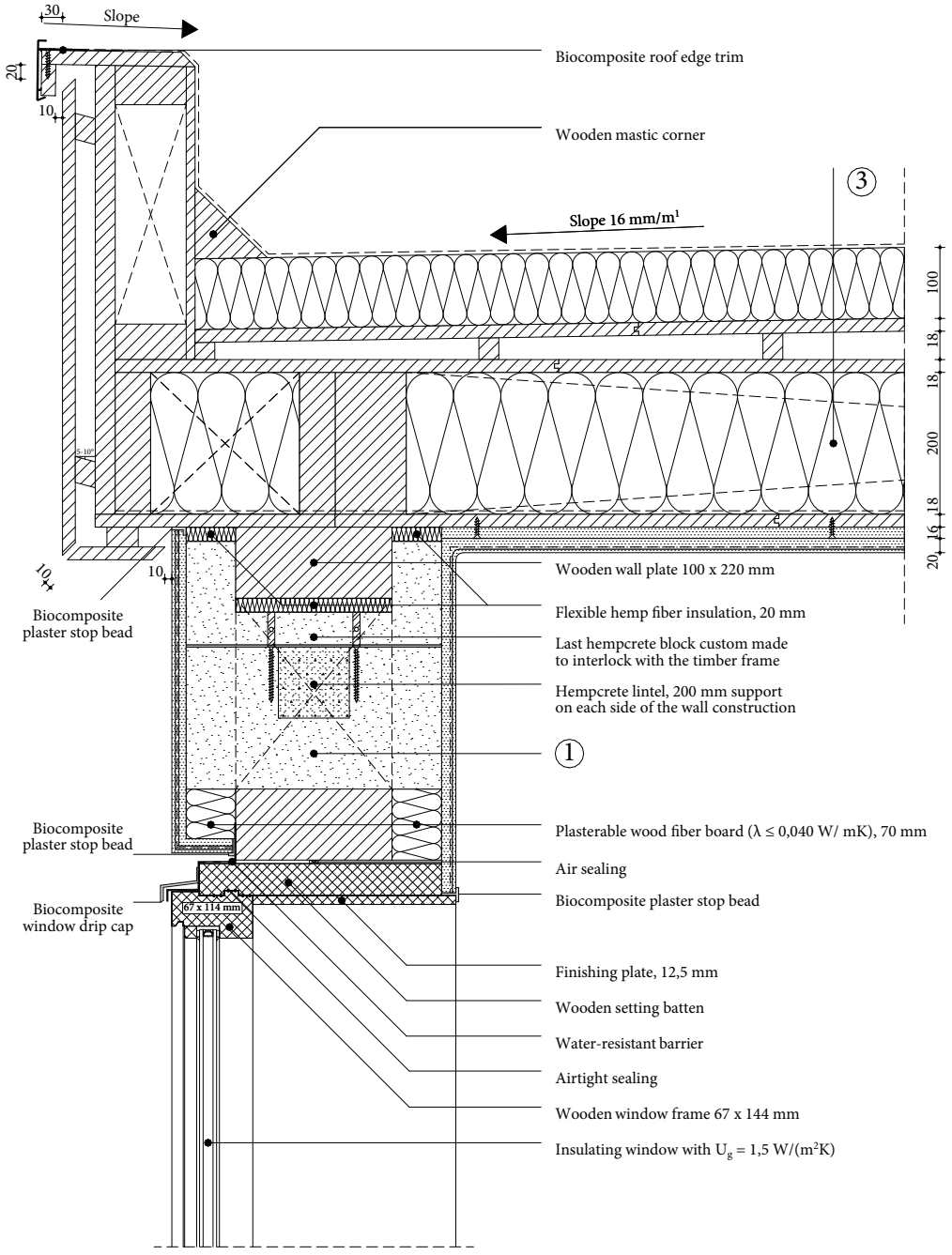

Figure A2, 1:10 detail of V2, configuration 2, own illustration

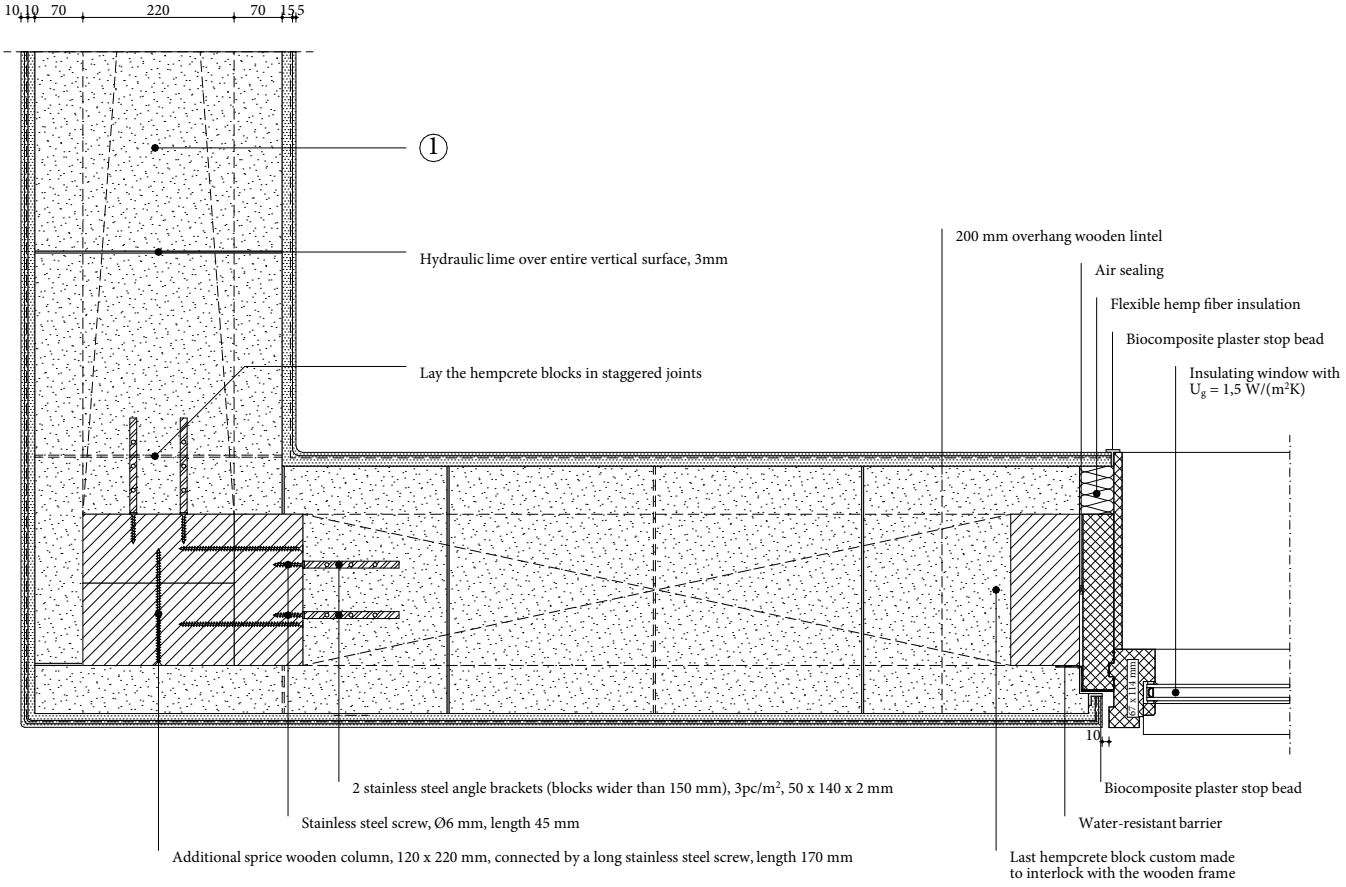

Figure A3, 1:10 detail of H1, configuration 2, own illustration

❶ Wall construction build-up, RC-value: 5.53 (m²K)/W

- Finishing lime plaster, 5 mm;
- Jute reinforcement mesh;
- Rough base lime plaster, 5 mm;
- Rough bonding lime plaster, 10 mm;
- Timber frame construction, 100 x 220 mm, center-to-center 3000 mm, placed 70 mm from outside;
- Hempcrete blocks ($\lambda \leq 0.071$ W/mK), 360 mm;
- Rough base clay plaster, 15 mm;
- Jute reinforcement mesh;
- Finishing clay plaster, 5 mm.

❷ Floor construction build-up, RC-value: 4.65 (m²K)/W

- Finishing board, 6 mm;
- Biobased wooden construction board, 12.5 mm;
- Biobased wooden construction board, perpendicular on the other plate, 12.5 mm;
- Vapour-retarding and airtight membrane with a variable vapour diffusion resistanance;
- Flexible hemp fiber insulation placed between construction ($\lambda \leq 0.043$ W/(mK), 250 mm;
- Wooden beams 100 x 250 mm, center-to-center 600 mm;
- Biobased wooden construction board, 12.5 mm.

❸ Roof construction build-up, RC-value: 6.71 (m²K)/W

- EPDM glued on underlayment to prevent roof covering from lifting;
- Pressure-resistant woodfibre insulation plate ($\lambda \leq 0.042$ W/(mK), 100 mm;
- Biobased wooden construction board, 18 mm;
- Sloped wooden battens for drainage at an angle of 16 mm/m^1, 28 x 24 mm;
- Biobased wooden construction board, 18 mm;
- Flexible hemp fiber insulation placed between construction ($\lambda \leq 0.043$ W/(mK), 200 mm;
- Wooden beams 100 x 200 mm, center-to-center 600 mm;
- Vapour-retarding and airtight membrane with a variable vapour diffusion resistanance;
- Biobased wooden construction board, 18 mm;
- Clay base plate, 16 mm;
- Rough base clay plaster, 15 mm;
- Jute reinforcement mesh;
- Finishing clay plaster, 5 mm.

$U_g = 1.50$ W/(m²K)

$U_w = 1.76$ W/(m²K)

f-factor ≥ 0.65

Ψ_{V1}: 0.082 W/(mK) Ψ_{V2}: 0.058 W/(mK) Ψ_{H1}: 0.095 W/(mK)

Isopleths: no risk of mould $f_{R,si} > f_{R,si,\,max}$; no risk of mould

Phase shift of the wall construction: 23.5 h

Density of the wall construction 153 kg/m³

Calculation RC-value wall construction build-up

❶ Wall construction build-up, RC-value: 5.53 (m²K)/W

Table A1, Calculation of the RC-value of the wall construction build-up

Material	Thickness [m]	Thermal conductivity [W/(mK)]	Thermal resistance [W/(m²K)]
Lime plaster	0,020	0,049	0,408
Timber frame construction, with hempcrete blocks	0,360	0,073	4,932
Clay plaster	0,020	0,910	0,022

Table A2, Calculation of the equivalent thermal conductivity of the individual layers in the relevant build-up

	Layer 1		Layer 2	
Material	Area [m²]	Thermal conductivity [W/(mK)]	Area [m²]	Thermal conductivity [W/(mK)]
Timber frame construction, with hempcrete blocks	1,072	0,071	0,036	0,130

Density mass per unit area of the wall construction

Table A3, Calculation of the density mass per unit area

Material	Thickness [m]	Density [kg/m³]
Lime plaster	0,020	200
Timber frame construction, with hempcrete blocks	0,360	326
Clay plaster	0,020	1600

By using the previously presented formula a **m'-value** of **153.36 kg/m²** can be given for the **second detail configuration**.

Phase-shift

Table A4, Calculation of the phase shift

Material	Thickness [m]	Thermal conductivity [W/(mK)]	Density [kg/m³]	Specific heat capacity [J/(kgK)]
Timber frame construction, with hempcrete blocks	0,360	0,073	326	1794

By using the presented phase shift formula, the resulting **φ-value** for **the second configuration** is **23.5 h.**

Geometry WUFI

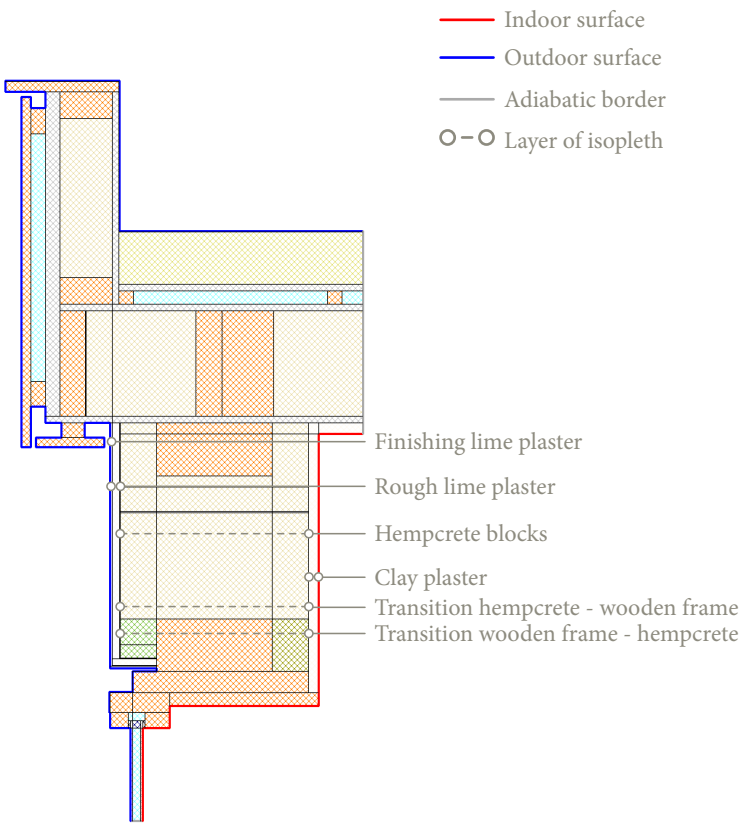

Figure A5, geometry detail V2 including location isopleths

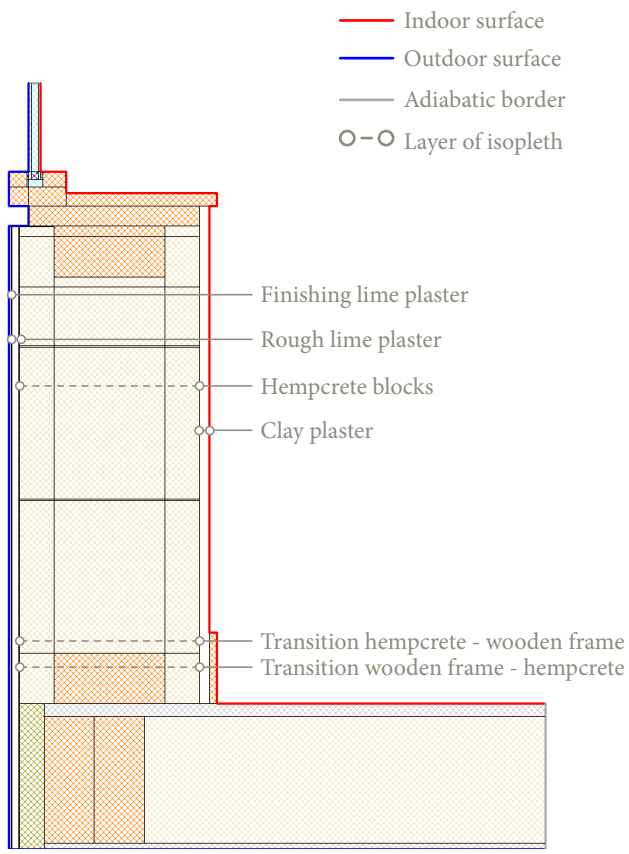

Figure A6, geometry detail V1 including location isopleths

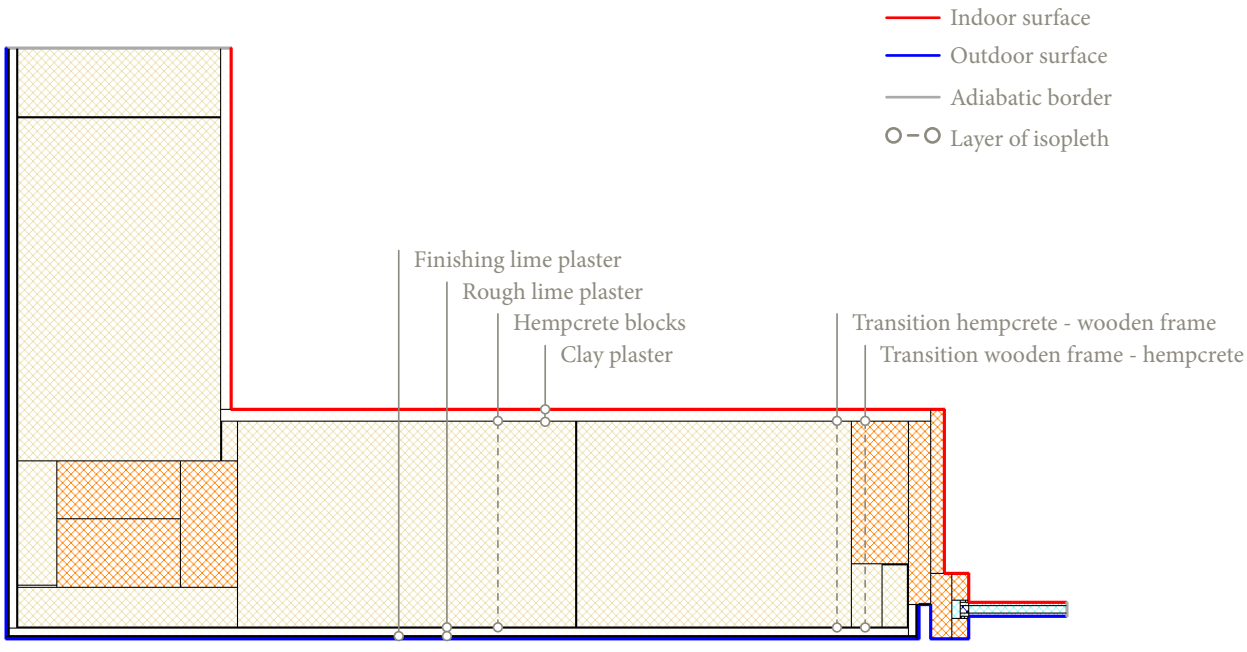

Figure A4, geometry detail H1including location isopleths

Isopleths - V1

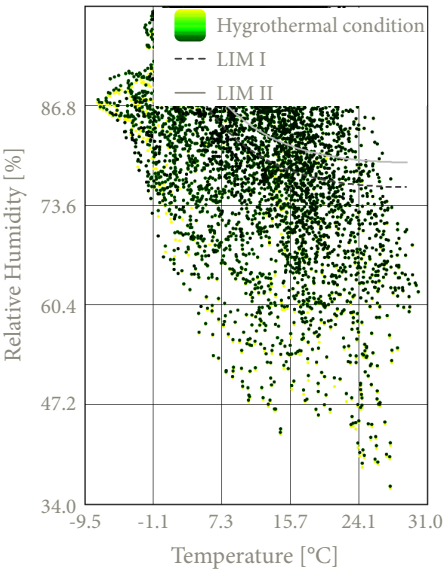

Figure A7, Isopleths finishing lime plaster

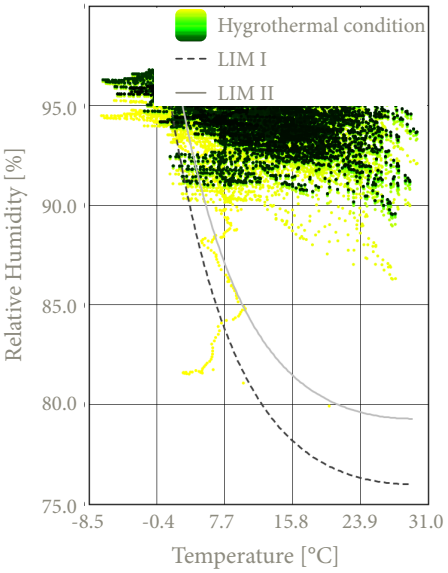

Figure A8, Isopleths rough bonding lime plaster

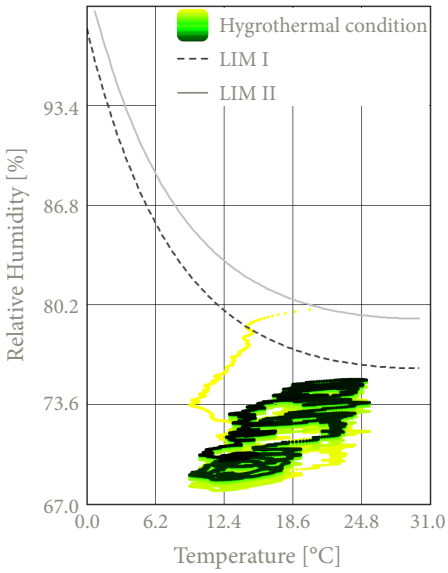

Figure A9, Isopleths hempcrete blocks

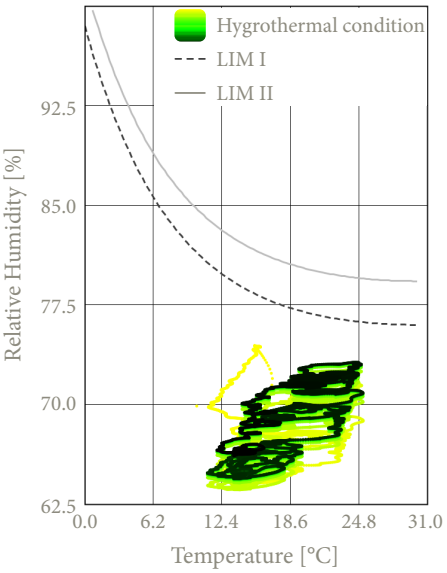

Figure A10, Isopleths hempcrete & transition frame

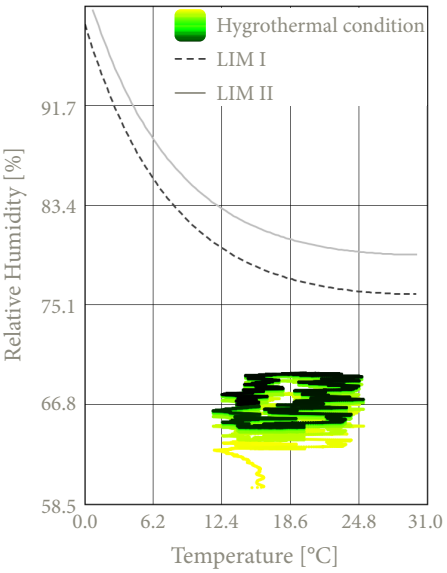

Figure A11, Isopleths transition frame & hempcrete

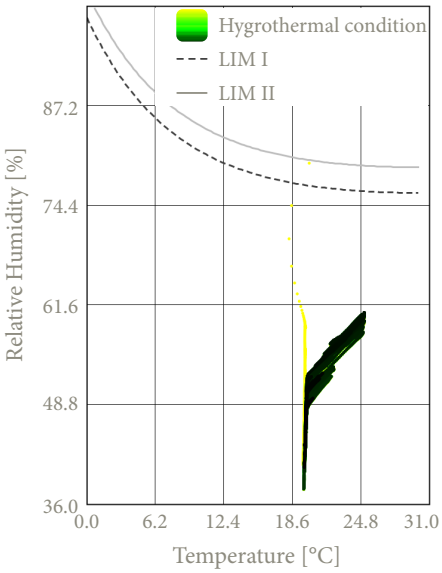

Figure A12, Isopleths clay plaster

Isopleths - V2

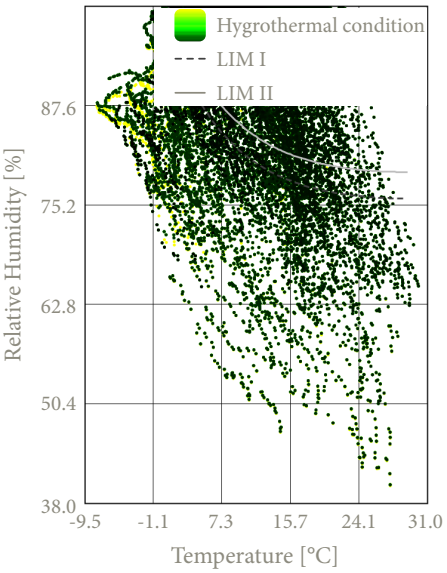

Figure A13, Isopleths finishing lime plaster

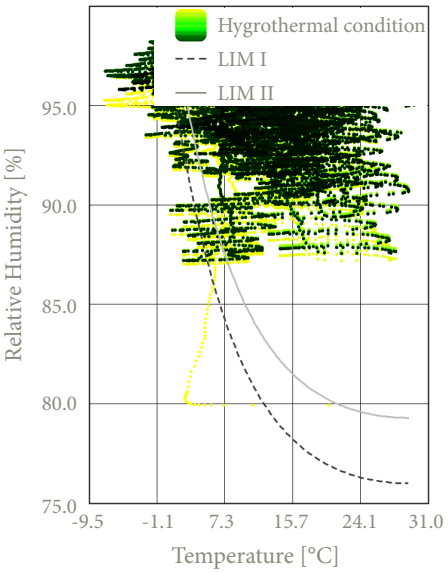

Figure A14, Isopleths rough bonding lime plaster

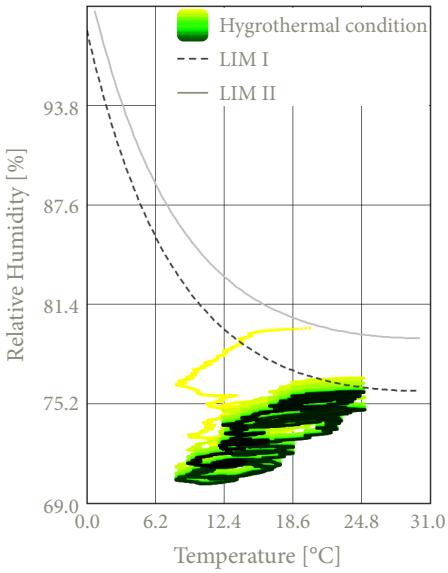

Figure A15, Isopleths hempcrete blocks

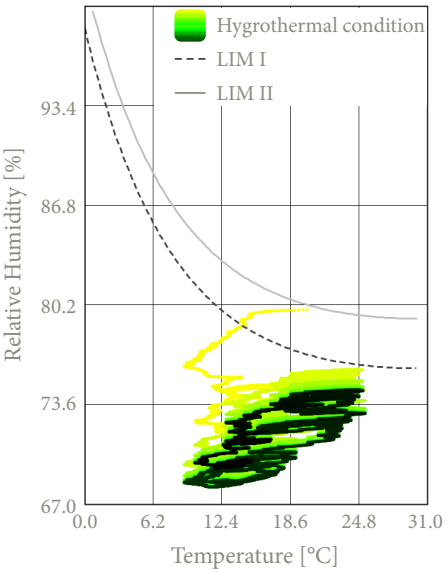

Figure A16, Isopleths hempcrete & transition frame

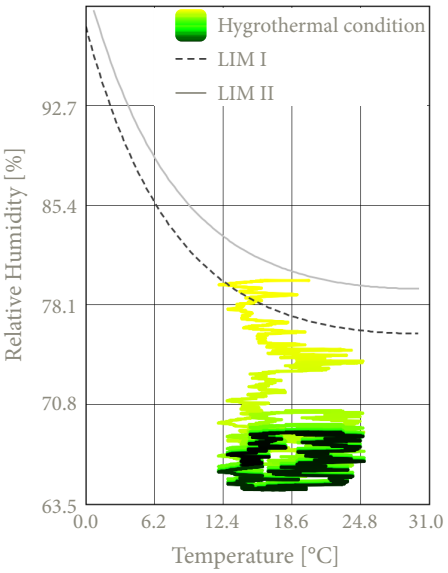

Figure A17, Isopleths transition frame & hempcrete

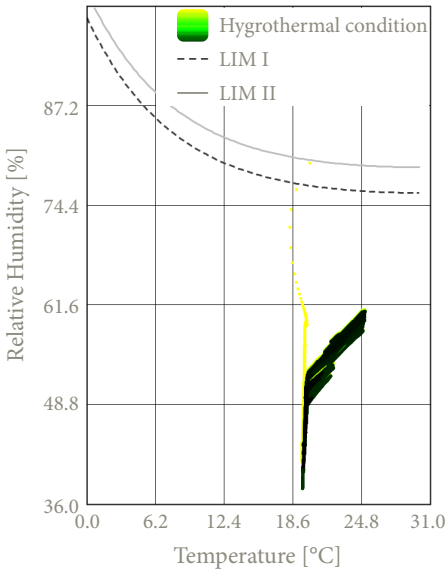

Figure A18, Isopleths clay plaster

Isopleths - H1

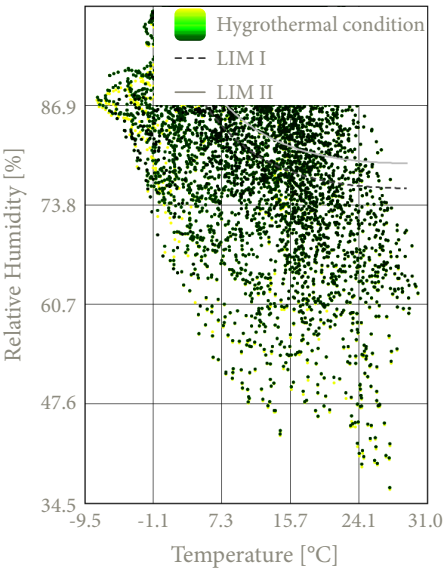

Figure A19, Isopleths finishing lime plaster

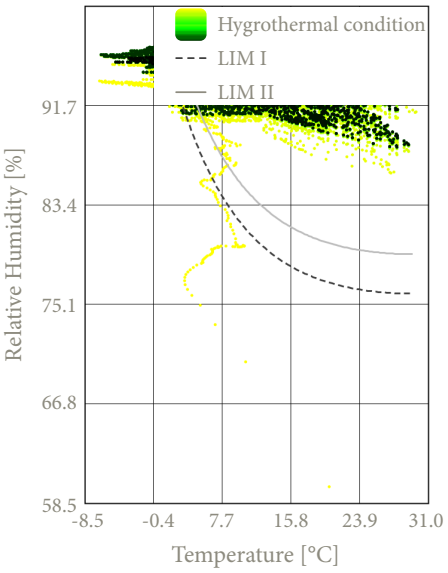

Figure A20, Isopleths rough bonding lime plaster

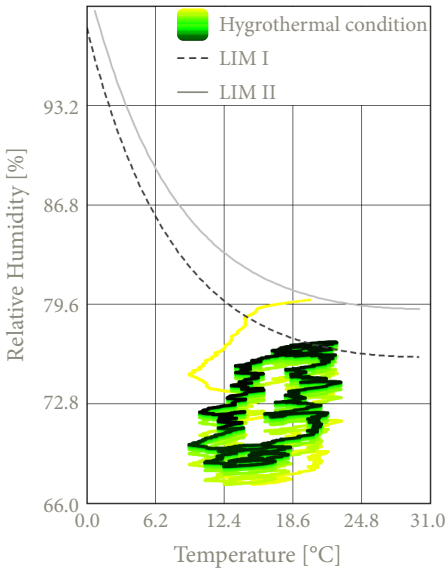

Figure A21, Isopleths hempcrete blocks

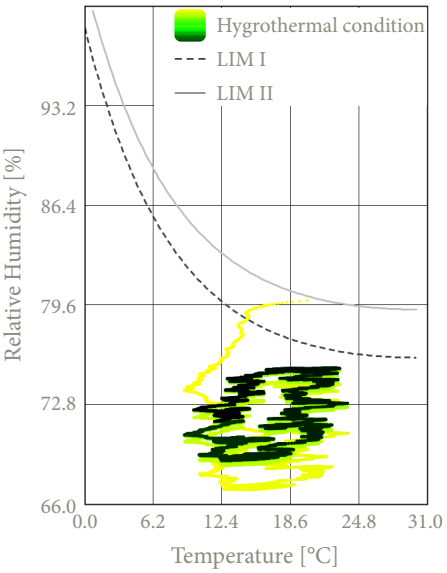

Figure A22, Isopleths hempcrete & transition frame

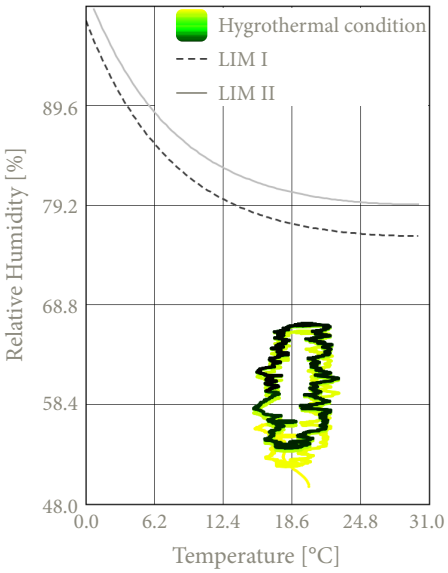

Figure A23, Isopleths transition frame & hempcrete

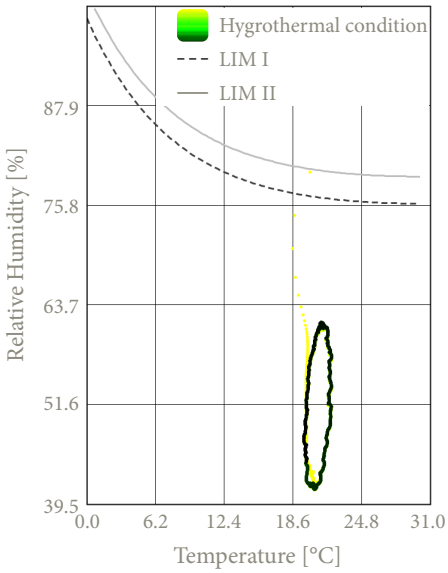

Figure A24, Isopleths clay plaster

Conclusion isoplteths

Based on the established and analysed isopleths of the various details within this construction **configuration**, it can be concluded that there is **no risk of mould growth** within the different material layers of V1 and H1. All isopleths located behind the outer plaster layer remain **below** the critical threshold values **LIM I** and **LIM II**, indicating that the details meet the established criteria.

For detail V2, however, a problem occurred during the simulation, causing the calculations to stop after four years. As a result, no further simulation was performed, and the total moisture content in the construction did not receive a value. A possible cause is a convergence issue. After P4, an attempt will be made to resolve this by reducing the time step from one hour to 30 minutes. This allows the influence of rain on the total moisture content to be calculated more accurately, which may contribute to solving the convergence issue.

With regard to the **finishing plaster**, the isopleths do **exceed** the **threshold values**. However, this is not fully representative of the intended construction scenario, as in practice a plaster with mould-resistant properties is applied. As previously mentioned, such specialised plasters can effectively inhibit microbial growth within the material. Additionally, in real-life applications an exterior plaster is used specifically designed to withstand weather conditions and fluctuations in relative humidity. These types of plasters are also recommended by hempcrete suppliers, with the combination of hempcrete and lime-based plaster being a commonly prescribed solution.

In the case of **hempcrete blocks**, the isopleths initially remain below LIM I and LIM II, followed by a slight upward trend. At the end of the simulation, the values briefly exceed the LIM I threshold but quickly go below the theshold. Since the values remain below the critical thresholds for the vast majority of the simulation period, the risk of **mould growth** is considered **very low** and practically **negligible**. This conclusion is further supported by the fact that the upward trend diminishes over time.

A similar upward trend is observed in the **transition zones between the hempcrete blocks and the wooden frame**, but in these areas the isopleth values remain below both LIM I and LIM II. Over time, this upward trend diminishes, further indicating stable hygrothermal performance in this layer. For the **timber frame**, the isopleths are well below the critical threshold values confirming that there is no risk of mould growth in this layer.

Finally, the isopleths in the **clay plaster** remain well below the LIM thresholds, indicating no risk of mould formation in this layer either.

To conclude, this construction configuration poses no risk of mould growth, as long as a mould-resistant exterior plaster is used. As such, the design complies with the required hygrothermal performance standards.

Surface condensation - V1, V2 & H1

The circle at each figure figures below, **figure 25**, **figure 27** and **figure 29**, show the coldest point of the interior surface at each detail in order to consider the f_{Rsi}. Below these graphs the corresponding surface temperature at this point is shown over a ten-year simulation below, **figure 26**, **figure 28** and **figure 30**.

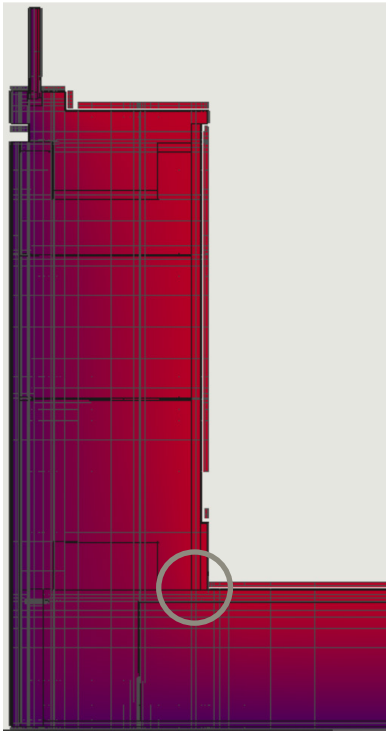

Figure A25, Highlight lowest point, V1

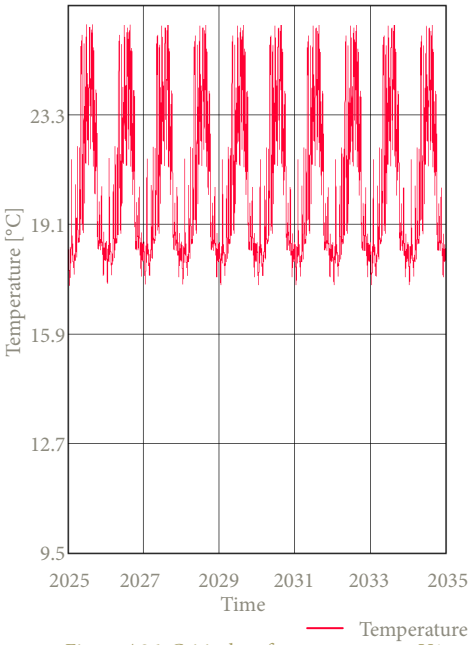

Figure A26, Critical surface temperature, V1

From this graph the lowest surface temperature of this detail is **16.11 °C**.

The resulting f_{Rsi} for this detail is **0.68** which exceeds the minimum requirement of 0.61. This indicates a negligible risk of mold growth.

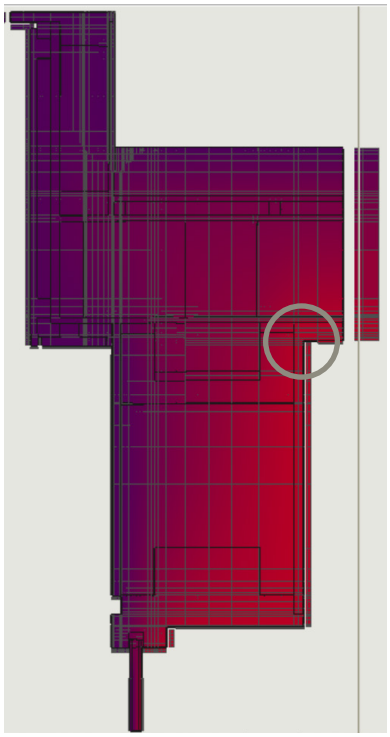

Figure A27, Highlight lowest point, V2

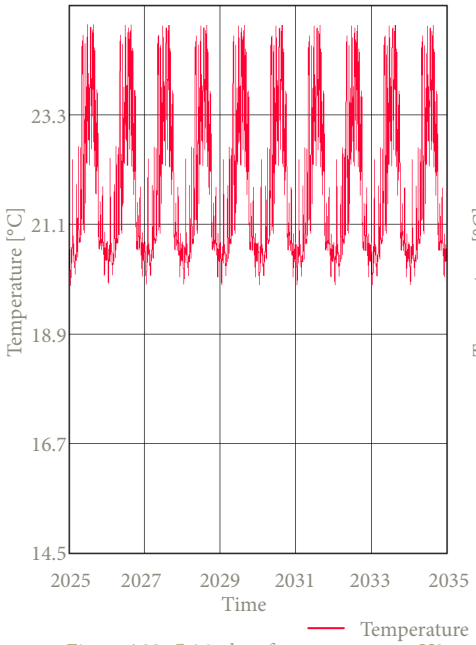

Figure A28, Critical surface temperature, V2

From this graph the lowest surface temperature of this detail is **15.31 °C**.

The resulting f_{Rsi} for this detail is **0.62** which exceeds the minimum requirement of 0.61. This indicates a negligible risk of mold growth.

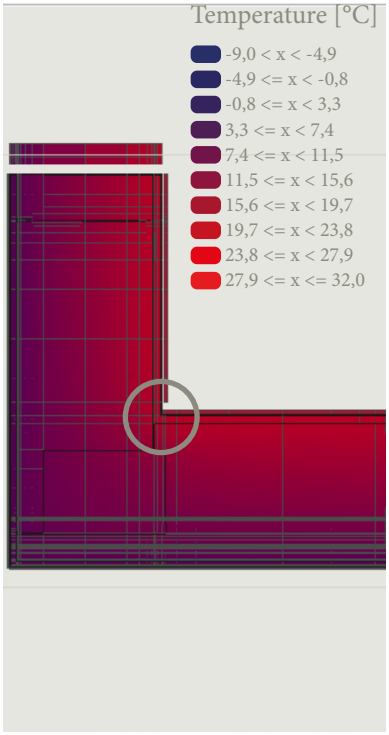

Figure A29, Highlight lowest point, H1

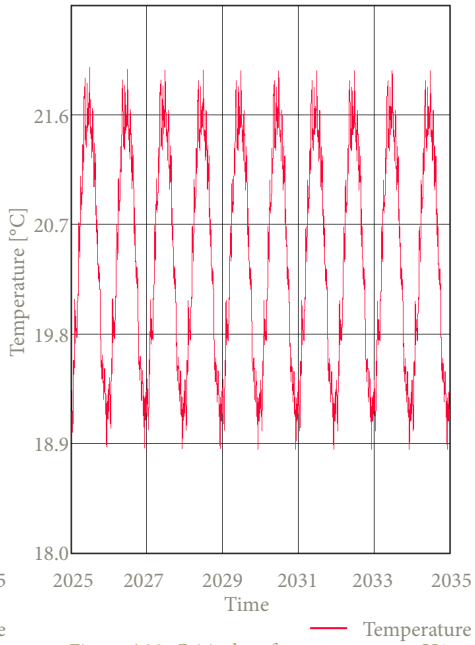

Figure A30, Critical surface temperature, H1

From this graph the lowest surface temperature of this detail is **18.51 °C**.

The resulting f_{Rsi} for this detail is **0.88** which exceeds the minimum requirement of 0.61. This indicates a negligible risk of mold growth.

F-factor - V1, V2 & H1

The resulting **f-factor** of **detail V1** is **0.91** for a temperature of **16.48 °C**. Next the resulting **f-factor** of **detail V2** is **0.95** for a temperature of **17.04 °C**. Lastly, the resulting **f-factor** of **detail H1** is **0.94** for a temperature of **17.07 °C**. This indicates a very limited thermal bridge is assessed within the details of this configuration.
Given that these values significantly all exceeds the required threshold of **0.65**, it can be concluded that the details within this configuration complies with the thermal performance requirements set by the Dutch Building Decree.

PSI-value - V1

Table A5, Calculation of the $Q_{ideal\ condition}$

$R_{construction,\ window}$ [(m²K)/W]	$A_{construction,\ window}$ [m²]	$R_{construction,\ wall}$ [(m²K)/W]	$A_{construction,\ wall}$ [m²]	$R_{construction,\ floor}$ [(m²K)/W]	$A_{construction,\ floor}$ [m²]
0.600	0.2425	5.532	1.019	4.648	0.731

The resulting $\mathbf{Q_{ideal\ condition}}$ is **13.421 W**

Q_{WUFI} represents the sum of all heat flows through the detail, resulting in a total heat flow of **14.899 W**.

These values give a **Ψ-value** of **0.082 W/(mK)** for **detail V1**, indicating that the detail can be characterised as a well-insulated building component.

PSI-value - V2

Table A6, Calculation of the $Q_{ideal\ condition}$

$R_{construction,\ window}$ [(m²K)/W]	$A_{construction,\ window}$ [m²]	$R_{construction,\ wall}$ [(m²K)/W]	$A_{construction,\ wall}$ [m²]	$R_{construction,\ roof}$ [(m²K)/W]	$A_{construction,\ roof}$ [m²]
0.600	0.2425	5.532	0.844	6.442	0.096

The resulting $\mathbf{Q_{ideal\ condition}}$ is **10.289 W**

Q_{WUFI} represents the sum of all heat flows through the detail, resulting in a total heat flow of **11.338 W**.

These values give a **Ψ-value** of **0.058 W/(mK)** for **detail V2**, indicating that the detail can be characterised as a well-insulated building component.

PSI-value - H1

Table A7, Calculation of the $Q_{ideal\ condition}$

$R_{construction,\ window}$ [(m²K)/W]	$A_{construction,\ window}$ [m²]	$R_{construction,\ wall}$ [(m²K)/W]	$A_{construction,\ wall}$ [m²]
0.600	0.2425	5.532	2.351

The resulting $\mathbf{Q_{ideal\ condition}}$ is **14.924 W**

Q_{WUFI} represents the sum of all heat flows through the detail, resulting in a total heat flow of **16.647 W**.

These values give a **Ψ-value** of **0.095 W/(mK)** for **detail H1**, indicating that the detail can be characterised as a well-insulated building component.

Assessment detail configuration

Important notes about the details

For the given configuration, **key considerations** are presented below in the form of bullet points. These points highlight specific aspects that need to be taken into account during detailing and construction.

- Apply 3 mm of hydraulic lime to all contact surfaces to ensure proper adhesion between the blocks.
- Place the blocks in staggered joints to distribute load correctly and minimize the thermal bridge.
- The blocks can be easily cut to size to fit for every project.
- Fill the gaps between the blocks and the timber structural frame with 20 mm of flexible hemp.
- Attach the water-resistant barrier of the window frame to the timber structural frame.
- The hempcrete lintel is equipped with a concrete core and needs to have 200 mm bearing.
- Fill the spaces beneath the lintel with plasterable wood fiber boards.
- Cover the wooden structure with at least 70 mm of hempcrete for adequate protection against moisture and weather.
- Use a hydraulic lime plaster for the outside with antifungal properties to prevent mould growth, this plaster needs to be also suitable for outdoor applications and resistant to moisture and weather.
- Apply biobased composite plaster stops for a neat and durable plaster finish.
- Use a jute reinforcement mesh between the rough and finishing clay & lime plaster to prevent cracking.

Assessment of the configuration

Additionally, the configuration is evaluated based on the following criteria:

1. **Weight**: The total mass per unit area of the wall construction.
2. **Construction time**: The time required for assembling the construction.
3. **Resistance Construction-value:** The combined thermal resistance of all layers in the construction.
4. **Phase shift**: The heat transfer delay of the structure.

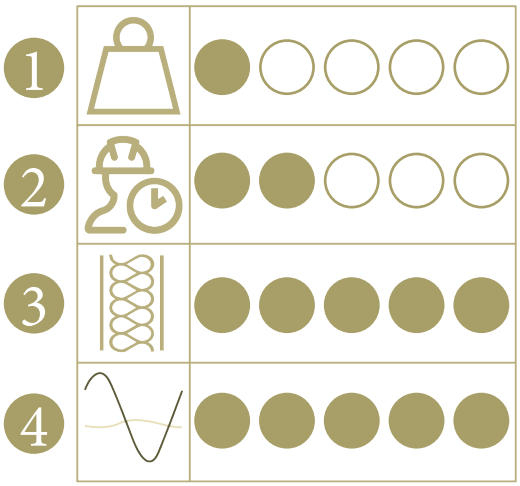

Axonometric view of the detail configuration

In addition to the presented details, an **axonometric view** of the respective detail is also shown. This is presented in the figure below, **figure 31**, and is intended to provide more clarity and insight into **detail V1, detail V2,** and **detail H1**.

Figure A31, Axonometric view of detail configuration 2

Detail configuration 3 - flexible hemp with wooden façade

The third detail configuration consists of flexible hemp fibre placed between the studs of the timber construction frame. The timber construction frame is then finished on the exterior with a pressure-resistant wood fibre board. This board protects the timber construction frame against moisture penetration and allows for the attachment of the wooden cladding. On the interior, the timber construction frame is finished with a biobased diffusion-open construction board to which a clay plate is screwed. A clay plaster can be applied on this plate, consisting of a rough layer and a finishing layer.

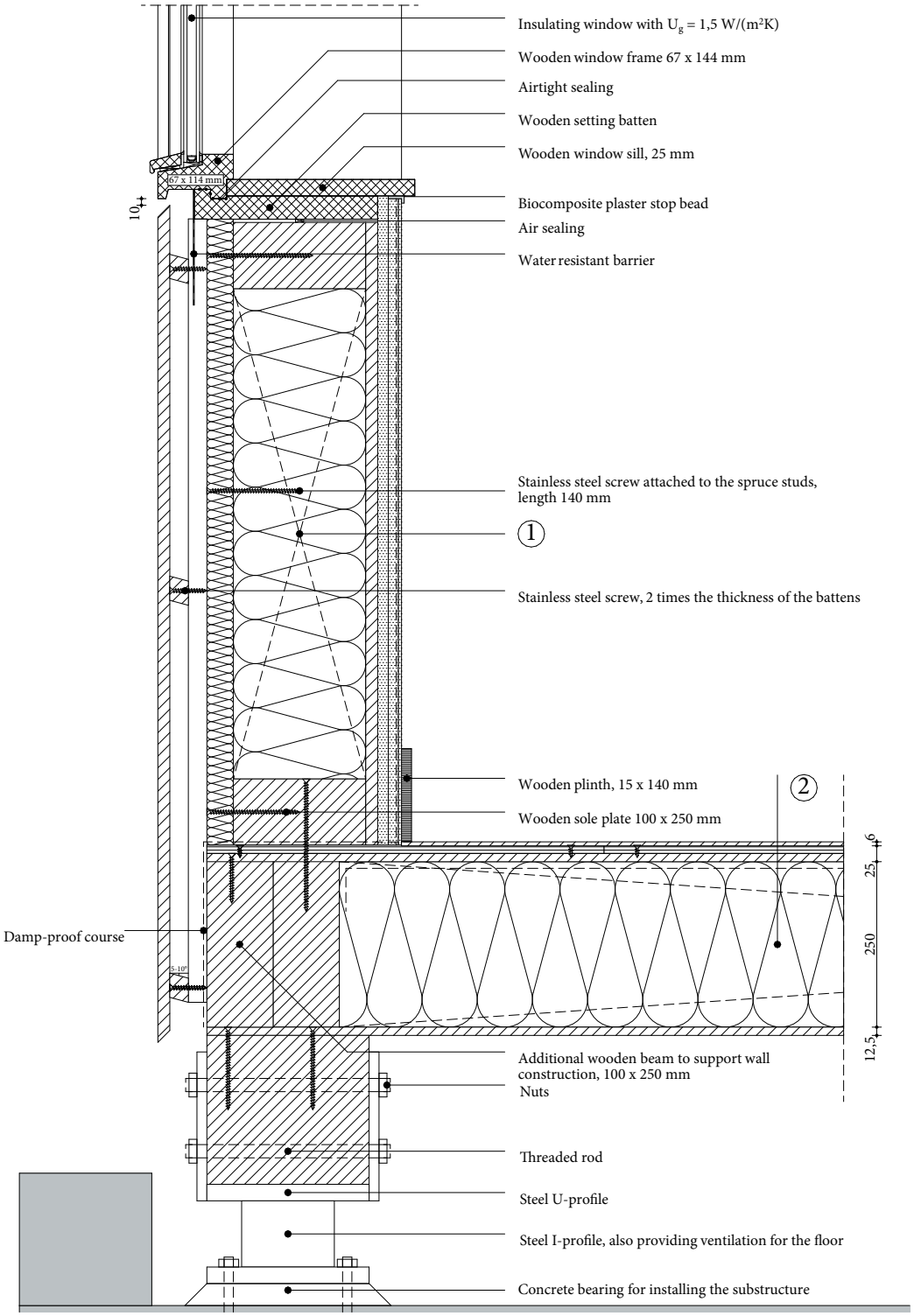

Figure A32, 1:10 detail of V1, configuration 3, own illustration

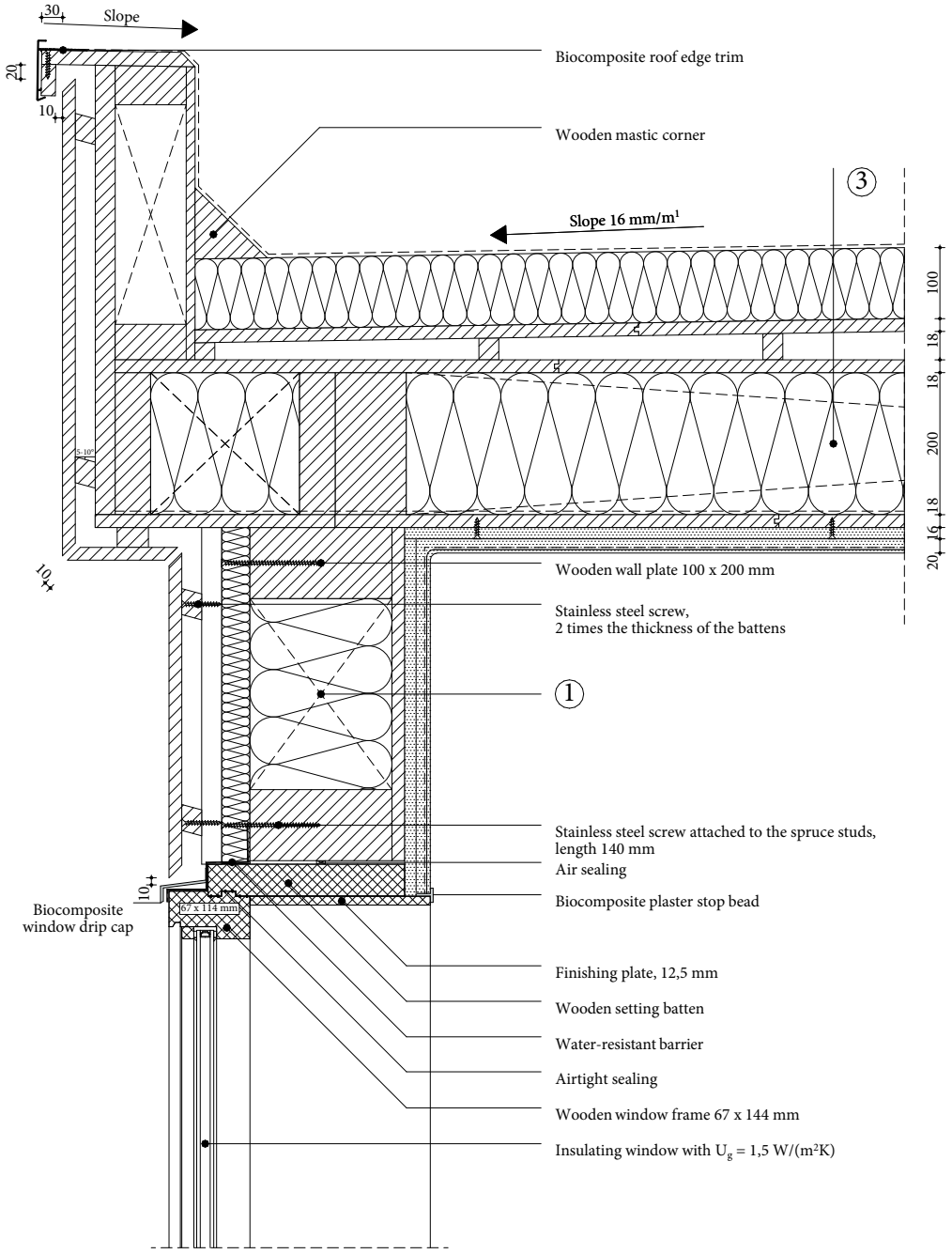

Figure A33, 1:10 detail of V2, configuration 3, own illustration

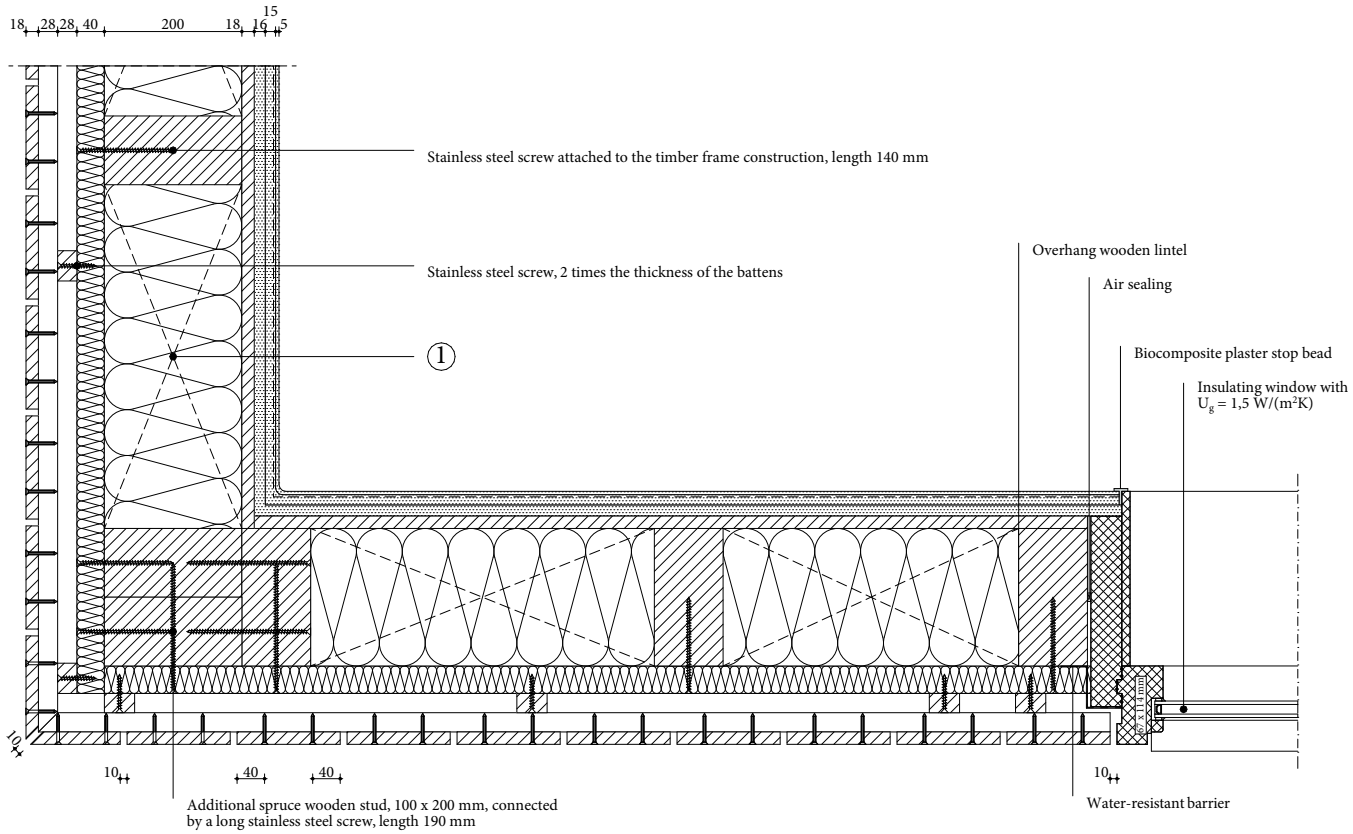

Figure A34, 1:10 detail of H1, configuration 3, own illustration

❶ Wall construction build-up, RC-value: 5.22 (m²K)/W

- Vertical wooden cladding, 18 mm;
- Horizontal spruce cladding batten cavity, 28 x 44 mm, center-to-center 600 mm;
- Vertical spruce cladding batten forming ventilated cavity, 28 x 44 mm, center-to-center 600 mm;
- Pressure-resistant woodfibre insulation plate (λ ≤ 0.042 W/mK), 40 mm;
- Timber frame construction, 100 x 200 mm, center-to-center 600 mm;
- Flexible hemp fibre insulation, placed between construction (λ ≤ 0.043 W/mK), 200 mm;
- Clay base plate, 16 mm;
- Rough base clay plaster, 15 mm;
- Jute reinforcement mesh;
- Finishing clay plaster, 5 mm.

❷ Floor construction build-up, RC-value: 4.65 (m²K)/W

- Finishing board, 6 mm;
- Biobased wooden construction board, 12.5 mm;
- Biobased wooden construction board, perpendicular on the other plate, 12.5 mm;
- Vapour-retarding and airtight membrane with a variable vapour diffusion resistanance;
- Flexible hemp fiber insulation placed between construction (λ ≤ 0.043 W/(mK), 250 mm;
- Wooden beams 100 x 250 mm, center-to-center 600 mm;
- Biobased wooden construction board, 12.5 mm.

❸ Roof construction build-up, RC-value: 6.71 (m²K)/W

- EPDM glued on underlayment to prevent roof covering from lifting;
- Pressure-resistant woodfibre insulation plate (λ ≤ 0.042 W/(mK), 100 mm;
- Biobased wooden construction board, 18 mm;
- Sloped wooden battens for drainage at an angle of 16 mm/m^1, 28 x 24 mm;
- Biobased wooden construction board, 18 mm;
- Flexible hemp fiber insulation placed between construction (λ ≤ 0.043 W/(mK), 200 mm;
- Wooden beams 100 x 200 mm, center-to-center 600 mm;
- Vapour-retarding and airtight membrane with a variable vapour diffusion resistanance;
- Biobased wooden construction board, 18 mm;
- Clay base plate, 16 mm;
- Rough base clay plaster, 15 mm;
- Jute reinforcement mesh;
- Finishing clay plaster, 5 mm.

U_g = 1.50 W/(m²K)

U_w = 1.76 W/(m²K)

f-factor ≥ 0.65

Ψ_{V1}: 0.079 W/(mK) Ψ_{V2}: 0.098 W/(mK) Ψ_{H1}: 0.064 W/(mK)

Isopleths: no risk of mould $f_{R,si} > f_{R,si,\,max}$; no risk of mould

Phase shift of the wall construction: 9.5 h

Density of the wall construction 102 kg/m³

Calculation RC-value wall construction build-up

❶ Wall construction build-up, RC-value: 5.22 (m²K)/W

Table A8, Calculation of the RC-value of the wall construction build-up

Material	Thickness [m]	Thermal conductivity [W/(mK)]	Thermal resistance [W/(m²K)]
Vertical wooden cladding	0,018	0,130	0,078
Ventilated cavity with horizontal wooden cladding batten, center-to-center 600 mm	0,024	0,313	0,076
Ventilated cavity with vertical wooden cladding batten, center-to-center 600 mm	0,024	0,313	0,076
Pressure-resistant woodfibre insulation plate	0,040	0,041	0,976
Timber frame construction, with flexible hemp	0,200	0,055	3,636
Biobased construction board	0,018	0,120	0,150
Clay base plate	0,016	0,470	0,034
Clay plaster	0,020	0,910	0,022

Table A9, Calculation of the equivalent thermal conductivity of the individual layers in the relevant build-up

	Layer 1		Layer 2	
Material	Area [m²]	Thermal conductivity [W/(mK)]	Area [m²]	Thermal conductivity [W/(mK)]
Ventilated cavity with horizontal wooden cladding batten, center-to-center 600 mm	0,0283	0,337	0,0037	0,130
Ventilated cavity with vertical wooden cladding batten, center-to-center 600 mm	0,0037	0,130	0,0283	0,337
Timber frame construction, with flexible hemp	0,1200	0,043	0,0200	0,013

Density mass per unit area of the wall construction

Table A10, Calculation of the density mass per unit area

Material	Thickness [m]	Density [kg/m³]
Vertical wooden cladding	0,018	520
Ventilated cavity with horizontal wooden cladding batten, center-to-center 600 mm	0,024	35
Ventilated cavity with vertical wooden cladding batten, center-to-center 600 mm	0,024	35
Pressure-resistant woodfibre insulation plate	0,040	140
Timber frame construction, with flexible hemp	0,200	107
Biobased construction board	0,018	621
Clay base plate	0,016	1300
Clay plaster	0,020	1600

By using the previously presented formula a **m'-value** of **102.02 kg/m²** can be given for the **third detail configuration**.

Phase-shift

Table A11, Calculation of the phase shift

Material	Thickness [m]	Thermal conductivity [W/(mK)]	Density [kg/m³]	Specific heat capacity [J/(kgK)]
Timber frame construction, with flexible hemp	0,200	0,055	107	2200

By using the presented phase shift formula, the resulting **φ-value** for **the third configuration** is **9.5 h.**

Geometry WUFI

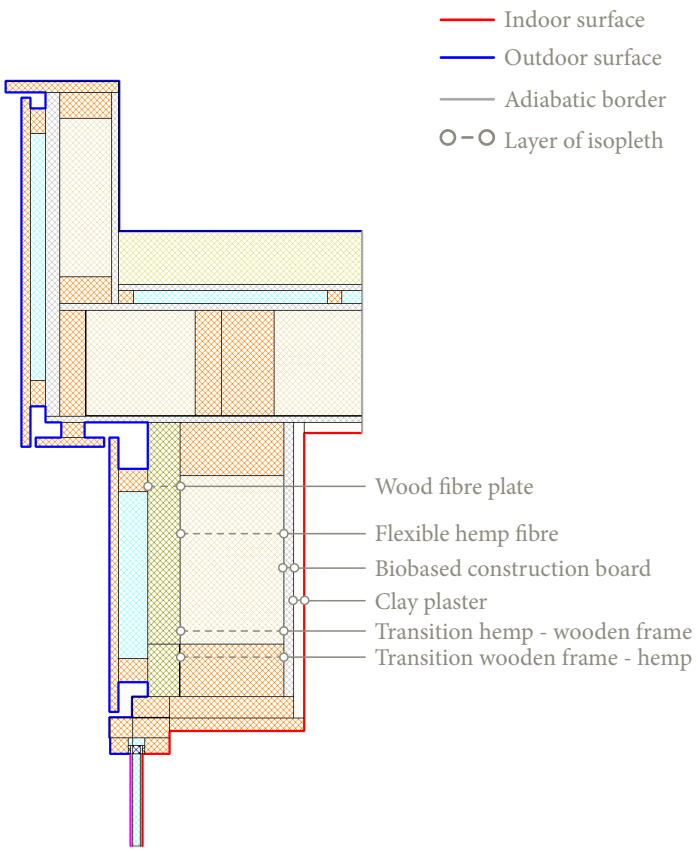

Figure A36, geometry detail V2 including location isopleths

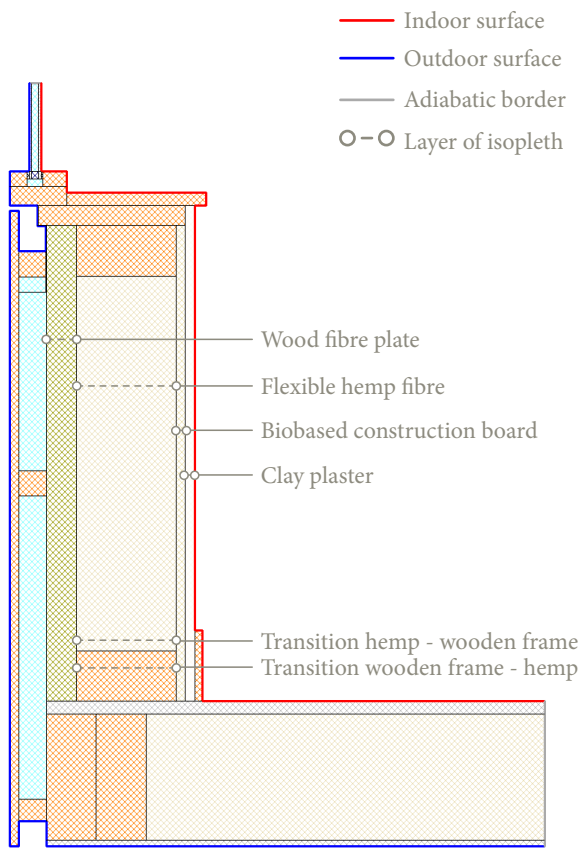

Figure A37, geometry detail V1 including location isopleths

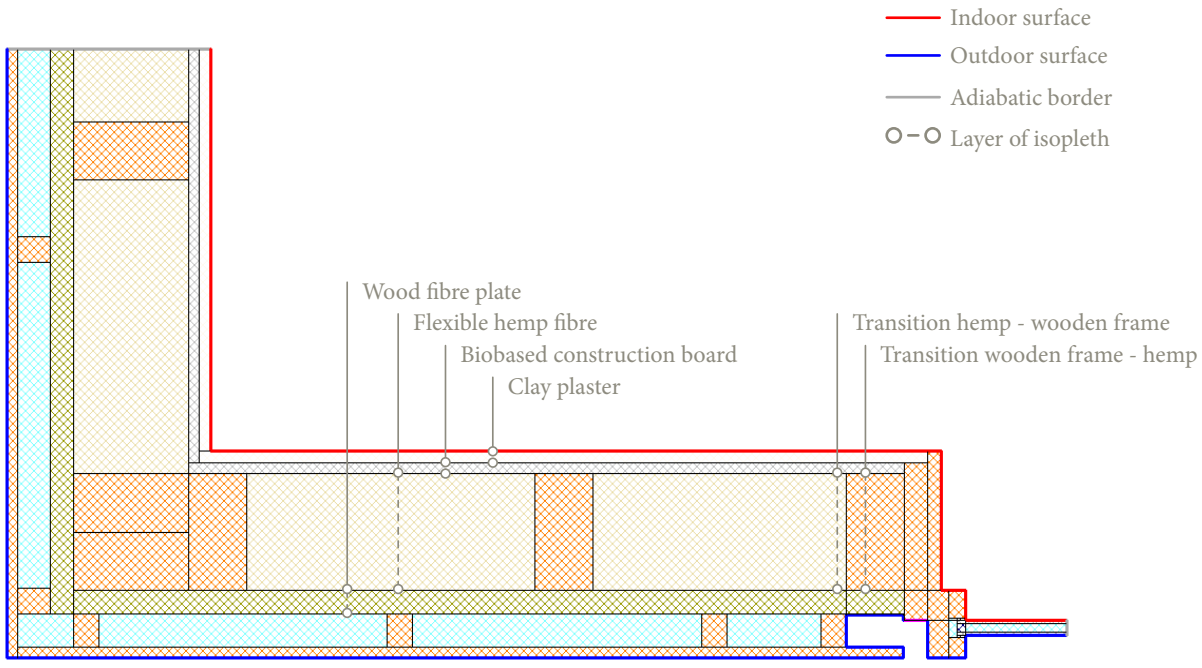

Figure A35, geometry detail H1including location isopleths

Isopleths - V1

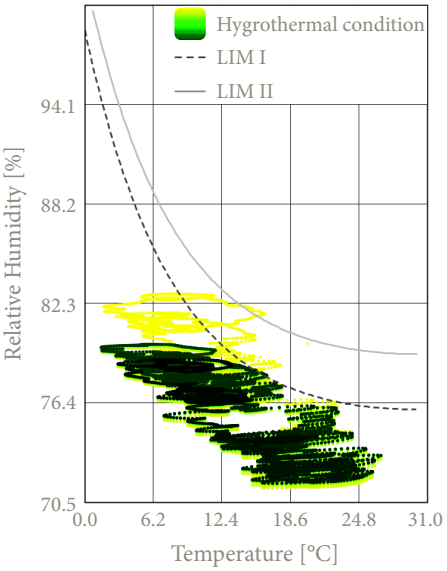

Figure A38, Isopleths wood fibre plate

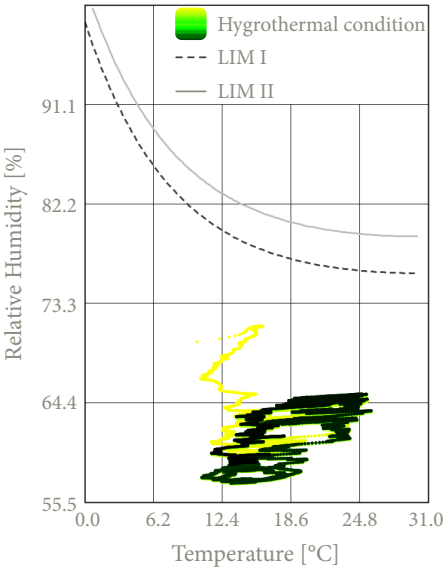

Figure A39, Isopleths flexible hemp

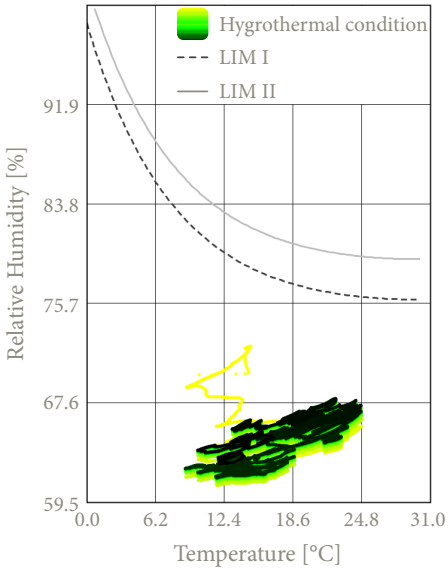

Figure A40, Isopleths hemp & transition frame

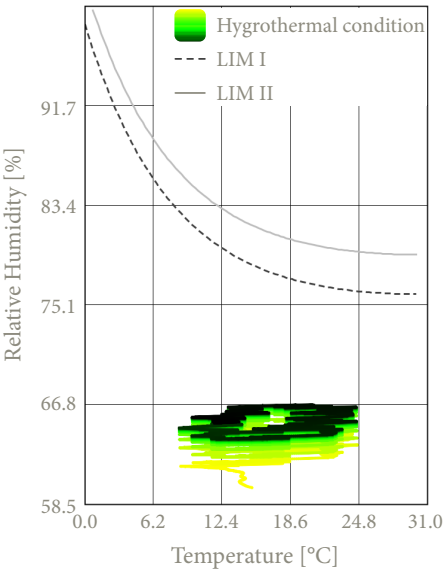

Figure A41, Isopleths transition frame & hemp

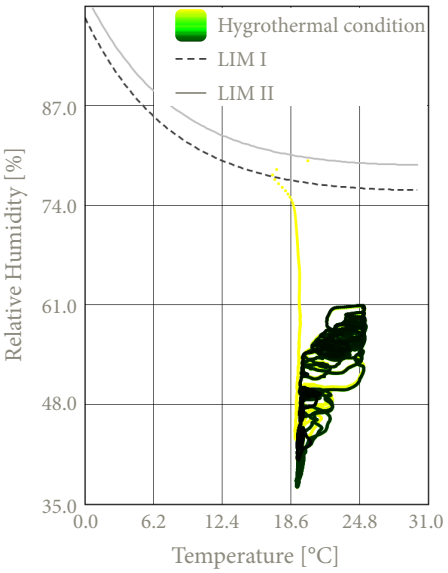

Figure A42, Isopleths biobased construction board

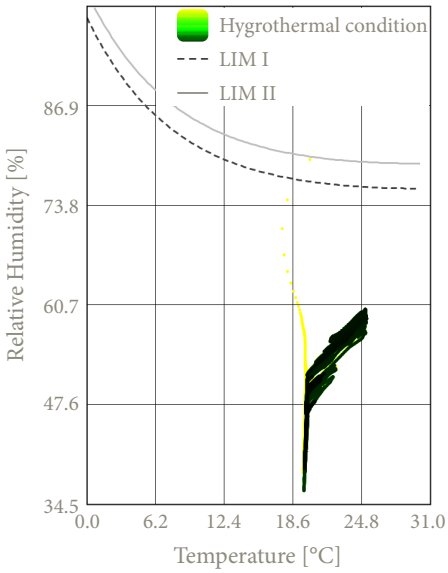

Figure A43, Isopleths clay plaster

Isopleths - V2

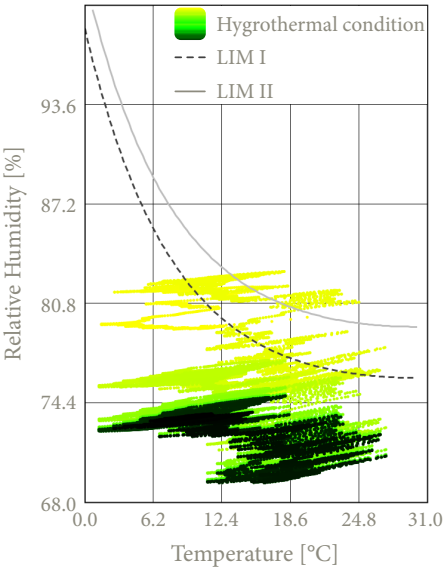

Figure A44, Isopleths wood fibre plate

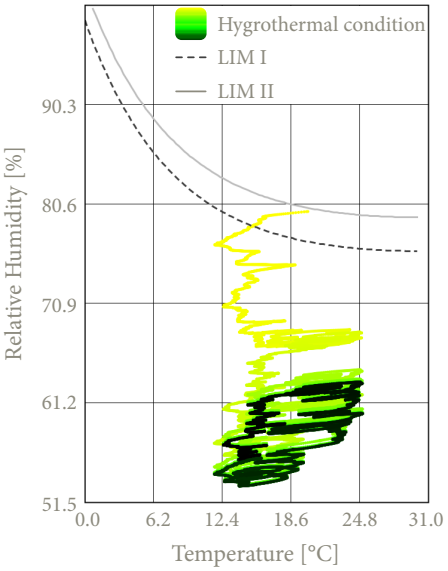

Figure A45, Isopleths flexible hemp

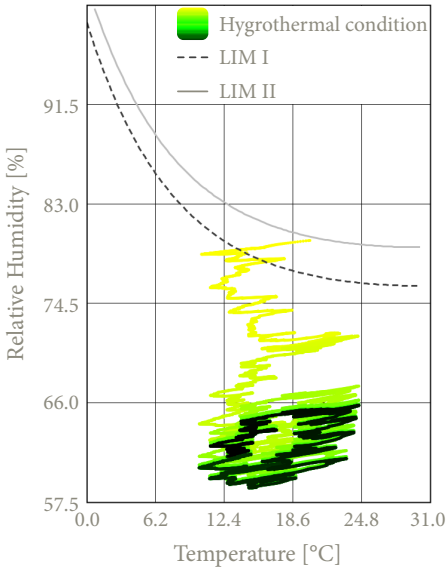

Figure A46, Isopleths hemp & transition frame

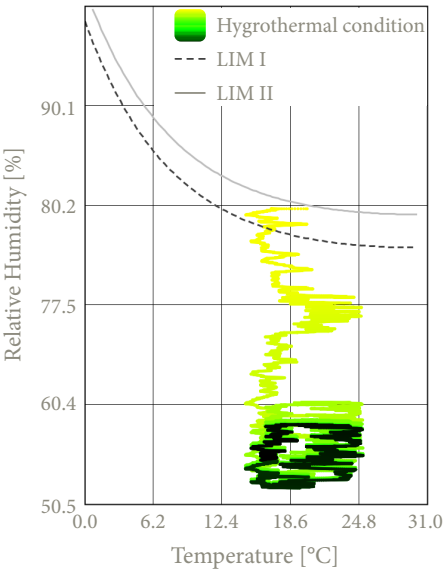

Figure A47, Isopleths transition frame & hemp

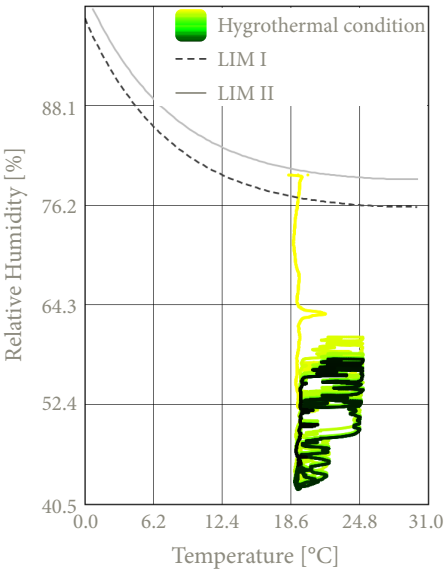

Figure A48, Isopleths biobased construction board

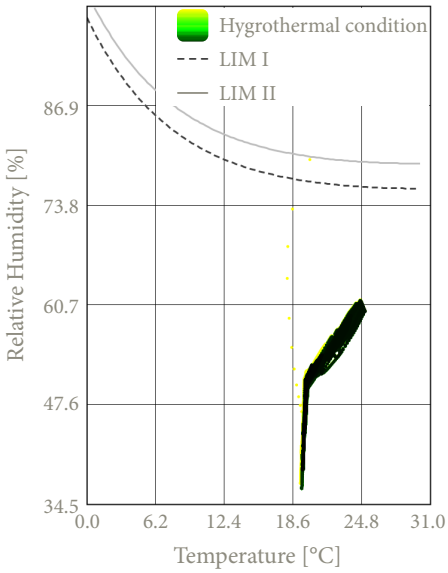

Figure A49, Isopleths clay plaster

Isopleths - H1

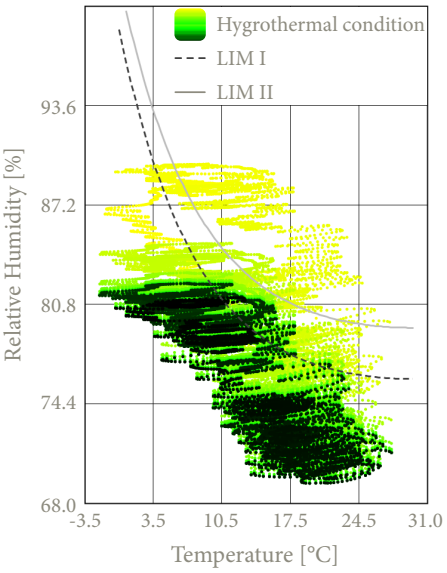

Figure A50, Isopleths wood fibre plate

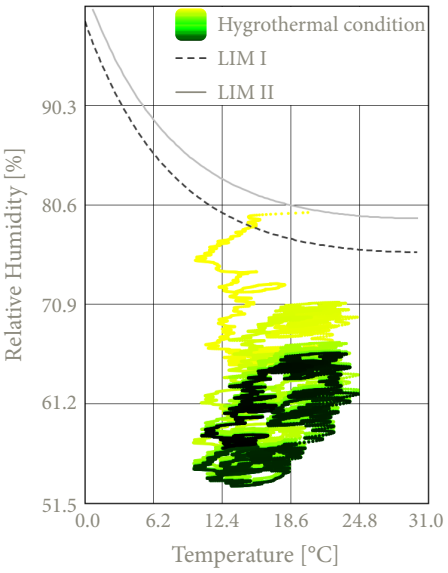

Figure A51, Isopleths flexible hemp

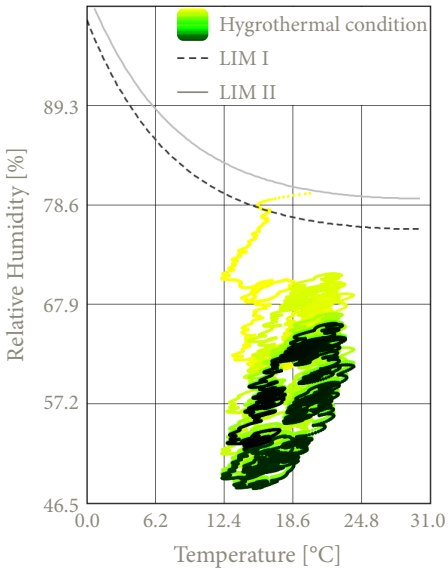

Figure A52, Isopleths hemp & transition frame

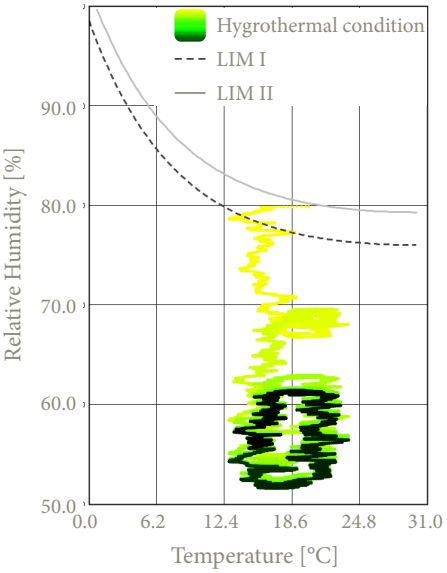

Figure A53, Isopleths transition frame & hemp

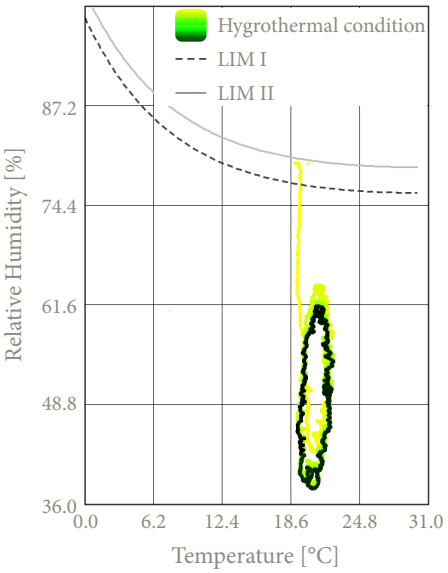

Figure A54, Isopleths biobased construction board

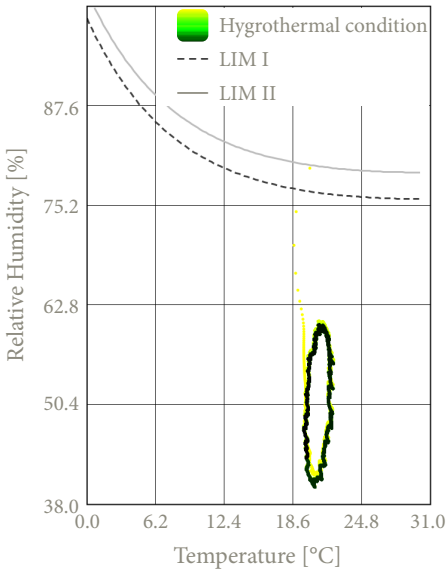

Figure A55, Isopleths clay plaster

Conclusion isoplteths

Based on the established and analysed isopleths of the various details within this construction **configuration**, it can be concluded that there is **no risk of mould growth** within the different material layers. All isopleths located behind the outer plaster layer remain **below** the critical threshold values **LIM I** and **LIM II**, indicating that the details meet the established criteria.

With regard to the isopleths of the **wood fibre plate** in each detail, it can be observed that the relative humidity exceeds the LIM I threshold at the beginning of the simulation. This trend can possibly be attributed to the initial conditions, where the initial moisture content in the wood fibre was approximately 80%. During the simulation, however, the relative humidity gradually decreases to below both LIM I and LIM II, indicating that moisture is being transported out of the material. Nevertheless, at the end of the simulation, the isopleths still slightly exceed the LIM I line. However, for the majority of the year, the isopleths remain below both LIM thresholds. The continuously decreasing trend and the fact that the isopleths are for the majority of the year below the thresholds, suggests that there is no long-term risk of mould development.

With respect to the isopleths of the **flexible hemp fibre**, as well as the t**ransition zones between the hemp fibre and the wooden construction frame**, the **biobased construction board**, and the **clay plaster**, the values remain well below both LIM threshold values. At the location of the hemp fibre and at the transition between the hemp fibre and the wooden frame, the isopleths show a slight upward trend. However, this increase gradually levels off across all three isopleths, with values remaining below the critical LIM thresholds.

In relation to the isopleths of the **biobased construction board**, it can be seen that they remain well below the LIM threshold values and continue to decrease further over the course of the ten years. A similar but smaller effect can be observed at the **clay plaster**.

In conclusion, it can be stated that this configuration poses no risk of mould growth and thus complies with the specified isopleth requirements. As such, the design complies with the required hygrothermal performance standards.

Surface condensation - V1, V2 & H1

The circle at each figure figures below, **figure 56**, **figure 58** and **figure 60**, show the coldest point of the interior surface at each detail in order to consider the f_{Rsi}. Below these graphs the corresponding surface temperature at this point is shown over a ten-year simulation below, **figure 57**, **figure 59** and **figure 61**.

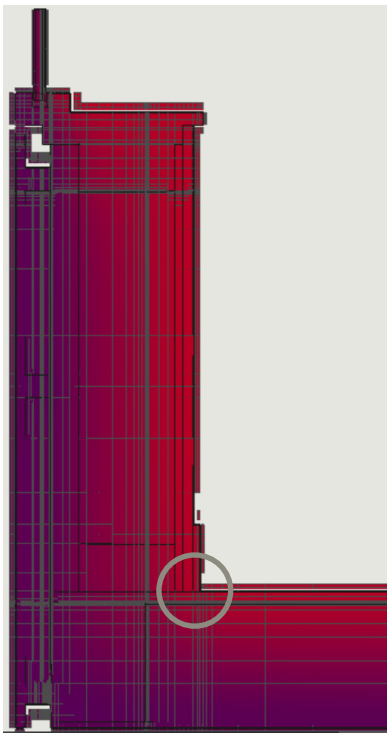

Figure A56, Highlight lowest point, V1

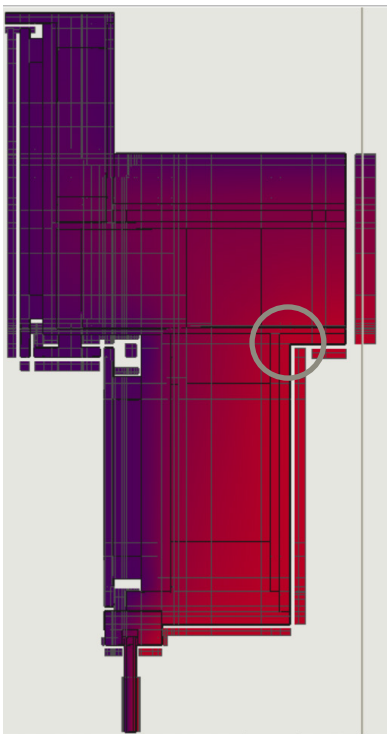

Figure A58, Highlight lowest point, V2

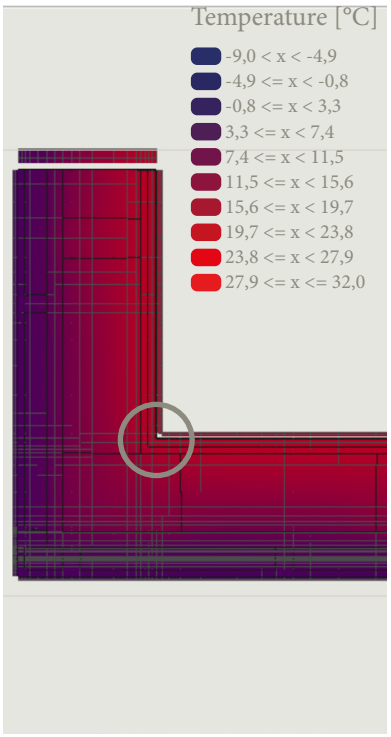

Figure A60, Highlight lowest point, H1

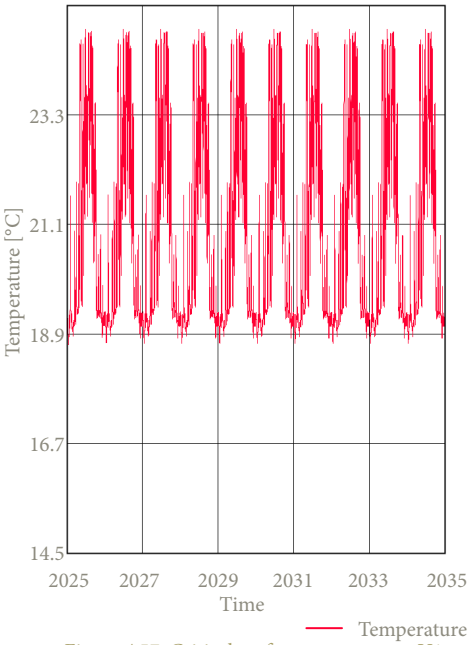

Figure A57, Critical surface temperature, V1

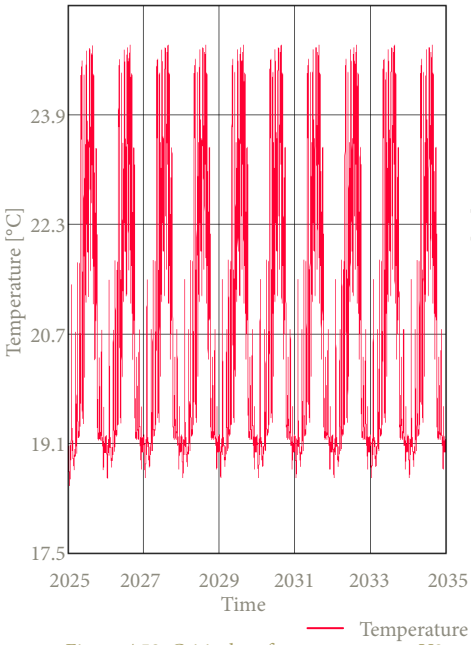

Figure A59, Critical surface temperature, V2

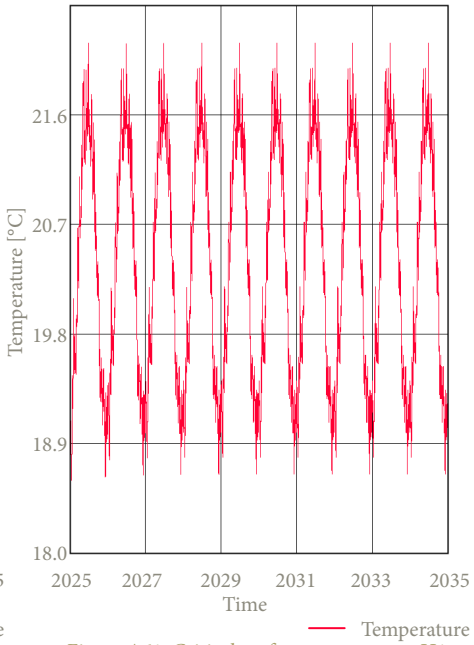

Figure A61, Critical surface temperature, H1

From this graph the lowest surface temperature of this detail is **17.49 °C**.

The resulting f_{Rsi} for this detail is **0.79** which exceeds the minimum requirement of 0.61. This indicates a negligible risk of mold growth.

From this graph the lowest surface temperature of this detail is **18.06 °C**.

The resulting f_{Rsi} for this detail is **0.84** which exceeds the minimum requirement of 0.61. This indicates a negligible risk of mold growth.

From this graph the lowest surface temperature of this detail is **18.59 °C**.

The resulting f_{Rsi} for this detail is **0.88** which exceeds the minimum requirement of 0.61. This indicates a negligible risk of mold growth.

F-factor - V1, V2 & H1

The resulting **f-factor** of **detail V1** is **0.91** for a temperature of **16.45 °C**. Next the resulting **f-factor** of **detail V2** is **0.93** for a temperature of **16.74 °C**. Lastly, the resulting **f-factor** of **detail H1** is **0.94** for a temperature of **16.99 °C**. This indicates a very limited thermal bridge is assessed within the details of this configuration.
Given that these values significantly all exceeds the required threshold of **0.65**, it can be concluded that the details within this configuration complies with the thermal performance requirements set by the Dutch Building Decree.

PSI-value - V1

Table A12, Calculation of the $Q_{ideal\ condition}$

$R_{construction,\ window}$ [(m²K)/W]	$A_{construction,\ window}$ [m²]	$R_{construction,\ wall}$ [(m²K)/W]	$A_{construction,\ wall}$ [m²]	$R_{construction,\ floor}$ [(m²K)/W]	$A_{construction,\ floor}$ [m²]
0.600	0.2425	5.218	1.298	4.648	0.717

The resulting $\mathbf{Q_{ideal\ condition}}$ is **14.592 W**

Q_{WUFI} represents the sum of all heat flows through the detail, resulting in a total heat flow of **15.953 W**.

These values give a **Ψ-value** of **0.079 W/(mK)** for **detail V1**, indicating that the detail can be characterised as a well-insulated building component.

PSI-value - V2

Table A13, Calculation of the $Q_{ideal\ condition}$

$R_{construction,\ window}$ [(m²K)/W]	$A_{construction,\ window}$ [m²]	$R_{construction,\ wall}$ [(m²K)/W]	$A_{construction,\ wall}$ [m²]	$R_{construction,\ roof}$ [(m²K)/W]	$A_{construction,\ roof}$ [m²]
0.600	0.2425	5.218	0.896	6.442	0.190

The resulting $\mathbf{Q_{ideal\ condition}}$ is **10.896 W**

Q_{WUFI} represents the sum of all heat flows through the detail, resulting in a total heat flow of **12.633 W**.

These values give a **Ψ-value** of **0.098 W/(mK)** for **detail V2**, indicating that the detail can be characterised as a well-insulated building component.

PSI-value - H1

Table A14, Calculation of the $Q_{ideal\ condition}$

$R_{construction,\ window}$ [(m²K)/W]	$A_{construction,\ window}$ [m²]	$R_{construction,\ wall}$ [(m²K)/W]	$A_{construction,\ wall}$ [m²]
0.600	0.2425	5.218	2.796

The resulting $\mathbf{Q_{ideal\ condition}}$ is **16.920 W**

Q_{WUFI} represents the sum of all heat flows through the detail, resulting in a total heat flow of **18.081 W**.

These values give a **Ψ-value** of **0.064 W/(mK)** for **detail H1**, indicating that the detail can be characterised as a well-insulated building component.

Assessment detail configuration

Important notes about the details

For the given configuration, **key considerations** are presented below in the form of bullet points. These points highlight specific aspects that need to be taken into account during detailing and construction.

- Place the flexible hemp between the studs of the wooden frame
- Finish the outside of the wooden frame with a pressure-resistant wood fibre insulation board.
- Finish the inside of the wooden frame with a pressure-resistant wood fibre board to allow for fixings.
- Attach the water-resistant barrier of the window frame to the timber structural frame.
- The wooden lintel needs to have 200 mm bearing.
- The screws of the wood fibre must reach the center of the timber frame to ensure secure attachment.
- Use stainless steel screws with 2 times the thickness of the battens to sufficient load-bearing capacity.
- Stainless steel nails must be at least 2.5 times the thickness of the cladding.
- The stainless steel nails must be placed 40 mm from the outer edge of the cladding.
- Ensure 10 mm gaps for ventilation both between cladding boards and at the window frame.
- Use a clay base plate to provide a correct underlayment for the clay plaster.
- Use a jute reinforcement mesh between the rough and finishing clay plaster to prevent cracking.

Assessment of the configuration

Additionally, the configuration is evaluated based on the following criteria:

1. **Weight**: The total mass per unit area of the wall construction.
2. **Construction time**: The time required for assembling the construction.
3. **Resistance Construction-value:** The combined thermal resistance of all layers in the construction.
4. **Phase shift**: The heat transfer delay of the structure.

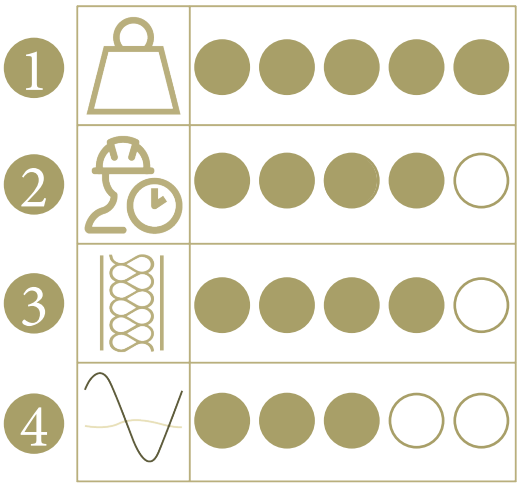

Axonometric view of the detail configuration

In addition to the presented details, an **axonometric view** of the respective detail is also shown. This is presented in the figure below, **figure 62**, and is intended to provide more clarity and insight into **detail V1, detail V2,** and **detail H1**.

Figure A62, Axonometric view of detail configuration 3

Detail configuration 4 - cork insulation with cork façade

The fourth detail configuration consists of cork insulation boards placed between the studs of the timber construction frame. In this configuration, the timber frame is finished with a pressure-resistant wood fibre board that protects the structure against moisture penetration. This board also enables the attachment of the cork cladding board, which is bonded using a cork mortar to a biobased, diffusion-open construction board with water-repellent properties. This board is attached with vertical spruce battens to the wood fibre plate On the interior side, the timber construction frame is finished with a biobased, diffusion-open construction board to which a clay board is screwed. A clay plaster can then be applied to this board, consisting of a rough layer and a finishing layer.

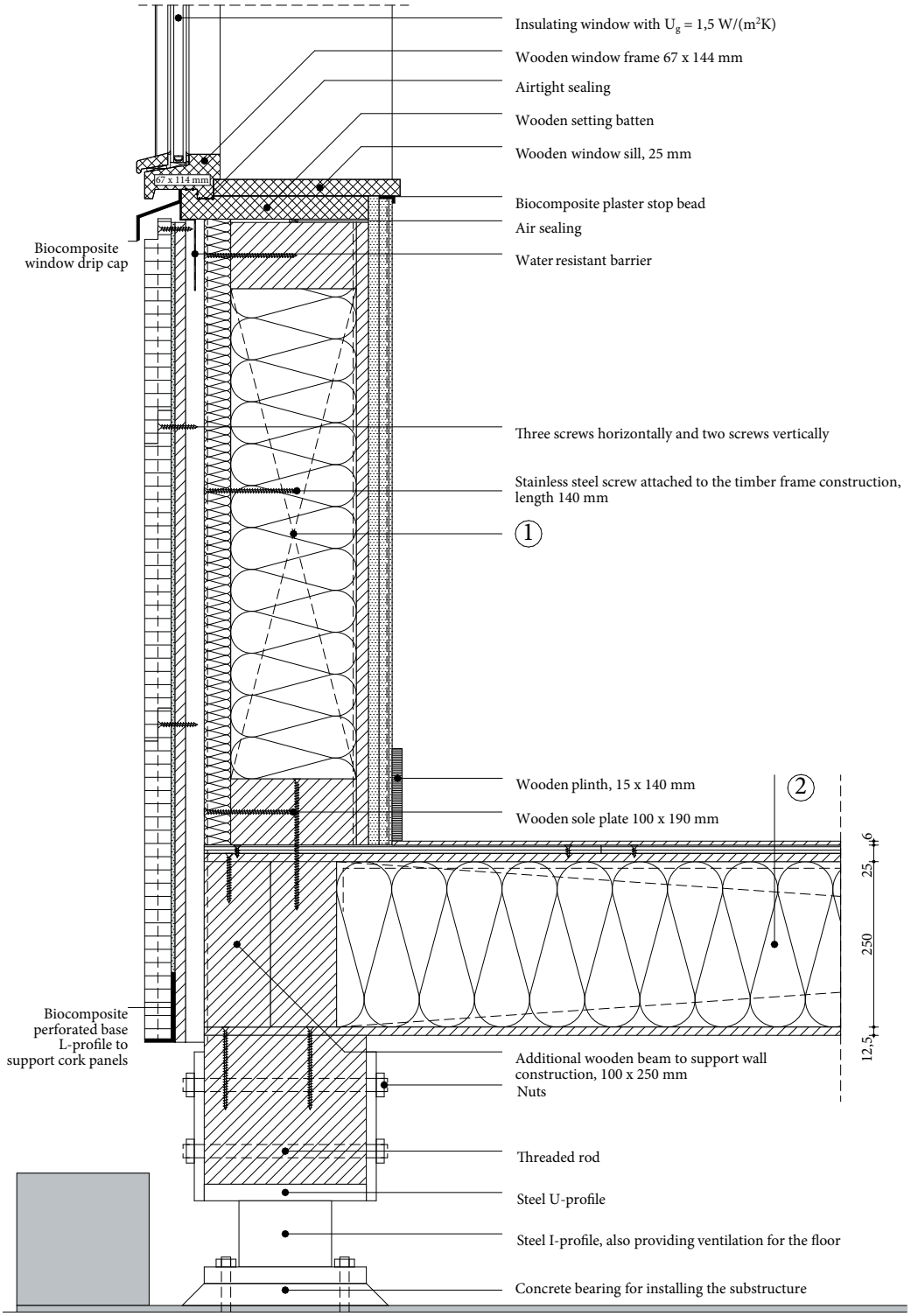

Figure A63, 1:10 detail of V1, configuration 4, own illustration

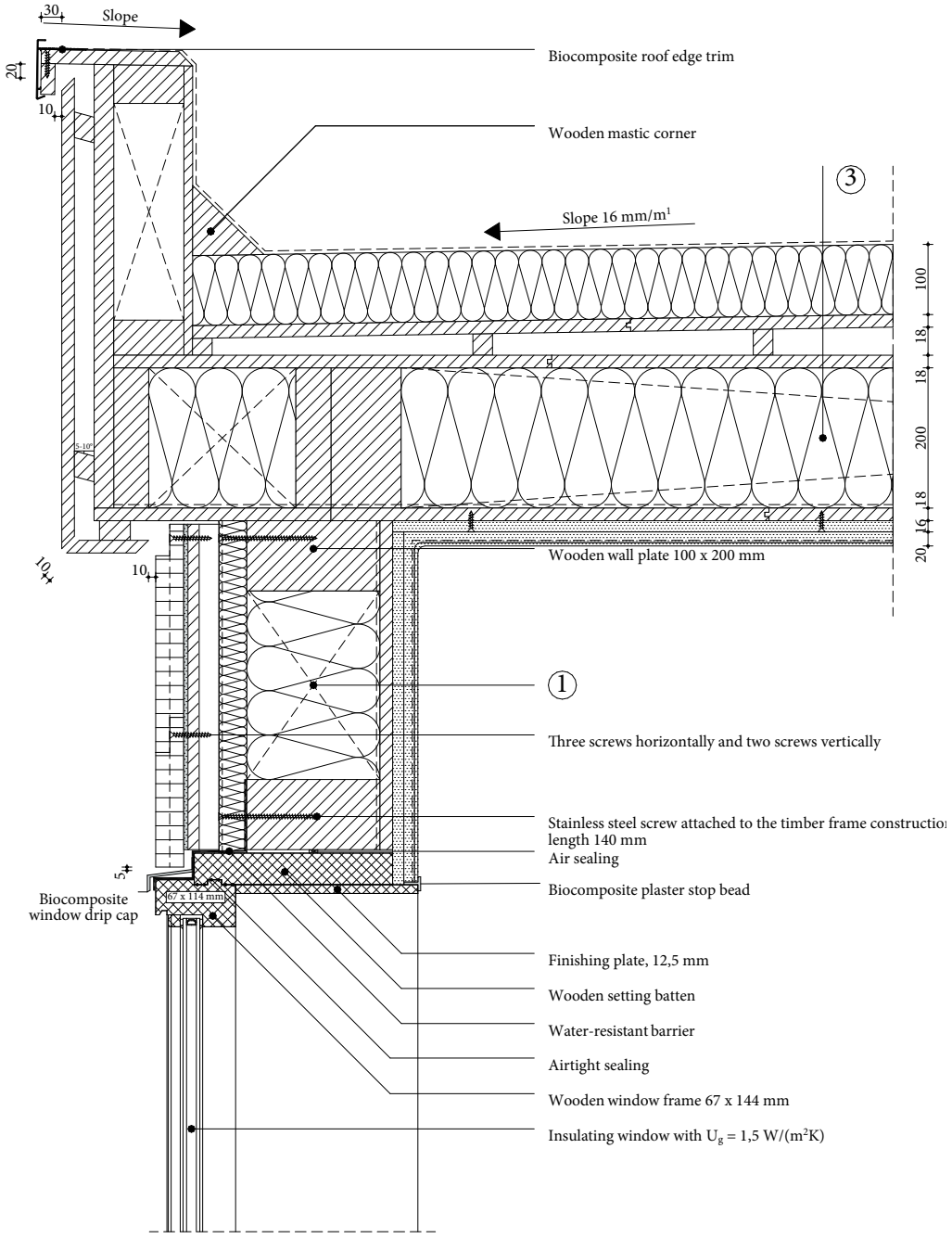

Figure A64, 1:10 detail of V2, configuration 4, own illustration

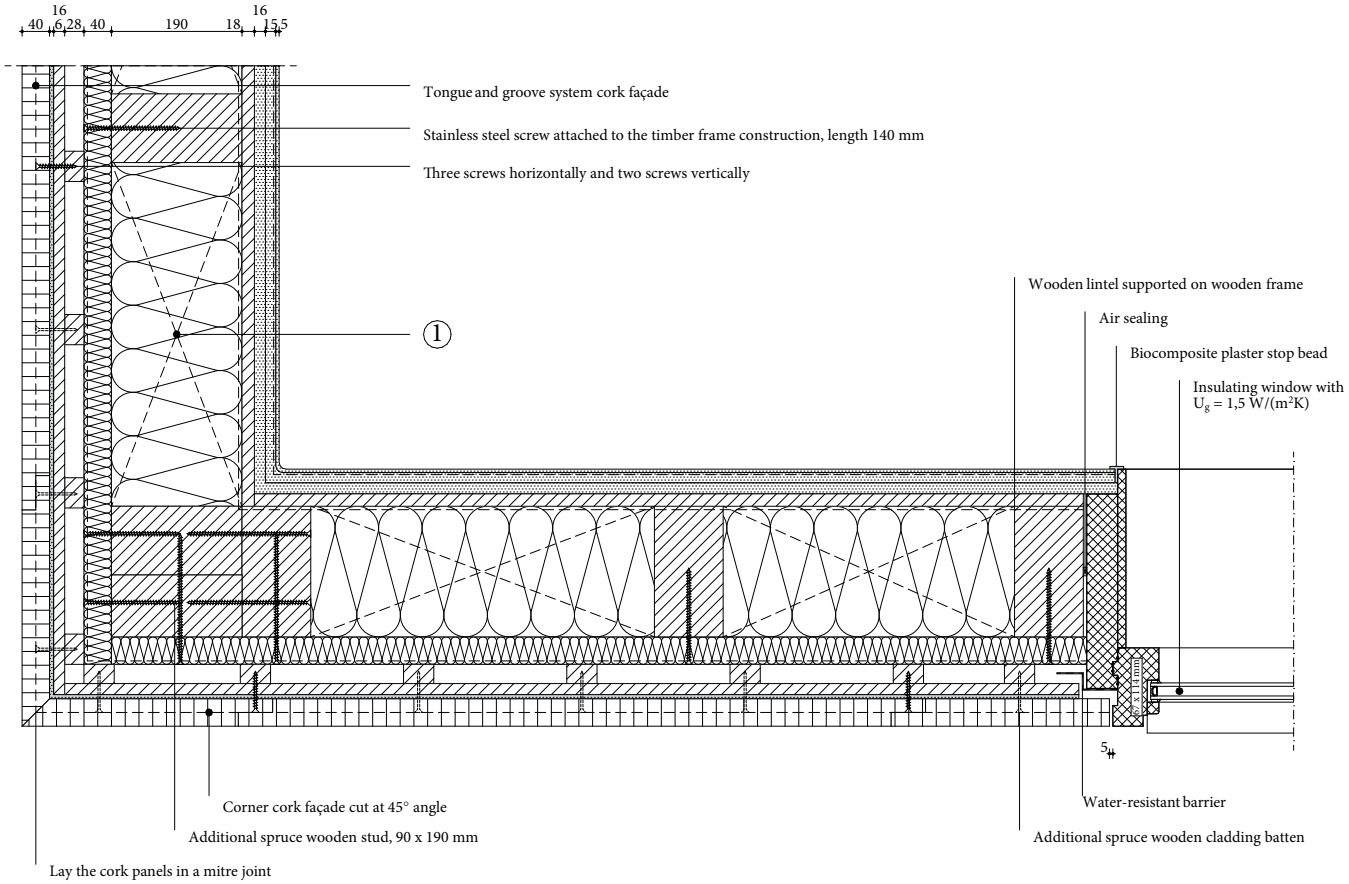

Figure A65, 1:10 detail of H1, configuration 4, own illustration

❶ Wall construction build-up, RC-value: 4.98 (m²K)/W

- Tongue and groove cork cladding panels (λ ≤ 0.043 W/mK), 40 mm;
- Cork mortar, 6mm;
- Biobased diffusion open construction board, 16mm;
- Vertical spruce cladding batten forming ventilated cavity, 28 x 44 mm, center-to-center 237 mm;
- Water resistant vapour-permeable membrane;
- Pressure-resistant woodfibre insulation plate (λ ≤ 0.042 W/mK), 40 mm;
- Timber frame construction, 100 x 190 mm, center-to-center 600 mm;
- Expanded insulation corkboard, placed between construction (λ ≤ 0.039 W/mK), 190 mm;
- Biobased construction board, 18 mm;
- Clay base plate, 16 mm;
- Rough base clay plaster, 15 mm;
- Jute reinforcement mesh;
- Finishing clay plaster, 5 mm.

❷ Floor construction build-up, RC-value: 4.65 (m²K)/W

- Finishing board, 6 mm;
- Biobased wooden construction board, 12.5 mm;
- Biobased wooden construction board, perpendicular on the other plate, 12.5 mm;
- Vapour-retarding and airtight membrane with a variable vapour diffusion resistanance;
- Flexible hemp fiber insulation placed between construction (λ ≤ 0.043 W/(mK), 250 mm;
- Wooden beams 100 x 250 mm, center-to-center 600 mm;
- Biobased wooden construction board, 12.5 mm.

❸ Roof construction build-up, RC-value: 6.71 (m²K)/W

- EPDM glued on underlayment to prevent roof covering from lifting;
- Pressure-resistant woodfibre insulation plate (λ ≤ 0.042 W/(mK), 100 mm;
- Biobased wooden construction board, 18 mm;
- Sloped wooden battens for drainage at an angle of 16 mm/m^1, 28 x 24 mm;
- Biobased wooden construction board, 18 mm;
- Flexible hemp fiber insulation placed between construction (λ ≤ 0.043 W/(mK), 200 mm;
- Wooden beams 100 x 200 mm, center-to-center 600 mm;
- Vapour-retarding and airtight membrane with a variable vapour diffusion resistanance;
- Biobased wooden construction board, 18 mm;
- Clay base plate, 16 mm;
- Rough base clay plaster, 15 mm;
- Jute reinforcement mesh;
- Finishing clay plaster, 5 mm.

U_g = 1.50 W/(m²K)

U_w = 1.76 W/(m²K)

f-factor ≥ 0.65

Ψ_{V1}: 0.057 W/(mK) Ψ_{V2}: 0.085 W/(mK) Ψ_{H1}: 0.085 W/(mK)

Isopleths: no risk of mould $f_{R,si} > f_{R,si,\,max}$; no risk of mould

Phase shift of the wall construction: 10.8 h

Density of the wall construction 123 kg/m³

Calculation RC-value wall construction build-up

❶ Wall construction build-up, RC-value: 4.98 (m²K)/W

Table A15, Calculation of the RC-value of the wall construction build-up

Material	Thickness [m]	Thermal conductivity [W/(mK)]	Thermal resistance [W/(m²K)]
Tongue and groove cork cladding panels	0,040	0,043	0,930
Cork mortar	0,006	0,250	0,024
Biobased diffusion open construction board	0,016	0,090	0,178
Ventilated cavity with vertical wooden cladding batten, center-to-center 237 mm	0,028	0,304	0,009
Pressure-resistant woodfibre insulation plate	0,040	0,042	0,952
Timber frame construction, with expanded insulation corkboard	0,190	0,052	3,654
Biobased construction board	0,018	0,120	0,150
Clay base plate	0,016	0,470	0,034
Clay plaster	0,020	0,910	0,022

Table A16, Calculation of the equivalent thermal conductivity of the individual layers in the relevant build-up

	Layer 1		Layer 2	
Material	Area [m²]	Thermal conductivity [W/(mK)]	Area [m²]	Thermal conductivity [W/(mK)]
Ventilated cavity with vertical wooden cladding batten, center-to-center 237 mm	0,0012	0,130	0,0066	0,337
Timber frame construction, with expanded insulation corkboard	0,114	0,039	0,019	0,130

Density mass per unit area of the wall construction

Table A17, Calculation of the density mass per unit area

Material	Thickness [m]	Density [kg/m³]
Tongue and groove cork cladding panels	0,040	140
Cork mortar	0,006	1000
Biobased diffusion open construction board	0,016	565
Ventilated cavity with vertical wooden cladding batten, center-to-center 237 mm	0,020	35
Pressure-resistant woodfibre insulation plate	0,040	140
Timber frame construction, with expanded insulation corkboard	0,190	169
Biobased construction board	0,018	621
Clay base plate	0,016	1300
Clay plaster	0,020	1600

By using the previously presented formula a **m'-value** of **123.03 kg/m²** can be given for the **fourth detail configuration**.

Phase-shift

Table A18, Calculation of the phase shift

Material	Thickness [m]	Thermal conductivity [W/(mK)]	Density [kg/m³]	Specific heat capacity [J/(kgK)]
Timber frame construction, with expanded insulation corkboard	0,190	0,052	169	1857

By using the presented phase shift formula, the resulting **φ-value** for **the fourth configuration** is **10.8 h.**

Geometry WUFI

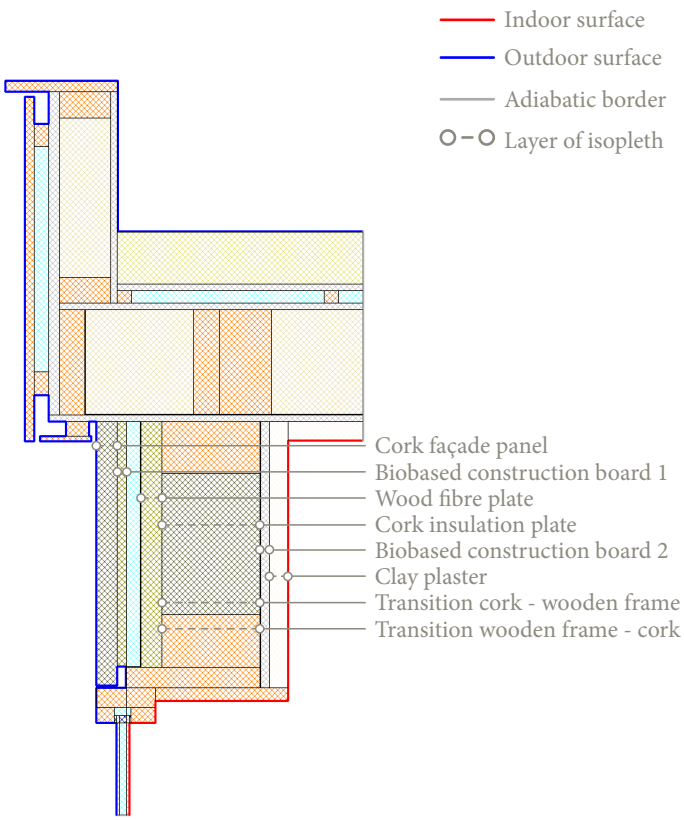

Figure A67, geometry detail V2 including location isopleths

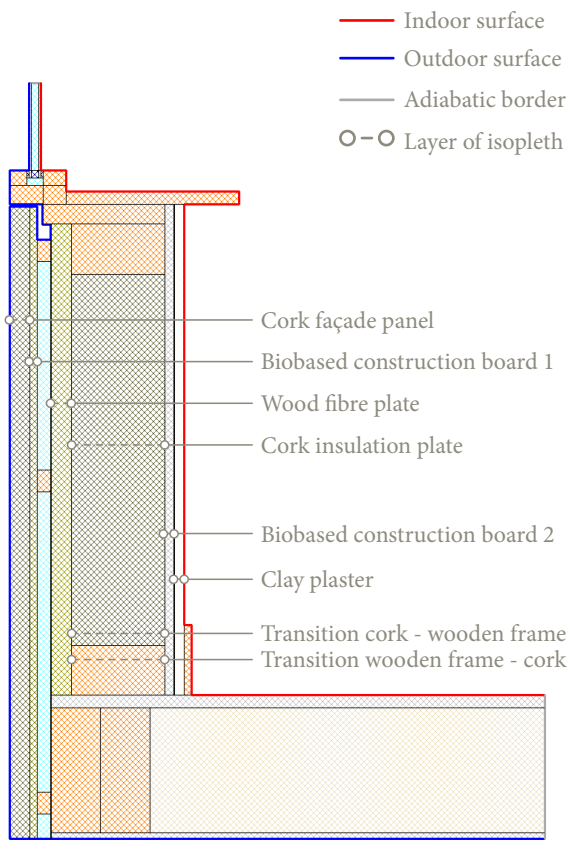

Figure A68, geometry detail V1 including location isopleths

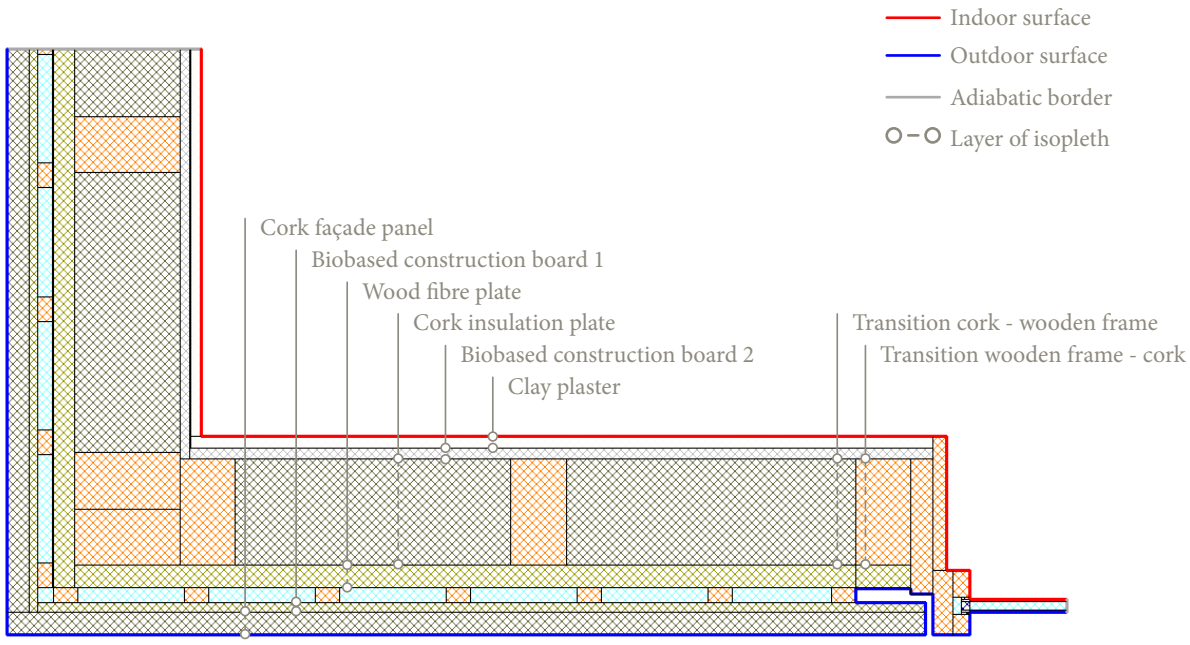

Figure A66, geometry detail H1including location isopleths

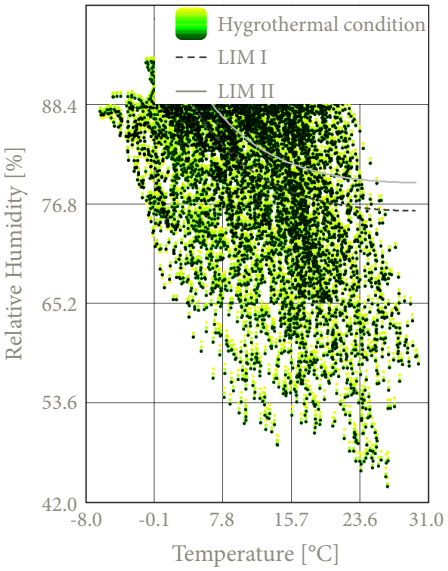

Figure A69, Isopleths cork façade panel

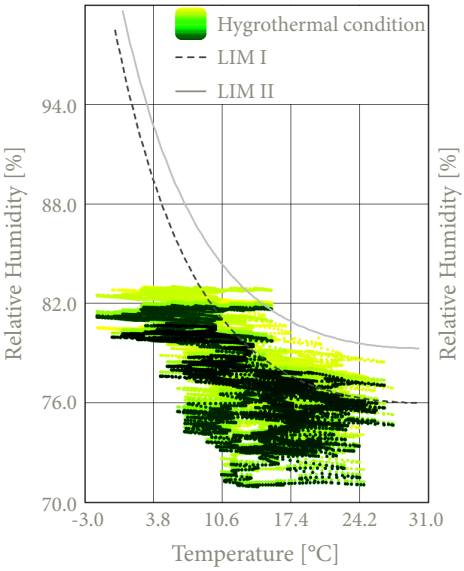

Figure A70, Isopleths biobased construction board 1

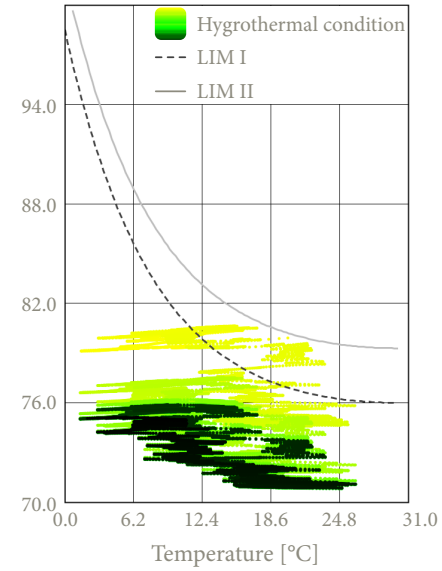

Figure A71, Isopleths wood fibre plate

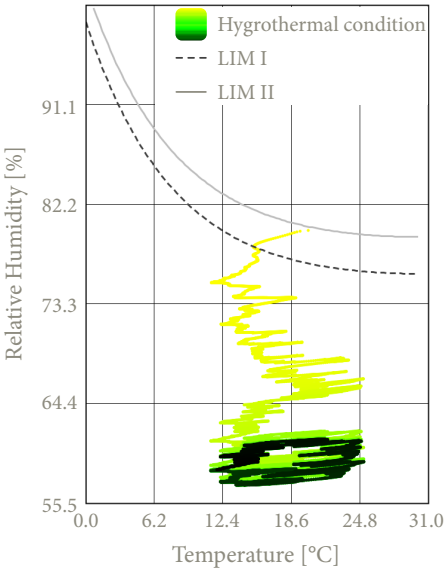

Figure A72, Isopleths cork insulation plate

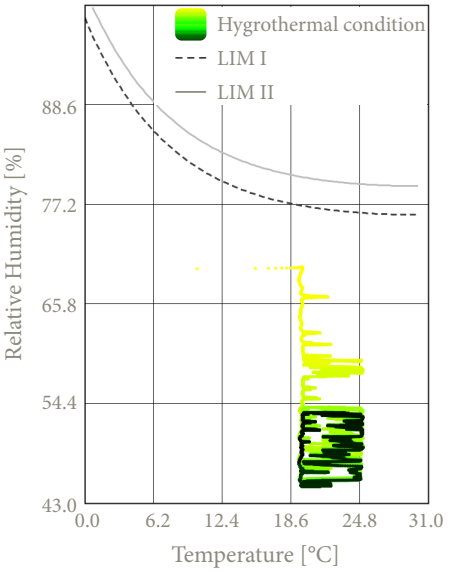

Figure A73, Isopleths biobased construction board 2

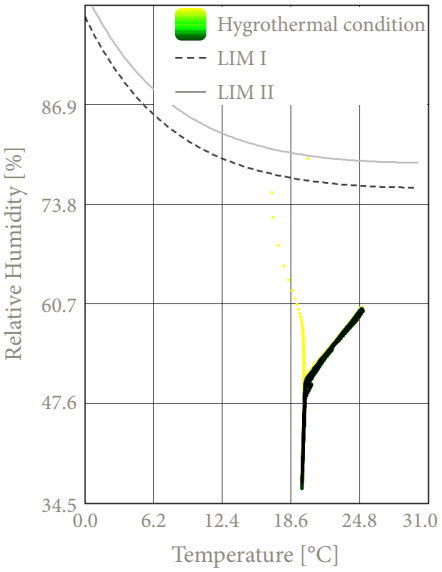

Figure A74, Clay plaster

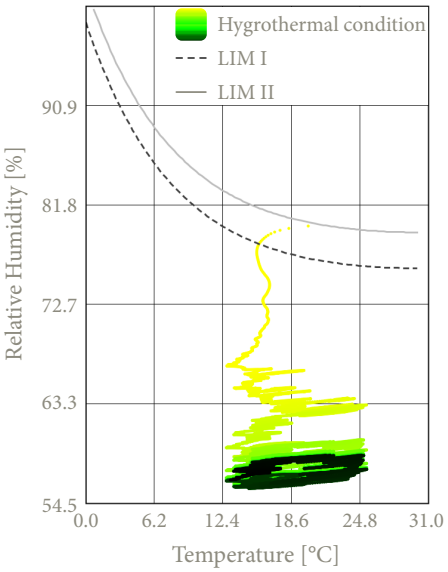

Figure A75, Isopleths transition cork & frame

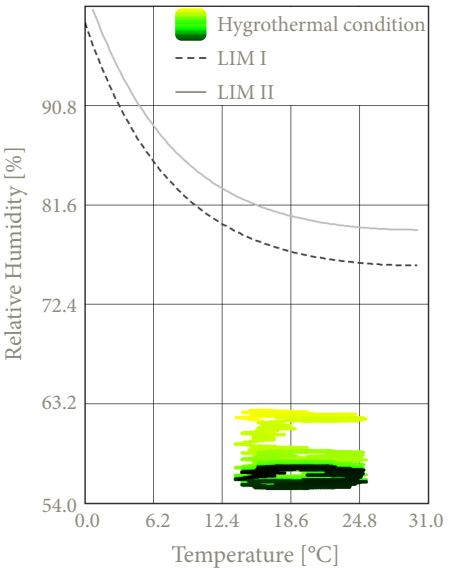

Figure A76, Isopleths transition frame & cork

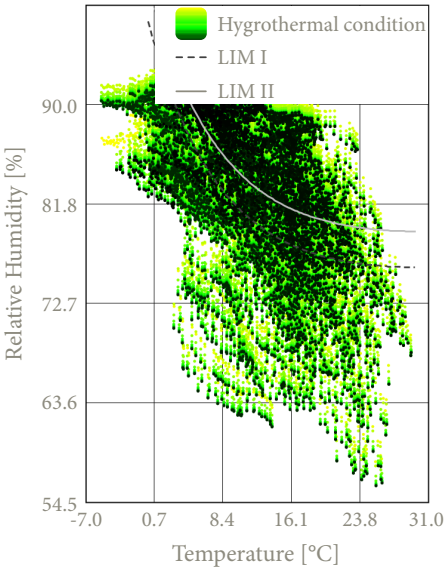

Figure A77, Isopleths cork façade panel

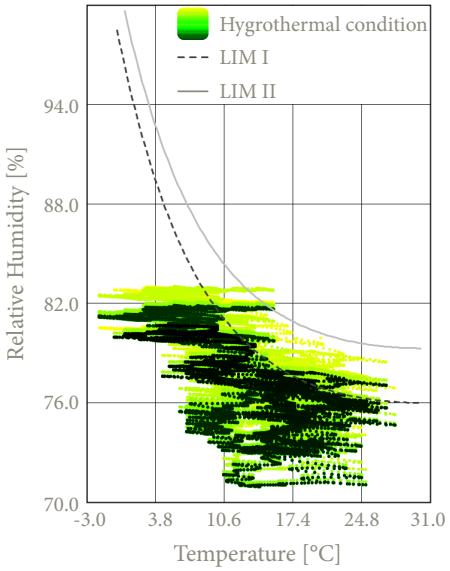

Figure A78, Isopleths biobased construction board 1

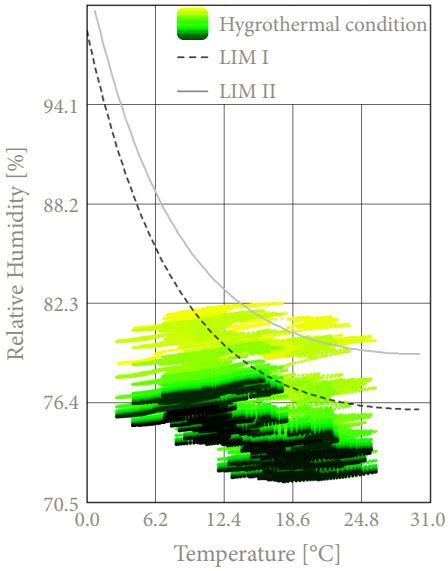

Figure A79, Isopleths wood fibre plate

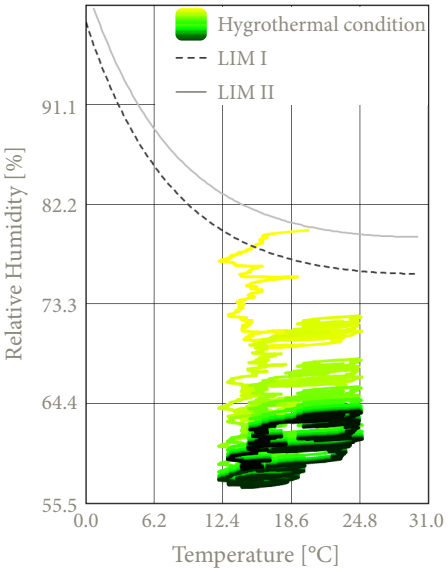

Figure A80, Isopleths cork insulation plate

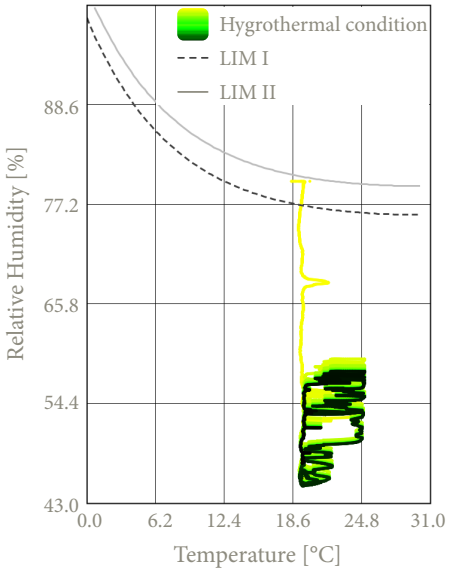

Figure A81, Isopleths biobased construction board 2

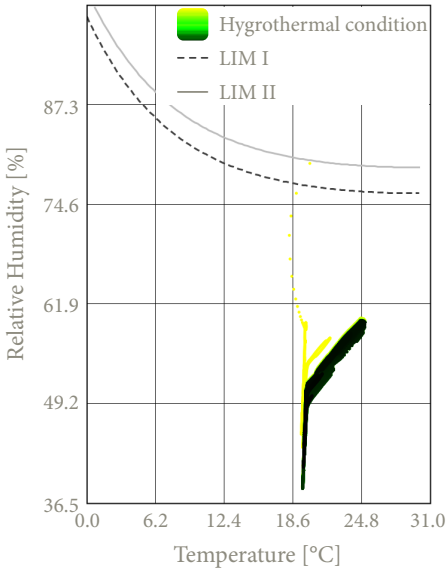

Figure A82, Clay plaster

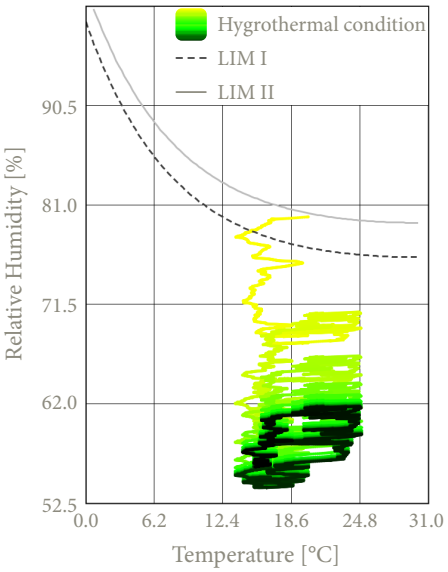

Figure A83, Isopleths transition cork & frame

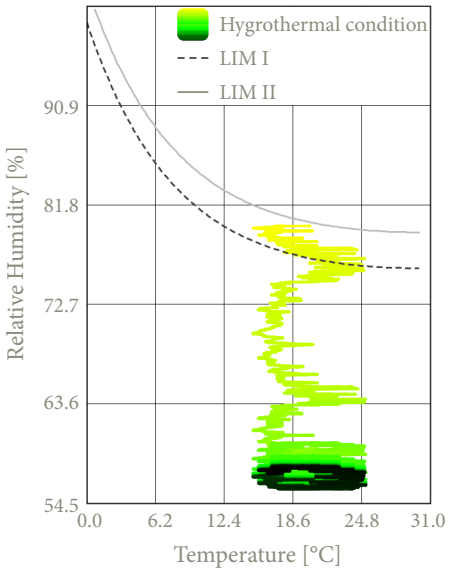

Figure A84, Isopleths transition frame & cork

Isopleths - H1

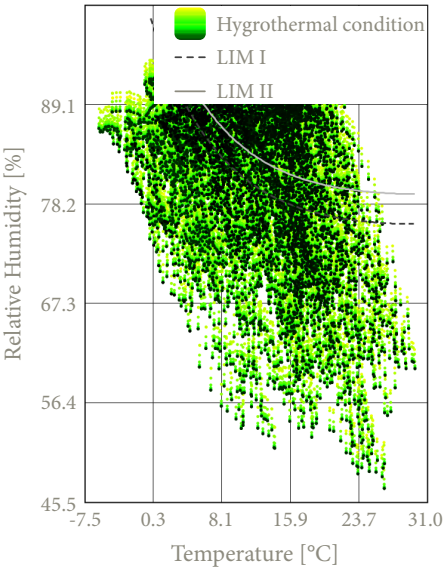

Figure A85, Isopleths cork façade panel

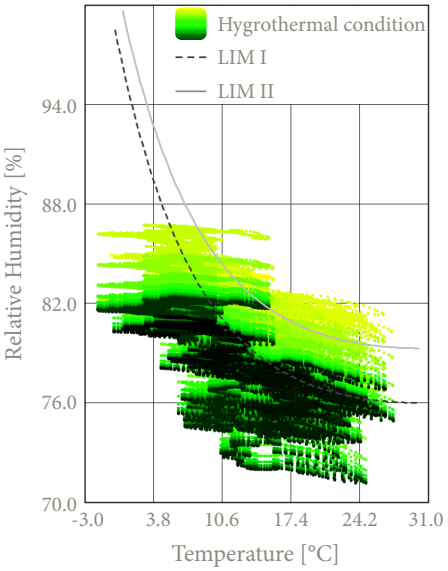

Figure A86, Isopleths biobased construction board 1

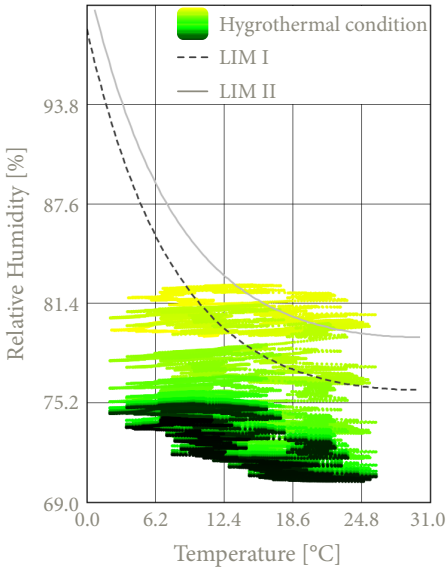

Figure A87, Isopleths wood fibre plate

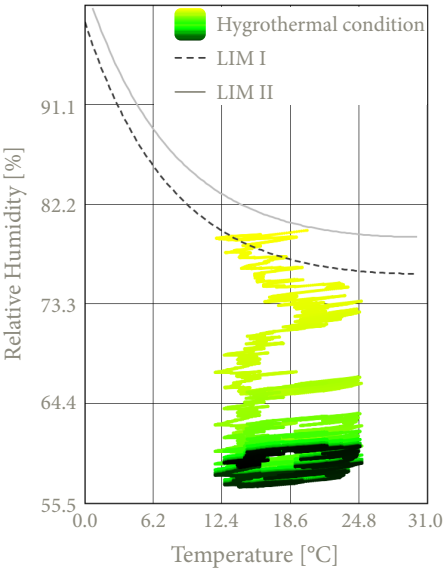

Figure A88, Isopleths cork insulation plate

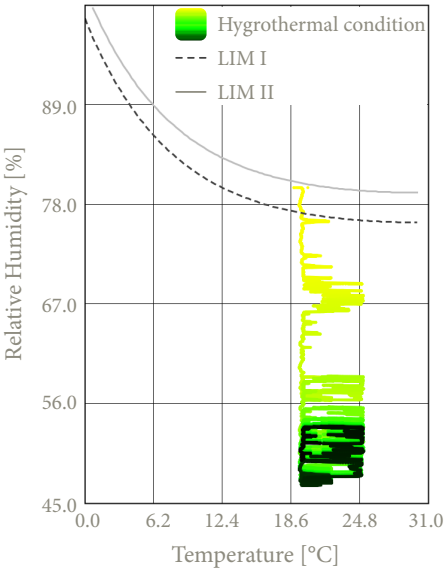

Figure A89, Isopleths biobased construction board 2

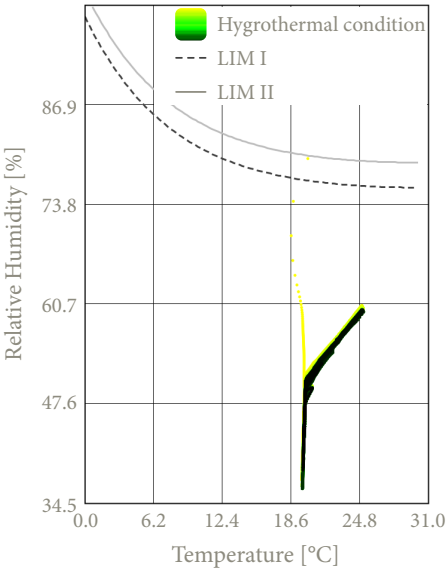

Figure A90, Clay plaster

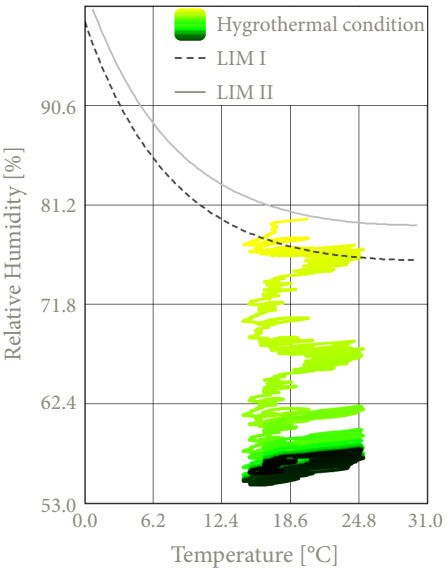

Figure A91, Isopleths transition cork & frame

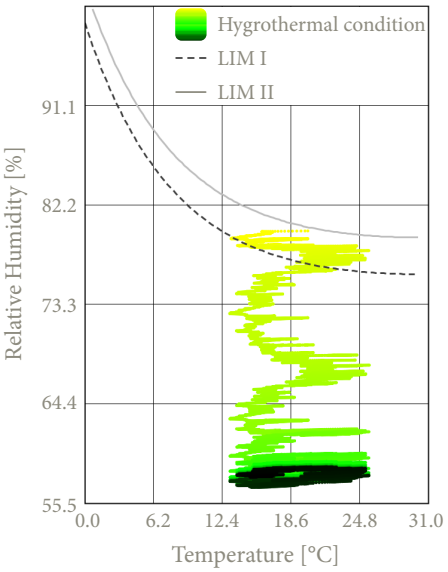

Figure A92, Isopleths transition frame & cork

Conclusion isoplteths

Based on the established and analysed isopleths of the various details within this construction **configuration**, it can be concluded that there is **no risk of mould growth** within the different material layers. All isopleths located behind the cork insulation plate remain mostly below the critical threshold values **LIM I** and **LIM II**, indicating that the details meet the established criteria.

With regards to the **cork façade panel**, it can be observed that the isopleths mostly exceed the LIM threshold values. However, (Hon, 2024) states that cork did not show any clear signs of degradation or mould growth even after four weeks of exposure to high humidity levels during which the material was placed inside a water-filled desiccator. Moreover, the study indicates that other literature reaches similar conclusions regarding the resistance to mould growth of cork. Since cork is a porous material it also is capable of absorbing fluctuations in relative humidity, further indicating good moisture buffering capacity. However, to be able to state with certainty that no mould growth occurs in cork used as an exterior panel material, additional research is required.

When examining the isopleths of the **outside biobased construction board**, it can be seen that the relative humidity exceeds LIM I and occasionally LIM II at the beginning of the simulation. This trend can possibly be attributed to the initial condition, where the initial moisture content in the construction board was approximately 80%. During the simulation, however, the relative humidity gradually decreases to below both LIM I and LIM II, indicating that moisture is being transported out of the material. Nevertheless, at the end of the simulation the isopleths still slightly exceed the LIM I line. However, for the majority of the year the isopleths remain below both LIM thresholds. The continuously decreasing trend and the fact that the isopleths are for the majority of the year below the thresholds suggest that there is no long-term risk of mould development.

With regard to the isopleths of the **wood fibre plate** in each detail, it can be observed that the same starting relative humidity also negatively affects the isopleths and cause the isopleths to exceed the LIM-thresholds. Over time, a downward trend in the isopleths is also visible in this material, indicating that no mould formation occurs in this layer. In contrast to the other wood fibre plates in the previous configurations, this build-up shows a decreasing trend instead of an increasing one. This suggests that this configuration performs better for the wood fibre plate than the previous configurations.

With regard to the isopleths of the **cork insulation plate**, as well as the **transition zones between the cork and the wooden construction frame**, the **inside biobased construction board**, and the **clay plaster**, the values remain well below both LIM threshold values. A downward trend in the isopleths is also visible for these layers of material.

In conclusion, it can be stated that this configuration poses no risk of mould growth and thus complies with the specified isopleth requirements. However, in order to fully confirm this, further research is needed regarding the cork panel used on the exterior. As such, the design complies with the required hygrothermal performance standards.

Surface condensation - V1, V2 & H1

The circle at each figure figures below, **figure 93**, **figure 95** and **figure 97**, show the coldest point of the interior surface at each detail in order to consider the f_{Rsi}. Below these graphs the corresponding surface temperature at this point is shown over a ten-year simulation below, **figure 94**, **figure 96** and **figure 98**.

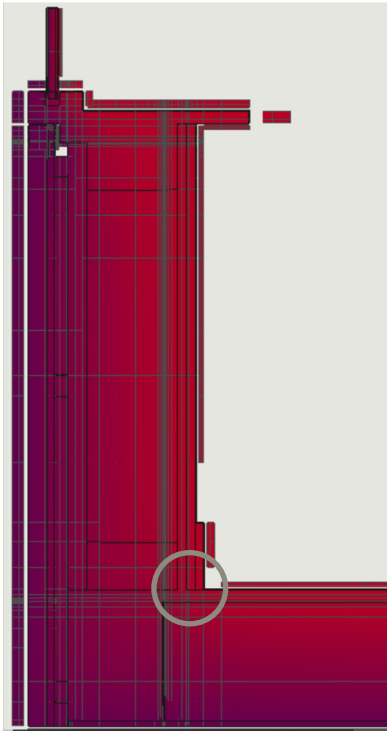

Figure A93, Highlight lowest point, V1

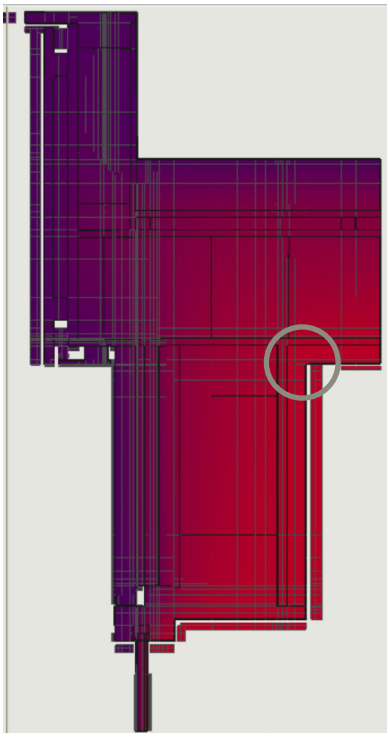

Figure A95, Highlight lowest point, V2

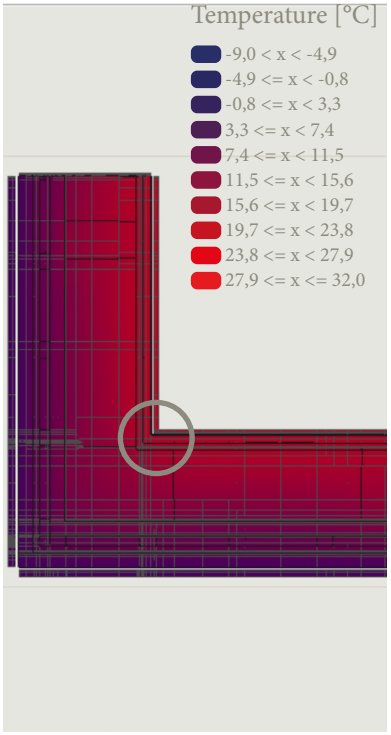

Figure A97, Highlight lowest point, H1

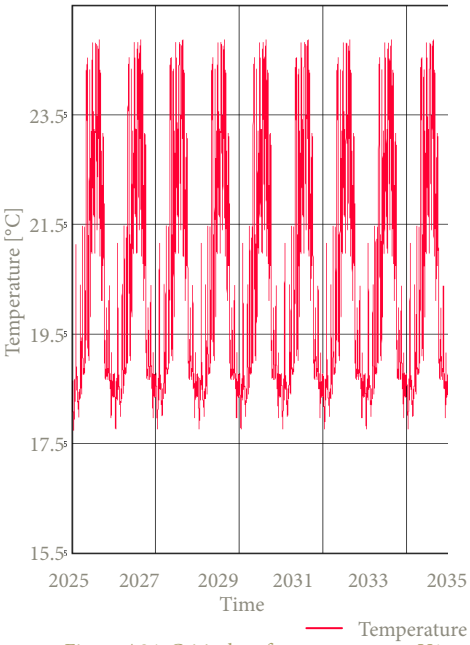

Figure A94, Critical surface temperature, V1

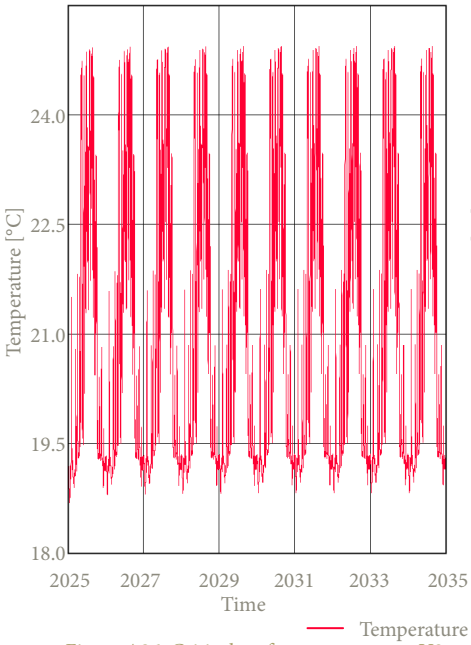

Figure A96, Critical surface temperature, V2

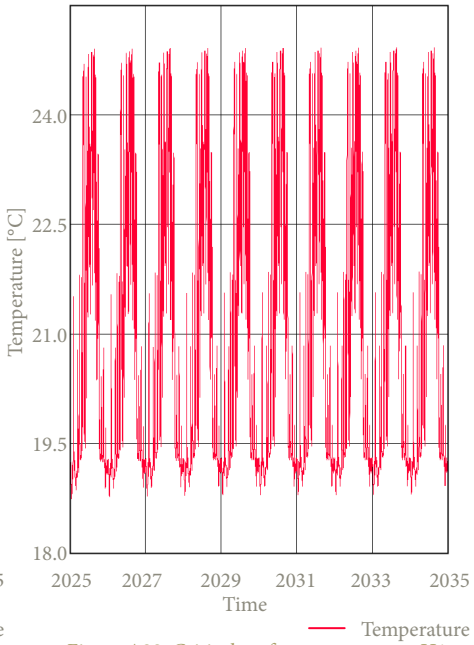

Figure A98, Critical surface temperature, H1

From this graph the lowest surface temperature of this detail is **16.02 °C**.

The resulting f_{Rsi} for this detail is **0.67** which exceeds the minimum requirement of 0.61. This indicates a negligible risk of surface condensation.

From this graph the lowest surface temperature of this detail is **18.69 °C**.

The resulting f_{Rsi} for this detail is **0.88** which exceeds the minimum requirement of 0.61. This indicates a negligible risk of surface condensation.

From this graph the lowest surface temperature of this detail is **18.54 °C**.

The resulting f_{Rsi} for this detail is **0.88** which exceeds the minimum requirement of 0.61. This indicates a negligible risk of surface condensation.

F-factor - V1, V2 & H1

The resulting **f-factor** of **detail V1** is **0.90** for a temperature of **16.26 °C**. Next the resulting **f-factor** of **detail V2** is **0.94** for a temperature of **17.09 °C**. Lastly, the resulting **f-factor** of **detail H1** is **0.94** for a temperature of **17.07 °C**. This indicates a very limited thermal bridge is assessed within the details of this configuration.
Given that these values significantly all exceeds the required threshold of **0.65**, it can be concluded that the details within this configuration complies with the thermal performance requirements set by the Dutch Building Decree.

PSI-value - V1

Table A19, Calculation of the $Q_{ideal\ condition}$

$R_{construction,\ window}$ [(m²K)/W]	$A_{construction,\ window}$ [m²]	$R_{construction,\ wall}$ [(m²K)/W]	$A_{construction,\ wall}$ [m²]	$R_{construction,\ floor}$ [(m²K)/W]	$A_{construction,\ floor}$ [m²]
0.600	0.2425	4.982	1.002	4.648	0.744

The resulting $\mathbf{Q_{ideal\ condition}}$ is **13.777 W**

Q_{WUFI} represents the sum of all heat flows through the detail, resulting in a total heat flow of **14.815 W**.

These values give a **Ψ-value** of **0.057 W/(mK)** for **detail V1**, indicating that the detail can be characterised as a well-insulated building component.

PSI-value - V2

Table A20, Calculation of the $Q_{ideal\ condition}$

$R_{construction,\ window}$ [(m²K)/W]	$A_{construction,\ window}$ [m²]	$R_{construction,\ wall}$ [(m²K)/W]	$A_{construction,\ wall}$ [m²]	$R_{construction,\ roof}$ [(m²K)/W]	$A_{construction,\ roof}$ [m²]
0.600	0.2425	4.982	0.923	6.442	0.171

The resulting $\mathbf{Q_{ideal\ condition}}$ is **11.087 W**

Q_{WUFI} represents the sum of all heat flows through the detail, resulting in a total heat flow of **12.626 W**.

These values give a **Ψ-value** of **0.085 W/(mK)** for **detail V2**, indicating that the detail can be characterised as a well-insulated building component.

PSI-value - H1

Table A21, Calculation of the $Q_{ideal\ condition}$

$R_{construction,\ window}$ [(m²K)/W]	$A_{construction,\ window}$ [m²]	$R_{construction,\ wall}$ [(m²K)/W]	$A_{construction,\ wall}$ [m²]
0.600	0.2425	4.982	2.462

The resulting $\mathbf{Q_{ideal\ condition}}$ is **16.170 W**

Q_{WUFI} represents the sum of all heat flows through the detail, resulting in a total heat flow of **17.712 W**.

These values give a **Ψ-value** of **0.085 W/(mK)** for **detail H1**, indicating that the detail can be characterised as a well-insulated building component.

Assessment detail configuration

Important notes about the details

For the given configuration, **key considerations** are presented below in the form of bullet points. These points highlight specific aspects that need to be taken into account during detailing and construction.

- Place the cork insulation board between the studs of the wooden frame.
- Finish the outside of the wooden frame with a pressure-resistant wood fibre insulation board.
- Finish the inside of the wooden frame with a pressure-resistant wood fibre board to allow for fixings.
- Attach the water-resistant barrier of the window frame to the timber structural frame.
- Apply a water-resistant, vapour-permeable membrane over the wood fibre insulation board.
- Apply vertical battens with 237 mm center-to-center spacing to attach the cork facade cladding.
- Apply a diffusion-open construction board with water-resistant properties onto the battens, over which cork mortar can be applied.
- Fix the cork façade panels using both 6mm cork mortar adhesive and use 3 screws horizontally and 2 vertically to mechanical fasten the cork facade.
- The wooden lintel must have proper bearing on the wooden frame.
- The screws of the wood fibre must reach the center of the timber frame to ensure secure attachment.
- Use stainless steel screws with twice the thickness of the battens to sufficient load-bearing capacity.
- Ensure 5 mm ventilation gaps both between cork panels and at the window frame.
- Use a clay base plate to provide a correct underlayment for the clay plaster.
- Use a jute reinforcement mesh between the rough and finishing clay plaster to prevent cracking.

Assessment of the configuration

Additionally, the configuration is evaluated based on the following criteria:

1. **Weight**: The total mass per unit area of the wall construction.
2. **Construction time**: The time required for assembling the construction.
3. **Resistance Construction-value:** The combined thermal resistance of all layers in the construction.
4. **Phase shift**: The heat transfer delay of the structure.

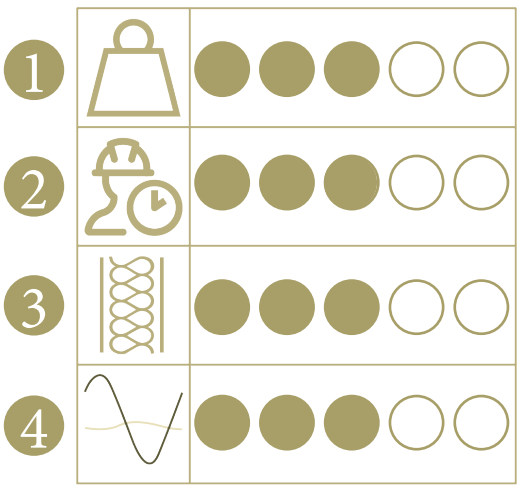

Axonometric view of the detail configuration

In addition to the presented details, an **axonometric view** of the respective detail is also shown. This is presented in the figure below, **figure 99**, and is intended to provide more clarity and insight into **detail V1, detail V2,** and **detail H1**.

Figure A99, Axonometric view of detail configuration 4

Detail configuration 5 - cork insulation with cork façade

The fifth detail configuration consists of cork insulation boards placed between the studs of the timber construction frame. In this configuration, a water-resistant, vapour-permeable membrane is used to protect the structure against moisture penetration. Next, a biobased, diffusion-open construction board with water-repellent properties is applied for structural stability and for the application of the cork façade system. This board enables the attachment of the expanded insulation corkboard, which is bonded using a cork mortar. On top of the expanded insulation corkboard, another layer of cork mortar is applied to bond the cork cladding panels. On the interior side, the timber construction frame is finished with a biobased, diffusion-open construction board to which a clay board is screwed. A clay plaster can then be applied to this board, consisting of a rough layer and a finishing layer.

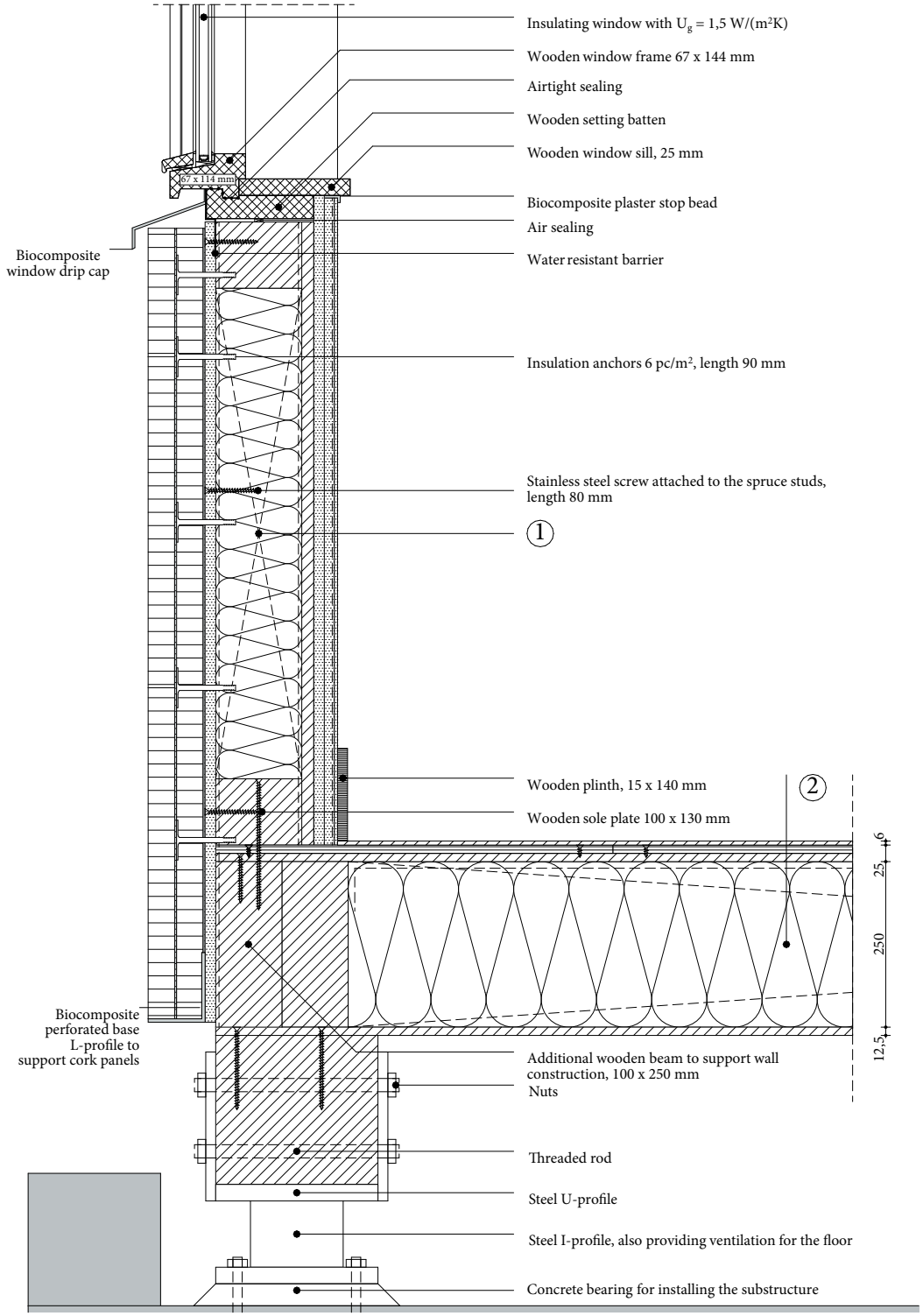

Figure A100, 1:10 detail of V1, configuration 5, own illustration

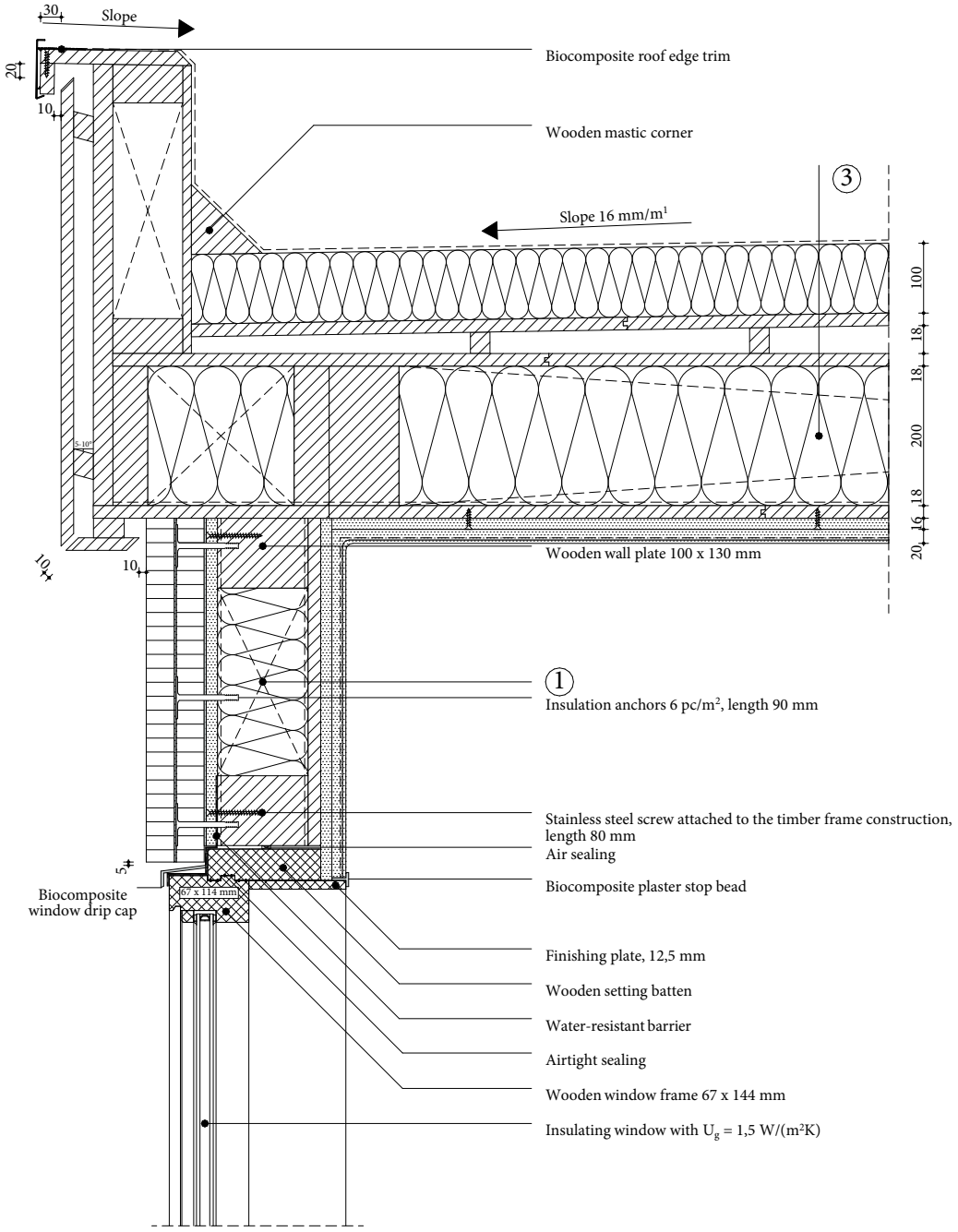

Figure A101, 1:10 detail of V2, configuration 5, own illustration

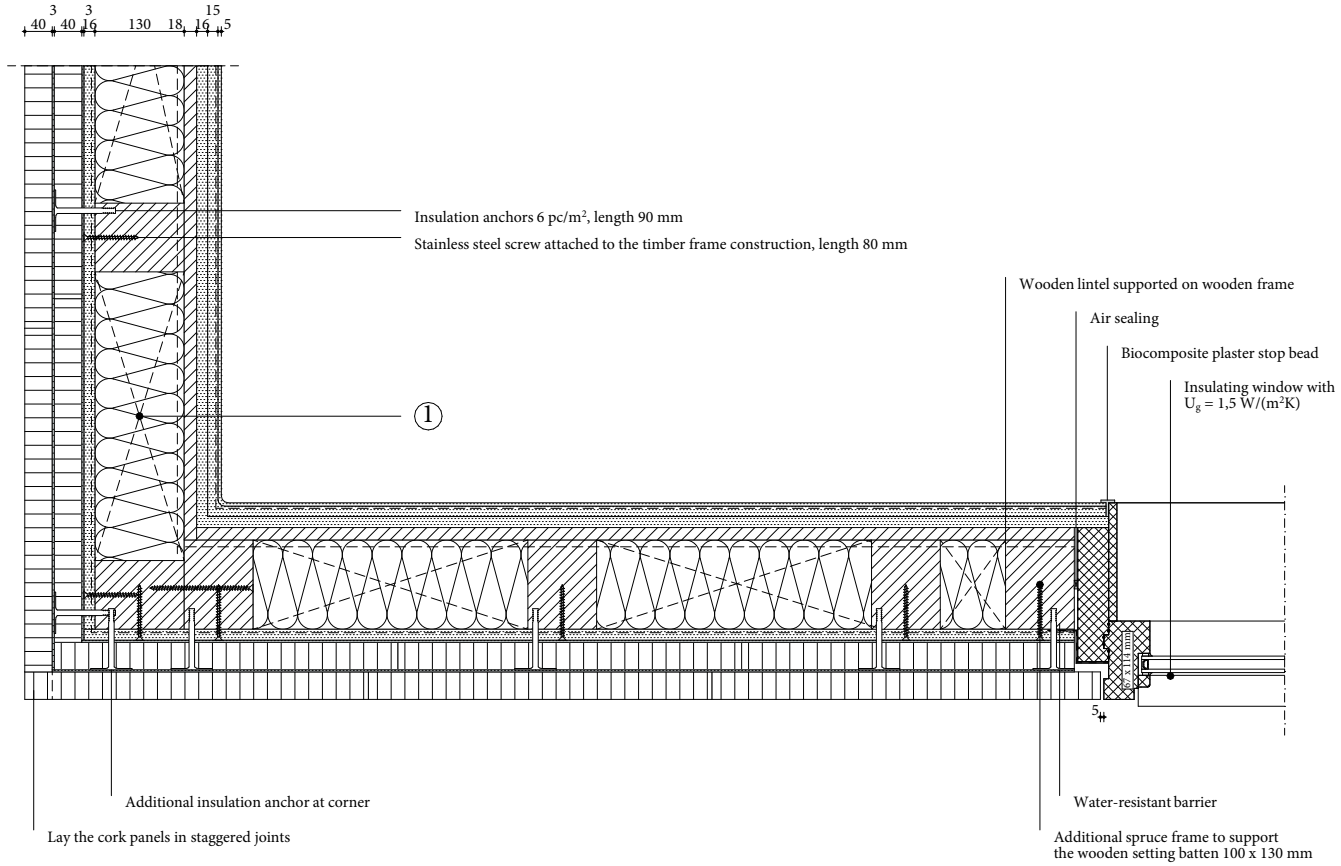

Figure A102, 1:10 detail of H1, configuration 5, own illustration

❶ Wall construction build-up, RC-value: 4.94 (m²K)/W

- Cork cladding panels (λ ≤ 0.043 W/mK), 40 mm;
- Cork mortar, 3 mm;
- Expanded insulation corkboard (λ ≤ 0.039 W/mK), 40 mm;
- Cork mortar, 3 mm;
- Biobased diffusion open construction board, 16mm;
- Water resistant vapour-permeable membrane;
- Timber frame construction, 100 x 130 mm, center-to-center 500 mm;
- Expanded insulation corkboard, placed between construction (λ ≤ 0.039 W/mK), 130 mm;
- Vapour-retarding and airtight membrane with a variable vapour diffusion resistance;
- Biobased construction board, 18 mm;
- Clay base plate, 16 mm;
- Rough base clay plaster, 15 mm;
- Jute reinforcement mesh;
- Finishing clay plaster, 5 mm.

❷ Floor construction build-up, RC-value: 4.65 (m²K)/W

- Finishing board, 6 mm;
- Biobased wooden construction board, 12.5 mm;
- Biobased wooden construction board, perpendicular on the other plate, 12.5 mm;
- Vapour-retarding and airtight membrane with a variable vapour diffusion resistanance;
- Flexible hemp fiber insulation placed between construction (λ ≤ 0.043 W/(mK), 250 mm;
- Wooden beams 100 x 250 mm, center-to-center 600 mm;
- Biobased wooden construction board, 12.5 mm.

❸ Roof construction build-up, RC-value: 6.71 (m²K)/W

- EPDM glued on underlayment to prevent roof covering from lifting;
- Pressure-resistant woodfibre insulation plate (λ ≤ 0.042 W/(mK), 100 mm;
- Biobased wooden construction board, 18 mm;
- Sloped wooden battens for drainage at an angle of 16 mm/m[1], 28 x 24 mm;
- Biobased wooden construction board, 18 mm;
- Flexible hemp fiber insulation placed between construction (λ ≤ 0.043 W/(mK), 200 mm;
- Wooden beams 100 x 200 mm, center-to-center 600 mm;
- Vapour-retarding and airtight membrane with a variable vapour diffusion resistanance;
- Biobased wooden construction board, 18 mm;
- Clay base plate, 16 mm;
- Rough base clay plaster, 15 mm;
- Jute reinforcement mesh;
- Finishing clay plaster, 5 mm.

U_g = 1.50 W/(m²K)

U_w = 1.76 W/(m²K)

f-factor ≥ 0.65

Ψ_{V1}: 0.061 W/(mK) Ψ_{V2}: 0.085 W/(mK) Ψ_{H1}: 0.071 W/(mK)

Isopleths: no risk of mould $f_{R,si} > f_{R,si,\,max}$; no risk of mould

Phase shift of the wall construction: 7.2 h

Density of the wall construction 112 kg/m³

Calculation RC-value wall construction build-up

❶ Wall construction build-up, RC-value: 4.94 (m²K)/W

Table A22, Calculation of the RC-value of the wall construction build-up

Material	Thickness [m]	Thermal conductivity [W/(mK)]	Thermal resistance [W/(m²K)]
Tongue and groove cork cladding panels	0,040	0,043	0,930
Cork mortar	0,003	0,250	0,012
Expanded insulation corkboard	0,040	0,039	1,025
Cork mortar	0,003	0,250	0,012
Biobased diffusion open constrution board	0,016	0,090	0,178
Timber frame construction, with expanded insulation corkboard	0,130	0,054	2,408
Biobased construction board	0,018	0,120	0,150
Clay base plate	0,016	0,470	0,034
Clay plaster	0,020	0,910	0,022

Table A23, Calculation of the equivalent thermal conductivity of the individual layers in the relevant build-up

	Layer 1		Layer 2	
Material	Area [m²]	Thermal conductivity [W/(mK)]	Area [m²]	Thermal conductivity [W/(mK)]
Timber frame construction, with expanded insulation corkboard	0,065	0,039	0,013	0,130

Density mass per unit area of the wall construction

Table A24, Calculation of the density mass per unit area

Material	Thickness [m]	Density [kg/m³]
Tongue and groove cork cladding panels	0,040	140
Cork mortar	0,003	1000
Expanded insulation corkboard	0,040	110
Cork mortar	0,003	1000
Biobased diffusion open construction board	0,016	565
Timber frame construction, with expanded insulation corkboard	0,130	178
Biobased construction board	0,018	621
Clay base plate	0,016	1300
Clay plaster	0,020	1600

By using the previously presented formula a **m'-value** of **112.16 kg/m²** can be given for the **fifth detail configuration**.

Phase-shift

Table A25, Calculation of the phase shift

Material	Thickness [m]	Thermal conductivity [W/(mK)]	Density [kg/m³]	Specific heat capacity [J/(kgK)]
Timber frame construction, with expanded insulation corkboard	0,130	0,054	178	1766

By using the presented phase shift formula, the resulting **φ-value** for **the fifth configuration** is **7.2 h.**

Geometry WUFI

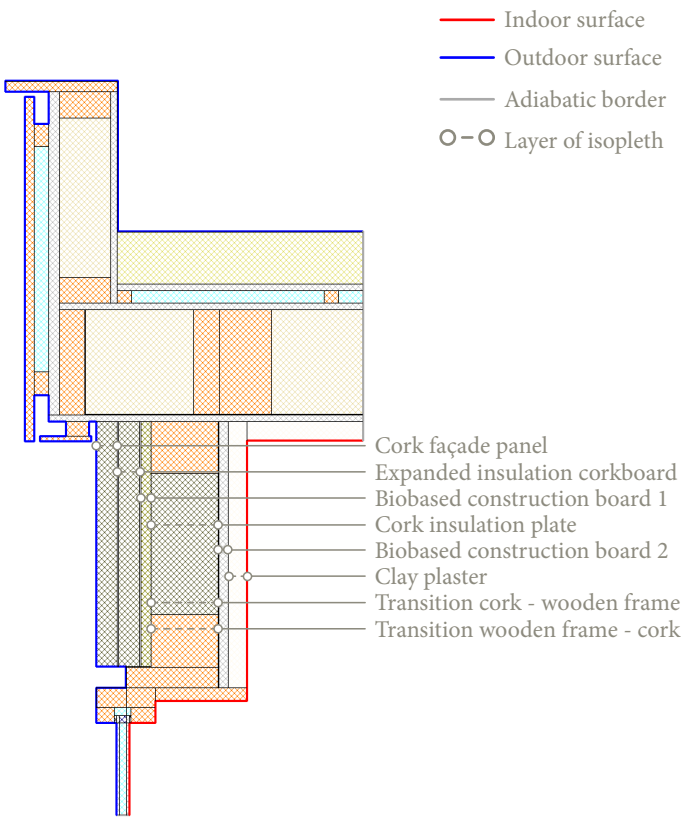

Figure A104, geometry detail V2 including location isopleths

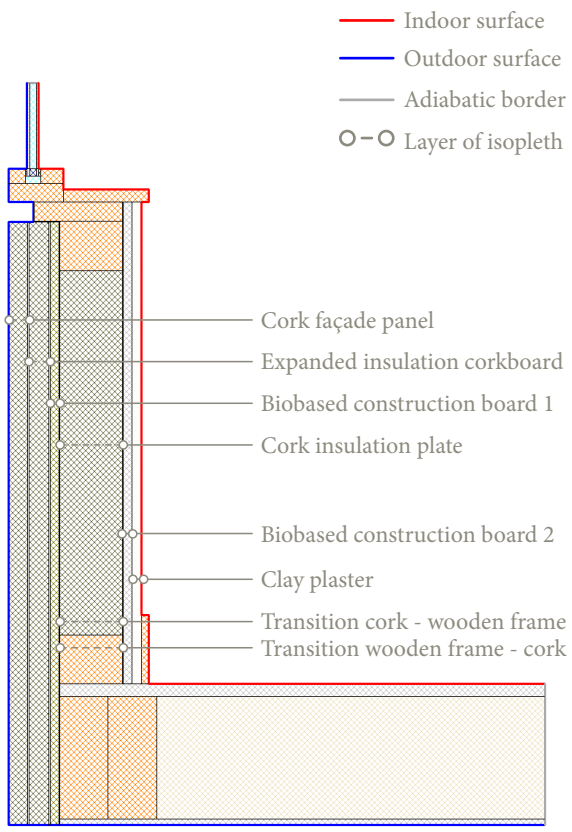

Figure A105, geometry detail V1 including location isopleths

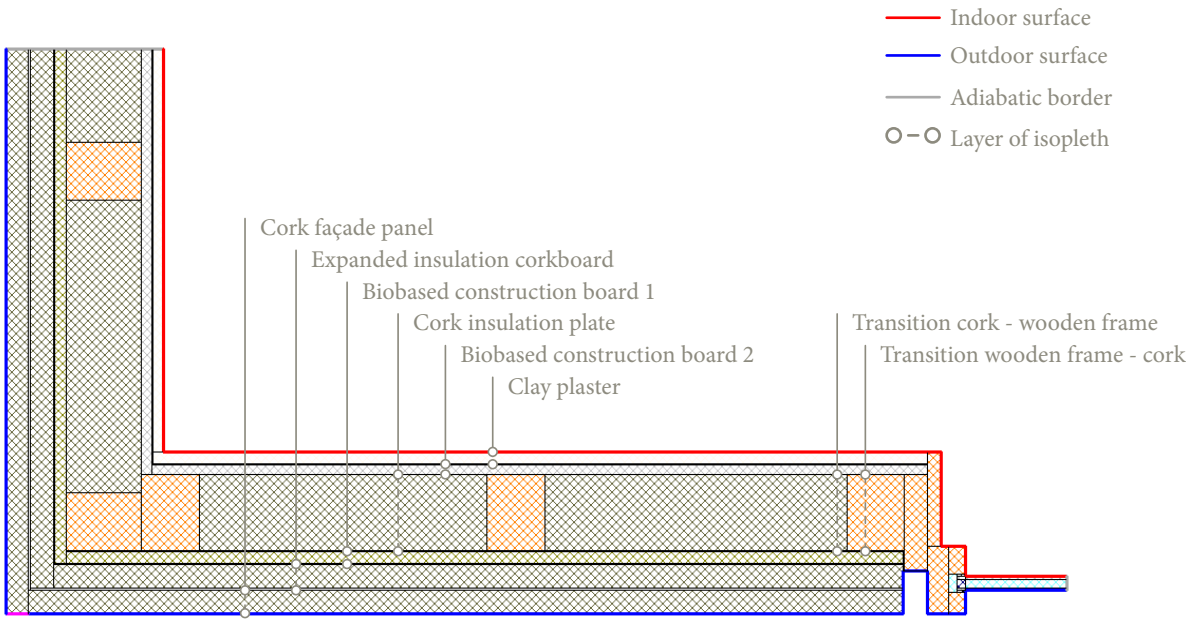

Figure A103, geometry detail H1including location isopleths

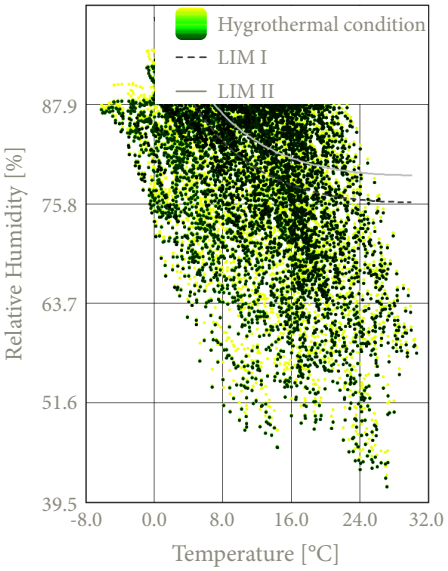

Figure A106, Isopleths cork façade panel

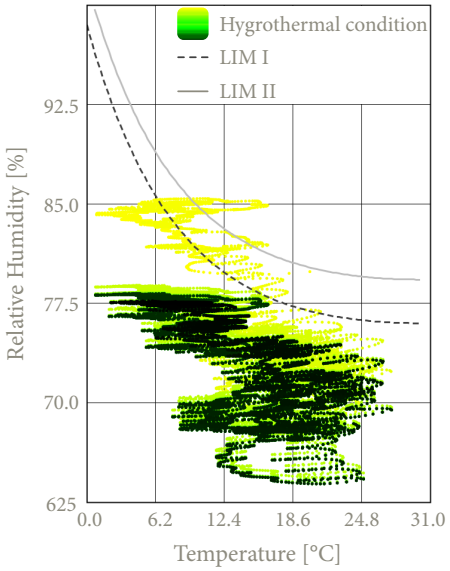

Figure A107, Isopleths expanded insulation corkboard

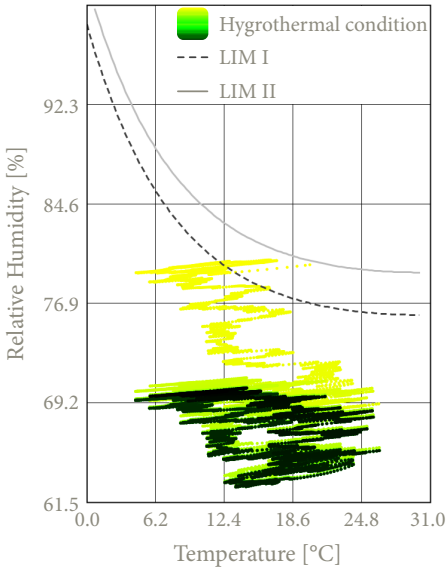

Figure A108, Isopleths biobased construction board 1

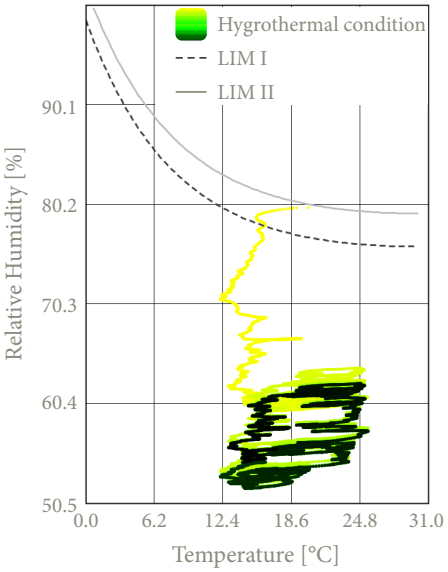

Figure A109, Isopleths cork insulation plate

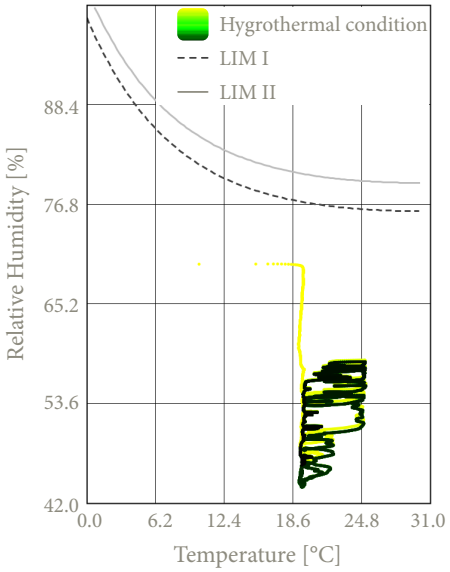

Figure A110, Isopleths biobased construction board 2

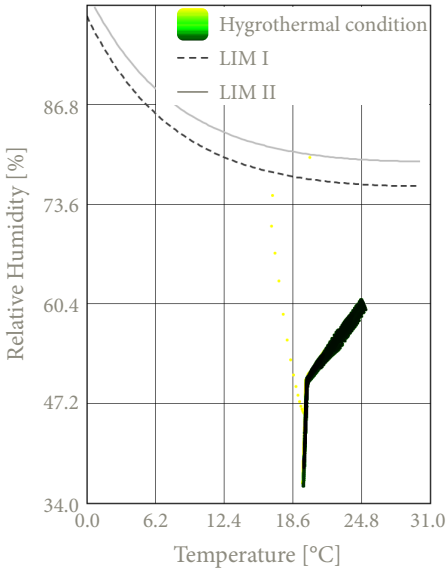

Figure A111, Clay plaster

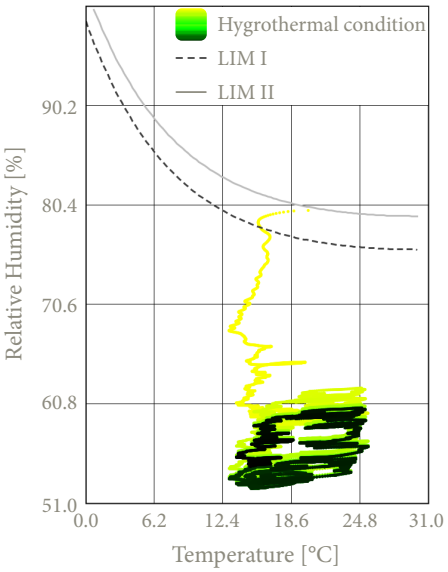

Figure A112, Isopleths transition cork & frame

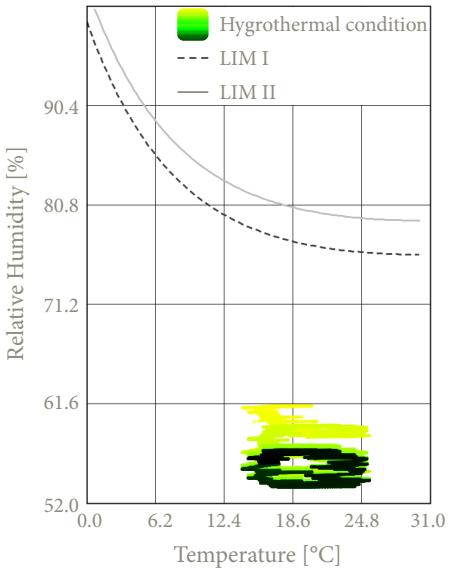

Figure A113, Isopleths transition frame & cork

Isopleths - V2

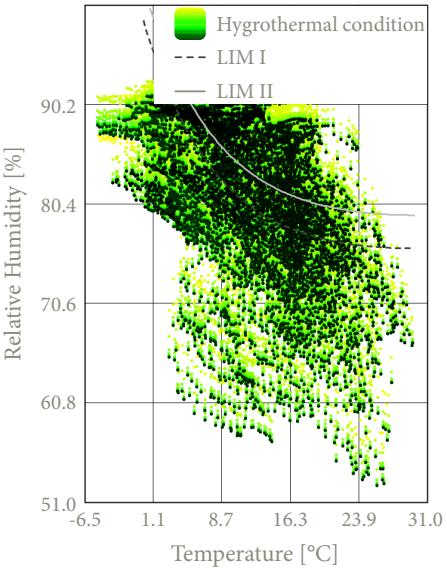

Figure A114, Isopleths cork façade panel

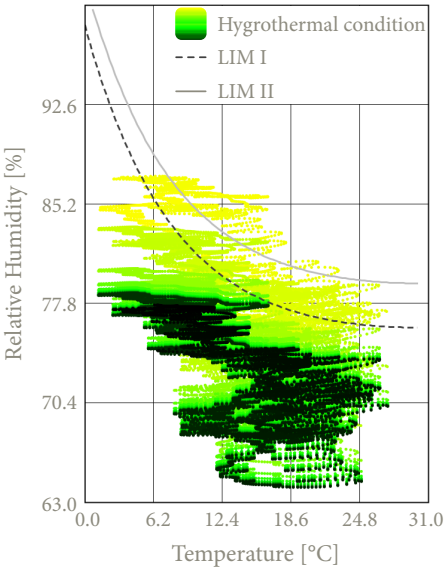

Figure A115, Isopleths expanded insulation corkboard

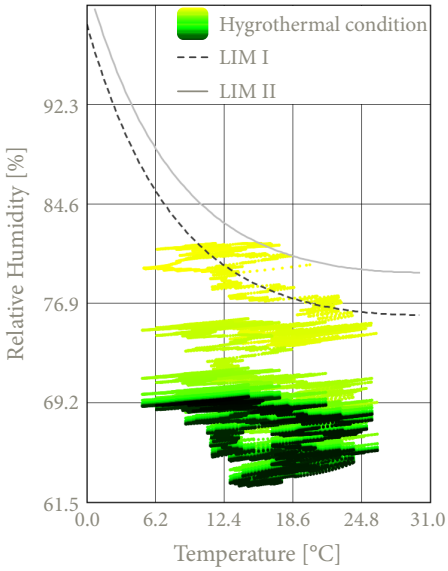

Figure A116, Isopleths biobased construction board 1

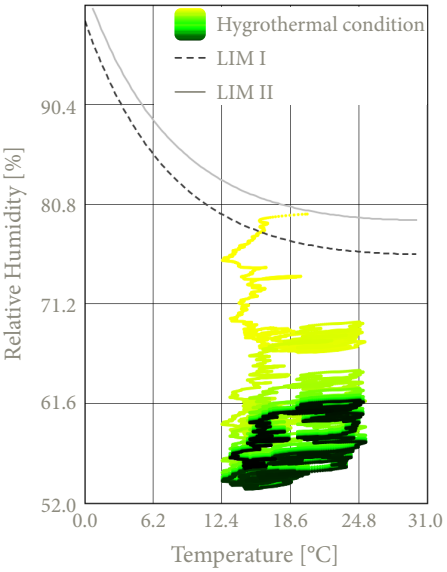

Figure A117, Isopleths cork insulation plate

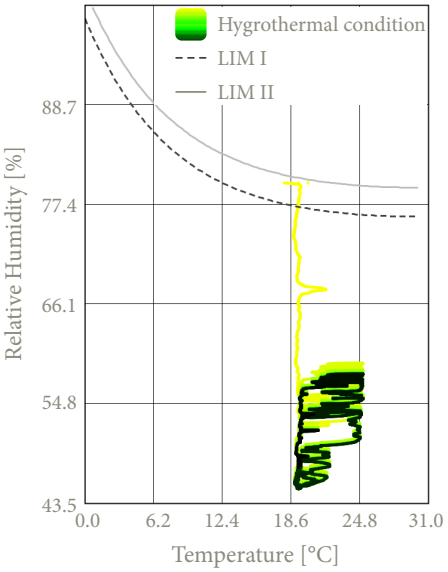

Figure A118, Isopleths biobased construction board 2

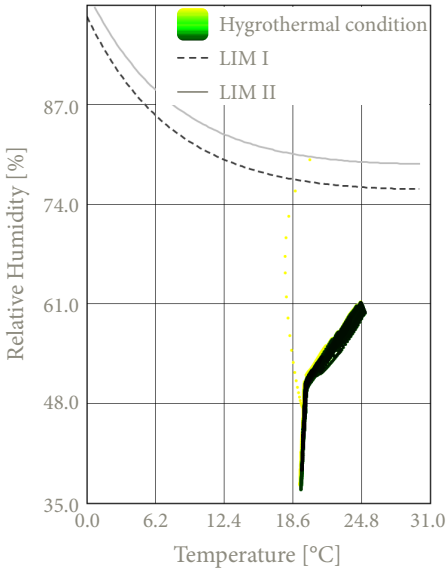

Figure A119, Clay plaster

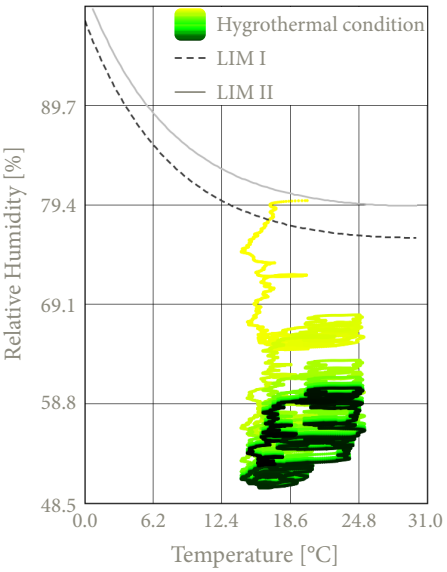

Figure A120, Isopleths transition cork & frame

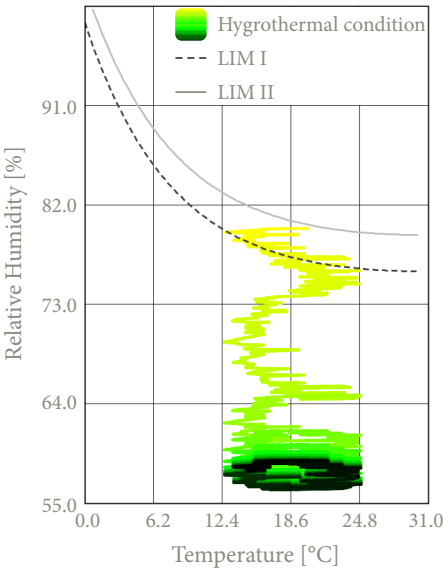

Figure A121, Isopleths transition frame & cork

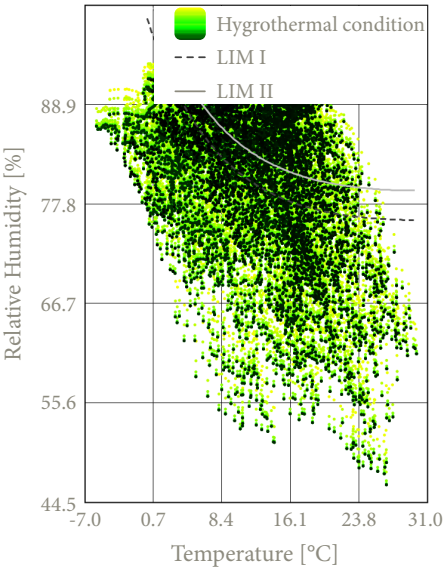

Figure A122, Isopleths cork façade panel

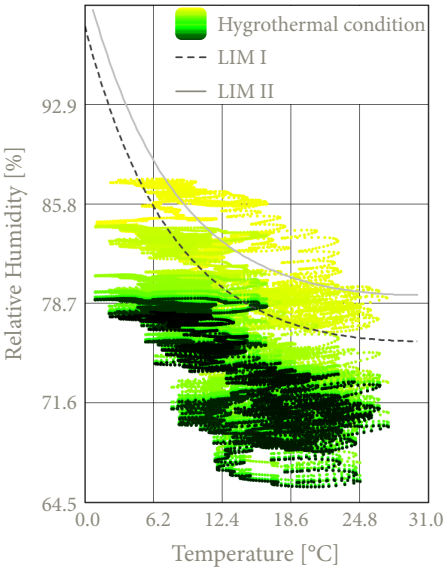

Figure A123, Isopleths expanded insulation corkboard

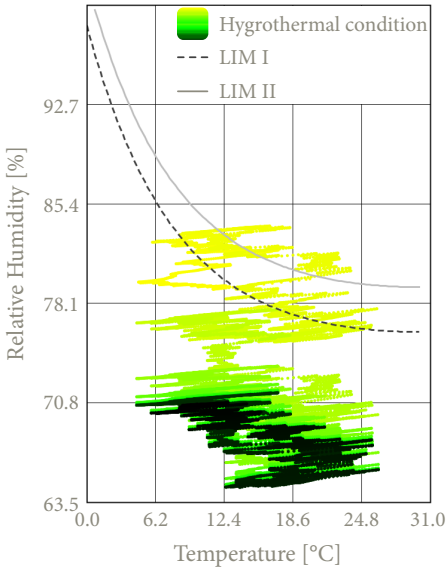

Figure A124, Isopleths biobased construction board 1

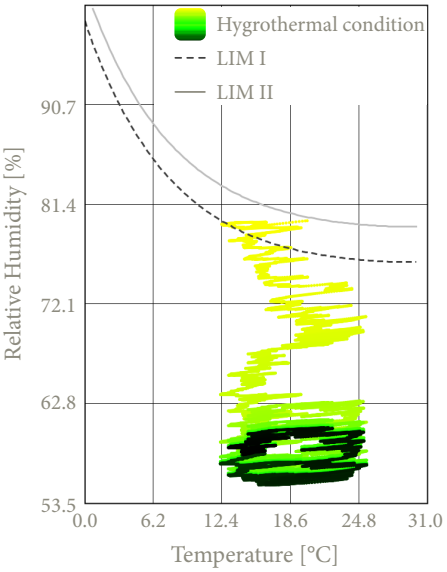

Figure A125, Isopleths cork insulation plate

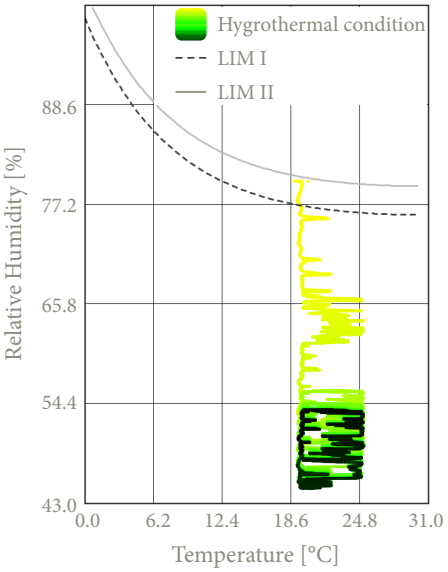

Figure A126, Isopleths biobased construction board 2

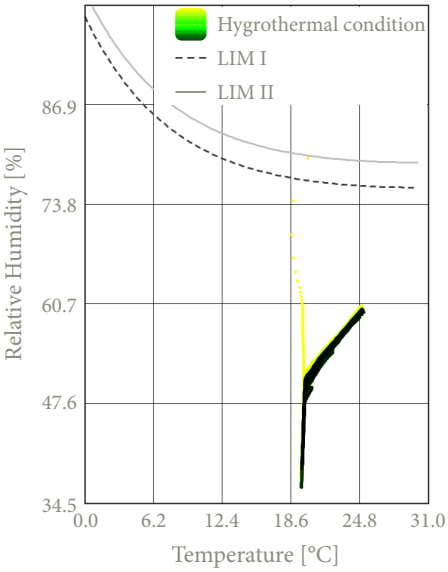

Figure A127, Clay plaster

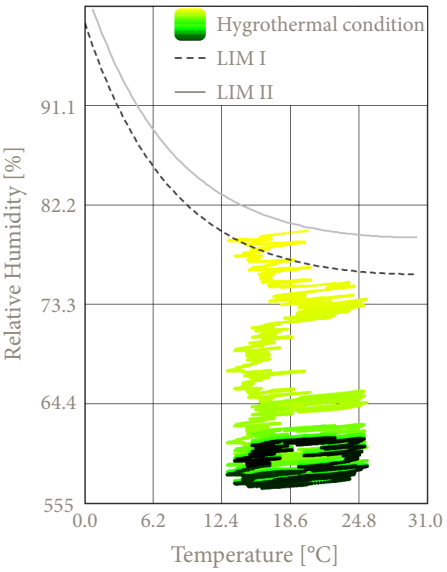

Figure A128, Isopleths transition cork & frame

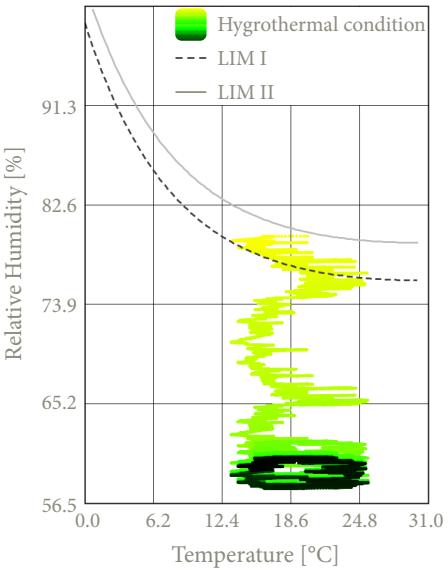

Figure A129, Isopleths transition frame & cork

Conclusion isoplteths

Based on the established and analysed isopleths of the various details within this construction **configuration** it can be concluded that there is no risk of mould growth within the different material layers. All isopleths located behind the cork insulation plate remain below the critical threshold values **LIM I** and **LIM II**, indicating that the details meet the established criteria.

With regards to the **cork façade panel**, it can be observed that the isopleths mostly exceed the LIM threshold values, the same as in the other cork configuration assessment. Therefore, a similar conclusion can be drawn as in the previous cork configuration based on the paper by (Hon, 2024). However, just like in the previous configuration, in order to state with certainty that no mould growth occurs in the cork as an exterior panel material, additional research is required.

The board that is glued with cork mortar behind the cork façade panel, the **expanded insulation corkboard**, shows isopleths exceeding the LIM lines at the initial conditions. However, over time the moisture present in the material at the start, approximately 80%, is transported out. This is because, as previously stated cork is a porous material making it capable of buffering fluctuations in relative humidity. As a result, the isopleths drop below the LIM lines over time. Although an upward trend is initially noticeable, it weakens after a few years of simulation. Therefore, it can be stated with some confidence that even after 10 years, the isopleths will remain below the LIM lines.

When examining the isopleths of the **outside biobased construction board**, it can be seen that the isopleths, apart from a short period at the beginning, remain below the LIM thresholds. When comparing the isopleths between this cork configuration and the previous cork configuration, it becomes clear that the outside biobased construction board in this configuration is much better protected against mould growth due to the additional expanded insulation corkboard and the cork mortar. Therefore, with regard to mould resistance, this configuration is preferable to the previous one. Although a slight upward trend is still noticeable in this isopleth analysis it remains well below the LIM thresholds and diminishes over time.

With regard to the isopleths of the **cork insulation plate**, as well as the **transition zones between the cork and the wooden construction frame**, the **inside biobased construction board**, and the **clay plaster**, the values remain well below both LIM threshold values. A downward trend in the isopleths is also visible for these layers of material.

In conclusion, it can be stated that this configuration poses no risk of mould growth and thus complies with the specified isopleth requirements. However, in order to fully confirm this, further research is needed regarding the cork panel used on the exterior. As such, the design complies with the required hygrothermal performance standards.

Surface condensation - V1, V2 & H1

The circle at each figure figures below, **figure 130**, **figure 132** and **figure 134**, show the coldest point of the interior surface at each detail in order to consider the f_{Rsi}. Below these graphs the corresponding surface temperature at this point is shown over a ten-year simulation below, **figure 131**, **figure 133** and **figure 135**.

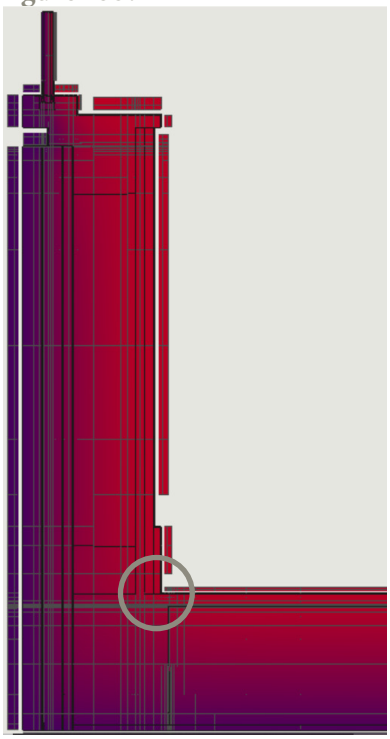

Figure A130, Highlight lowest point, V1

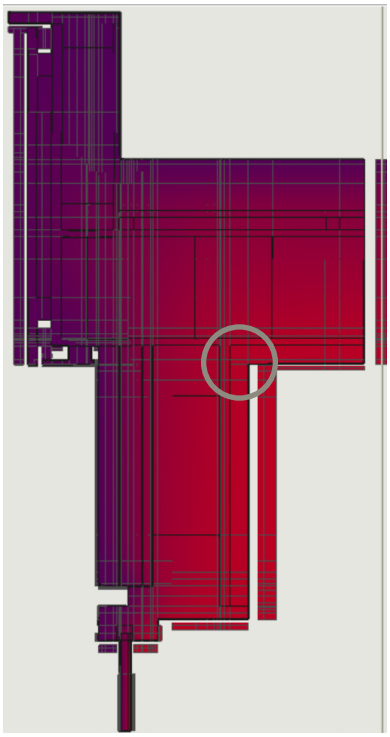

Figure A132, Highlight lowest point, V2

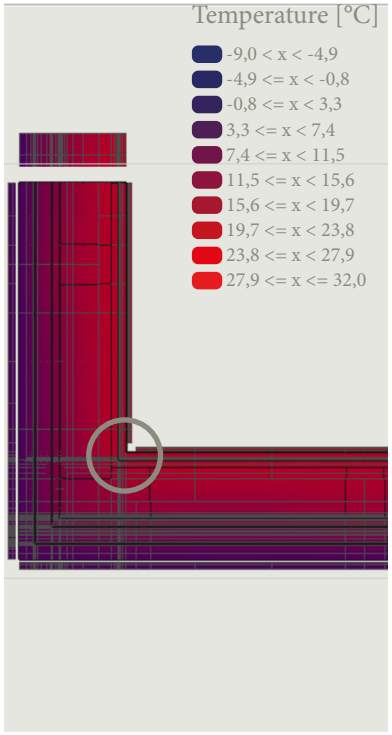

Figure A134, Highlight lowest point, H1

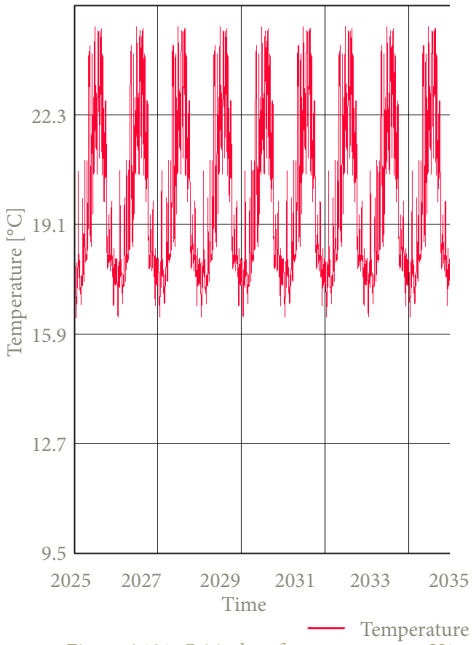

Figure A131, Critical surface temperature, V1

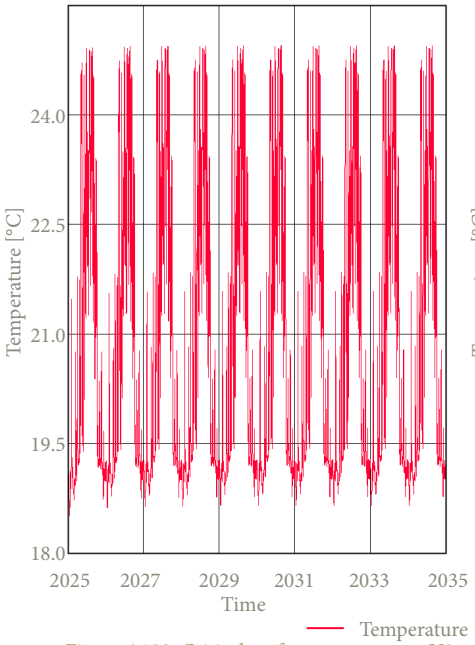

Figure A133, Critical surface temperature, V2

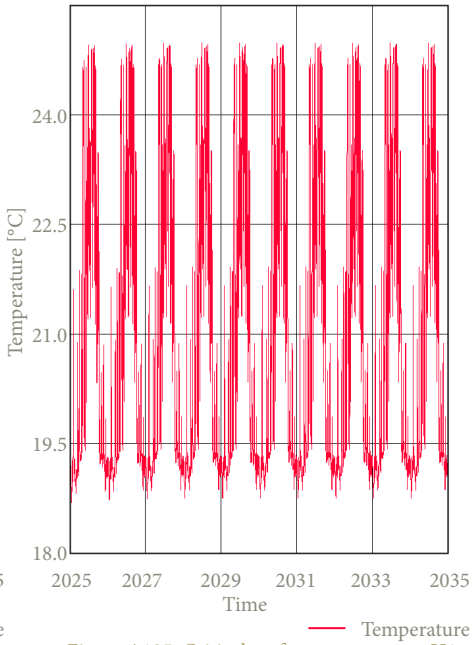

Figure A135, Critical surface temperature, H1

From this graph the lowest surface temperature of this detail is **15.73 °C**.

The resulting f_{Rsi} for this detail is **0.64** which exceeds the minimum requirement of 0.61. This indicates a negligible risk of surface condensation.

From this graph the lowest surface temperature of this detail is **18.51 °C**.

The resulting f_{Rsi} for this detail is **0.88** which exceeds the minimum requirement of 0.61. This indicates a negligible risk of surface condensation.

From this graph the lowest surface temperature of this detail is **18.67 °C**.

The resulting f_{Rsi} for this detail is **0.89** which exceeds the minimum requirement of 0.61. This indicates a negligible risk of surface condensation.

F-factor - V1, V2 & H1

The resulting **f-factor** of **detail V1** is **0.88** for a temperature of **15.99 °C**. Next the resulting **f-factor** of **detail V2** is **0.94** for a temperature of **16.98 °C**. Lastly, the resulting **f-factor** of **detail H1** is **0.94** for a temperature of **17.05 °C**. This indicates a very limited thermal bridge is assessed within the details of this configuration.
Given that these values significantly all exceeds the required threshold of **0.65**, it can be concluded that the details within this configuration complies with the thermal performance requirements set by the Dutch Building Decree.

PSI-value - V1

Table A26, Calculation of the $Q_{ideal\ condition}$

$R_{construction,\ window}$ [(m²K)/W]	$A_{construction,\ window}$ [m²]	$R_{construction,\ wall}$ [(m²K)/W]	$A_{construction,\ wall}$ [m²]	$R_{construction,\ floor}$ [(m²K)/W]	$A_{construction,\ floor}$ [m²]
0.600	0.2425	4.941	0.978	4.648	0.841

The resulting $\mathbf{Q_{ideal\ condition}}$ is **14.095 W**

Q_{WUFI} represents the sum of all heat flows through the detail, resulting in a total heat flow of **15.197 W**.

These values give a **Ψ-value** of **0.061 W/(mK)** for **detail V1**, indicating that the detail can be characterised as a well-insulated building component.

PSI-value - V2

Table A27, Calculation of the $Q_{ideal\ condition}$

$R_{construction,\ window}$ [(m²K)/W]	$A_{construction,\ window}$ [m²]	$R_{construction,\ wall}$ [(m²K)/W]	$A_{construction,\ wall}$ [m²]	$R_{construction,\ roof}$ [(m²K)/W]	$A_{construction,\ roof}$ [m²]
0.600	0.2425	5.532	0.844	6.442	0.096

The resulting $\mathbf{Q_{ideal\ condition}}$ is **11.056 W**

Q_{WUFI} represents the sum of all heat flows through the detail, resulting in a total heat flow of **12.592 W**.

These values give a **Ψ-value** of **0.085 W/(mK)** for **detail V2**, indicating that the detail can be characterised as a well-insulated building component.

PSI-value - H1

Table A28, Calculation of the $Q_{ideal\ condition}$

$R_{construction,\ window}$ [(m²K)/W]	$A_{construction,\ window}$ [m²]	$R_{construction,\ wall}$ [(m²K)/W]	$A_{construction,\ wall}$ [m²]
0.600	0.2425	4.941	2.304

The resulting $\mathbf{Q_{ideal\ condition}}$ is **15.668 W**

Q_{WUFI} represents the sum of all heat flows through the detail, resulting in a total heat flow of **16.951 W**.

These values give a **Ψ-value** of **0.071 W/(mK)** for **detail H1**, indicating that the detail can be characterised as a well-insulated building component.

Assessment detail configuration

Important notes about the details

For the given configuration, **key considerations** are presented below in the form of bullet points. These points highlight specific aspects that need to be taken into account during detailing and construction.

- Place the cork insulation board between the studs of the wooden frame.
- Finish the outside of the wooden frame with a pressure-resistant wood fibre insulation board.
- Finish the inside of the wooden frame with a pressure-resistant wood fibre board to allow for fixings.
- Attach the water-resistant barrier of the window frame to the timber structural frame.
- Apply a water-resistant, vapour-permeable membrane over the timber frame construction.
- Apply a diffusion-open construction board with water-resistant properties onto the timber frame, over which cork mortar can be applied.
- Attach the cork façade panels using 3 mm cork mortar adhesive onto the cork insulation boards.
- Fix the cork insulation boards using both 3 mm cork mortar adhesive and mechanical fastening with insulation anchors to ensure a structurally secure base layer for the cork façade panels.
- Use 6 insulation anchors per m^2, with anchor lengths equal to the insulation board thickness plus 30 mm embedment depth.
- The wooden lintel must have proper bearing on the wooden frame.
- Ensure 5 mm ventilation gaps both between cork panels and at the window frame.
- Use a clay base plate to provide a correct underlayment for the clay plaster.
- Use a jute reinforcement mesh between the rough and finishing clay plaster to prevent cracking.

Assessment of the configuration

Additionally, the configuration is evaluated based on the following criteria:

1. **Weight**: The total mass per unit area of the wall construction.
2. **Construction time**: The time required for assembling the construction.
3. **Resistance Construction-value:** The combined thermal resistance of all layers in the construction.
4. **Phase shift**: The heat transfer delay of the structure.

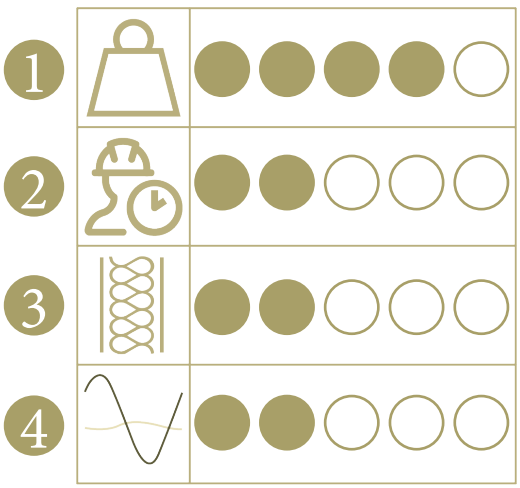

Axonometric view of the detail configuration

In addition to the presented details, an **axonometric view** of the respective detail is also shown. This is presented in the figure below, **figure 136**, and is intended to provide more clarity and insight into **detail V1, detail V2,** and **detail H1**.

Figure A136, Axonometric view of detail configuration 5

Detail configuration 6 - flax insulation with wooden façade

The sixth detail configuration consists of flexible flax insulation placed between the studs of the timber construction frame. To protect the flax against water and mould growth a water-resistant vapour-permeable membrane is placed at the outside of the timber frame construction. In this configuration the cladding battens can be attached on which the horizontal wooden cladding can be placed.
On the interior side, the timber construction frame is finished with a biobased, diffusion-open construction board to which a clay board is screwed. A clay plaster can then be applied to this board, consisting of a rough layer and a finishing layer.

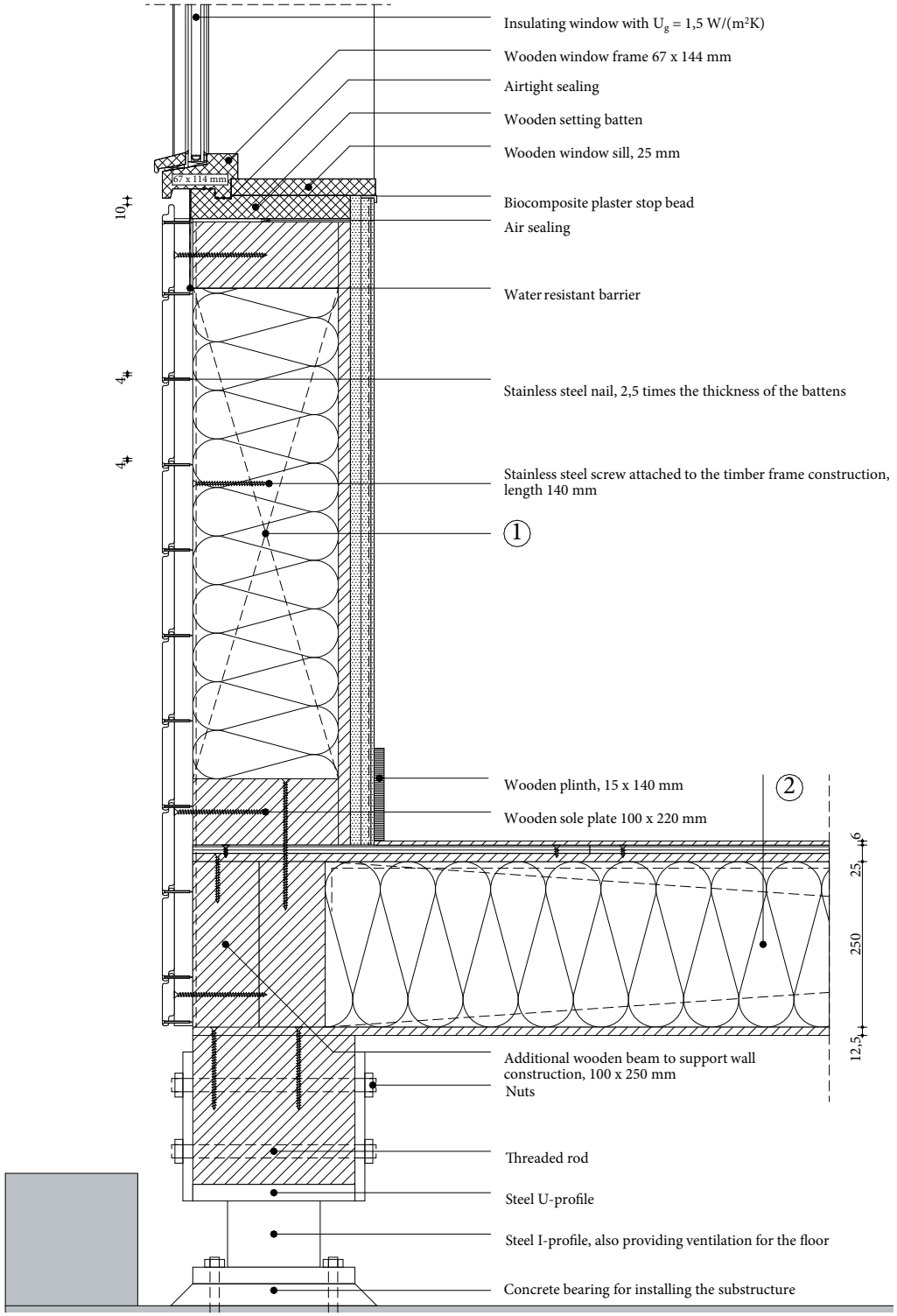

Figure A137, 1:10 detail of V1, configuration 6, own illustration

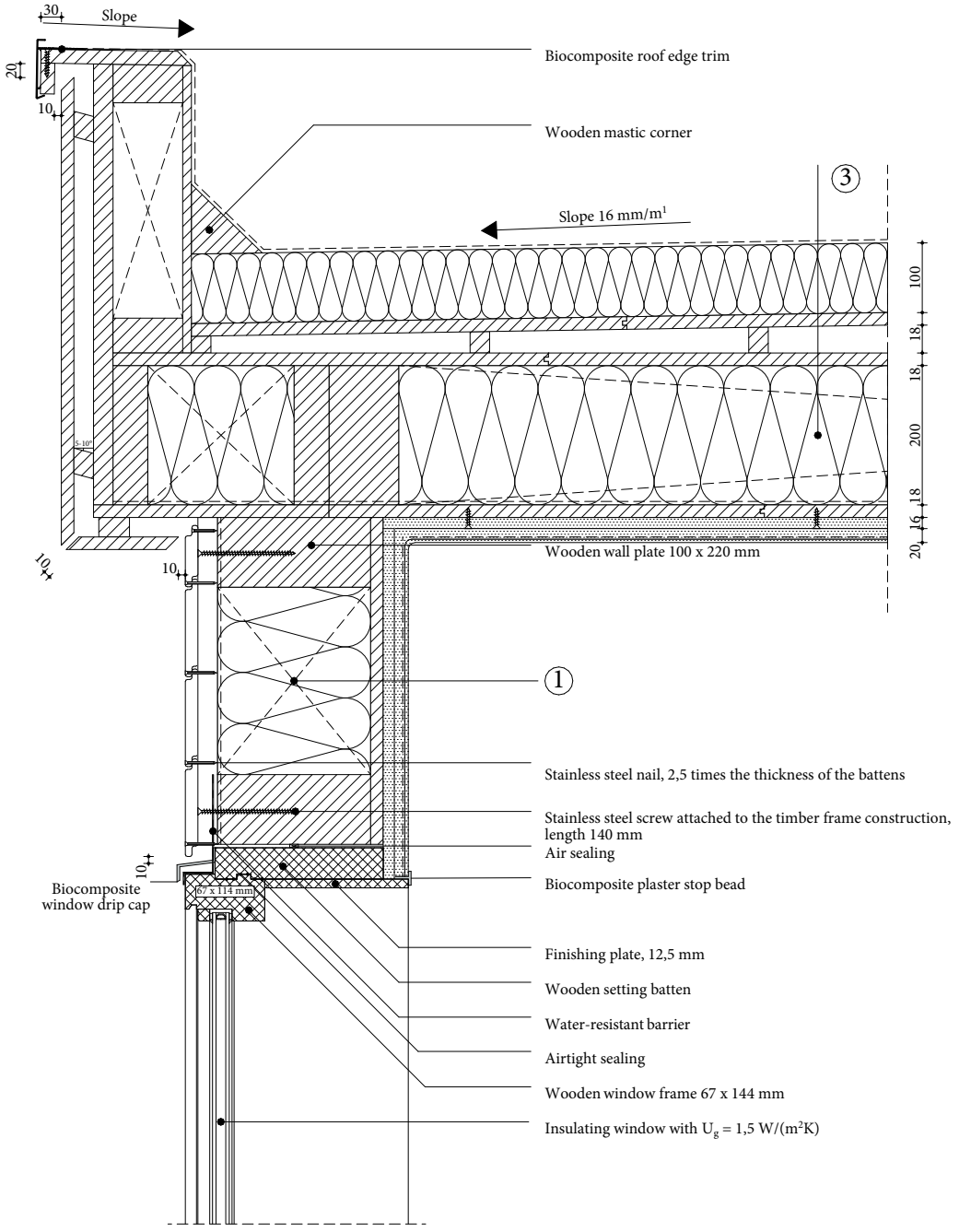

Figure A138, 1:10 detail of V2, configuration 6, own illustration

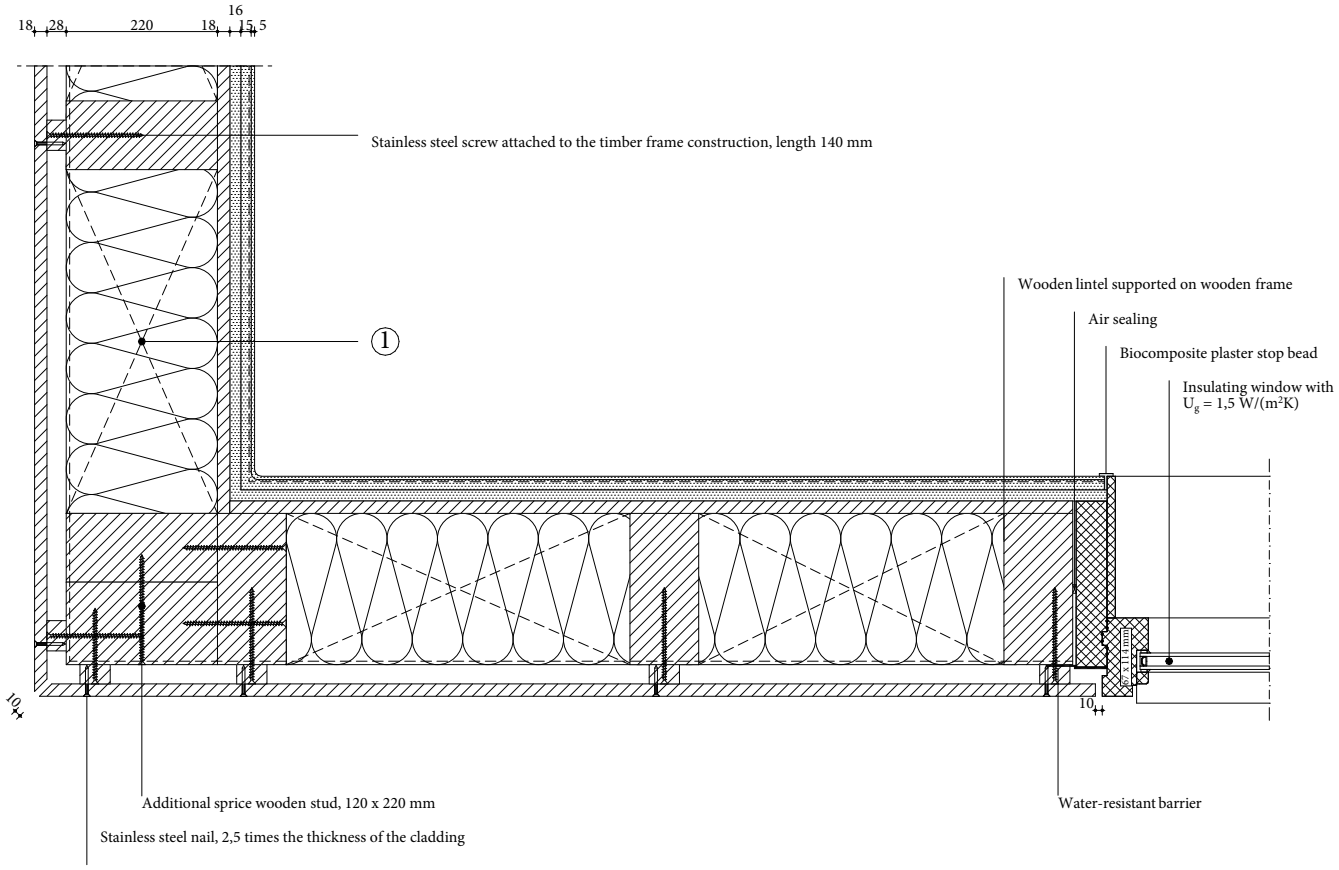

Figure A139, 1:10 detail of H1, configuration 6, own illustration

❶ Wall construction build-up, RC-value: 5.09 (m²K)/W

- Horizontal wooden cladding, 18 mm;
- Vertical spruce cladding batten forming ventilated cavity, 28 x 44 mm, center-to-center 600 mm;
- Water resistant vapour-permeable membrane;
- Timber frame construction, 100 x 220 mm, center-to-center 600 mm;
- Flexible flax insulation, placed between construction (λ ≤ 0.035 W/mK), 180 + 40 mm;
- Biobased construction board, 18 mm;
- Clay base plate, 16 mm;
- Rough base clay plaster, 15 mm;
- Jute reinforcement mesh;
- Finishing clay plaster, 5 mm.

❷ Floor construction build-up, RC-value: 4.65 (m²K)/W

- Finishing board, 6 mm;
- Biobased wooden construction board, 12.5 mm;
- Biobased wooden construction board, perpendicular on the other plate, 12.5 mm;
- Vapour-retarding and airtight membrane with a variable vapour diffusion resistanance;
- Flexible hemp fiber insulation placed between construction (λ ≤ 0.043 W/(mK), 250 mm;
- Wooden beams 100 x 250 mm, center-to-center 600 mm;
- Biobased wooden construction board, 12.5 mm.

❸ Roof construction build-up, RC-value: 6.71 (m²K)/W

- EPDM glued on underlayment to prevent roof covering from lifting;
- Pressure-resistant woodfibre insulation plate (λ ≤ 0.042 W/(mK), 100 mm;
- Biobased wooden construction board, 18 mm;
- Sloped wooden battens for drainage at an angle of 16 mm/m^1, 28 x 24 mm;
- Biobased wooden construction board, 18 mm;
- Flexible hemp fiber insulation placed between construction (λ ≤ 0.043 W/(mK), 200 mm;
- Wooden beams 100 x 200 mm, center-to-center 600 mm;
- Vapour-retarding and airtight membrane with a variable vapour diffusion resistanance;
- Biobased wooden construction board, 18 mm;
- Clay base plate, 16 mm;
- Rough base clay plaster, 15 mm;
- Jute reinforcement mesh;
- Finishing clay plaster, 5 mm.

U_g = 1.50 W/(m²K)

U_w = 1.76 W/(m²K)

f-factor ≥ 0.65

Ψ_{V1}: 0.062 W/(mK) Ψ_{V2}: 0.083 W/(mK) Ψ_{H1}: 0.063 W/(mK)

Isopleths: no risk of mould $f_{R,si} > f_{R,si,\,max}$; no risk of mould

Phase shift of the wall construction: 9.7 h

Density of the wall construction 99 kg/m³

Calculation RC-value wall construction build-up

❶ Wall construction build-up, RC-value: 5.09 (m²K)/W

Table A29, Calculation of the RC-value of the wall construction build-up

Material	Thickness [m]	Thermal conductivity [W/(mK)]	Thermal resistance [W/(m²K)]
Vertical wooden cladding	0,018	0,130	0,138
Ventilated cavity with vertical wooden cladding batten, center-to-center 600 mm	0,028	0,322	0,087
Timber frame construction, with flexible flax insulation	0,220	0,049	4,489
Biobased construction board	0,018	0,120	0,150
Clay base plate	0,016	0,470	0,034
Clay plaster	0,020	0,910	0,022

Table A30, Calculation of the equivalent thermal conductivity of the individual layers in the relevant build-up

	Layer 1		Layer 2	
Material	Area [m²]	Thermal conductivity [W/(mK)]	Area [m²]	Thermal conductivity [W/(mK)]
Ventilated cavity with vertical wooden cladding batten, center-to-center 600 mm	0,0012	0,130	0,0168	0,337
Timber frame construction, with flexible flax	0,1320	0,071	0,0220	0,130

Density mass per unit area of the wall construction

Table A31, Calculation of the density mass per unit area

Material	Thickness [m]	Density [kg/m³]
Vertical wooden cladding	0,018	520
Ventilated cavity with vertical wooden cladding batten, center-to-center 600 mm	0,024	35
Timber frame construction, with flexible flax insulation	0,220	113
Biobased construction board	0,018	621
Clay base plate	0,016	1300
Clay plaster	0,020	1600

By using the previously presented formula a **m'-value** of **99.04 kg/m²** can be given for the **sixth detail configuration**.

Phase-shift

Table A32, Calculation of the phase shift

Material	Thickness [m]	Thermal conductivity [W/(mK)]	Density [kg/m³]	Specific heat capacity [J/(kgK)]
Timber frame construction, with flexible flax insulation	0,220	0,049	113	1600

By using the presented phase shift formula, the resulting **φ-value** for **the sixth configuration** is **9.7 h.**

Geometry WUFI

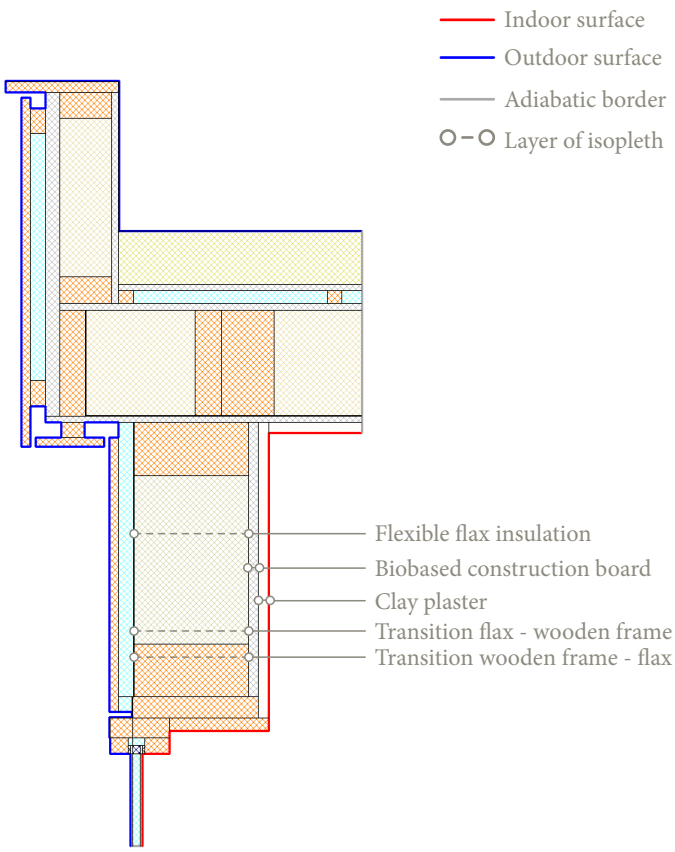

Figure A141, geometry detail V2 including location isopleths

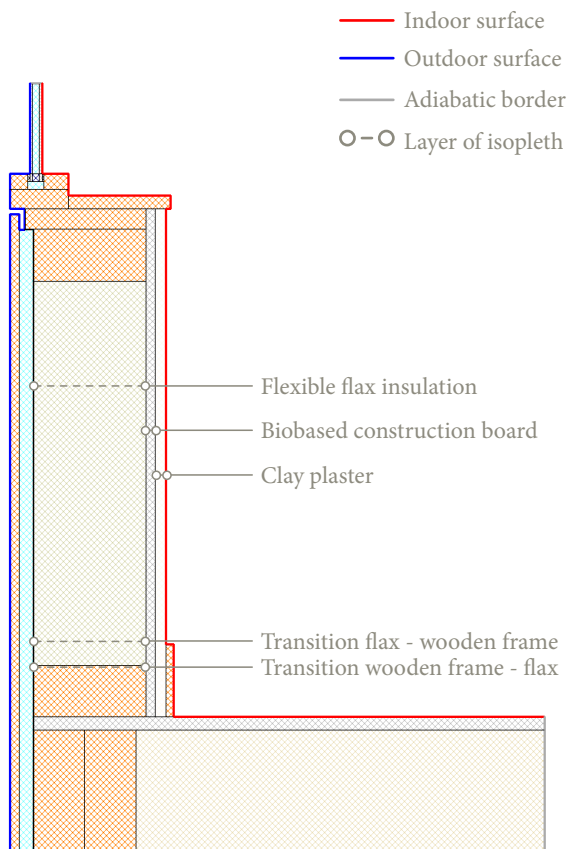

Figure A142, geometry detail V1 including location isopleths

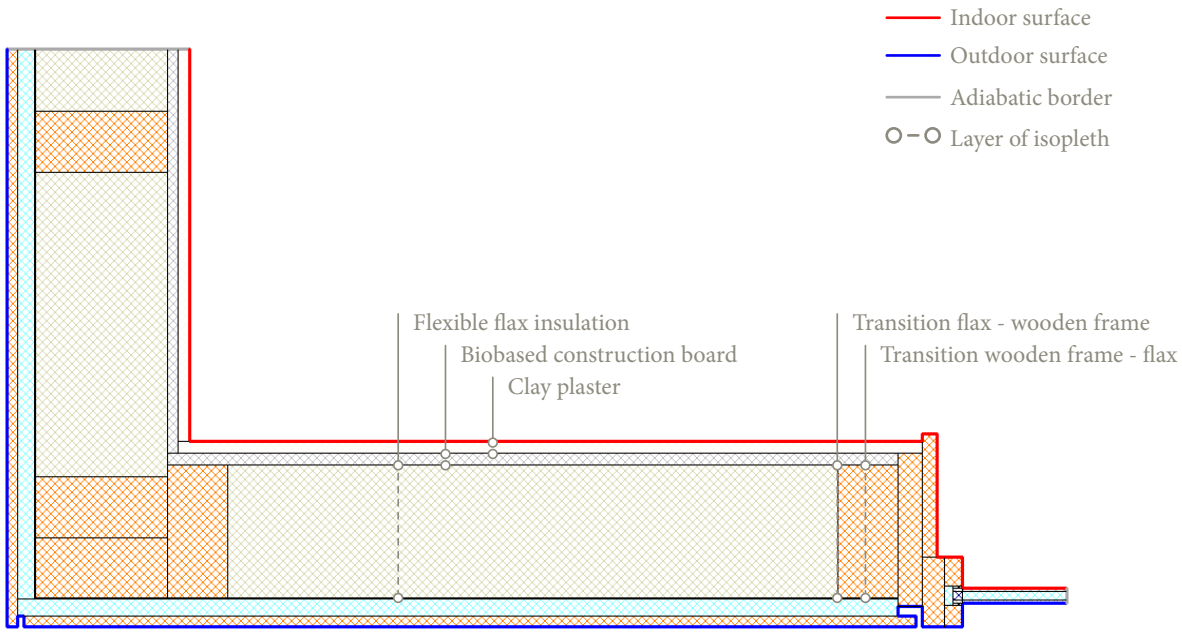

Figure A140, geometry detail H1including location isopleths

Isopleths - V1

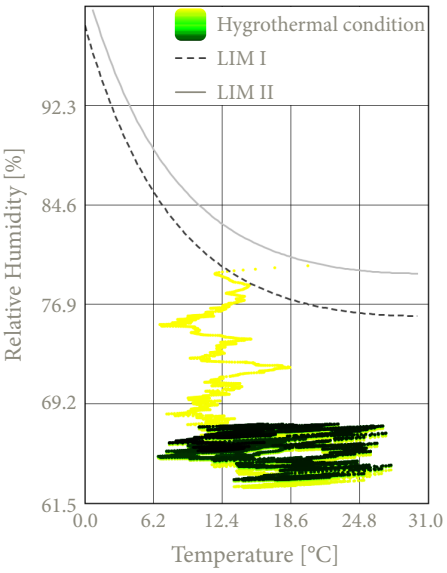

Figure A143, Isopleths flexible flax insulation

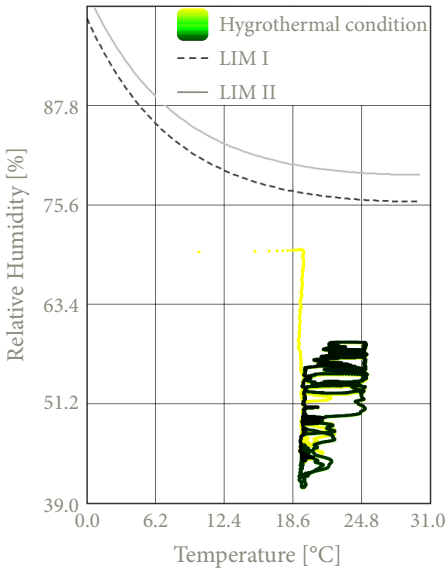

Figure A144, Isopleths biobased construction board

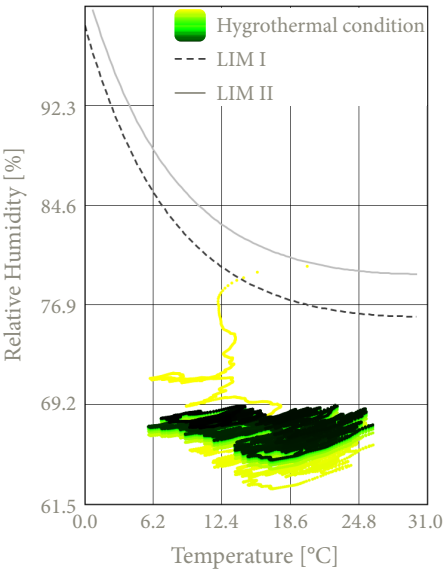

Figure A145, Isopleths transition flax & frame

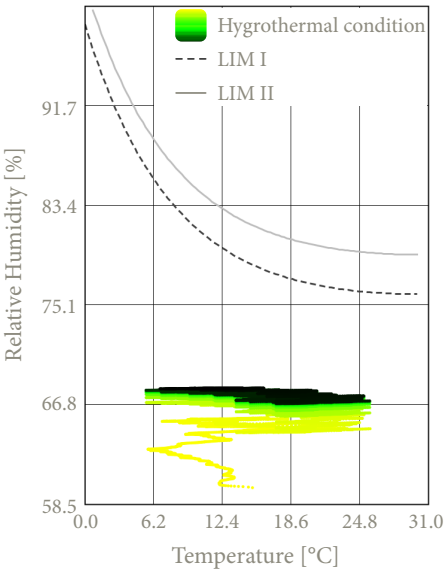

Figure A146, Isopleths transition frame & flax

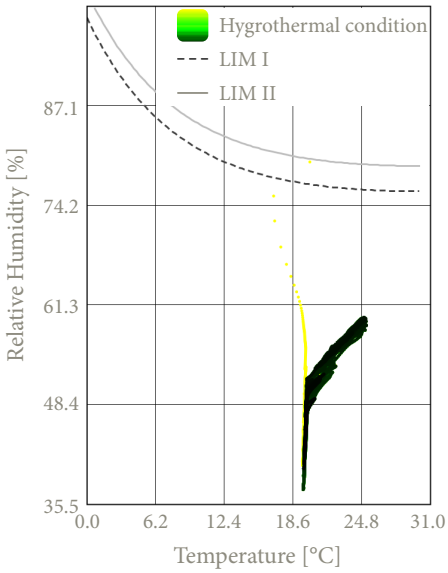

Figure A147, Isopleths clay plaster

Isopleths - V2

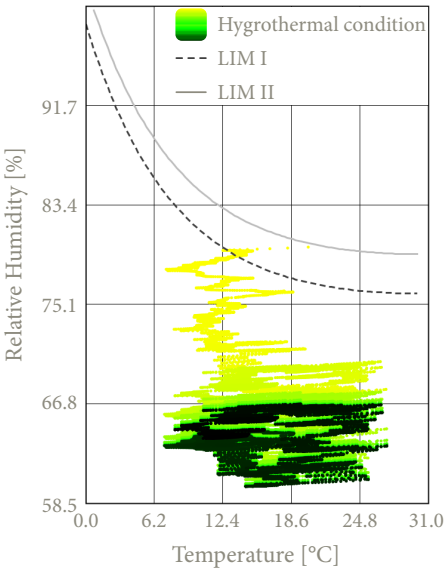

Figure A148, Isopleths flexible flax insulation

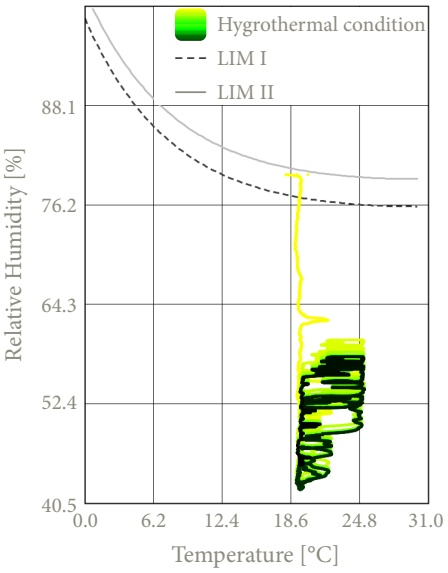

Figure A149, Isopleths biobased construction board

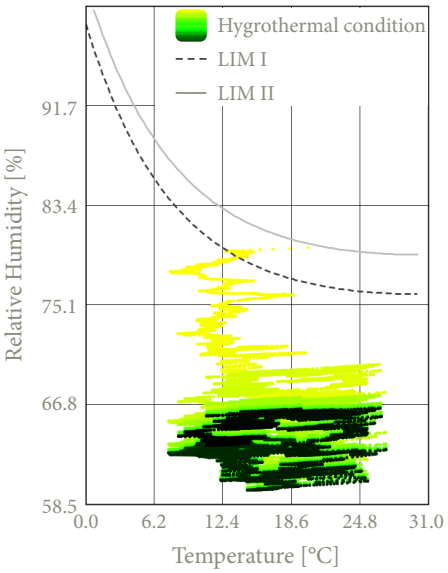

Figure A150, Isopleths transition flax & frame

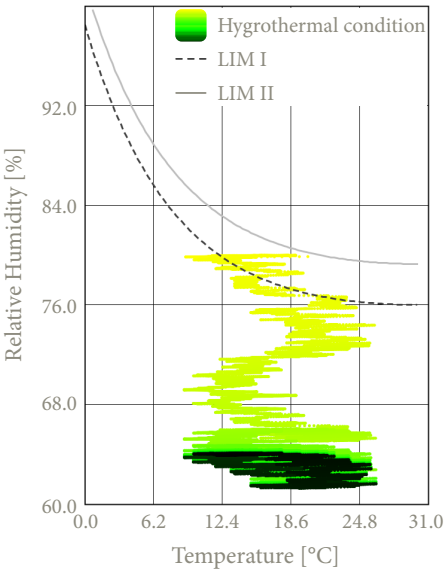

Figure A151, Isopleths transition frame & flax

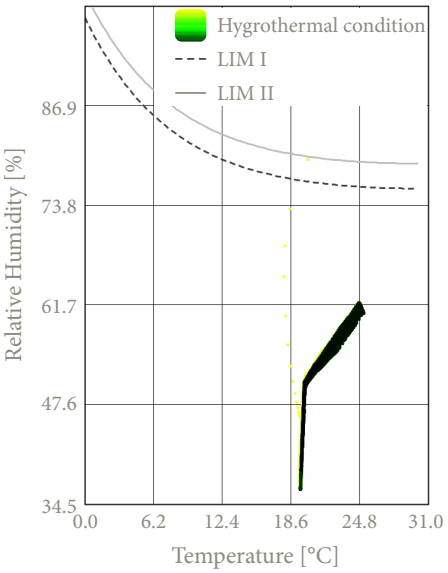

Figure A152, Isopleths clay plaster

Isopleths - H1

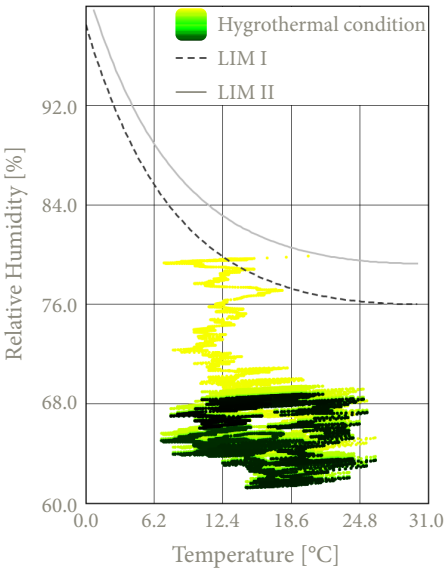

Figure A153, Isopleths flexible flax insulation

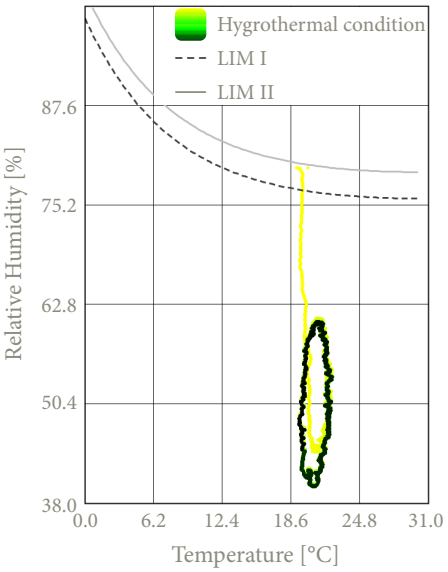

Figure A154, Isopleths biobased construction board

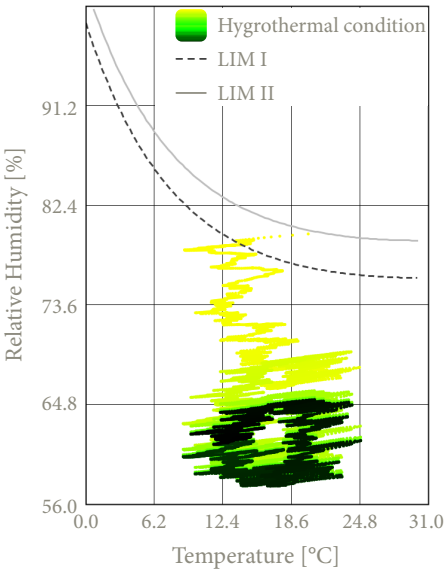

Figure A155, Isopleths transition flax & frame

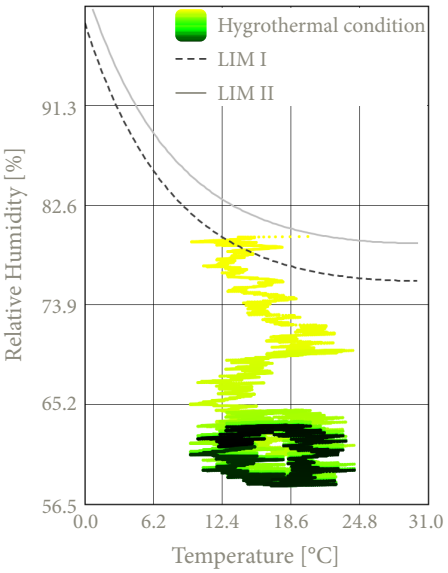

Figure A156, Isopleths transition frame & flax

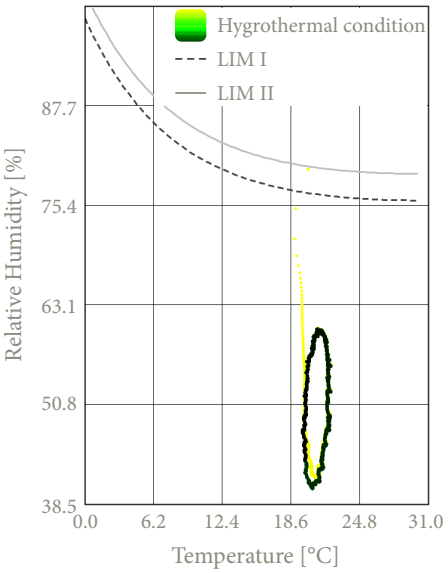

Figure A157, Isopleths clay plaster

Conclusion isoplteths

Based on the established and analysed isopleths of the various details within this construction **configuration**, it can be concluded that there is no risk of mould growth within the different material layers. All isopleths remain below the critical threshold values **LIM I** and **LIM II**, indicating that the details meet the established criteria.

With regards to the **flax insulation** and the **transition between the flax and the timber frame** construction, the isopleths for these layers all remain below the LIM threshold values. However, a small upward trend is visible in the isopleths of the flax and the transition between the flax and the timber frame in details V1 & V2. Although an upward trend is initially noticeable it weakens after a few years of simulation. In contrast, a downward trend is observed in the isopleths of the layers in detail V2. While V1 and H1 show a slight upward trend, which eventually weakens, the isopleths remain well below the LIM threshold values. Therefore, it can be stated with some confidence that even after 10 years the isopleths will remain below the LIM lines.

With regard to the isopleths of the **inside biobased construction board** and the **clay plaster**, the values remain well below both LIM threshold values. A downward trend in the isopleths is also visible for the biobased construction board at V2. For the isopleths of V1 and H1, the values remain consistent throughout the ten-year simulation period.

In conclusion, it can be stated that this configuration poses no risk of mould growth and thus complies with the specified isopleth requirements. As such, the design complies with the required hygrothermal performance standards.

Surface condensation - V1, V2 & H1

The circle at each figure figures below, **figure 158**, **figure 160** and **figure 162**, show the coldest point of the interior surface at each detail in order to consider the f_{Rsi}. Below these graphs the corresponding surface temperature at this point is shown over a ten-year simulation below, **figure 159**, **figure 161** and **figure 163**.

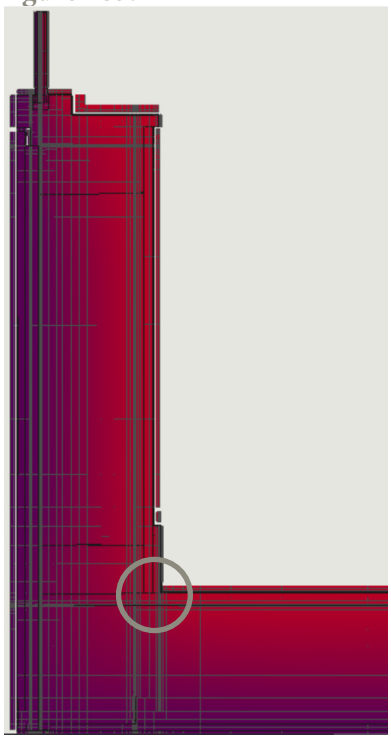

Figure A158, Highlight lowest point, V1

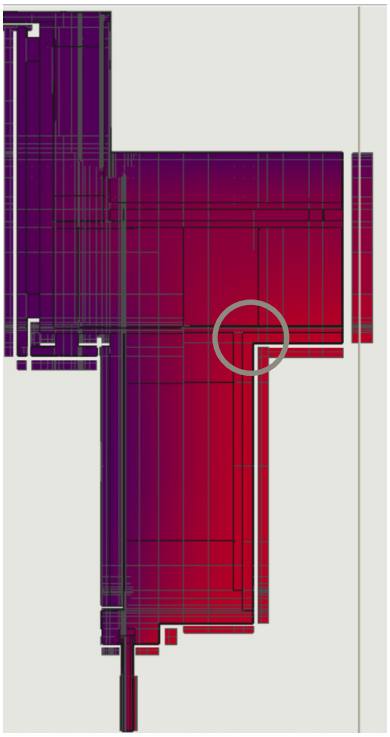

Figure A160, Highlight lowest point, V2

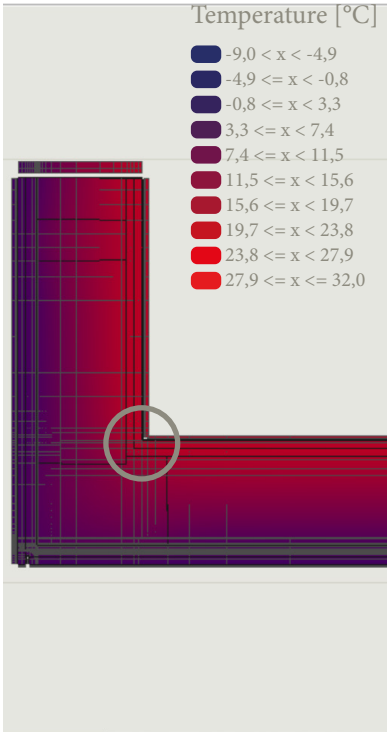

Figure A162, Highlight lowest point, H1

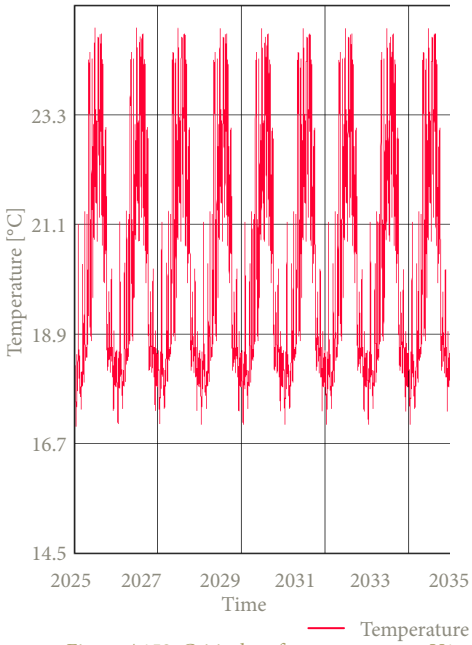

Figure A159, Critical surface temperature, V1

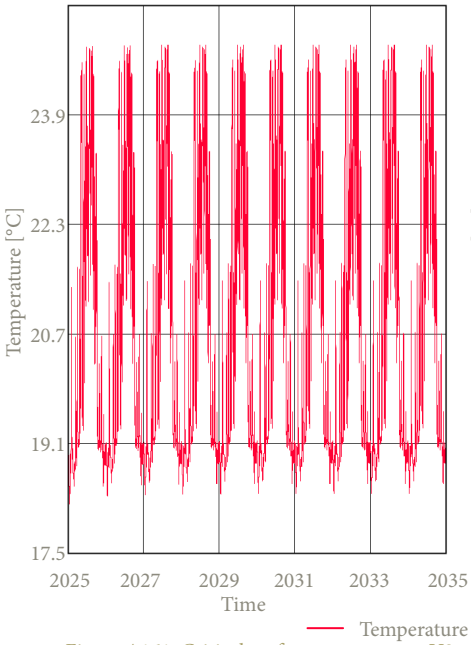

Figure A161, Critical surface temperature, V2

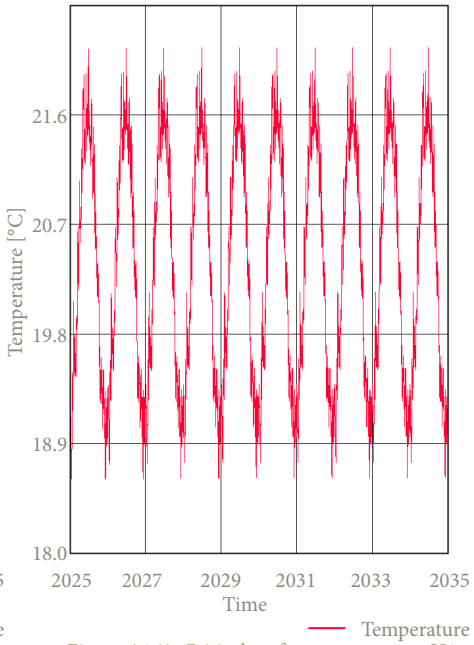

Figure A163, Critical surface temperature, H1

From this graph the lowest surface temperature of this detail is **15.58 °C**.

The resulting f_{Rsi} for this detail is **0.63** which exceeds the minimum requirement of 0.61. This indicates a negligible risk of surface condensation.

From this graph the lowest surface temperature of this detail is **18.09 °C**.

The resulting f_{Rsi} for this detail is **0.84** which exceeds the minimum requirement of 0.61. This indicates a negligible risk of surface condensation.

From this graph the lowest surface temperature of this detail is **18.60 °C**.

The resulting f_{Rsi} for this detail is **0.88** which exceeds the minimum requirement of 0.61. This indicates a negligible risk of surface condensation.

F-factor - V1, V2 & H1

The resulting **f-factor** of **detail V1** is **0.88** for a temperature of **15.93 °C**. Next the resulting **f-factor** of **detail V2** is **0.93** for a temperature of **16.74 °C**. Lastly, the resulting **f-factor** of **detail H1** is **0.93** for a temperature of **16.86 °C**. This indicates a very limited thermal bridge is assessed within the details of this configuration.
Given that these values significantly all exceeds the required threshold of **0.65**, it can be concluded that the details within this configuration complies with the thermal performance requirements set by the Dutch Building Decree.

PSI-value - V1

Table A33, Calculation of the $Q_{ideal\ condition}$

$R_{construction,\ window}$ [(m²K)/W]	$A_{construction,\ window}$ [m²]	$R_{construction,\ wall}$ [(m²K)/W]	$A_{construction,\ wall}$ [m²]	$R_{construction,\ floor}$ [(m²K)/W]	$A_{construction,\ floor}$ [m²]
0.600	0.2425	5.090	1.019	4.648	0.747

The resulting $\mathbf{Q_{ideal\ condition}}$ is **13.771 W**

Q_{WUFI} represents the sum of all heat flows through the detail, resulting in a total heat flow of **14.891 W**.

These values give a **Ψ-value** of **0.062 W/(mK)** for **detail V1**, indicating that the detail can be characterised as a well-insulated building component.

PSI-value - V2

Table A34, Calculation of the $Q_{ideal\ condition}$

$R_{construction,\ window}$ [(m²K)/W]	$A_{construction,\ window}$ [m²]	$R_{construction,\ wall}$ [(m²K)/W]	$A_{construction,\ wall}$ [m²]	$R_{construction,\ roof}$ [(m²K)/W]	$A_{construction,\ roof}$ [m²]
0.600	0.2425	5.090	0.887	6.442	0.190

The resulting $\mathbf{Q_{ideal\ condition}}$ is **10.872 W**

Q_{WUFI} represents the sum of all heat flows through the detail, resulting in a total heat flow of **12.370 W**.

These values give a **Ψ-value** of **0.083 W/(mK)** for **detail V2**, indicating that the detail can be characterised as a well-insulated building component.

PSI-value - H1

Table A35, Calculation of the $Q_{ideal\ condition}$

$R_{construction,\ window}$ [(m²K)/W]	$A_{construction,\ window}$ [m²]	$R_{construction,\ wall}$ [(m²K)/W]	$A_{construction,\ wall}$ [m²]
0.600	0.2425	5.090	2.149

The resulting $\mathbf{Q_{ideal\ condition}}$ is **14.875 W**

Q_{WUFI} represents the sum of all heat flows through the detail, resulting in a total heat flow of **16.008 W**.

These values give a **Ψ-value** of **0.063 W/(mK)** for **detail H1**, indicating that the detail can be characterised as a well-insulated building component.

Assessment detail configuration

Important notes about the details

For the given configuration, **key considerations** are presented below in the form of bullet points. These points highlight specific aspects that need to be taken into account during detailing and construction.

- Place the flexible flax between the studs of the wooden frame.
- Finish the inside of the wooden frame with a pressure-resistant wood fibre board to allow for fixings.
- Attach the water-resistant barrier of the window frame to the timber structural frame.
- Apply a water-resistant, vapour-permeable membrane over the timber frame construction to protect the flexible flax against mould growth.
- Use one 180 mm flax board and one 40 mm flax board to achieve the required insulation thickness.
- The wooden lintel must have proper bearing on the wooden frame.
- The screws of the battens must reach the center of the timber frame to ensure secure attachment.
- Stainless steel nails must be at least 2.5 times the thickness of the cladding.
- The stainless steel nails must be placed 40 mm from the outer edge of the cladding.
- Ensure 4 mm gaps between the cladding to accommodate the movement of the wood.
- Ensure 10 mm gaps for ventilation both between cladding boards and at the window frame.
- Use a clay base plate to provide a correct underlayment for the clay plaster.
- Use a jute reinforcement mesh between the rough and finishing clay plaster to prevent cracking.

Assessment of the configuration

Additionally, the configuration is evaluated based on the following criteria:

1. **Weight**: The total mass per unit area of the wall construction.
2. **Construction time**: The time required for assembling the construction.
3. **Resistance Construction-value:** The combined thermal resistance of all layers in the construction.
4. **Phase shift**: The heat transfer delay of the structure.

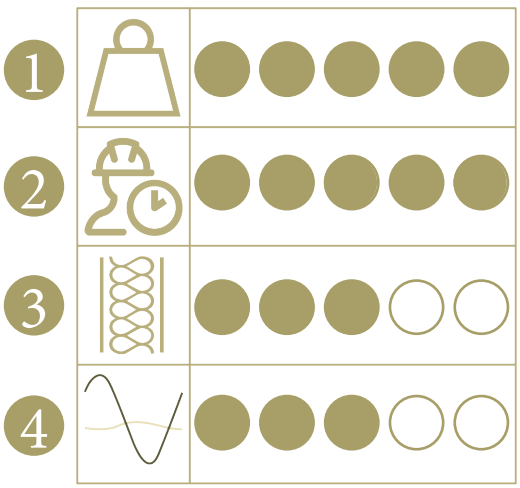

Axonometric view of the detail configuration

In addition to the presented details, an **axonometric view** of the respective detail is also shown. This is presented in the figure below, **figure 164**, and is intended to provide more clarity and insight into **detail V1, detail V2,** and **detail H1**.

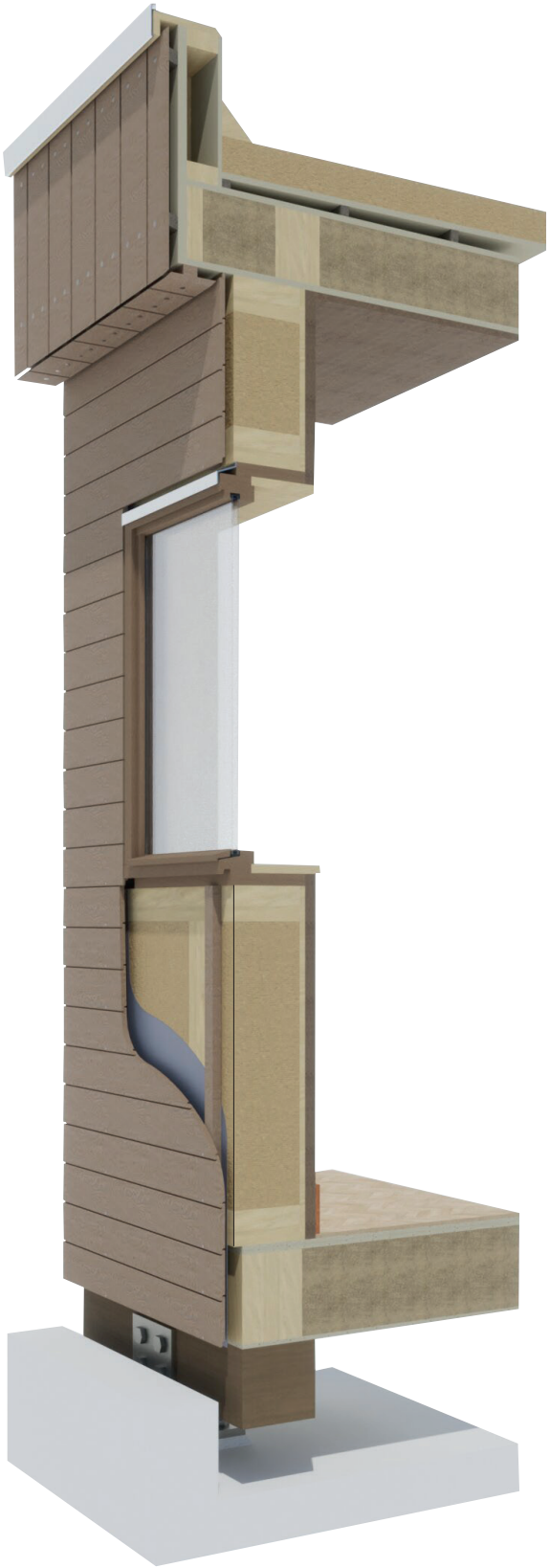

Figure A164, Axonometric view of detail configuration 6

Detail configuration 7 - flax insulation with cork façade

The seventh detail configuration consists of flexible flax insulation placed between the studs of the timber construction frame. To protect the flax against water and mould growth a water-resistant vapour-permeable membrane is placed at the outside of the timber frame construction. Next, a biobased, diffusion-open construction board is applied for structural stability and for the application of the cork façade system. This board enables the attachment of the expanded insulation corkboard, which is bonded using a cork mortar. On top of the expanded insulation corkboard, another layer of cork mortar is applied to bond the cork cladding panels. On the interior side, the timber construction frame is finished with a biobased, diffusion-open construction board to which a clay board is screwed. A clay plaster can then be applied to this board, consisting of a rough layer and a finishing layer.

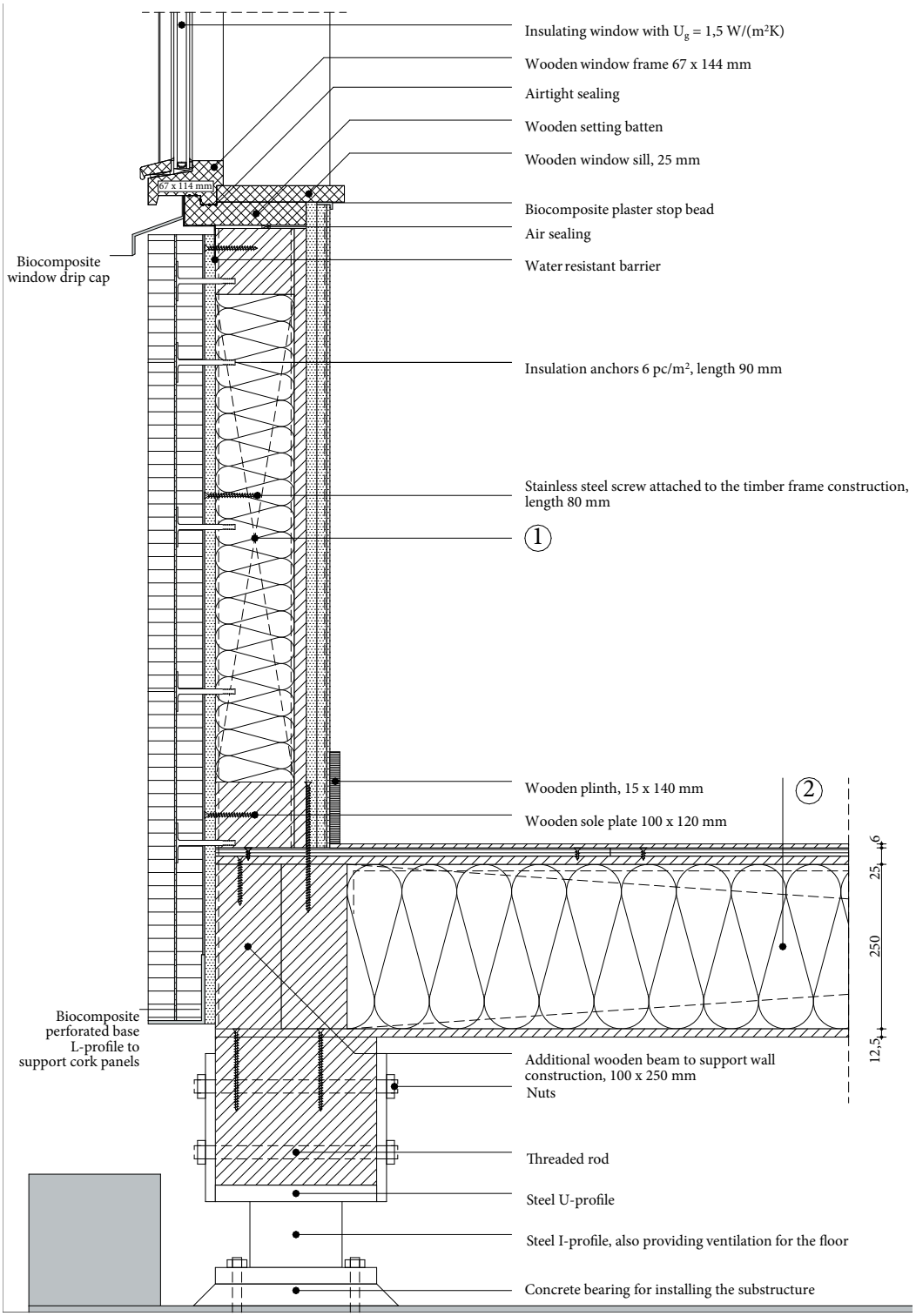

Figure A165, 1:10 detail of V1, configuration 7, own illustration

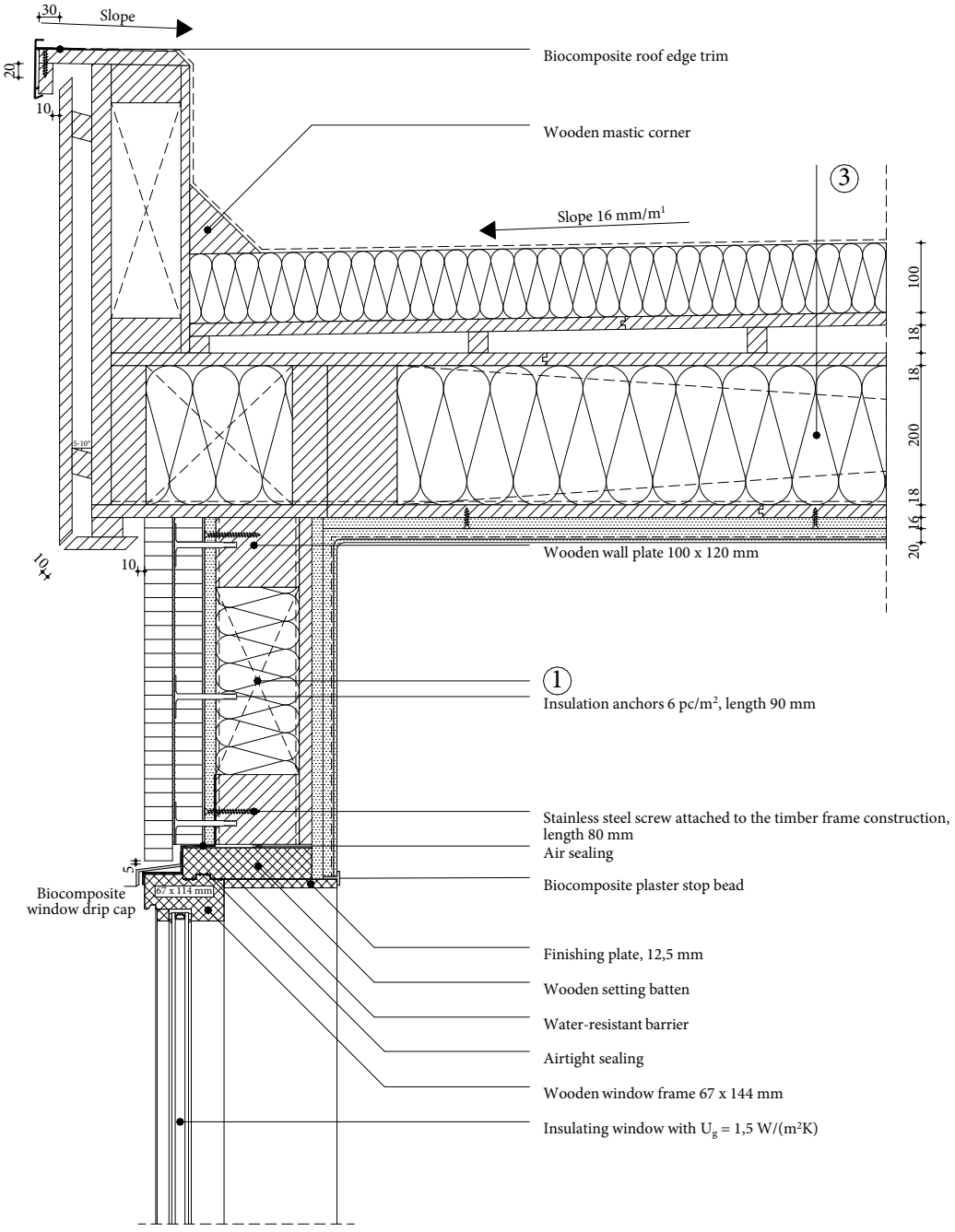

Figure A166, 1:10 detail of V2, configuration 7, own illustration

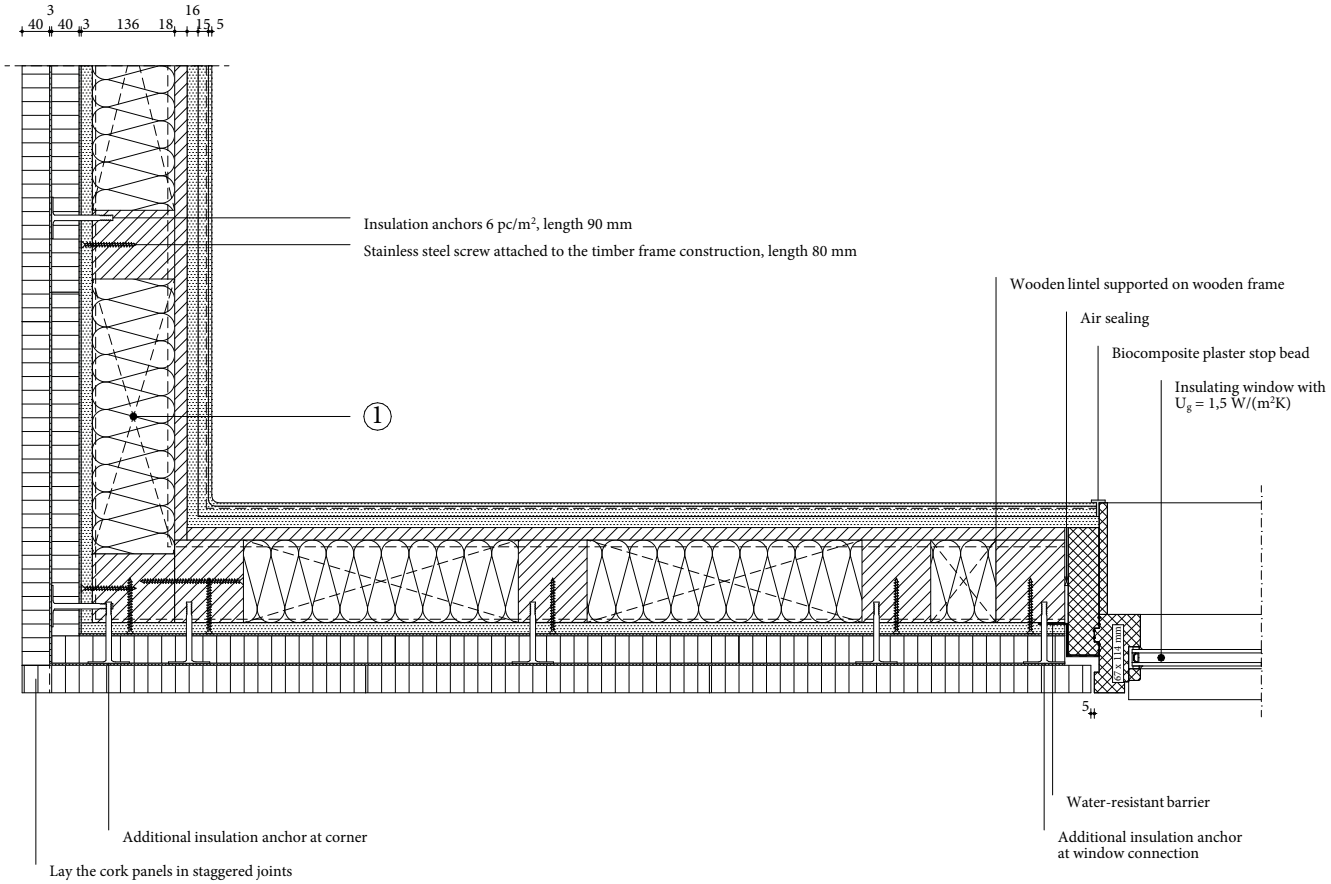

Figure A167, 1:10 detail of H1, configuration 7, own illustration

❶ Wall construction build-up, RC-value: 4.89 (m²K)/W

- Cork cladding panels (λ ≤ 0.043 W/mK), 40 mm;
- Cork mortar, 3 mm;
- Expanded insulation corkboard (λ ≤ 0.039 W/mK), 40 mm;
- Cork mortar, 3 mm;
- Biobased diffusion open construction board, 16mm;
- Water resistant vapour-permeable membrane;
- Timber frame construction, 100 x 120 mm, center-to-center 500 mm;
- Flexible flax insulation, placed between construction (λ ≤ 0.035 W/mK), 120 mm;
- Vapour-retarding and airtight membrane with a variable vapour diffusion resistance;
- Biobased construction board, 18 mm;
- Clay base plate, 16 mm;
- Rough base clay plaster, 15 mm;
- Jute reinforcement mesh;
- Finishing clay plaster, 5 mm.

❷ Floor construction build-up, RC-value: 4.65 (m²K)/W

- Finishing board, 6 mm;
- Biobased wooden construction board, 12.5 mm;
- Biobased wooden construction board, perpendicular on the other plate, 12.5 mm;
- Vapour-retarding and airtight membrane with a variable vapour diffusion resistanance;
- Flexible hemp fiber insulation placed between construction (λ ≤ 0.043 W/(mK), 250 mm;
- Wooden beams 100 x 250 mm, center-to-center 600 mm;
- Biobased wooden construction board, 12.5 mm.

❸ Roof construction build-up, RC-value: 6.71 (m²K)/W

- EPDM glued on underlayment to prevent roof covering from lifting;
- Pressure-resistant woodfibre insulation plate (λ ≤ 0.042 W/(mK), 100 mm;
- Biobased wooden construction board, 18 mm;
- Sloped wooden battens for drainage at an angle of 16 mm/m^1, 28 x 24 mm;
- Biobased wooden construction board, 18 mm;
- Flexible hemp fiber insulation placed between construction (λ ≤ 0.043 W/(mK), 200 mm;
- Wooden beams 100 x 200 mm, center-to-center 600 mm;
- Vapour-retarding and airtight membrane with a variable vapour diffusion resistanance;
- Biobased wooden construction board, 18 mm;
- Clay base plate, 16 mm;
- Rough base clay plaster, 15 mm;
- Jute reinforcement mesh;
- Finishing clay plaster, 5 mm.

U_g = 1.50 W/(m²K)

U_w = 1.76 W/(m²K)

f-factor ≥ 0.65

Ψ_{V1}: 0.061 W/(mK) Ψ_{V2}: 0.078 W/(mK) Ψ_{H1}: 0.085 W/(mK)

Isopleths: no risk of mould $f_{R,si} > f_{R,si,\,max}$; no risk of mould

Phase shift of the wall construction: 5.5 h

Density of the wall construction 104 kg/m³

Calculation RC-value wall construction build-up

❶ Wall construction build-up, RC-value: 4.89 (m²K)/W

Table A36, Calculation of the RC-value of the wall construction build-up

Material	Thickness [m]	Thermal conductivity [W/(mK)]	Thermal resistance [W/(m²K)]
Tongue and groove cork cladding panels	0,040	0,043	0,930
Cork mortar	0,003	0,250	0,012
Expanded insulation corkboard	0,040	0,039	1,025
Cork mortar	0,003	0,250	0,012
Biobased diffusion open construction board	0,016	0,090	0,178
Timber frame construction, with expanded insulation corkboard	0,120	0,051	2,353
Biobased construction board	0,018	0,120	0,150
Clay base plate	0,016	0,470	0,034
Clay plaster	0,020	0,910	0,022

Table A37, Calculation of the equivalent thermal conductivity of the individual layers in the relevant build-up

	Layer 1		Layer 2	
Material	Area [m²]	Thermal conductivity [W/(mK)]	Area [m²]	Thermal conductivity [W/(mK)]
Ventilated cavity with vertical wooden cladding batten, center-to-center 600 mm	0,0012	0,130	0,0168	0,337
Timber frame construction, with flexible flax	0,1320	0,071	0,0220	0,130

Density mass per unit area of the wall construction

Table A138, Calculation of the density mass per unit area

Material	Thickness [m]	Density [kg/m³]
Tongue and groove cork cladding panels	0,040	140
Cork mortar	0,003	1000
Expanded insulation corkboard	0,040	110
Cork mortar	0,003	1000
Biobased diffusion open construction board	0,016	565
Timber frame construction, with expanded insulation corkboard	0,120	124
Biobased construction board	0,018	621
Clay base plate	0,016	1300
Clay plaster	0,020	1600

By using the previously presented formula a **m'-value** of **103.90 kg/m²** can be given for the **seventh detail configuration**.

Phase-shift

Table A139, Calculation of the phase shift

Material	Thickness [m]	Thermal conductivity [W/(mK)]	Density [kg/m³]	Specific heat capacity [J/(kgK)]
Timber frame construction, with flexible flax insulation	0,120	0,051	124	1600

By using the presented phase shift formula, the resulting **φ-value** for **the seventh configuration** is **5.5 h.**

Geometry WUFI

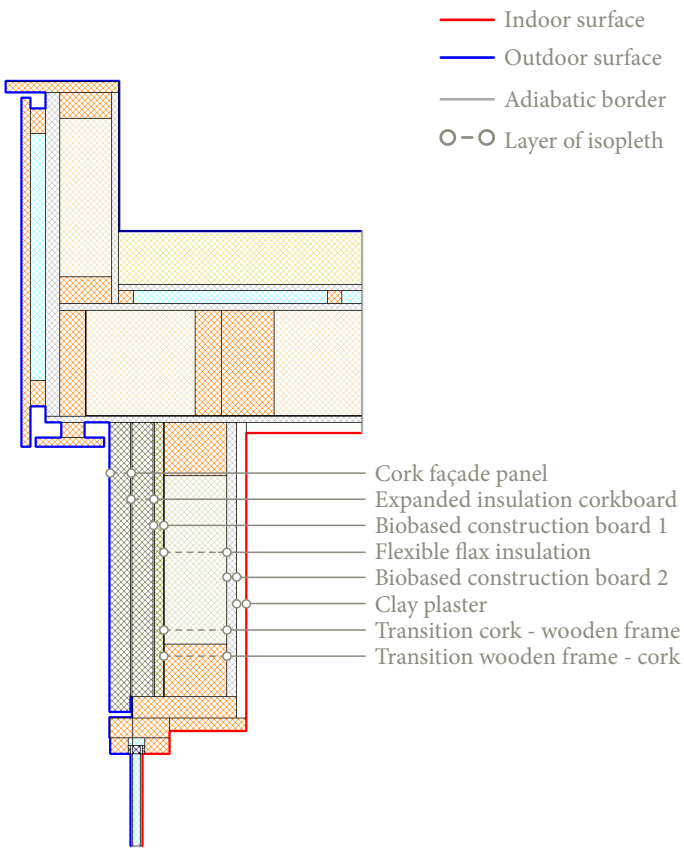

Figure A169, geometry detail V2 including location isopleths

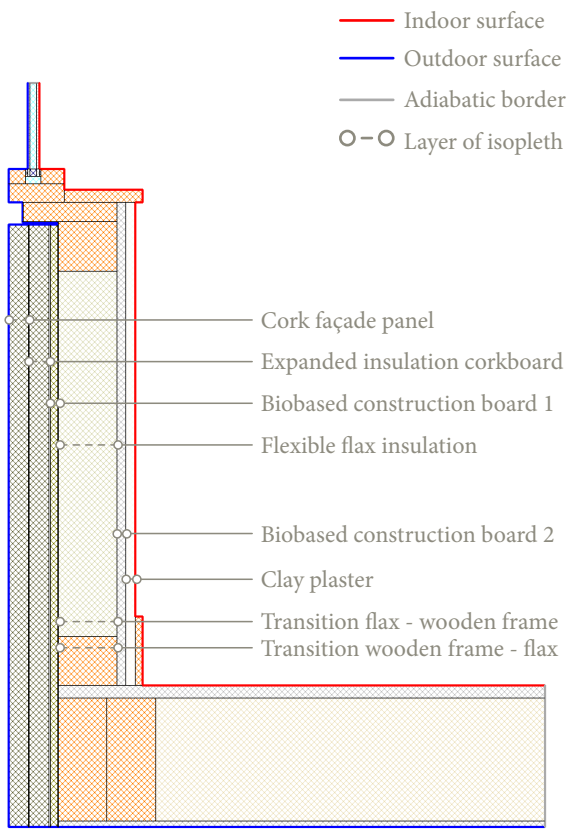

Figure A170, geometry detail V1 including location isopleths

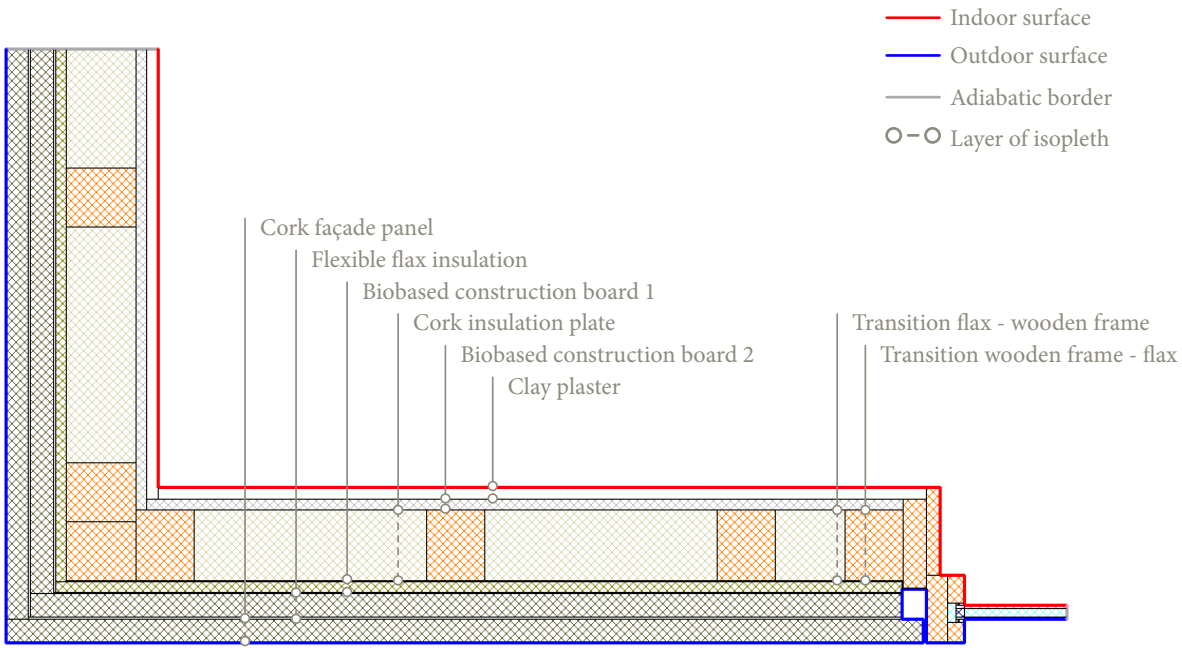

Figure A168, geometry detail H1 including location isopleths

Isopleths - V1

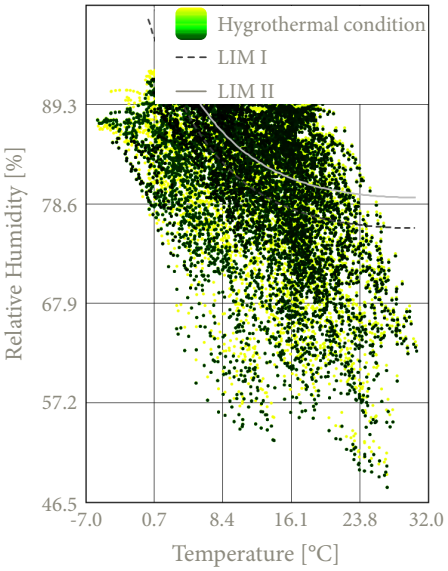

Figure A171, Isopleths cork façade panel

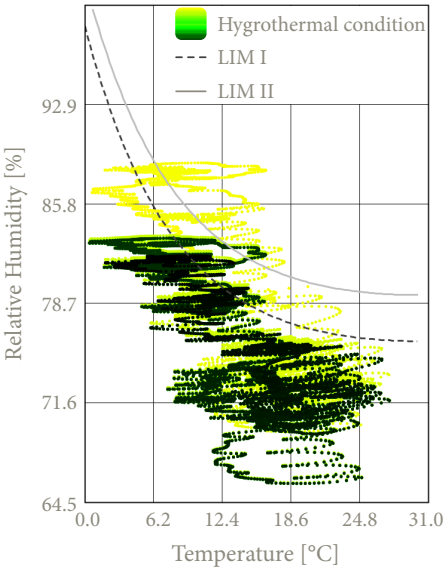

Figure A172, Isopleths expanded insulation corkboard

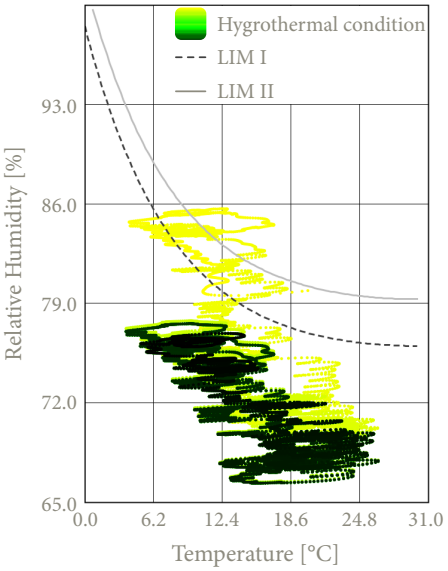

Figure A173, Isopleths biobased construction board 1

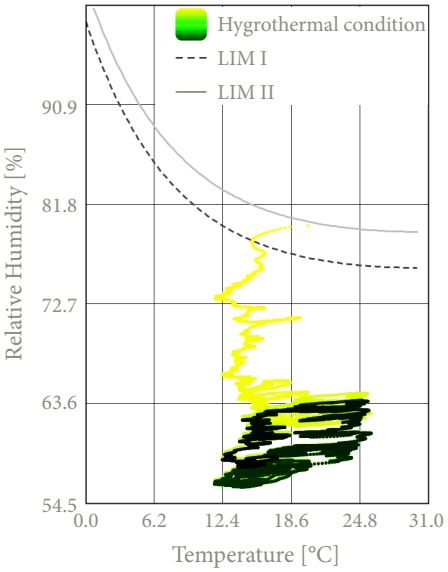

Figure A174, Isopleths flexible flax insulation

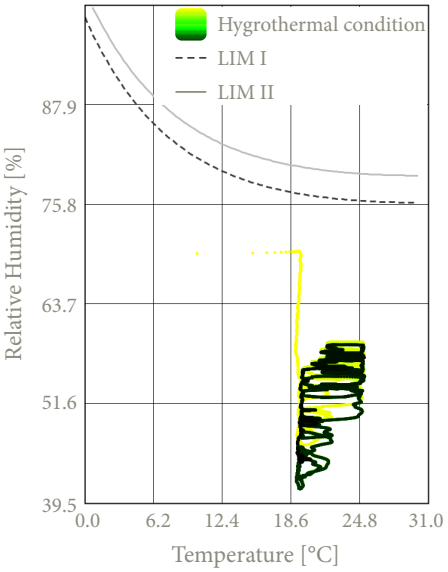

Figure A175, Isopleths biobased construction board 2

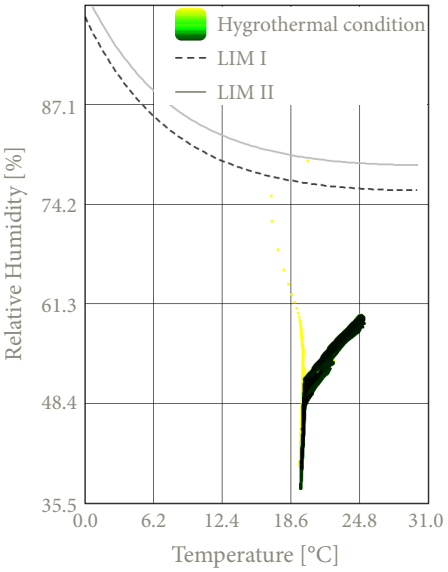

Figure A176, Clay plaster

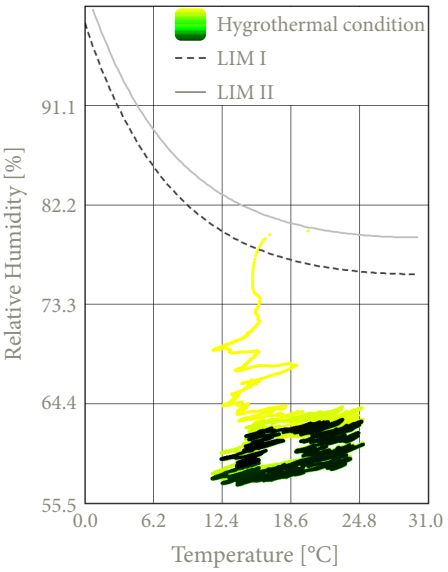

Figure A177, Isopleths transition flax & frame

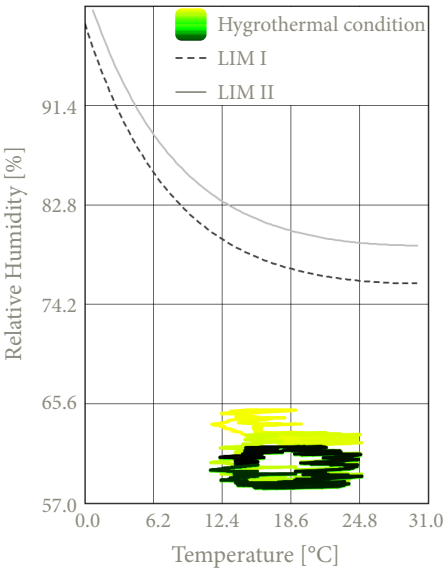

Figure A178, Isopleths transition frame & flax

Isopleths - V2

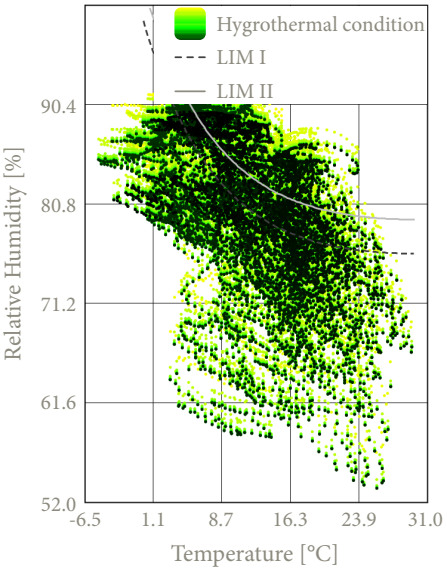

Figure A179, Isopleths cork façade panel

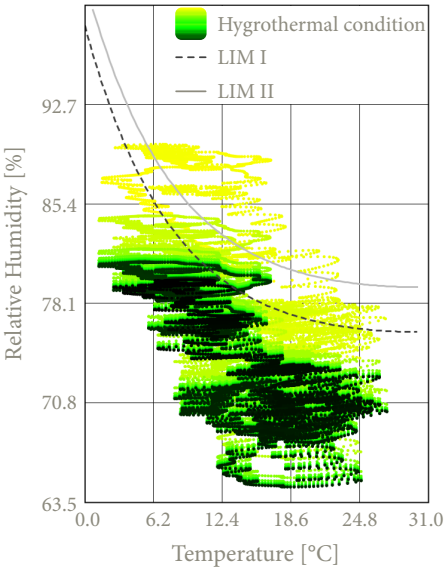

Figure A180, Isopleths expanded insulation corkboard

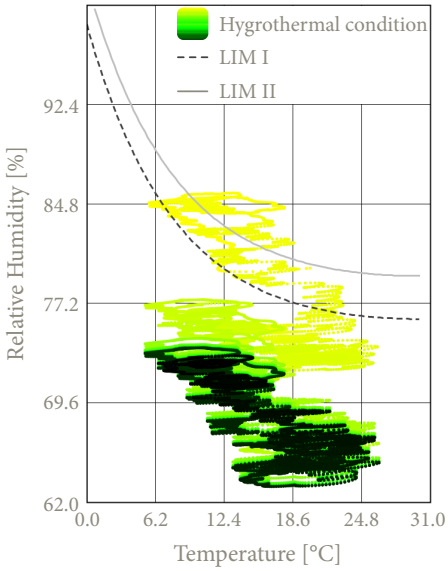

Figure A181, Isopleths biobased construction board 1

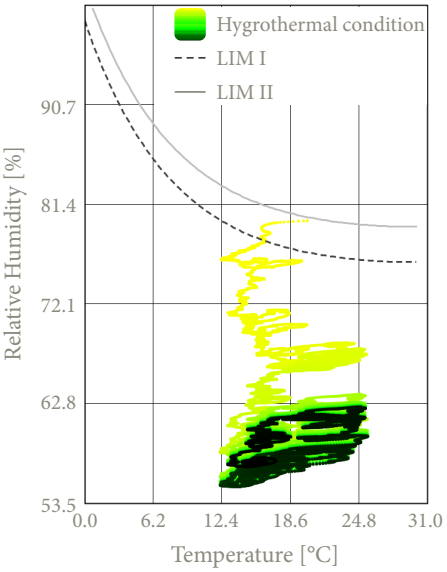

Figure A182, Isopleths flexible flax insulation

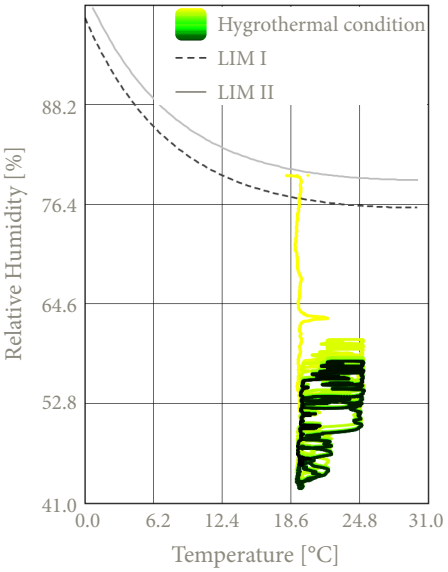

Figure A183, Isopleths biobased construction board 2

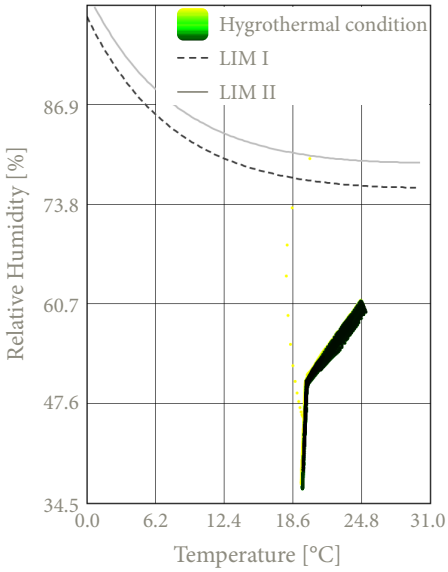

Figure A184, Clay plaster

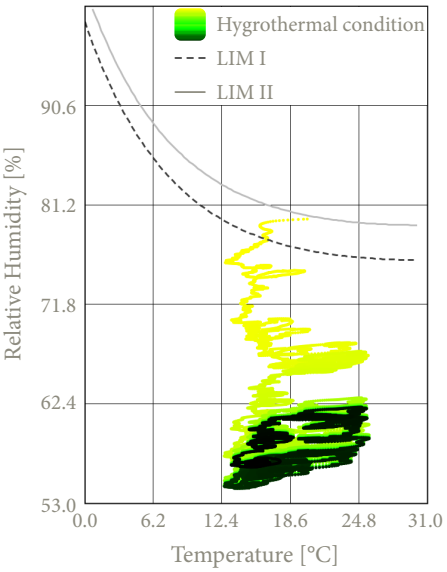

Figure A185, Isopleths transition flax & frame

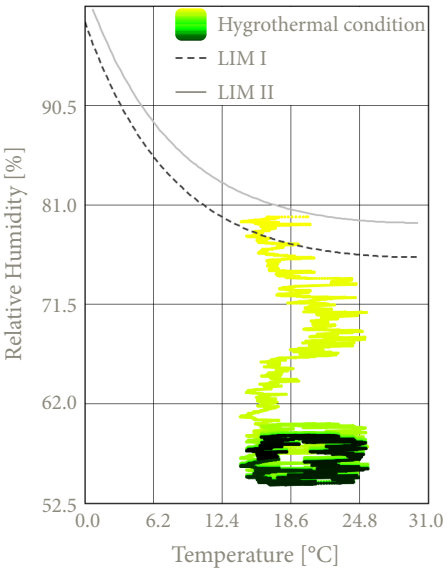

Figure A186, Isopleths transition frame & flax

Isopleths - H1

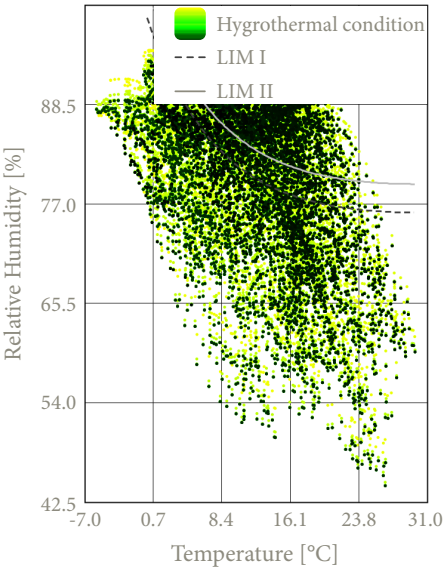

Figure A187, Isopleths cork façade panel

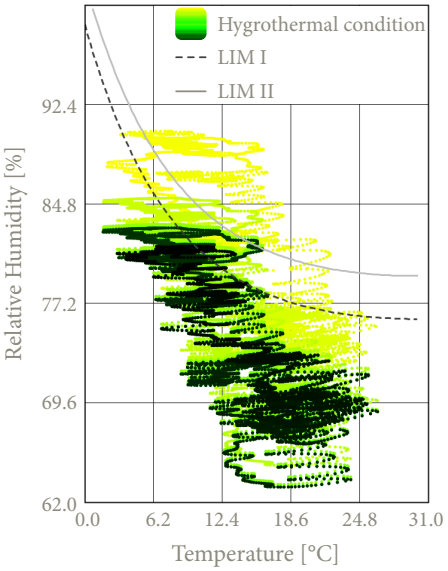

Figure A188, Isopleths expanded insulation corkboard

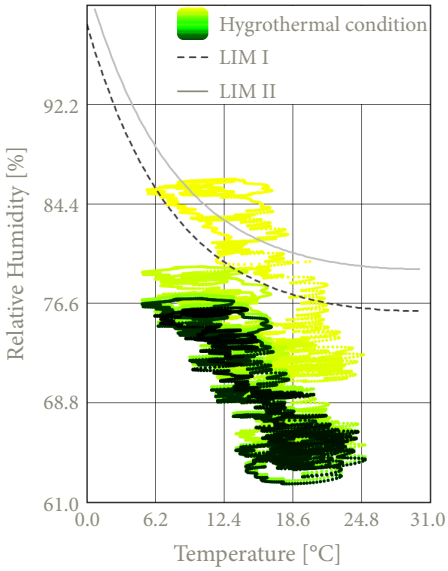

Figure A189, Isopleths biobased construction board 1

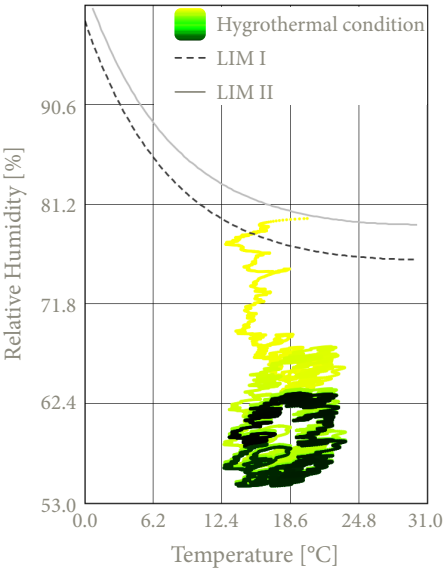

Figure A190, Isopleths flexible flax insulation

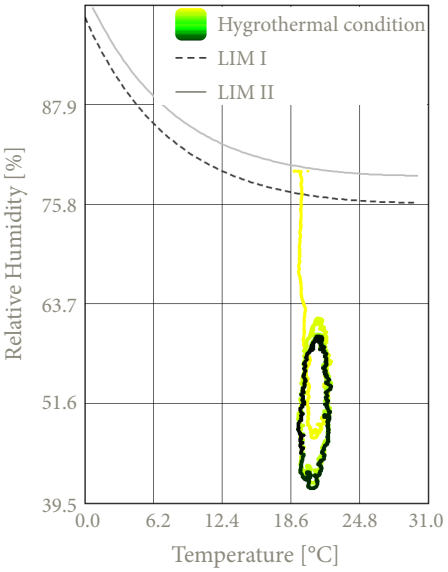

Figure A191, Isopleths biobased construction board 2

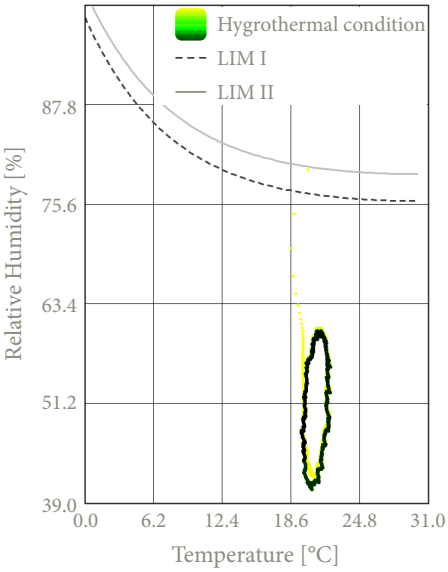

Figure A192, Clay plaster

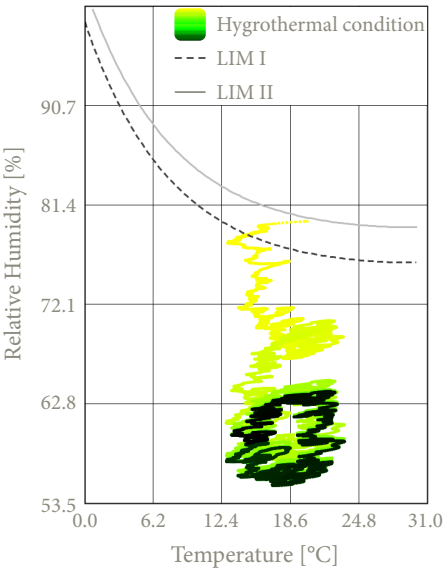

Figure A193, Isopleths transition flax & frame

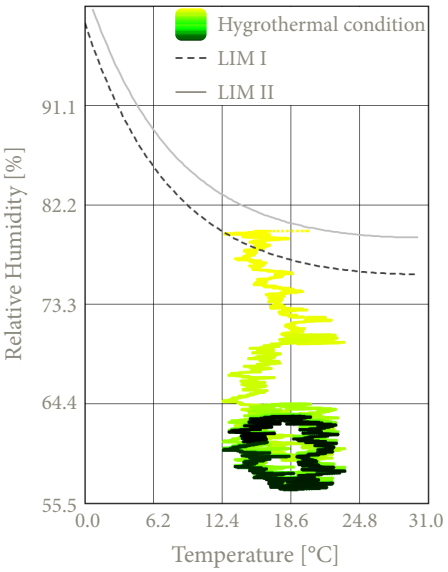

Figure A194, Isopleths transition frame & flax

Conclusion isoplteths

Based on the established and analysed isopleths of the various details within this construction **configuration**, it can be concluded that there is no risk of mould growth within the different material layers. All isopleths located behind the cork insulation plate remain below the critical threshold values **LIM I** and **LIM II**, indicating that the details meet the established criteria.

With regards to the **cork façade panel** it can be observed that the isopleths mostly exceed the LIM threshold values, which is the same as in the other two cork configuration assessments. Therefore, a similar conclusion can be drawn as in the previous cork configurations based on the paper by (Hon, 2024). Just like in both the previous cork configurations, in order to state with certainty that no mould growth occurs in the cork as an exterior panel material, additional research is required.

The board that is glued with cork mortar behind the cork façade panel, the **expanded insulation corkboard**, shows primarily in V2 and H1 that the isopleths exceed the LIM lines at the initial conditions. The isopleths of the expanded insulation corkboard in V1 show a small exceedance at the beginning. However, over time the moisture present in the material at the start, approximately 80%, is transported out. This is because, as previously stated, cork is a porous material making it capable of buffering fluctuations in relative humidity. As a result, the isopleths drop below the LIM lines over time. In V2 and H1 a relatively strong downward trend is visible compared to V1, however, for all three isopleths the values fall below the LIM thresholds for most of the simulation period. Nevertheless, at the end of the simulation, the isopleths still slightly exceed the LIM I line. However, for the majority of the year, the isopleths remain below both LIM thresholds. The continuously decreasing trend and the fact that the isopleths are for the majority of the year below the thresholds, suggests that there is no long-term risk of mould development.

When examining the isopleths of the **outside biobased construction board**, it can be seen that the isopleths, apart from a short period at the beginning, remain below the LIM thresholds and all show a downward trend. When comparing the isopleths between this flax configuration and the previous cork configurations with a cork cladding it becomes clear that this configuration has the same effect on the biobased construction board as the second cork configuration. This means that the construction board is better protected against mould growth due to the additional expanded insulation corkboard and the cork mortar. In this configuration, a downward trend is also visible in the isopleths. Therefore, with regard to mould resistance the outside construction board has no risk of mould growth.

With regard to the isopleths of the **flexible flax insulation**, as well as the **transition zones between the flax and the wooden construction frame**, the values remain well below both LIM threshold values and a downward trend is visible in these isopleths. Lastly, the isopleths of the **inside biobased construction board**, and the **clay plaster**, also remain well below the LIM lines with a slight upward trend visible in the inside biobased construction board. However, the isopleths remain far below the LIM lines so this upward trend does nog negatively affect the risk of mould growth.

In conclusion, it can be stated that this configuration poses no risk of mould growth and thus complies with the specified isopleth requirements. However, in order to fully confirm this, further research is needed regarding the cork panel used on the exterior. As such, the design complies with the required hygrothermal performance standards.

Surface condensation - V1, V2 & H1

The circle at each figure figures below, **figure 195**, **figure 197** and **figure 199**, show the coldest point of the interior surface at each detail in order to consider the f_{Rsi}. Below these graphs the corresponding surface temperature at this point is shown over a ten-year simulation below, **figure 196**, **figure 198** and **figure 200**.

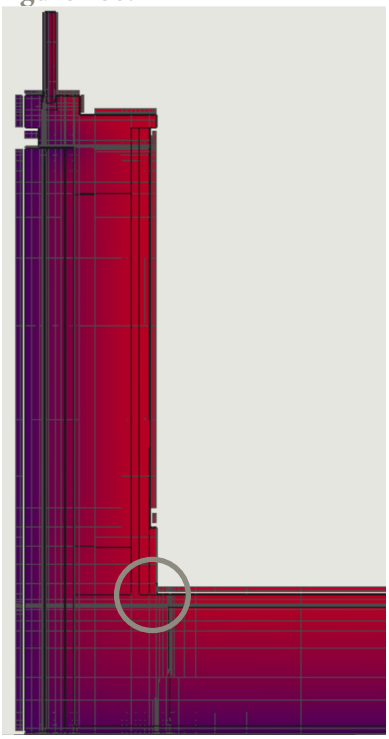

Figure A195, Highlight lowest point, V1

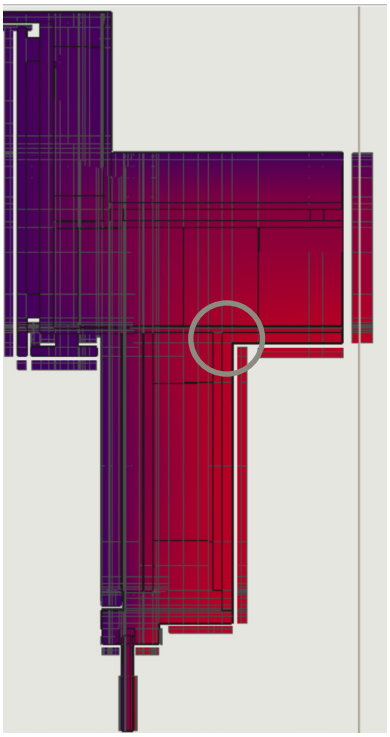

Figure A197, Highlight lowest point, V2

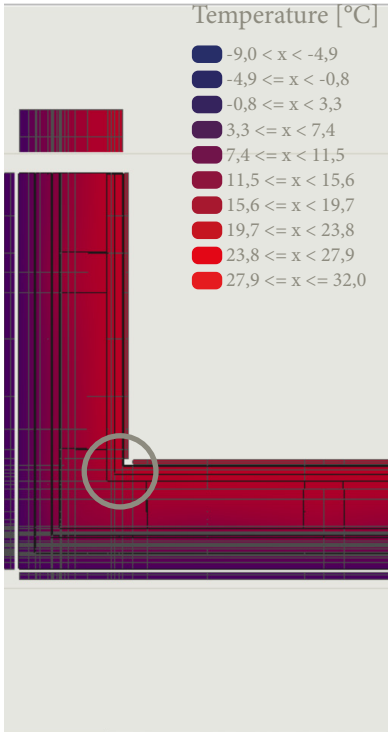

Figure A199, Highlight lowest point, H1

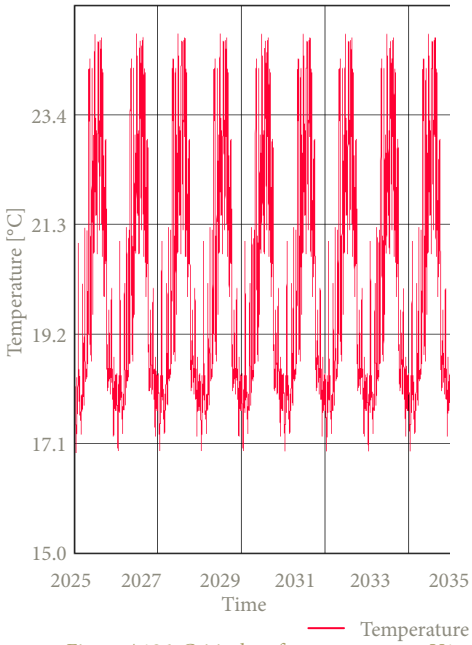

Figure A196, Critical surface temperature, V1

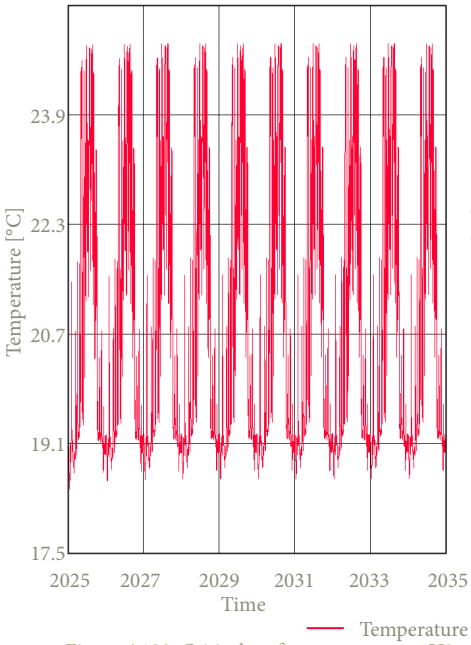

Figure A198, Critical surface temperature, V2

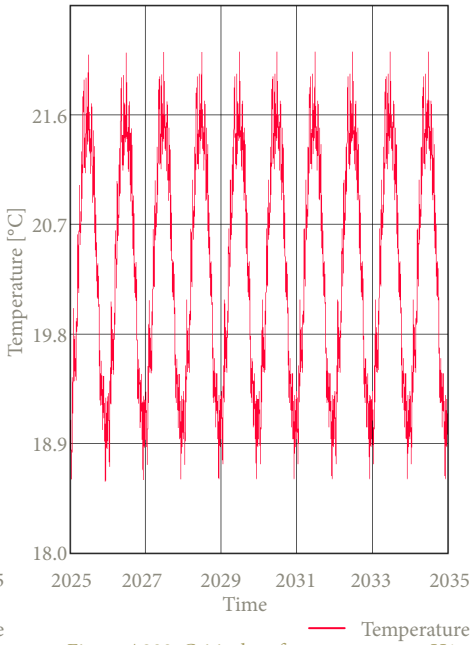

Figure A200, Critical surface temperature, H1

From this graph the lowest surface temperature of this detail is **15.36 °C**.

The resulting f_{Rsi} for this detail is **0.61** which is the same as the minimum requirement of 0.61. This indicates a negligible risk of surface condensation.

From this graph the lowest surface temperature of this detail is **18.10 °C**.

The resulting f_{Rsi} for this detail is **0.84** which exceeds the minimum requirement of 0.61. This indicates a negligible risk of surface condensation.

From this graph the lowest surface temperature of this detail is **18.58 °C**.

The resulting f_{Rsi} for this detail is **0.88** which exceeds the minimum requirement of 0.61. This indicates a negligible risk of surface condensation.

F-factor - V1, V2 & H1

The resulting **f-factor** of **detail V1** is **0.88** for a temperature of **15.82 °C**. Next the resulting **f-factor** of **detail V2** is **0.88** for a temperature of **16.92 °C**. Lastly, the resulting **f-factor** of **detail H1** is **0.93** for a temperature of **16.86 °C**. This indicates a very limited thermal bridge is assessed within the details of this configuration.
Given that these values significantly all exceeds the required threshold of **0.65**, it can be concluded that the details within this configuration complies with the thermal performance requirements set by the Dutch Building Decree.

PSI-value - V1

Table A40, Calculation of the $Q_{ideal\ condition}$

$R_{construction,\ window}$ [(m²K)/W]	$A_{construction,\ window}$ [m²]	$R_{construction,\ wall}$ [(m²K)/W]	$A_{construction,\ wall}$ [m²]	$R_{construction,\ floor}$ [(m²K)/W]	$A_{construction,\ floor}$ [m²]
0.600	0.2425	4.886	1.019	4.648	0.857

The resulting $\mathbf{Q_{ideal\ condition}}$ is **14.348 W**

Q_{WUFI} represents the sum of all heat flows through the detail, resulting in a total heat flow of **15.443 W**.

These values give a **Ψ-value** of **0.061 W/(mK)** for **detail V1**, indicating that the detail can be characterised as a well-insulated building component.

PSI-value - V2

Table A41, Calculation of the $Q_{ideal\ condition}$

$R_{construction,\ window}$ [(m²K)/W]	$A_{construction,\ window}$ [m²]	$R_{construction,\ wall}$ [(m²K)/W]	$A_{construction,\ wall}$ [m²]	$R_{construction,\ roof}$ [(m²K)/W]	$A_{construction,\ roof}$ [m²]
0.600	0.2425	4.886	0.867	6.442	0.221

The resulting $\mathbf{Q_{ideal\ condition}}$ is **11.087 W**

Q_{WUFI} represents the sum of all heat flows through the detail, resulting in a total heat flow of **12.491 W**.

These values give a **Ψ-value** of **0.078 W/(mK)** for **detail V2**, indicating that the detail can be characterised as a well-insulated building component.

PSI-value - H1

Table A42, Calculation of the $Q_{ideal\ condition}$

$R_{construction,\ window}$ [(m²K)/W]	$A_{construction,\ window}$ [m²]	$R_{construction,\ wall}$ [(m²K)/W]	$A_{construction,\ wall}$ [m²]
0.600	0.2425	4.886	2.283

The resulting $\mathbf{Q_{ideal\ condition}}$ is **15.686 W**

Q_{WUFI} represents the sum of all heat flows through the detail, resulting in a total heat flow of **17.219 W**.

These values give a **Ψ-value** of **0.085 W/(mK)** for **detail H1**, indicating that the detail can be characterised as a well-insulated building component.

Assessment detail configuration

Important notes about the details

For the given configuration, **key considerations** are presented below in the form of bullet points. These points highlight specific aspects that need to be taken into account during detailing and construction.

- Place the flexible flax between the studs of the wooden frame.
- Finish the inside of the wooden frame with a pressure-resistant wood fibre board to allow for fixings.
- Attach the water-resistant barrier of the window frame to the timber structural frame.
- Apply a water-resistant, vapour-permeable membrane over the timber frame construction to protect the flexible flax against mould growth.
- Apply a diffusion-open construction board with water-resistant properties onto the timber frame, over which cork mortar can be applied.
- Attach the cork façade panels using 3 mm cork mortar adhesive onto the cork insulation boards.
- Fix the cork insulation boards using both 3 mm cork mortar adhesive and mechanical fastening with insulation anchors to ensure a structurally secure base layer for the cork façade panels.
- Use 6 insulation anchors per m^2, with anchor lengths equal to the insulation board thickness plus 30 mm embedment depth.
- The wooden lintel must have proper bearing on the wooden frame.
- The screws of the biobased construction board must reach the center of the timber frame to ensure secure attachment.
- Ensure 5 mm ventilation gaps both between cork panels and at the window frame.
- Use a clay base plate to provide a correct underlayment for the clay plaster.
- Use a jute reinforcement mesh between the rough and finishing clay plaster to prevent cracking.

Assessment of the configuration

Additionally, the configuration is evaluated based on the following criteria:

1. **Weight**: The total mass per unit area of the wall construction.
2. **Construction time**: The time required for assembling the construction.
3. **Resistance Construction-value:** The combined thermal resistance of all layers in the construction.
4. **Phase shift**: The heat transfer delay of the structure.

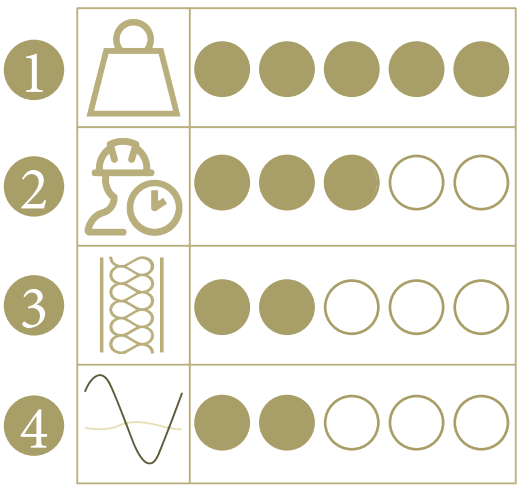

Axonometric view of the detail configuration

In addition to the presented details, an **axonometric view** of the respective detail is also shown. This is presented in the figure below, **figure 201**, and is intended to provide more clarity and insight into **detail V1, detail V2,** and **detail H1**.

Figure A201, Axonometric view of detail configuration 7

Detail configuration 8 - wood fibre insulation with wooden façade

The eighth detail configuration consists of flexible wood fibre insulation placed between the studs of the timber construction frame. To protect the timber frame construction against water and mould growth a pressure-resistant wood fibre board is placed at the outside of the timber frame construction. This board also enables the attachment of the wooden battens and the wooden façade. On the interior side, the timber construction frame is finished with a biobased, diffusion-open construction board to which a clay board is screwed. A clay plaster can then be applied to this board, consisting of a rough layer and a finishing layer.

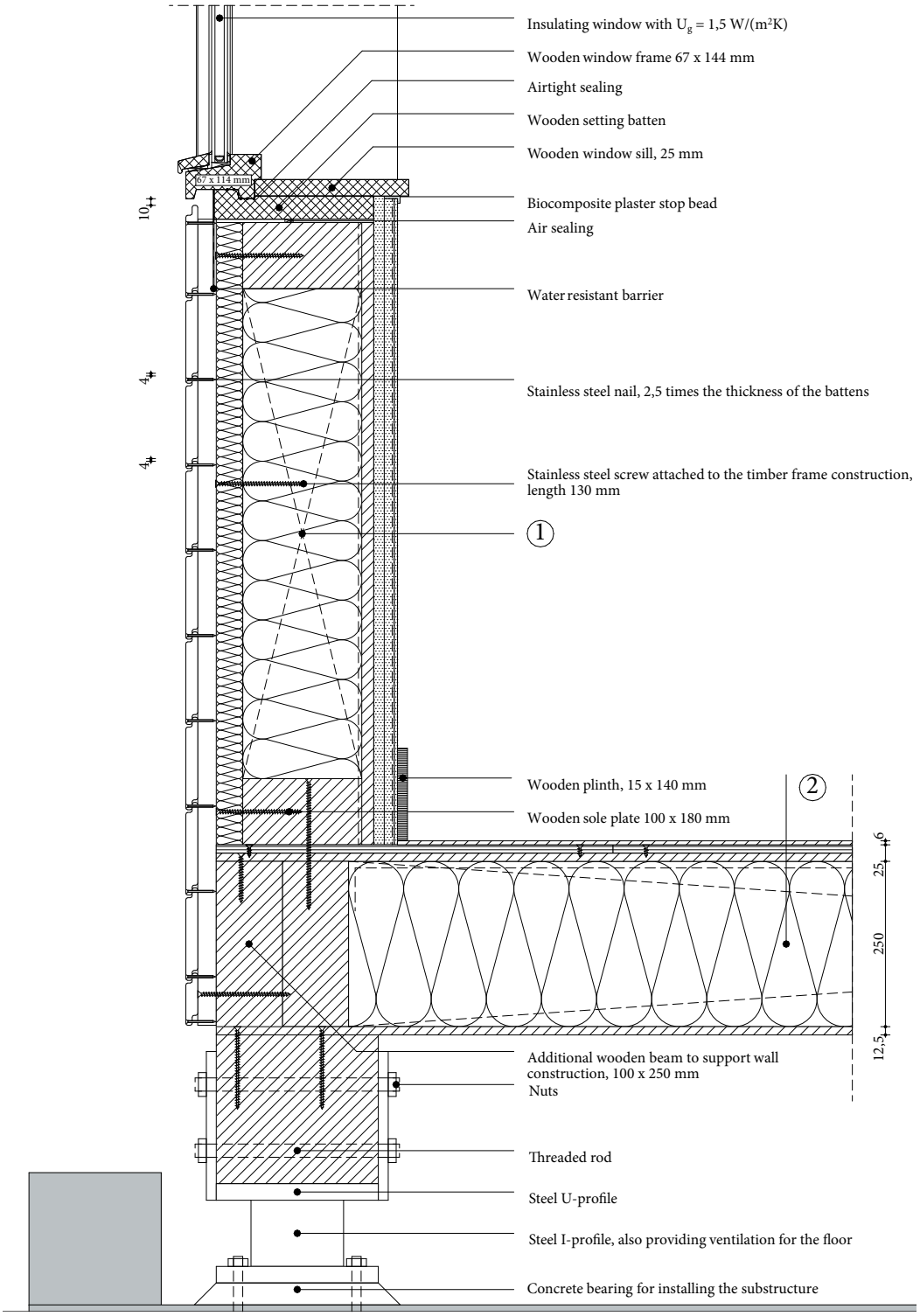

Figure A202, 1:10 detail of V1, configuration 8, own illustration

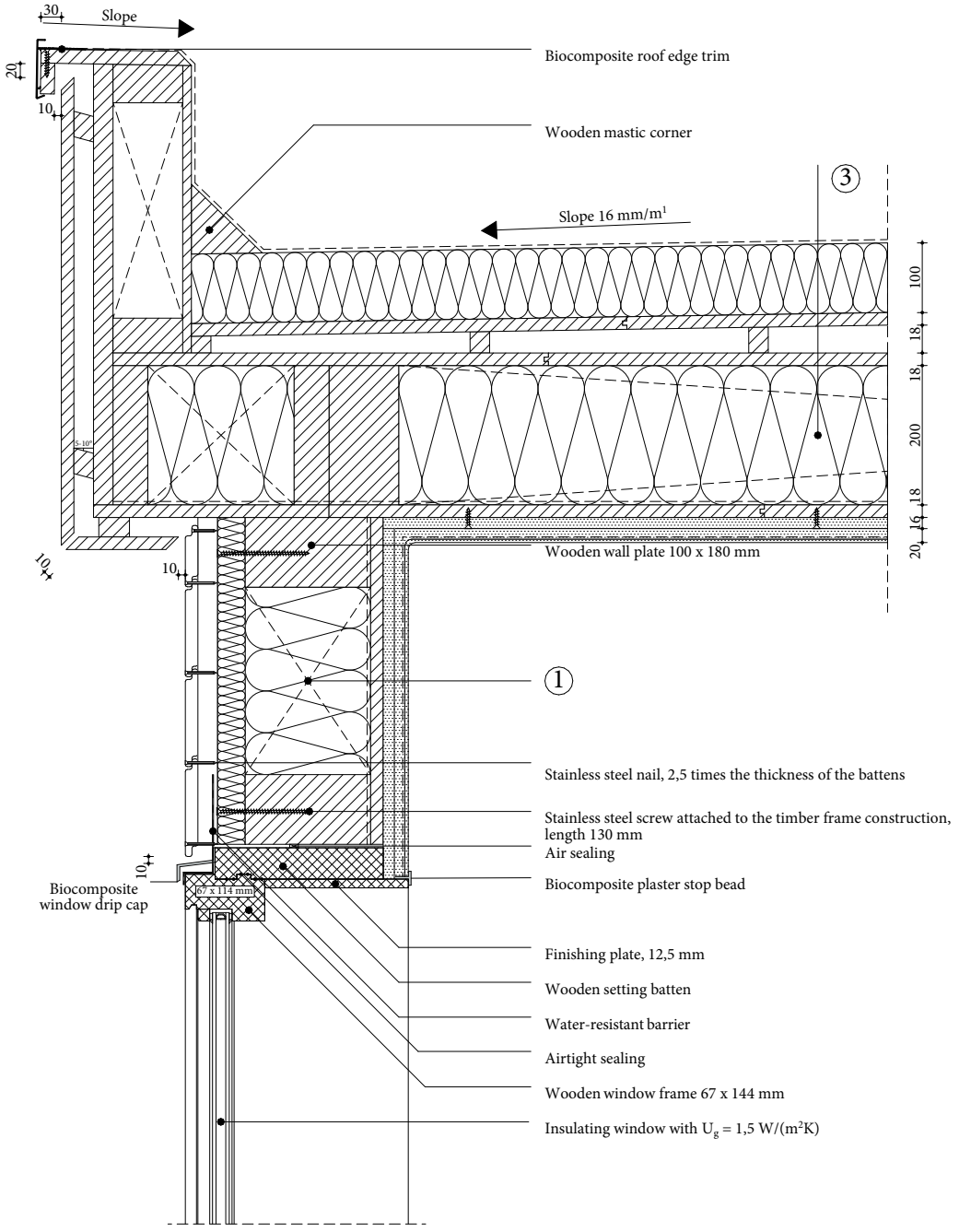

Figure A203, 1:10 detail of V2, configuration 8, own illustration

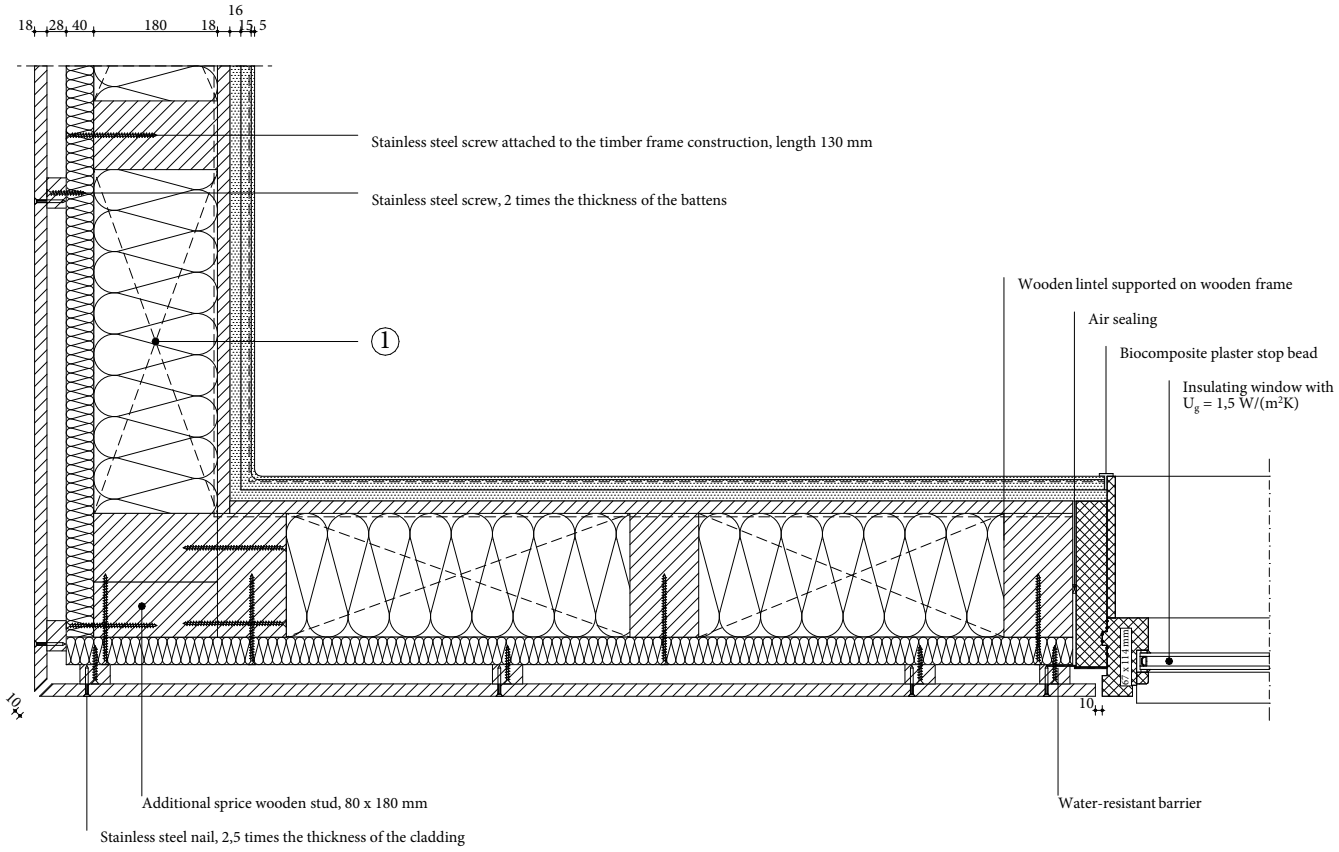

Figure A204, 1:10 detail of H1, configuration 8, own illustration

❶ Wall construction build-up, RC-value: 5.08 (m²K)/W

- Horizontal wooden cladding, 18 mm;
- Vertical spruce cladding batten forming ventilated cavity, 28 x 44 mm, center-to-center 600 mm;
- Pressure-resistant woodfibre insulation plate (λ ≤ 0.042 W/mK), 40 mm;
- Timber frame construction, 100 x 180 mm, center-to-center 600 mm;
- Flexible wood fibre insulation, placed between construction (λ ≤ 0.038 W/mK), 180 mm;
- Vapour-retarding and airtight membrane with a variable vapour diffusion resistance;
- Biobased construction board, 18 mm;
- Clay base plate, 16 mm;
- Rough base clay plaster, 15 mm;
- Jute reinforcement mesh;
- Finishing clay plaster, 5 mm.

❷ Floor construction build-up, RC-value: 4.65 (m²K)/W

- Finishing board, 6 mm;
- Biobased wooden construction board, 12.5 mm;
- Biobased wooden construction board, perpendicular on the other plate, 12.5 mm;
- Vapour-retarding and airtight membrane with a variable vapour diffusion resistanance;
- Flexible hemp fiber insulation placed between construction (λ ≤ 0.043 W/(mK), 250 mm;
- Wooden beams 100 x 250 mm, center-to-center 600 mm;
- Biobased wooden construction board, 12.5 mm.

❸ Roof construction build-up, RC-value: 6.71 (m²K)/W

- EPDM glued on underlayment to prevent roof covering from lifting;
- Pressure-resistant woodfibre insulation plate (λ ≤ 0.042 W/(mK), 100 mm;
- Biobased wooden construction board, 18 mm;
- Sloped wooden battens for drainage at an angle of 16 mm/m^1, 28 x 24 mm;
- Biobased wooden construction board, 18 mm;
- Flexible hemp fiber insulation placed between construction (λ ≤ 0.043 W/(mK), 200 mm;
- Wooden beams 100 x 200 mm, center-to-center 600 mm;
- Vapour-retarding and airtight membrane with a variable vapour diffusion resistanance;
- Biobased wooden construction board, 18 mm;
- Clay base plate, 16 mm;
- Rough base clay plaster, 15 mm;
- Jute reinforcement mesh;
- Finishing clay plaster, 5 mm.

U_g = 1.50 W/(m²K)

U_w = 1.76 W/(m²K)

f-factor ≥ 0.65

Ψ_{V1}: 0.066 W/(mK) Ψ_{V2}: 0.082 W/(mK) Ψ_{H1}: 0.078 W/(mK)

Isopleths: no risk of mould $f_{R,si} > f_{R,si,\,max}$; no risk of mould

Phase shift of the wall construction: 8.5 h

Density of the wall construction 100 kg/m³

Calculation RC-value wall construction build-up

❶ Wall construction build-up, RC-value: 5.08 (m²K)/W

Table A43, Calculation of the RC-value of the wall construction build-up

Material	Thickness [m]	Thermal conductivity [W/(mK)]	Thermal resistance [W/(m²K)]
Vertical wooden cladding	0,018	0,130	0,138
Ventilated cavity with vertical wooden cladding batten, center-to-center 600 mm	0,028	0,322	0,087
Pressure-resistant woodfibre insulation plate	0,040	0,042	0,952
Timber frame construction, with flexible wood fibre insulation	0,180	0,051	3,529
Biobased construction board	0,018	0,120	0,150
Clay base plate	0,016	0,470	0,034
Clay plaster	0,020	0,910	0,022

Table A44, Calculation of the equivalent thermal conductivity of the individual layers in the relevant build-up

	Layer 1		Layer 2	
Material	Area [m²]	Thermal conductivity [W/(mK)]	Area [m²]	Thermal conductivity [W/(mK)]
Ventilated cavity with vertical wooden cladding batten, center-to-center 600 mm	0,0168	0,337	0,0012	0,130
Timber frame construction, with flexible wood fibre insulation	0,1080	0,038	0,0180	0,130

Density mass per unit area of the wall construction

Table A45, Calculation of the density mass per unit area

Material	Thickness [m]	Density [kg/m³]
Vertical wooden cladding	0,018	520
Ventilated cavity with vertical wooden cladding batten, center-to-center 600 mm	0,024	35
Pressure-resistant woodfibre insulation plate	0,040	140
Timber frame construction, with flexible wood fibre insulation	0,180	117
Biobased construction board	0,018	621
Clay base plate	0,016	1300
Clay plaster	0,020	1600

By using the previously presented formula a **m'-value** of **100.84 kg/m²** can be given for the **eighth detail configuration**.

Phase-shift

Table A46, Calculation of the phase shift

Material	Thickness [m]	Thermal conductivity [W/(mK)]	Density [kg/m³]	Specific heat capacity [J/(kgK)]
Timber frame construction, with flexible wood fibre insulation	0,180	0,051	117	2028

By using the presented phase shift formula, the resulting **φ-value** for **the eighth configuration** is **8.5 h.**

Geometry WUFI

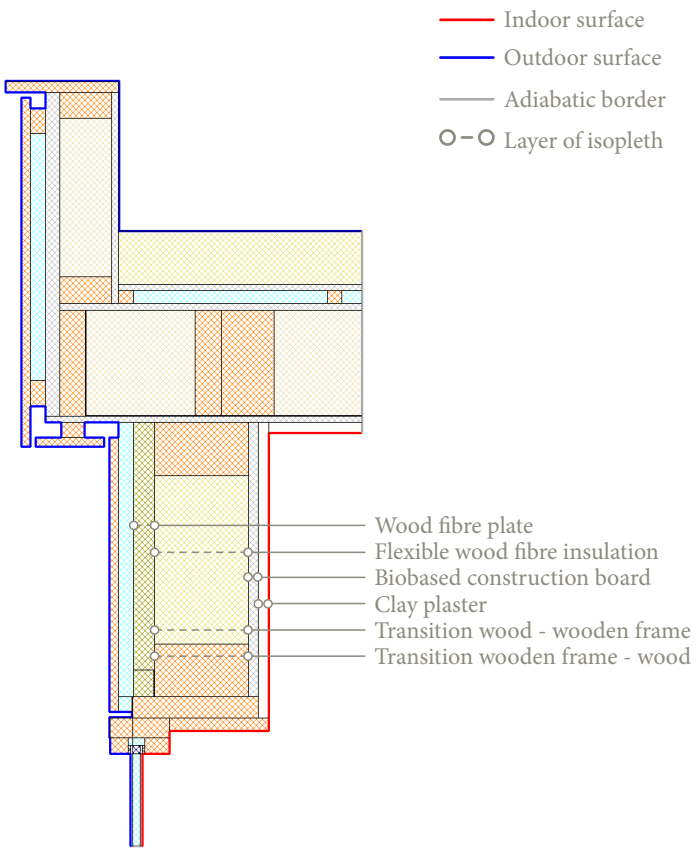

Figure A206, geometry detail V2 including location isopleths

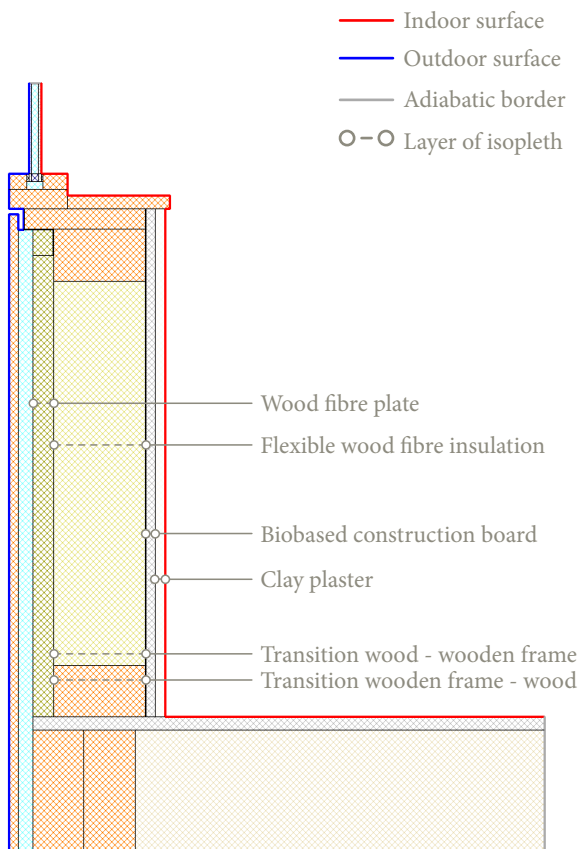

Figure A207, geometry detail V1 including location isopleths

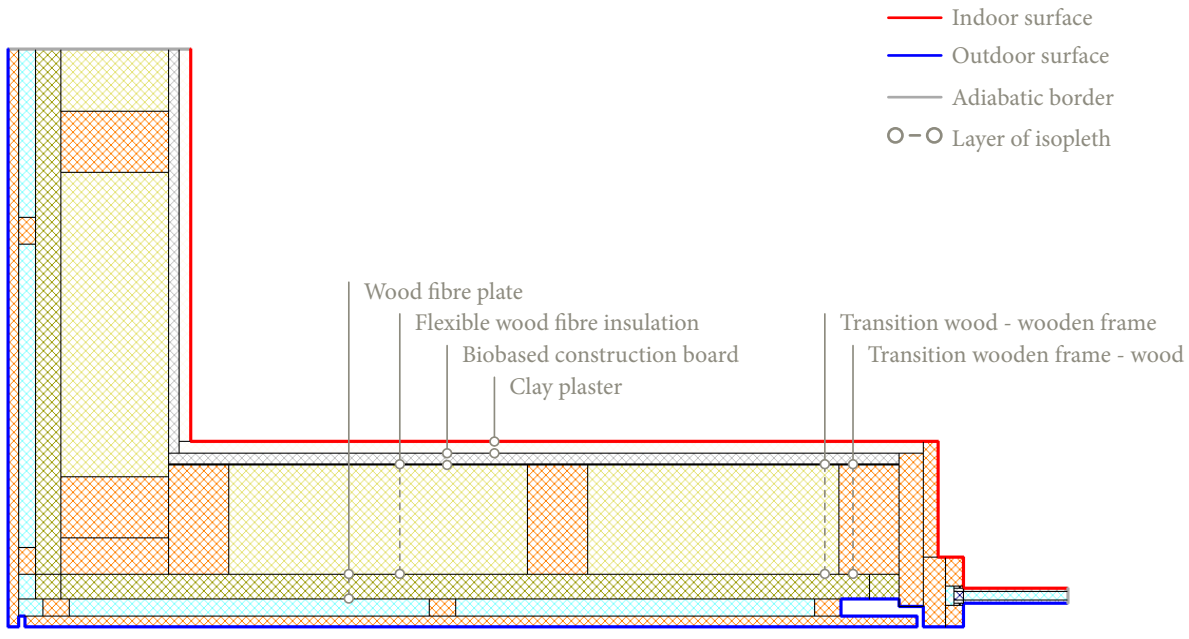

Figure A205, geometry detail H1including location isopleths

Isopleths - V1

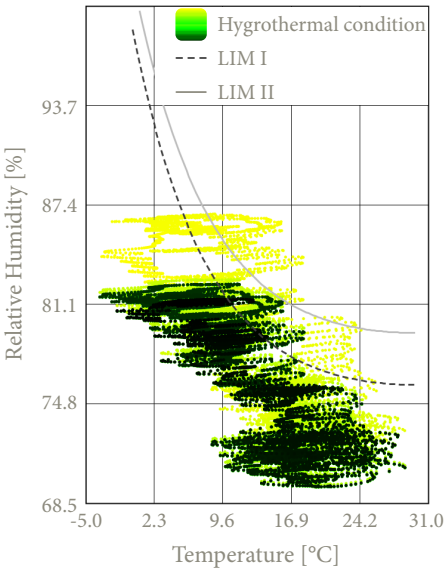

Figure A208, Isopleths wood fibre plate

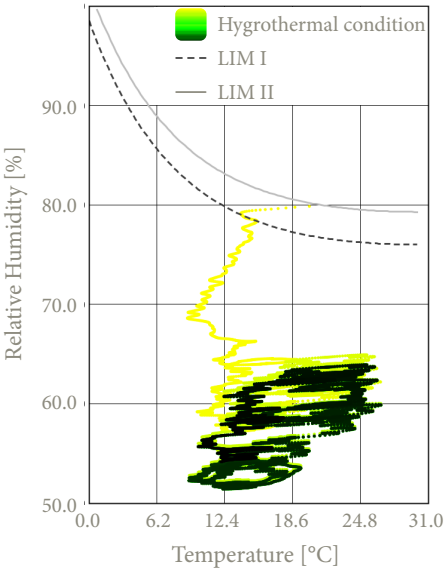

Figure A209, Isopleths flexible wood fibre

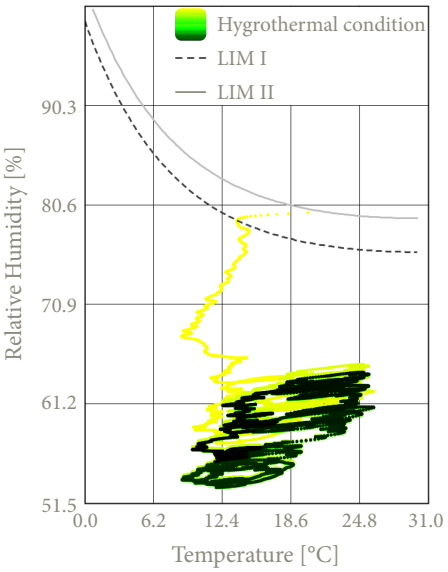

Figure A210, Isopleths wood fibre & transition frame

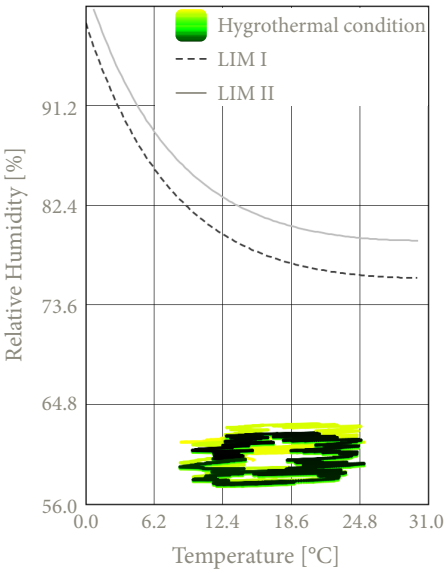

Figure A211, Isopleths transition frame & wood fibre

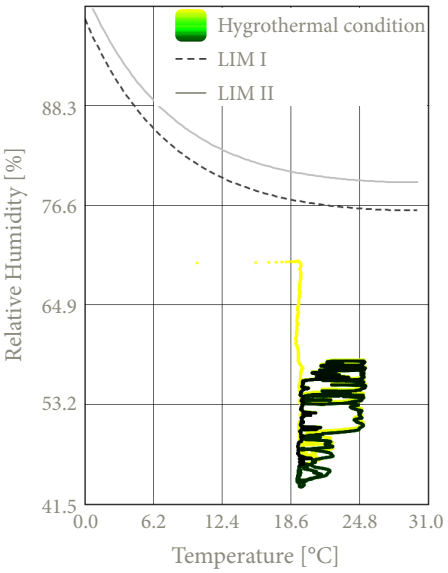

Figure A212, Isopleths biobased construction board

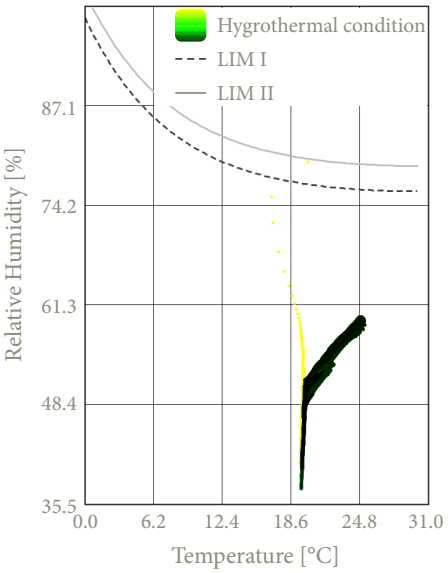

Figure A213, Isopleths clay plaster

Isopleths - V2

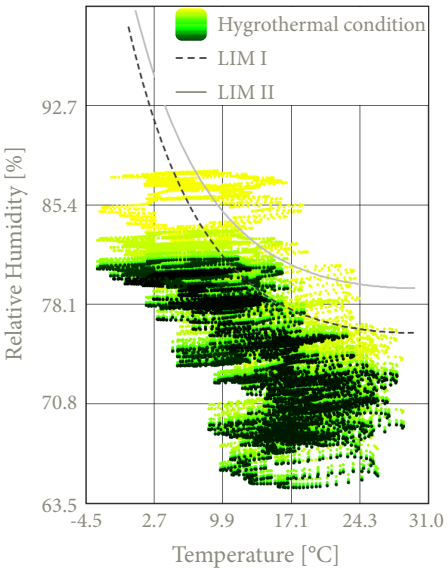

Figure A214, Isopleths wood fibre plate

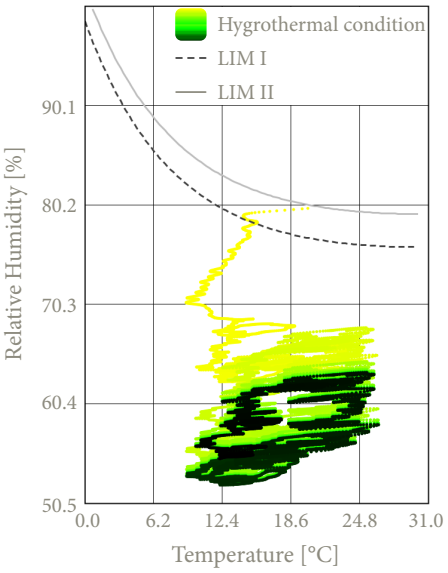

Figure A215, Isopleths flexible wood fibre

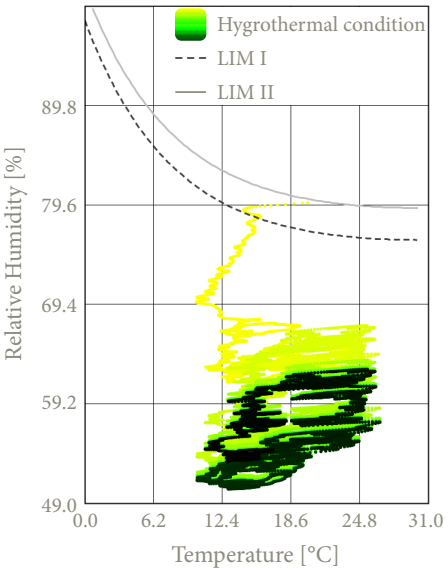

Figure A216, Isopleths wood fibre & transition frame

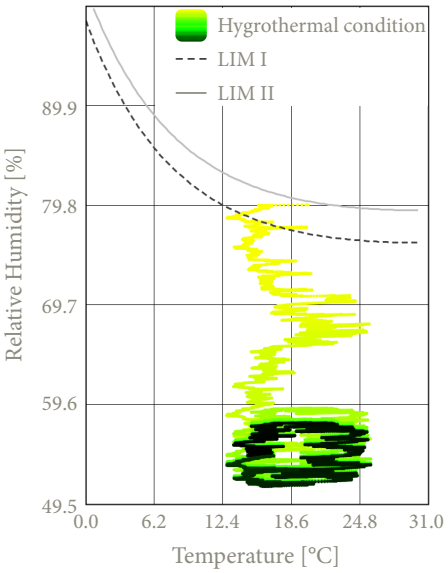

Figure A217, Isopleths transition frame & wood fibre

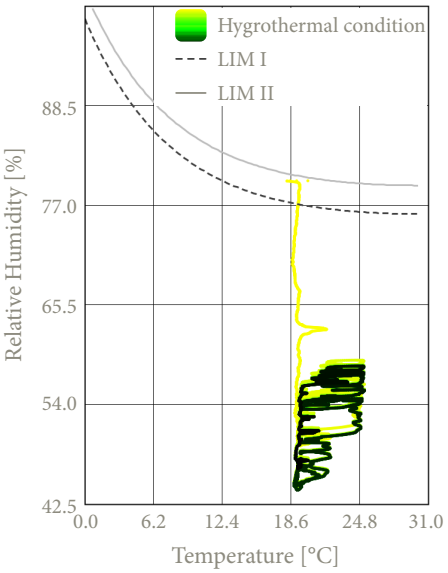

Figure A218, Isopleths biobased construction board

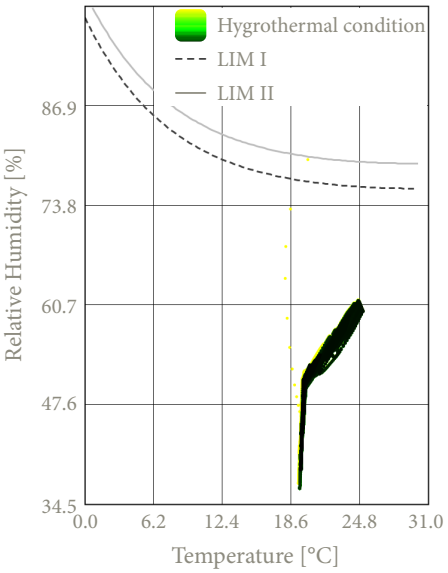

Figure A219, Isopleths clay plaster

Isopleths - H1

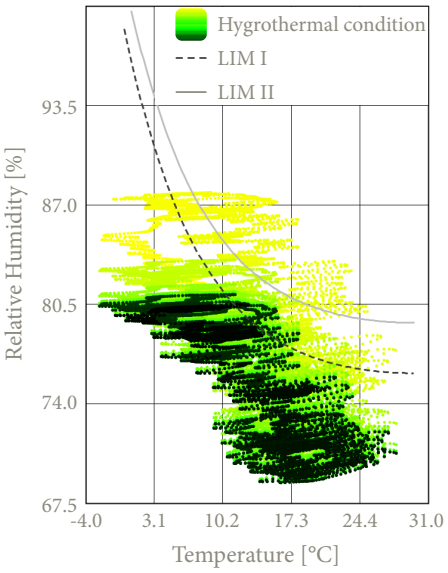

Figure A220, Isopleths wood fibre plate

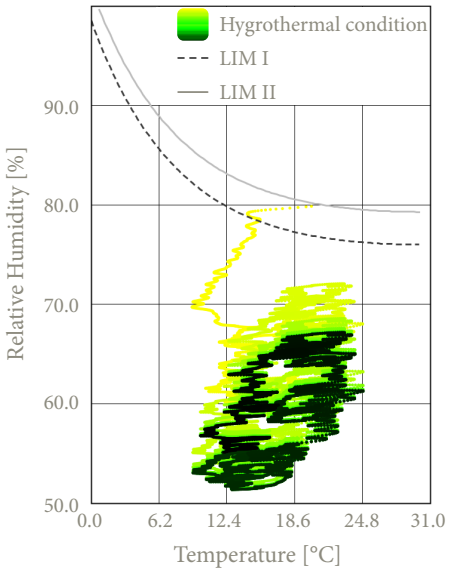

Figure A221, Isopleths flexible wood fibre

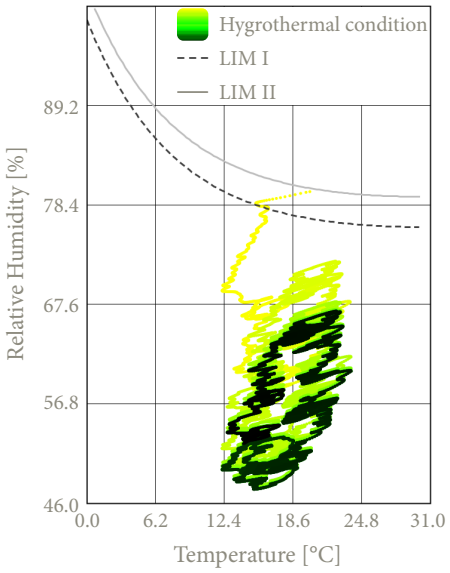

Figure A222, Isopleths wood fibre & transition frame

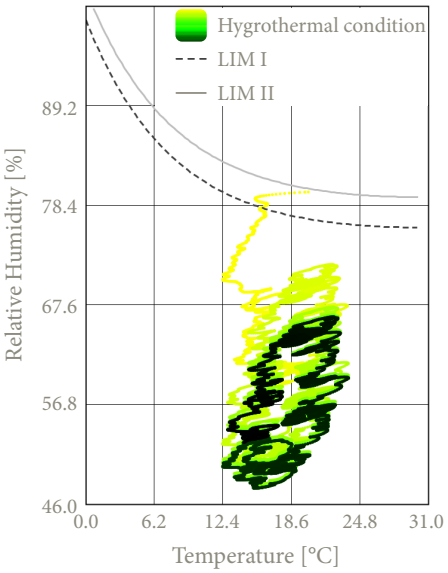

Figure A223, Isopleths transition frame & wood fibre

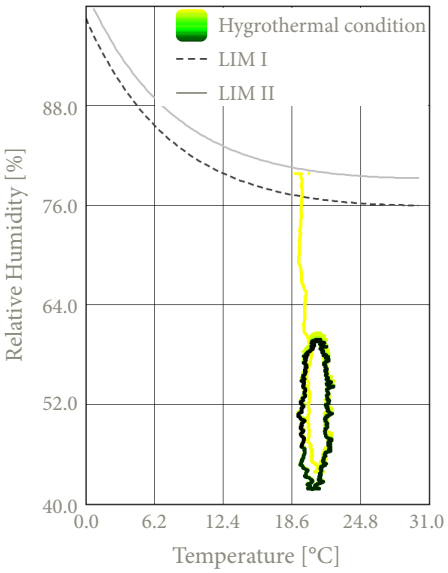

Figure A224, Isopleths biobased construction board

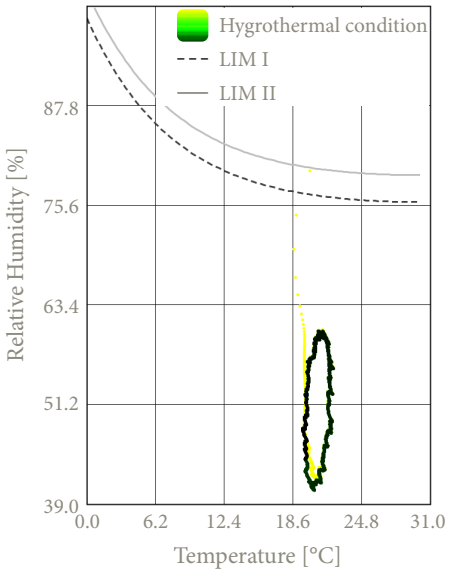

Figure A225, Isopleths clay plaster

Conclusion isoplteths

Based on the established and analysed isopleths of the various details within this construction **configuration**, it can be concluded that there is **no risk of mould growth** within the different material layers. All isopleths remain below the critical threshold values **LIM I** and **LIM II**, indicating that the details meet the established criteria.

With regard to the isopleths of the **wood fibre plate** in each detail, it can be observed that the relative humidity exceeds the LIM I threshold at the beginning of the simulation. This trend can possibly be attributed to the initial conditions, where the initial moisture content in the wood fibre was approximately 80%. During the simulation, however, the relative humidity gradually decreases to below both LIM I and LIM II, indicating that moisture is being transported out of the material. Nevertheless, at the end of the simulation, the isopleths still slightly exceed the LIM I line. However, for the majority of the year, the isopleths remain below both LIM thresholds. The continuously decreasing trend and the fact that the isopleths are for the majority of the year below the thresholds, suggests that there is no long-term risk of mould development.

With respect to the isopleths of the **flexible wood fibre**, as well as the **transition zones between the wood fibre and the wooden construction frame**, the **biobased construction board**, and the **clay plaster**, the values remain well below both LIM threshold values. At the location of the transition between the wood fibre and the wooden frame, the isopleths show a slight upward trend at V1. However, this increase gradually levels off, with values remaining below the critical LIM thresholds. With regard to the isopleths at V2 and H1 a decreasing trend can be observed at the location of the transition zone between the wood fibre and the wooden frame.

In relation to the isopleths of the **biobased construction board**, it can be seen that they remain well below the LIM threshold values and continue to decrease further over the course of the ten years. A similar but smaller effect can be observed at the **clay plaster**.

In conclusion, it can be stated that this configuration poses no risk of mould growth and thus complies with the specified isopleth requirements. As such, the design complies with the required hygrothermal performance standards.

Surface condensation - V1, V2 & H1

The circle at each figure figures below, **figure 226**, **figure 228** and **figure 230**, show the coldest point of the interior surface at each detail in order to consider the f_{Rsi}. Below these graphs the corresponding surface temperature at this point is shown over a ten-year simulation below, **figure 227**, **figure 229** and **figure 231**.

Figure A226, Highlight lowest point, V1

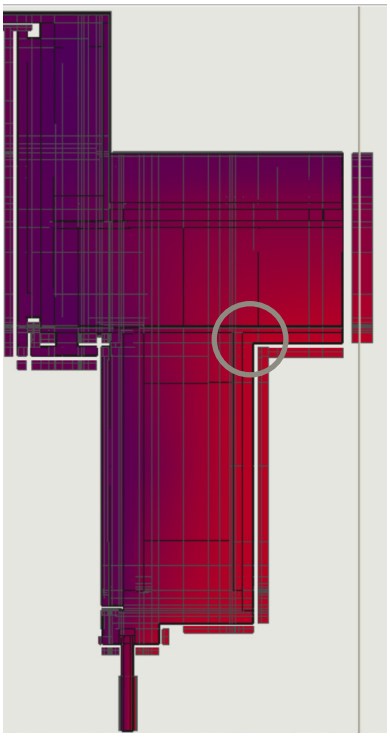

Figure A228, Highlight lowest point, V2

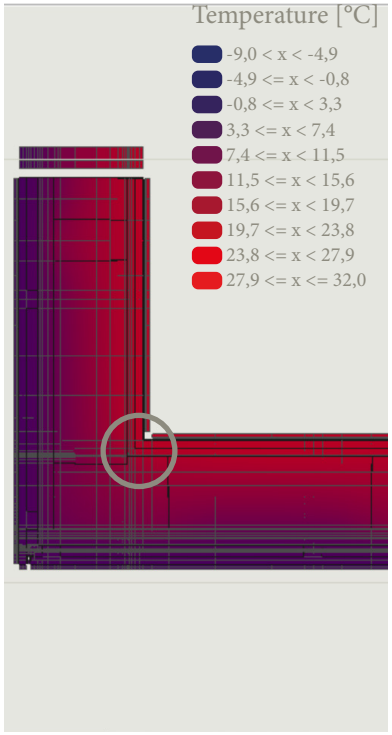

Figure A230, Highlight lowest point, H1

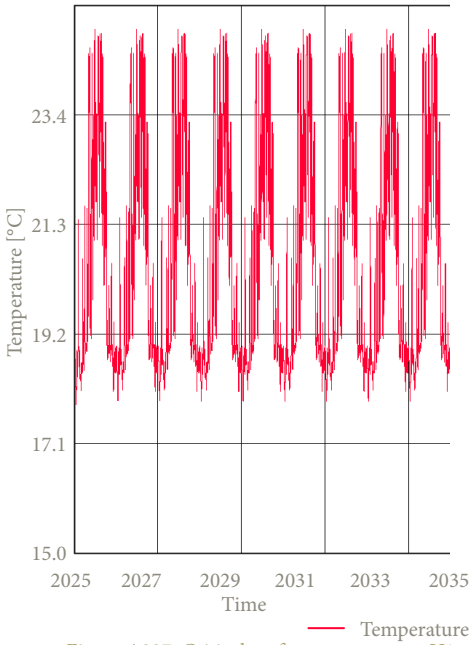

Figure A227, Critical surface temperature, V1

From this graph the lowest surface temperature of this detail is **15.33 °C**.

The resulting f_{Rsi} for this detail is **0.61** which is the same as the minimum requirement of 0.61. This indicates a negligible risk of surface condensation.

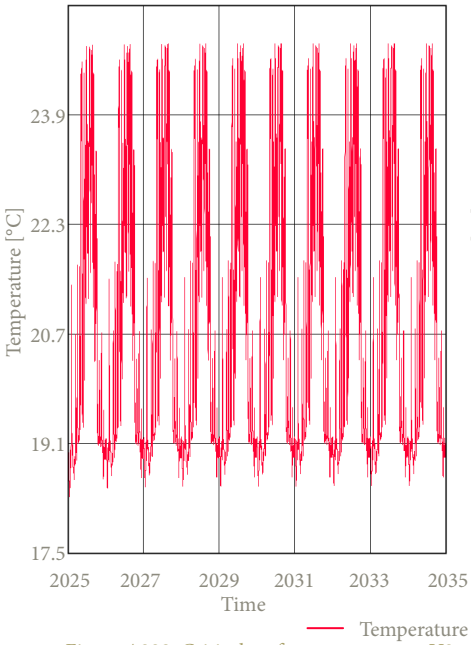

Figure A229, Critical surface temperature, V2

From this graph the lowest surface temperature of this detail is **18.11 °C**.

The resulting f_{Rsi} for this detail is **0.84** which exceeds the minimum requirement of 0.61. This indicates a negligible risk of surface condensation.

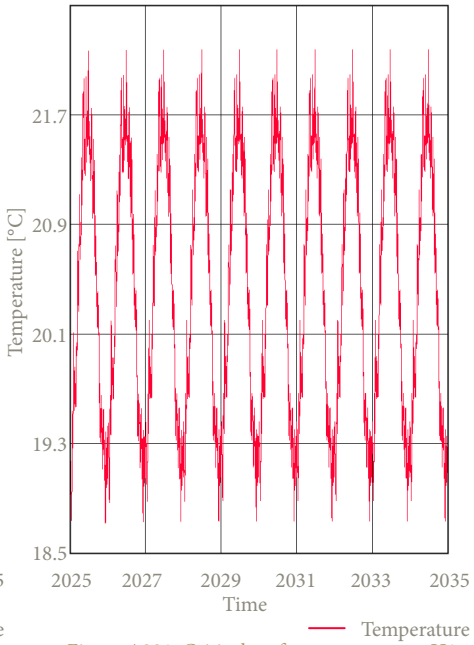

Figure A231, Critical surface temperature, H1

From this graph the lowest surface temperature of this detail is **18.70 °C**.

The resulting f_{Rsi} for this detail is **0.89** which exceeds the minimum requirement of 0.61. This indicates a negligible risk of surface condensation.

F-factor - V1, V2 & H1

The resulting **f-factor** of **detail V1** is **0.91** for a temperature of **16.49 °C**. Next the resulting **f-factor** of **detail V2** is **0.93** for a temperature of **16.84 °C**. Lastly, the resulting **f-factor** of **detail H1** is **0.94** for a temperature of **16.97 °C**. This indicates a very limited thermal bridge is assessed within the details of this configuration.
Given that these values significantly all exceeds the required threshold of **0.65**, it can be concluded that the details within this configuration complies with the thermal performance requirements set by the Dutch Building Decree.

PSI-value - V1

Table A47, Calculation of the $Q_{ideal\ condition}$

$R_{construction,\ window}$ [(m²K)/W]	$A_{construction,\ window}$ [m²]	$R_{construction,\ wall}$ [(m²K)/W]	$A_{construction,\ wall}$ [m²]	$R_{construction,\ floor}$ [(m²K)/W]	$A_{construction,\ floor}$ [m²]
0.600	0.2425	5.082	1.011	4.648	0.756

The resulting $\mathbf{Q_{ideal\ condition}}$ is **14.206 W**

Q_{WUFI} represents the sum of all heat flows through the detail, resulting in a total heat flow of **14.979 W**.

These values give a **Ψ-value** of **0.042 W/(mK)** for **detail V1**, indicating that the detail can be characterised as a well-insulated building component.

PSI-value - V2

Table A48, Calculation of the $Q_{ideal\ condition}$

$R_{construction,\ window}$ [(m²K)/W]	$A_{construction,\ window}$ [m²]	$R_{construction,\ wall}$ [(m²K)/W]	$A_{construction,\ wall}$ [m²]	$R_{construction,\ roof}$ [(m²K)/W]	$A_{construction,\ roof}$ [m²]
0.600	0.2425	5.082	0.836	6.442	0.204

The resulting $\mathbf{Q_{ideal\ condition}}$ is **10.806 W**

Q_{WUFI} represents the sum of all heat flows through the detail, resulting in a total heat flow of **12.290 W**.

These values give a **Ψ-value** of **0.082 W/(mK)** for **detail V2**, indicating that the detail can be characterised as a well-insulated building component.

PSI-value - H1

Table A49, Calculation of the $Q_{ideal\ condition}$

$R_{construction,\ window}$ [(m²K)/W]	$A_{construction,\ window}$ [m²]	$R_{construction,\ wall}$ [(m²K)/W]	$A_{construction,\ wall}$ [m²]
0.600	0.2425	5.082	2.237

The resulting $\mathbf{Q_{ideal\ condition}}$ is **15.198 W**

Q_{WUFI} represents the sum of all heat flows through the detail, resulting in a total heat flow of **16.606 W**.

These values give a **Ψ-value** of **0.078 W/(mK)** for **detail H1**, indicating that the detail can be characterised as a well-insulated building component.

Assessment detail configuration

Important notes about the details

For the given configuration, **key considerations** are presented below in the form of bullet points. These points highlight specific aspects that need to be taken into account during detailing and construction.

- Place the flexible flax between the studs of the wooden frame.
- Finish the inside of the wooden frame with a pressure-resistant wood fibre board to allow for fixings.
- Attach the water-resistant barrier of the window frame to the timber structural frame.
- The wooden lintel must have proper bearing on the wooden frame.
- The screws of the wood fibre plate must reach the center of the timber frame to ensure secure attachment.
- Stainless steel screws must be at least 2 times the thickness of the battens.
- Stainless steel nails must be at least 2.5 times the thickness of the cladding.
- The stainless steel nails must be placed 40 mm from the outer edge of the cladding.
- Ensure 4 mm gaps between the cladding to accommodate the movement of the wood.
- Ensure 10 mm gaps for ventilation both between cladding boards and at the window frame.
- Use a clay base plate to provide a correct underlayment for the clay plaster.
- Use a jute reinforcement mesh between the rough and finishing clay plaster to prevent cracking.

Assessment of the configuration

Additionally, the configuration is evaluated based on the following criteria:

1. **Weight**: The total mass per unit area of the wall construction.
2. **Construction time**: The time required for assembling the construction.
3. **Resistance Construction-value:** The combined thermal resistance of all layers in the construction.
4. **Phase shift**: The heat transfer delay of the structure.

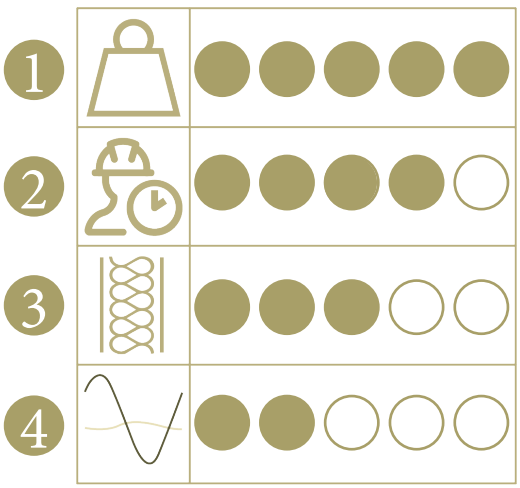

Axonometric view of the detail configuration

In addition to the presented details, an **axonometric view** of the respective detail is also shown. This is presented in the figure below, **figure 232**, and is intended to provide more clarity and insight into **detail V1, detail V2,** and **detail H1**.

Figure 232, Axonometric view of detail configuration 8

Detail configuration 9 - wood fibre insulation with cork façade

The ninth detail configuration consists of flexible wood fibre insulation placed between the studs of the timber construction frame. To protect the wood fibre against water and mould growth a water-resistant vapour-permeable membrane is placed at the outside of the timber frame construction. Next, a biobased, diffusion-open construction board is applied for structural stability and for the application of the cork façade system. This board enables the attachment of the expanded insulation corkboard, which is bonded using a cork mortar. On top of the expanded insulation corkboard, another layer of cork mortar is applied to bond the cork cladding panels. On the interior side, the timber construction frame is finished with a biobased, diffusion-open construction board to which a clay board is screwed. A clay plaster can then be applied to this board, consisting of a rough layer and a finishing layer.

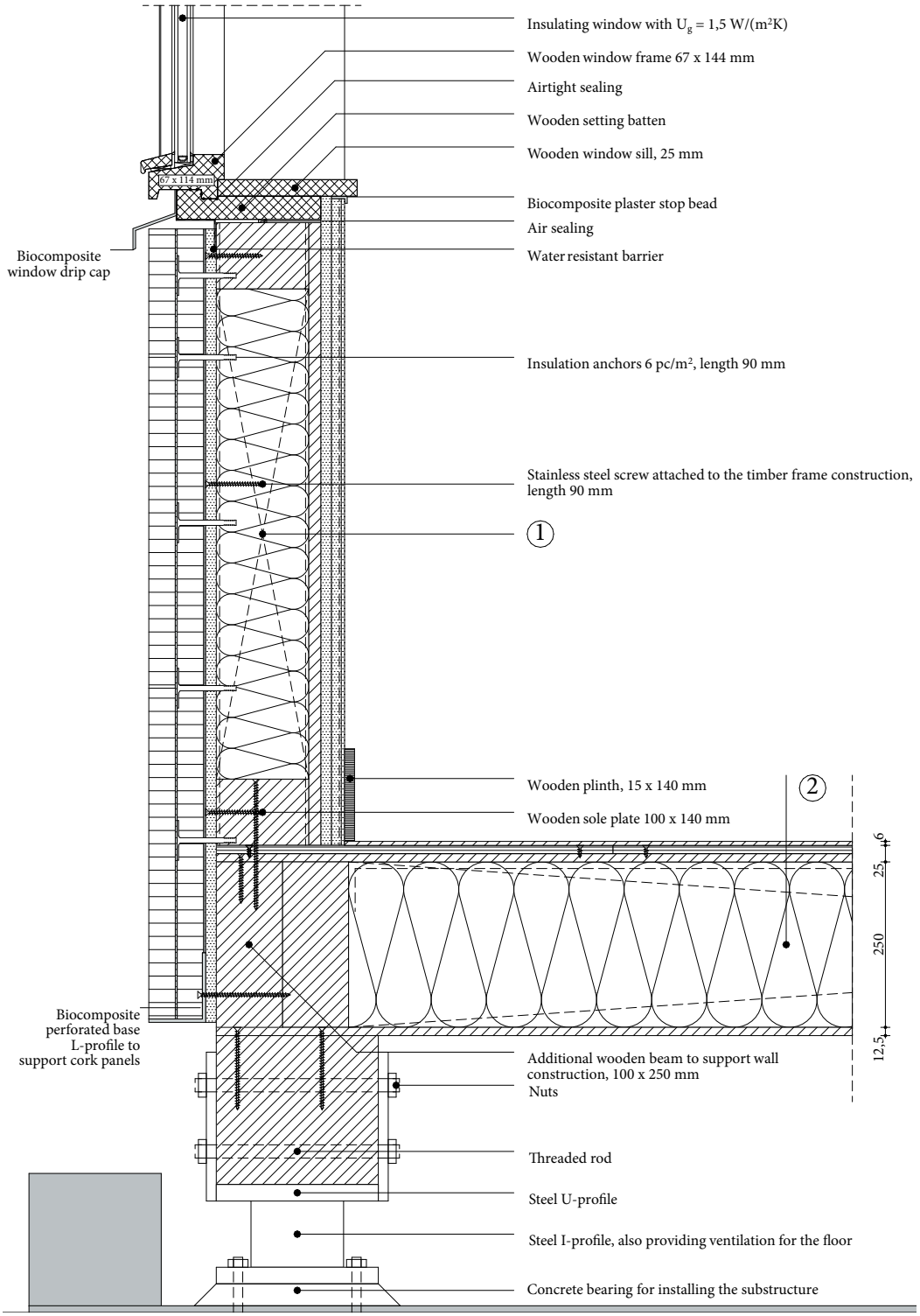

Figure A233, 1:10 detail of V1, configuration 9, own illustration

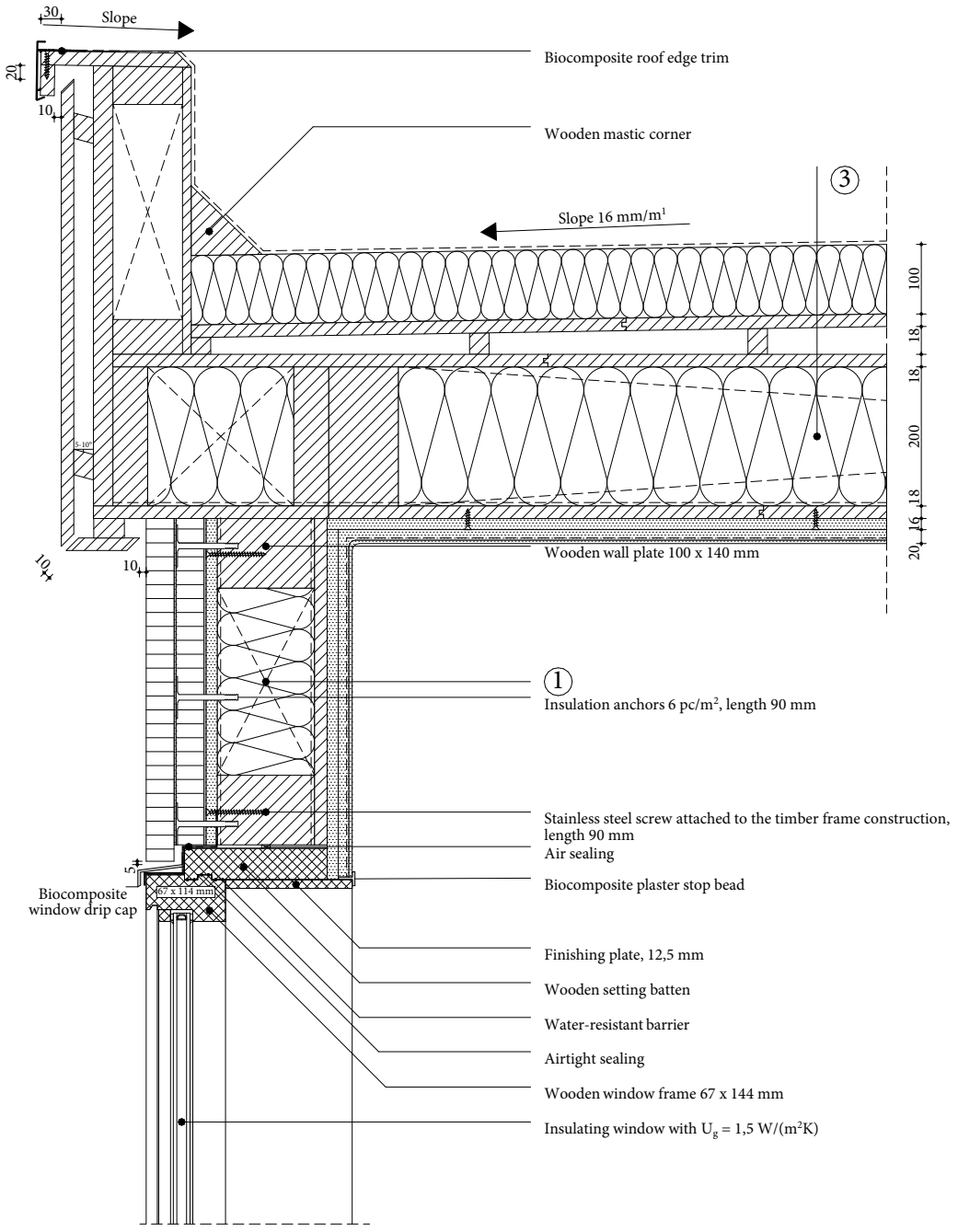

Figure A234, 1:10 detail of V2, configuration 9, own illustration

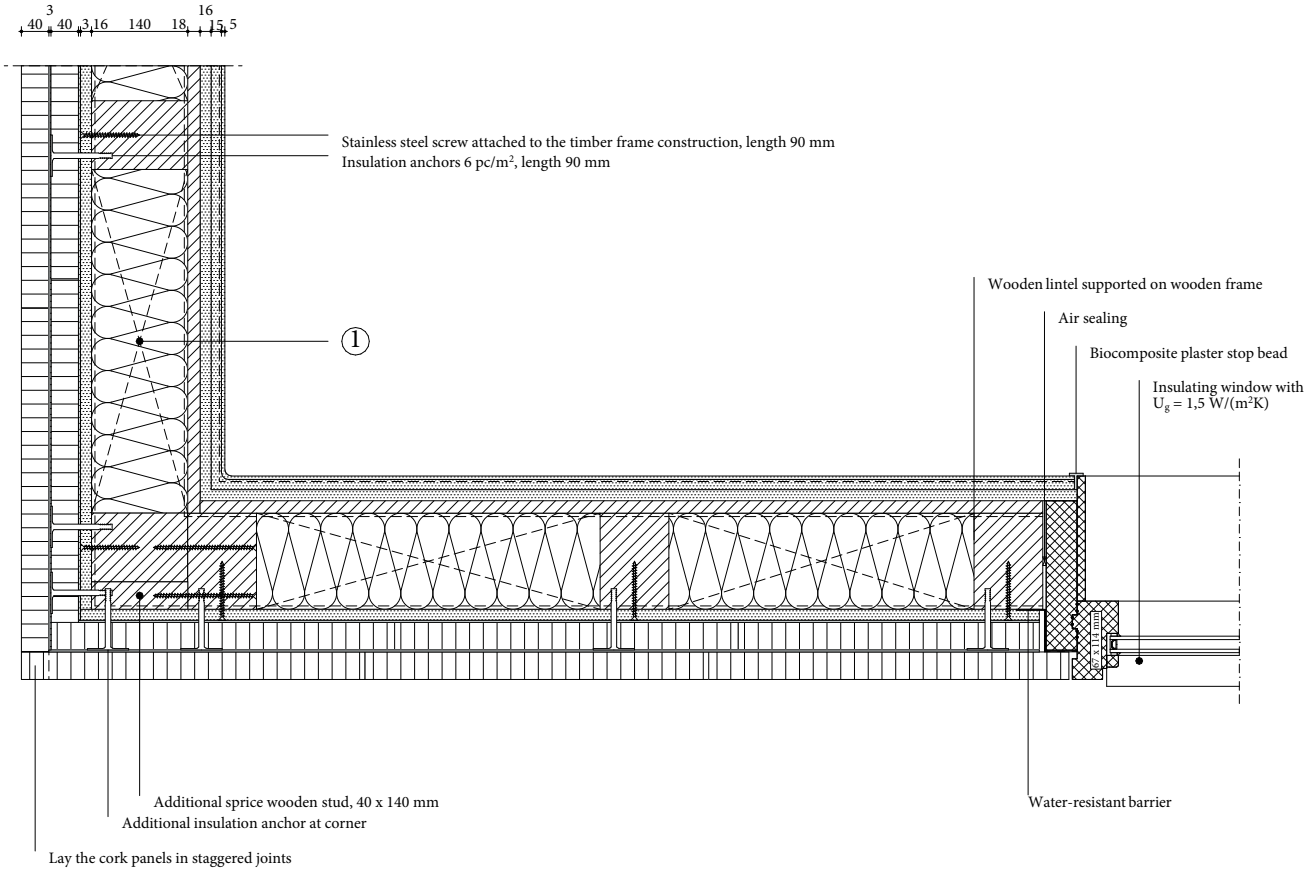

Figure A235, 1:10 detail of H1, configuration 9, own illustration

❶ Wall construction build-up, RC-value: 5.28 (m²K)/W

- Cork cladding panels (λ ≤ 0.043 W/mK), 40 mm;
- Cork mortar, 3 mm;
- Expanded insulation corkboard (λ ≤ 0.039 W/mK), 40 mm;
- Cork mortar, 3 mm;
- Biobased diffusion open construction board, 16mm;
- Water resistant vapour-permeable membrane;
- Timber frame construction, 100 x 140 mm, center-to-center 600 mm;
- Wood fibre insulation, placed between construction (λ ≤ 0.038 W/mK), 140 mm;
- Vapour-retarding and airtight membrane with a variable vapour diffusion resistance;
- Biobased construction board, 18 mm;
- Clay base plate, 16 mm;
- Rough base clay plaster, 15 mm;
- Jute reinforcement mesh;
- Finishing clay plaster, 5 mm.

❷ Floor construction build-up, RC-value: 4.65 (m²K)/W

- Finishing board, 6 mm;
- Biobased wooden construction board, 12.5 mm;
- Biobased wooden construction board, perpendicular on the other plate, 12.5 mm;
- Vapour-retarding and airtight membrane with a variable vapour diffusion resistanance;
- Flexible hemp fiber insulation placed between construction (λ ≤ 0.043 W/(mK), 250 mm;
- Wooden beams 100 x 250 mm, center-to-center 600 mm;
- Biobased wooden construction board, 12.5 mm.

❸ Roof construction build-up, RC-value: 6.71 (m²K)/W

- EPDM glued on underlayment to prevent roof covering from lifting;
- Pressure-resistant woodfibre insulation plate (λ ≤ 0.042 W/(mK), 100 mm;
- Biobased wooden construction board, 18 mm;
- Sloped wooden battens for drainage at an angle of 16 mm/m^1, 28 x 24 mm;
- Biobased wooden construction board, 18 mm;
- Flexible hemp fiber insulation placed between construction (λ ≤ 0.043 W/(mK), 200 mm;
- Wooden beams 100 x 200 mm, center-to-center 600 mm;
- Vapour-retarding and airtight membrane with a variable vapour diffusion resistanance;
- Biobased wooden construction board, 18 mm;
- Clay base plate, 16 mm;
- Rough base clay plaster, 15 mm;
- Jute reinforcement mesh;
- Finishing clay plaster, 5 mm.

U_g = 1.50 W/(m²K)

U_w = 1.76 W/(m²K)

f-factor ≥ 0.65

Ψ_{V1}: 0.057 W/(mK) Ψ_{V2}: 0.076 W/(mK) Ψ_{H1}: 0.085 W/(mK)

Isopleths: no risk of mould $f_{R,si} > f_{R,si,\,max}$; no risk of mould

Phase shift of the wall construction: 7.0 h

Density of the wall construction 105 kg/m³

Calculation RC-value wall construction build-up

❶ Wall construction build-up, RC-value: 5.28 (m²K)/W

Table A50, Calculation of the RC-value of the wall construction build-up

Material	Thickness [m]	Thermal conductivity [W/(mK)]	Thermal resistance [W/(m²K)]
Tongue and groove cork cladding panels	0,040	0,043	0,930
Cork mortar	0,003	0,250	0,012
Expanded insulation corkboard	0,040	0,039	1,025
Cork mortar	0,003	0,250	0,012
Biobased diffusion open construction board	0,016	0,090	0,178
Timber frame construction, with flexible wood fibre insulation	0,140	0,051	2,745
Biobased construction board	0,018	0,120	0,150
Clay base plate	0,016	0,470	0,034
Clay plaster	0,020	0,910	0,022

Table A51, Calculation of the equivalent thermal conductivity of the individual layers in the relevant build-up

	Layer 1		Layer 2	
Material	Area [m²]	Thermal conductivity [W/(mK)]	Area [m²]	Thermal conductivity [W/(mK)]
Timber frame construction, with flexible wood fibre insulation	0,084	0,038	0,014	0,130

Density mass per unit area of the wall construction

Table A52, Calculation of the density mass per unit area

Material	Thickness [m]	Density [kg/m³]
Tongue and groove cork cladding panels	0,040	140
Cork mortar	0,003	1000
Expanded insulation corkboard	0,040	110
Cork mortar	0,003	1000
Biobased diffusion open construction board	0,016	565
Timber frame construction, with flexible wood fibre insulation	0,140	117
Biobased construction board	0,018	621
Clay base plate	0,016	1300
Clay plaster	0,020	1600

By using the previously presented formula a **m'-value** of **105.39 kg/m²** can be given for the **ninth detail configuration**.

Phase-shift

Table A53, Calculation of the phase shift

Material	Thickness [m]	Thermal conductivity [W/(mK)]	Density [kg/m³]	Specific heat capacity [J/(kgK)]
Timber frame construction, with flexible wood fibre insulation	0,140	0,051	117	2029

By using the presented phase shift formula, the resulting **φ-value** for **the ninth configuration** is **7.0 h.**

Geometry WUFI

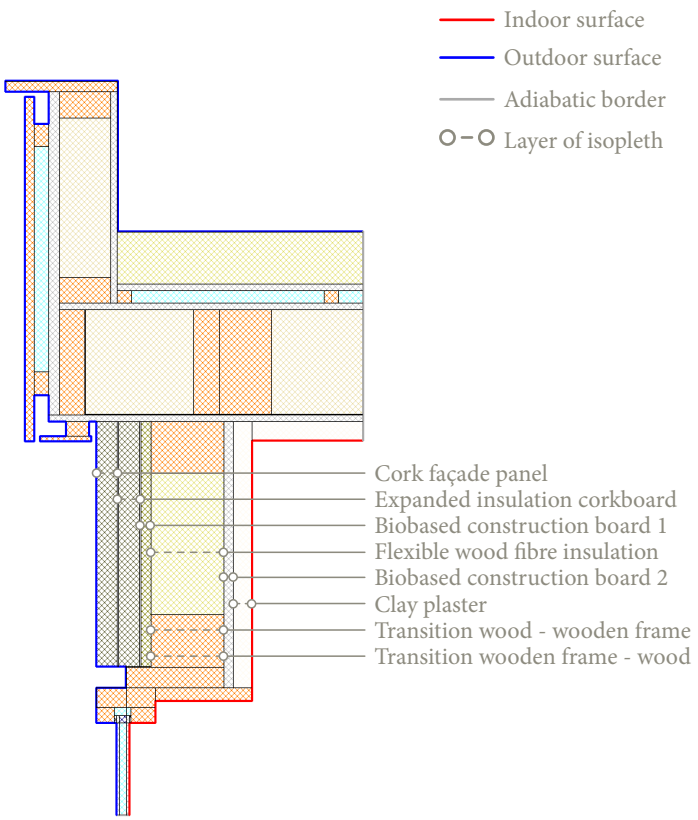

Figure A237, geometry detail V2 including location isopleths

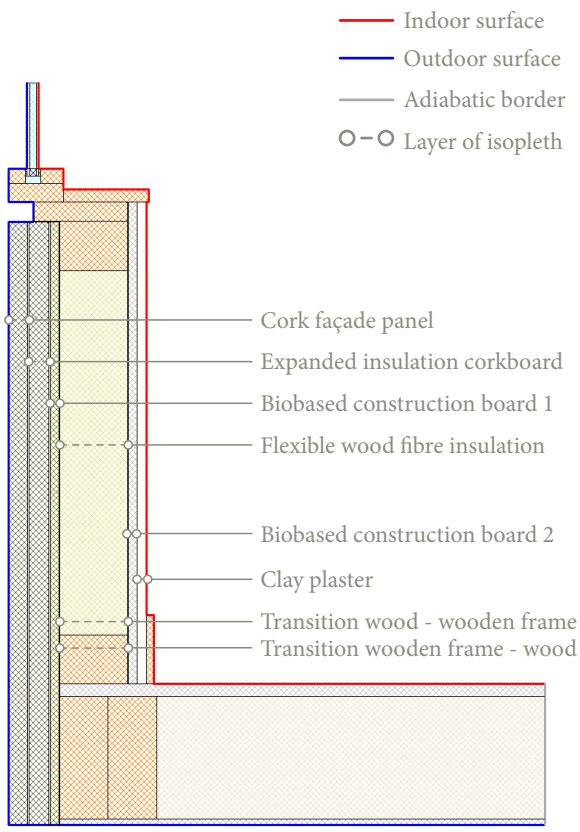

Figure A238, geometry detail V1 including location isopleths

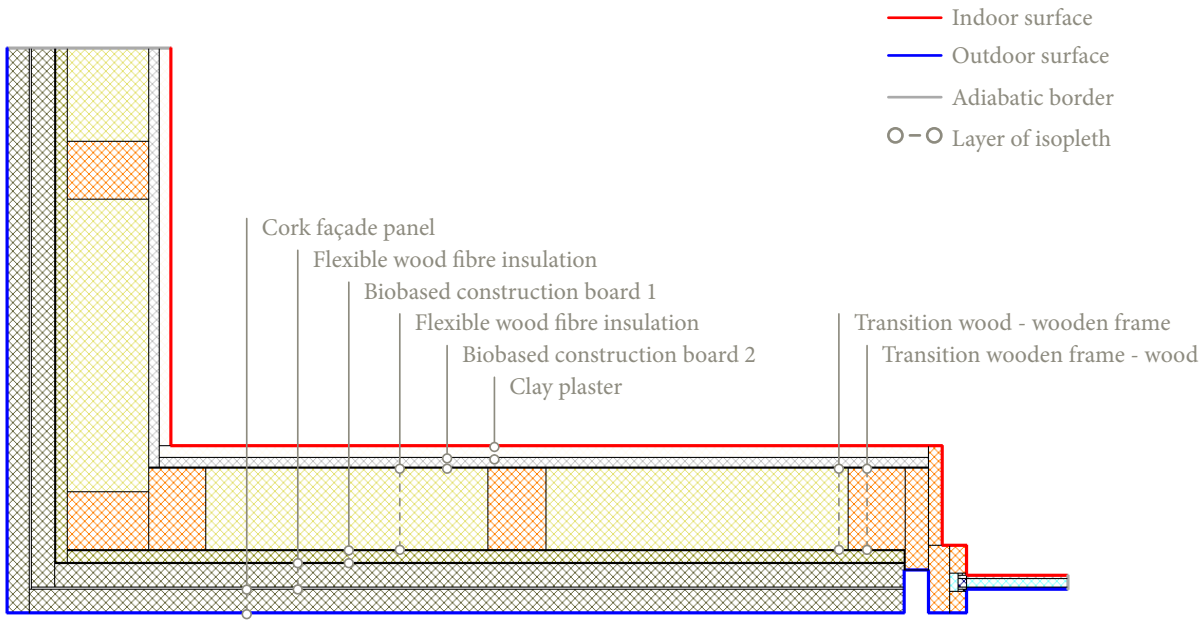

Figure A236, geometry detail H1including location isopleths

Isopleths - V1

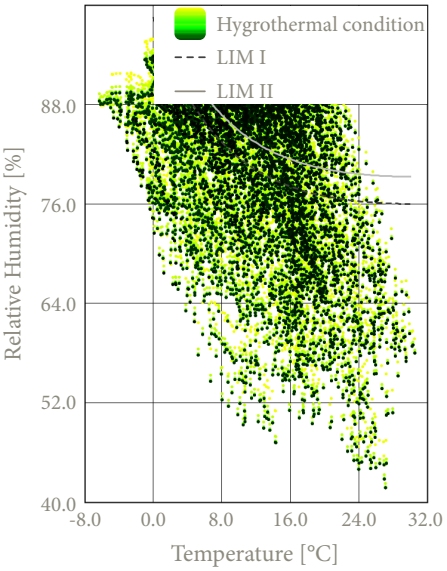

Figure A239, Isopleths cork façade panel

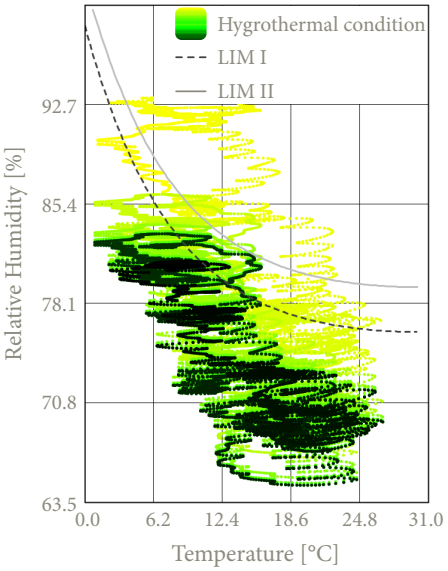

Figure A240, Isopleths expanded insulation corkboard

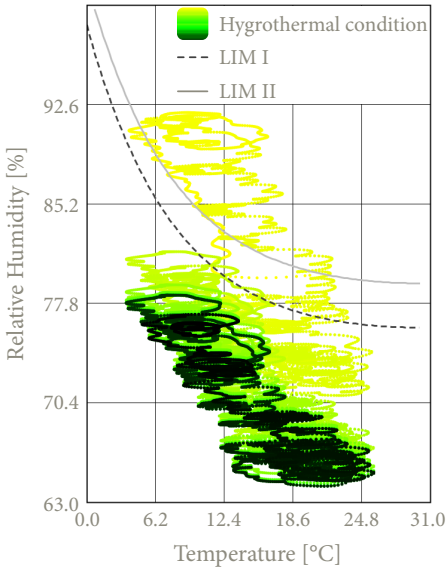

Figure A241, Isopleths biobased construction board 1

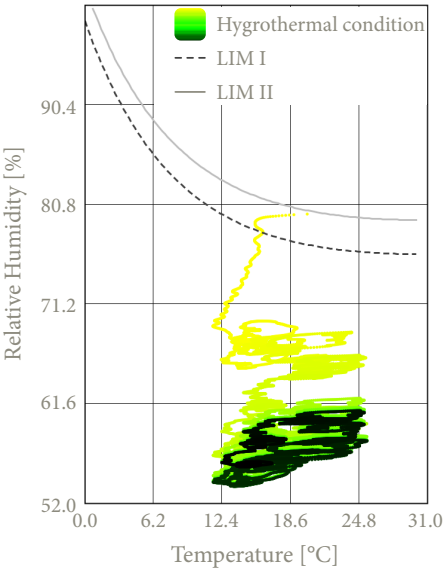

Figure A242, Isopleths flexible wood fibre insulation

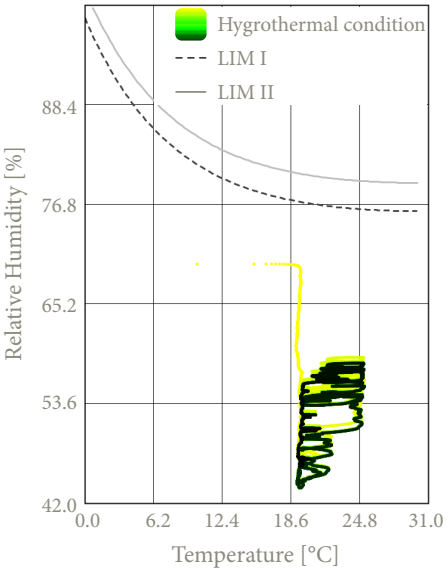

Figure A243, Isopleths biobased construction board 2

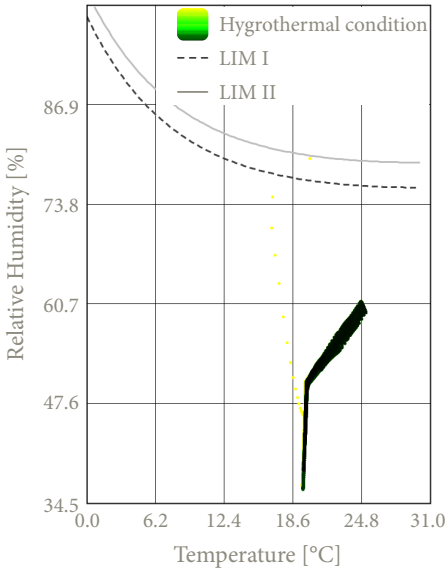

Figure A244, Clay plaster

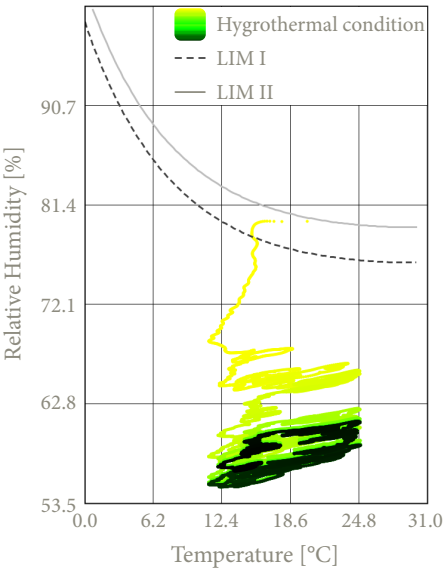

Figure A245, Isopleths transition wood & frame

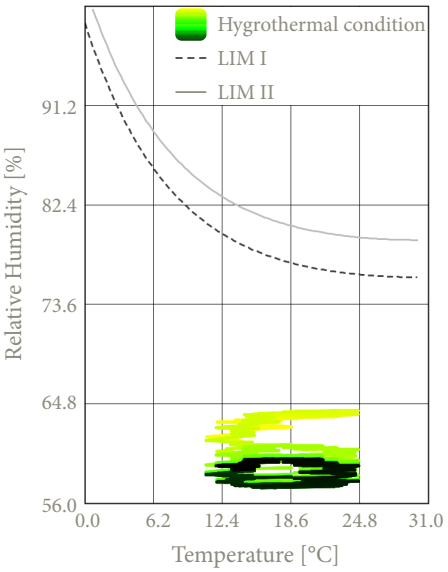

Figure A246, Isopleths transition frame & wood

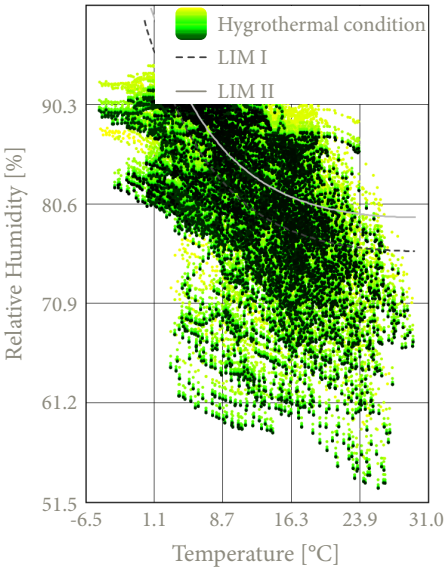

Figure A247, Isopleths cork façade panel

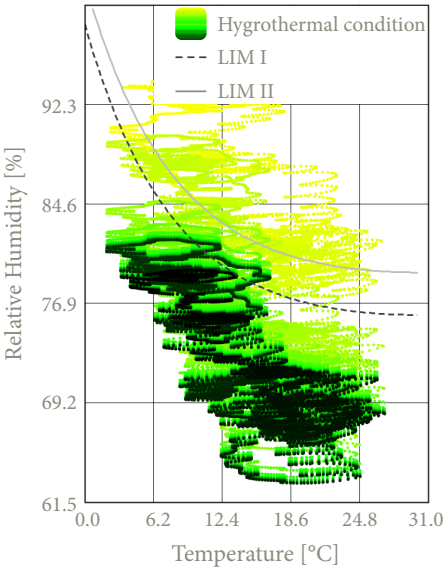

Figure A248, Isopleths expanded insulation corkboard

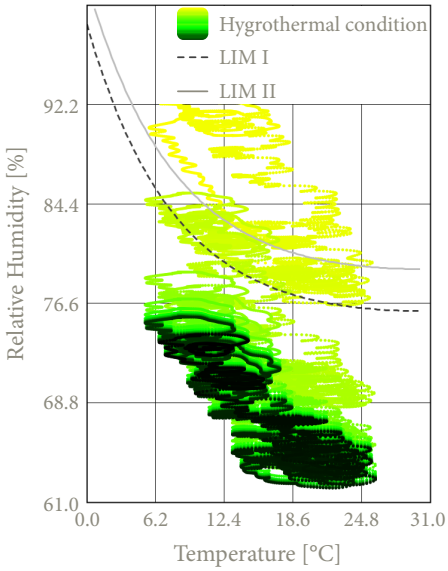

Figure A249, Isopleths biobased construction board 1

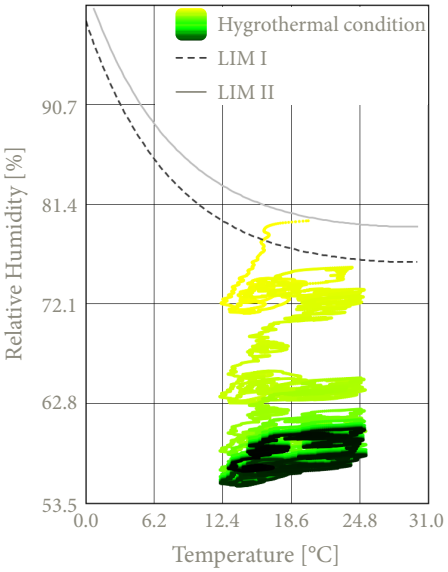

Figure A250, Isopleths flexible wood fibre insulation

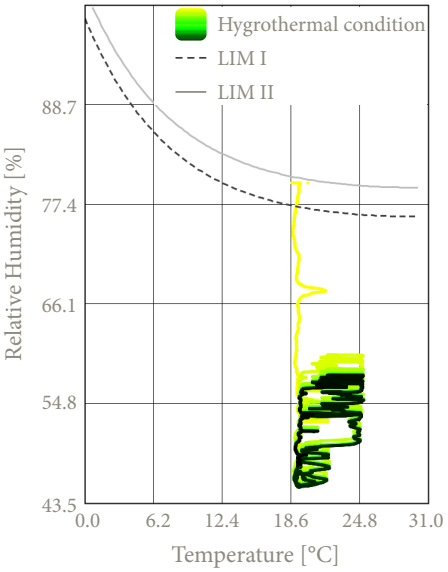

Figure A251, Isopleths biobased construction board 2

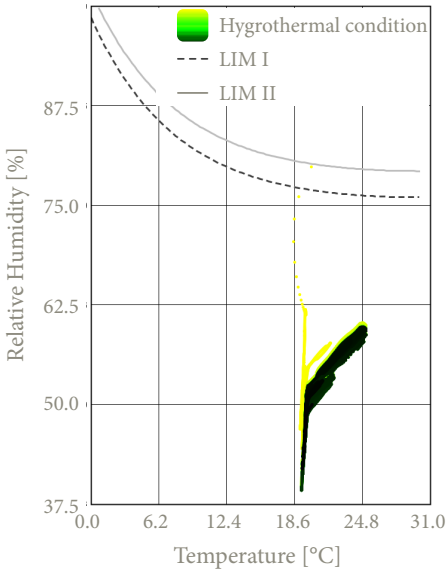

Figure A252, Clay plaster

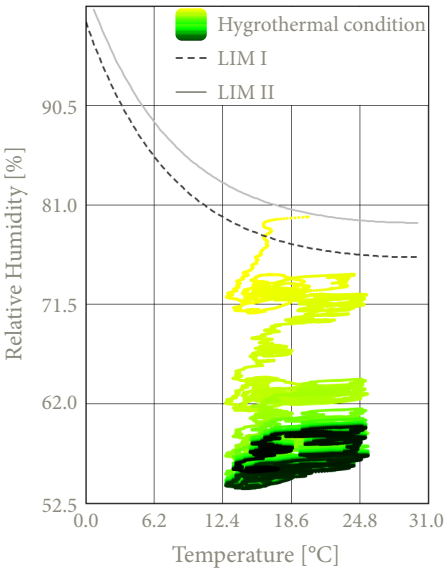

Figure A253, Isopleths transition wood & frame

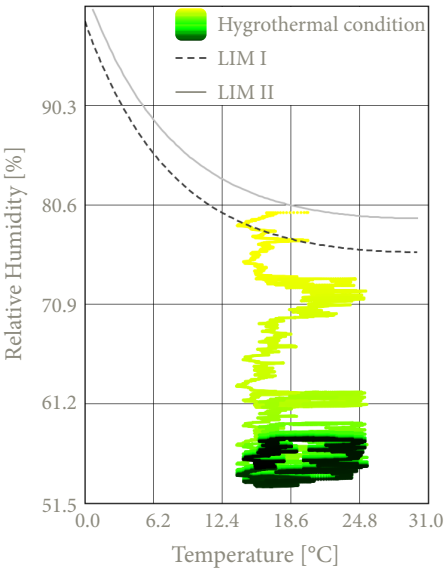

Figure A254, Isopleths transition frame & wood

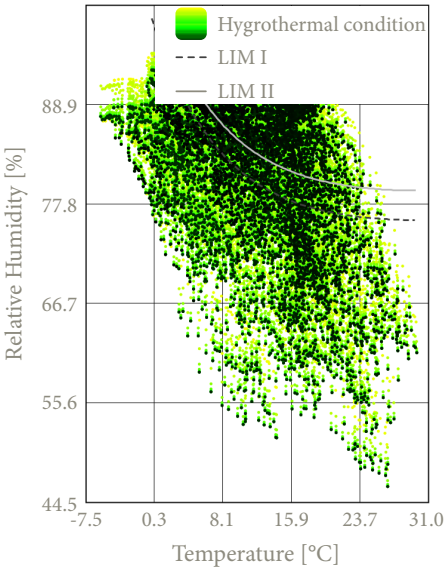

Figure A255, Isopleths cork façade panel

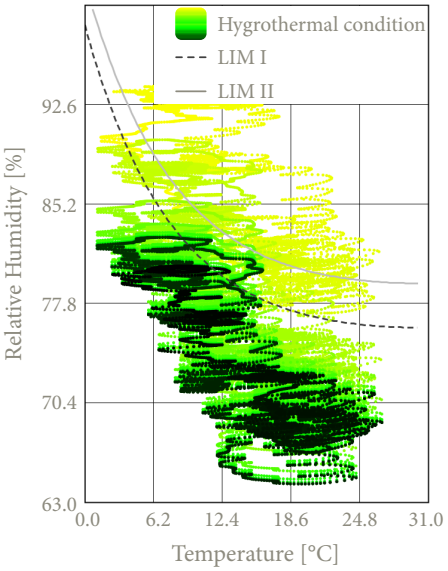

Figure A256, Isopleths expanded insulation corkboard

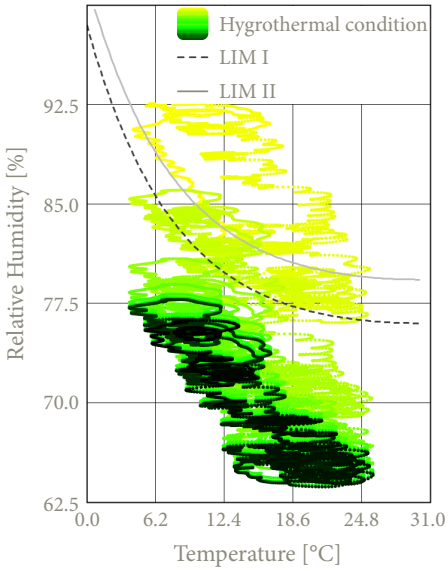

Figure A257, Isopleths biobased construction board 1

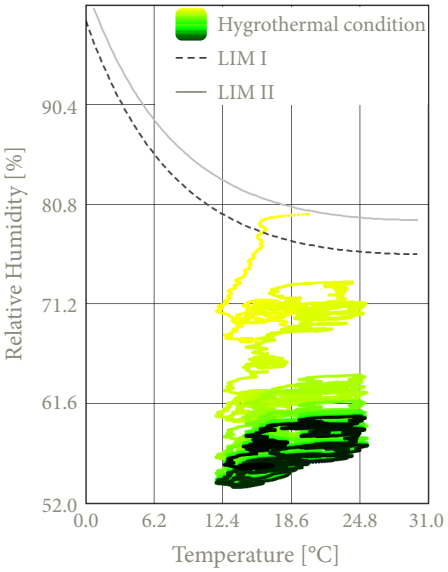

Figure A258, Isopleths flexible wood fibre insulation

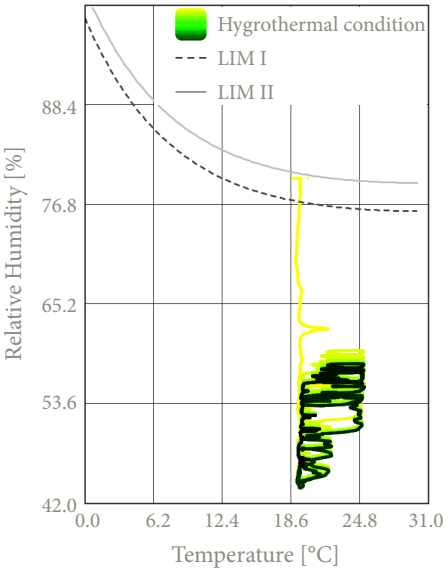

Figure A259, Isopleths biobased construction board 2

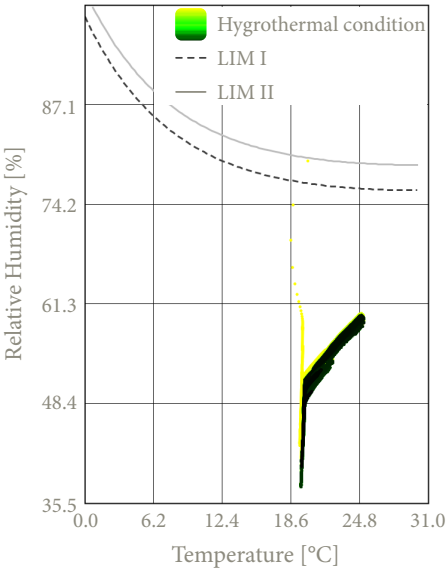

Figure A260, Clay plaster

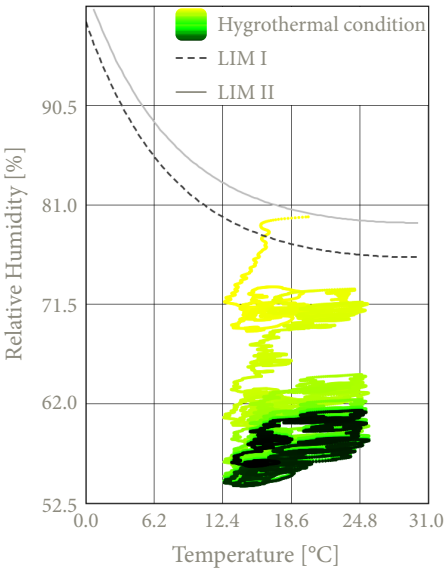

Figure A261, Isopleths transition wood & frame

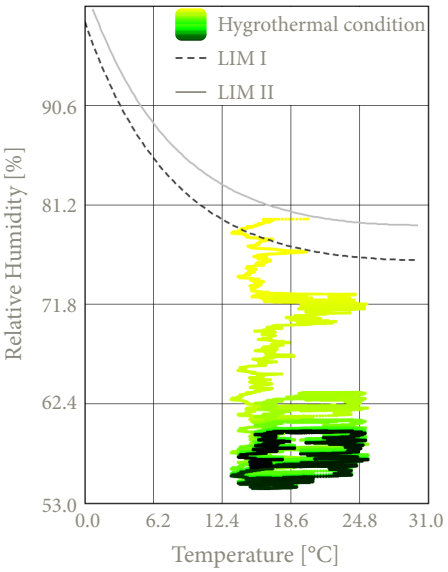

Figure A262, Isopleths transition frame & wood

Conclusion isoplteths

Based on the established and analysed isopleths of the various details within this construction **configuration**, it can be concluded that there is no risk of mould growth within the different material layers. All isopleths located behind the cork insulation plate remain below the critical threshold values **LIM I** and **LIM II**, indicating that the details meet the established criteria.

With regards to the **cork façade panel** it can be observed that the isopleths mostly exceed the LIM threshold values, which is the same as in the other three cork configuration assessments. Therefore, a similar conclusion can be drawn as in the previous cork configurations based on the paper by (Hon, 2024). Just like in the previous cork configurations, in order to state with certainty that no mould growth occurs in the cork as an exterior panel material, additional research is required.

The board that is glued with cork mortar behind the cork façade panel, the **expanded insulation corkboard**, shows in all three details similair results. The isopleths show a small exceedance at the beginning of the simulation. However, over time the moisture present in the material at the start, approximately 80%, is transported out. This is because, as previously stated, cork is a porous material making it capable of buffering fluctuations in relative humidity. Nevertheless, at the end of the simulation, the isopleths still slightly exceed the LIM I line. However, for the majority of the year, the isopleths remain below both LIM thresholds. The continuously decreasing trend and the fact that the isopleths are for the majority of the year below the thresholds, suggests that there is no long-term risk of mould development.

When examining the isopleths of the **outside biobased construction board**, it can be seen that the isopleths, apart from a short period at the beginning, remain below the LIM thresholds and all show a downward trend. When comparing the isopleths between this wood fibre configuration and the previous flax cork configurations with a cork cladding it becomes clear that this configuration has the same effect on the biobased construction board as the flax configuration and the second cork configuration. This means that the construction board is better protected against mould growth due to the additional expanded insulation corkboard and the cork mortar. In this configuration, a downward trend is also visible in the isopleths. Therefore, with regard to mould resistance the outside construction board has no risk of mould growth.

With regard to the isopleths of the **flexible wood fibre insulation**, as well as the **transition zones between the wood fibre and the wooden construction frame**, the values remain well below both LIM threshold values and for all of these isopleths a downward trend is visible. Lastly, the isopleths of the **inside biobased construction board**, and the **clay plaster**, also remain well below the LIM lines with a slight downward trend visible in the inside biobased construction board. However, the isopleths remain far below the LIM lines.

In conclusion, it can be stated that this configuration poses no risk of mould growth and thus complies with the specified isopleth requirements. However, in order to fully confirm this, further research is needed regarding the cork panel used on the exterior. As such, the design complies with the required hygrothermal performance standards.

Surface condensation - V1, V2 & H1

The circle at each figure figures below, **figure 263**, **figure 265** and **figure 267**, show the coldest point of the interior surface at each detail in order to consider the f_{Rsi}. Below these graphs the corresponding surface temperature at this point is shown over a ten-year simulation below, **figure 264**, **figure 266** and **figure 268**.

Figure A263, Highlight lowest point, V1

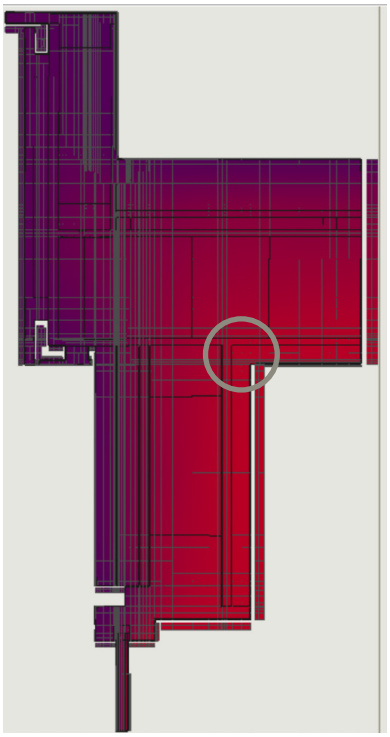

Figure A265, Highlight lowest point, V2

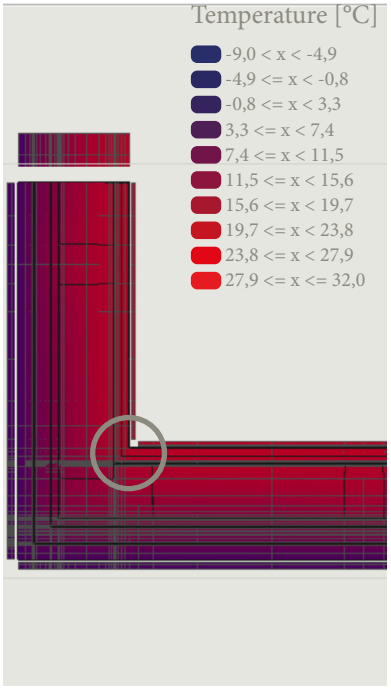

Figure A267, Highlight lowest point, H1

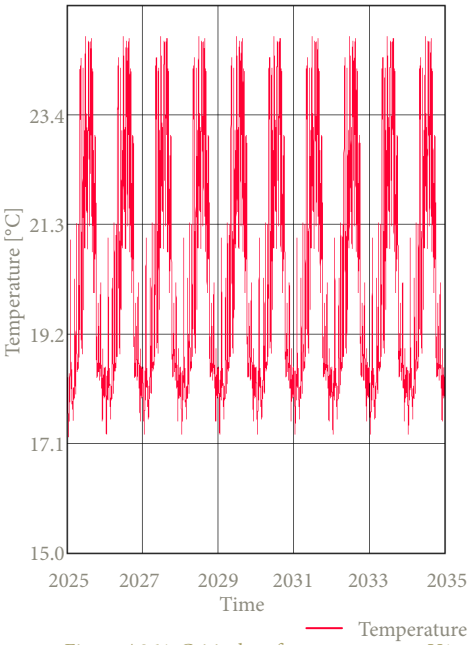

Figure A264, Critical surface temperature, V1

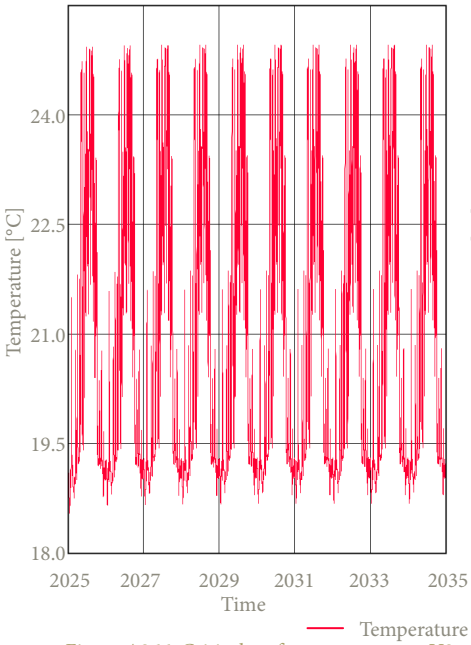

Figure A266, Critical surface temperature, V2

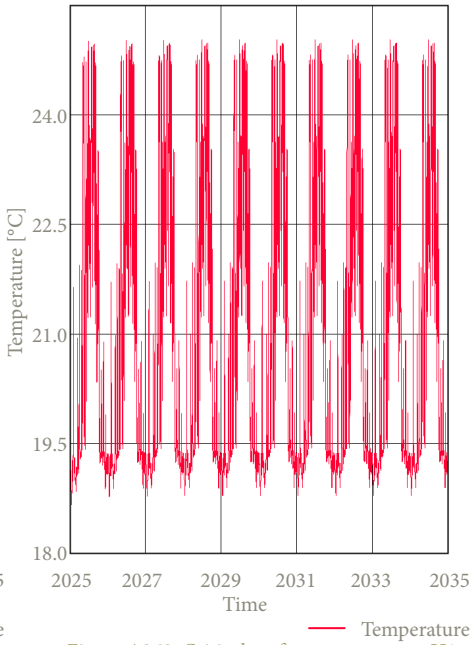

Figure A268, Critical surface temperature, H1

From this graph the lowest surface temperature of this detail is **15.76 °C**.

The resulting f_{Rsi} for this detail is **0.65** which exceeds the minimum requirement of 0.61. This indicates a negligible risk of surface condensation.

From this graph the lowest surface temperature of this detail is **18.54 °C**.

The resulting f_{Rsi} for this detail is **0.88** which exceeds the minimum requirement of 0.61. This indicates a negligible risk of surface condensation.

From this graph the lowest surface temperature of this detail is **18.60 °C**.

The resulting f_{Rsi} for this detail is **0.88** which exceeds the minimum requirement of 0.61. This indicates a negligible risk of surface condensation.

F-factor - V1, V2 & H1

The resulting **f-factor** of **detail V1** is **0.89** for a temperature of **16.03 °C**. Next the resulting **f-factor** of **detail V2** is **0.94** for a temperature of **17.00 °C**. Lastly, the resulting **f-factor** of **detail H1** is **0.95** for a temperature of **17.10 °C**. This indicates a very limited thermal bridge is assessed within the details of this configuration.
Given that these values significantly all exceeds the required threshold of **0.65**, it can be concluded that the details within this configuration complies with the thermal performance requirements set by the Dutch Building Decree.

PSI-value - V1

Table A54, Calculation of the $Q_{ideal\ condition}$

$R_{construction,\ window}$ [(m²K)/W]	$A_{construction,\ window}$ [m²]	$R_{construction,\ wall}$ [(m²K)/W]	$A_{construction,\ wall}$ [m²]	$R_{construction,\ floor}$ [(m²K)/W]	$A_{construction,\ floor}$ [m²]
0.600	0.2425	5.278	1.018	4.648	0.845

The resulting $\mathbf{Q_{ideal\ condition}}$ is **14.019 W**

Q_{WUFI} represents the sum of all heat flows through the detail, resulting in a total heat flow of **15.050 W**.

These values give a **Ψ-value** of **0.057 W/(mK)** for **detail V1**, indicating that the detail can be characterised as a well-insulated building component.

PSI-value - V2

Table A55, Calculation of the $Q_{ideal\ condition}$

$R_{construction,\ window}$ [(m²K)/W]	$A_{construction,\ window}$ [m²]	$R_{construction,\ wall}$ [(m²K)/W]	$A_{construction,\ wall}$ [m²]	$R_{construction,\ roof}$ [(m²K)/W]	$A_{construction,\ roof}$ [m²]
0.600	0.2425	5.278	0.943	6.442	0.198

The resulting $\mathbf{Q_{ideal\ condition}}$ is **11.044 W**

Q_{WUFI} represents the sum of all heat flows through the detail, resulting in a total heat flow of **12.423 W**.

These values give a **Ψ-value** of **0.076 W/(mK)** for **detail V2**, indicating that the detail can be characterised as a well-insulated building component.

PSI-value - H1

Table A56, Calculation of the $Q_{ideal\ condition}$

$R_{construction,\ window}$ [(m²K)/W]	$A_{construction,\ window}$ [m²]	$R_{construction,\ wall}$ [(m²K)/W]	$A_{construction,\ wall}$ [m²]
0.600	0.2425	5.278	2.278

The resulting $\mathbf{Q_{ideal\ condition}}$ is **15.044 W**

Q_{WUFI} represents the sum of all heat flows through the detail, resulting in a total heat flow of **16.580 W**.

These values give a **Ψ-value** of **0.085 W/(mK)** for **detail H1**, indicating that the detail can be characterised as a well-insulated building component.

Assessment detail configuration

Important notes about the details

For the given configuration, **key considerations** are presented below in the form of bullet points. These points highlight specific aspects that need to be taken into account during detailing and construction.

- Place the flexible wood fibre between the studs of the wooden frame.
- Finish the inside of the wooden frame with a pressure-resistant wood fibre board to allow for fixings.
- Attach the water-resistant barrier of the window frame to the timber structural frame.
- Apply a water-resistant, vapour-permeable membrane over the timber frame construction to protect the flexible wood fibre against mould growth.
- Apply a diffusion-open construction board with water-resistant properties onto the timber frame, over which cork mortar can be applied.
- Attach the cork façade panels using 3 mm cork mortar adhesive onto the cork insulation boards.
- Fix the cork insulation boards using both 3 mm cork mortar adhesive and mechanical fastening with insulation anchors to ensure a structurally secure base layer for the cork façade panels.
- Use 6 insulation anchors per m^2, with anchor lengths equal to the insulation board thickness plus 30 mm embedment depth.
- The wooden lintel must have proper bearing on the wooden frame.
- The screws of the biobased construction board must reach the center of the timber frame to ensure secure attachment.
- Ensure 5 mm ventilation gaps both between cork panels and at the window frame.
- Use a clay base plate to provide a correct underlayment for the clay plaster.
- Use a jute reinforcement mesh between the rough and finishing clay plaster to prevent cracking.

Assessment of the configuration

Additionally, the configuration is evaluated based on the following criteria:

1. **Weight**: The total mass per unit area of the wall construction.
2. **Construction time**: The time required for assembling the construction.
3. **Resistance Construction-value:** The combined thermal resistance of all layers in the construction.
4. **Phase shift**: The heat transfer delay of the structure.

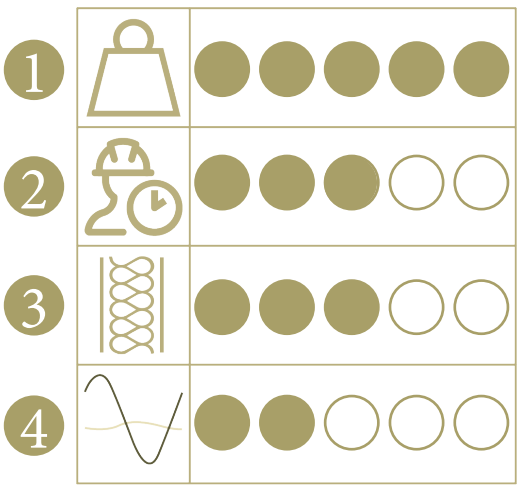

Axonometric view of the detail configuration

In addition to the presented details, an **axonometric view** of the respective detail is also shown. This is presented in the figure below, **figure 269**, and is intended to provide more clarity and insight into **detail V1, detail V2,** and **detail H1**.

Figure A269, Axonometric view of detail configuration 9

Detail configuration 10 - straw insulation with wooden façade

The tenth detail configuration consists of blow-in straw insulation that is sprayed between the studs of the timber construction frame and the construction boards with a density of 100 kg/m³. The straw only needs to be protected against water and mould growth by placing a diffusion-open construction board on the exterior side of the timber frame. This board also provides structural stability and serves as a base for the timber façade system. On the interior side, the timber construction frame is finished with a biobased, vapour-open construction board onto which a clay board is screwed. A clay plaster can then be applied to this board, consisting of a base layer and a finishing layer.

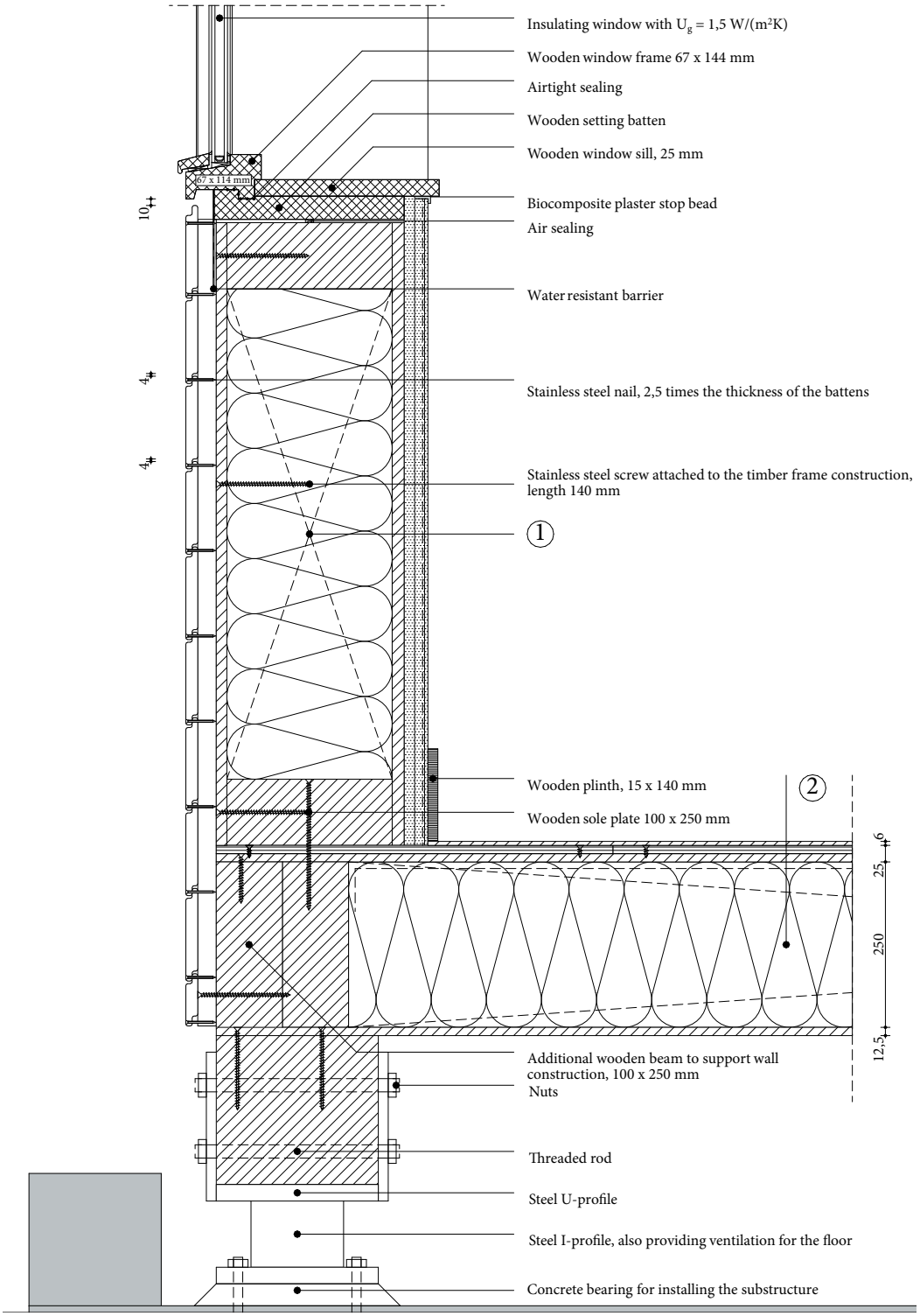

Figure A270, 1:10 detail of V1, configuration 10, own illustration

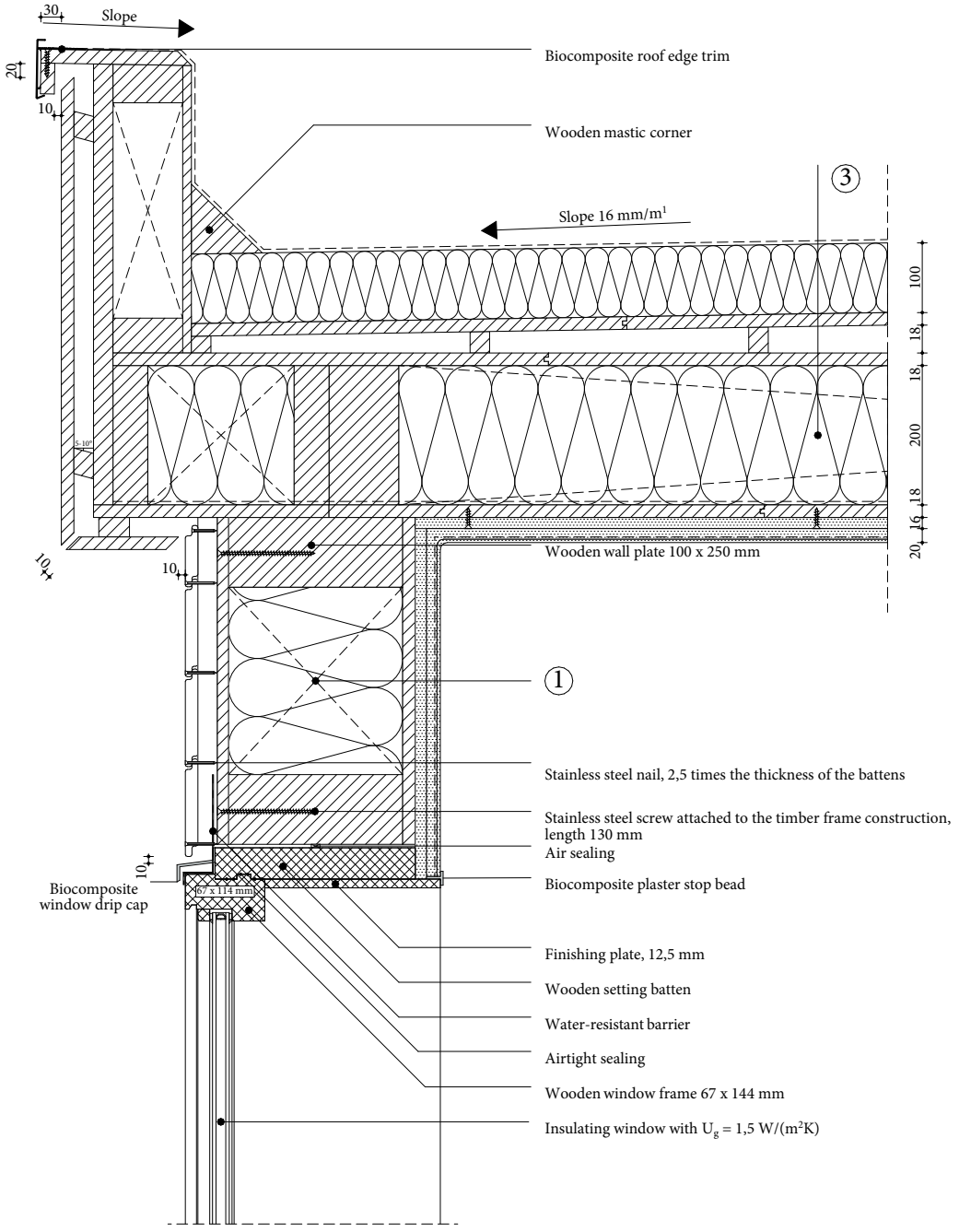

Figure A271, 1:10 detail of V2, configuration 10, own illustration

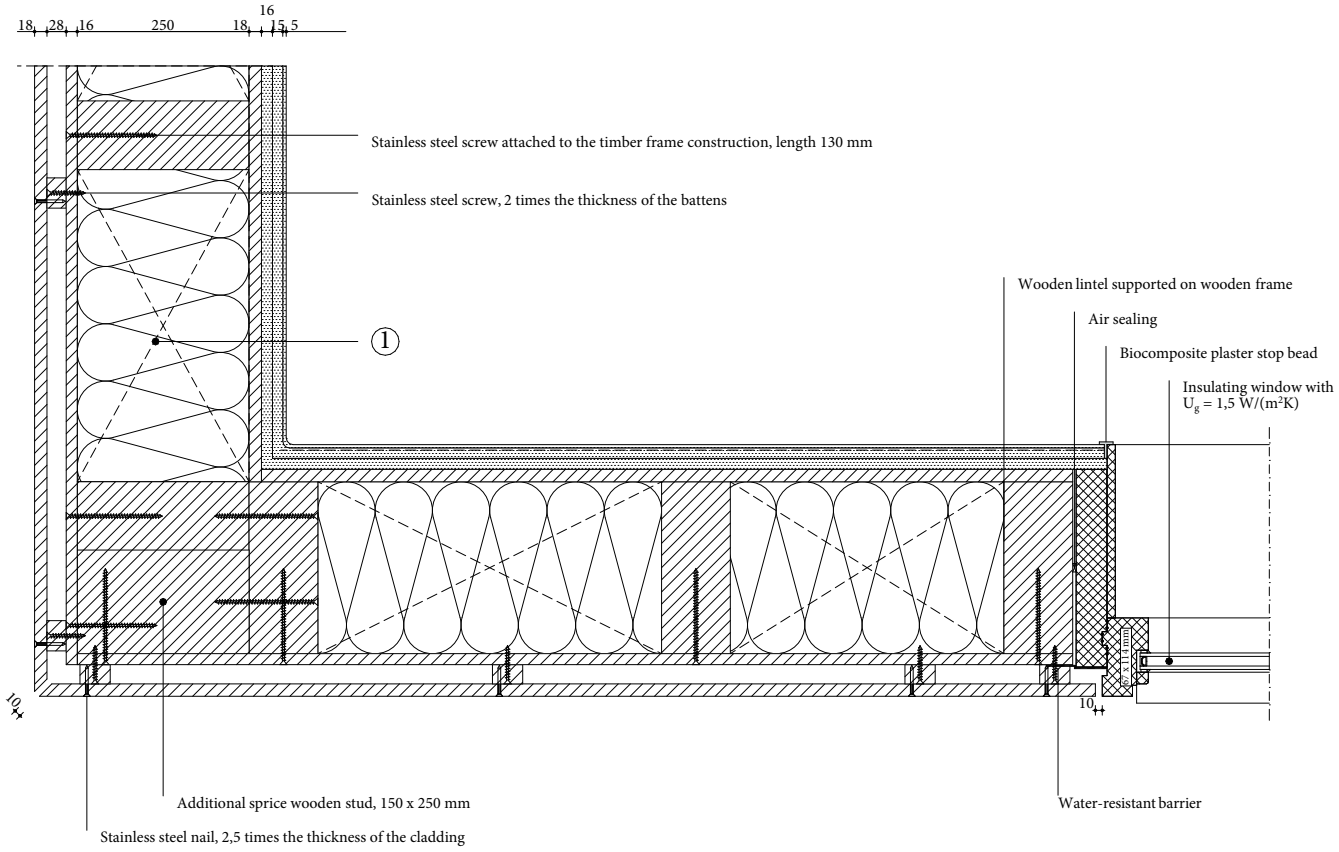

Figure A272, 1:10 detail of H1, configuration 10, own illustration

❶ Wall construction build-up, RC-value: 4.92 (m²K)/W

- Horizontal wooden cladding, 18 mm;
- Vertical spruce cladding batten forming ventilated cavity, 28 x 44 mm, center-to-center 600 mm;
- Biobased diffusion open construction board, 16mm;
- Timber frame construction, 100 x 250 mm, center-to-center 600 mm;
- Blow in straw blown between construction & construction boards (λ ≤ 0.043 W/mK), 250 mm;
- Biobased construction board, 18 mm;
- Clay base plate, 16 mm;
- Rough base clay plaster, 15 mm;
- Jute reinforcement mesh;
- Finishing clay plaster, 5 mm.

❷ Floor construction build-up, RC-value: 4.65 (m²K)/W

- Finishing board, 6 mm;
- Biobased wooden construction board, 12.5 mm;
- Biobased wooden construction board, perpendicular on the other plate, 12.5 mm;
- Vapour-retarding and airtight membrane with a variable vapour diffusion resistanance;
- Flexible hemp fiber insulation placed between construction (λ ≤ 0.043 W/(mK), 250 mm;
- Wooden beams 100 x 250 mm, center-to-center 600 mm;
- Biobased wooden construction board, 12.5 mm.

❸ Roof construction build-up, RC-value: 6.71 (m²K)/W

- EPDM glued on underlayment to prevent roof covering from lifting;
- Pressure-resistant woodfibre insulation plate (λ ≤ 0.042 W/(mK), 100 mm;
- Biobased wooden construction board, 18 mm;
- Sloped wooden battens for drainage at an angle of 16 mm/m^1, 28 x 24 mm;
- Biobased wooden construction board, 18 mm;
- Flexible hemp fiber insulation placed between construction (λ ≤ 0.043 W/(mK), 200 mm;
- Wooden beams 100 x 200 mm, center-to-center 600 mm;
- Vapour-retarding and airtight membrane with a variable vapour diffusion resistanance;
- Biobased wooden construction board, 18 mm;
- Clay base plate, 16 mm;
- Rough base clay plaster, 15 mm;
- Jute reinforcement mesh;
- Finishing clay plaster, 5 mm.

U_g = 1.50 W/(m²K)

U_w = 1.76 W/(m²K)

f-factor ≥ 0.65

Ψ_{V1}: 0.067 W/(mK) Ψ_{V2}: 0.078 W/(mK) Ψ_{H1}: 0.094 W/(mK)

Isopleths: no risk of mould $f_{R,si} > f_{R,si,\,max}$; no risk of mould

Phase shift of the wall construction: 10.2 h

Density of the wall construction 123 kg/m³

Calculation RC-value wall construction build-up

❶ Wall construction build-up, RC-value: 4.92 (m²K)/W

Table A57, Calculation of the RC-value of the wall construction build-up

Material	Thickness [m]	Thermal conductivity [W/(mK)]	Thermal resistance [W/(m²K)]
Vertical wooden cladding	0,018	0,130	0,138
Ventilated cavity with vertical wooden cladding batten, center-to-center 600 mm	0,028	0,322	0,087
Biobased diffusion open construction board	0,016	0,090	0,178
Timber frame construction, with blow in straw insulation	0,250	0,058	4,310
Biobased construction board	0,018	0,120	0,150
Clay base plate	0,016	0,470	0,034
Clay plaster	0,020	0,910	0,022

Table A58, Calculation of the equivalent thermal conductivity of the individual layers in the relevant build-up

	Layer 1		Layer 2	
Material	Area [m²]	Thermal conductivity [W/(mK)]	Area [m²]	Thermal conductivity [W/(mK)]
Timber frame construction, with blow in straw insulation	0,15	0,046	0,025	0,130

Density mass per unit area of the wall construction

Table A59, Calculation of the density mass per unit area

Material	Thickness [m]	Density [kg/m³]
Vertical wooden cladding	0,018	520
Ventilated cavity with vertical wooden cladding batten, center-to-center 600 mm	0,024	35
Biobased diffusion open construction board	0,016	565
Timber frame construction, with blow in straw insulation	0,250	160
Biobased construction board	0,018	621
Clay base plate	0,016	1300
Clay plaster	0,020	1600

By using the previously presented formula a **m'-value** of **123.22 kg/m²** can be given for the **tenth detail configuration**.

Phase-shift

Table A60, Calculation of the phase shift

Material	Thickness [m]	Thermal conductivity [W/(mK)]	Density [kg/m³]	Specific heat capacity [J/(kgK)]
Timber frame construction, with blow in straw insulation	0,250	0,058	160	1143

By using the presented phase shift formula, the resulting **φ-value** for **the tenth configuration** is **10.2 h.**

Geometry WUFI

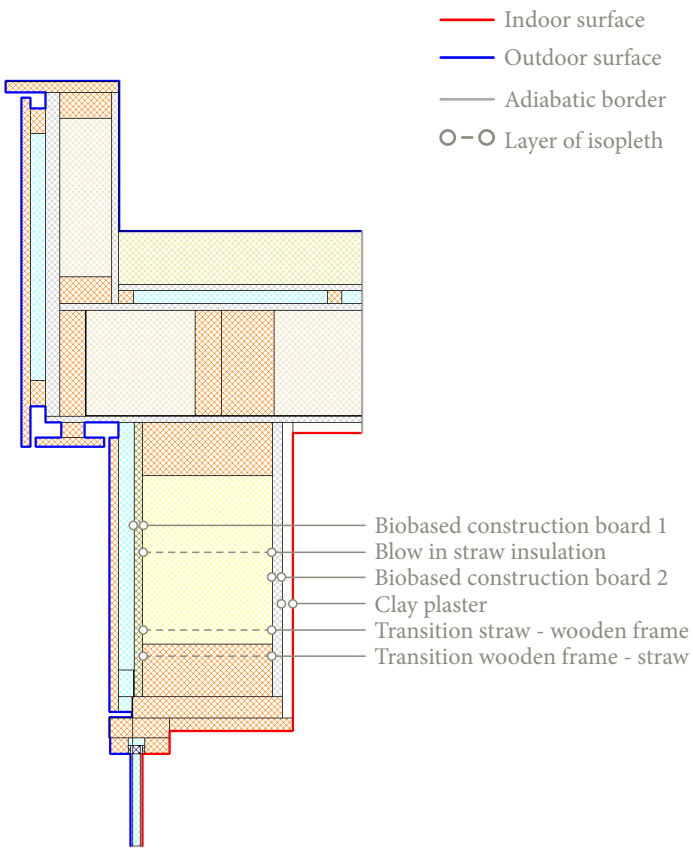

Figure A274, geometry detail V2 including location isopleths

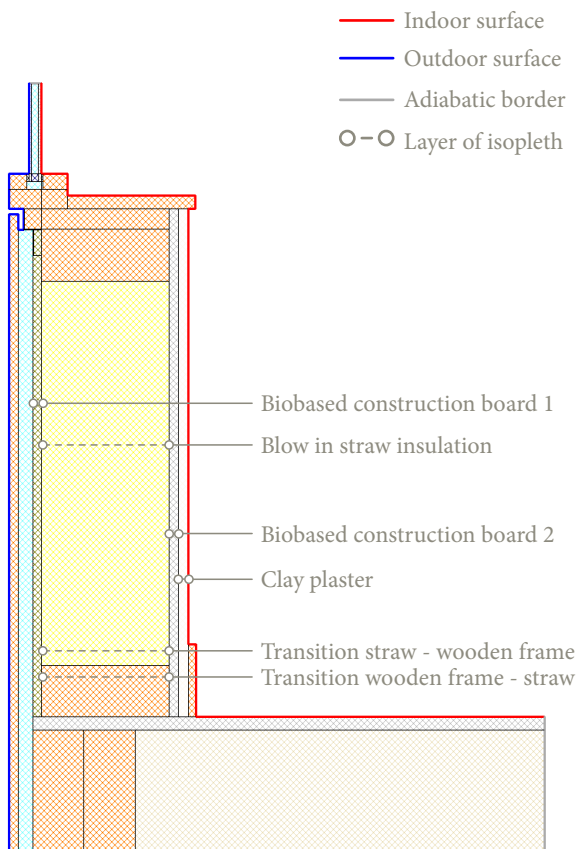

Figure A275, geometry detail V1 including location isopleths

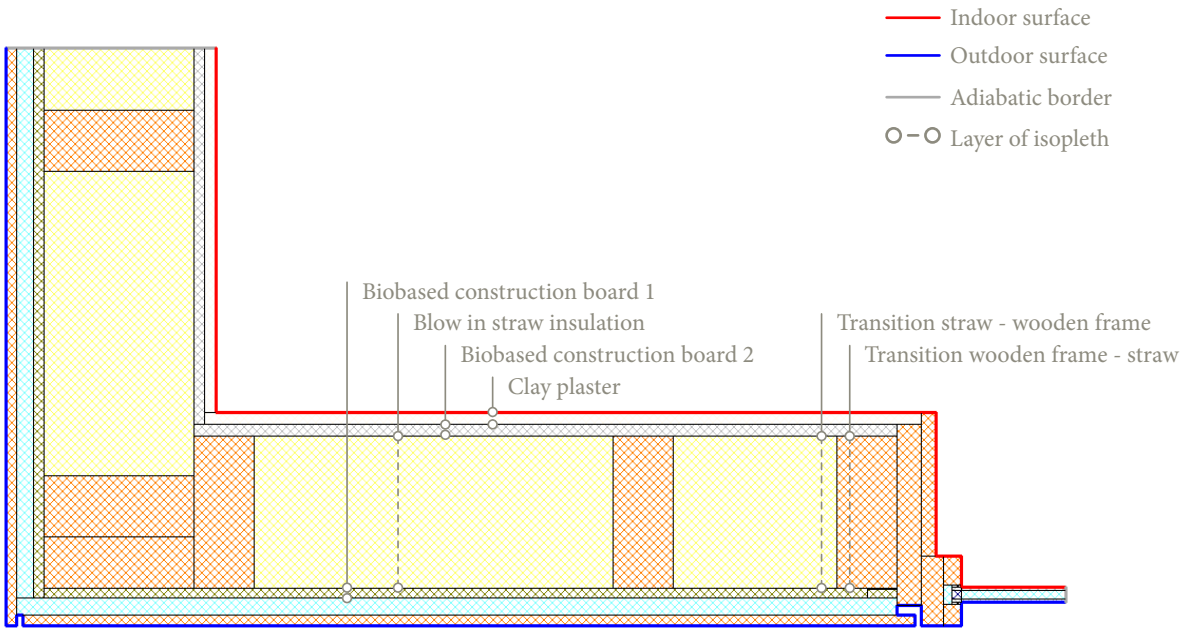

Figure A273, geometry detail H1including location isopleths

Isopleths - V1

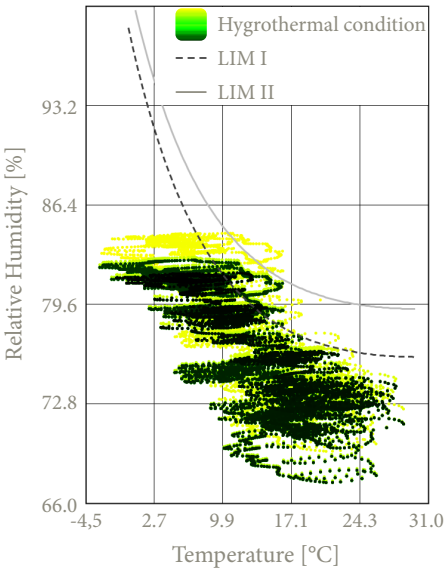

Figure A276, Isopleths biobased construction board 1

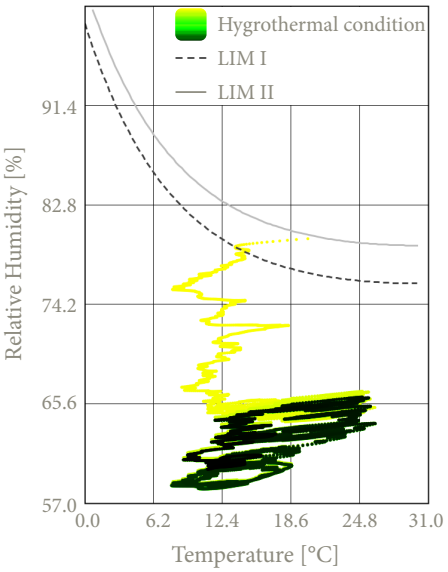

Figure A277, Isopleths blow in straw

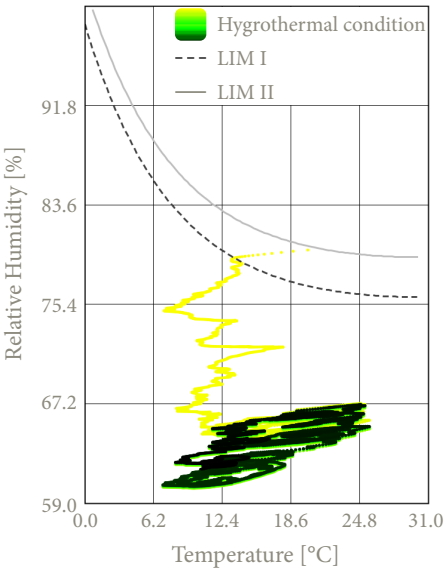

Figure A278, Isopleths straw & transition frame

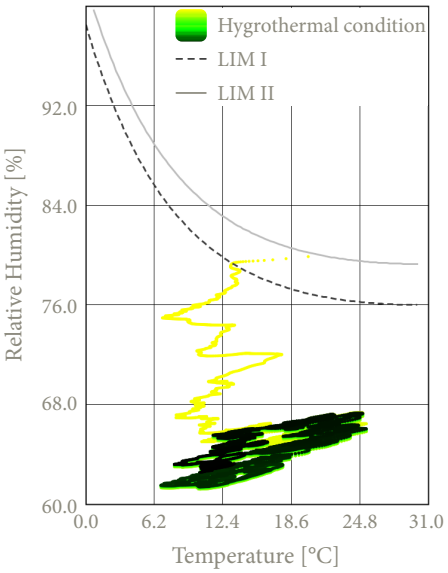

Figure A279, Isopleths transition frame & straw

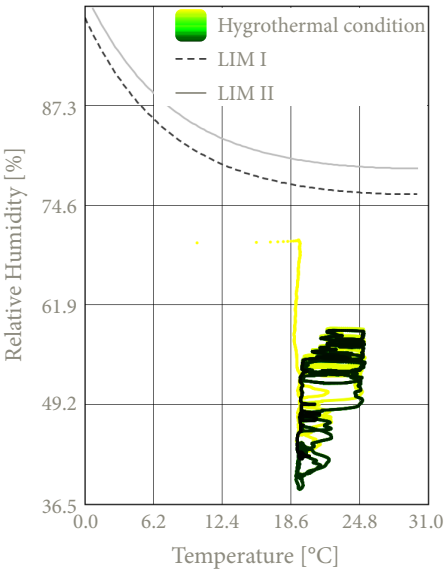

Figure A280, Isopleths biobased construction board 2

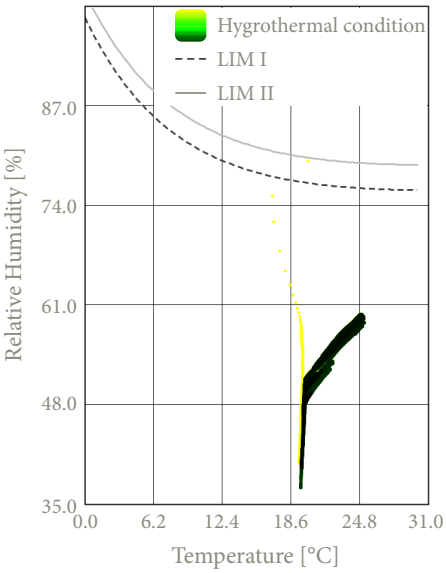

Figure A281, Isopleths clay plaster

Isopleths - V2

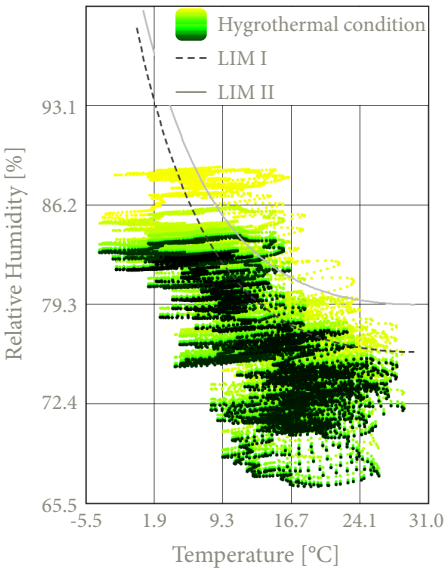

Figure A282, Isopleths biobased construction board 1

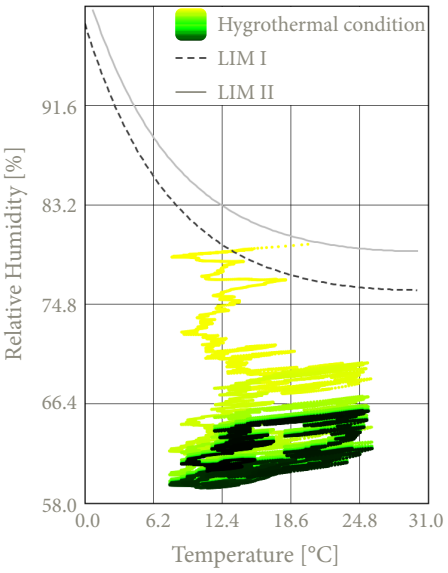

Figure A283, Isopleths blow in straw

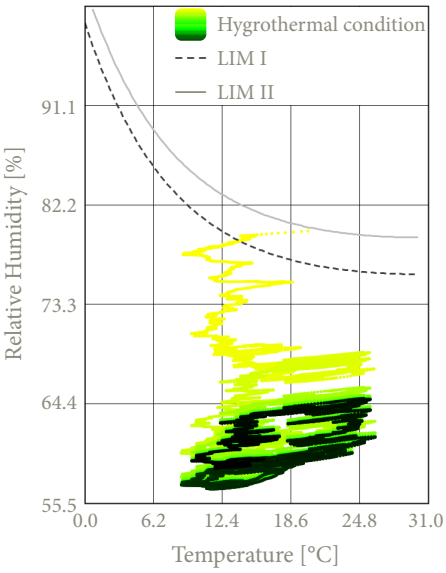

Figure A284, Isopleths straw & transition frame

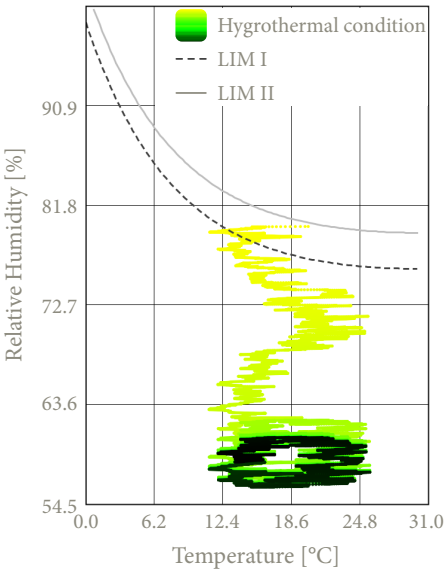

Figure A285, Isopleths transition frame & straw

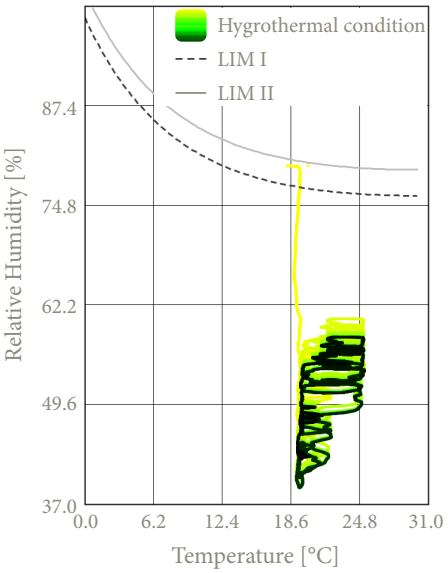

Figure A286, Isopleths biobased construction board 2

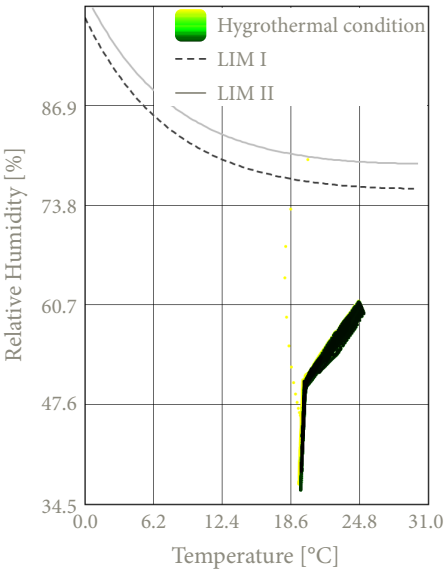

Figure A287, Isopleths clay plaster

Isopleths - H1

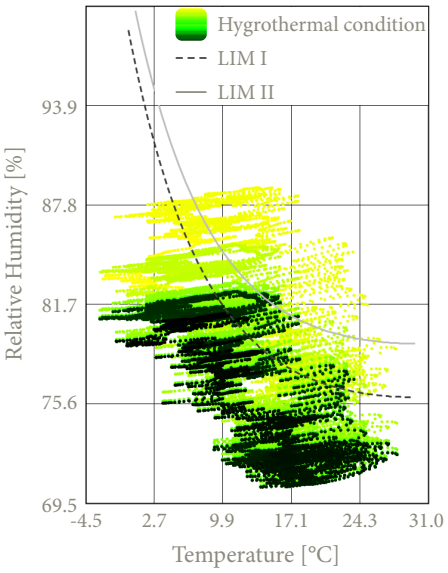

Figure A288, Isopleths biobased construction board 1

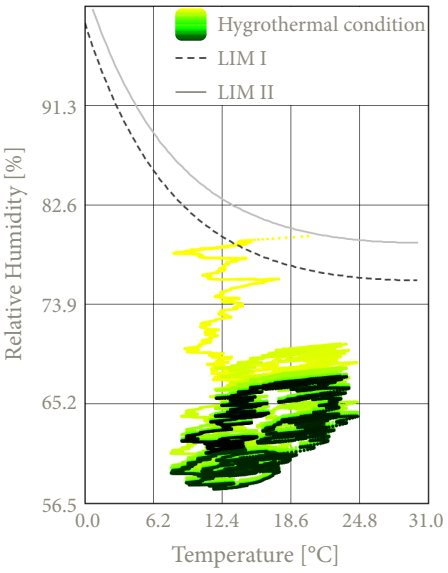

Figure A289, Isopleths blow in straw

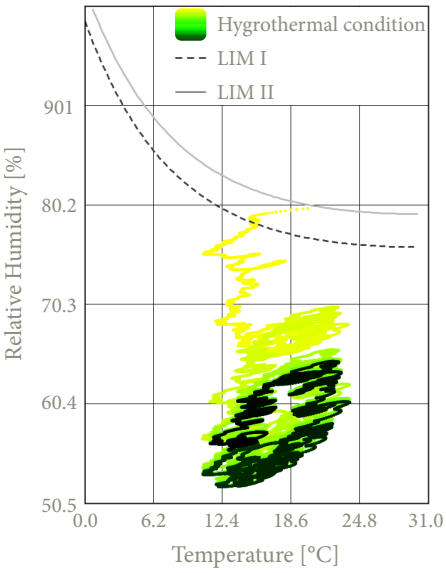

Figure A290, Isopleths straw & transition frame

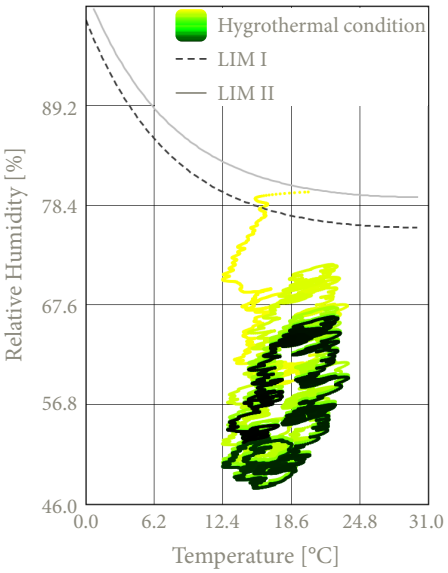

Figure A291, Isopleths transition frame & straw

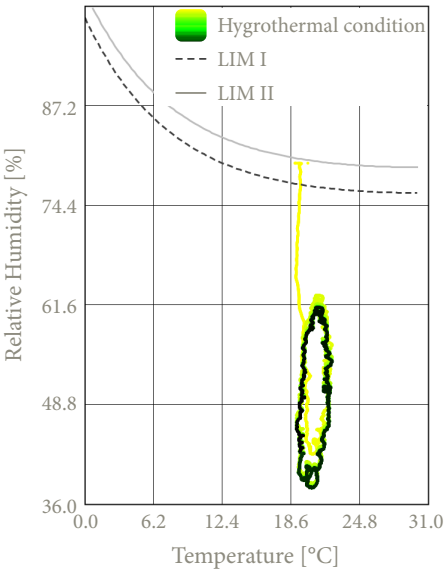

Figure A292, Isopleths biobased construction board 2

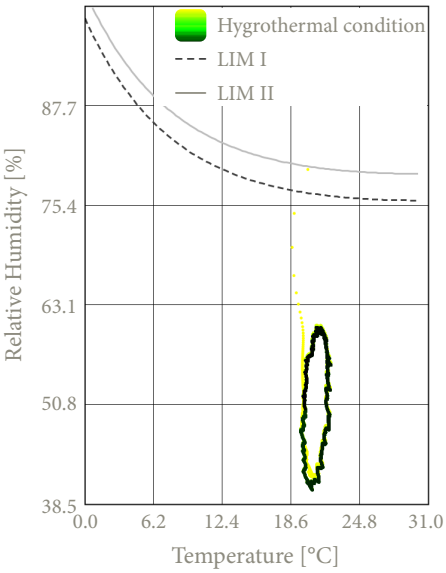

Figure A293, Isopleths clay plaster

Conclusion isoplteths

Based on the established and analysed isopleths of the various details within this construction **configuration**, it can be concluded that there is **no risk of mould growth** within the different material layers. All isopleths remain below the critical threshold values **LIM I** and **LIM II**, indicating that the details meet the established criteria.

With regard to the isopleths of the **biobased construction board on the outside** in each detail, it can be observed that the relative humidity exceeds the LIM I threshold at the beginning of the simulation. This trend can possibly be attributed to the initial conditions, where the initial moisture content in the wood fibre was approximately 80%. During the simulation, however, the relative humidity gradually decreases to below both LIM I and LIM II, indicating that moisture is being transported out of the material. Nevertheless, at the end of the simulation, the isopleths still slightly exceed the LIM I line. However, for the majority of the year, the isopleths remain below both LIM thresholds. The continuously decreasing trend and the fact that the isopleths are for the majority of the year below the thresholds, suggests that there is no long-term risk of mould development.

With respect to the isopleths of the **blow in straw insulation**, as well as the **transition zones between the straw and the wooden construction frame**, the **biobased construction board on the inside**, and the **clay plaster**, the values remain well below both LIM threshold values. At the location of the transition between the straw and the wooden frame, the isopleths show a slight upward trend at V1. However, this increase gradually levels off, with values remaining below the critical LIM thresholds. With regard to the isopleths at V2 and H1 a decreasing trend can be observed at the location of the transition zone between the wood fibre and the wooden frame.

In relation to the isopleths of the **biobased construction board on the inside**, it can be seen that they remain well below the LIM threshold values and continue to decrease further over the course of the ten years. A similar but smaller effect can be observed at the **clay plaster**.

In conclusion, it can be stated that this configuration poses no risk of mould growth and thus complies with the specified isopleth requirements. As such, the design complies with the required hygrothermal performance standards.

Surface condensation - V1, V2 & H1

The circle at each figure figures below, **figure 294**, **figure 296** and **figure 298**, show the coldest point of the interior surface at each detail in order to consider the f_{Rsi}. Below these graphs the corresponding surface temperature at this point is shown over a ten-year simulation below, **figure 295**, **figure 297** and **figure 299**.

Figure A294, Highlight lowest point, V1

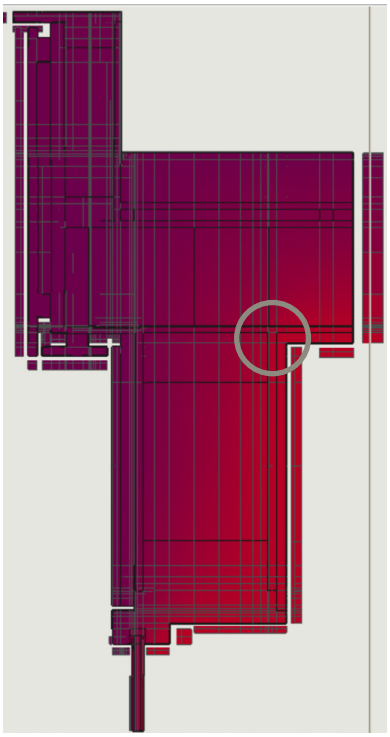

Figure A296, Highlight lowest point, V2

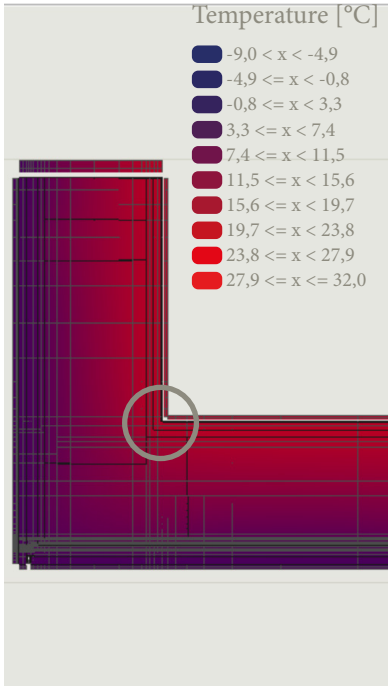

Figure A298, Highlight lowest point, H1

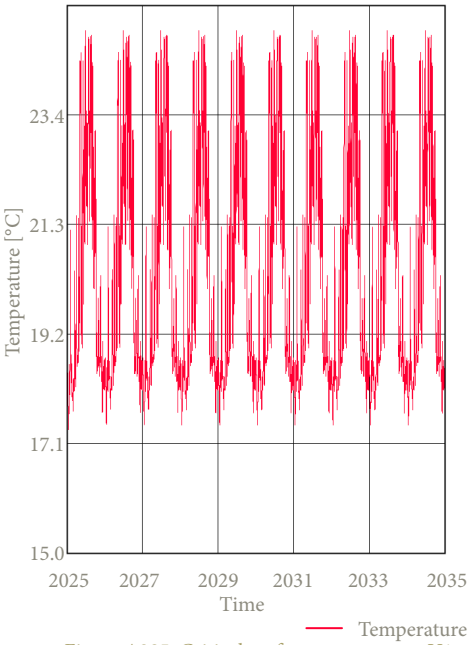

Figure A295, Critical surface temperature, V1

From this graph the lowest surface temperature of this detail is **15.75 °C**.

The resulting f_{Rsi} for this detail is **0.65** which exceeds the minimum requirement of 0.61. This indicates a negligible risk of surface condensation.

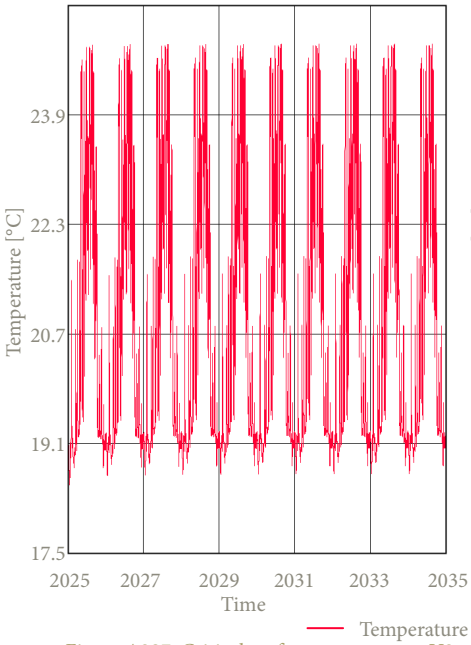

Figure A297, Critical surface temperature, V2

From this graph the lowest surface temperature of this detail is **18.05 °C**.

The resulting f_{Rsi} for this detail is **0.84** which exceeds the minimum requirement of 0.61. This indicates a negligible risk of surface condensation.

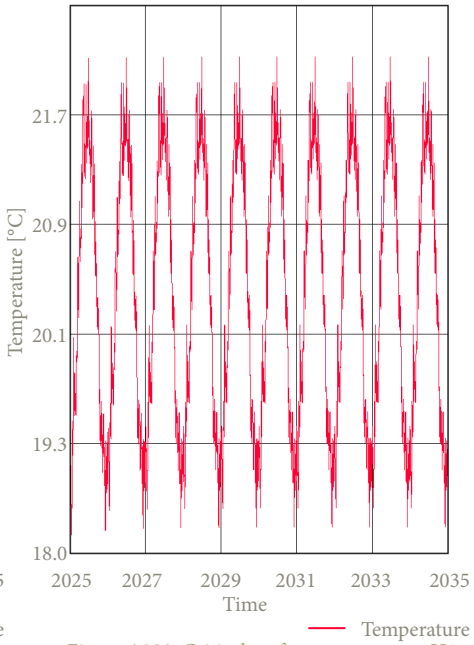

Figure A299, Critical surface temperature, H1

From this graph the lowest surface temperature of this detail is **18.63 °C**.

The resulting f_{Rsi} for this detail is **0.89** which exceeds the minimum requirement of 0.61. This indicates a negligible risk of surface condensation.

F-factor - V1, V2 & H1

The resulting **f-factor** of **detail V1** is **0.89** for a temperature of **16.17 °C**. Next the resulting **f-factor** of **detail V2** is **0.94** for a temperature of **16.95 °C**. Lastly, the resulting **f-factor** of **detail H1** is **0.93** for a temperature of **16.88 °C**. This indicates a very limited thermal bridge is assessed within the details of this configuration.
Given that these values significantly all exceeds the required threshold of **0.65**, it can be concluded that the details within this configuration complies with the thermal performance requirements set by the Dutch Building Decree.

PSI-value - V1

Table A61, Calculation of the $Q_{ideal\ condition}$

$R_{construction,\ window}$ [(m²K)/W]	$A_{construction,\ window}$ [m²]	$R_{construction,\ wall}$ [(m²K)/W]	$A_{construction,\ wall}$ [m²]	$R_{construction,\ floor}$ [(m²K)/W]	$A_{construction,\ floor}$ [m²]
0.600	0.2425	4.919	1.018	4.648	0.711

The resulting $\mathbf{Q_{ideal\ condition}}$ is **13.754 W**

Q_{WUFI} represents the sum of all heat flows through the detail, resulting in a total heat flow of **14.962 W**.

These values give a **Ψ-value** of **0.067 W/(mK)** for **detail V1**, indicating that the detail can be characterised as a well-insulated building component.

PSI-value - V2

Table A62, Calculation of the $Q_{ideal\ condition}$

$R_{construction,\ window}$ [(m²K)/W]	$A_{construction,\ window}$ [m²]	$R_{construction,\ wall}$ [(m²K)/W]	$A_{construction,\ wall}$ [m²]	$R_{construction,\ roof}$ [(m²K)/W]	$A_{construction,\ roof}$ [m²]
0.600	0.2425	4.919	0.883	6.442	0.202

The resulting $\mathbf{Q_{ideal\ condition}}$ is **11.071 W**

Q_{WUFI} represents the sum of all heat flows through the detail, resulting in a total heat flow of **12.472 W**.

These values give a **Ψ-value** of **0.078 W/(mK)** for **detail V2**, indicating that the detail can be characterised as a well-insulated building component.

PSI-value - H1

Table A63, Calculation of the $Q_{ideal\ condition}$

$R_{construction,\ window}$ [(m²K)/W]	$A_{construction,\ window}$ [m²]	$R_{construction,\ wall}$ [(m²K)/W]	$A_{construction,\ wall}$ [m²]
0.600	0.2425	4.919	2.119

The resulting $\mathbf{Q_{ideal\ condition}}$ is **15.029 W**

Q_{WUFI} represents the sum of all heat flows through the detail, resulting in a total heat flow of **16.725 W**.

These values give a **Ψ-value** of **0.094 W/(mK)** for **detail H1**, indicating that the detail can be characterised as a well-insulated building component.

Assessment detail configuration

Important notes about the details

For the given configuration, **key considerations** are presented below in the form of bullet points. These points highlight specific aspects that need to be taken into account during detailing and construction.

- Blow the straw between the studs of the wooden frame and the construction boards at a density of 100 kg/m3 by creating a hole in the inner construction board.
- Finish the inside of the wooden frame with a pressure-resistant wood fibre board to allow for fixings.
- Attach the water-resistant barrier of the window frame to the timber structural frame.
- Apply a diffusion-open construction board with water-resistant properties onto the timber frame, over which cork mortar can be applied.
- The wooden lintel must have proper bearing on the wooden frame.
- The screws of the outdoor biobased construction board must reach the center of the timber frame to ensure secure attachment.
- Stainless steel screws must be at least 2 times the thickness of the battens.
- Stainless steel nails must be at least 2.5 times the thickness of the cladding.
- The stainless steel nails must be placed 40 mm from the outer edge of the cladding.
- Ensure 4 mm gaps between the cladding to accommodate the movement of the wood.
- Ensure 10 mm gaps for ventilation both between cladding boards and at the window frame.
- Use a clay base plate to provide a correct underlayment for the clay plaster.
- Use a jute reinforcement mesh between the rough and finishing clay plaster to prevent cracking.

Assessment of the configuration

Additionally, the configuration is evaluated based on the following criteria:

1. **Weight**: The total mass per unit area of the wall construction.
2. **Construction time**: The time required for assembling the construction.
3. **Resistance Construction-value:** The combined thermal resistance of all layers in the construction.
4. **Phase shift**: The heat transfer delay of the structure.

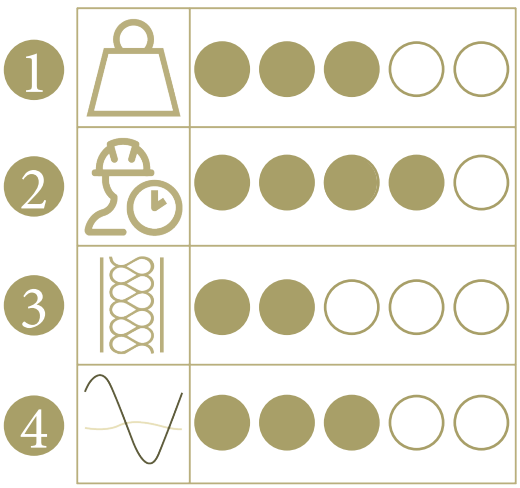

Axonometric view of the detail configuration

In addition to the presented details, an **axonometric view** of the respective detail is also shown. This is presented in the figure below, **figure 300**, and is intended to provide more clarity and insight into **detail V1, detail V2,** and **detail H1**.

Figure A300, Axonometric view of detail configuration 10

Detail configuration 11 - straw insulation with cork façade

The eleventh detail configuration consists of straw insulation that is sprayed between the studs of the timber construction frame and the construction boards with a density of 100 kg/m^3. The straw only needs to be protected against water and mould growth by placing a diffusion-open construction board on the exterior side of the timber frame. This board also provides structural stability and serves for the application of the cork façade system. Cork mortar can be applied over this board for the attachment of the expanded insulation corkboard. On top of the expanded insulation corkboard, another layer of cork mortar is applied to bond the cork cladding panels. On the interior side, the timber construction frame is finished with a biobased, diffusion-open construction board to which a clay board is screwed. A clay plaster can then be applied to this board, consisting of a rough layer and a finishing layer.

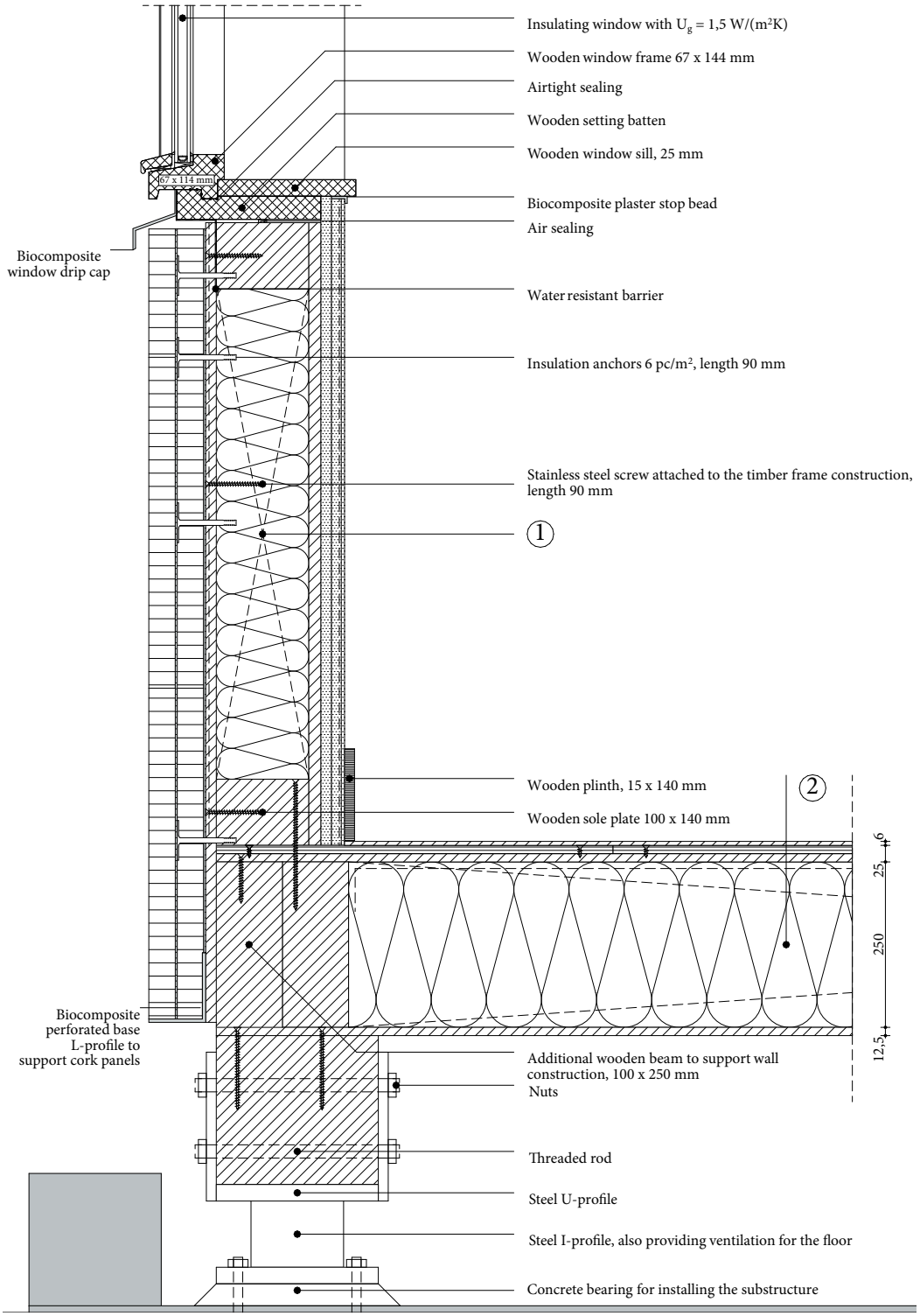

Figure A301, 1:10 detail of V1, configuration 11, own illustration

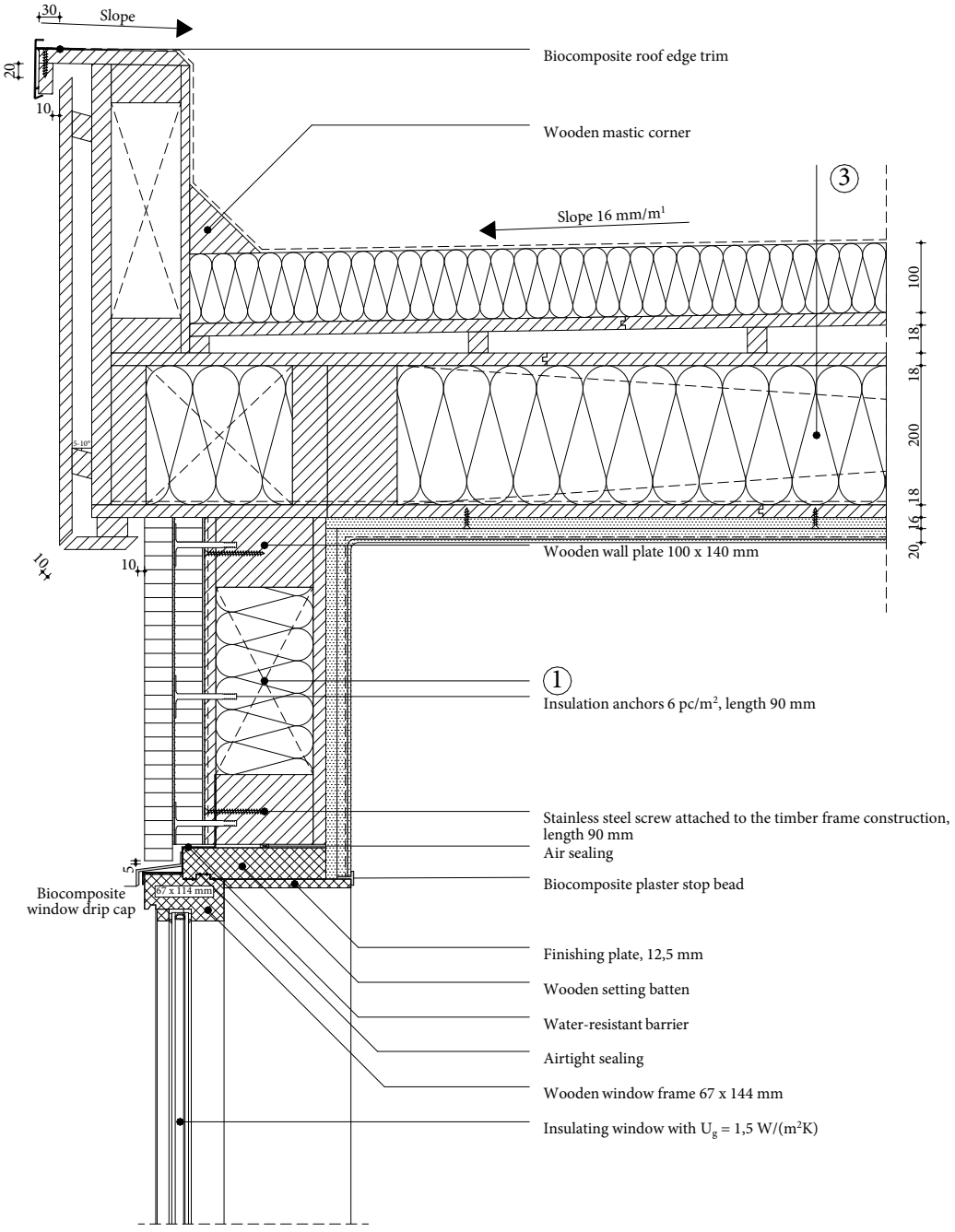

Figure A302, 1:10 detail of V2, configuration 11, own illustration

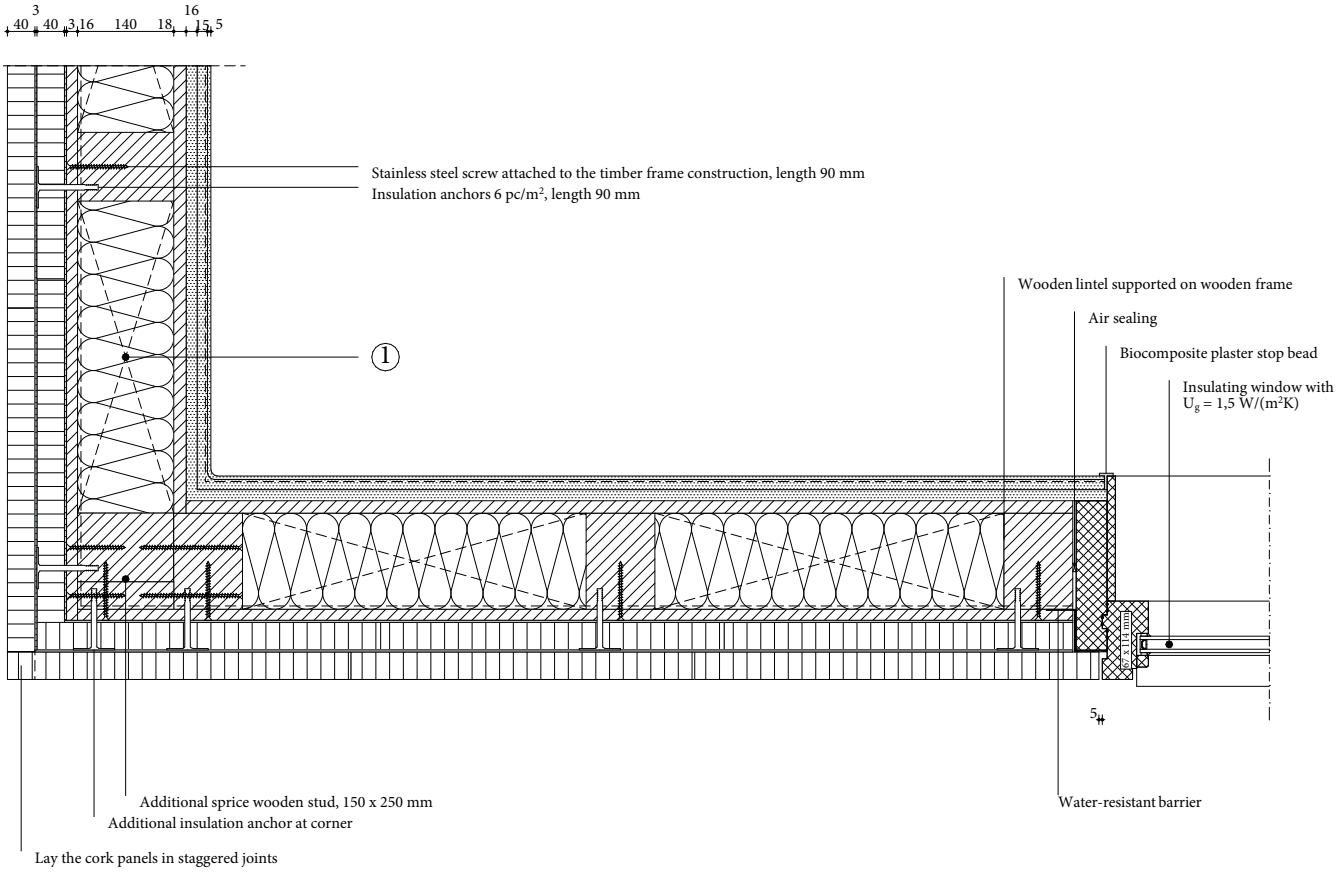

Figure A303, 1:10 detail of H1, configuration 11, own illustration

❶ Wall construction build-up, RC-value: 4.78 (m²K)/W

- Cork cladding panels (λ ≤ 0.043 W/mK), 40 mm;
- Cork mortar, 3 mm;
- Expanded insulation corkboard (λ ≤ 0.039 W/mK), 40 mm;
- Cork mortar, 3 mm;
- Biobased diffusion open construction board, 16mm;
- Water resistant vapour-permeable membrane;
- Timber frame construction, 100 x 140 mm, center-to-center 600 mm;
- Blow in straw placed between construction & construction boards (λ ≤ 0.043 W/mK), 140 mm;
- Biobased construction board, 18 mm;
- Clay base plate, 16 mm;
- Rough base clay plaster, 15 mm;
- Jute reinforcement mesh;
- Finishing clay plaster, 5 mm.

❷ Floor construction build-up, RC-value: 4.65 (m²K)/W

- Finishing board, 6 mm;
- Biobased wooden construction board, 12.5 mm;
- Biobased wooden construction board, perpendicular on the other plate, 12.5 mm;
- Vapour-retarding and airtight membrane with a variable vapour diffusion resistanance;
- Flexible hemp fiber insulation placed between construction (λ ≤ 0.043 W/(mK), 250 mm;
- Wooden beams 100 x 250 mm, center-to-center 600 mm;
- Biobased wooden construction board, 12.5 mm.

❸ Roof construction build-up, RC-value: 6.71 (m²K)/W

- EPDM glued on underlayment to prevent roof covering from lifting;
- Pressure-resistant woodfibre insulation plate (λ ≤ 0.042 W/(mK), 100 mm;
- Biobased wooden construction board, 18 mm;
- Sloped wooden battens for drainage at an angle of 16 mm/m^1, 28 x 24 mm;
- Biobased wooden construction board, 18 mm;
- Flexible hemp fiber insulation placed between construction (λ ≤ 0.043 W/(mK), 200 mm;
- Wooden beams 100 x 200 mm, center-to-center 600 mm;
- Vapour-retarding and airtight membrane with a variable vapour diffusion resistanance;
- Biobased wooden construction board, 18 mm;
- Clay base plate, 16 mm;
- Rough base clay plaster, 15 mm;
- Jute reinforcement mesh;
- Finishing clay plaster, 5 mm.

U_g = 1.50 W/(m²K)

U_w = 1.76 W/(m²K)

f-factor ≥ 0.65

Ψ_{V1}: 0.062 W/(mK) Ψ_{V2}: 0.087 W/(mK) Ψ_{H1}: 0.078 W/(mK)

Isopleths: no risk of mould $f_{R,si} > f_{R,si,\,max}$; no risk of mould

Phase shift of the wall construction: 5.7 h

Density of the wall construction 111 kg/m³

Calculation RC-value wall construction build-up

❶ Wall construction build-up, RC-value: 4.78 (m²K)/W

Table A64, Calculation of the RC-value of the wall construction build-up

Material	Thickness [m]	Thermal conductivity [W/(mK)]	Thermal resistance [W/(m²K)]
Tongue and groove cork cladding panels	0,040	0,043	0,930
Cork mortar	0,003	0,250	0,012
Expanded insulation corkboard	0,040	0,039	1,025
Cork mortar	0,003	0,250	0,012
Biobased diffusion open construction board	0,016	0,090	0,178
Timber frame construction, with blow in straw insulation	0,140	0,058	2,414
Biobased construction board	0,018	0,120	0,150
Clay base plate	0,016	0,470	0,034
Clay plaster	0,020	0,910	0,022

Table A65, Calculation of the equivalent thermal conductivity of the individual layers in the relevant build-up

	Layer 1		Layer 2	
Material	Area [m²]	Thermal conductivity [W/(mK)]	Area [m²]	Thermal conductivity [W/(mK)]
Timber frame construction, with blow in straw insulation	0,084	0,046	0,014	0,130

Density mass per unit area of the wall construction

Table A66, Calculation of the density mass per unit area

Material	Thickness [m]	Density [kg/m³]
Tongue and groove cork cladding panels	0,040	140
Cork mortar	0,003	1000
Expanded insulation corkboard	0,040	110
Cork mortar	0,003	1000
Biobased diffusion open construction board	0,016	565
Timber frame construction, with blow in straw insulation	0,140	160
Biobased construction board	0,018	621
Clay base plate	0,016	1300
Clay plaster	0,020	1600

By using the previously presented formula a **m'-value** of **111.42 kg/m²** can be given for the **eleventh detail configuration**.

Phase-shift

Table A67, Calculation of the phase shift

Material	Thickness [m]	Thermal conductivity [W/(mK)]	Density [kg/m³]	Specific heat capacity [J/(kgK)]
Timber frame construction, with blow in straw insulation	0,140	0,058	160	1143

By using the presented phase shift formula, the resulting **φ-value** for **the eleventh configuration** is **5.7 h.**

Geometry WUFI

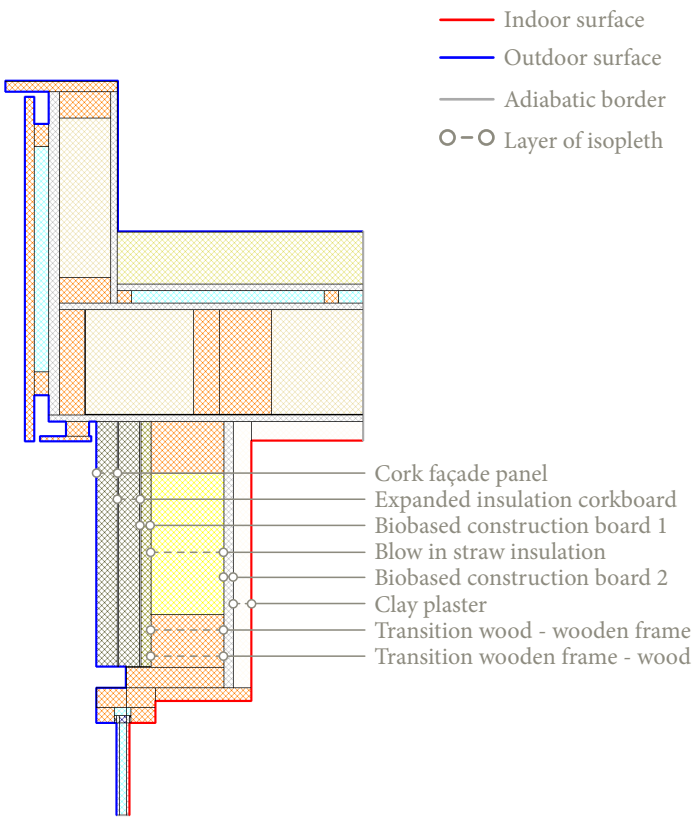

Figure A305, geometry detail V2 including location isopleths

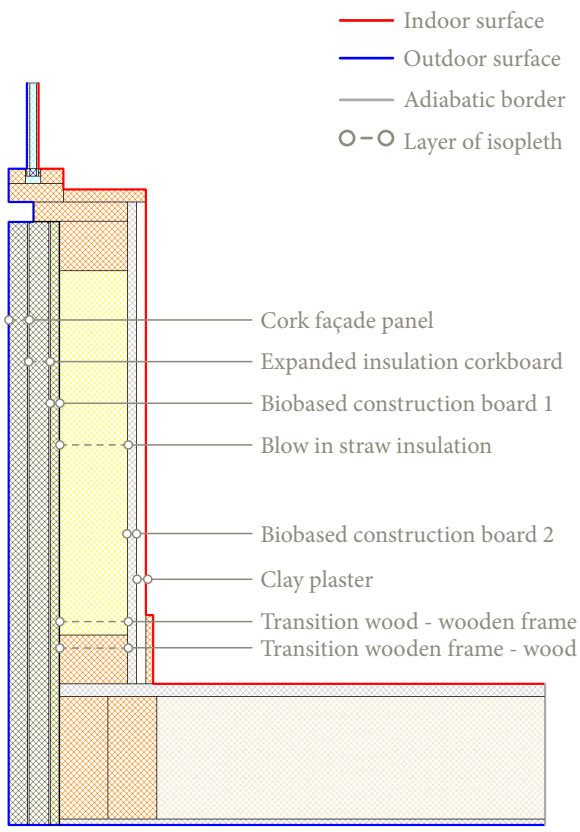

Figure A306, geometry detail V1 including location isopleths

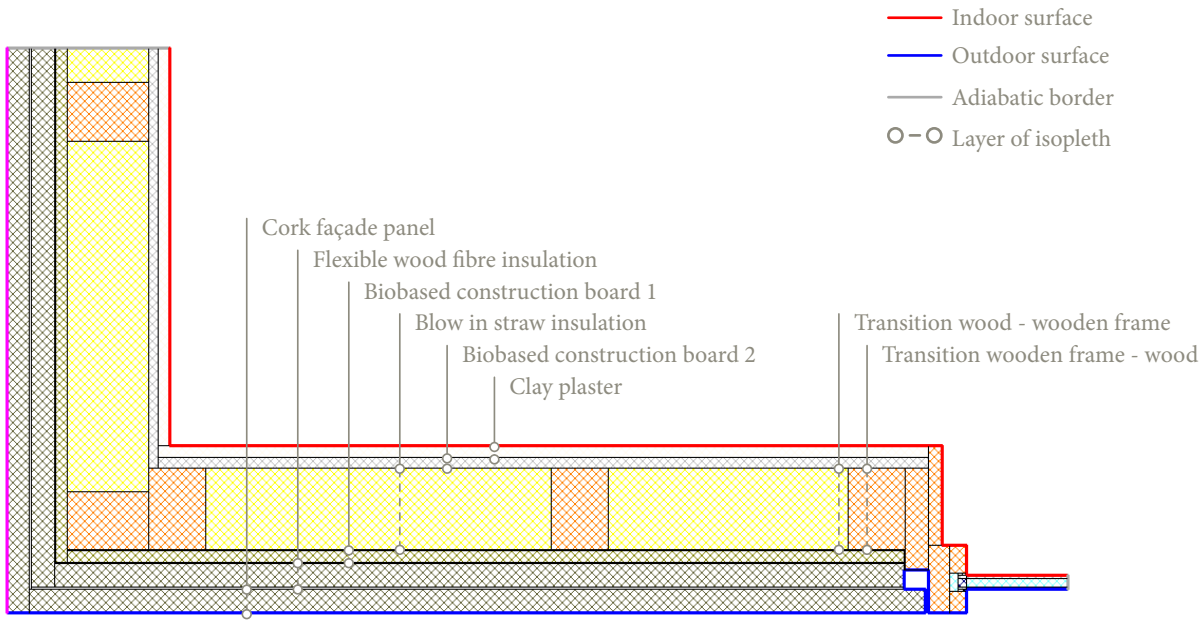

Figure A304, geometry detail H1including location isopleths

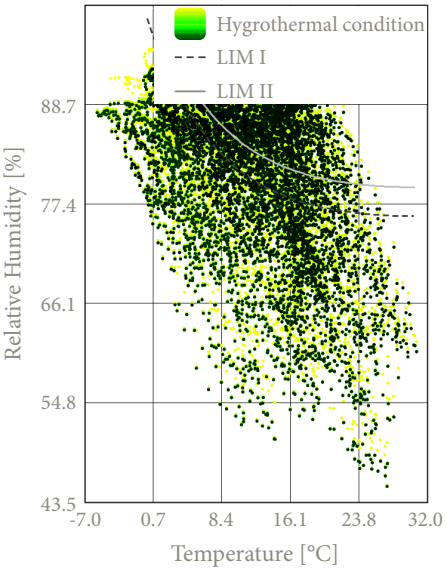

Figure A307, Isopleths cork façade panel

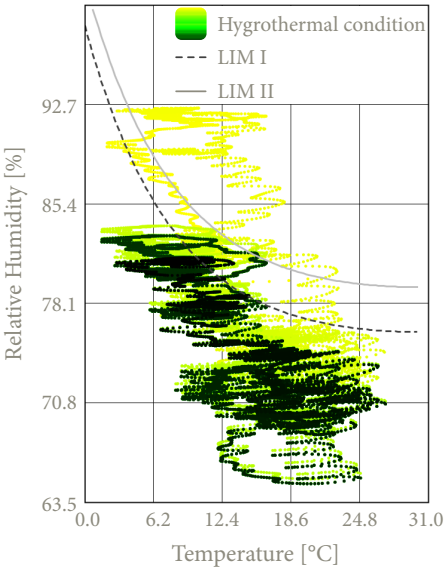

Figure A308, Isopleths expanded insulation corkboard

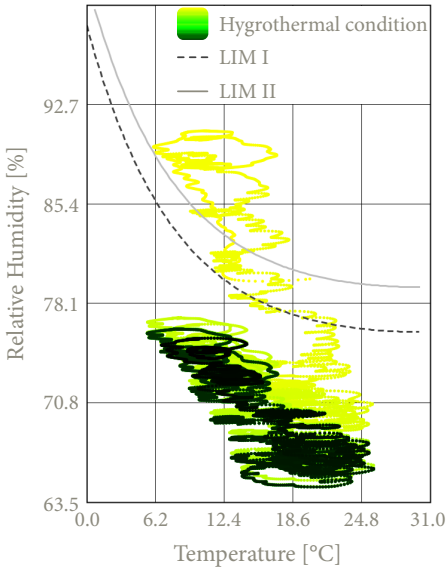

Figure A309, Isopleths biobased construction board 1

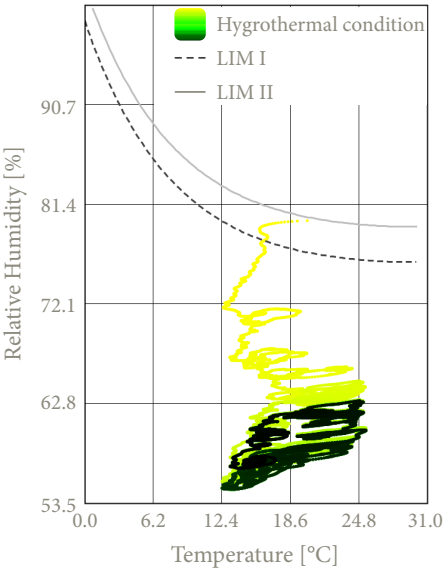

Figure A310, Isopleths blow in straw

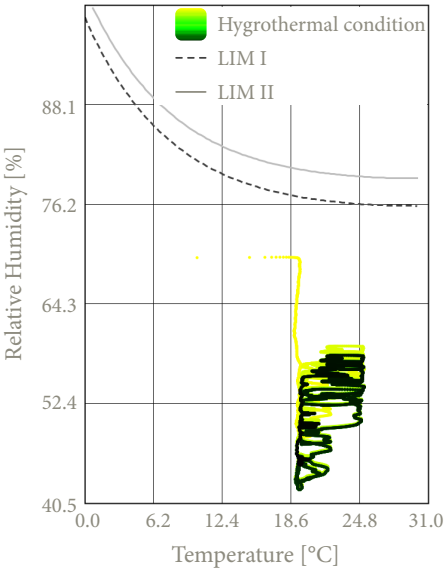

Figure A311, Isopleths biobased construction board 2

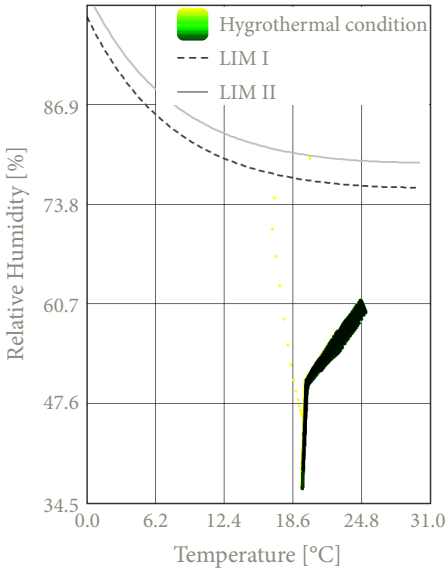

Figure A312, Clay plaster

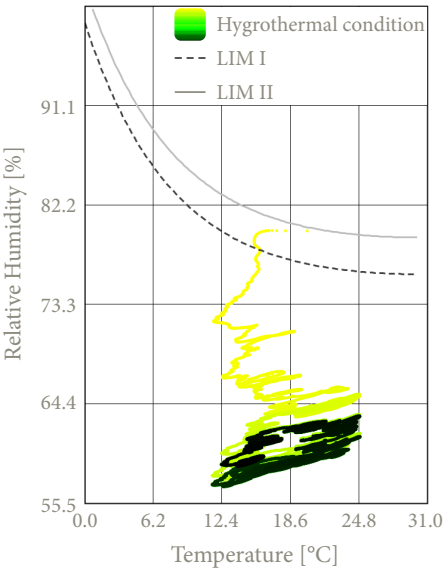

Figure A313, Isopleths transition straw & frame

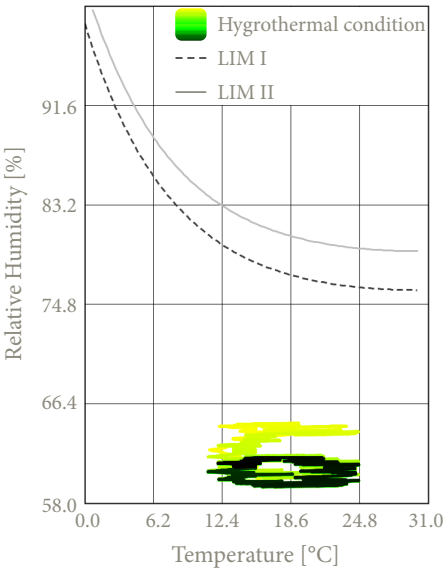

Figure A314, Isopleths transition frame & straw

Isopleths - V2

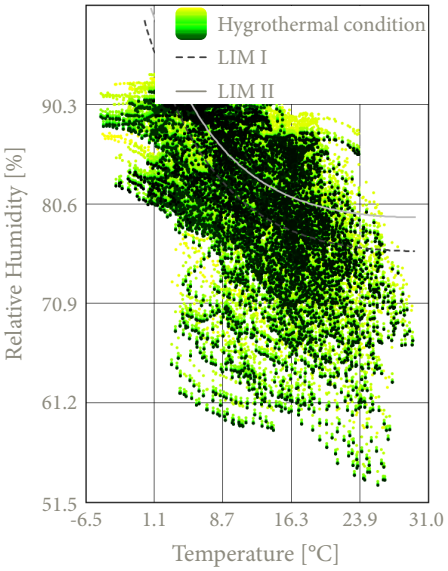

Figure A315, Isopleths cork façade panel

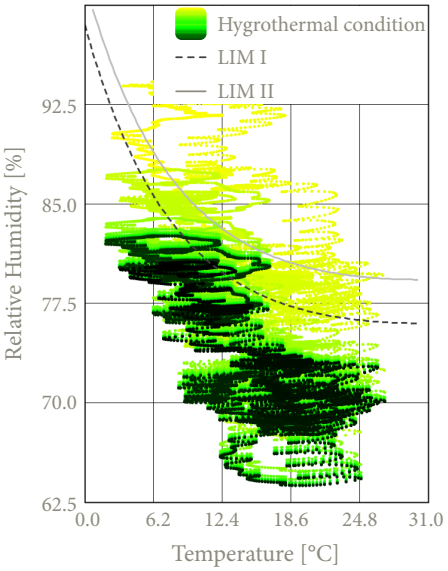

Figure A316, Isopleths expanded insulation corkboard

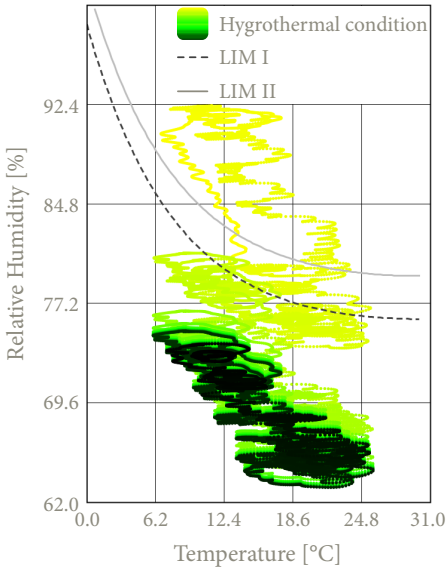

Figure A317, Isopleths biobased construction board 1

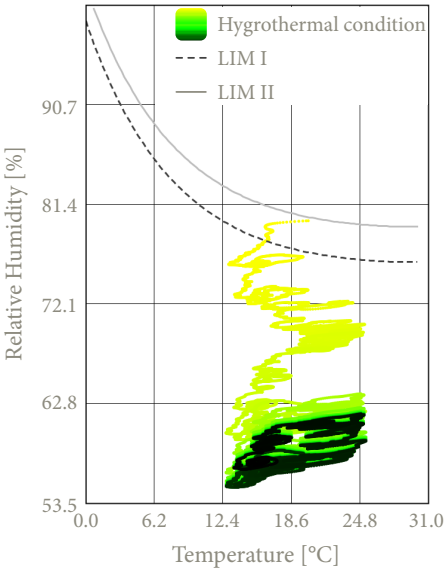

Figure A318, Isopleths blow in straw

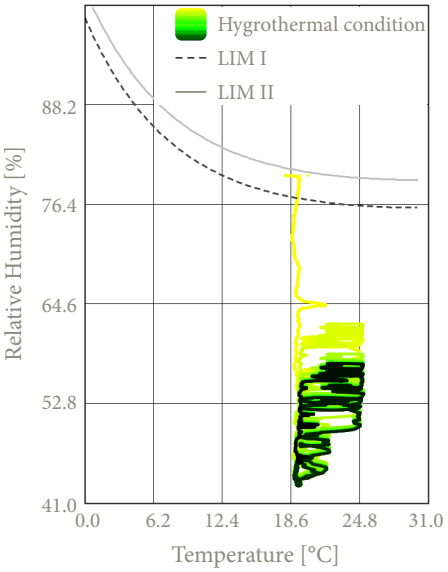

Figure A319, Isopleths biobased construction board 2

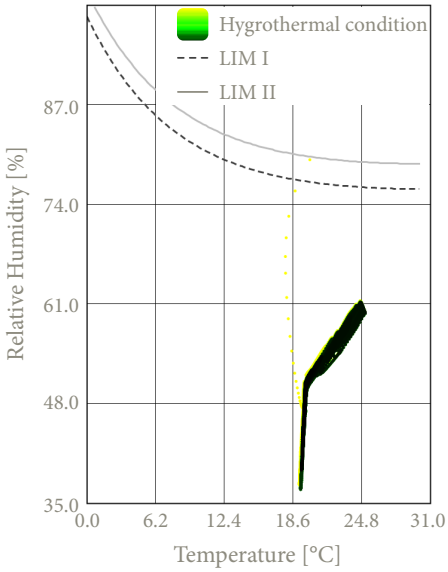

Figure A320, Clay plaster

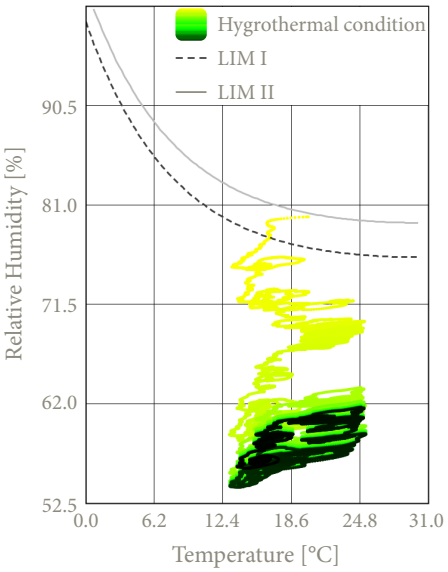

Figure A321, Isopleths transition straw & frame

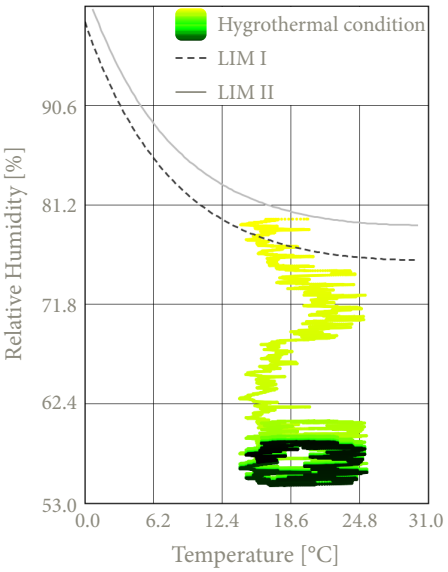

Figure A322, Isopleths transition frame & straw

Isopleths - H1

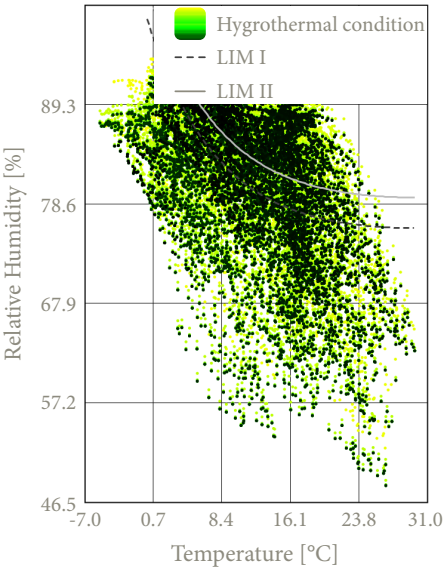

Figure A323, Isopleths cork façade panel

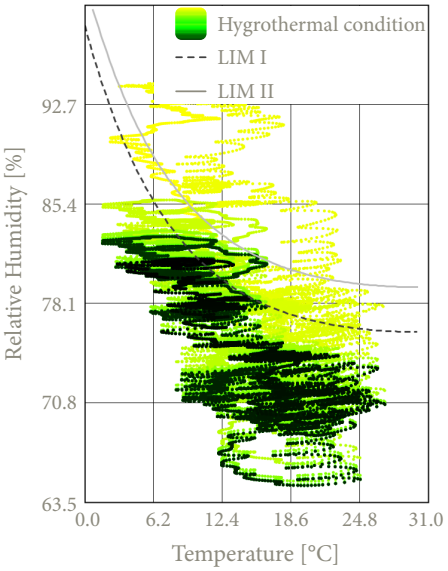

Figure A324, Isopleths expanded insulation corkboard

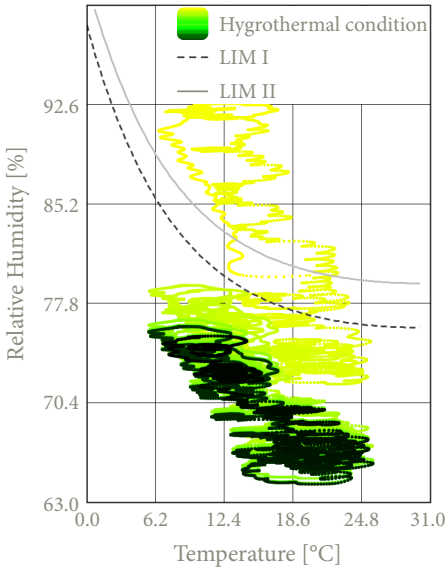

Figure A325, Isopleths biobased construction board 1

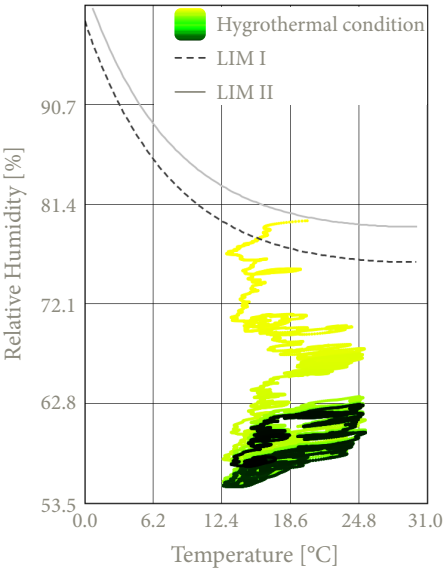

Figure A326, Isopleths blow in straw

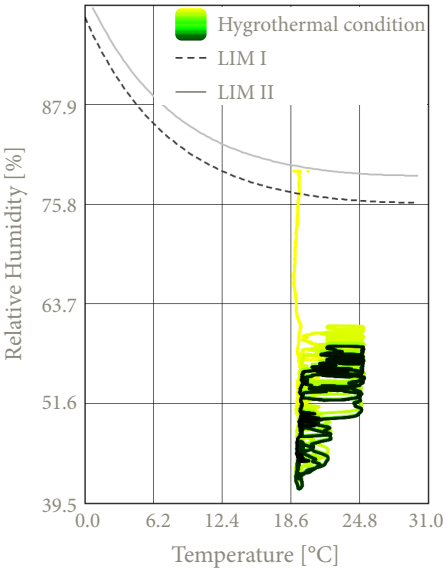

Figure A327, Isopleths biobased construction board 2

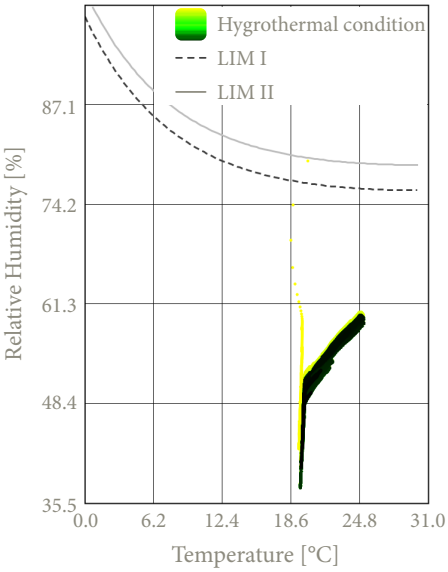

Figure A328, Clay plaster

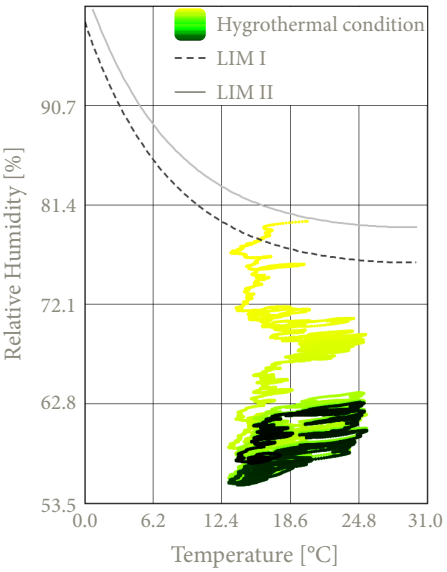

Figure A329, Isopleths transition straw & frame

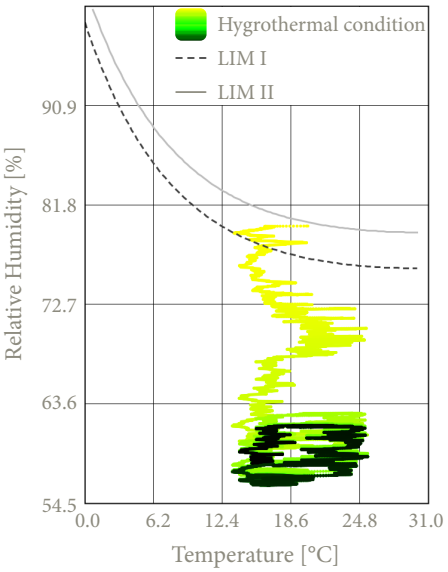

Figure A330, Isopleths transition frame & straw

Conclusion isoplteths

Based on the established and analysed isopleths of the various details within this construction **configuration**, it can be concluded that there is no risk of mould growth within the different material layers. All isopleths located behind the cork insulation plate remain below the critical threshold values **LIM I** and **LIM II**, indicating that the details meet the established criteria.

With regards to the **cork façade panel** it can be observed that the isopleths mostly exceed the LIM threshold values, which is the same as in the other three cork configuration assessments. Therefore, a similar conclusion can be drawn as in the previous cork configurations based on the paper by (Hon, 2024). Just like in the previous cork configurations, in order to state with certainty that no mould growth occurs in the cork as an exterior panel material, additional research is required.

The board that is glued with cork mortar behind the cork façade panel, the **expanded insulation corkboard**, shows in all three details similair results. The isopleths show a small exceedance at the beginning of the simulation. However, over time the moisture present in the material at the start, approximately 80%, is transported out. This is because, as previously stated, cork is a porous material making it capable of buffering fluctuations in relative humidity. Nevertheless, at the end of the simulation, the isopleths still slightly exceed the LIM I line. However, for the majority of the year, the isopleths remain below both LIM thresholds. The continuously decreasing trend and the fact that the isopleths are for the majority of the year below the thresholds, suggests that there is no long-term risk of mould development.

When examining the isopleths of the **outside biobased construction board**, it can be seen that the isopleths, apart from a short period at the beginning, remain below the LIM thresholds and all show a downward trend. When the results of this configuration are compared with those of the assemblies using wood fibre and cork, it can be seen that this configuration has a similar effect on the biobased construction board as the second configurations of flax, cork, and wood fibre with a cork façade. It is also evident that the construction board is better protected against mould growth compared to the first straw configuration. This is due to the additional expanded insulation cork board and the cork board. In this configuration, a downward trend is also visible in the isopleths. Therefore, with regard to mould resistance the outside construction board has no risk of mould growth.

With regard to the isopleths of the **blow in straw insulation**, as well as the **transition zones between the straw and the wooden construction frame**, the values remain well below both LIM threshold values and for all of these isopleths a downward trend is visible. Lastly, the isopleths of the **inside biobased construction board**, and the **clay plaster**, also remain well below the LIM lines with a slight downward trend visible in the inside biobased construction board. However, the isopleths remain far below the LIM lines.

In conclusion, it can be stated that this configuration poses no risk of mould growth and thus complies with the specified isopleth requirements. However, in order to fully confirm this, further research is needed regarding the cork panel used on the exterior. As such, the design complies with the required hygrothermal performance standards.

Surface condensation - V1, V2 & H1

The circle at each figure figures below, **figure 331**, **figure 333** and **figure 335**, show the coldest point of the interior surface at each detail in order to consider the f_{Rsi}. Below these graphs the corresponding surface temperature at this point is shown over a ten-year simulation below, **figure 332**, **figure 334** and **figure 336**.

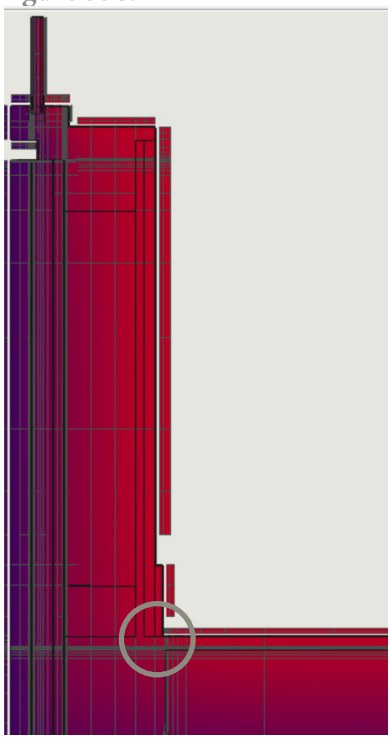

Figure A331, Highlight lowest point, V1

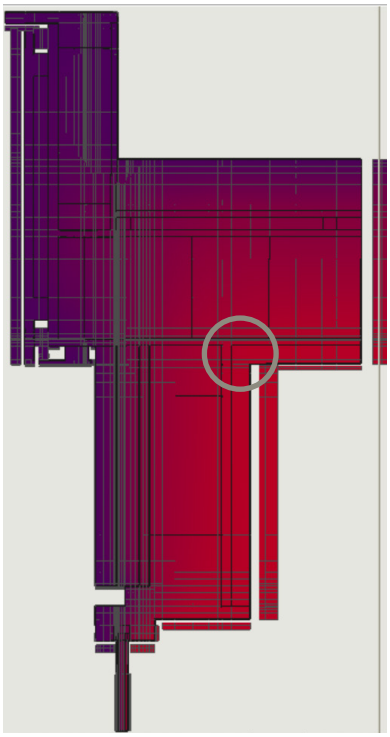

Figure A333, Highlight lowest point, V2

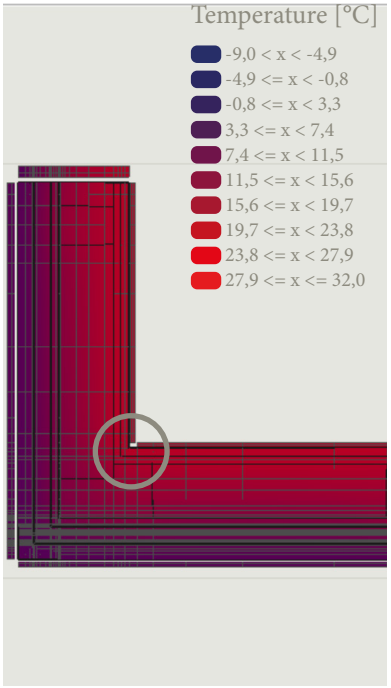

Figure A335, Highlight lowest point, H1

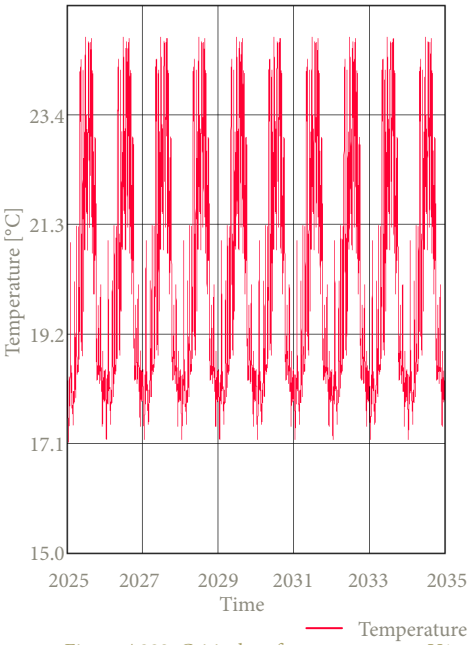

Figure A332, Critical surface temperature, V1

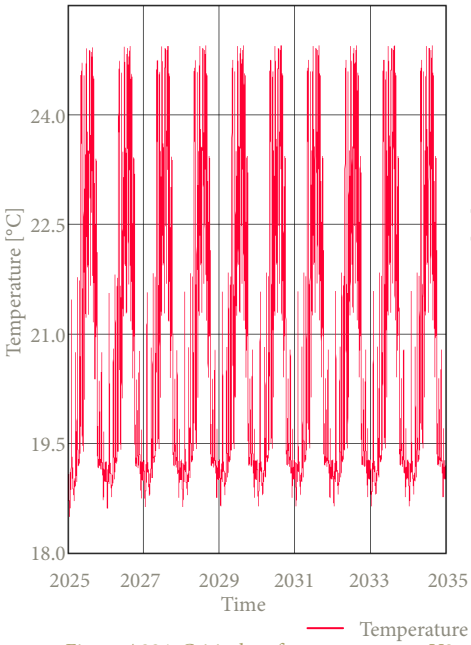

Figure A334, Critical surface temperature, V2

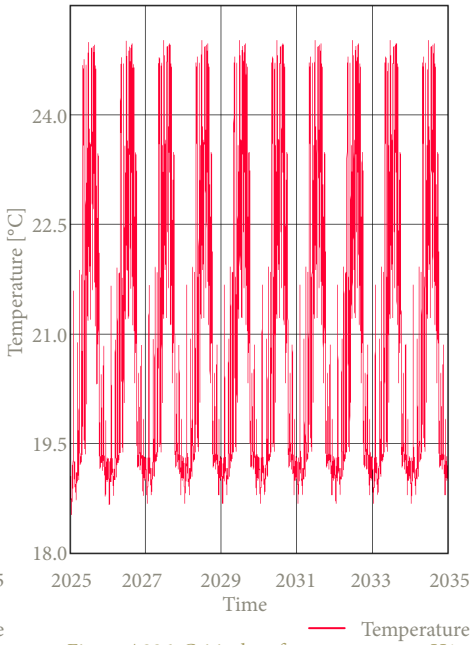

Figure A336, Critical surface temperature, H1

From this graph the lowest surface temperature of this detail is **15.66 °C**.

The resulting f_{Rsi} for this detail is **0.64** which exceeds the minimum requirement of 0.61. This indicates a negligible risk of surface condensation.

From this graph the lowest surface temperature of this detail is **18.50 °C**.

The resulting f_{Rsi} for this detail is **0.83** which exceeds the minimum requirement of 0.61. This indicates a negligible risk of surface condensation.

From this graph the lowest surface temperature of this detail is **18.52 °C**.

The resulting f_{Rsi} for this detail is **0.88** which exceeds the minimum requirement of 0.61. This indicates a negligible risk of surface condensation.

F-factor - V1, V2 & H1

The resulting **f-factor** of **detail V1** is **0.88** for a temperature of **15.95 °C**. Next the resulting **f-factor** of **detail V2** is **0.94** for a temperature of **16.92 °C**. Lastly, the resulting **f-factor** of **detail H1** is **0.94** for a temperature of **17.00 °C**. This indicates a very limited thermal bridge is assessed within the details of this configuration.
Given that these values significantly all exceeds the required threshold of **0.65**, it can be concluded that the details within this configuration complies with the thermal performance requirements set by the Dutch Building Decree.

PSI-value - V1

Table A68, Calculation of the $Q_{ideal\ condition}$

$R_{construction,\ window}$ [(m²K)/W]	$A_{construction,\ window}$ [m²]	$R_{construction,\ wall}$ [(m²K)/W]	$A_{construction,\ wall}$ [m²]	$R_{construction,\ floor}$ [(m²K)/W]	$A_{construction,\ floor}$ [m²]
0.600	0.2425	4.780	1.019	4.648	0.86

The resulting $\mathbf{Q_{ideal\ condition}}$ is **14.249 W**

Q_{WUFI} represents the sum of all heat flows through the detail, resulting in a total heat flow of **15.367 W**.

These values give a **Ψ-value** of **0.048 W/(mK)** for **detail V1**, indicating that the detail can be characterised as a well-insulated building component.

PSI-value - V2

Table A69, Calculation of the $Q_{ideal\ condition}$

$R_{construction,\ window}$ [(m²K)/W]	$A_{construction,\ window}$ [m²]	$R_{construction,\ wall}$ [(m²K)/W]	$A_{construction,\ wall}$ [m²]	$R_{construction,\ roof}$ [(m²K)/W]	$A_{construction,\ roof}$ [m²]
0.600	0.2425	4.780	0.883	6.442	0.221

The resulting $\mathbf{Q_{ideal\ condition}}$ is **12.218 W**

Q_{WUFI} represents the sum of all heat flows through the detail, resulting in a total heat flow of **12.789 W**.

These values give a **Ψ-value** of **0.087 W/(mK)** for **detail V2**, indicating that the detail can be characterised as a well-insulated building component.

PSI-value - H1

Table A70, Calculation of the $Q_{ideal\ condition}$

$R_{construction,\ window}$ [(m²K)/W]	$A_{construction,\ window}$ [m²]	$R_{construction,\ wall}$ [(m²K)/W]	$A_{construction,\ wall}$ [m²]
0.600	0.2425	4.780	2.283

The resulting $\mathbf{Q_{ideal\ condition}}$ is **15.987 W**

Q_{WUFI} represents the sum of all heat flows through the detail, resulting in a total heat flow of **17.282 W**.

These values give a **Ψ-value** of **0.071 W/(mK)** for **detail H1**, indicating that the detail can be characterised as a well-insulated building component.

Assessment detail configuration

Important notes about the details

For the given configuration, **key considerations** are presented below in the form of bullet points. These points highlight specific aspects that need to be taken into account during detailing and construction.

- Blow the straw between the studs of the wooden frame and the construction boards at a density of 100 kg/m^3 by creating a hole in the inner construction board.
- Finish the inside of the wooden frame with a pressure-resistant wood fibre board to allow for fixings.
- Attach the water-resistant barrier of the window frame to the timber structural frame.
- Apply a diffusion-open construction board with water-resistant properties onto the timber frame, over which cork mortar can be applied.
- The wooden lintel must have proper bearing on the wooden frame.
- The screws of the outdoor biobased construction board must reach the center of the timber frame to ensure secure attachment.
- Stainless steel screws must be at least 2 times the thickness of the battens.
- Stainless steel nails must be at least 2.5 times the thickness of the cladding.
- The stainless steel nails must be placed 40 mm from the outer edge of the cladding.
- Ensure 4 mm gaps between the cladding to accommodate the movement of the wood.
- Ensure 10 mm gaps for ventilation both between cladding boards and at the window frame.
- Use a clay base plate to provide a correct underlayment for the clay plaster.
- Use a jute reinforcement mesh between the rough and finishing clay plaster to prevent cracking.

Assessment of the configuration

Additionally, the configuration is evaluated based on the following criteria:

1. **Weight**: The total mass per unit area of the wall construction.
2. **Construction time**: The time required for assembling the construction.
3. **Resistance Construction-value:** The combined thermal resistance of all layers in the construction.
4. **Phase shift**: The heat transfer delay of the structure.

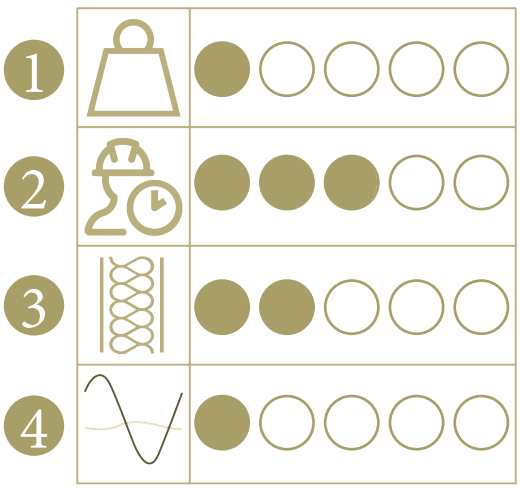

Axonometric view of the detail configuration

In addition to the presented details, an **axonometric view** of the respective detail is also shown. This is presented in the figure below, **figure 337**, and is intended to provide more clarity and insight into **detail V1, detail V2,** and **detail H1**.

Figure A337, Axonometric view of detail configuration 11

Appendix B
Not assessed details

Detail configuration 1.4 - hempcrete with wooden façade

Since not all 66 details can be tested, this appendix presents the details that have been formulated but could not be examined. Based on the simulation results, it can be stated that these 33 details will achieve similar results to the 33 tested details. To confirm this with certainty, these details must also be tested using WUFI. The same methodology presented in this thesis can be applied for this purpose.

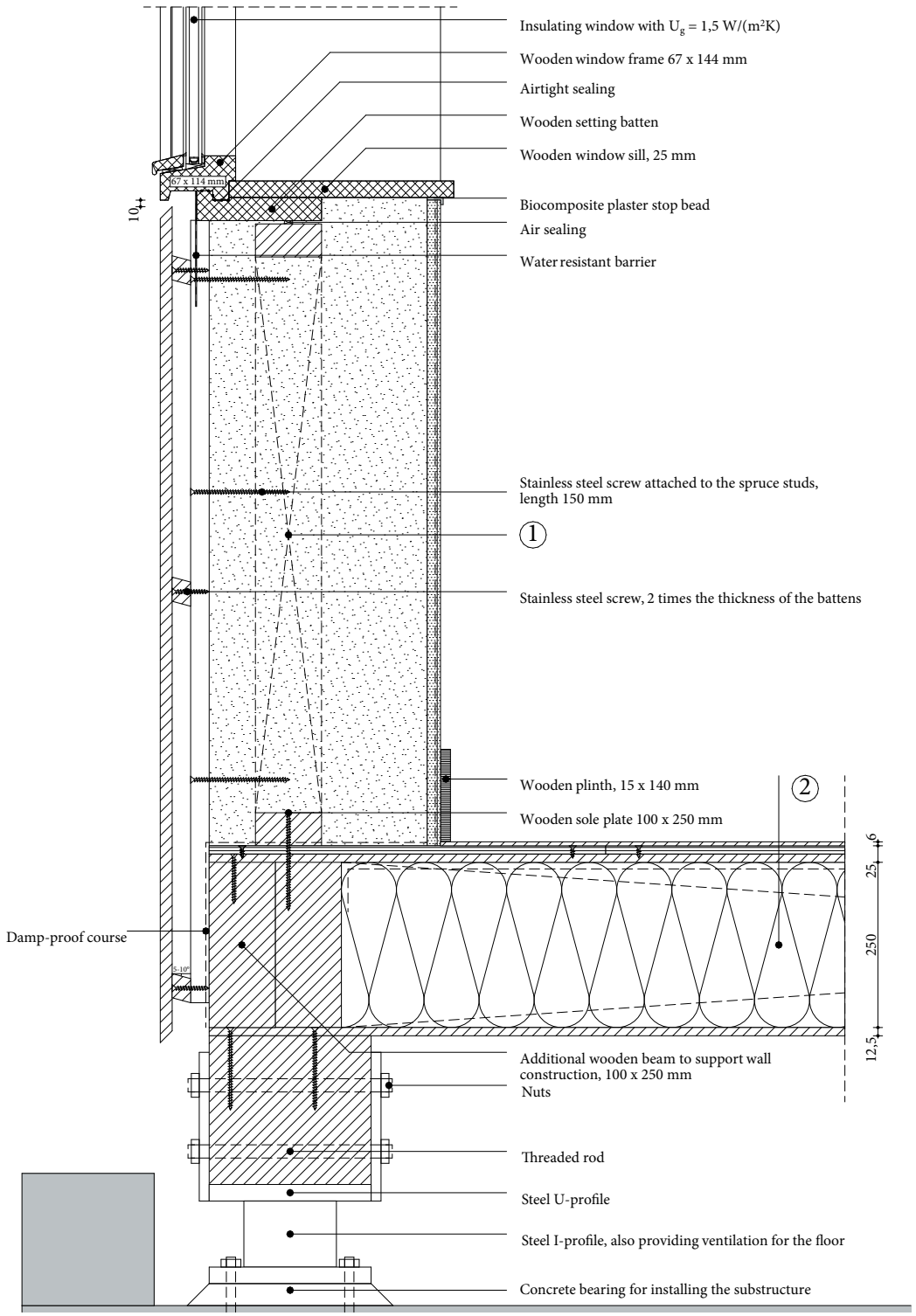

Figure A338, 1:10 detail of V1, configuration 1.4, own illustration

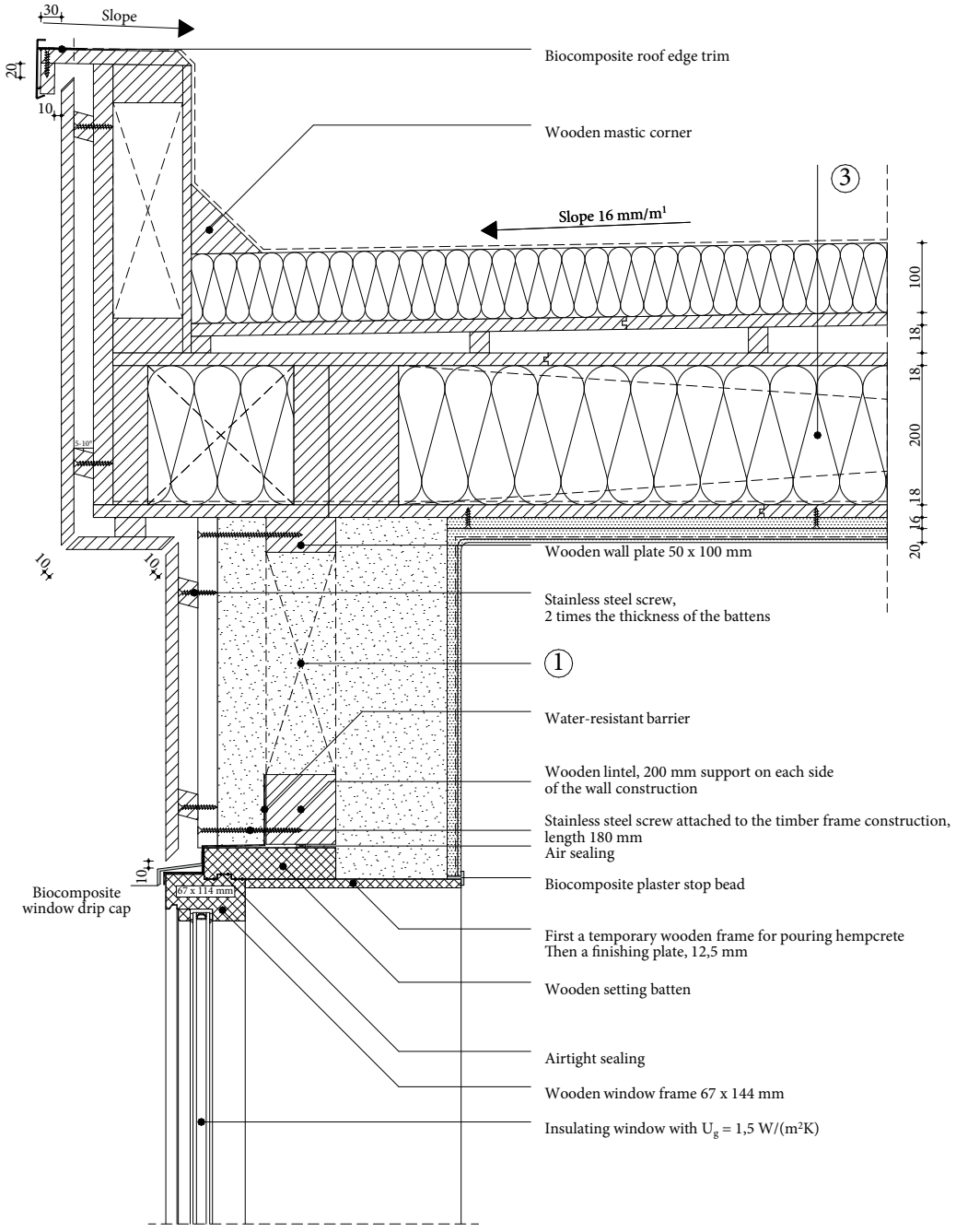

Figure A339, 1:10 detail of V2, configuration 1.4, own illustration

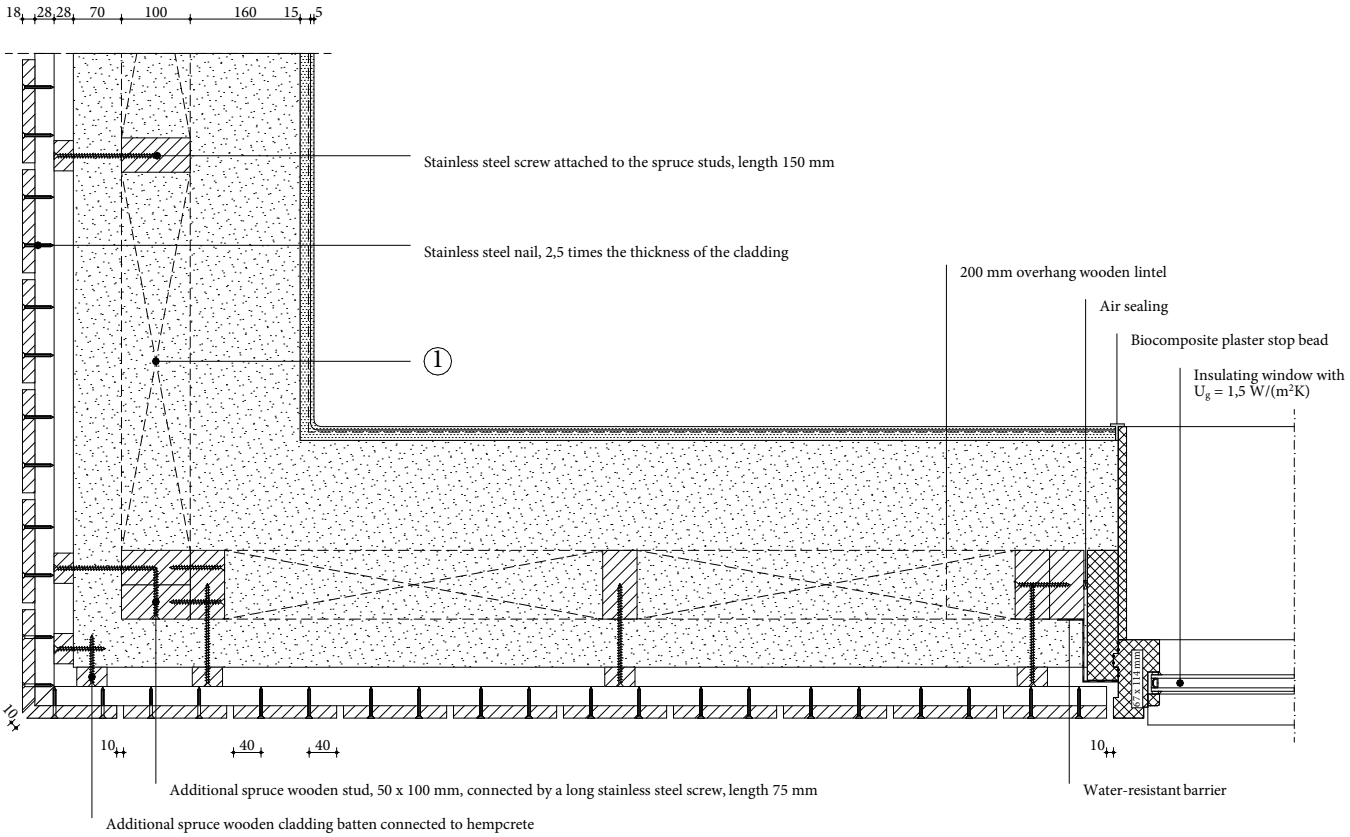

Figure A340, 1:10 detail of H1, configuration 1.4, own illustration

1 Wall construction build-up, RC-value: 4.83 (m²K)/W

- Vertical wooden cladding, 18 mm;
- Horizontal spruce cladding batten cavity, 28 x 44 mm, center-to-center 600 mm;
- Vertical spruce cladding batten forming ventilated cavity, 28 x 44 mm, center-to-center 600 mm;
- Pressure-resistant woodfibre insulation plate ($\lambda \leq 0.042$ W/mK), 40 mm;
- Timber frame construction, 100 x 200 mm, center-to-center 600 mm;
- Flexible hemp fiber insulation placed between construction ($\lambda \leq 0.043$ W/mK), 200 mm;
- Biobased wooden construction board, 18 mm;
- Clay base plate, 16 mm;
- Rough base clay plaster, 15 mm;
- Jute reinforcement mesh;
- Finishing clay plaster, 5 mm.

Detail configuration 1.5 - flexible hemp with wooden façade

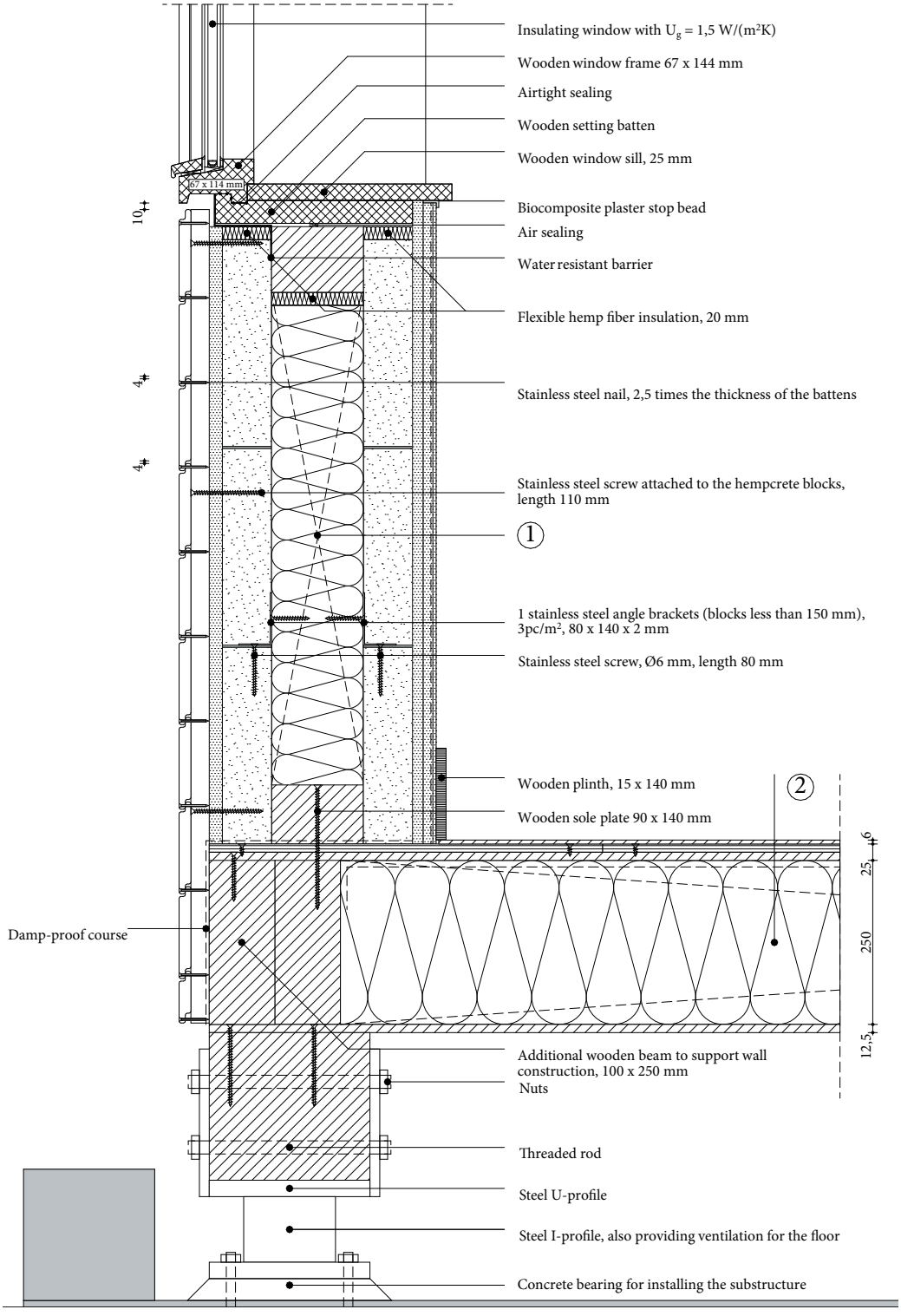

Figure A341, 1:10 detail of V1, configuration 1.5, own illustration

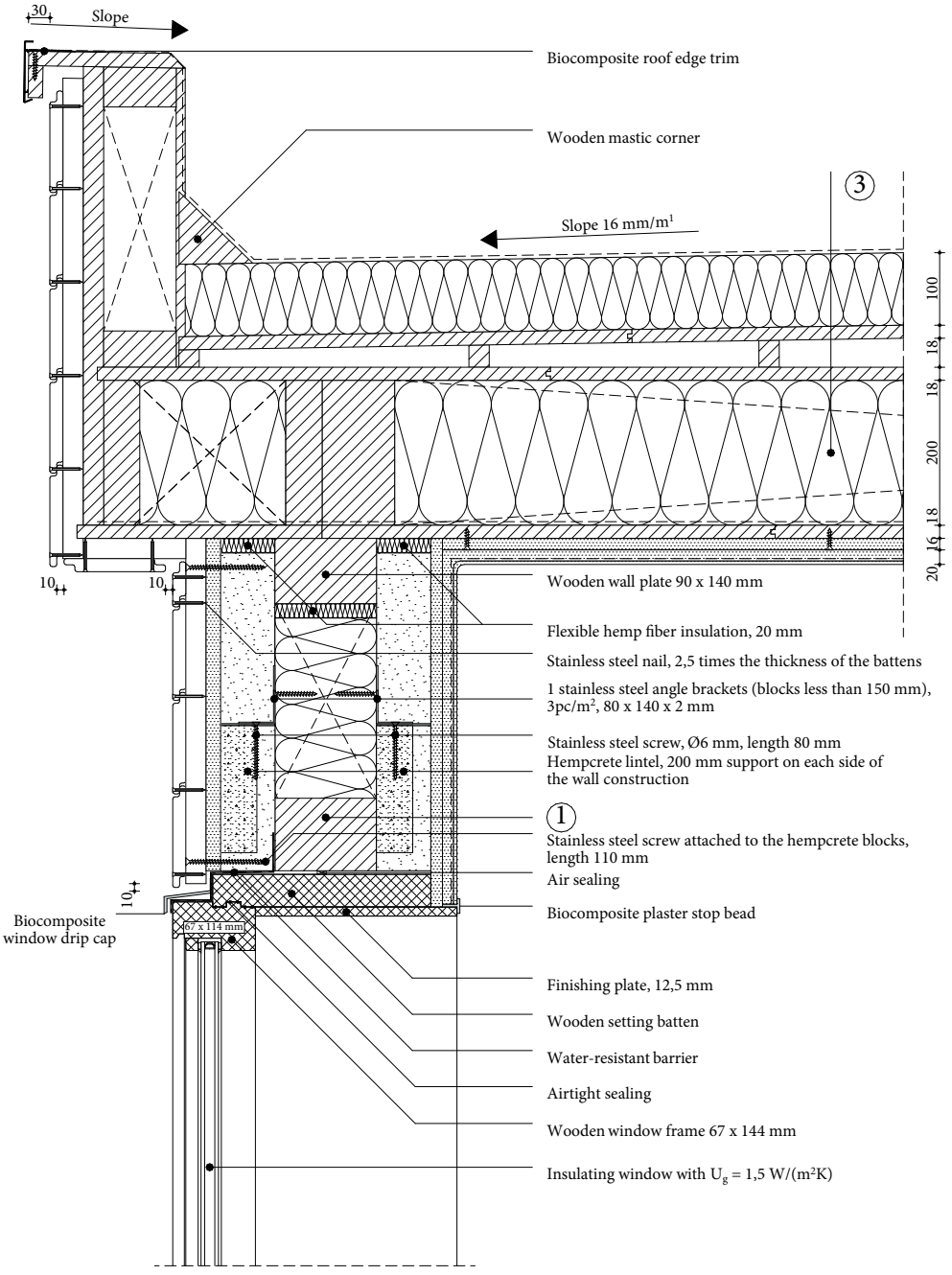

Figure A342, 1:10 detail of V2, configuration 1.5, own illustration

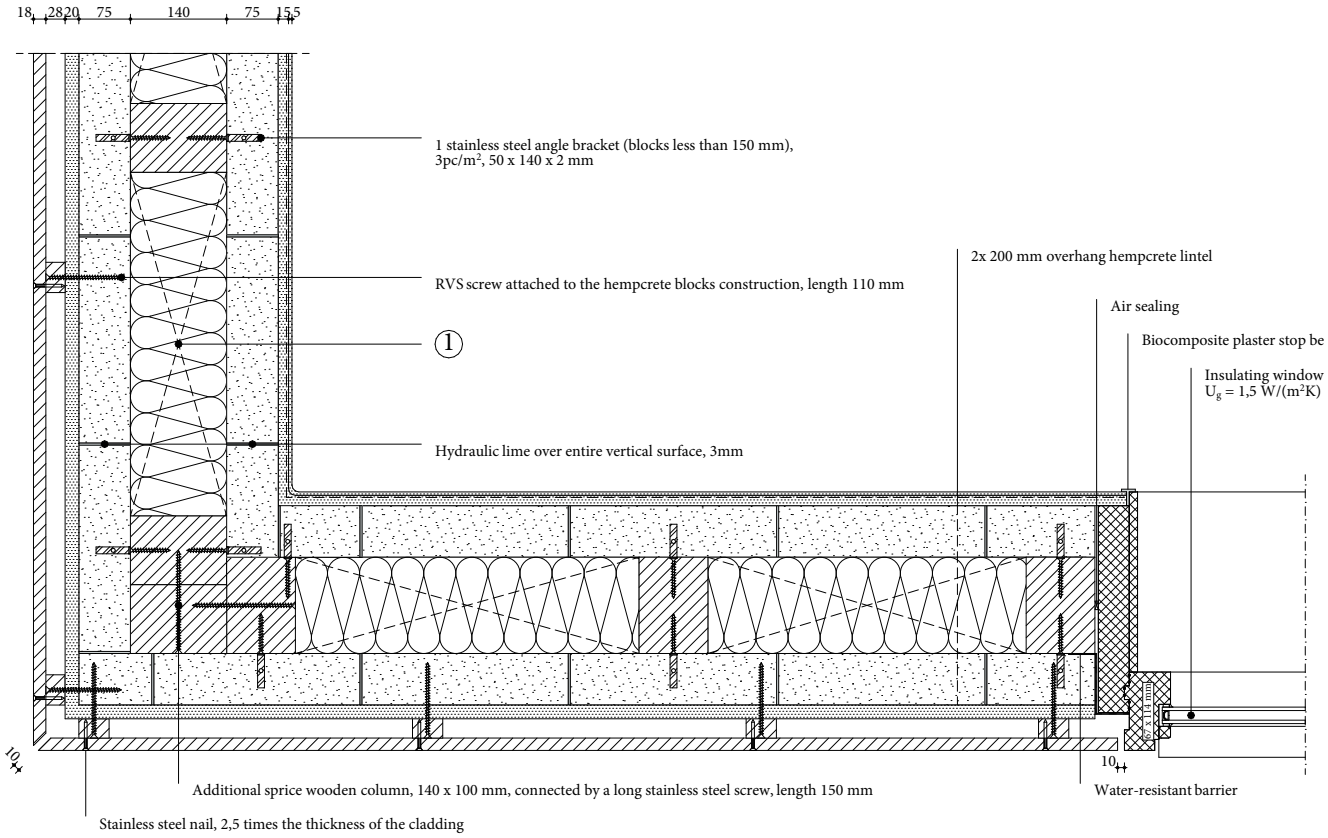

Figure A343, 1:10 detail of H1, configuration 1.5, own illustration

❶ Wall construction build-up, RC-value: 4.82 (m²K)/W

- Closed horizontal wooden cladding, 18 mm;
- Vertical spruce cladding batten forming ventilated cavity, 28 x 44 mm, center-to-center 600 mm;
- Rough lime plaster render, 20 mm;
- Hempcrete blocks (λ ≤ 0.071 W/mK), 75 mm;
- Timber frame construction, 100 x 140 mm, center-to-center 600 mm;
- Flexible hemp fiber insulation placed between construction (λ ≤ 0.043 W/mK), 140 mm;
- Hempcrete blocks (λ ≤ 0.071 W/mK), 75 mm;
- Clay base plate, 16 mm;
- Rough base clay plaster, 15 mm;
- Jute reinforcement mesh;
- Finishing clay plaster, 5 mm.

Detail configuration 2.3 - hempcrete with cork façade

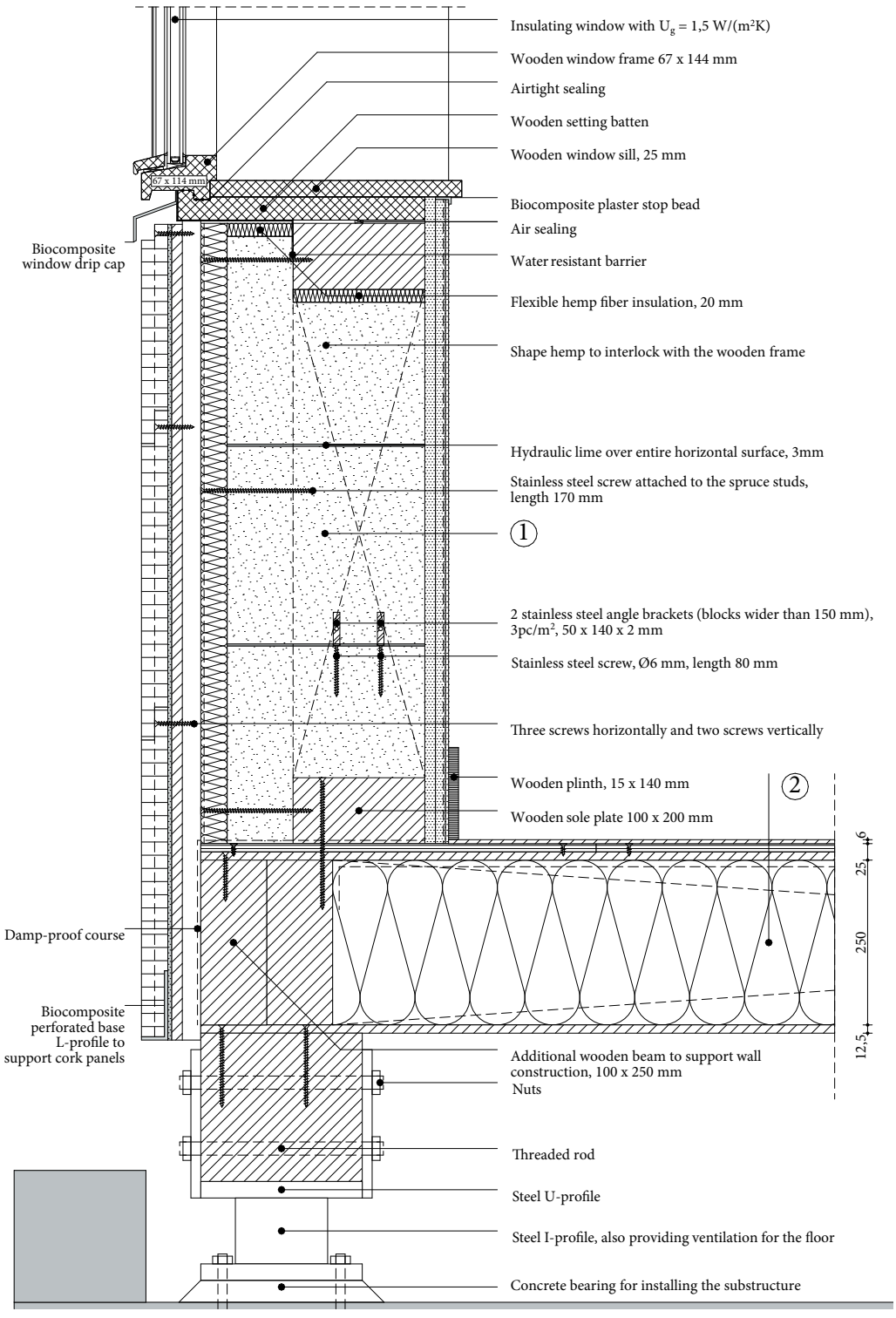

Figure A344, 1:10 detail of V1, configuration 2.3, own illustration

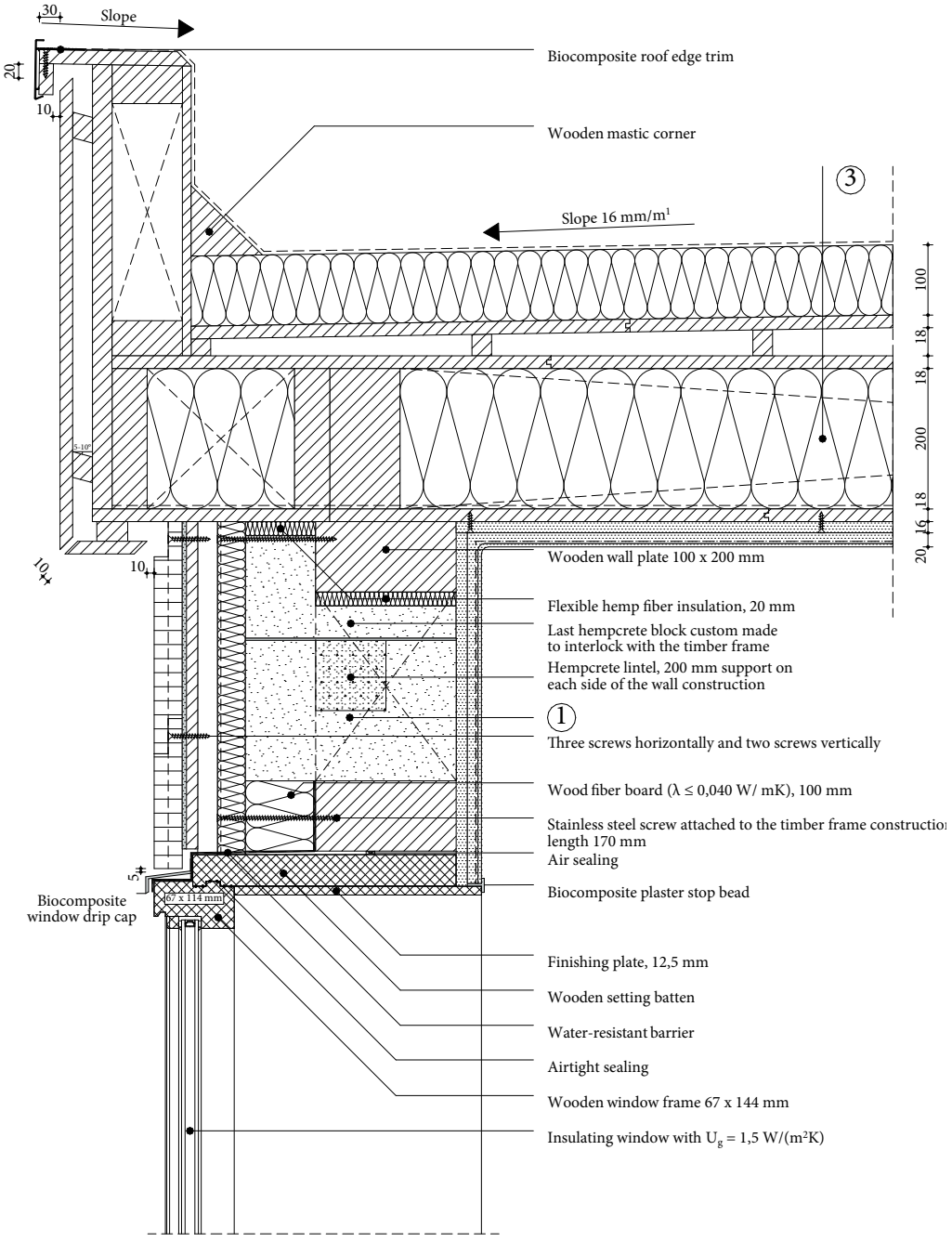

Figure A345, 1:10 detail of V2, configuration 2.3, own illustration

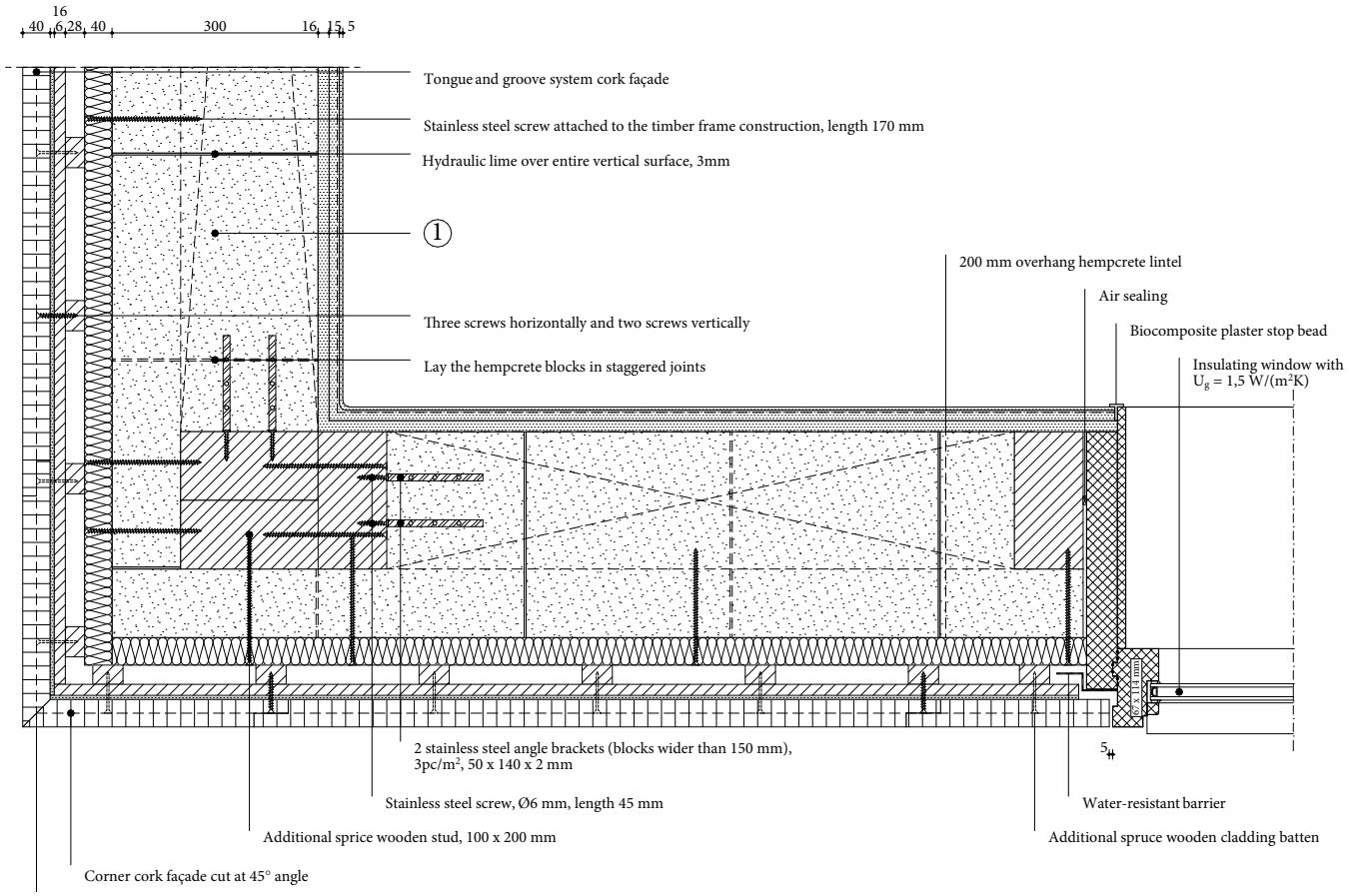

Figure A346, 1:10 detail of H1, configuration 2.3, own illustration

❶ Wall construction build-up, RC-value: 5.18 (m²K)/W

- Tongue and groove cork cladding panels, 40 mm;
- Cork mortar, 6 mm;
- Biobased diffusion open construction board, 16 mm;
- Vertical spruce cladding batten forming ventilated cavity, 28 x 44 mm, center-to-center 237 mm;
- Water-resistant vapour-permeable membrane;
- Pressure-resistant woodfibre insulation plate ($\lambda \leq 0.042$ W/mK), 40 mm;
- Timber frame construction, 100 x 200 mm, center-to-center 3000 mm, placed 70 mm from outside to protect the wood for moisture;
- Hempcrete blocks placed between construction ($\lambda \leq 0.071$ W/mK), 300 mm;
- Clay base plate, 16 mm;
- Rough base clay plaster, 15 mm;
- Jute reinforcement mesh;
- Finishing clay plaster, 5 mm.

Detail configuration 2.4 - cork insulation with wooden façade

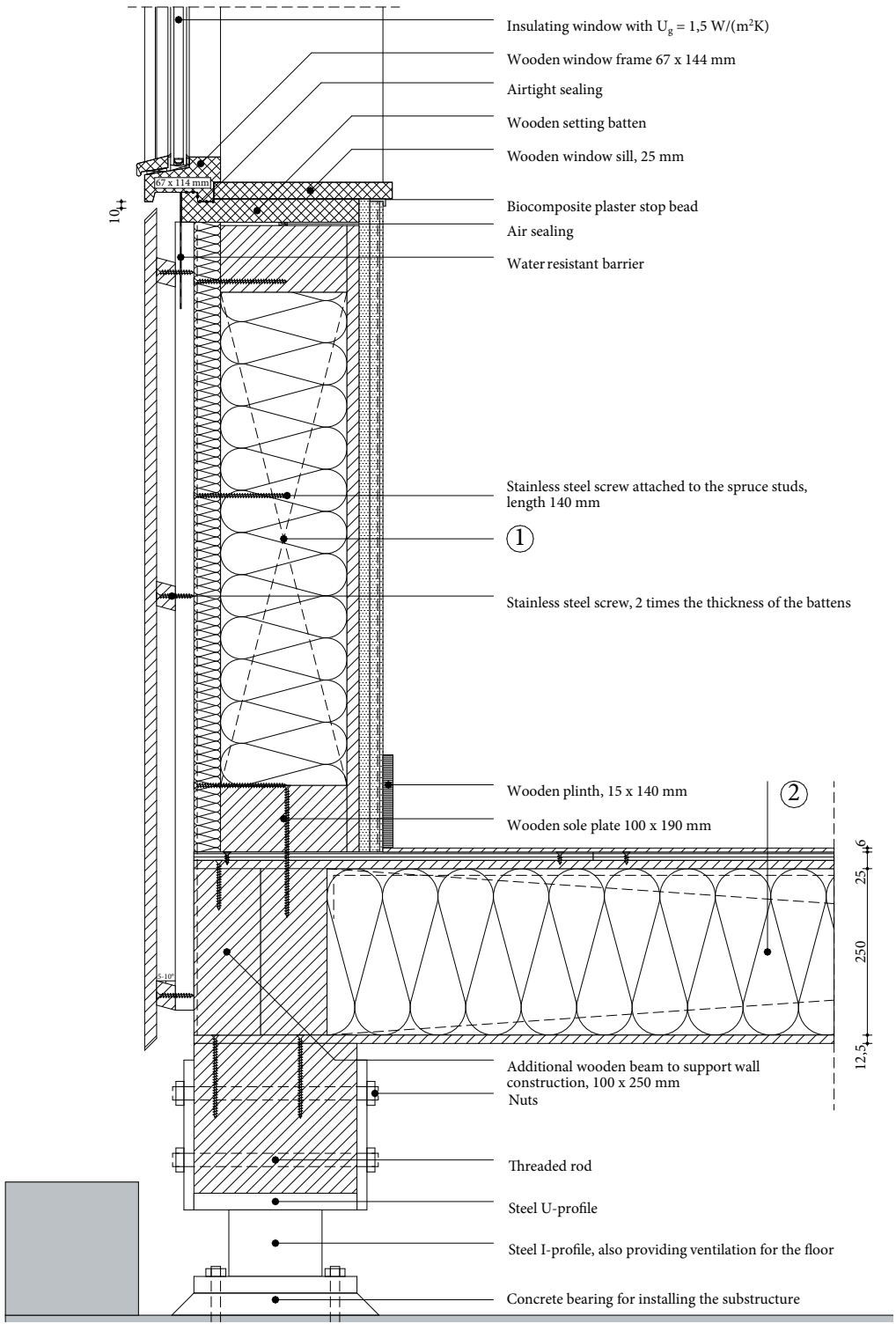

Figure A347, 1:10 detail of V1, configuration 2.4, own illustration

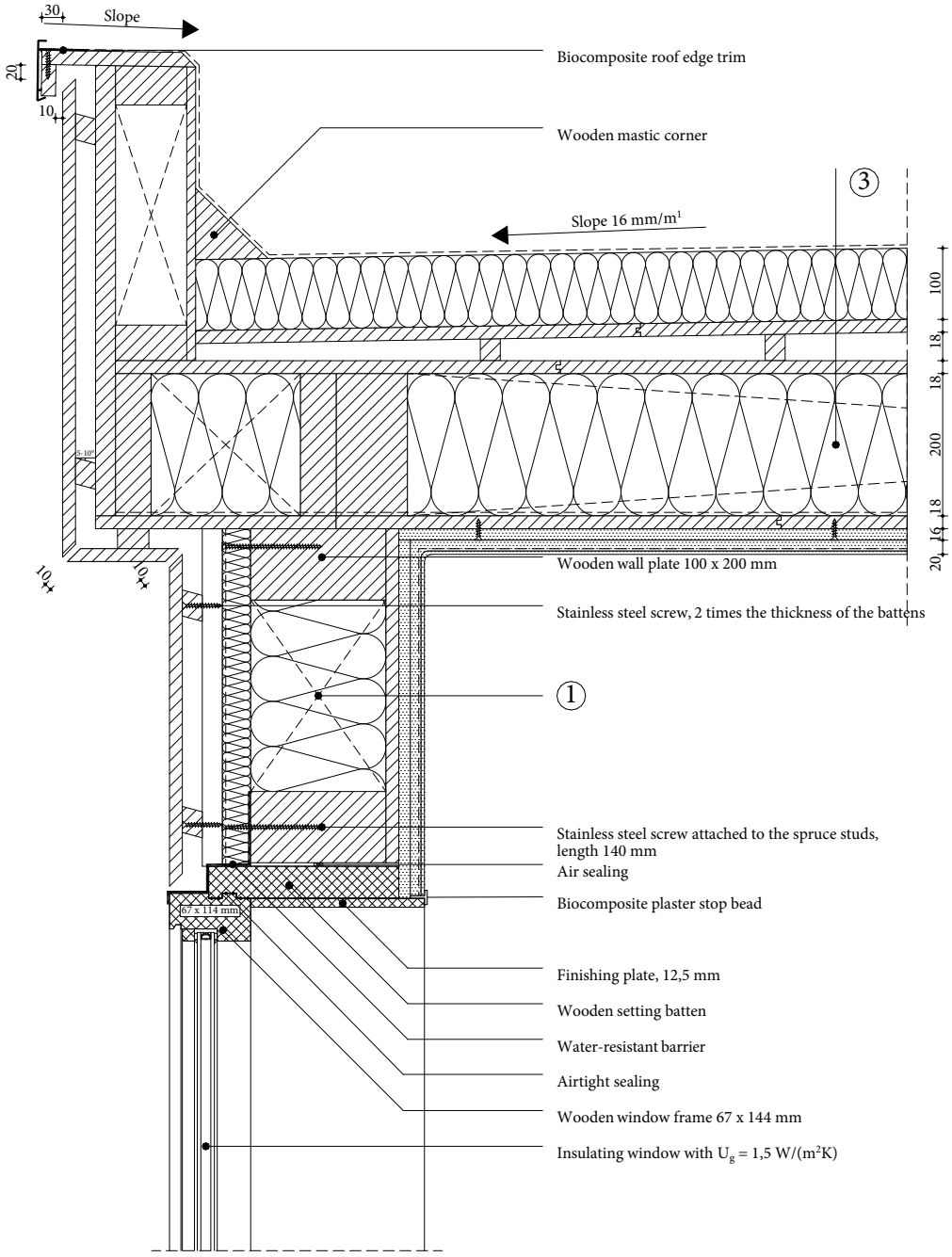

Figure A348, 1:10 detail of V1, configuration 2.4, own illustration

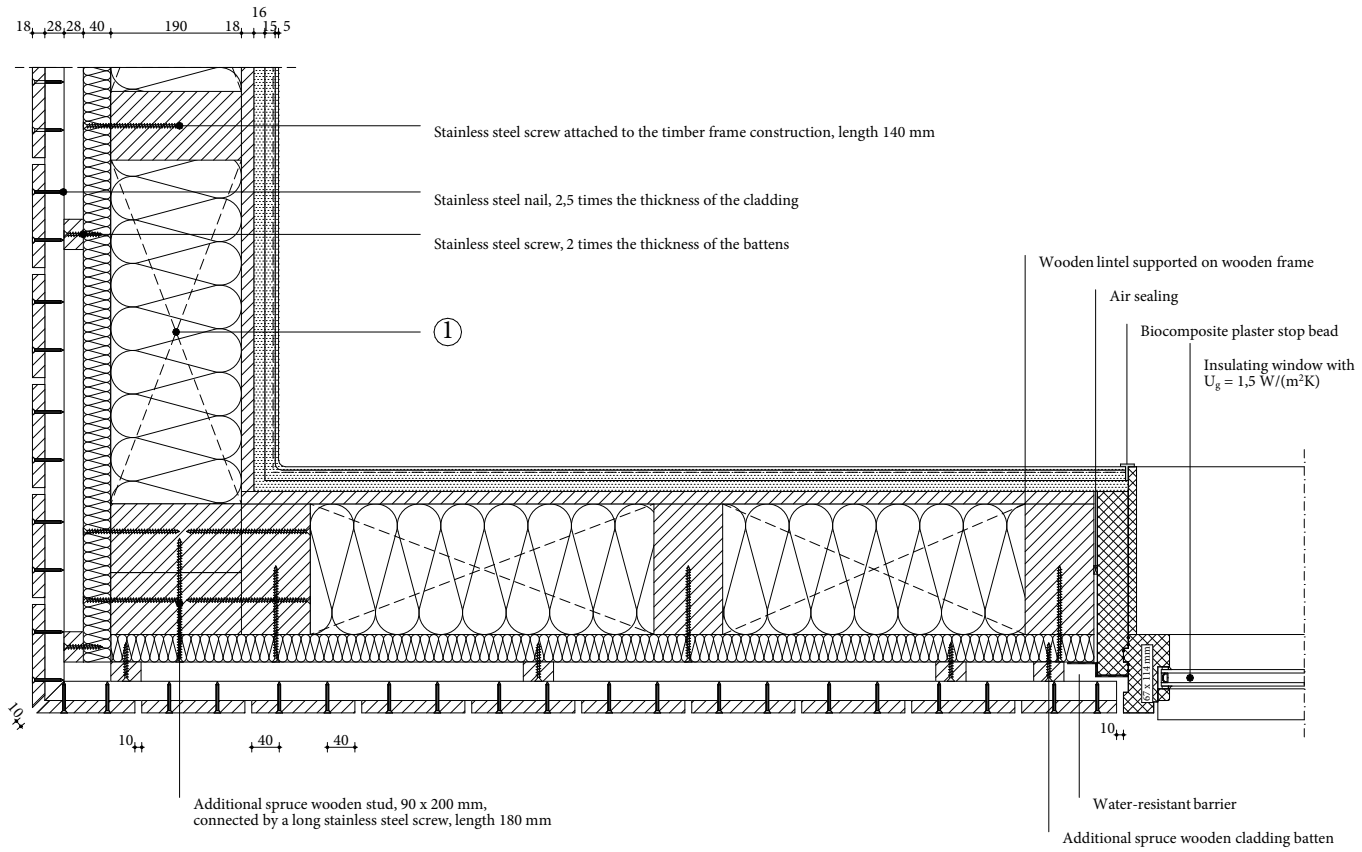

Figure A349, 1:10 detail of V1, configuration 2.4, own illustration

❶ Wall construction build-up, RC-value: 4.91 (m²K)/W

- Vertical wooden cladding, 18 mm;
- Horizontal spruce cladding batten cavity, 28 x 44 mm, center-to-center 600 mm;
- Vertical spruce cladding batten forming ventilated cavity, 28 x 44 mm, center-to-center 600 mm;
- Water resistant vapour-permeable membrane;
- Pressure-resistant woodfibre insulation plate ($\lambda \leq 0.042$ W/mK), 40 mm;
- Timber frame construction, 100 x 190 mm, center-to-center 600 mm;
- Expanded insulation corkboard placed between construction ($\lambda \leq 0.040$ W/mK), 190 mm;
- Biobased construction board, 18 mm;
- Clay base plate, 16 mm;
- Rough base clay plaster, 15 mm;
- Jute reinforcement mesh;
- Finishing clay plaster, 5mm.

Detail configuration 2.5 - hemp insulation with cork façade

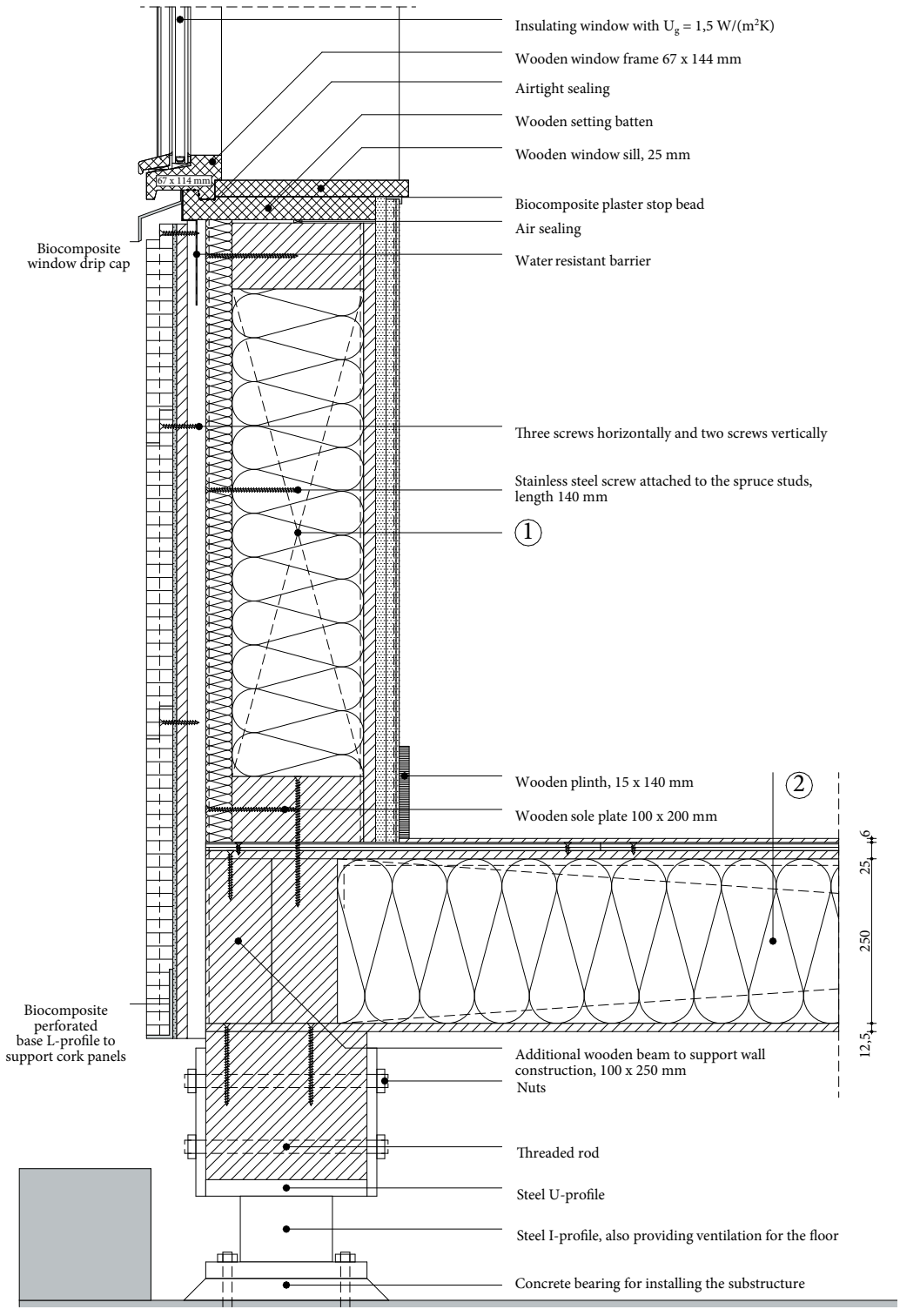

Figure A350, 1:10 detail of V1, configuration 2.5, own illustration

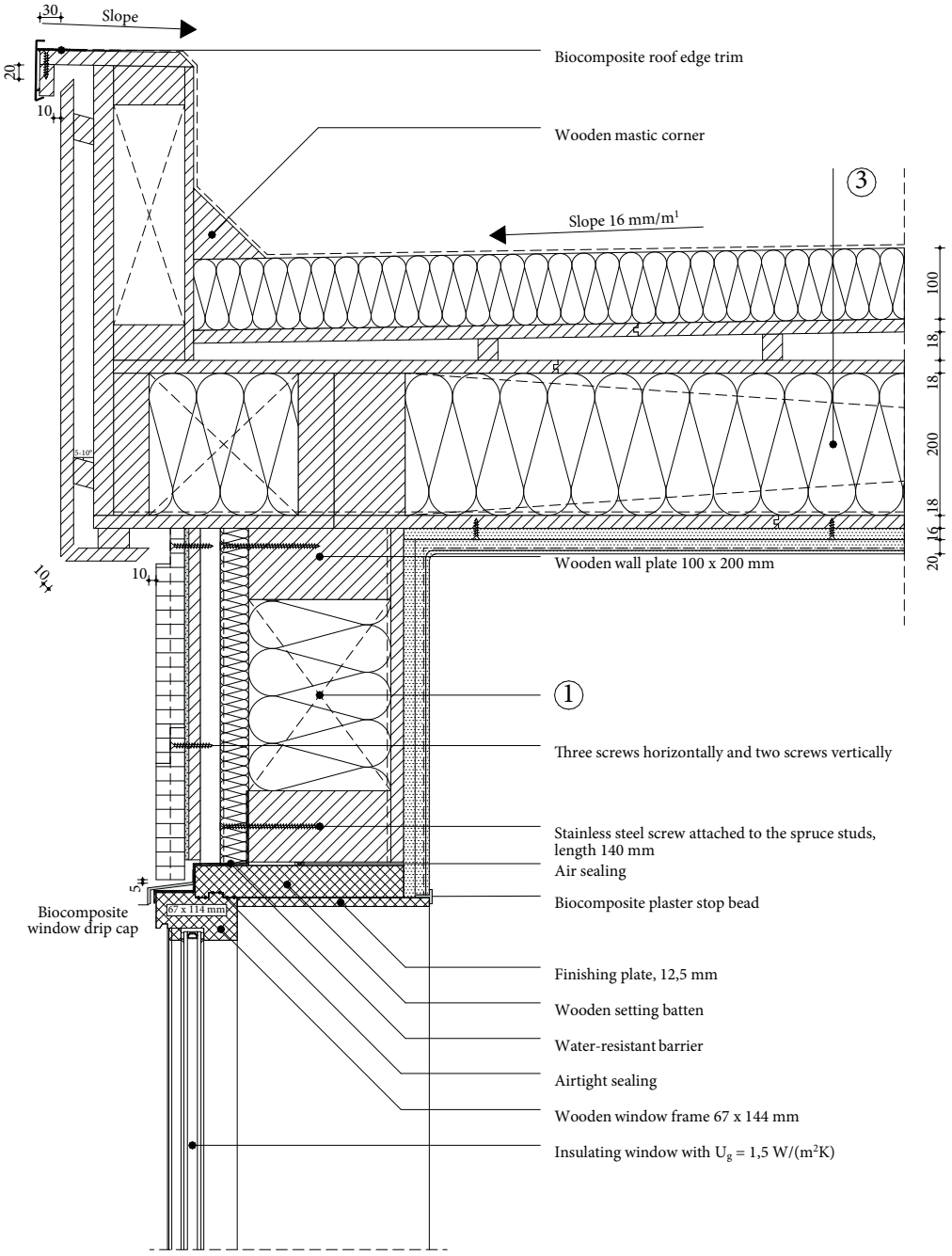

Figure A351, 1:10 detail of V2, configuration 2.5, own illustration

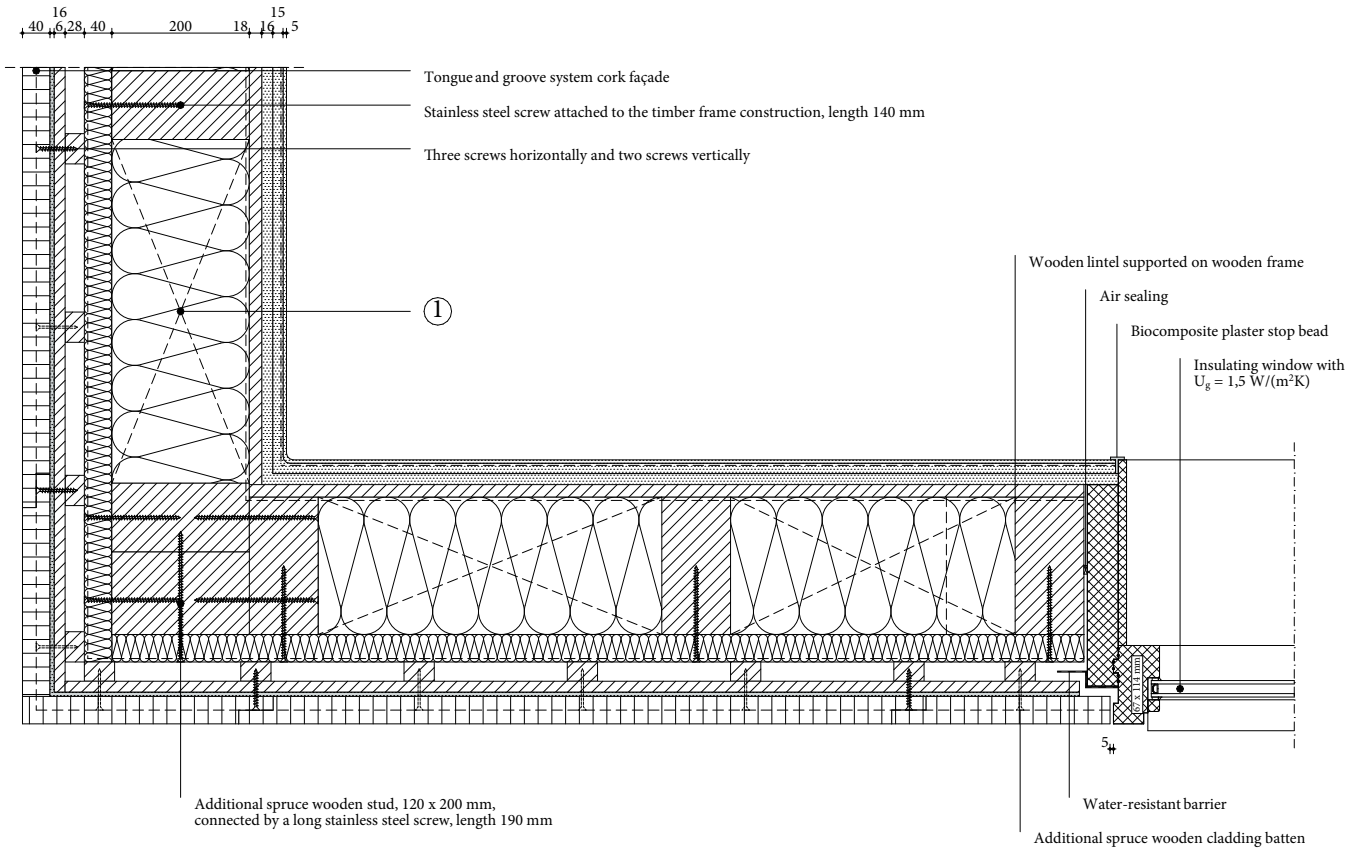

Figure A352, 1:10 detail of H1, configuration 2.5, own illustration

❶ Wall construction build-up, RC-value: 4.89 (m²K)/W

- Tongue and groove cork cladding panels, 40 mm;
- Cork mortar, 3 mm;
- Biobased diffusion open construction board, 16 mm;
- Vertical spruce cladding batten forming ventilated cavity, 28 x 44 mm, center-to-center 237 mm;
- Water resistant vapour-permeable membrane;
- Pressure-resistant woodfibre insulation plate ($\lambda \leq 0.042$ W/mK), 40 mm;
- Timber frame construction, 100 x 200 mm, center-to-center 600 mm;
- Flexible hemp fiber insulation placed between construction ($\lambda \leq 0.043$ W/mK), 200 mm;
- Vapour-retarding and airtight membrane with a variable vapour diffusion resistance;
- Biobased construction board, 18 mm;
- Clay base plate, 16 mm;
- Rough base clay plaster, 15 mm;
- Jute reinforcement mesh;
- Finishing clay plaster, 5mm.

Detail configuration 2.6 - hempcrete with cork façade

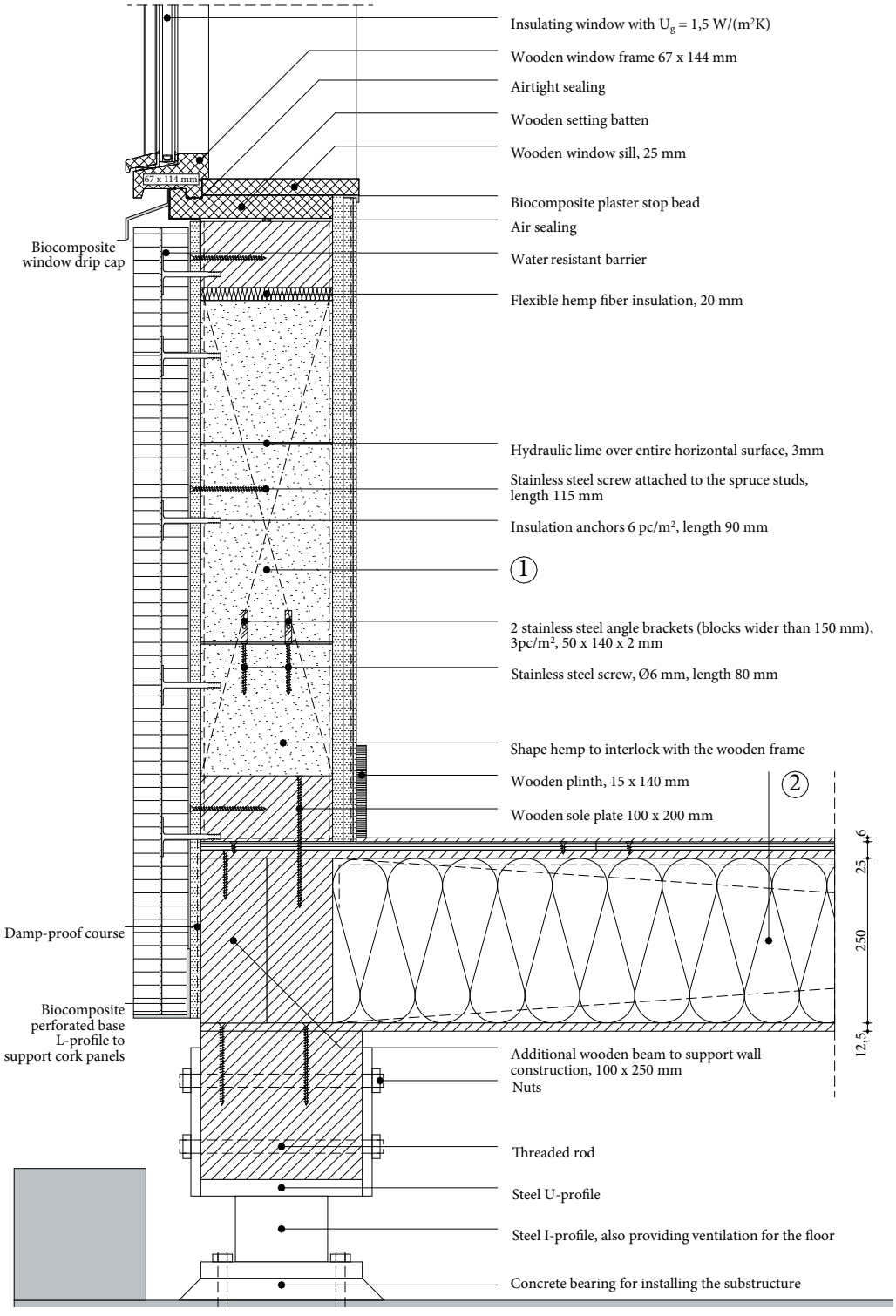

Figure A353, 1:10 detail of V1, configuration 2.6, own illustration

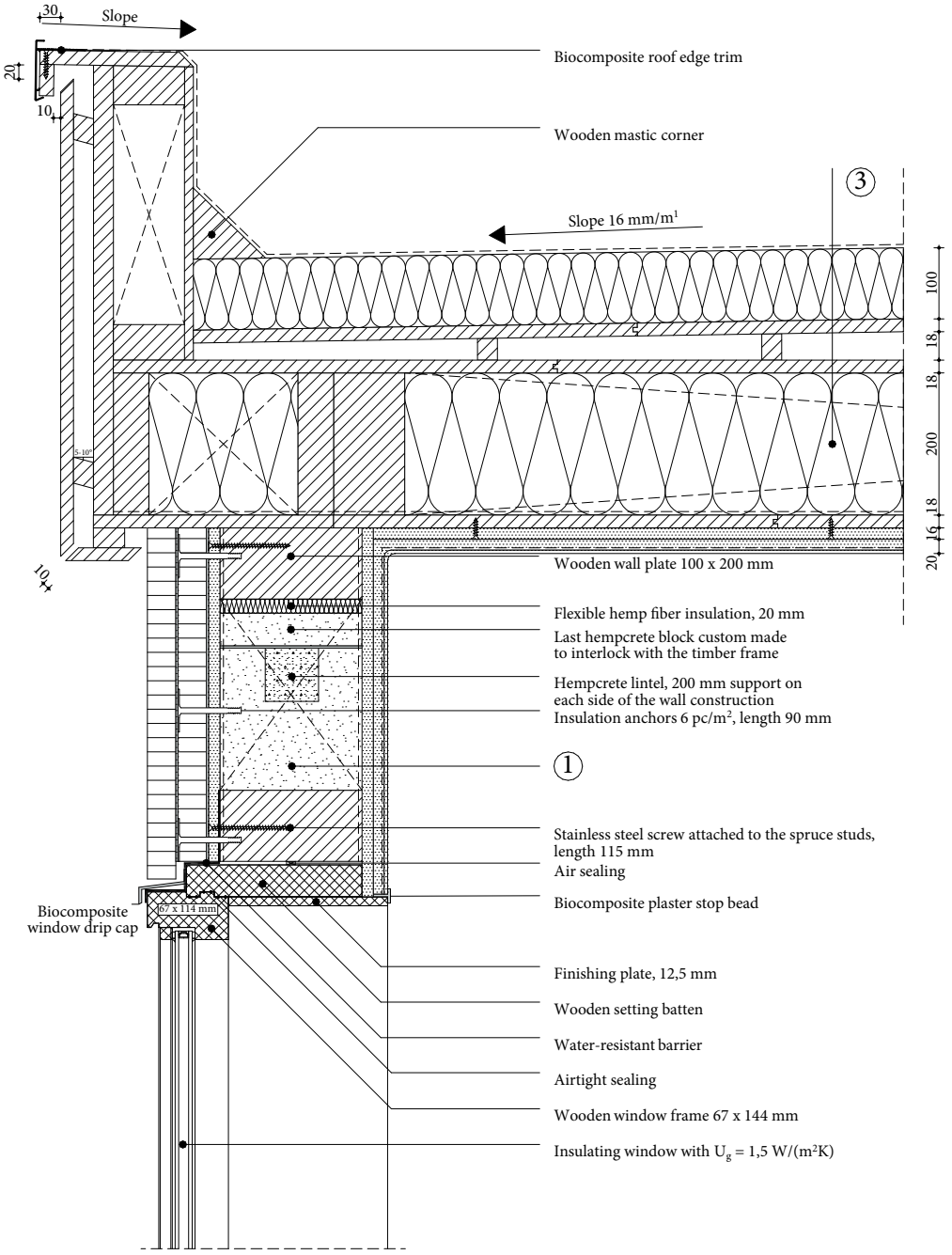

Figure A354, 1:10 detail of V2, configuration 2.6, own illustration

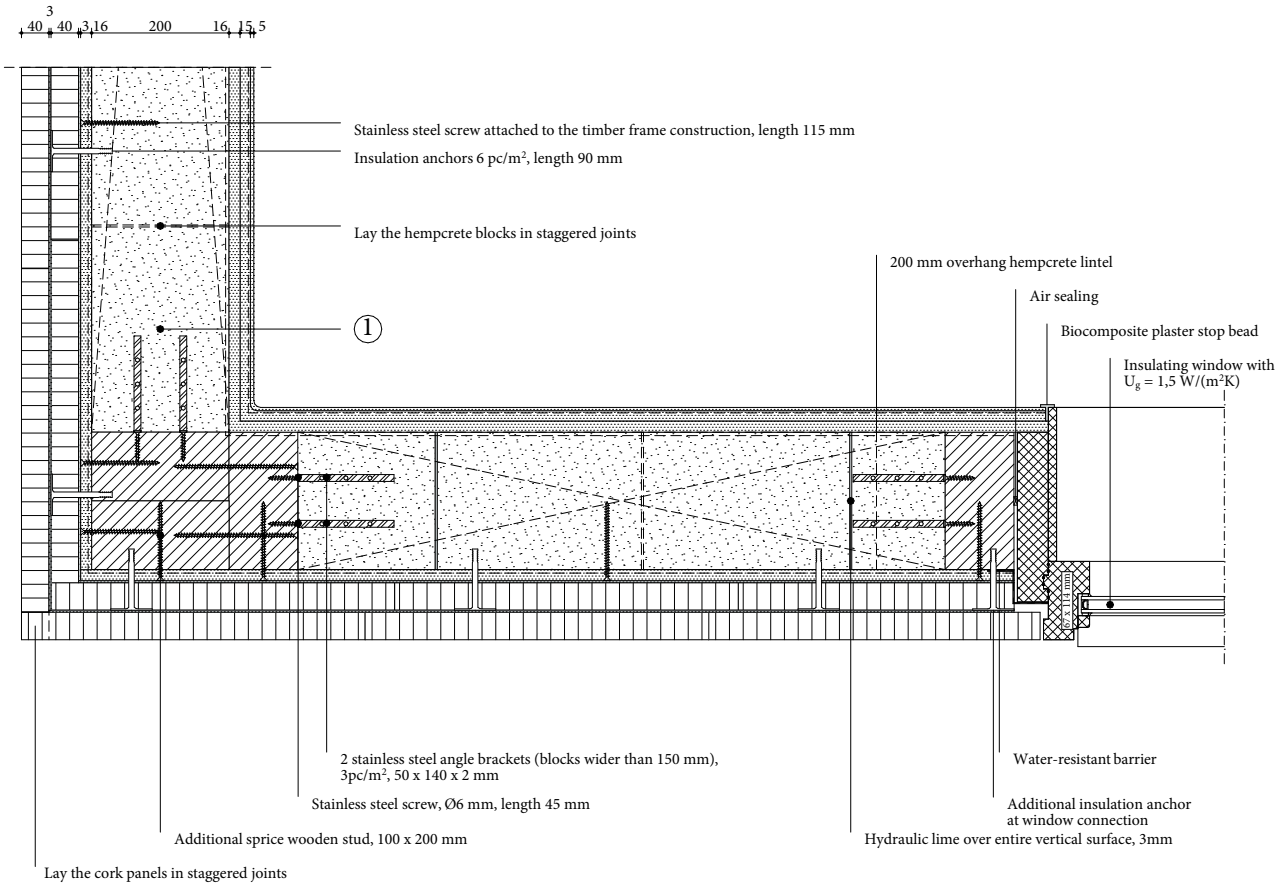

Figure A355, 1:10 detail of H1, configuration 2.6, own illustration

❶ Wall construction build-up, RC-value: 4.94 (m²K)/W

- Cork cladding panels (λ ≤ 0.043 W/mK), 40 mm;
- Cork underlayment mortar, 3 mm;
- Expanded insulation corkboard (λ ≤ 0.039 W/mK), 40 mm;
- Cork underlayment mortar, 3 mm;
- Biobased diffusion open construction board, 16 mm;
- Water-resistant vapour-permeable membrane;
- Timber frame construction, 100 x 200 mm, center-to-center 3000 mm;
- Hempcrete blocks placed between construction (λ ≤ 0.071 W/mK), 200 mm;
- Vapour-retarding and airtight membrane with a variable vapour diffusion resistance;
- Biobased construction board, 18 mm;- Clay base plate, 16 mm;
- Rough base clay plaster, 15 mm;
- Jute reinforcement mesh;
- Finishing clay plaster, 5mm.

Detail configuration 3.3 - flax insulation with cork façade

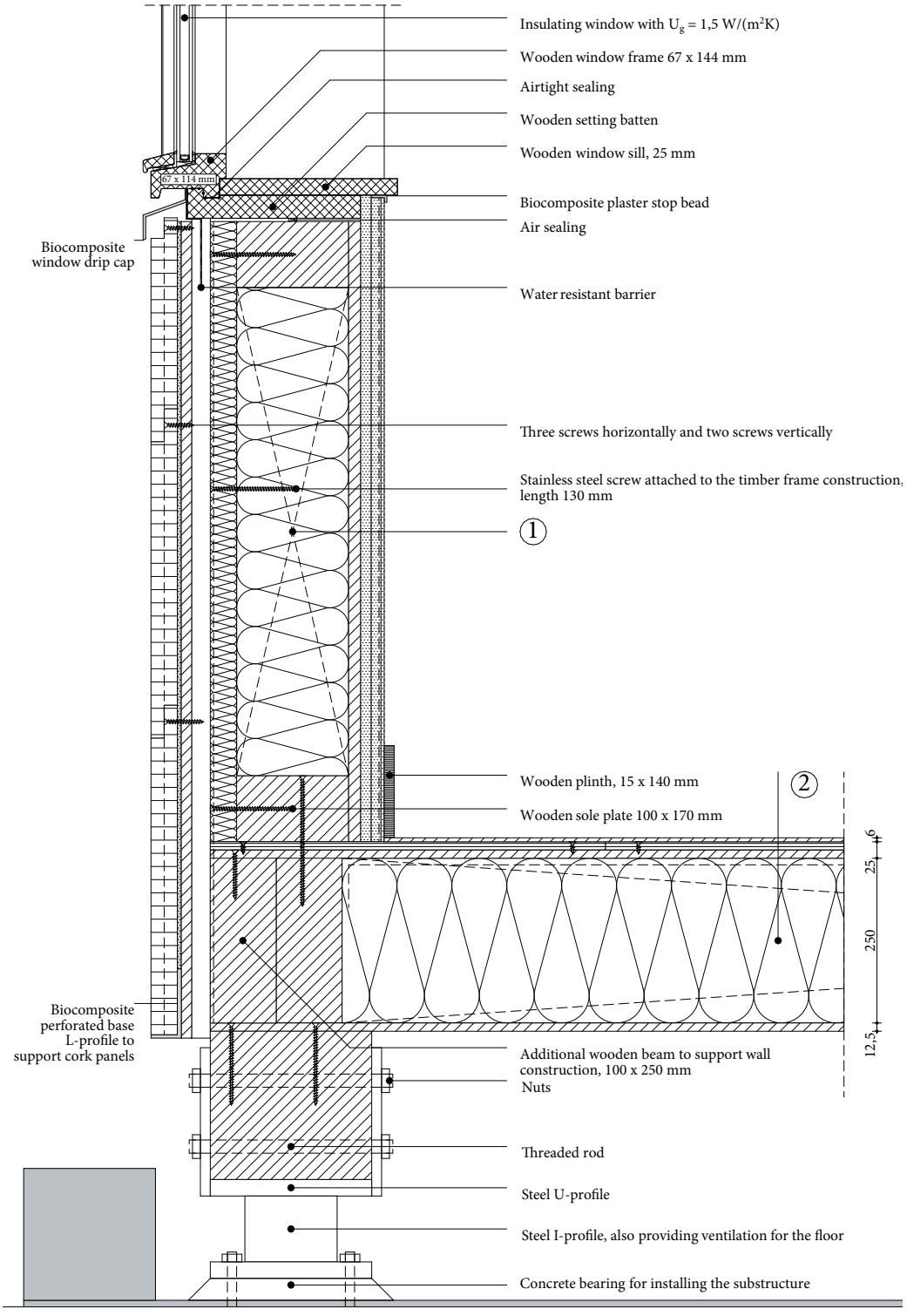

Figure A356, 1:10 detail of V1, configuration 3.3, own illustration

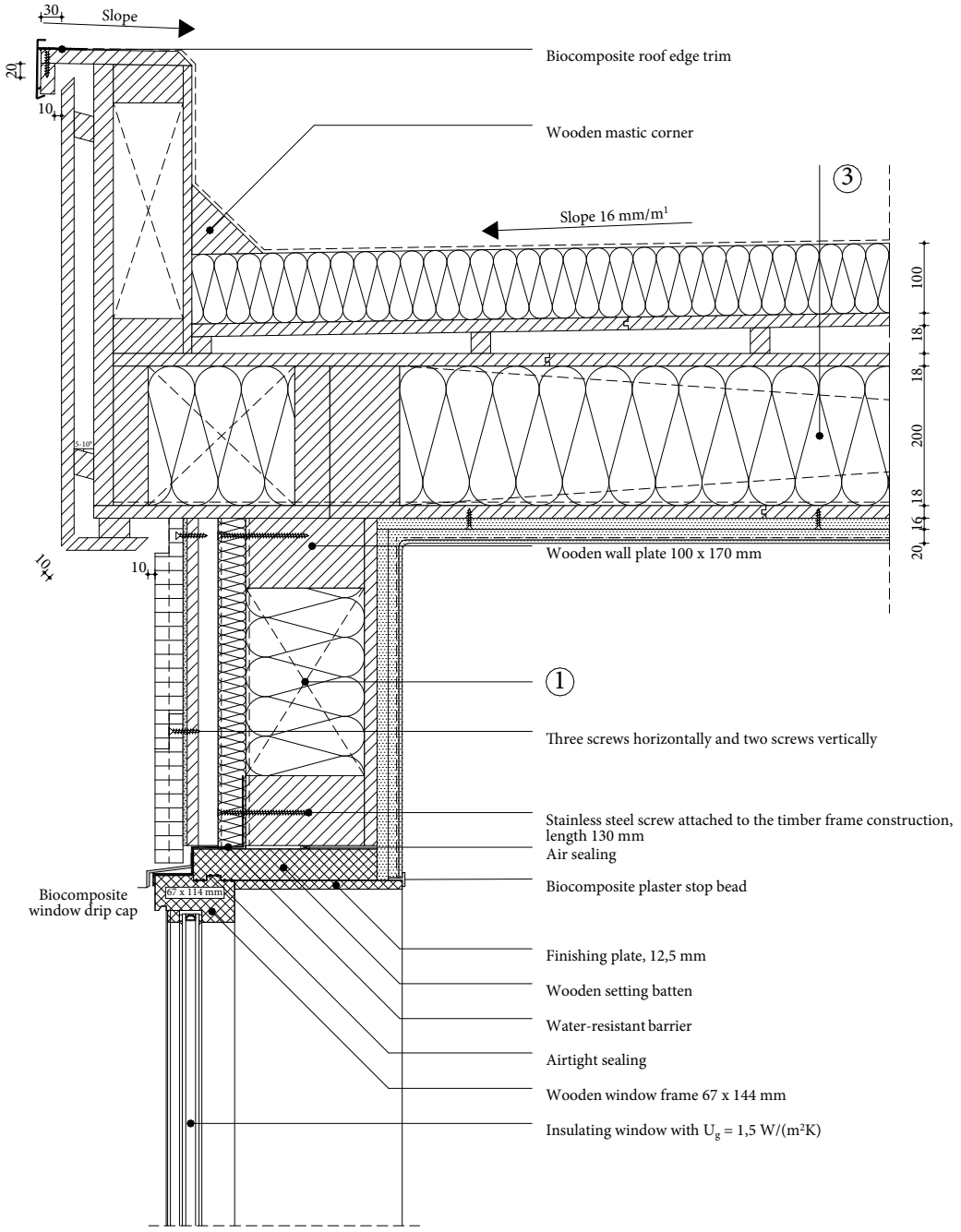

Figure A357, 1:10 detail of V2, configuration 3.3, own illustration

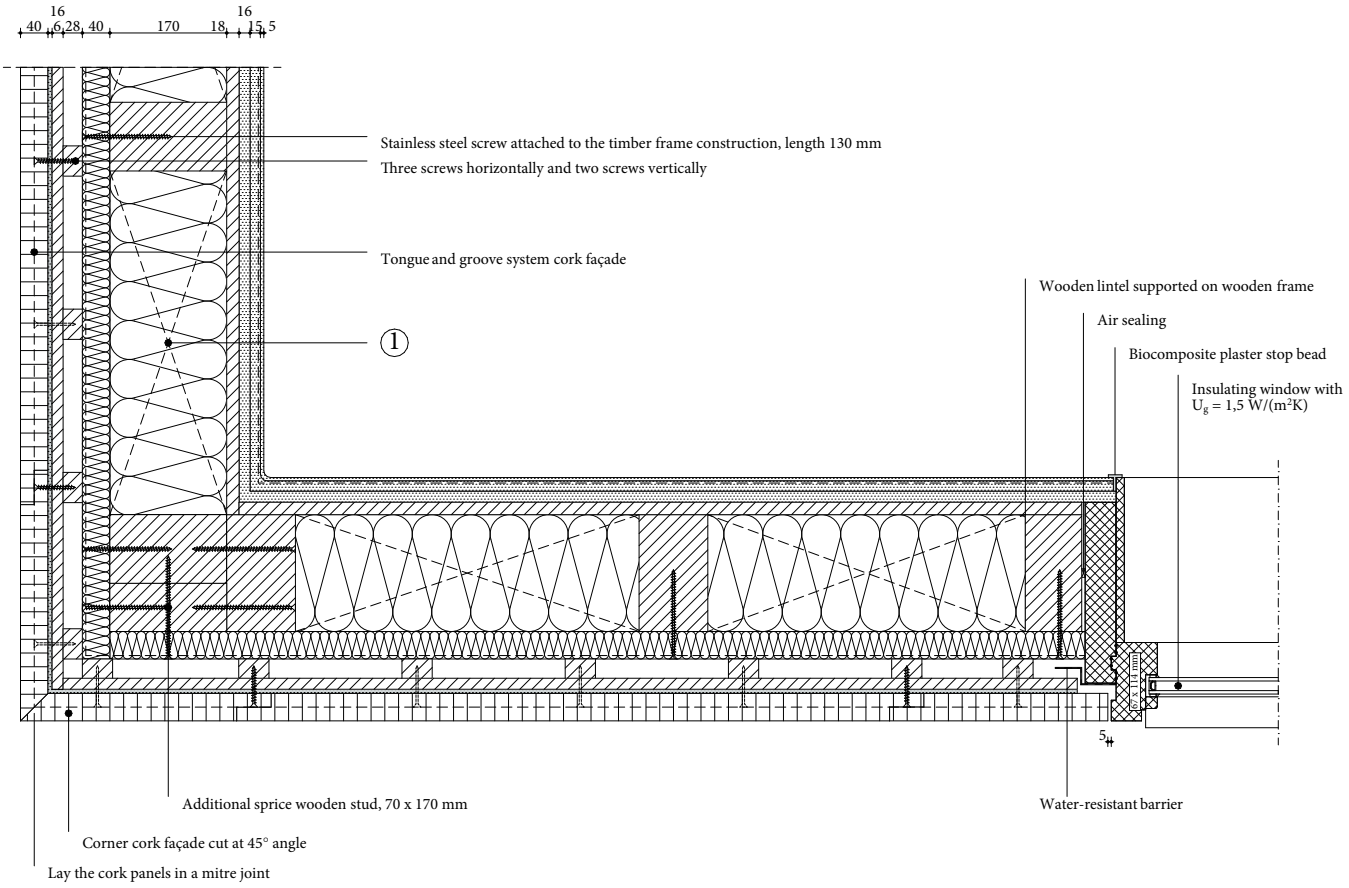

Figure A358, 1:10 detail of H1, configuration 3.3, own illustration

❶ Wall construction build-up, RC-value: 4.85 (m²K)/W

- Tongue and groove cork cladding panels, 40 mm;
- Cork mortar, 6 mm;
- Biobased diffusion open construction board, 16 mm;
- Vertical spruce cladding batten forming ventilated cavity, 28 x 44 mm, center-to-center 237 mm;
- Water-resistant vapour-permeable membrane;
- Pressure-resistant woodfibre insulation plate ($\lambda \leq 0.042$ W/mK), 40 mm;
- Timber frame construction, 100 x 170 mm, center-to-center 600 mm;
- Flax insulation placed between construction ($\lambda \leq 0.035$ W/mK), 170 mm;
- Biobased wooden construction board, 18 mm;
- Clay base plate, 16 mm;
- Rough base clay plaster, 15 mm;
- Jute reinforcement mesh;
- Finishing clay plaster, 5mm.

Detail configuration 3.4 - flax insulation with plaster façade

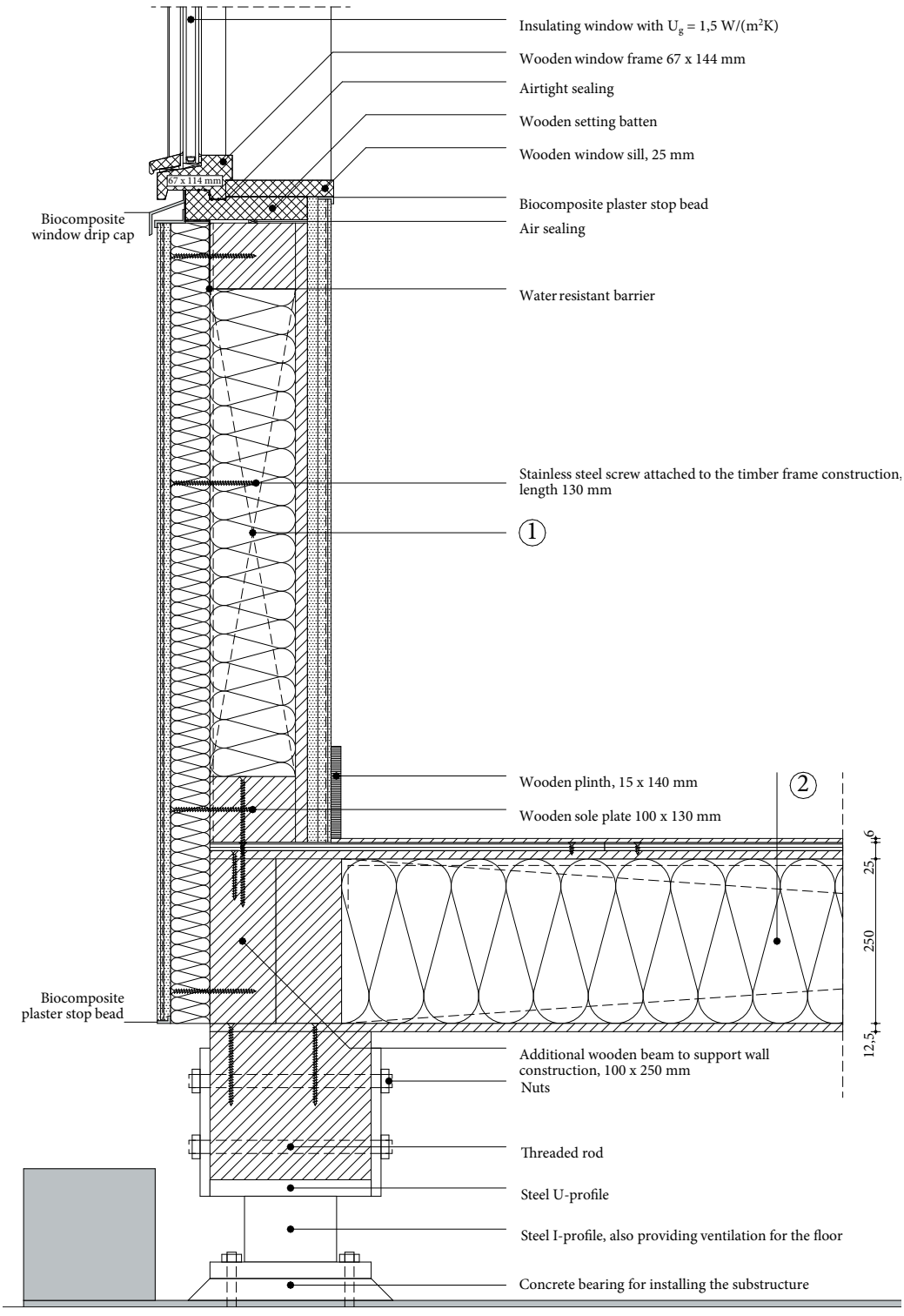

Figure A359, 1:10 detail of V1, configuration 3.4, own illustration

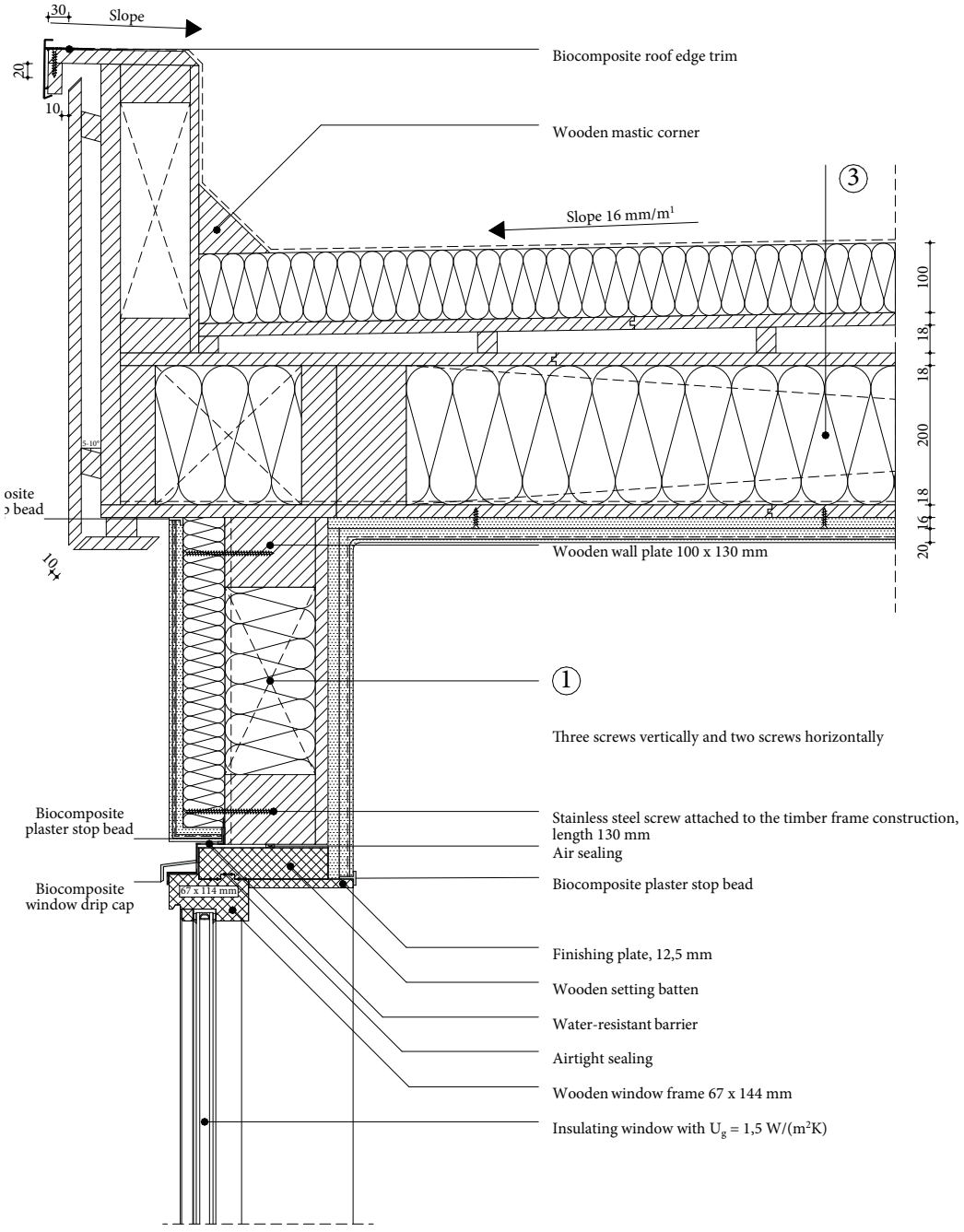

Figure A360, 1:10 detail of V2, configuration 3.4, own illustration

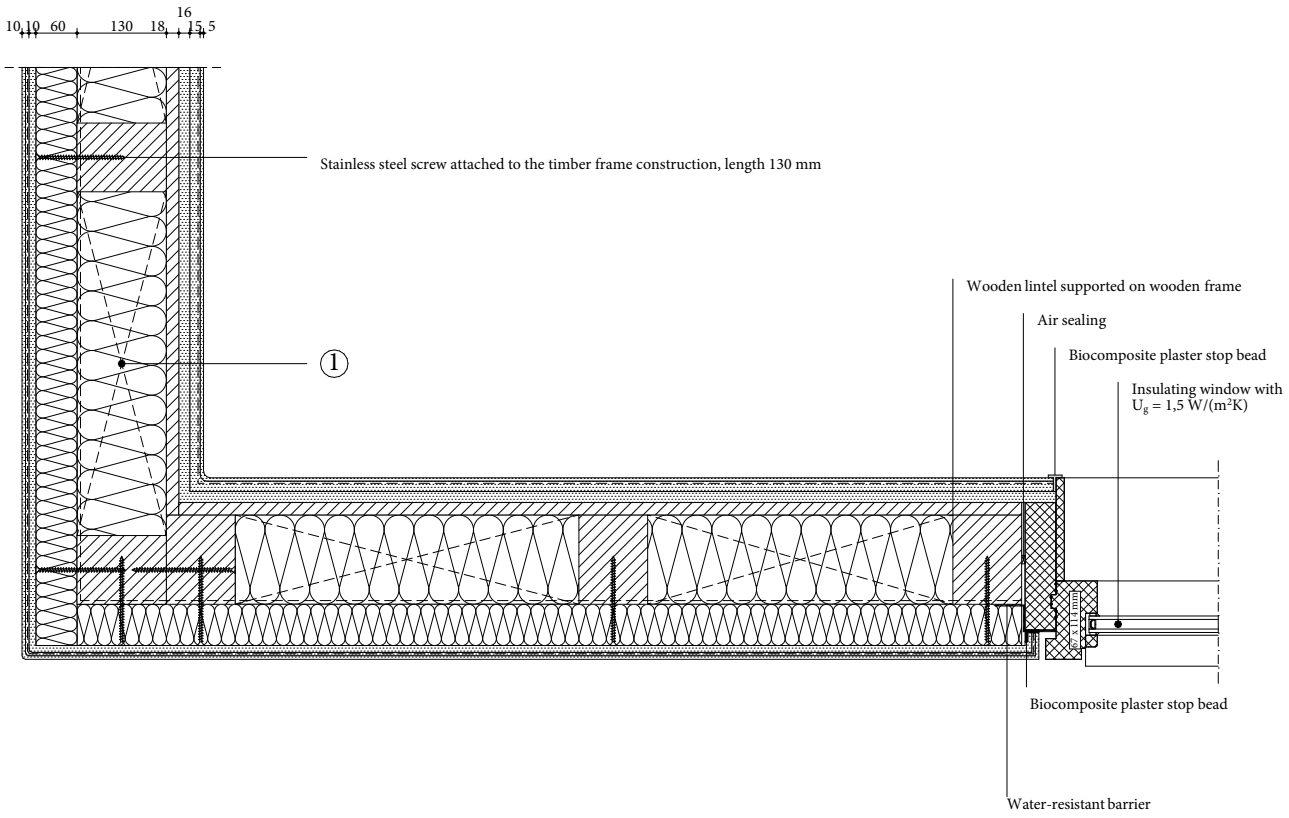

Figure A361, 1:10 detail of H1, configuration 3.4, own illustration

❶ Wall construction build-up, RC-value: 4.92 (m²K)/W

- Finishing lime plaster, 5 mm;
- Jute reinforcement mesh;
- Rough base lime plaster, 5 mm;
- Rough bonding lime plaster, 10 mm;
- Plasterable wood fibre insulation (λ ≤ 0.042 W/mK), 60 mm;
- Water-resistant vapour-permeable membrane;
- Timber frame construction, 100 x 130 mm, center-to-center 600 mm;
- Flax insulation placed between construction (λ ≤ 0.035 W/mK), 130 mm;
- Biobased wooden construction board, 18 mm;
- Clay base plate, 16 mm;
- Rough base clay plaster, 15 mm;
- Jute reinforcement mesh;
- Finishing clay plaster, 5mm.

Detail configuration 4.3 - wood fibre insulation with plaster façade

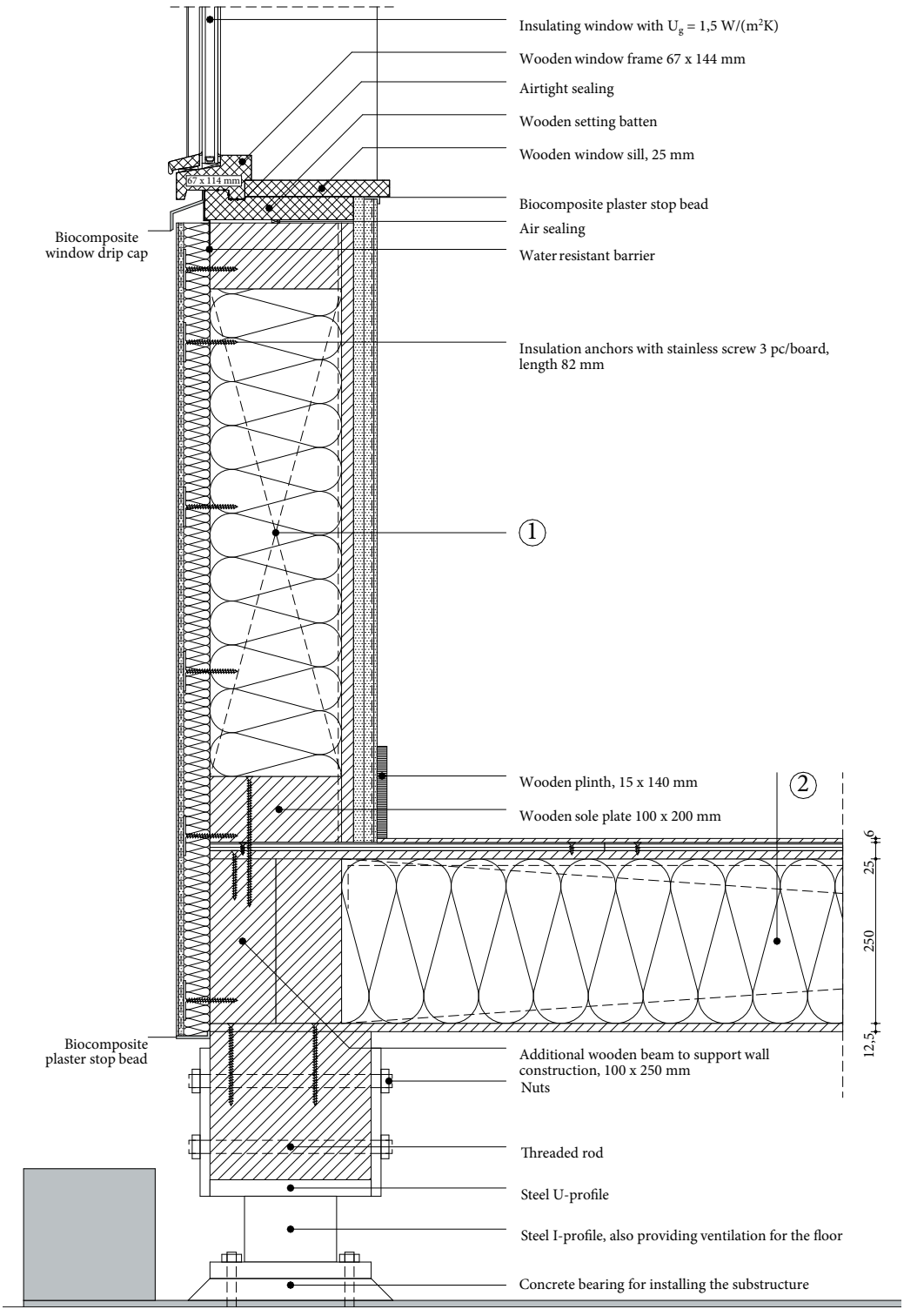

Figure A362, 1:10 detail of V1, configuration 4.3, own illustration

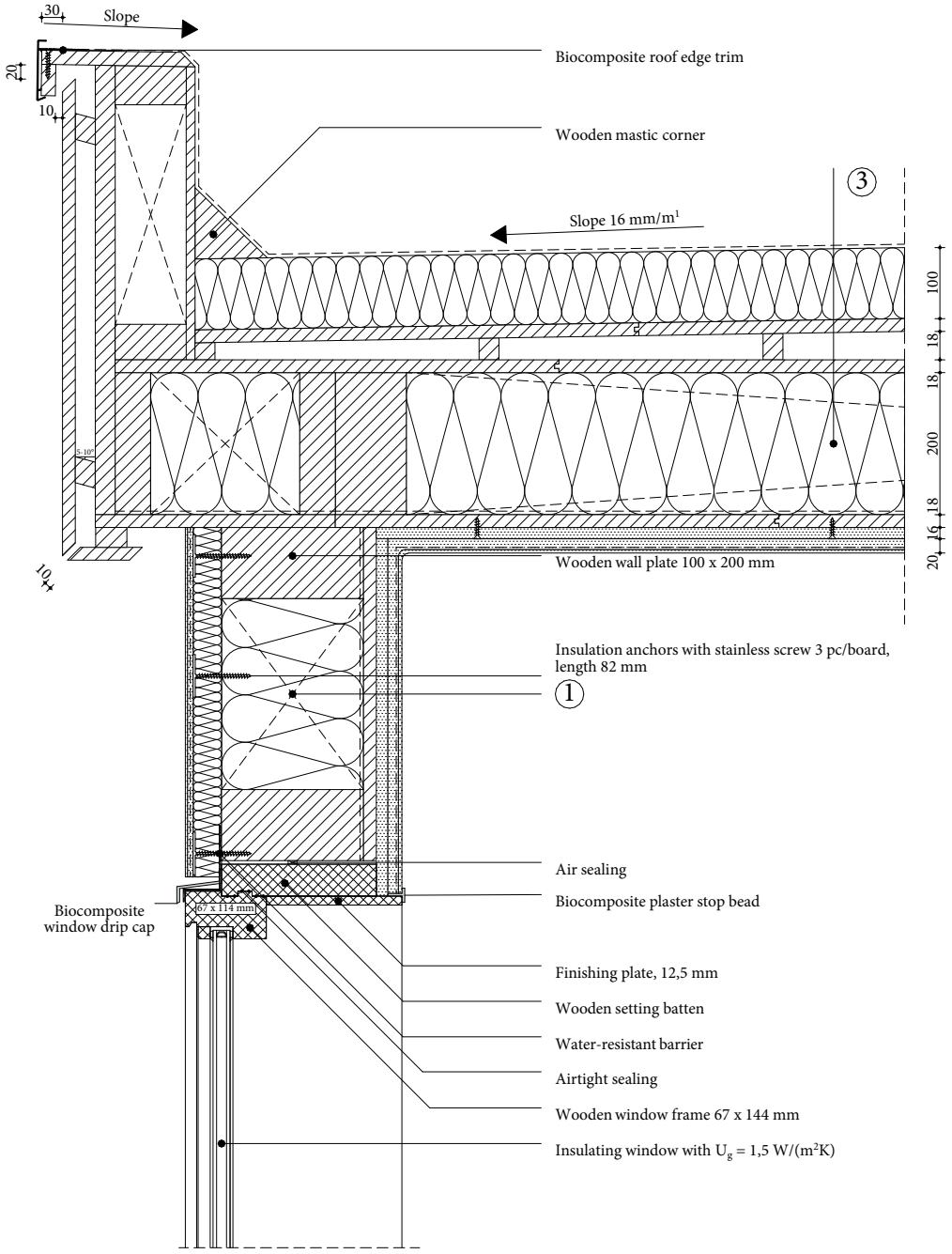

Figure A363, 1:10 detail of V2, configuration 4.3, own illustration

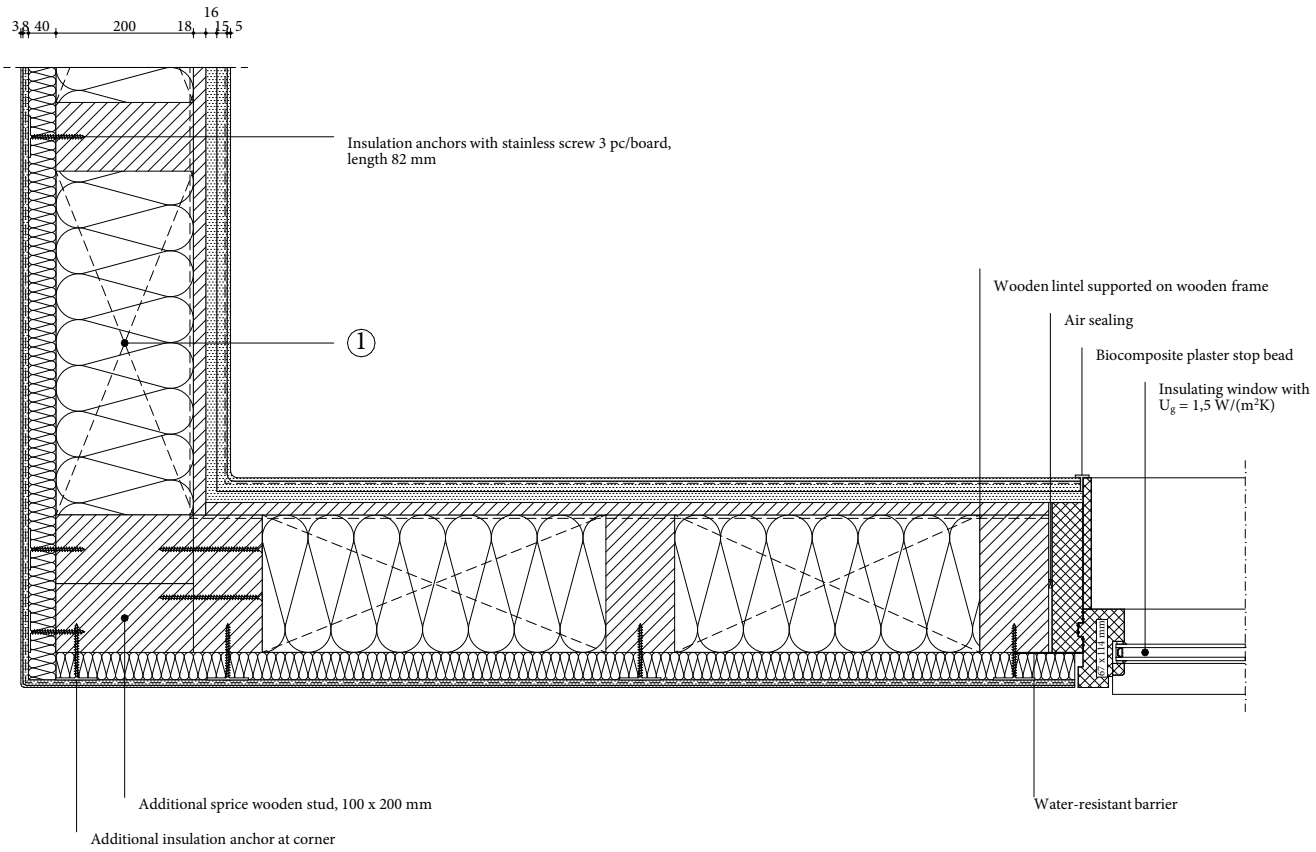

Figure A364, 1:10 detail of H1, configuration 4.3, own illustration

❶ Wall construction build-up, RC-value: 5.08 (m²K)/W

- Weather protective paint;
- Finishing mineral plaster, 3 mm;
- Rough base mineral plaster, 4 mm;
- Reinforcement glassfibre mesh;
- Rough base mineral plaster, 4 mm;
- Pressure-resistant plasterable wood fibre insulation (λ ≤ 0.045 W/mK), 40 mm;
- Timber frame construction, 100 x 200 mm, center-to-center 600 mm;
- Wood fibre insulation placed between construction (λ ≤ 0.038 W/mK), 200mm;
- Vapour-retarding and airtight membrane with a variable vapour diffusion resistance;
- Biobased wooden construction board, 18 mm;
- Clay base plate, 16 mm;
- Rough base clay plaster, 15 mm;
- Jute reinforcement mesh;
- Finishing clay plaster, 5mm.

Bibliography Appendices

Figure references

Table references

1. Calculation of the RC-value of the wall construction build-up. Own table
2. Calculation of the equivalent thermal conductivity of the individual layers in the relevant build-up. Own table
3. Calculation of the density mass per unit area. Own table
4. Calculation of the phase shift. Own table
5. Calculation of the $Q_{ideal\ condition}$ V1. Own table
6. Calculation of the $Q_{ideal\ condition}$ V2. Own table
7. Calculation of the $Q_{ideal\ condition}$ H1. Own table
8. Calculation of the RC-value of the wall construction build-up. Own table
9. Calculation of the equivalent thermal conductivity of the individual layers in the relevant build-up. Own table
10. Calculation of the density mass per unit area. Own table
11. Calculation of the phase shift. Own table
12. Calculation of the $Q_{ideal\ condition}$ V1. Own table
13. Calculation of the $Q_{ideal\ condition}$ V2. Own table
14. Calculation of the $Q_{ideal\ condition}$ H1. Own table
15. Calculation of the RC-value of the wall construction build-up. Own table
16. Calculation of the equivalent thermal conductivity of the individual layers in the relevant build-up. Own table
17. Calculation of the density mass per unit area. Own table
18. Calculation of the phase shift. Own table
19. Calculation of the $Q_{ideal\ condition}$ V1. Own table
20. Calculation of the $Q_{ideal\ condition}$ V2. Own table
21. Calculation of the $Q_{ideal\ condition}$ H1. Own table
22. Calculation of the RC-value of the wall construction build-up. Own table
23. Calculation of the equivalent thermal conductivity of the individual layers in the relevant build-up. Own table
24. Calculation of the density mass per unit area. Own table
25. Calculation of the phase shift. Own table
26. Calculation of the $Q_{ideal\ condition}$ V1. Own table
27. Calculation of the $Q_{ideal\ condition}$ V2. Own table
28. Calculation of the $Q_{ideal\ condition}$ H1. Own table
29. Calculation of the RC-value of the wall construction build-up. Own table
30. Calculation of the equivalent thermal conductivity of the individual layers in the relevant build-up. Own table
31. Calculation of the density mass per unit area. Own table
32. Calculation of the phase shift. Own table

33. Calculation of the $Q_{ideal\ condition}$ V1. Own table
34. Calculation of the $Q_{ideal\ condition}$ V2. Own table
35. Calculation of the $Q_{ideal\ condition}$ H1. Own table
36. Calculation of the RC-value of the wall construction build-up. Own table
37. Calculation of the equivalent thermal conductivity of the individual layers in the relevant build-up. Own table
38. Calculation of the density mass per unit area. Own table
39. Calculation of the phase shift. Own table
40. Calculation of the $Q_{ideal\ condition}$ V1. Own table
41. Calculation of the $Q_{ideal\ condition}$ V2. Own table
42. Calculation of the $Q_{ideal\ condition}$ H1. Own table
43. Calculation of the RC-value of the wall construction build-up. Own table
44. Calculation of the equivalent thermal conductivity of the individual layers in the relevant build-up. Own table
45. Calculation of the density mass per unit area. Own table
46. Calculation of the phase shift. Own table
47. Calculation of the $Q_{ideal\ condition}$ V1. Own table
48. Calculation of the $Q_{ideal\ condition}$ V2. Own table
49. Calculation of the $Q_{ideal\ condition}$ H1. Own table
50. Calculation of the RC-value of the wall construction build-up. Own table
51. Calculation of the equivalent thermal conductivity of the individual layers in the relevant build-up. Own table
52. Calculation of the density mass per unit area. Own table
53. Calculation of the phase shift. Own table
54. Calculation of the $Q_{ideal\ condition}$ V1. Own table
55. Calculation of the $Q_{ideal\ condition}$ V2. Own table
56. Calculation of the $Q_{ideal\ condition}$ H1. Own table
57. Calculation of the RC-value of the wall construction build-up. Own table
58. Calculation of the equivalent thermal conductivity of the individual layers in the relevant build-up. Own table
59. Calculation of the density mass per unit area. Own table
60. Calculation of the phase shift. Own table
61. Calculation of the $Q_{ideal\ condition}$ V1. Own table
62. Calculation of the $Q_{ideal\ condition}$ V2. Own table
63. Calculation of the $Q_{ideal\ condition}$ H1. Own table
64. Calculation of the RC-value of the wall construction build-up. Own table

65. Calculation of the equivalent thermal conductivity of the individual layers in the relevant build-up. Own table
66. Calculation of the density mass per unit area. Own table
67. Calculation of the phase shift. Own table
68. Calculation of the $Q_{ideal\ condition}$ V1. Own table
69. Calculation of the $Q_{ideal\ condition}$ V2. Own table
70. Calculation of the $Q_{ideal\ condition}$ H1. Own table

Bio-based reference façade wall details

Design and analysis of moisture transport and thermal bridges for Dutch residential top-up buildings

With a special thanks to:

Dr. Ing. O. (Olga) Ioannou

&

Prof. Dr. Ir. M. (Martin) Tenpierik

Master thesis
MSc. Architecture, Urbanism and Building Sciences
Master track: Buidling Technology
19-06-2025

Mark de Kanter